

A mis aïtonas

Regioselective Synthesis and Functionalization of 2- and 3-Aryl Benzo[*b*]furans. Application to Medicinal Chemistry

DOCTORAL THESIS

Leire Lidia Arias Echeverría
Donostia – San Sebastián
2014

Index

Autorización del director de tesis para su presentación.....	13
Conformidad del Departamento.....	17
Acta de grado de doctora acta de defensa de tesis doctoral.....	19
Resumen (Spanish Summary).....	21
Acknowledgements.....	37
Abbreviations.....	41
Chapter 1: General Introduction to Benzo[<i>b</i>]furans and Objectives.....	47
1.1. General introduction to benzo[<i>b</i>]furans.....	49
1.1.1. The benzo[<i>b</i>]furan, a “privileged structure”.....	49
1.1.2. Applications of benzo[<i>b</i>]furans.....	51
1.1.3. Preparation of benzo[<i>b</i>]furans.....	57
1.1.3.1. Construction of the benzo[<i>b</i>]furan core.....	57
1.1.3.1.1. Methods based on the O-C ₂ bond formation (A).....	58
1.1.3.1.2. Methods based on the C ₂ -C ₃ bond formation (B).....	69
1.1.3.1.3. Methods based on the C ₃ -C _{3a} bond formation (C).....	75
1.1.3.1.4. Methods based on the O-C _{7a} bond formation (D).....	81
1.1.3.1.5. Methods based on the construction of the benzene ring (E).....	84
1.1.3.1.6. Methods based on the transformation of bi- or tricyclic oxygen-containing ring systems (F).....	87
1.1.3.2. Substituents in the benzo[<i>b</i>]furan structure.....	89
1.1.3.2.1. Halogens.....	89
1.1.3.2.2. Hydroxy groups.....	91
1.2. Objectives.....	93
Chapter 2: Regioselective Preparation of 2- and 3-Aryl Benzo[<i>b</i>]furans.....	95
2.1. Short introduction and objectives.....	97
2.2. Experimental study: reaction conditions and products.....	98
2.2.1. General considerations.....	98
Microwave irradiation.....	98
Alumina.....	100
2.2.2. Optimization of the reaction conditions.....	102
2.2.3. Two families of compounds: 2-aryl and 3-aryl benzo[<i>b</i>]furans.....	109
2.2.4. Characterization: NMR spectroscopy study and X-ray diffraction analysis.....	113
NMR spectroscopy study.....	113
X-ray diffraction analysis.....	120
2.2.5. Graphical overview.....	121
2.3. Computational study: mechanisms.....	122
2.3.1. General considerations.....	122
2.3.2. Reaction path in the absence of alumina.....	123

2.3.3. Reaction path in the presence of alumina.....	125
2.3.4. Graphical overview.....	131
2.4. Broadening the scope of the reaction: naphthofuran synthesis.....	132
2.4.1. Experimental study.....	132
2.4.2. Insight into the reaction mechanism.....	133
2.5. Conclusions.....	137
Chapter 3: Chemical Transformations on 2- and 3-Aryl Benzo[<i>b</i>]furans.....	139
3.1. Short introduction and objectives.....	141
3.2. <i>N</i> -halosuccinimides-mediated aromaticity driven regioselective halogenation of substituted benzo[<i>b</i>]furans.....	144
3.2.1. Preparation of halogenated benzofurans overview.....	144
3.2.1.1. Formation of the heterocyclic framework after the introduction of the halogen(s).....	144
3.2.1.2. Introduction of the halogen(s) to the preformed heterocycle.....	145
3.2.2. Experimental study: <i>N</i> -halosuccinimides (NXS).....	149
3.2.2.1. General considerations.....	149
<i>N</i> -halosuccinimides: general features.....	149
<i>N</i> -halosuccinimides and C-halogenations (background).....	150
3.2.2.2. Two families of compounds: 2-aryl and 3-aryl halobenzofurans.....	153
2-aryl halobenzofurans.....	154
3-aryl halobenzofurans.....	158
3.2.2.3. Structural elucidation: NMR spectroscopy study.....	162
Monohalogenation of 124a (126a) and 125a (127a,d-e)	162
Dibromination of 124a (126b) and 125a (127b)	163
Dichlorination of 124a : major (126f) and minor (126g) isomers.....	168
Combined dihalogenation: monobromination of 127e (127f)	173
3.2.2.4. Graphical overview.....	176
3.2.3. Computational study.....	177
3.2.3.1. General considerations.....	177
3.2.3.2. Assessment of the aromaticity of the starting benzofurans 124a and 125a	179
3.2.3.3. Energy profiles of the bromination reactions of 124a and 125a using NBS....	181
3.2.3.4. Graphical overview.....	190
3.2.4. Conclusions.....	192
3.3. Hypervalent iodine-mediated oxidative dearomatization of monohydroxylated benzo[<i>b</i>]furans.....	194
3.3.1. Oxidative dearomatization of phenols overview.....	194
3.3.1.1. Basic concepts.....	194
3.3.1.2. The reaction of oxidative dearomatization of phenols.....	197
3.3.1.3. Hypervalent iodine-based reagents.....	199
3.3.2. Experimental study: λ^3 -Iodanes.....	201
3.3.2.1. General considerations.....	201
3.3.2.2. Preparation of the starting 2- and 3- phenylbenzofuran-6-ols 124a and 125p ..	205

3.3.2.3. Reaction of 2- and 3-phenylbenzofuran-6-ols 124s and 125p with λ^3 -iodanes.....	207
2-phenylbenzofuran-6-ol (124s) as starting material.....	207
Methanol.....	207
Other nucleophiles.....	211
3-phenylbenzofuran-6-ol (125p) as starting material.....	213
Methanol.....	213
Other nucleophiles.....	214
3.3.2.4. Structural elucidation and characterization.....	216
Compounds cis-170a and trans-170a	216
Compound 171a	221
3.3.2.5. Graphical overview.....	223
3.3.2.6. Insight into the reaction mechanism.....	224
2-phenylbenzofuran-6-ol (124s) as starting material.....	224
3-phenylbenzofuran-6-ol (125p) as starting material.....	225
3.3.3. Experimental study: λ^5 -Iodanes (preliminary results).....	228
3.3.3.1. General considerations.....	228
3.3.3.2. Reaction of 2- and 3- phenylbenzofuran-6-ols 124s and 125p with λ^5 -iodanes.....	231
2-phenylbenzofuran-6-ol (124s) as starting material.....	232
3-phenylbenzofuran-6-ol (125p) as starting material.....	234
3.3.4. Conclusions.....	236
3.4. Boron tribromide-mediated demethylation of methoxy groups in benzo[<i>b</i>]furans.....	238
3.4.1. Preparation of hydroxylated benzofurans overview.....	238
3.4.2. Experimental study: boron tribromide (BBr ₃).....	242
3.4.2.1. General considerations.....	242
3.4.2.2. Synthesis of 2-aryl and 3-aryl hydroxybenzofurans.....	243
2-aryl hydroxybenzofurans (128).....	244
3-aryl hydroxybenzofurans (129).....	246
3.4.3. Conclusions.....	248
Chapter 4: Benzo[<i>b</i>]furans as Resveratrol Analogues: Biological Assays.....	249
4.1. Short introduction and objectives.....	251
4.2. Resveratrol overview.....	254
Getting to know resveratrol.....	254
Biological activity of resveratrol.....	256
Bioavailability of resveratrol.....	259
Resveratrol analogues.....	260
4.3. Enzymatic assays: modulation of SIRT1.....	262
4.3.1. General considerations: sirtuins.....	262
Getting to know sirtuins.....	262
Biological activity of sirtuins.....	263
Sirtuin modulators.....	264

4.3.2. Experimental procedure of the enzymatic assays.....	267
4.3.2.1. Tested compounds.....	267
4.3.2.2. SIRT1 modulation assay.....	267
4.3.3. Results and discussion of the enzymatic assays.....	269
4.3.3.1. General considerations.....	269
4.3.3.2. SIRT1 inhibitors.....	270
4.3.3.3. SIRT1 activators.....	271
4.3.4. Controversy: uncertain validity of the fluorescence assays.....	273
4.4. Cell-based assays: anticancer properties.....	277
4.4.1. General considerations: cancer.....	277
Cancer in few words.....	277
Carcinogenesis stages and the metastatic process.....	277
Colon tumor model for the evaluation of anticancer agents.....	280
4.2. Experimental procedures of the cell-based assays.....	281
4.4.2.1. Treatments: benzofuran analogues of resveratrol at various concentrations..	281
4.4.2.2. Cancer cell line: murine colon carcinoma C26.....	282
4.4.2.3. Tumor cell adhesion assay to primary cultured LSECs.....	282
Primary culture, isolation and purification of LSECs.....	282
Adhesion assay.....	283
4.4.2.4. Proliferation assay.....	284
4.4.2.5. <i>In vitro</i> migration assay.....	284
4.4.3. Results and discussion of the cell-based assays.....	286
4.4.3.1. Effect of the resveratrol analogues on the adhesion of murine colon carcinoma C26 cells to primary cultures of LSECs.....	286
4.4.3.2. Effect of the resveratrol analogues on the net proliferation rate of murine colon carcinoma C26 cells.....	287
4.4.3.3. Effect of the resveratrol analogues on the migration of murine colon carcinoma C26 cells.....	291
4.4.4. Graphical overview.....	293
4.5. Conclusions.....	295
Chapter 5: Experimental Section.....	297
5.1. Analytical techniques and reagents.....	299
5.2. Regioselective synthesis of 2- and 3-aryl benzo[<i>b</i>]furans.....	303
5.2.1. General procedure for the preparation of α -bromoketones 123b-c,h-j	303
5.2.2. Procedure for the preparation of 2-aryl benzo[<i>b</i>]furans 124a-n and 2-aryl naphtho[1,2- <i>b</i>] and 2-aryl naphtho[2,1- <i>b</i>] furans 124q-r	305
5.2.3. Procedure for the preparation of α -phenoxyketones 130a-l and α -naphthoxyketones 130n-o	322
5.2.4. Procedure for the preparation of 3-aryl benzo[<i>b</i>]furans 125a-i and 3-aryl naphtho[1,2- <i>b</i>] and 3-aryl naphtho[2,1- <i>b</i>] furans 125n-o	336
5.3. <i>N</i> -halosuccinimides (NXS)-mediated regioselective halogenation of 2- and 3-aryl benzo[<i>b</i>]furans 124a and 125a	347
5.3.1. Procedure for the monohalogenation of 2-aryl benzo[<i>b</i>]furan 124a and 3-aryl benzo[<i>b</i>]furan 125a with NXS leading to products 126a and 127a,d-e	347

5.3.2. Procedure for the dihalogenation of 2-aryl benzo[<i>b</i>]furan 124a and 3-aryl benzo[<i>b</i>]furan 125a with NXS leading to products 126b,f-g and 127b	354
5.3.3. Procedure for the tribromination of 2-aryl benzo[<i>b</i>]furan 124a with NBS leading to product 126c	361
5.3.4. Procedure for the monobromination of 2-chloro 3-aryl benzo[<i>b</i>]furan 127e with NBS leading to product 127f	363
5.4. Hypervalent iodine reagents-mediated oxidative dearomatization of 2- and 3-aryl benzo[<i>b</i>]furans 124s and 125p	365
5.4.1. Procedure for the preparation of 2-phenylbenzofuran-6-ol 124s	365
5.4.2. Procedure for the preparation of 3-phenylbenzofuran-6-ol 125p	366
5.4.3. Procedure for the preparation of <i>cis/trans</i> -2,3-dialkoxy-2-phenyl-2,3-dihydrobenzofuran-6-ols <i>cis/trans</i>-170a-d	367
5.4.4. Procedure for the preparation of 2-alkoxy-3-phenylbenzofuran-6-ols 171a-f	377
5.4.5. Methylation of 2- and 3-phenyl benzo[<i>b</i>]furans 124s and 125p with methyl iodide	386
5.4.6. Synthesis of <i>o</i> -iodoxybenzoic acid IBX.....	387
5.4.7. Procedure for the preparation of 2-phenylbenzofuran-6,7-dione 141	388
5.4.8. Procedure for the preparation of 3-phenylbenzofuran-6,7-diol 186	390
5.5. Boron tribromide (BBr ₃)-mediated demethylation of methoxy groups of 2- and 3-aryl benzo[<i>b</i>]furans 124a-e,i-k,q and 125a,d,i	392
5.6. Characterization reports.....	408
5.6.1. X-ray diffraction analysis report of compound 124a	408
5.6.2. X-ray diffraction analysis report of compound 125a	413
5.6.3. X-ray diffraction analysis report of compound <i>cis</i>-170a	417
5.6.4. X-ray diffraction analysis report of compound <i>trans</i>-170a	422
5.6.5. HRMS report of <i>cis/trans</i> mixtures of compounds 170c and 170d	429



**AUTORIZACIÓN DEL DIRECTOR DE TESIS
PARA SU PRESENTACIÓN**

Dr. Fernando P. Cossío Mora con N.I.F. 18010287-E como Director de la Tesis Doctoral: “Regioselective Synthesis and Functionalization of 2- and 3-Aryl Benzo[*b*]furans. Application to Medicinal Chemistry” realizada en el Departamento de Química Orgánica I por la Doctoranda Doña Leire Lidia Arias Echeverría, autorizo la presentación de la citada Tesis Doctoral, dado que reúne las condiciones necesarias para su defensa.

En Donostia – San Sebastián, a 16 de septiembre de 2014

EL DIRECTOR/A DE LA TESIS

Fdo.: Fernando P. Cossío Mora



**AUTORIZACIÓN DEL DIRECTOR DE TESIS
PARA SU PRESENTACIÓN**

Dr. Yosu Ion Vara Salazar con N.I.F. 72479673-A como Director de la Tesis Doctoral: “Regioselective Synthesis and Functionalization of 2- and 3-Aryl Benzo[*b*]furans. Application to Medicinal Chemistry” realizada en el Departamento de Química Orgánica I por la Doctoranda Doña Leire Lidia Arias Echeverría, autorizo la presentación de la citada Tesis Doctoral, dado que reúne las condiciones necesarias para su defensa.

En Donostia – San Sebastián, a 16 de septiembre de 2014

EL DIRECTOR/A DE LA TESIS

Fdo.: Yosu Ion Vara Salazar



CONFORMIDAD DEL DEPARTAMENTO

El Consejo del Departamento de Química Orgánica I, Universidad del País Vasco – Euskal Herriko Unibertsitatea, en reunión celebrada el día 17 de septiembre de 2014 ha acordado dar la conformidad a la admisión a trámite de presentación de la Tesis Doctoral titulada: “Regioselective Synthesis and Functionalization of 2- and 3-Aryl Benzo[b]furans. Application to Medicinal Chemistry” dirigida por el Dr. Fernando P. Cossío Mora y el Dr. Yosu Ion Vara Salazar y presentada por Doña Leire Lidia Arias Echeverría ante este Departamento.

En Donostia – San Sebastián a 19 de septiembre de 2014

Vº Bº DIRECTOR/A DEL DEPARTAMENTO SECRETARIO/A DEL DEPARTAMENTO

Fdo.: Claudio Palomo Nicolau

Fdo.: Antonia Mielgo Vicente



ACTA DE GRADO DE DOCTORA
ACTA DE DEFENSA DE TESIS DOCTORAL

DOCTORANDA DÑA. Leire Lidia Arias Echeverría

TÍTULO DE LA TESIS: "Regioselective Synthesis and Functionalization of 2- and 3-Aryl Benzo[b]furans. Application to Medicinal Chemistry"

El Tribunal designado por la Comisión de Postgrado de la UPV/EHU para calificar la Tesis Doctoral arriba indicada y reunido en el día de la fecha, una vez efectuada la defensa por el/la doctorando/a y contestadas las objeciones y/o sugerencias que se le han formulado, ha otorgado por _____ la calificación de:

unanimidad o mayoría

SOBRESALIENTE / NOTABLE / APROBADO / NO APTO

Idioma/s de defensa (en caso de más de un idioma, especificar porcentaje defendido en cada idioma): _____

En Donostia – San Sebastián a ____ de _____ de 2014

EL/LA PRESIDENTE/A,

EL/LA SECRETARIO/A,

Fdo.:

Fdo.:

Dr/a: _____

Dr/a: _____

VOCAL 1º,

VOCAL 2º,

VOCAL 3º,

Fdo.:

Fdo.:

Fdo.:

Dr/a: _____ Dr/a: _____ Dr/a: _____

LA DOCTORANDA,

Fdo.: Leire Lidia Arias Echeverría

Resumen (Spanish Summary)

En esta Tesis se aborda el estudio de diversas reacciones dirigidas a la síntesis y posterior funcionalización de benzo[*b*]furanos parcialmente sustituidos, así como la posible aplicación en el campo de la biomedicina de algunos de los compuestos preparados. Este resumen está organizado siguiendo el esquema que se detalla a continuación:

Introducción

Memoria

Resultados y Discusión

1. Preparación regioselectiva de benzo[*b*]furanos 2- y 3-aril sustituidos (capítulo 2)

1.1. Estudio experimental

1.2. Estudio computacional

2. Transformaciones con 2- y 3-aril benzo[*b*]furanos (capítulo 3)

2.1. Halogenación regioselectiva de benzo[*b*]furanos sustituidos mediada por *N*-halosuccinimidias

2.2. Desaromatización oxidante de benzo[*b*]furanos monohidroxilados mediada por reactivos de iodo hipervalente

2.3. Desmetilación de grupos metoxilo presentes en benzo[*b*]furanos mediada por tribromuro de boro

3. Benzo[*b*]furanos como análogos del resveratrol: ensayos biológicos (capítulo 4)

3.1. Ensayos enzimáticos: modulación de SIRT1

3.1. Ensayos celulares: propiedades antitumorales

Bibliografía Seleccionada

Mencionar también que en este resumen se mantiene la numeración de los compuestos y de las referencias empleada en el manuscrito original.

INTRODUCCIÓN

Un benzofurano es un compuesto heterocíclico aromático con estructura bicíclica que consiste en un anillo de benceno fusionado con un anillo de furano. El término benzofurano engloba, estrictamente hablando, dos tipos de compuestos: benzo[*b*]furanos y benzo[*c*]furanos, dependiendo de la posición que ocupa el oxígeno respecto al enlace que comparten los anillos de benceno y de furano. Sin embargo, cuando no se especifica, se emplea el término benzofurano para referirse al benzo[*b*]furano (o 1-benzofurano) e isobenzofurano para el benzo[*c*]furano (o 2-benzofurano). En cualquier caso, esta tesis se centra exclusivamente en el isómero benzo[*b*]furano, por lo que de ahora en adelante se considerará este de forma exclusiva (figura 1).

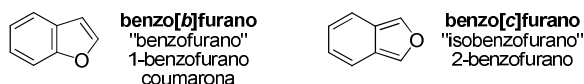


Figura 1. Estructura y nomenclatura de los benzofuranos.

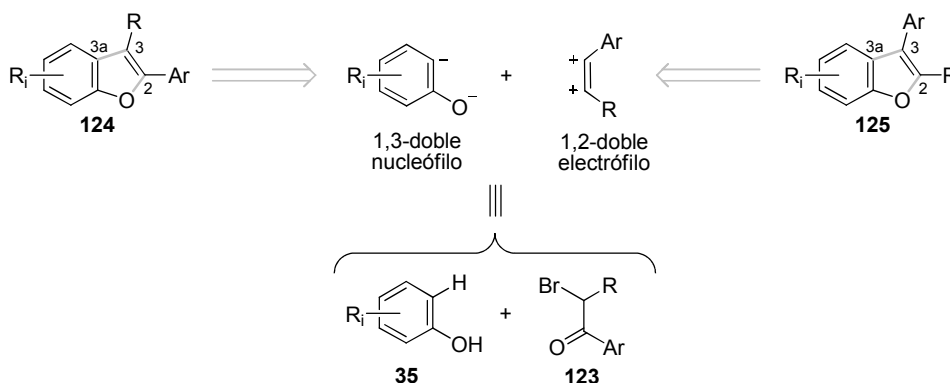
Los benzo[*b*]furanos y sus análogos se encuentran ampliamente distribuidos en la naturaleza. Además su estructura está incluida en cantidad de compuestos, tanto naturales como sintéticos, que presentan diversas actividades biológicas lo que les ha hecho encontrar aplicaciones en diferentes áreas. Una de las vertientes más prolíficas de los benzo[*b*]furanos, en cuanto a aplicaciones se refiere, es su empleo (o potencial empleo) como fármacos dirigidos a diversas afecciones. En este campo destacan por ejemplo compuestos que han demostrado tener propiedades antitumorales, antioxidantes o antiinflamatorias y que han dado lugar a un elevado número de publicaciones (artículos y patentes) en los últimos años^{8,26a}.

La gran variedad de aplicaciones (actuales y potenciales) de los benzo[*b*]furanos ha generado un interés y un esfuerzo amplio y duradero en el desarrollo de métodos para su preparación. A este respecto, cabe destacar que la mayoría de las síntesis convergentes de benzo[*b*]furanos parten de compuestos carbonílicos y fenoles o derivados fenólicos funcionalizados en *orto* (halógenos, grupos formilo o trimetilsililo, por ejemplo)^{40a,d}.

MEMORIA

Teniendo todo esto en cuenta la tesis se plantea, como se detalla a continuación, en tres grandes bloques.

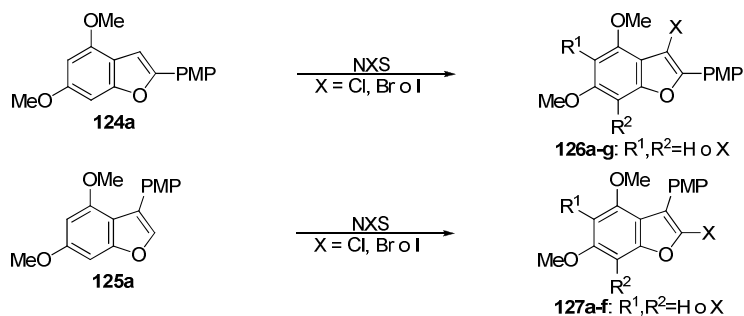
El primer objetivo es desarrollar y optimizar una metodología experimental de preparación regioselectiva de benzo[*b*]furanos 2- ó 3-aril sustituidos (**124** y **125**, respectivamente), partiendo de compuestos fácilmente accesibles como son los fenoles **35** y las α -bromoacetofenonas **123** (esquema 1).



Esquema 1. Análisis retrosintético propuesto para los 2- y 3-arilbenzo[*b*]furanos **124** y **125**, basado en la desconexión de los enlaces O₁-C₂ y C₃-C_{3a}.

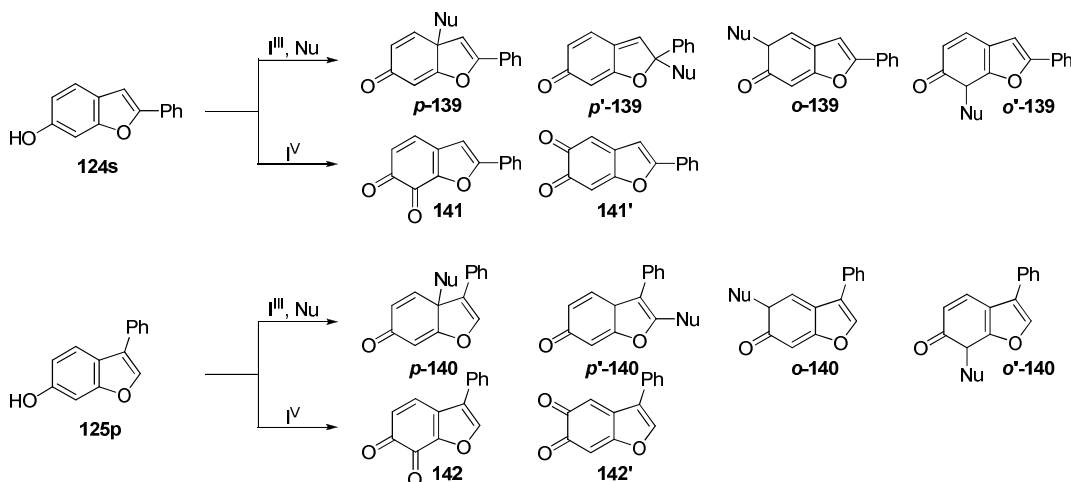
La segunda línea de trabajo, consiste en derivatizar algunos de los benzo[*b*]furanos preparados con el fin de conseguir una mayor variabilidad en cuanto a su patrón de sustitución, de manera que los compuestos resultantes puedan ser interesantes por sí mismos o de cara a futuras transformaciones. Así, se pensó estudiar:

- la halogenación de benzo[*b*]furanos sustituidos mediada por *N*-halosuccinimidias (NXS) (esquema 2),



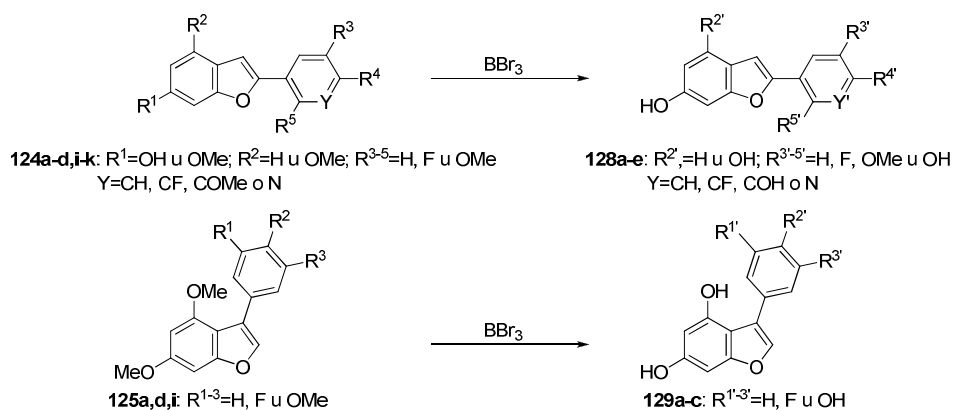
Esquema 2. Esquema general de las reacciones de halogenación de los benzo[*b*]furanos **124a** y **125a**.

- la desaromatización oxidante de benzo[*b*]furanos monohidroxilados mediada por reactivos de iodo hipervalente (esquema 3) y



Esquema 3. Predicción de los posibles productos de la reacción de desaromatización de los benzo[*b*]furanos **124s** y **125p** mediada por iodanos- λ^3 y λ^5 (I^{III} y I^{V} , respectivamente).

- la desmetilación de los grupos metoxilo presentes en algunos de los benzo[*b*]furanos sintetizados mediada por tribromuro de boro (BBr_3) (esquema 4).



Esquema 4. Esquema general de las reacciones de desmetilación de los grupos metoxilo presentes en los benzo[*b*]furanos **124** y **125**.

En tercer y último lugar, teniendo en cuenta la gran similitud estructural y electrónica de algunos de los benzo[*b*]furanos sintetizados con un compuesto con contrastada actividad biológica como es el resveratrol (figura 2), se pensó en llevar a cabo ensayos para testar la posible actividad biológica de algunos de los compuestos sintetizados.

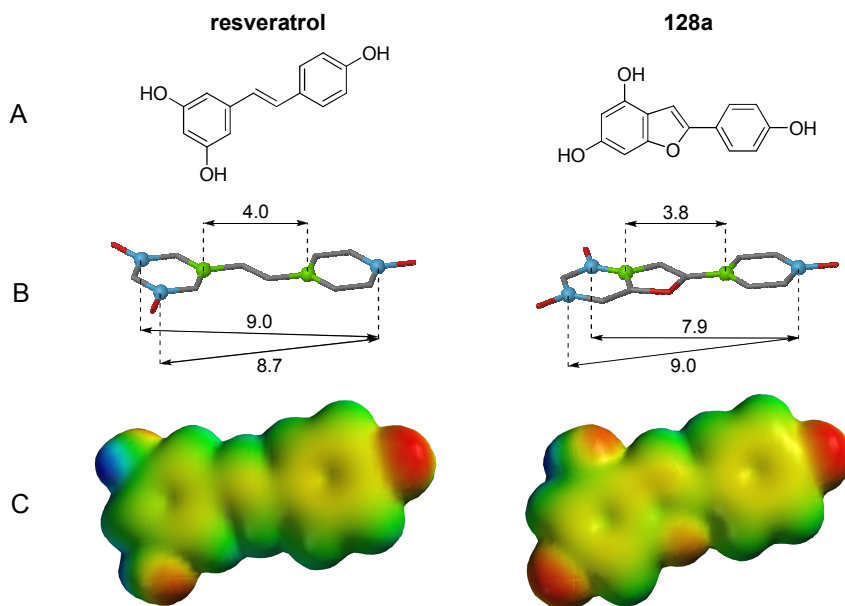


Figura 2. (A) Estructuras del resveratrol y del compuesto cabeza de serie **128a**. (B) Estructuras optimizadas (método semi-empírico PM3) del resveratrol y del compuesto **128a**. Las esferas azules indican los átomos de carbono que soportan los grupos hidroxilo y las verdes los átomos de carbono unidos a la estructura central. Las distancias están dadas en Å. (C) Estructuras optimizadas del resveratrol y del compuesto **128a** que muestran el potencial electrostático proyectado sobre su densidad electrónica. Los potenciales negativos y positivos están dados en rojo y en azul, respectivamente.

RESULTADOS Y DISCUSIÓN

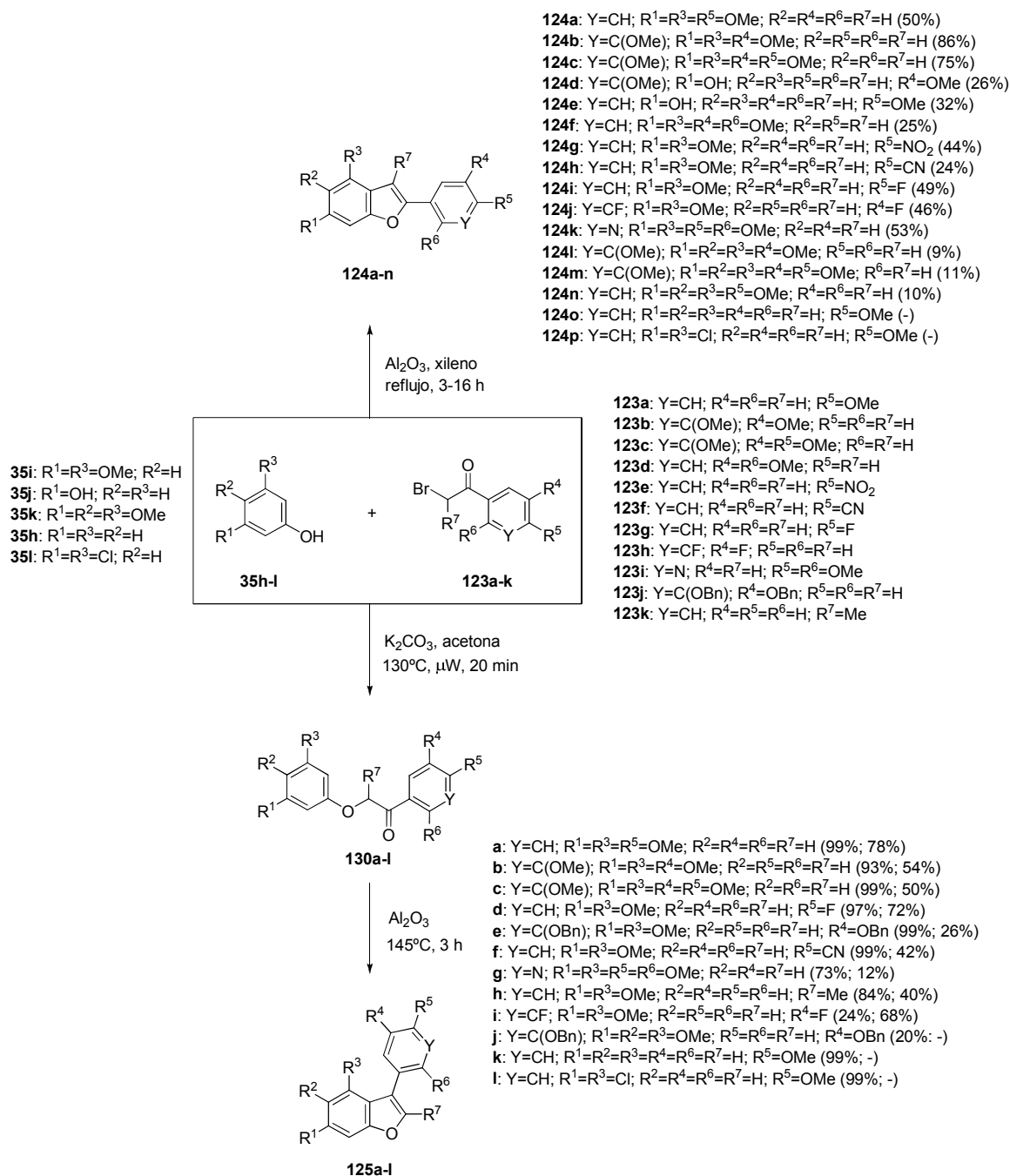
1. Preparación regioselectiva de benzo[b]furanos 2- y 3-aril sustituidos (capítulo 2)

1.1. Estudio experimental

A la hora de abordar el estudio experimental de un nuevo protocolo para la síntesis de benzo[b]furanos 2- ó 3-aril sustituidos, por un lado se pensó en utilizar fenoles no sustituidos en *orto* **35** y α -bromoacetofenonas **123** como productos de partida (por tratarse de reactivos comerciales o fácilmente sintetizables) y por otro, se trató de combinar dos herramientas: la utilización de radicación de microondas y el empleo de alúmina (que habían mostrado tener ventajas significativas en síntesis orgánica)^{168a-b,173a}.

Con esto en mente, se optimizaron las condiciones de reacción para la obtención de benzo[b]furanos atendiendo a diferentes parámetros. Las diversas pruebas realizadas nos llevaron a concluir que las condiciones óptimas de reacción para obtener regioselectivamente los benzo[b]furanos 2- ó 3-aril sustituidos son las que se muestran en el esquema 5.

Es decir, que la reacción entre fenoles **35** y α -bromoacetofenonas **123** en presencia de alúmina neutra permite la obtención exclusiva de los 2-aril benzofuranos **124** (esquema 5, parte superior). Y que los análogos 3-arilados correspondientes **125** en cambio, se obtienen regioselectivamente siguiendo una secuencia reacción de Williamson – ciclación en dos etapas: empleando carbonato potásico¹⁷⁵ como aditivo, la reacción entre fenoles **35** y α -bromoacetofenonas **124** da las α -fenoxicetonas **130**, que en presencia de alúmina ciclan dando lugar a los 3-arilbenzo[b]furanos **125** (esquema 5, parte inferior).



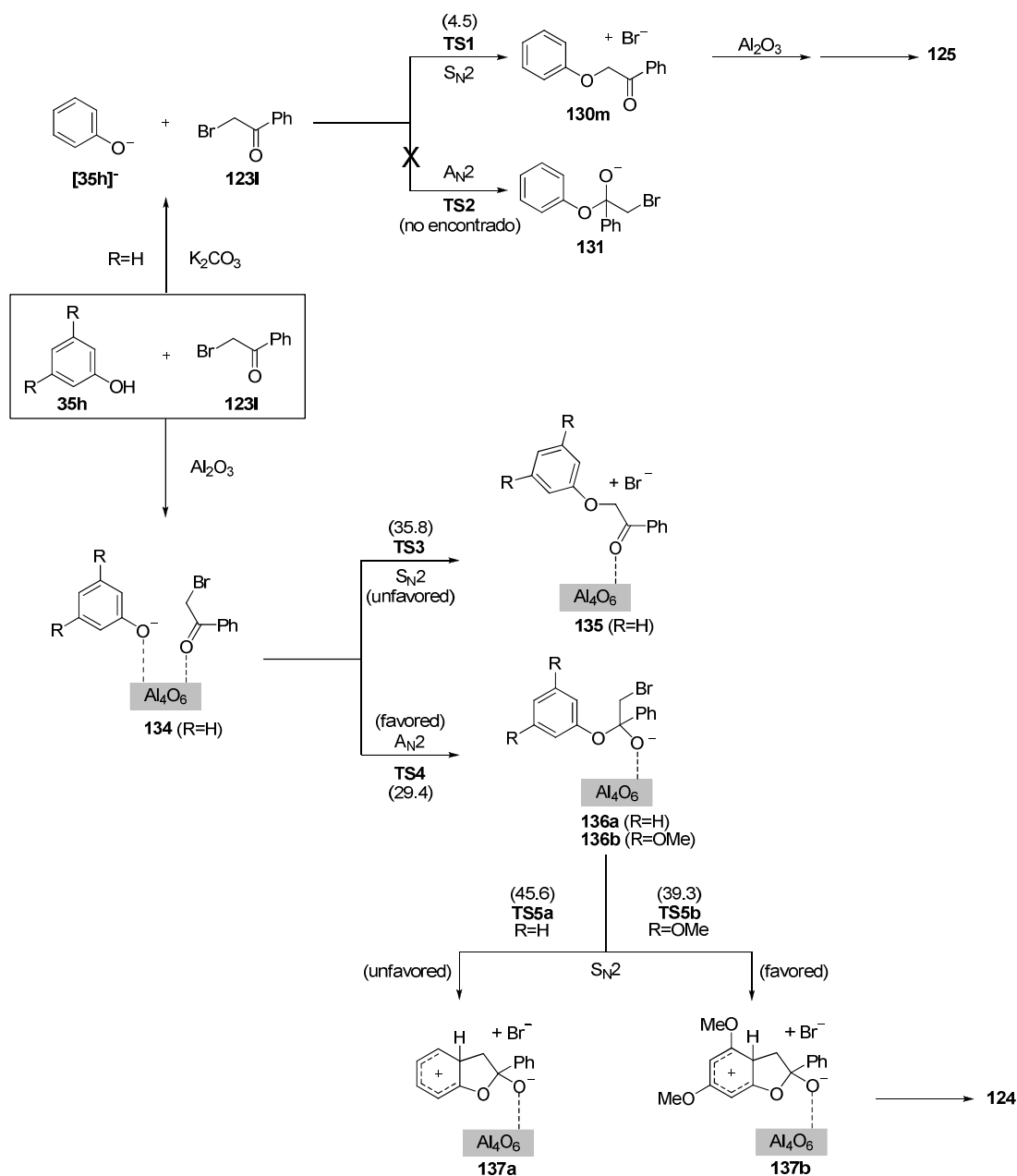
Esquema 5. Esquema general del estudio experimental de la síntesis de los 2- y 3- arilbenzo[*b*]furanos **124** y **125**, respectivamente. Los rendimientos están dados entre paréntesis.

Con el fin de caracterizar y determinar la estructura de estas dos series de compuestos, se llevó a cabo un estudio exhaustivo de resonancia magnética nuclear (RMN) de los compuestos cabeza de serie **124a** y **125a** cuyas estructuras se confirmaron además por análisis de difracción de rayos X.

1.2. Estudio computacional

Además, con el fin de comprender mejor las rutas sintéticas por las cuales se obtienen estos dos regioisómeros, se llevó a cabo un estudio computacional basado en cálculos DFT para evaluar las

posibles vías por las que podrían transcurrir las reacciones en ausencia y en presencia de la alúmina (Esquema 6).



Esquema 6. Esquema general del estudio computacional de la síntesis de los 2- y 3- arilbenzo[*b*]furanos **124** y **125**, respectivamente. Las energías de activación vienen dadas en kcal/mol entre paréntesis y se calcularon al nivel de teoría B3LYP/6-31+G*+ Δ ZPVE. TS = estructura de transición.

Los resultados de este estudio concluyeron que, en ausencia de alúmina, la preparación de los 3- arilbenzo[*b*]furanos **125** comienza, con una sustitución nucleófila (S_N2) (esquema 6, parte superior). En presencia de alúmina, en cambio, los cálculos revelaron una preferencia por la adición nucleófila (A_{N2}) sobre el carbono carbonílico frente a la sustitución nucleófila (S_N2) en el primer paso hacia la síntesis de los 2- aril benzo[*b*]furanos **124** (esquema 6, parte inferior).

2. Transformaciones con 2- y 3-aril benzo[*b*]furanos (capítulo 3)

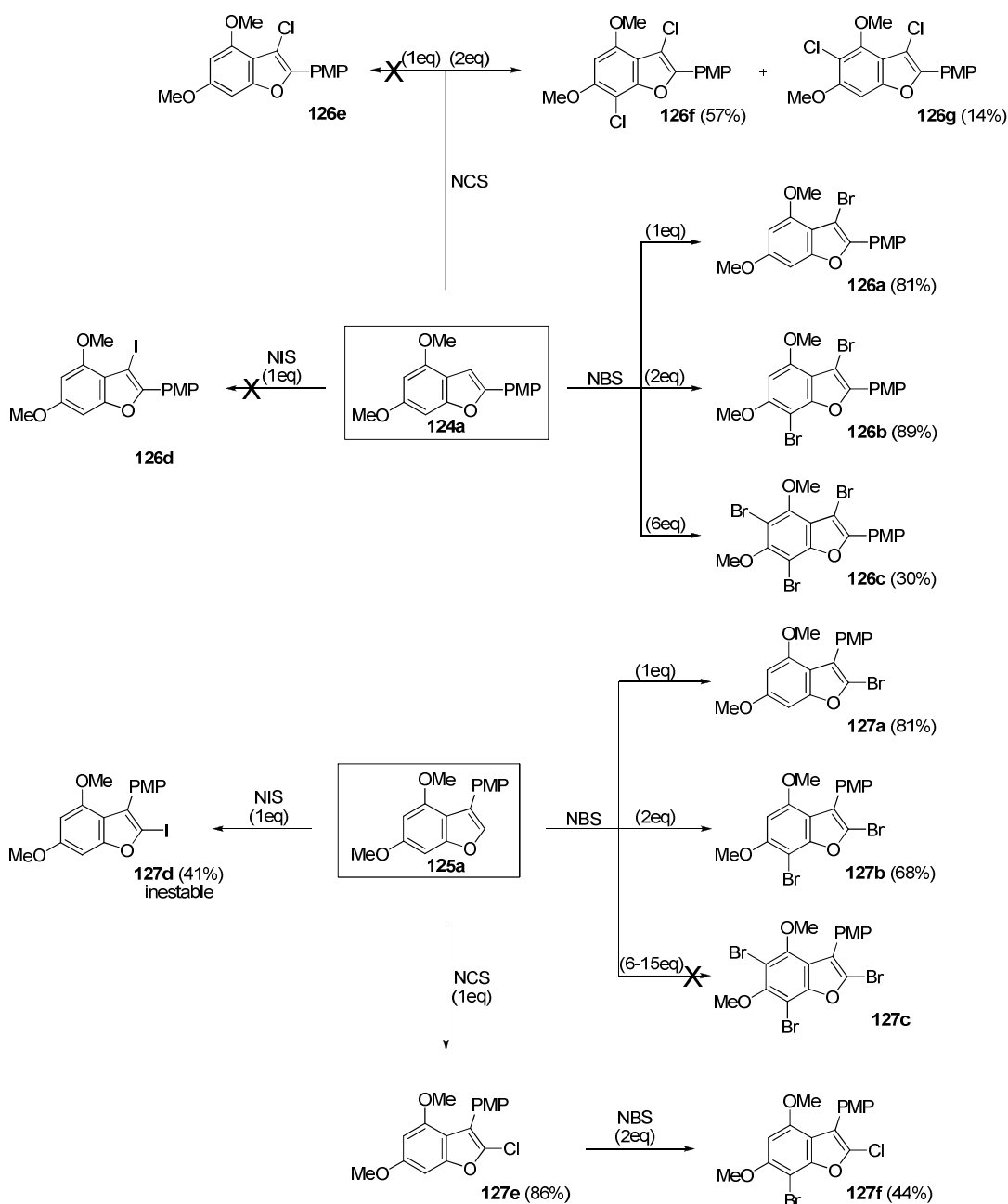
2.1. Halogenación regioselectiva de benzo[*b*]furanos sustituidos mediada por *N*-halosuccinimidas

Para llevar a cabo el estudio sobre la halogenación de benzo[*b*]furanos sustituidos, se eligieron las *N*-halosuccinimidas como fuente de los halógenos, debido a su disponibilidad, fácil manejo y a los buenos resultados que estos reactivos habían presentado en reacciones equivalentes de C-halogenación con otros compuestos^{183,192,194-195}. Así, siguiendo la línea de algunos protocolos de halogenación descritos previamente para las *N*-halosuccinimidas, se llevaron a cabo las reacciones empleando diclorometano como disolvente, a temperatura ambiente y adicionando una disolución de este reactivo lentamente. Las *N*-halosuccinimidas (NXS) probadas fueron la *N*-bromosuccinimida (NBS), la *N*-clorosuccinimida (NCS) y la *N*-iodosuccinimida (NIS).

El estudio se realizó empleando en primer lugar *N*-bromosuccinimida (NBS) y los benzo[*b*]furanos 2- y 3-aril sustituidos cabezas de serie **124a** y **125a**. La modificación del número de equivalentes de NBS adicionado permitió, en la mayoría de los casos obtener de manera exclusiva los correspondientes productos mono- y di- bromados derivados de **124a** (**126a-b**) y **125a** (**127a-b**) e incluso la del producto de tribromación derivado de **124a** (**126c**). A continuación se ensayó el empleo de otras *N*-halosuccinimidas (NXS) (esquema 7).

Partiendo de **124a**, el empleo de *N*-iodosuccinimida (NIS) condujo en todas nuestras pruebas a mezclas complejas de productos de degradación. Al emplear un equivalente de *N*-clorosuccinimida (NCS), en cambio, no se observó producto de reacción considerable ni siquiera aumentando el tiempo de reacción, mientras que el empleo de dos equivalentes de la misma condujo a la formación de dos productos diclorados **126f-g**, en proporción 1:4.

Partiendo de **125a**, el empleo de *N*-iodosuccinimida (NIS) condujo a la formación del correspondiente producto de monoiodación **127d**, que resultó ser bastante inestable. La utilización de *N*-clorosuccinimida (NCS) condujo a la formación del derivado monoclorado **127e**. Un último experimento de este apartado consistió en bromar el producto clorado **127e**, dando lugar al producto dihalogenado **127f**.



Esquema 7. Esquema general del estudio experimental de la halogenación de los benzo[*b*]furanos **124a** y **125a** empleando *N*-halosuccinimidias (NXS). Los rendimientos están dados entre paréntesis.

Para elucidación estructural de todos estos compuestos se recurrió a la técnica de resonancia magnética nuclear (RMN), y se registraron los experimentos pertinentes de la siguiente serie: ^1H -RMN, ^{13}C -RMN, COSY, HSQC, HMBC y NOE selectivo.

Además, para tratar comprender la selectividad en las posiciones de bromación, así como la posibilidad de obtener los productos de monohalogenación (ajustando los equivalentes de *N*-halosuccinimida) con preferencia sobre posibles productos polihalogenados, paralelamente se llevó a cabo un estudio computacional basado en cálculos DFT para las reacciones de bromación. Los resultados obtenidos del mismo están de acuerdo con los datos obtenidos experimentalmente.

2.2. Desaromatización oxidante de benzo[*b*]furanos monohidroxilados mediada por reactivos de iodo hipervalente

Teniendo presente la reacción de desaromatización oxidante de fenoles, se pensó que los benzo[*b*]furanos monohidroxilados podrían ser interesantes productos de partida para probar esta transformación, con la particularidad añadida de presentar en su estructura varios posibles sitios de reacción de cara a la entrada del nucleófilo.

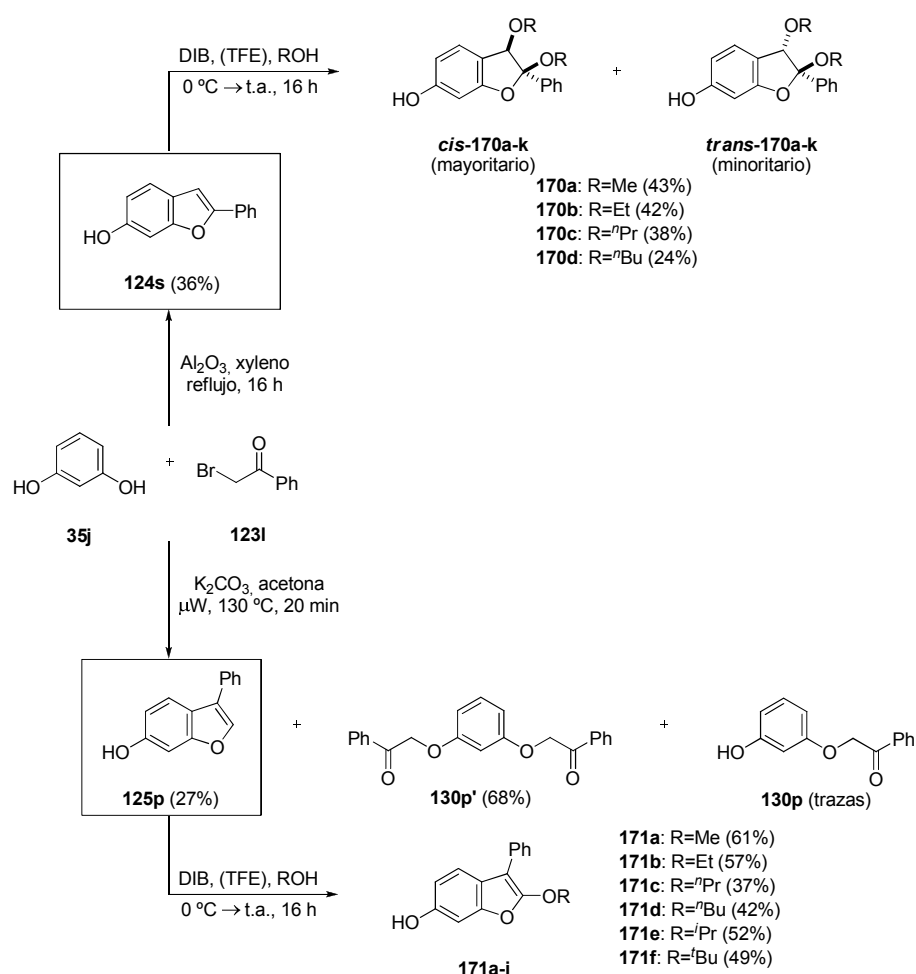
La desaromatización oxidante de fenoles es una reacción que ha sido ampliamente estudiada y para la que en los últimos años los reactivos de iodo hipervalente han demostrado ser de gran utilidad, debido a que combinan los criterios de electrofilia y nucleofugalidad, además de ser de fácil manejo y ser capaces de actuar bajo condiciones de reacción suaves^{214d,219,222a}.

Así, tras preparar los benzofuranos monohidroxilados **124s** y **125p**, siguiendo los procedimientos descritos en el primer apartado, se procedió a optimizar las condiciones de reacción para su desaromatización oxidativa empleando un reactivo de iodo hipervalente (III) o iodano- λ^3 (se ensayaron diacetoxiidobenceno, DIB, y bistrifluoroacetoxiidobenceno, BTI) y metanol (MeOH) como disolvente y nucleófilo, atendiendo a diferentes parámetros.

Partiendo del 2-fenilbenzo[*b*]furan-6-ol **124s** (esquema 8, parte superior), bajo las condiciones optimizadas que se muestran en el esquema, se obtuvo una mezcla de isómeros *cis/trans* de los correspondientes 2,3-dimetoxi-2,3-dihidrobenzo[*b*]furan-6-oles correspondientes, ***cis*-170a** y ***trans*-170a**, y ningún compuesto carbonílico resultante de la oxidación del grupo hidroxilo del fenol que cabía esperar (compuestos **139**, esquema 3). La estructura tanto del isómero mayoritario (***cis*-170a**) como la del minoritario (***trans*-170a**) fue confirmada por análisis de difracción de rayos X. La extensión de esta metodología al empleo de otros nucleófilos resultó en mezclas de dos isómeros **170b-d** análogas en el caso de otros alcoholes lineales (EtOH, ⁿPrOH y ⁿBuOH), mientras que en el caso de emplear otros nucleófilos como los alcoholes ramificados ⁱPrOH, ^tBuOH y el fenol, el diol HOEtOH, los tioles EtSH y PhSH y la dietilamina se recuperaron los productos de partida sin reaccionar.

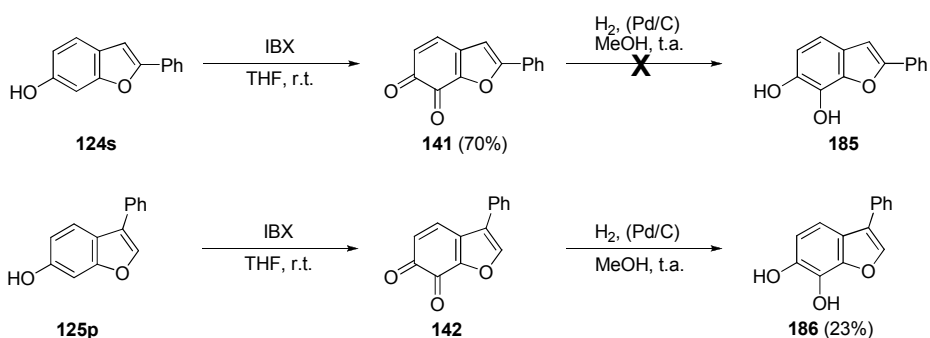
Partiendo del 3-fenilbenzo[*b*]furan-6-ol **125p** (esquema 8, parte inferior), bajo las mismas condiciones optimizadas que se muestran en el esquema, se obtuvo el correspondientes 2-metoxi-2,3-dihidrobenzo[*b*]furan-6-ol correspondientes **171a**, y de nuevo ningún compuesto carbonílico resultante de la oxidación del grupo hidroxilo del fenol que cabía esperar (compuestos **140**, esquema 3). La extensión de esta metodología al empleo de otros nucleófilos resultó en los correspondientes 3-fenilbenzo[*b*]furan-6-oles alcoxilados en posición 2 **171b-d** al emplear otros alcoholes lineales (EtOH, ⁿPrOH y ⁿBuOH). En esta ocasión, los alcoholes ramificados ⁱPrOH,

t BuOH dieron lugar a los productos **171e-f**. Sin embargo, cuando se emplearon otros nucleófilos como, fenol, etanotiol o dietilamina, se recuperaron los productos de partida sin reaccionar.



Esquema 8. Esquema general del estudio experimental de la desaromatización oxidante de los benzo[*b*]furanos **124s** y **125p** empleando el iodano- λ^3 DIB. Los rendimientos están dados entre paréntesis.

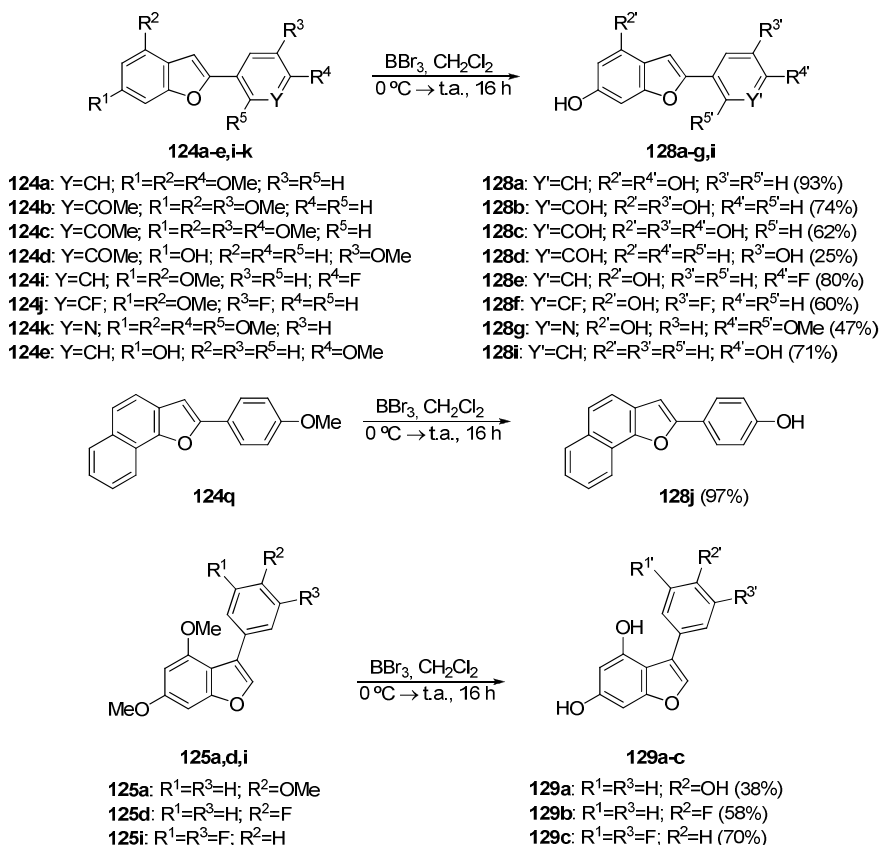
Además también se probó la reacción de los benzo[*b*]furan-6-oles **124s** y **125p** con el iodano- λ^5 ácido *o*-iodoxibenzoico IBX y su versión estabilizada SIBX, obteniéndose prometedores crudos de reacción de los que resulta complicado aislar las correspondientes benzo[*b*]furan-6,7-dionas **141** y **142**. Ante la dificultad de purificación de estas dionas, se procedió a su hidrogenación catalítica con el fin de reducirlas a sus correspondientes dioles. De esta forma se obtuvo el producto **186**, aunque no el **185** (esquema 9).



Esquema 9. Esquema del estudio experimental de la desaromatización oxidante de los benzo[*b*]furanos **124s** y **125p** empleando el iodano- λ^5 IBX. Los rendimientos están dados entre paréntesis.

2.3. Desmetilación de grupos metoxilo presentes en benzo[*b*]furanos mediada por tribromuro de boro

El objetivo de esta sección estaba dirigido a la obtención de benzo[*b*]furanos polihidroxilados. Para ello se utilizaron los benzo[*b*]furanos polimetoxilados sintetizados previamente como productos de partida, dado que los grupos metoxilo se presentaban como buenos precursores de grupos hidroxilo para este tipo de compuestos, compatibles con el procedimiento sintético que habíamos desarrollado.



Esquema 10. Esquema general del estudio experimental de la desmetilación de los grupos metilo presentes en los benzo[*b*]furanos **124** y **125** empleando BBr₃. Los rendimientos están dados entre paréntesis.

Así, la revisión bibliográfica nos condujo al empleo de tribromuro de boro (BBr_3) para llevar a cabo esta transformación²⁵¹⁻²⁵³, obteniéndose, bajo las condiciones indicadas en el esquema 10, los benzo[b]furanos polihidroxilados **128a-j** y **129a-c**.

3. Benzo[b]furanos como análogos del resveratrol: ensayos biológicos

Dada la analogía de algunos de los productos sintetizados con el resveratrol, un polifenol natural que ha demostrado presentar diversas actividades biológicas (atribuidas por muchos autores principal aunque no exclusivamente a sus propiedades antioxidantes)^{267b,272}, se pensó en evaluar la posible actividad biológica de algunos compuestos seleccionados.

3.1. Ensayos enzimáticos: modulación de SIRT1

En primer lugar se llevaron a cabo unos ensayos enzimáticos para evaluar la actividad de los compuestos **128a-g** y **129a-c** como reguladores (inhibidores o activadores) de SIRT1. Brevemente, SIRT1 es un tipo de sirtuinas, desacetilasas de histonas de clase II, cuya actividad biológica está asociada a multitud de procesos celulares implicados en el envejecimiento y en las enfermedades asociadas al mismo (como pueden ser el cáncer, las enfermedades neurodegenerativas, cardiovasculares o metabólicas). Esto hace que la regulación de las sirtuinas (tanto la inhibición como la activación, que pueden tener distintas aplicaciones terapéuticas) despierte un gran interés^{264,265d,267a,289d}.

Las pruebas fueron realizadas por Reaction Biology (Malvern, PA) empleando el ensayo de fluorescencia basado en el fluoróforo Fluor-de-Lys. Se utilizó suramin sódico como control positivo de inhibición y resveratrol como control positivo de activación.

De los compuestos testados, **128c,f** y **129a-c** presentaron un efecto inhibitor sobre la actividad de la enzima SIRT1, siendo **128c** el compuesto más potente a este respecto con un IC_{50} (concentración de compuesto requerida para reducir en un 50% la actividad de la enzima) de 1.84 μM (figura 3).

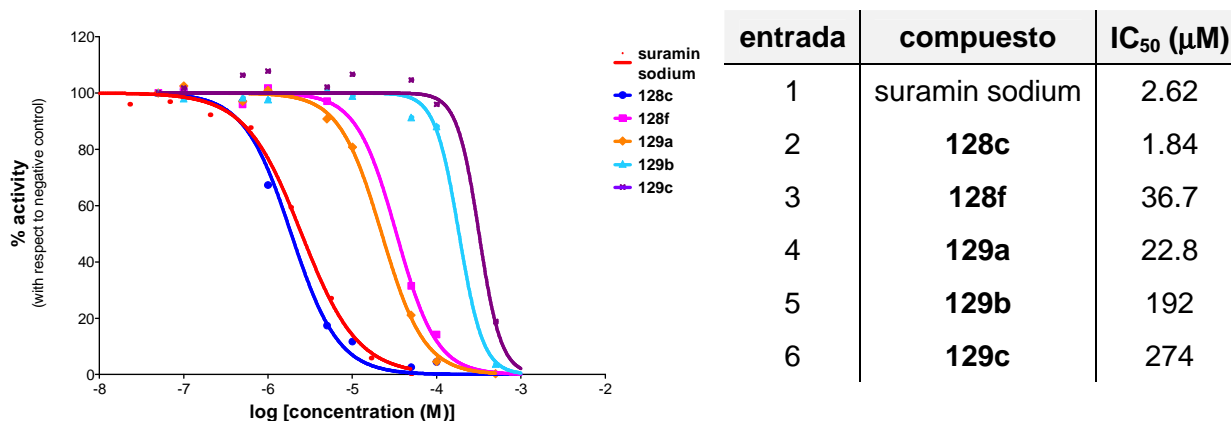


Figura 3. Ensayos enzimáticos de los inhibidores de SIRT1 (se utilizó suramin sódico como control positivo de inhibición). Valores de IC₅₀.

Los compuestos **128a-b,d-e,g** tenían, por su parte, un efecto activador sobre la actividad de la enzima SIRT1. En el caso de la activación, los compuestos más prometedores fueron **128a y b**, que presentaron un interesante compromiso entre los dos parámetros de estudio EC_{1.5} (concentración de compuesto requerida para aumentar en un 50% la actividad de la enzima) y % Max (porcentaje máximo de activación alcanzado), comparables a los del resveratrol empleado como control (figura 4).

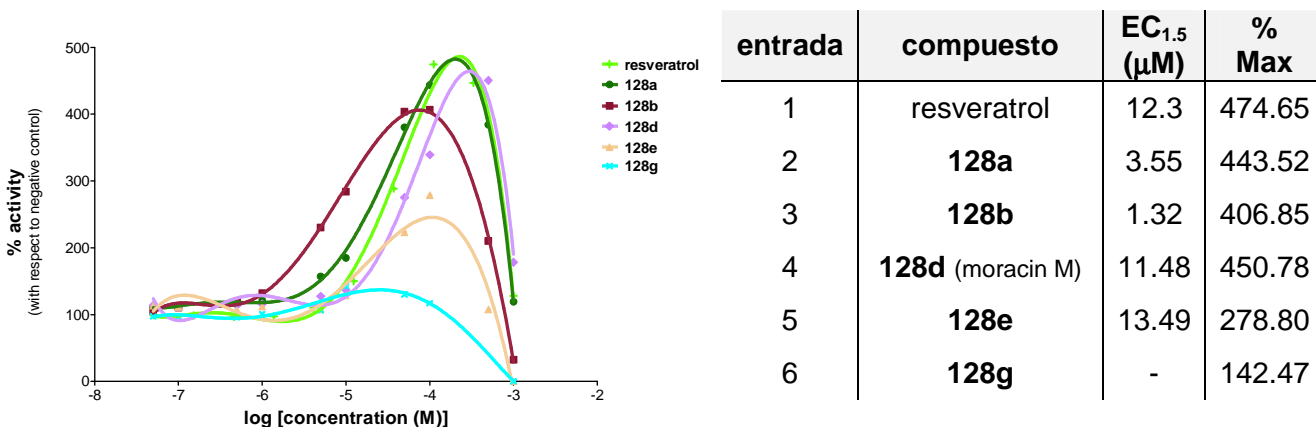


Figura 4. Ensayos enzimáticos de los activadores de SIRT1 (se utilizó resveratrol como control positivo de inhibición). Valores de EC_{1.5} y % Max.

Lamentablemente, durante el desarrollo de este proyecto la capacidad del resveratrol (y por extensión de sus análogos) para activar directamente las sirtuinas se puso en entredicho, ya que el ensayo de fluorescencia utilizado para medir su actividad *in vitro* (empleado también en nuestro estudio) se encuentra actualmente cuestionado (se sospecha que puede dar lugar a falsos positivos o artefactos)^{258c,289b-c}.

3.1. Ensayos celulares: propiedades antitumorales

Confiando en el potencial de los compuestos sintetizados, se llevaron a cabo otro tipo de ensayos biológicos. Recordando que el resveratrol ha demostrado tener propiedades contra el cáncer^{258a,261,271}, en este caso se optó por ensayos celulares para testar las propiedades antitumorales de los compuestos **128a-c** y **129a** y sus precursores metoxilados **124a-c** y **125a** a distintos niveles como son la adhesión, proliferación y migración de células tumorales.

Esta ocasión los compuestos se testaron en el modelo de carcinoma de colon C26 en el Departamento de Biología Celular e Histología de la Facultad de Medicina y Odontología de la Universidad del País Vasco (UPV/EHU) en el grupo de la profesora Beatriz Arteta. Las diferentes pruebas realizadas con estos ocho compuestos revelaron que presentan diferentes y significativos efectos en los parámetros pro-metastáticos estudiados, resultando complicado establecer una pauta o tendencia general. Un resumen de los resultados se recoge en la tabla 1. De modo general, se puede concluir que los compuestos metoxilados **124a** y **125a** son más prometedores que sus análogos metoxilados pero que, en cualquier caso, sería necesario llevar a cabo más ensayos.

Tabla 1. Tabla resumen de los ensayos celulares.

ensayo	con respecto a	entrada	conc. (µM)	hidroxilados (disolvente: EtOH)				metoxilados (disolvente: DMSO)			
				128a	128b	128c	129a	124a	124b	124c	125a
adhesión	control	1	0.5	↓	–	↓	↓	–	–	–	–
		2	2.5	↓	↓	↓	↓	↓	–	–	–
		3	12.5	–	↓	↓	↑	↓	–	–	–
proliferación	control	4	0.5	–	–	–	–	–	–	–	–
		5	2.5	–	–	–	–	–	↑	↑	↓
		6	12.5	↓	–	↓	–	–	↑	↑	↓
		7	25	↓	↓	↓	↓	–	↑	↑	↓
		8	50	↓	↓	↓	↓	–	–	–	↓
	nº inicial	9	0.5	↑	↑	↑	↑	↑	↑	↑	↑
		10	2.5	↑	↑	↑	↑	↑	↑	↑	–
		11	12.5	↑	↑	–	↑	↑	↑	↑	–
		12	25	↓	–	↓	–	↑	↑	↑	–
		13	50	↓	↓	↓	↓	↑	↑	↑	
migración	control	14	2.5	↓	↓	↓	–	↓	–	–	

↓ = inhibición o disminución en nº significativa

↑ = activación o aumento en nº significativa

– = sin efecto significativo

■ = inhibidor

■ = activador

■ = citotóxico

control = 0 µM

conc. = concentración

nº = número

BIBLIOGRAFÍA SELECCIONADA

- ⁸ Dawood, K.M. *Expert Opin. Ther. Patents* **2013**, *23*, 1133-1156
- ²⁶ (a) Katrizky, A. R.; Rees, C. W.; Scriven, E. F. V. *Comprehensive Heterocyclic Chemistry II* (Pergamon Press, Oxford) **1996**, *2*, 413-436
- ⁴⁰ (a) Katrizky, A. R.; Rees, C. W.; Scriven, E. F. V. *Comprehensive Heterocyclic Chemistry II* (Pergamon Press, Oxford) **1996**, *2*, 368-378 (d) De Luca, L.; Nieddu, G.; Porcheddu, A.; Giacomelli, G. *Curr. Med. Chem.* **2009**, *16*, 1-20
- ¹⁶⁸ (a) Srinivasan, K. V.; Chaskar, P. K.; Dighe, S. N.; Rane, D. S.; Khade, P. V.; Jain, K. S. *Heterocycles* **2011**, *83*, 2451-2488; (b) Kappe, C. O. *Angew. Chem. Int. Ed.* **2004**, *43*, 6250-6284
- ¹⁷³ (a) Trueba, M.; Trasatti, S. P. *Eur. J. Inorg. Chem.* **2005**, 3393-3403
- ¹⁷⁵ Leadbeter, N. E.; Schmink, J. R. *Tetrahedron* **2007**, *63*, 6764-6773
- ¹⁸³ Prakash, G. K. S.; Mathew, T.; Hoole, D.; Esteves, P. M.; Wang, Q.; Rasul, G.; Olah, G. A. *J. Am. Chem. Soc.* **2004**, *126*, 15770-15776
- ¹⁹² Koval', I. V. *Russ. J. Org. Chem.* **2002**, *38*, 301-337
- ¹⁹⁴ Zhang, Y.; Shibatomi, K.; Yamamoto, H. *Synlett* **2005**, *18*, 2837-2842
- ¹⁹⁵ Kalyani, D.; Dick, A. R.; Anani, W. Q.; Sanford, M. S. *Org. Lett.* **2006**, *8*, 2523-2526
- ²¹⁴ (d) Quideau, S.; Pouységu, L.; Deffieux, D. *Synlett* **2008**, 467-495
- ²¹⁹ Pouységu, L.; Deffieux, D.; Quideau, S. *Tetrahedron* **2010**, *66*, 2235-2261
- ²²² (a) Ding, Q.; Ye, Y.; Fan, R. *Synthesis* **2013**, *45*, 1-16
- ²⁵¹ McOmie, J. F. W.; Watts, M. L.; West, D. E. *Tetrahedron* **1968**, *24*, 2289-2292
- ²⁵² Yao, M.-L.; Kabalka, G. W. *Boron Science* **2012**, 579-621
- ²⁵³ García, E. *Synlett* **2005**, 1636-1637
- ²⁵⁸ (a) Aggarwal, B. B.; Bhardwaj, A.; Aggarwal, R. S.; Seeram, N. P.; Shishodia, S.; Takada, Y. *Anticancer Res.* **2004**, *24*, 2783-2840 (c) Quideau, S.; Defieux, D.; Pouységu, L. *Angew. Chem. Int. Ed.* **2012**, *51*, 6824-6826
- ²⁶¹ Jang, M.; Cai, L.; Udeani, G. O.; Slowing, K. V.; Thomas, C. F.; Beecher, C. W. W.; Fong, H. H. S. Farnsworth, N. R.; Kinghorn, A. D.; Mehta, R. G.; Moon, R. C.; Pezzuto, J. M. *Science* **1997**, *275*, 218-220
- ²⁶⁴ Howitz, K. T.; Bitterman, K. J.; Cohen, H. Y.; Lamming, D. W.; Lavu, S.; Wood, J. G.; Zipkin, R. E.; Chung, P.; Kisielewski, A.; Zhang, L.-L.; Scherer, B.; Sinclair, D. A. *Nature* **2003**, *425*, 191-196
- ²⁶⁵ (d) Cantó, C.; Auwerx, J. *Trends Endocrinol. Metab.* **2009**, *20*, 325-331
- ²⁶⁷ (a) Wood, J. G.; Rogina, B.; Lavu, S.; Howitz, K.; Helfand, S. L.; Tatar, M.; Sinclair, D. *Nature* **2004**, *430*, 686-689 (b) Baur, J. A.; Sinclair, D. A. *Nat. Rev. Drug Discov.* **2006**, *5*, 493-506
- ²⁷¹ Kundu, J. K.; Surh, Y.-J. *Cancer Lett.* **2008**, *269*, 243-261
- ²⁷² Saiko, P.; Szakmary, A.; Jaeger, W.; Szekeres, T. *Mutat. Res.* **2008**, *658*, 68-94
- ²⁷⁶ Baur, J. A. *Mech. Ageing Dev.* **2010**, *131*, 261-269
- ²⁸⁹ (b) Kaeberlein, M.; McDonagh, T.; Heltweg, B.; Hixon, J.; Westman, E. A.; Caldwell, S. D.; Napper, A.; Curtis, R.; DiStefano, P. S.; Fields, S.; Bedalov, A.; Kennedy, B. K. *J. Biol. Chem.* **2005**, *280*, 17038-17045 (c) Borra, M. T.; Smith, B. C.; Denu, J. M. *J. Biol. Chem.* **2005**, *280*, 17187-17195 (d) Pallàs, M.; Verdaguer, E.; Tajés, M.; Gutierrez-Cuesta, J.; Camins, A. *Recent Pat. CNS Drug Discov.* **2008**, *3*, 61-69

Acknowledgements

The work presented in this dissertation manuscript was developed in the Department of Organic Chemistry I of the University of the Basque Country (UPV/ EHU) in Donostia – San Sebastián, under the supervision of Professor Fernando P. Cossío and Doctor Yosu I. Vara.

Firstly, I want to thank the economical support that made this project possible. On the one hand, the Spanish Ministry of Education, Culture and Sport for the 4-year predoctoral fellowship they granted me and on the other hand Fernando and Professor Ana Arrieta for finding some extra funding when it was over.

However, much more importantly, I would like to express my most sincere gratitude to Fernando, and of course Ana, for the opportunity offered to take my first steps in the research world. Thank you so much for opening the doors of your laboratory for me and for all the help and understanding provided throughout these years. Thank you also for your guidance and for all the organic chemistry, the passion for knowledge and the fighting spirit I have learnt along the way by your side.

I owe a huge, really huge, thank you to Yosu. I apologize in advance because I know that my words will not do justice to him. So, to my at first lab-mate, then co-director and always friend, thank you. Thank you for sharing with me the fantastic chemist and the even better person that you are.

During the development of this work, I was lucky to do a short stay in the research group of Professor Stéphane Quideau at the “Institute Européen de Chimie et Biologie” (IECB, University of Bordeaux) for the last months of 2010. To him, his research group and some of their “voisins”, merci de votre accueil et de votre hospitalité ces mois-làs. Among all of them, the two Spanish-speakers in the team earned reading their names here, Professor Laurent Pouységou and the already Doctor Melanie Delannoy, not for their language skills but for being always there to lend a hand both inside and outside the laboratory.

I am also grateful to Associated Professor Beatriz Arteta and her research group in the Department of Cell Biology and Histology of the School of Medicine and Dentistry of the University of the Basque Country (UPV/ EHU), who agreed to collaborate with us and performed the cell-based assays included in this thesis. Thank you for so quickly and kindly solving my doubts on the reports of the results, too.

The computational studies in this manuscript would not be here without the hours invested by both Fernando and Doctor Abel de Cozar. For your time and dedication, thank you.

I think that it is now time to express my gratitude to the work of all the technicians and professionals who participated in the development of this thesis (NMR, X-rays, elemental analysis, HRMS, etc.). I think that in the everyday rush we do not say it enough so I want to sincerely add that “technical and human support provided by SGIker (UPV/EHU, MICINN, GV/EJ, ESF) is gratefully acknowledged”, using your own words. Also to Maite, of course, for always helping with the unappreciated paperwork. And not only for her efficiency at doing it, but also for her smile and nice chat.

I owe a massive thank you to all the people I spent so long hours in the laboratory with. Thank you to the ones who are yet there but more especially to the ones who are already gone. Also to the ones who were temporarily part of the group or joined it later. With you I shared a great period of my life and from all of you I learnt a lot about how to face both work and life.

The veterans when I landed here, the “Ikerchem boys & girls”, deserve a special mention. Thank you for taking your time to teach me chemistry and laboratory practice and for creating such a magical working atmosphere. Even now, years later, you keep helping and showing concern for me, thank you all. In particular, besides Yosu, I will always be in debt with Aizpea and Eneko for many things, including all the free time dedicated to revise this manuscript. That is just priceless.

To my generation lab-mates thank you. You made the everyday so pleasant and funny at times, so much more bearable at another times. Although I am definitely taking something of all of you with me, I want to especially thank my “table-surrounding”-mates. When I said that my desk in the laboratory was the best, it was not only for its physical location.

To the “rookies” and “sophomores” thank you too. I might not have shared that much with you but anytime I went on a “visit”, you kindly made room for me, never complaint about the print queues I created and always had encouraging words for me. I would not like to get out of our laboratory without mentioning Celsi who has always taken care both of keeping our mess clean and of us.

A couple paragraphs before I started saying “hours «in» the laboratory” but I really meant in and out of it. At this point I must also include our organic neighbors “living” on the other side of the aisle and in the Faculty. Impossible to forget the countless coffee and/or lunch-time talks, dinners, our particular St Albert’s celebrations, the master year, congresses and trips, bachelor(ette) parties, weddings, ... Unforgettable maybe because of the about 50 GB in photos at my computer, but obviously not only for that. Thank you all for such a great collection of memories. Among all of

them, Friday's "frontenis" games and lunches will always take up a special place in my heart, probably because sometime along the way the players-diners became a family to me.

In fact, I pride myself on being member of more than one family and I would like to have an extremely brief word of thanks to the rest of them. Sanpedrotarras, salconmigueros and fmm-members, thank you because we share(d) a way. Jai, cma and camp-mates, thank you because we share(d) a mission. Friends I found in all these groups, at university or in basketball teams, thank you because we share(d) experiences. Heterogeneous group of friends called "cuadrilla" thank you because, more than a quarter of century later, we still share our lives! A "rôpla" to that ;-)

But above all, THANK YOU to the family I did not choose but I was blessed with. To the ones that are around and the ones that I carry forever in my heart. Few but always close together through thick and thin, through anything, through everything. I hope you know what you mean to me because, honestly, it cannot be put down in words.

THANK YOU / MERCI BEAUCOUP / MUCHAS GRACIAS / MILA ESKER

Abbreviations

1D	1 dimensional (NMR experiment)
2D	2 dimensional (NMR experiment)
2'-OAADPr	2'-O-acetyl-adenosine diphosphate-ribose
3'-OAADPr	3'-O-acetyl-adenosine diphosphate-ribose
% Max	percentage of maximum activation (of enzyme activity)
a	axial position
a.u.	atomic unit (NBO charges)
Ac	acetyl (group)
AceCS1	acetyl-CoA (coenzyme A) synthetase 1
AD	Alzheimer's disease
Ad _N 2	bimolecular nucleophilic addition
Alk	alkyl
AMC	7-amino-4-methylcoumarin
AMPK	AMP (5'-adenosine monophosphate)-activated protein kinase
Ar	aryl, aromatic group
Arg	arginine, R (amino acid residue)
Assoc. Prof.	Associated professor
ATCC	ATCC private, nonprofit biological resource center and research organization
ATP	adenosine-5'-triphosphate
Aβ	amyloid beta peptide
Å	ångström
B3LYP	Becke, three-parameter, Lee-Yang-Parr hybrid functional
BARF	tetrakis[3,5-bis(trifluoromethyl)phenyl] borate anion
Bcl-2	B-cell lymphoma 2
BINAP	2,2'-bis(diphenylphosphino)-1,1'-binaphthalene
[BMIM]BF ₄	1-Butyl-3-methylimidazolium tetrafluoroborate
Bn	benzyl (group)
Boc	<i>tert</i> -butoxycarbonyl
bphen	bathophenanthroline
BQ	1,4-benzoquinone (<i>para</i> -benzoquinone)
bs	broad signal (NMR)
Bt	benzotriazolyl
BTI	bis(trifluoroacetoxy)iodobenzene (also PIFA)
C	cubic (coordination of Al atoms in alumina)
C26	colon carcinoma cell line (also CT26 and MCA26)
CamKKβ	Ca ²⁺ /calmodulin-dependent kinase beta
cAMP	cyclic adenosine monophosphate
Cat.	Catalogue
CCD	charge-coupled detector (X-ray diffraction analysis)
CCK	cholecystokinin
cod	1,5-cyclooctadiene
compd.	compound
conc.	concentration
COSY	correlation spectroscopy (NMR experiment)
COX	cyclooxygenase
Cp*	pentamethylcyclopentadienyl
CR	calorie restriction (also dietary restriction)
CSFE	carboxyfluorescein diacetate succinimidyl ester, fluorescent probe (also CFDA, SE)
CYP	cytochrome P450

d	doublet (NMR)
DAPI	4',6-diamidino-2-phenylindole
dba	dibenzylideneacetone
DCE	1,2-dichloroethane
DCN	1,4-dicyanonaphthalene
dd	doublet of doublets (NMR)
DDQ	2,3-dichloro-5,6-dicyano-1,4-benzoquinone
DEA	<i>N,N</i> -diethylaniline
dec.	decomposition (decomposition temperature, instead of melting point, m.p.)
degrad.	degradation
DEPT	Distortionless Enhancement by Polarization Transfer (NMR experiment)
DFT	Density Functional Theory
DIB	diacetoxyiodobenzene (also PIDA)
diglyme	diethylene glycol dimethyl ether
DMA	<i>N,N</i> -dimethylacetamide
DMAP	4-dimethylaminopyridine
DMF	<i>N,N</i> -dimethylformamide
DMP	Dess-Martin periodinane
DMSO	dimethyl sulfoxide
DNA	deoxyribonucleic acid
DPEphos	bis[(2-diphenylphosphino)phenyl] ether
dppe	1,2-bis(diphenylphosphino)ethane
DR	dietary restriction (also calorie restriction)
δ	chemical shift (NMR spectroscopy)
ΔE_{rxn}	reaction energy
ΔG^\ddagger	activation energy (Gibbs free energy)
e	equatorial position
E	electrophile
E_a	activation energy (internal energy)
EAS	electrophilic aromatic substitution (also $S_{\text{E}}\text{Ar}$)
$\text{EC}_{1.5}$	50% activatory concentration (concentration of compound required to increase the enzyme activity by 50%)
eNOS	endothelial nitric oxide synthase
E_{N}^{T}	normalized empirical parameter of solvent polarity
Epac1	c-AMP-dependent guanine nucleotide exchange factor
eq	equivalent
ESI	electrospray ionization (mass spectrometry)
Et	ethyl (group)
EWG	electron-withdrawing group
F	fluorofore
FBS	fetal bovine serum
FdL	Fluor de Lys
FMO	frontier molecular orbital
FOXO	Forkhead transcription factor (also FKRH)
G_0	Gap 0 (quiescent or senescent state of the cell cycle)
G_1	Gap 1 (stage of the interphase state of the cell cycle)
G_2	Gap 2 (stage of the interphase state of the cell cycle)
GHz	gigahertz
GIAO	gauge-independent atomic orbital
h	hour
H	histidine, His (amino acid residue)
HC	Herrmann's catalyst (Pd(0) catalyst)
HD	Huntington's disease

HDAC	histone deacetylase
HDP	hydroxylative dearomatization of phenol (reaction)
HIF- α	hypoxia inducible factor alpha
His	histidine, H (amino acid residue)
HIV	human immunodeficiency virus
HMBC	Heteronuclear Multiple Bond Correlation (NMR experiment)
HO-1	heme oxygenase 1
HOMO	highest occupied molecular orbital
HPLC	high performance liquid chromatography
HRMS	high resolution mass spectrometry
HSQC	Heteronuclear Single Quantum Coherence (NMR experiment)
HVC	hepatitis C virus
Hx	hexane
Hz	hertz
\sim H ⁺	prototropy
IBA	2-iodosobenzoic acid
IBX	<i>ortho</i> -iodoxybenzoic acid
IC ₅₀	half maximal inhibitory concentration (concentration of compound required to reduce the enzyme activity by 50%)
ICAM-1	intercellular cell adhesion molecule 1
IL	interleukin
iNOS	inducible nitric oxide synthase
INT	intermediate
<i>i</i> Pr	<i>iso</i> -propyl (group)
IPr	1,3-bis(diisopropylphenyl)imidazolium tetrafluoroborate
IR	infrared (spectroscopy)
IUPAC	International Union of Pure and Applied Chemistry
<i>J</i>	Coupling constant (NMR)
K	Lysine, Lys (amino acid residue)
KC	Kupffer cell
kcal	kilocalorie
Ki67	protein, cellular marker for proliferation (also MKI67)
K _m	Michaelis-Menten constant
Ku70	ATP-dependent DNA helicase 2 subunit 1
L	ligand
LDA	lithium diisopropylamide
LDL	low-density lipoprotein
LFA-1	lymphocyte function-associated antigen 1
LOX-5	lipoxygenase 5
LSEC	liver sinusoidal endothelial cell
LTA	lead tetraacetate (Pb(OAc) ₄)
LUMO	lowest unoccupied molecular orbital
Lys	Lysine, K (amino acid residue)
λ	wavelength
<i>m</i>	multiplet (NMR)
M	Molar (when related to concentration) or mitosis (when related to cell division state of the cell cycle)
m.p.	melting point
mA	miliampere
maj	major
MAO	monoamine oxidase A
MAOS	microwave assisted organic synthesis

<i>m</i> CPBA	<i>meta</i> -chloroperbenzoic acid
MD	Maryland (USA state)
Me	methyl (group)
MHz	megahertz
min	minute (when related to time) or minor (when related to proportion of product)
mM	milimolar
MO	Missouri (USA state)
mmol	milimol
μM	micromolar
μW	microwave (irradiation)
NAD ⁺	nicotinamide adenine dinucleotide
NBO	natural bond orbital
NBS	<i>N</i> -bromosuccinimide
ⁿ Bu	<i>n</i> -butyl (group)
NCS	<i>N</i> -chlorosuccinimide
Nfr2	nuclear factor (erythroid-derived 2)-like factor 2
NF-κB	nuclear factor kappa B
NICS	nucleus-independent chemical shifts
NIS	<i>N</i> -iodosuccinimide
nM	nanomolar
NMP	1-methyl-2-pyrrolidinone
NMR	nuclear magnetic resonance (spectroscopy)
ⁿ Pr	<i>n</i> -propyl (group)
NO	nitric oxide
no.	number
NOE	Nuclear Overhauser Effect (NMR experiment)
NPC	nonparenchymal cell
NTf ₂	bis(trifluoromethanesulfonyl)imide
Nu/NuH	nucleophile
NXS	<i>N</i> -halosuccinimide
[O]	oxidant, oxidation
OAc	acetate (group)
ODC	ornithine decarboxylase
ORTEP	Oak Ridge Thermal Ellipsoid Plot Program (molecular modelling)
OTf	triflate (trifluoromethanesulfonate)
p	statistical parameter
p21	cyclin-dependent kinase inhibitor 1
p27	cyclin-dependent kinase inhibitor 1B
p53	tumor suppressor protein 53
PBS-EDTA	phosphate buffered saline ethylenediaminetetraacetic acid
PC	parenchymal cell
PD	Parkinson's disease
PDA	photodiode array (mass spectrometry)
PDE	phosphodiesterase
PEG	polyethyleneglycol
PET	Polyethylene terephthalate (membrane, for the migration cell-based assays)
PGC-1α	PPAR-γ transcriptional coactivator
Ph	phenyl (group)
phen	phenantroline
PIDA	diacetoxyiodobenzene (also DIB)
pK _a	is equal to -log ₁₀ K _a , being K _a the acid dissociation constant
PIFA	bis(trifluoroacetoxy)iodobenzene (also BTI)
PLC	phospholipase C or preparative thin layer chromatography

PM3	parameterized model number 3 (semi-empirical method for the quantum calculation of molecular electronic structure in computational chemistry)
PMC	polarization continuum model
PMP	<i>para</i> -methoxyphenyl or 4-methoxyphenyl (group)
PPA	(poly)phosphoric acid
PPAR- γ	nuclear receptor peroxisome proliferator-activated receptor gamma
ppm	parts per million
prod	product
PTSA	<i>para</i> -toluenesulfonic acid
Py·HCl	pyridine hydrochloride
pyr	pyridine
q	quartet (NMR) or charge
QTOF	quadrupole time-of-flight (mass spectrometry)
R	arginine, Arg (amino acid residue)
R110	rhodamine 110
r.t.	room temperature
rcp	ring critical point
rDNA	ribosomal deoxyribonucleic acid
ref.	reference
react.	reaction
RIMA	reversible inhibitor of monoamine oxidase A
RNA	ribonucleic acid
RNS	reactive nitrogen species
ROS	reactive oxygen species
rpm	revolutions per minute
RPMI-1640	Roswell Park Memorial Institute cell culture medium
s	singlet (NMR)
S	synthesis (stage of the interphase state of the cell cycle)
SCRf	self-consistent reaction field
SET	single-electron transfer
S _E Ar	electrophilic aromatic substitution (also EAS)
SIBX	stabilized <i>ortho</i> -iodoxybenzoic acid
Sir2	silent information regulator 2
SIRT1	silent information regulator human homologue 1
SM	starting material
S _N 2	bimolecular nucleophilic substitution
St.	Saint
STAC	sirtuin-activating compound
t	triplet (NMR)
T	temperature or tetrahedral (coordination of Al atoms in alumina)
^t AmOH	<i>tert</i> -amyl alcohol
TBAF	tetra- <i>n</i> -butylammonium fluoride
TBS	<i>tert</i> -butyldimethylsilyl
^t Bu	<i>tert</i> -butyl (group)
td	triplet of doublets (NMR)
TFA	trifluoroacetic acid
TFAT	trifluoroacetyl triflate
TFE	2,2,2-trifluoroethanol
THF	tetrahydrofuran
TLC	thin layer chromatography
TMEDA	<i>N,N,N',N'</i> -tetramethylethylenediamine
TMHD	2,2,7,7-tetramethylhepta-2,5-dione
TMP	3,4,5-trimethoxyphenyl or 2,2,6,6-tetramethylpiperidine (only in section 3.2)

TMS	tetramethylsilane
TNF	tumor necrosis factor
Ts	tosyl (4-toluenesulfonyl)
TS	transition structure
tt	triplet of triplets (NMR)
TTN	thallium trinitrate ($Tl(NO_3)_3$)
TxA ₂	thromboxane A ₂
UPLC	ultra high performance liquid chromatography
USA	United States of America
VA	Virginia (USA state)
VCAM-1	vascular cell adhesion molecule 1
VEGF	vascular endothelial growth factor
W	Watt
WHO	World Health Organization

Chapter 1:

General Introduction to Benzo[*b*]furans and Objectives

1.1. General introduction to benzo[*b*]furans

1.1.1. The benzo[*b*]furan, a “privileged structure”

1.1.2. Applications of benzo[*b*]furans

1.1.3. Preparation of benzo[*b*]furans

1.1.3.1. Construction of the benzo[*b*]furan core

1.1.3.1.1. Methods based on the O-C₂ bond formation (A)

1.1.3.1.2. Methods based on the C₂-C₃ bond formation (B)

1.1.3.1.3. Methods based on the C₃-C_{3a} bond formation (C)

1.1.3.1.4. Methods based on the O-C_{7a} bond formation (D)

1.1.3.1.5. Methods based on the construction of the benzene ring (E)

1.1.3.1.6. Methods based on the transformation of bi- or tricyclic oxygen-containing ring systems (F)

1.1.3.2. Substituents in the benzo[*b*]furan structure

1.1.3.2.1. Halogens

1.1.3.2.2. Hydroxy groups

1.2. Objectives

1.1. GENERAL INTRODUCTION to BENZO[b]FURANS

1.1.1. The benzo[b]furan, a “privileged structure”

A benzofuran is an aromatic heterocyclic compound with bicyclic structure that consists of a benzene fused with a furan ring. Roughly, two kinds of benzofurans can be differentiated, benzo[b]furans and benzo[c]furans, depending on the position of the oxygen atom with respect to the bond shared by the benzene and furan rings. Although strictly both are benzofurans, when not specified, the term benzofuran usually refers to the benzo[b]furan (also 1-benzofuran or coumarone) whilst the benzo[c]furan is denoted by its trivial name isobenzofuran (also 2-benzofuran) (Figure 1.1).

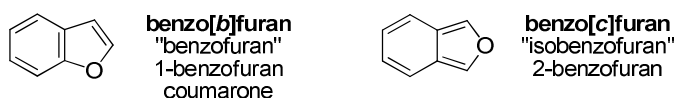


Figure 1.1. Structure and alternative names of benzo[b]furan and benzo[c]furan.

According to a study that assessed the role of aromaticity on the relative stability of position isomers, benzo[b]furan is 14.4 kcal/mol more stable than benzo[c]furan. The difference was attributed to a large decrease of aromaticity of the benzene ring in benzo[c]furan¹. Indeed, benzo[c]furan itself is not stable and rapidly polymerizes², although it has been identified³, prepared and trapped at low temperature⁴. Nevertheless, during the development of this thesis, our work was focused on benzo[b]furans so we will exclusively consider this isomer from now on.

Benzo[b]furan is found as building unit in a great variety of natural and synthetic products with biological activity. So much so that it was included in the “privileged structure” list, a term first coined by Evans to refer to a single molecular framework capable of providing useful ligands for diverse receptors⁵. In the seminal paper, a substituted benzodiazepine (inspired by the natural product lead asperlicin⁶) was identified as a key structure to

¹ Mandado, M.; Otero, N.; Morquera, R. A. *Tetrahedron* **2006**, *62*, 12204-12210

² Choi, H.-G.; Amara, J. P.; Swager, T. M.; Klavs F. Jensen, K. F. *Macromolecules* **2006**, *39*, 4400-4410

³ Fieser, L. F.; Haddadin, M. J. *J. Am Chem. Soc.* **1964**, *86*, 2181-2082

⁴ Wege, D. *Tetrahedron Lett.* **1971**, *12*, 2337-2338

⁵ (a) Evans, B. E.; Rittle, K. E.; Bock, M. G.; DiPardo, R. M.; Freidinger, R. M.; Whitter, W. L.; Lundell, G. F.; Veber, D. F.; Anderson, P. S.; Chang, R. S. L.; Lotti, V. J.; Cerino, D. J.; Chen, T. B.; Kling, P. J.; Kunkel, K. A.; Springer, J. P.; Hirshfield, J. *J. Med. Chem.* **1988**, *31*, 2235-2246 (b) Kubinyi, H.; Müller, G. (Eds) *Chemogenomics in Drug Discovery – a Medicinal Chemistry Perspective* **2004**, Wiley-VHC, Weinheim

⁶ Chang, R. S. L.; Lotti, V. J.; Monaghan, R. L.; Birnbaum, J.; Stapley, E. O.; Goetz, M. A.; Albers-Schönberg, G.; Patchett, A. A.; Liesch, J. M.; Hensens, O. D.; Springer, J. P. *Science* **1985**, *230*, 177-179

develop peptide hormone cholecystinin (CCK) antagonists. Besides, the potential of certain regularly occurring structural motifs as templates for derivatization in the search for new receptor agonists and antagonists was envisaged^{5a}. However, the definition has evolved over time and it gives now the notion of a particular scaffold present in multiple molecules having bioactivity.

Ever since then, the exploration of privileged structures in drug discovery has emerged as a trending topic in medicinal chemistry, as they represent an ideal source of lead compounds. Among all the scaffolds that have progressively joined this category, bicyclic fused ring systems (including benzo[*b*]furan), have drawn special attention (Figure 1.2). Their most remarkable feature is probably that they combine the ideal size (and its consequent relatively low molecular weight) with the intrinsic molecular rigidity of cycles (which allows less entropic cost upon binding and provides a better bioavailability). Moreover, they have a small enough molecular weight to either provide scope for improved specificity and affinity through the attachment of suitable substituents in a wide variety of topologies or to be used as substituents of other scaffolds⁷.

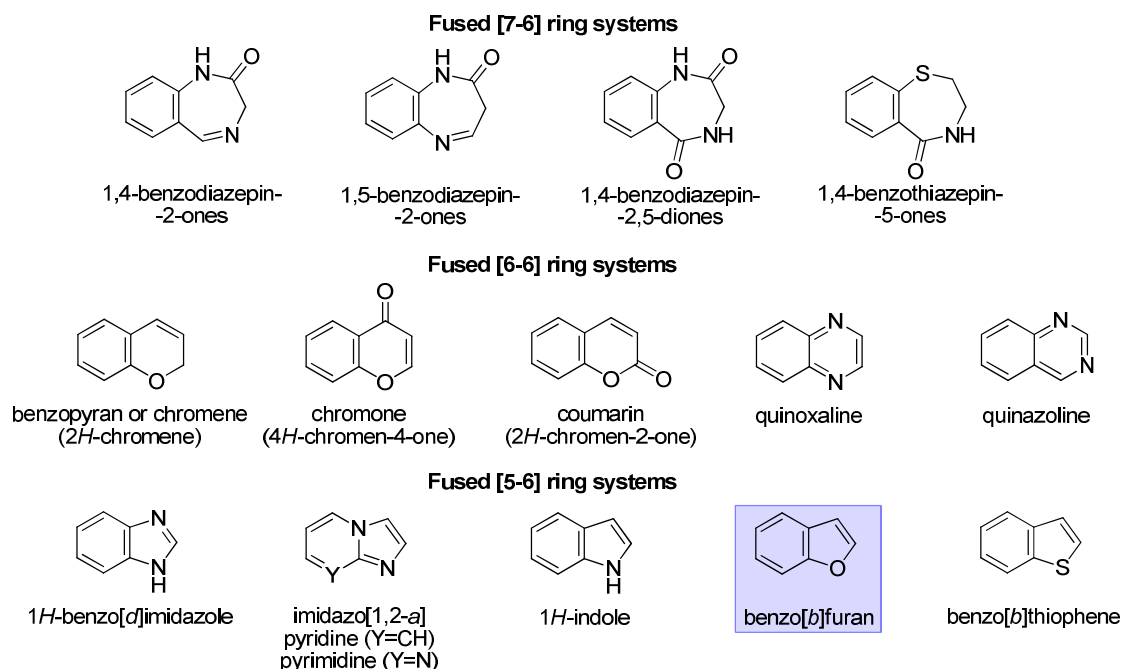


Figure 1.2. Examples of bicyclic fused ring systems considered privileged structures or substructures.

⁷ (a) Horton, D. A.; Bourne, G. T.; Smythe, M. L. *Chem. Rev.* **2003**, *103*, 893-930 (b) Sharma, S.; Saha, B.; Sawant, D.; Kundu, B. *J. Comb. Chem.* **2007**, *9*, 783-792

1.1.2. Applications of benzo[*b*]furans

A great variety of both synthetic and naturally occurring molecules that include the benzo[*b*]furan motif in their structure have been reported to show diverse biological activities and other special features, which provide them with potential applications in the fields of biomedicine and material sciences. In fact, the large number of references found on this topic makes it virtually impossible to carry out an exhaustive review of the literature. Therefore, only a selection of examples will be shown here.

Numerous publications reported the benzo[*b*]furans to have anti-inflammatory, antitumor, cytotoxic, antimicrobial, antitubercular, antioxidant, antiplasmodial and hepatitis C virus (HVC) and human immunodeficiency virus (HIV) inhibitory activities⁸.

As examples of this, in the area of biomedicine, interesting natural products such as cicerfuran, ailanthoidol, some furanocoumarins (psoralen, angelicin) and isomeric furanochromones (khellin, visnagin) or moracins C and M can be found (Figure 1.3).

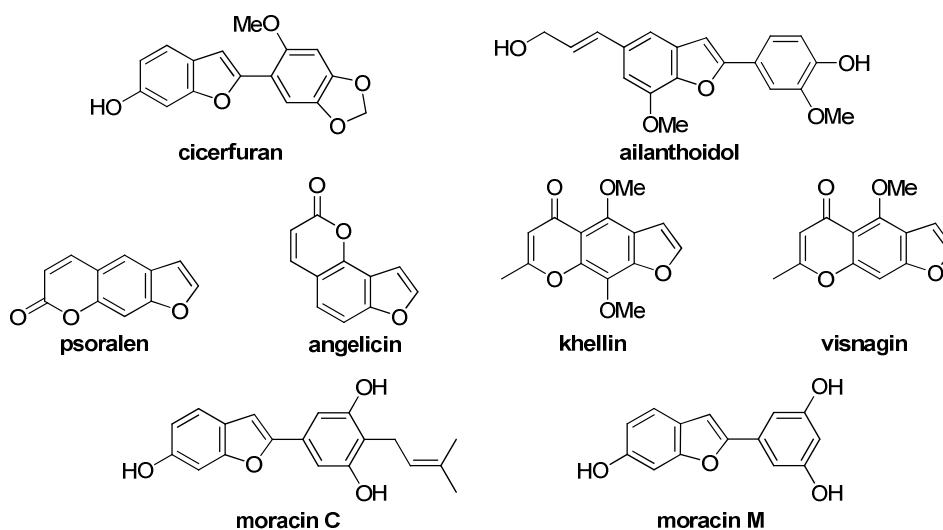


Figure 1.3. Examples of natural benzo[*b*]furans with (potential) pharmaceutical applications.

Cicerfuran, a hydroxylated benzo[*b*]furan derivative first obtained from the roots of wild species of chickpea (*Cicer bijugum*), is an antifungal phytoalexin (a substance synthesized

⁸ Dawood, K. M. *Expert Opin. Ther. Patents* **2013**, 23, 1133-1156

de novo by plants in response to a stress, injury, ultraviolet irradiation and/or fungal infection) which also presented antimicrobial activity⁹.

Ailanthoidol, a neolignan extracted from the stem woods of *Zanthoxylum ailanthoides*, was reported to be an anti-inflammatory which, belonging to the neolignan family, is also likely to possess a variety of other biological activities such as anticancer, antiviral, immunosuppressive, antioxidant or antifungal¹⁰.

Furanocoumarins, compounds having as core isomeric psoralen (linear furanocoumarins) or angelicin (angular furanocoumarins) structures among others, are produced by plants as a defense mechanism against various types of predators. They also showed interesting properties: psoralen itself combined with UVA irradiation proved useful in the treatment of vitiligo and psoriasis¹¹ whilst angelicin and some derivatives of it presented antifungal activity¹².

Furanochromones, like khellin and visnagin, are mainly found in the plant *Ammi visnaga* (also known by one of its common names Khella). Khellin found application as photosensitizer in the treatment of the aforementioned skin diseases (vitiligo and psoriasis)¹³, as well as coronary vasodilator¹⁴. Visnagin also listed vascular vasodilatation among its biological activities¹⁵. In addition, these two furanochromones are reportedly the

⁹ (a) Stevenson, P. C.; Veitch, N. C. *Phytochemistry* **1998**, *48*, 947-951 (b) Aslam, S. N.; Stevenson, P. C.; Phythian, S. J.; Veitch, N. C.; Hall, D. R. *Tetrahedron* **2006**, *62*, 4214-4226 (c) Aslam, S. N.; Stevenson, P. C.; Kokubun, T.; Hall, D. R. *Microbiol. Res.* **2009**, *164*, 191-195

¹⁰ (a) Sheen, W. S.; Tsai, I. L.; Teng, C. M.; Chen, I. S. *Phytochemistry* **1994**, *36*, 213-215 (b) Kao, C.-L.; Chern, J.-W. *Tetrahedron Lett.* **2001**, *42*, 1111-1113 (c) Kao, C.-L.; Chern, J.-W. *J. Org. Chem.* **2002**, *67*, 6772-6787 (d) Hwang, J. W.; Choi, D. H.; Jeon, J.-H.; Kim, J.-K.; Jun, J.-G. *Bull. Korean Chem. Soc.* **2010**, *31*, 965-970

¹¹ Bethea, D.; Fullmer, B.; Syed, S.; Seltzer, G.; Tiano, J.; Rischko, C.; Gillespie, L.; Brown, D.; Gasparro, F. *P. J. Dermatol. Sci.* **1999**, *19*, 78-88

¹² Sardari, S.; Mori, Y.; Horita, K.; Micetich, R. G.; Nishibe, S.; Daneshtalab, M. *Bioorg. Med. Chem.* **1999**, *7*, 1933-1940

¹³ (a) Abdel-Fattah, A.; Aboul-Enein, M. N.; Wassel, G.; El-Menshaw, B. *Dermatologica* **1983**, *167*, 109-110 (b) Ortel, B.; Tanew, A.; Hönigsmann, H. *J. Am. Acad. Dermatol.* **1988**, *18*, 693-701 (c) Morliere, P.; Hönigsmann, H.; Averbeck, D.; Dardalhon, M.; Hüppe, B. A.; Ortel, B.; Santus, R.; Dubertret, L. *J. Invest. Dermatol.* **1988**, *90*, 720-724 (d) Röcken, M.; Walchner, M.; Messer, G. *Patent* **2000** WO 00/30682A1

¹⁴ (a) Krul, E. S. *Patent* **2003** US 2003/0162824 A1 (b) Anrep, G. V.; Kenawy, M. R.; Barsoum, G. S. *Am. Heart J.* **1949**, *37*, 531-542

¹⁵ (a) Duarte, J.; Pérez-Vizcaino, F.; Torres, A. I.; Zarzuelo, A.; Jiménez, J.; Tamargo, J. *Eur. J. Pharmacol.* **1995**, *286*, 115-122 (b) Duarte, J.; Torres, A. I.; Zarzuelo, A. *Planta Med.* **2000**, *66*, 35-39 (c) Lee, J.-K.; Jung, J.-S.; Park, Sang-Hee; Park, Soo-Hyun; Sim, Y.-B.; Kim, S.-M.; Ha, T.-S.; Suh, H.-W. *Arch. Pharm. Res.* **2010**, *33*, 1843-1850

active ingredients of khella extract used in traditional medicine in the prevention and treatment of kidney stones¹⁶.

Moracins, compounds with a benzo[*b*]furan core occurring in *Morus* species, show a wide range of biological activities such as antifungal¹⁷, antioxidant¹⁸, antimicrobial¹⁹ or antidiabetic²⁰.

Besides, medicinal applications of synthetic benzo[*b*]furan derivatives like befunolol, bufuralol, cloridarol, amidarone, dronedarone, oxetorone, becliconazole, brofaromine or furaprofen were reported (Figure 1.4).

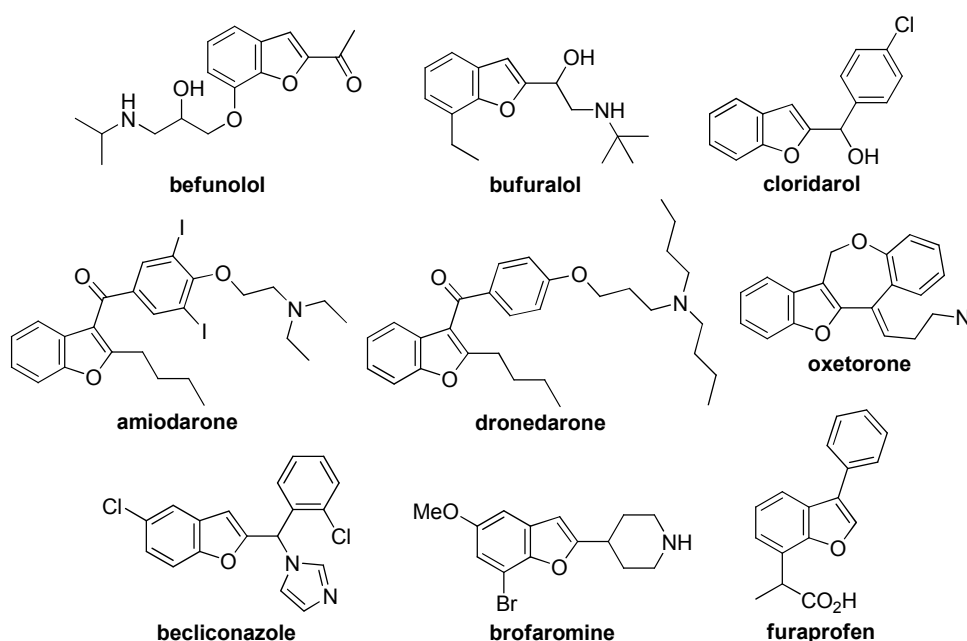


Figure 1.4. Examples of synthetic benzo[*b*]furans with (potential) pharmaceutical applications.

Befunolol is a β -blocker (β -adrenoceptor antagonist) used in the treatment of glaucoma²¹. The also β -blocker bufuralol is included in the antianginal and antihypertensive therapeutic

¹⁶ (a) Abdel-Aal, E. A.; Daosukho, S.; El-Shall, H. *J. Cryst. Growth.* **2009**, *311*, 2673-2681 (b) Vanachayangkul, P.; Chow, N.; Khan, S. R.; Butterweck, V. *Urol. Res.* **2011**, *39*, 189-195 (c) Haug, K. G.; Weber, B.; Hochhaus, G.; Butterweck, V. *Eur. J. Pharm. Sci.* **2012**, *45*, 79-89

¹⁷ Tkasugi, M.; Nagao, S.; Ueno, S.; Masamune, T.; Shirata, A.; Takahashi, K. *Chem. Lett.* **1978**, 1239-1240

¹⁸ Sharma, R.; Sharma, A.; Shono, T.; Takasugi, M.; Shirata, A.; Fujimura, T.; Machii, H. *Biosci. Biotechnol. Biochem.* **2001**, *65*, 1402-1405

¹⁹ Kuetea, V.; Fozingb, D. C.; Kapchec, W. F. G. D.; Mbavengd, A. T.; Kuatea, J. R.; Ngadjuib, B. T.; Abegaze, B. M. *J. Ethnopharmacol.* **2009**, *124*, 551-555

²⁰ Yang, Z.; Wang, Yingchao; Wang, Yi; Zhang, Y. *Food Chem.* **2012**, *131*, 617-625

²¹ (a) Reichl, S.; Müller-Goymann, C. C. *Int. J. Pharm.* **2003**, *250*, 191-201; (b) Welsch, W. E.; Snyder, S. A.; Stockwell, B. R. *Curr. Op. Chem. Biol.* **2010**, *14*, 347-361

categories^{21b,22} whilst cloridarol was reported to be useful in the treatment of lipidemia (abnormally elevated levels of any or all lipids and/or lipoproteins in the blood) and as anticoagulant²³.

Among synthetic benzo[*b*]furans, 3-ketobenzo[*b*]furans acquired importance as therapeutically valuable cardiac drugs. In this vein, we found amiodarone, one of the most effective antiarrhythmic drug ever developed²⁴, or the also antiarrhythmic agent dronedarone, pharmacologically related to amiodarone which was developed to reduce its side effects²⁵.

The tetracyclic oxetorone is included in the analgesic therapeutic category, being specific in migraine^{21b} and becliconazole is an antimycotic and antibiotic with activity against *Staphylococcus aureus* and *Pseudomonas aeruginosa*²⁶. Brofaromine, in contrast, is a reversible inhibitor of monoamine oxidase A (reversible MAO inhibitor or RIMA) primarily researched in the treatment of depression²⁷ and other psychological disorders (such as post-traumatic stress disorder²⁸). As a last example, we found furaprofen, a nonsteroidal anti-inflammatory drug analogue of the well-known Ibuprofen²⁹.

In any case, these constitute just a sample of biologically active compounds having the benzo[*b*]furan moiety as core. They are well-known due to their (potential) medicinal

²² (a) Pringle, T. H.; Francis, R. J.; East, P. B.; Shanks, R. G. *Br. J. Clin. Pharmacol.* **1986**, *22*, 527-534 (b) Narimatsu, S.; Takemi, C.; Kuramoto, S.; Tsuzuki, D.; Hichiya, H.; Tamagake, K.; Yamamoto, S. *Chirality* **2003**, *15*, 333-339

²³ Ghelardoni, M.; Pestellini, V.; Del Soldato, P.; Volterra, G.; Meli, A. *Patent* **1981**, DE 3029421 A1 19810226

²⁴ (a) Singh, B. N.; Vaughan Williams, E. M. *Br. J. Pharmac.* **1970**, *39*, 657-667 (b) Rosenbaum, M. B.; Chiale, P. A.; Halpern, M. S.; Nau, G. J.; Przybylski, J.; Levi, R. J.; Lázzari, J. O.; Elizari, M. V. *Am. J. Cardiol.* **1976**, *38*, 934-944 (c) Rosenbaum, M. B.; Chiale, P. A.; Haedo, A.; Lázzari, J. O.; Elizari, M. V. *Am. Heart J.* **1983**, *106*, 957-964

²⁵ (a) Kathofer, S.; Thomas, D.; Karle, C. A. *Cardiovasc. Drug Rev.* **2005**, *23*, 217-230 (b) Singh, B. N.; Connolly, S. J.; Crijns, H. J. G. M.; Roy, D.; Kowey, P. R.; Capucci, A.; Radzik, D.; Aliot, E. M.; Hohnloser, S. H. *N. Engl. J. Med.* **2007**, *357*, 987-999 (c) Patel, C.; Yan, G.-X.; Kowey, P. R. *Circulation* **2009**, *120*, 636-644 (d) Hohnloser, S. H.; Crijns, H. J. G. M.; van Eickels, M.; Gaudin, C.; Page, R. L.; Torp-Pedersen, C.; Connolly, S. J. *N. Engl. J. Med.* **2009**, *360*, 668-678

²⁶ (a) Katritzky, A. R.; Rees, C. W.; Scriven, E. F. V. *Comprehensive Heterocyclic Chemistry II* Pergamon Press, Oxford **1996**, *2*, 413-436 (b) Pestellini, V.; Ghelardoni, M.; Giannotti, D.; Giolitti, A.; Barzanti, A.; Ciappi, R.; Ortolani, C. *Patent* **1988**, EP0257171 A1

²⁷ (a) Schenker, K.; Bernasconi, R. *Patent* **1980**, US 4610655 A (b) Papp, M.; Moryl, E.; Willner, P. *Eur. J. Pharmacol.* **1996**, *296*, 129-136 (c) Lotufo-Neto, F.; Trivedi, M.; Thase, M. E. *Neuropsychopharmacol.* **1999**, *20*, 226-247

²⁸ Katz, R. *Patent* **1993**, WO 9316695 A1

²⁹ (a) Kaltenbronn, J. S.; Short, F. W. *Patent* **1972** US 3682976 (b) Scherrer, R. A. *Patent* **1975** US 3920828 (c) Swingle, K. F.; Scherrer, R. A.; Grant T. J. *Arch. Int. Pharmacodyn. Ther.* **1975**, *214*, 240-249 (d) Ringold, H. J.; Waterbury, L. D. *Patent* **1982** DE 3026402 A1 (e) Wang, T.; Lai, C.-S. *Patent* **2004** WO 2004000215 A2

applications and even have their own trivial (non-systematic) name, but many more have been identified and reported throughout the past decades^{8,26a}.

Although pharmaceuticals can seem the most prolific field of application of benzo[*b*]furans, their biological activities have also been applied to the development of agrochemical bioregulators, as trypanocidal (antiprotozoal). Insecticidal activities were also identified in some benzo[*b*]furans (Figure 1.5).

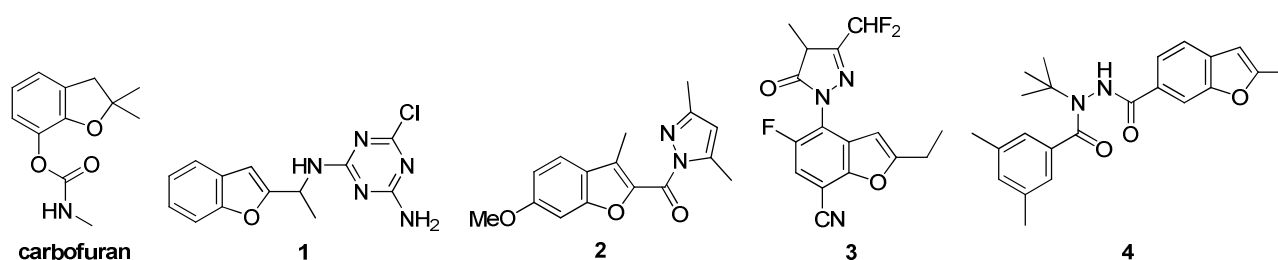


Figure 1.5. Examples of agrochemical bioregulators including a benzo[*b*]furan (or benzo[*b*]furan derivative) unit.

Some examples of these could be the renowned, and extremely toxic (there is now a ban on its use on crops grown for human consumption almost worldwide), carbofuran carbamate pesticide³⁰; triazine **1**, which was reported to be a herbicide useful in protecting rice paddies³¹; benzo[*b*]furan-2-carboxylic acid derivative **2**, a compound with insecticidal activity against adult sweet potato weevils (*Cylas formicarius elegantulus*)³²; substituted benzo[*b*]furan **3**, a potential herbicide showing a very strong effect against weeds³³; or carbohydrazide derivative **4**, which exhibited an excellent larvicidal (insecticidal) activity against beet armyworm (*Spodoptera exigua*)³⁴.

In the field of material sciences, it is worth mentioning that several benzo[*b*]furan derivatives have found utility as dyes and photographic materials or as subunits in the preparation of polymers (Figure 1.6).

³⁰ (a) Heiss, R.; Boecker, E.; Behrenz, W.; Unterstenhoefer, G. *Patent 1964* BE 649260 A (b) "EPA Bans Carbofuran Pesticide Residues on Food". Environmental News Service. 11 May 2009. Retrieved 5 June 2009 (<http://www.ens-newswire.com/ens/may2009/2009-05-11-093.asp>)

³¹ Takematsu, T.; Nishii, M.; Kobayashi, I. *Patent 1987* EP 021659 A1

³² Jackson, Y. A.; Williams, M. F.; Williams, L. A. D.; Morgan, K.; Redway, F. A. *Pestic. Sci.* **1998**, *53*, 241-244

³³ Linker, K.-H.; Andree, R.; Reubke, K.-J.; Schallner, O.; Drewes, M. W.; Dahmen, P.; Feucht, D.; Pontzen, R. *Patent 2001* WO 01/10862 A2

³⁴ Huang, Z.; Liu, Y.; Li, Y.; Xiong, L.; Cui, Z.; Song, H.; Liu, H.; Zhao, Q.; Wang, Q. *J. Agric. Food Chem.* **2011**, *59*, 635-644

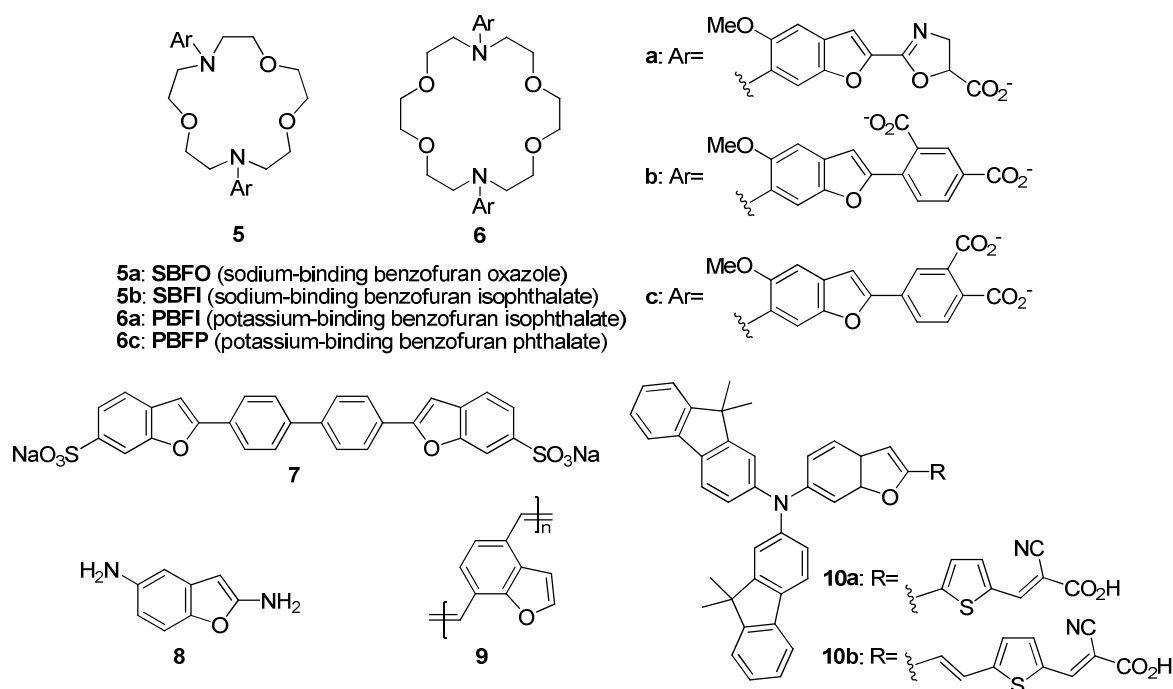


Figure 1.6. Examples of organic dyes and polymers including a benzo[*b*]furan unit.

On the one hand, compounds combining one heterocyclic unit with two benzo[*b*]furanyl substituents like **5** and **6** proved to be adequate fluorescent indicators (dyes) sensitive to cytosolic concentrations of free Na^+ and K^+ ³⁵. Bis(sulfobenzofuranyl)biphenyls such as **7** have been used as fluorescent brighteners in stable bleach solutions³⁶. Benzo[*b*]furan unit is also present in compounds **10**, prepared in an effort to develop more efficient (in terms of solar-to-electric conversion) metal-free organic dyes for dye-sensitized solar cells (DSSCs)³⁷.

On the other hand, the combination of benzofuranamine **8** with some bisanhydrides resulted in polyimides with good glass transition temperatures and solvent resistance³⁸. Poly(4,7-benzofuran vinylene) **9** was prepared in the search for conducting polyphenylenes³⁹.

Again, these are just some selected examples of products including the benzo[*b*]furan scaffold with actual and/or promising usefulness in different fields, but the list is and progressively grows longer.

³⁵ Minta, A.; Tsien, R. Y. *J. Biol. Chem.* **1989**, *264*, 19449-19457

³⁶ Clemens, A. H. *Patent* **1990** EP 0364027 A2

³⁷ Jung, I.; Lee, J. K.; Song, K. H.; Song, K.; Kang, S. O.; Ko, J. *J. Org. Chem.* **2007**, *72*, 3652-3658

³⁸ Berdahi, D. R. *Patent* **1988** EP 0264836 A1

³⁹ Sarker, A.; Lahti, P. M.; Karasz, F. E. *J. Polym. Sci., Polym. Chem., Part A* **1994**, *32*, 65-71

1.1.3. Preparation of benzo[*b*]furans

Due to the increasing number of compounds including the benzo[*b*]furan motif with current and/or potential applications in diverse economically relevant areas, there has been (and still is) an extensive and enduring effort in the preparation of these multiple carbon-substituted heterocycles^{21b,40}.

The synthetic approaches towards (multiply) substituted heterocycles can be crudely divided into two categories. The first aims at the construction of the heterocyclic core after the substituents have been installed, and the second is based on the attachment of substituents (in successive order) to the preformed heterocyclic scaffold.

The latest includes for example traditional aromatic substitution chemistry, directed metalation methods, halogen-metal exchange reactions, cross-coupling reactions, as well as protecting groups removal. Nevertheless, at some point the benzo[*b*]furan core must be built, which lead us to the methods described for the first approach. These involve an overwhelming great variety of strategies in which transition-metal, particularly palladium and to a lesser extent copper, catalyzed reactions have played a remarkable and ever growing role. A selection of some of the reported synthetic approaches for the construction of the benzo[*b*]furan core will be shown in the following section.

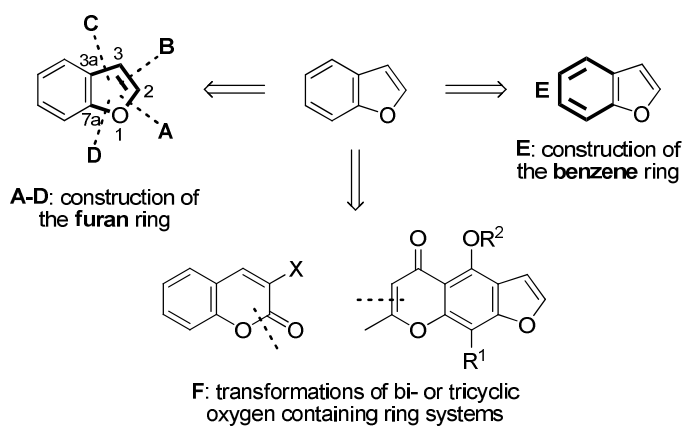
1.1.3.1. Construction of the benzo[*b*]furan core

On looking at the methods for the preparation of the benzo[*b*]furan core described in the literature, it becomes evident that most of them are based on the construction of the furan ring that is incorporated into a benzene moiety (Scheme 1.1. A-D). This benzene moiety is often included in an open-chain precursor (usually a substituted phenol derivative), which is cyclized into the bicyclic aromatic compound. Nevertheless, it can also be just one of the starting materials (typically a substituted or unsubstituted phenol) of a multi-component

⁴⁰ (a) Katritzky, A. R.; Rees, C. W.; Scriven, E. F. V. *Comprehensive Heterocyclic Chemistry II* Pergamon Press, Oxford **1996**, 2, 368-378 (b) Hou, X.-L.; Yang, Z.; Yeung, K.-S.; Wong, H. N. C. *Progr. Heterocycl. Chem.* **2007**, 18, 187-217 (c) Hou, X.-L.; Yang, Z.; Yeung, K.-S.; Wong, H. N. C. *Progr. Heterocycl. Chem.* **2008**, 19, 176-207 (d) De Luca, L.; Nieddu, G.; Porcheddu, A.; Giacomelli, G. *Curr. Med. Chem.* **2009**, 16, 1-20 (e) Hou, X.-L.; Yang, Z.; Yeung, K.-S.; Wong, H. N. C. *Progr. Heterocycl. Chem.* **2009**, 20, 152-189 (f) Hou, X.-L.; Yang, Z.; Yeung, K.-S.; Wong, H. N. C. *Progr. Heterocycl. Chem.* **2009**, 21, 179-223 (g) Yeung, K.-S.; Yang, Z.; Peng, X.-S.; Hou, X.-L. *Progr. Heterocycl. Chem.* **2011**, 22, 181-216 (h) Yeung, K.-S.; Peng, X.-S.; Wu, J.; Hou, X.-L. *Progr. Heterocycl. Chem.* **2011**, 23, 195-229 (i) Yeung, K.-S.; Peng, X.-S.; Wu, J.; Hou, X.-L. *Progr. Heterocycl. Chem.* **2012**, 24, 205-241

reaction. In any case, if the synthetic route is considered at an earlier step, a great majority of the approaches use phenols as starting building blocks.

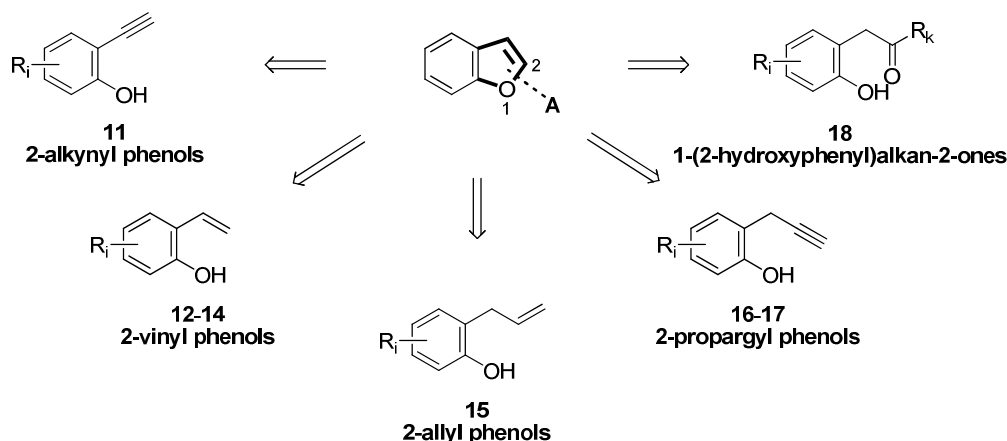
Though more scarcely, methods based on the construction of the benzene ring have also been reported. In them the starting material is or comprises the furan moiety (Scheme 1.1. E). As an alternative approach, we can also find methods based on the transformation of bi- or tricyclic oxygen-containing condensed ring systems (Scheme 1.1. F). Nevertheless, taking into account the relative shortage (and expensiveness) of the starting materials, they are used only in rather specific cases and, therefore, are not generally considered of preparative significance.



Scheme 1.1. Retrosynthetic approaches for the synthesis of the benzo[*b*]furan scaffold based on the construction of the furan ring (A-D), construction of the benzene ring (E) and transformation of bi- or tricyclic oxygen-containing ring systems (F).

1.1.3.1.1. Methods based on the O–C₂ bond formation (A)

The retrosynthetic approaches having a benzenoid scaffold as starting material based on the O–C₂ bond discussed below are presented in Scheme 1.2. Although in scheme 1.2 all the precursors shown are in phenolic form, reactions from derivatives having the hydroxy group protected were also described in some cases.



Scheme 1.2. Retrosynthetic approaches having a benzenoid scaffold as starting material, based on the construction of the O–C₂ bond.

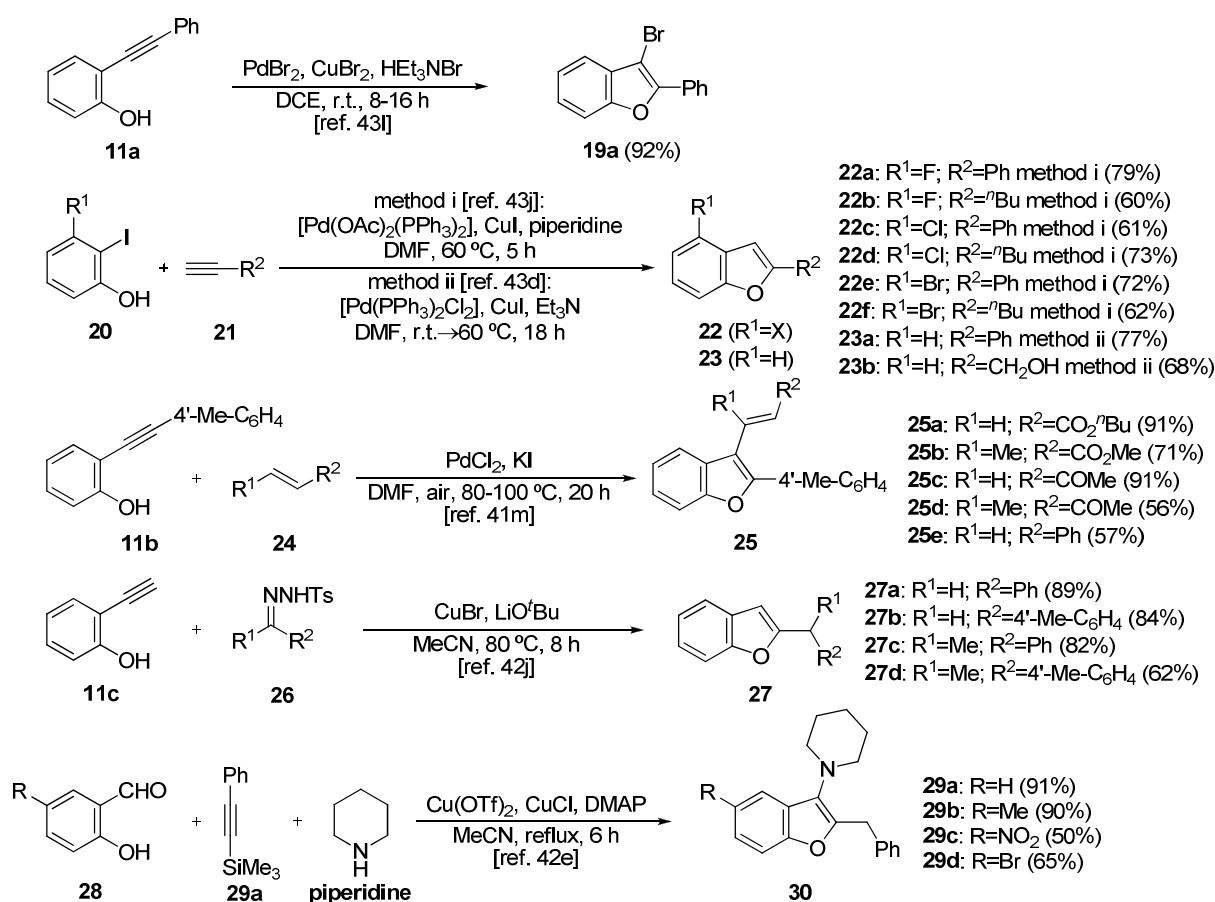
When considering the routes based on the O–C₂ bond formation, the most widely used approach involves the intramolecular addition of the phenolic moiety to a triple C–C bond in a 2-alkynylphenol (**11**). The most employed strategies to carry out this heterocyclization turn to transition metal catalysis. Catalytic systems based on palladium⁴¹, copper⁴² or a combination of both⁴³ are the most popular ones. It is noteworthy that, taking advantage of

⁴¹ (a) Arcadi, A.; Cacchi, S.; Del Rosario, M.; Fabrizi, G.; Marinelli, F. *J. Org. Chem.* **1996**, *61*, 9280-9288 (b) Bishop, B. C.; Cottrell, I. F.; Hands, D. *Synthesis* **1997**, *11*, 1315-1320 (c) Cacchi, S.; Fabrizi, G.; Moro, L. *Synlett* **1998**, 741-745 (d) Nan, Y.; Miao, H.; Yang, Z. *Org. Lett.* **2000**, *2*, 297-299 (e) Hu, Y.; Zhang, Y.; Yang, Z.; Fathi, R. *J. Org. Chem.* **2002**, *67*, 2365-2368 (f) Pal, M.; Subramanian, V.; Yeleswarapu, K. R. *Tetrahedron Lett.* **2002**, *44*, 8221-8225 (g) Hu, Y.; Nawoschik, K. J.; Liao, Y.; Ma, J.; Fathi, R.; Yang, Z. *J. Org. Chem.* **2004**, *69*, 2235-2239 (h) Yoshida, M.; Morishita, Y.; Fujita, M.; Ihara, M. *Tetrahedron Lett.* **2004**, *45*, 1861-1864 (i) Liao, Y.; Smith, J.; Fathi, R.; Yang, Z. *Org. Lett.* **2005**, *7*, 2707-2709 (j) Yoshida, M.; Morishita, Y.; Fujita, M.; Ihara, M. *Tetrahedron* **2005**, *7*, 4381-4393 (k) Anderson, K. W.; Ikawa, T.; Tundel, R. E.; Buchwald, S. L. *J. Am. Chem. Soc.* **2006**, *128*, 10694-10695 (l) Du, H.-A.; Zhang, X.-G.; Tang, R.-Y.; Li, J.-H. *J. Org. Chem.* **2009**, *74*, 7844-7848 (m) Martínez, C.; Álvarez, R.; Aurrecoechea, J. M. *Org. Lett.* **2009**, *11*, 1083-1086 (n) Álvarez, R.; Martínez, C.; Madich, Y.; Denis, J. G.; Aurrecoechea, J. M.; de Lera, A. R. *Chem. Eur. J.* **2010**, *16*, 12746-12753 (o) Malona, J. A.; Cariou, K.; Spencer III, W. T.; Frontier, A. J. *J. Org. Chem.* **2012**, *77*, 1891-1908 (p) Kusakabe, T.; Sekiyama, E.; Ishino, Y.; Motodate, S.; Kato, S.; Mochida, T.; Kato, K. *Synthesis* **2012**, *44*, 1825-1832

⁴² (a) Castro, C. E.; Gaughan, E. J.; Owsley, D. C. *J. Org. Chem.* **1966**, *31*, 4071-4076 (b) Kabalka, G. W.; Wang, L.; Pagni, R. M. *Tetrahedron Lett.* **2001**, *42*, 6049-6051 (c) Hiroya, K.; Itoha, S.; Sakamoto, T. *Tetrahedron* **2005**, *61*, 10958-10964 (d) Kabalka, G. W.; Zhou, L.-L.; Wang, L.; Pagni, R. M. *Tetrahedron* **2006**, *62*, 857-867 (e) Sakai, N.; Uchida, N.; Konakahara, T. *Tetrahedron Lett.* **2008**, *49*, 3437-3440 (f) Hirano, K.; Satoh, T.; Miura, M. *Org. Lett.* **2011**, *13*, 2395-2397 (g) Hachiya, H.; Hirano, K.; Satoh, T.; Miura, M. *Org. Lett.* **2011**, *13*, 3076-3079 (h) Matsuda, N.; Hirano, K.; Satoh, T.; Miura, M. *J. Org. Chem.* **2012**, *77*, 617-625 (i) Matsuda, N.; Hirano, K.; Satoh, T.; Miura, M. *Synthesis* **2012**, *44*, 1792-1797 (j) Xiao, Y.; Donga, X.; Zhou, L. *Org. Biomol. Chem.* **2013**, *11*, 1490-1497

⁴³ (a) Arcadi, A.; Marinelli, F. *Synthesis* **1986**, 749-751 (b) Kondo, Y.; Sakamoto, T.; Yamanaka, H. *Heterocycles* **1989**, *29*, 1013-1016 (c) Villemin, D.; Goussu, D. *Heterocycles* **1989**, *29*, 1255-1261 (d) Kundu, N. G.; Pal, M.; Mahanty, J. S.; Dasgupta, S. K. *J. Chem. Soc., Chem. Commun.* **1992**, 41-42 (e) Torii, S.; Xu, L. H.; Okumoto, H. *Synlett* **1992**, 515-516 (f) Kondo, Y.; Shiga, F.; Murata, N.; Sakamoto, T.; Yamanaka, H. *Tetrahedron* **1994**, *50*, 11803-11812 (g) Fancelli, D.; Fagnola, M. C.; Severino, D.; Bedeschi, A. *Tetrahedron Lett.* **1997**, *38*, 2311-2314 (h) Lütjens, H.; Scammells, P. J. *Synlett* **1999**, 1079-1081 (i) Kabalka, G. W.; Wang, L.; Pagni, R. M. *Tetrahedron* **2001**, *57*, 8017-8028 (j) Sanz, R.; Castroviejo, M. P.; Fernández, Y.; Fañanás, F. J. *J. Org. Chem.* **2005**, *70*, 6548-6551 (k) Liang, Y.; Tang, S.; Zhang, X.-D.; Mao, L.-Q.; Xie, Y.-X.; Li, J.-H. *Org. Lett.* **2006**, *8*, 3017-3020 (l) Sun, Y.-Y.; Liao, J.-H.; Fang, J.-M.; Chou, P.-T.; Shen, C.-H.; Hsu, C.-W.; Chen, L.-C. *Org. Lett.* **2006**, *8*, 3713-3716 (m) Bernini, R.; Cacchi, S.; De Salve, I.; Fabrizi, G. *Synthesis* **2007**, 873-882 (n) Liang, Y.; Tao, L.-M.; Zhang, Y.-H.; Li, J.-H. *Synthesis* **2008**, 3988-3994 (o) Grigg, R.; Sridharan, V.; Sykes, D. A. *Tetrahedron* **2008**, *64*, 8952-8962 (p) Berliner, M. A.; Cordi, E. M.;

the transition metal catalysis powerful tool, in many cases one-pot tandem procedures were reported either combining the 2-alkynylphenol preparation (from 2-iodophenols via Sonogashira couplings for example) and the heterocyclization, or the heterocyclization and the introduction of another substituent in the benzo[*b*]furan (through a Heck or a carbonylation reaction, for example) (Scheme 1.3).



Scheme 1.3. Examples of Pd and/or Cu-catalyzed benzo[*b*]furan preparation methods based on the formation of O–C₂ bond starting from, or having as intermediate, 2-alkynyl phenols of type **11**.

In addition to palladium and copper, many other transition metals proved successful at performing the cyclization step. These include: platinum⁴⁴, silver⁴⁵, gold⁴⁶, ruthenium⁴⁷,

Dunetz, J. R.; Price, K. E. *Org. Process. Res. Rev.* **2010**, *14*, 180-187 (q) Tréguier, B.; Rasolofonjatovo, E.; Hamze, A.; Provot, O.; Wdzieczak-Bakala, J.; Dubois, J.; Brion, J.-D.; Alami, M. *Eur. J. Org. Chem.* **2011**, 4868-4876 (r) Fischer, J.; Savage, G. P.; Coster, M. J. *Org. Lett.* **2011**, *13*, 3376-3379

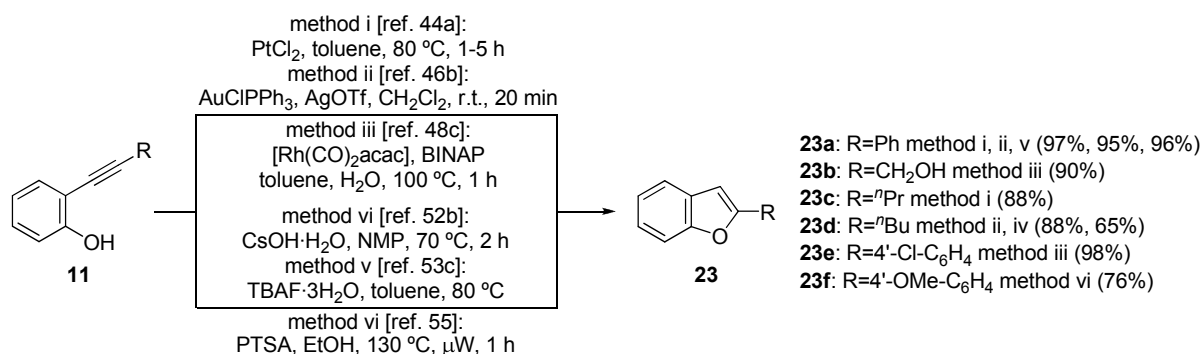
⁴⁴ (a) Fürstner, A.; Davies, P. W. *J. Am. Chem. Soc.* **2005**, *127*, 15024-15025 (b) Li, Y.; Liu, J. H.-C.; Witham, C. A.; Huang, W.; Marcus, M. A.; Fakra, S. C.; Alayoglu, P.; Zhu, Z.; Thompson, C. M.; Arjun, A.; Lee, K.; Gross, E.; Toste, F. D.; Somorjai, G. A. *J. Am. Chem. Soc.* **2011**, *133*, 13527-13533 (c) Zatochnaya, O. V.; Gevorgyan, V. *Org. Lett.* **2013**, *15*, 2562-2565

⁴⁵ Ye, Y.; Fan, R. *Chem. Commun.* **2011**, *47*, 5626-5628

⁴⁶ (a) Belting, V.; Krause, N. *Org. Lett.* **2006**, *8*, 4489-4492 (b) Zhang, Y.; Xin, Z.-J.; Xue, J.-J.; Li, Y. *Chin. J. Chem.* **2008**, *26*, 1461-1464 (c) Hashmi, A. S. K.; Ramamurthi, T. D.; Rominger, F. *Adv. Synth. Catal.* **2010**, *352*, 971-975 (d) Auzias, M. G.; Neuburger, M.; Wegner, H. A. *Synlett* **2010**, 2443-2448

⁴⁷ (a) Varela-Fernández, A.; González-Rodríguez, C.; Varela, J. A.; Castedo, L.; Saá, C. *Org. Lett.* **2009**, *11*, 5350-5353 (b) Nair, R. N.; Lee, P. J.; Rheingold, A. L.; Grotjahn, D. B. *Chem. Eur. J.* **2010**, *16*, 7992-7995 (c) Nair, R. N.; Lee, P. J.; Grotjahn, D. B. *Top Catal.* **2010**, *53*, 1045-1047

rhodium⁴⁸, iridium⁴⁹, zinc⁵⁰, and mercury⁵¹ (Scheme 1.4). Moreover, transition metal-free procedures were described. In the absence of a transition metal catalyst some of the reagents reported to promote the heterocyclization are: sodium, potassium and cesium salts (e. g. cesium hydroxide, sodium hydroxide, potassium *tert*-butoxide and potassium carbonate)⁵², tetra-*n*-butylammonium fluoride⁵³, boron trichloride⁵⁴ and *para*-toluenesulfonic acid⁵⁵ (Scheme 1.4).



Scheme 1.4. Examples of benzo[*b*]furan preparation methods based on the formation of O–C₂ bond starting from 2-alkynyl phenols of type **11** promoted by transition metals different from Pd and Cu and transition metal-free procedures.

In the case of vinyl phenols, *gem*-dihaloolefins **12** proved excellent starting materials to yield the corresponding 2-halobenzo[*b*]furans **31** via a base-promoted intramolecular cyclization (elimination-intramolecular addition process). Bromine is the most common halogen in these starting materials. Some of the bases employed in this transformation are butyllithium⁵⁶, sodium hydride⁵⁷ and tetra-*n*-butylammonium fluoride⁵⁸. Transition metals

⁴⁸ (a) Trost, B. M.; McClory, A. *Angew. Chem. Int. Ed.* **2007**, *46*, 2074-2077 (b) Isono, N.; Lautens, M. *Org. Lett.* **2009**, *11*, 1329-1331 (c) Boyer, A.; Isono, N.; Lackner, S.; Lautens, M. *Tetrahedron* **2010**, *66*, 6468-6482

⁴⁹ Li, X.; Chianese, A. R.; Vogel, T.; Crabtree, R. H. *Org. Lett.* **2005**, *7*, 5437-5440

⁵⁰ (a) Nakamura, M.; Ilies, L.; Otsubo, S.; Nakamura, E. *Angew. Chem. Int. Ed.* **2006**, *8*, 2803-2805 (b) Nakamura, M.; Ilies, L.; Otsubo, S.; Nakamura, E. *Org. Lett.* **2006**, *45*, 944-947

⁵¹ Atta, A. K.; Kim, S.-B.; Heo, J.; Cho, D.-G. *Org. Lett.* **2013**, *15*, 1072-1075

⁵² (a) Dai, W.-M.; Lai, K. W. *Tetrahedron Lett.* **2002**, *43*, 9377-9380 (b) Koradin, C.; Dohle, W.; Rodriguez, A. L.; Schmid, B.; Knochel, P. *Tetrahedron* **2003**, *59*, 1571-1587 (c) Anderson, S.; Taylor, P. N.; Verschoor, G. L. B. *Chem. Eur. J.* **2004**, *10*, 518-527 (d) Zhou, H.; Niu, J.-J.; Xu, J.-W.; Hu, S.-J. *Synth. Commun.* **2009**, *39*, 716-732 (e) Inamoto, K.; Asano, N.; Nakamura, Y.; Yonemoto, M.; Kondo, Y. *Org. Lett.* **2012**, *14*, 2622-2625 (f) Siddiqui, I. R.; Waseem, M. A.; Shamim, S.; Shireen; Srivastava, Arjita; Srivastava, Anjali *Tetrahedron Lett.* **2013**, *54*, 4154-4158

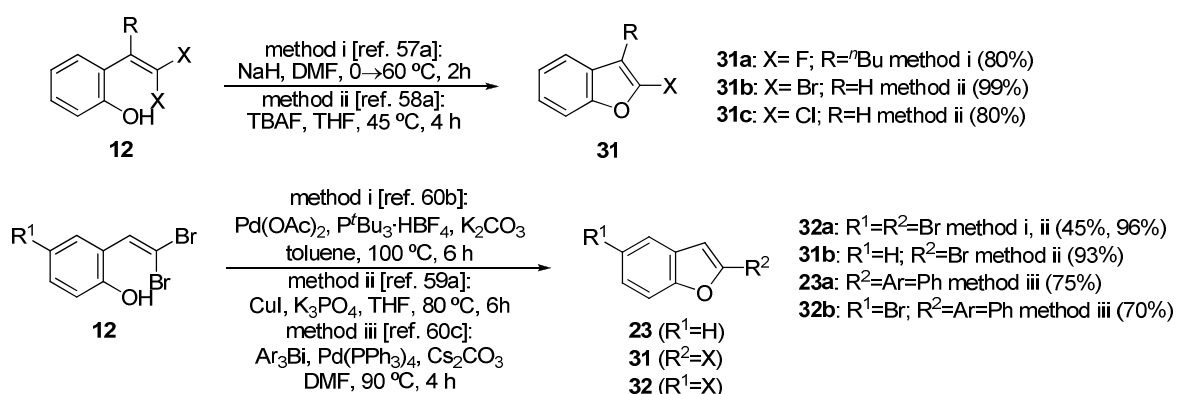
⁵³ (a) Hiroya, K.; Suzuki, N.; Yasuhara, A.; Egawa, Y.; Kasano, A.; Sakamoto, T. *Perkin 1* **2000**, 4339-4346 (b) Fiandanese, V.; Bottalico, D.; Marchese, G.; Punzi, A. *Tetrahedron* **2007**, *64*, 53-60 (c) Csékei, M.; Novák, Z.; Kotschy, A. *Tetrahedron* **2008**, *64*, 8992-8996 (d) Gunawan, C.; Rizzacasa, M. A. *Org. Lett.* **2010**, *12*, 1388-1391 (e) Boonsri, S.; Gunawan, C.; Krenske, E. H.; Rizzacasa, M. A. *Org. Biomol. Chem.* **2012**, *10*, 6010-6021

⁵⁴ Colobert, F.; Castanet, A.-S.; Abillard, O. *Eur. J. Org. Chem.* **2005**, 3334-3341

⁵⁵ Jacobert, M.; Hamze, A.; Provot, O.; Peyrat, J.-F.; Brion, J.-D.; Alami, M. *Tetrahedron Lett.* **2009**, *50*, 3588-3592

⁵⁶ Topolski, M. *J. Org. Chem.* **1995**, *60*, 5588-5594

such as copper (intramolecular Ullmann reaction)⁵⁹, palladium⁶⁰ or a combination of both⁶¹ were also reported to successfully catalyze these intramolecular cyclizations. Moreover, the halogen in position 2 of the resulting benzo[*b*]furan was in many cases further derivatized via transition metal-catalyzed C–C bond forming coupling reactions, even in one-pot reactions. The catalyst for the second step can be the one already employed for the cyclization or can be sequentially added, if the cyclization was a base-promoted transition metal-free process (Scheme 1.5).



Scheme 1.5. Examples of benzo[*b*]furan preparation methods based on the formation of O–C₂ bond starting from *gem*-halogenated vinyl phenols **12**.

When the geminal position of the vinyl phenol is not halogenated (**13**), several oxidants were employed to mediate the cyclization. These include copper halides⁶², molecular iodine⁶³, hypervalent iodine reagents (such as diacetoxyiodobenzene)⁶⁴, DDQ⁶⁵ and meta-

⁵⁷ (a) Ichikawa, J.; Wada, Y.; Okauchi, T.; Minami, T. *Chem. Commun.* **1997**, 1537-1538 (b) Ichikawa, J.; Wada, Y.; Fujiwara, M.; Sakoda, K. *Synthesis* **2002**, 1917-1936

⁵⁸ (a) Chen, W.; Zhang, Y.; Zhang, L.; Wang, M.; Wang, L. *Chem. Commun.* **2011**, 47, 1476-1478 (b) Liu, J.; Chen, W.; Ji, Y.; Wang, L. *Adv. Synth. Catal.* **2012**, 354, 1585-1592 (c) Chen, W.; Li, P.; Miao, T.; Meng, L.-G.; Wang, L. *Org. Biomol. Chem.* **2013**, 11, 420-424

⁵⁹ (a) Newman, S. G.; Aureggi, V.; Bryan, C. S.; Lautens, M. *Chem. Commun.* **2009**, 5236-5238 (b) Qin, X.; Cong, X.; Zhao, D.; You, J.; Lan, J. *Chem. Commun.* **2011**, 47, 5611-5613 (c) Zhou, W.; Chena, W.; Wang, L. *Org. Biomol. Chem.* **2012**, 10, 4172-4178 (d) Ye, S.; Liu, G.; Pu, S.; Wu, J. *Org. Lett.* **2012**, 14, 70-73 (e) Ji, Y.; Li, P.; Zhang, X.; Wang, L. *Org. Biomol. Chem.* **2013**, 11, 4095-4101 (f) Liu, J.; Zhang, N.; Yue, Y.; Wang, D.; Zhang, Y.; Zhanga, X.; Zhuo, K. *R. Soc. Chem. Adv.* **2013**, 3, 3865-3868 (g) Liu, J.; Chen, W.; Wang, L. *R. Soc. Chem. Adv.* **2013**, 3, 4723-4730

⁶⁰ (a) Thielges, S.; Meddah, E.; Bisseret, P.; Eustache, J. *Tetrahedron Lett.* **2004**, 45, 907-910 (b) Newman, S. G.; Lautens, M. *J. Am. Chem. Soc.* **2010**, 132, 11416-11417 (c) Rao, M. L. N.; Jadhav, D. N.; Dasgupta, P. *Eur. J. Org. Chem.* **2013**, 781-788

⁶¹ (a) Nagamochi, M.; Fang, Y.-Q.; Lautens, M. *Org. Lett.* **2007**, 9, 2955-2958 (b) Chen, W.; Wang, M.; Li, P.; Wang, L. *Tetrahedron Lett.* **2011**, 67, 5913-5919

⁶² (a) Bahatt, S.; Roy, K.; Nayak, S. K. *Synth. Commun.* **2010**, 40, 2736-2746 (b) Li, H.-S.; Liu, G. *J. Org. Chem.* **2014**, 79, 509-516

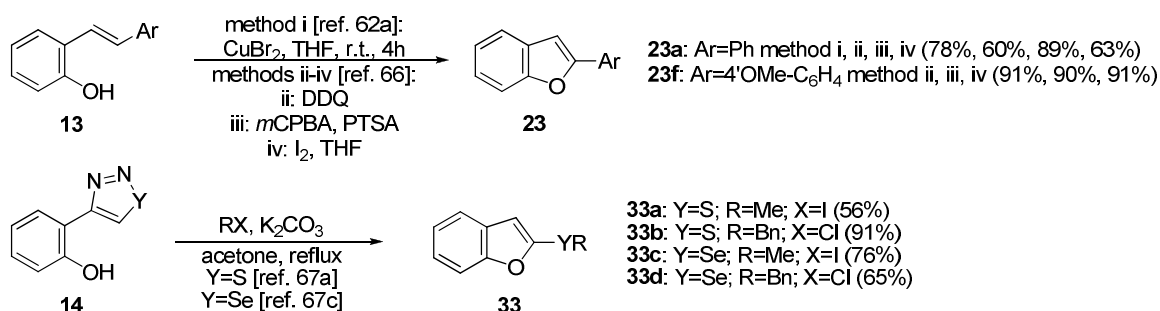
⁶³ (a) Pan, C.; Yu, J.; Zhou, Y.; Wang, Z.; Zhou, M.-M. *Synlett* **2006**, 1657-1662 (b) Duan, X.-F.; Shen, G.; Zhang, Z.-B. *Synthesis* **2010**, 1181-1187 (c) Duan, X.-F.; Shen, G.; Zhang, Z.-B. *Synthesis* **2010**, 2547-2552 (d) Liu, J.; Jiang, F.; Jiang, X.; Zhang, W.; Liu, J.; Liu, W.; Fu, L. *Eur. J. Med. Chem.* **2012**, 54, 879-886

⁶⁴ Singh, F. V.; Wirth, T. *Synthesis* **2012**, 44, 1171-1177

⁶⁵ Cardillo, G.; Criccio, R.; Merlini, L. *Tetrahedron* **1971**, 27, 1875-1883

chloroperbenzoic acid / *para*-toluenesulfonic acid system⁶⁶ for example (Scheme 1.6 above).

Reactions in which the starting vinyl group is included in a seleno- or thia- diazole system [4-(*ortho*-hydroxyaryl)-1,2,3-selena- or -thia- diazoles **14**] were also reported. These proceeded in the presence of a base (typically potassium carbonate) and an alkyl or benzyl halide to afford the corresponding benzo[*b*]furan-2-selenoates or thiolates **33**⁶⁷ (Scheme 1.6 below).



Scheme 1.6. Examples of benzo[*b*]furan preparation methods based on the formation of O–C₂ bond starting from non-*gem*-halogenated vinyl phenols **13** and **14**.

Starting from 2-allyl phenols **15** both acid-mediated cyclizations⁶⁸ and palladium-catalyzed oxidative cyclizations⁶⁹ were reported. When the oxidant employed in the second approach is molecular oxygen, the sequence is referred to as Wacker-type oxidation / intramolecular aldol cyclization⁷⁰ (Scheme 1.7).

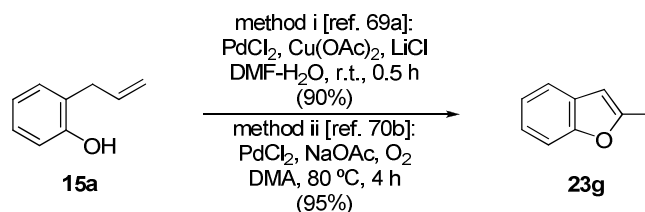
⁶⁶ Duan, X.-F.; Zeng, J.; Zhang, Z.-B.; Zi, G.-F. *J. Org. Chem.* **2007**, *72*, 10283-10286

⁶⁷ (a) D'hooge, B.; Smeets, S.; Toppet, S.; Dehaen, W. *Chem. Commun.* **1997**, 1753-1754 (b) Petrov, M. L.; Abramov, M. A.; Dehaen, W.; Toppet, S. *Tetrahedron Lett.* **1999**, *40*, 3903-3904 (c) Abramov, M. A.; Dehaen, W.; D'hooge, B.; Petrov, M. L.; Smeets, S.; Toppet, S.; Voets, M. *Tetrahedron* **2000**, *56*, 3933-3940 (d) Petrov, M. L.; Abramov, M. A.; Abramova, I. P.; Dehaen, W.; Lyakhovetskii, Y. I. *Russ. J. Org. Chem.* **2001**, *37*, 1643-1648 (e) Petrov, M. L.; Dehaen, W.; Abramov, M. A.; Abramova, I. P.; Androsov, D. A. *Russ. J. Org. Chem.* **2002**, *38*, 1510-1518 (f) Petrov, M. L.; Abramov, M. A.; Abramova, I. P.; Dehaen, W. *Russ. J. Org. Chem.* **2002**, *39*, 261-268 (g) Petrov, M. L. D.; Androsov, A.; Abramov, M. A.; Abramova, I. P.; Dehaen, W.; Lyakhovetskii, Y. I. *Russ. J. Org. Chem.* **2006**, *42*, 1521-1527 (h) Petrov, M. L.; Teplyakov, F. S.; Androsov, D. A.; Yekhlief, M. *Russ. J. Org. Chem.* **2009**, *45*, 1727-1729 (i) Petrov, M. L.; Iekhlief, M.; Teplyakov, F. S.; Androsov, D. A. *Russ. J. Org. Chem.* **2012**, *48*, 728-735

⁶⁸ (a) Anderson, W. K.; LaVoie, E. J.; Bottaro, J. C. *J. Chem. Soc., Perkin Trans 1* **1976**, 1-4 (b) Abaev, V. T.; Gutnov, A. V.; Butin, A. V. *Chem. Heterocycl. Compd.* **1998**, *34*, 529-532 (c) Gutnov, A. V.; Butin, A. V.; Abaev, V. T.; Krapivin, G. D.; Zavodnik, V. E. *Molecules* **1999**, *4*, 204-218

⁶⁹ (a) Roshchin, A. I.; Kel'chevski, S. M.; Bumagin, N. A. *J. Organomet. Chem.* **1998**, *560*, 163-167 (b) Durand, T.; Diouf, O.; Lemeune, S.; Marcoux, J.-F.; Henryon, V.; Monbrun, J.; Delamare, M. *Patent* **2008**, WO200813956 A1

⁷⁰ (a) Meulemans, T. M.; Kiers, N.H.; Feringa, B. L.; van Leeuwen, P. W. N. M. *Tetrahedron Lett.* **1994**, *35*, 455-458 (b) Mitsudome, T.; Umetani, T.; Nosaka, N.; Mori, K.; Mizugaki, T.; Ebitani, K.; Kaneda, K. *Angew. Chem. Int. Ed.* **2006**, *45*, 481-485 (c) Chang, M.-Y.; Chan, C.-K.; Lin, S.-Y. *Tetrahedron* **2013**, *69*, 1532-1538 (d) Chang, M.-Y.; Lin, S.-Y.; Chan, C.-K. *Tetrahedron* **2013**, *69*, 2933-2940



Scheme 1.7. Examples of benzo[*b*]furan preparation methods based on the formation of O–C₂ bond starting from 2-allyl phenols of type **15**.

2-propargyl phenols **16** can be converted into the corresponding 2-substituted benzo[*b*]furans via base-mediated cyclizations. The bases reported to successfully perform in these reactions include, for example, potassium hydroxide⁷¹ and potassium *tert*-butoxide⁷² (Scheme 1.8 above). The transformation worked with high yields when the base was combined with a phase-transfer-catalyst⁷³.

Besides, 2-propargyl phenols **16** can be prepared either from phenols and benzylic propargylic amine derivatives⁷⁴ or from phenols and propargylic alcohols⁷⁵ via Lewis acid-promoted Friedel-Crafts alkylation. Once formed, these compounds cyclized into the corresponding benzo[*b*]furans in one-pot fashion, under the same reaction conditions or by sequentially adding a base (Scheme 1.8 middle).

Another approach consists of carrying out a metal-catalyzed cycloisomerization of the 2-propargyl phenols **17** to afford 2-methylene-2,3-dihydrobenzofuran-3-ols **36**. Subsequent one-pot acid-promoted allylic isomerization (or nucleophilic substitution) of these compounds furnished benzo[*b*]furans⁷⁶ (Scheme 1.8 below).

⁷¹ Salom-Roig, X. J.; Reanud, P. *Synthesis* **2006**, 3419-3424

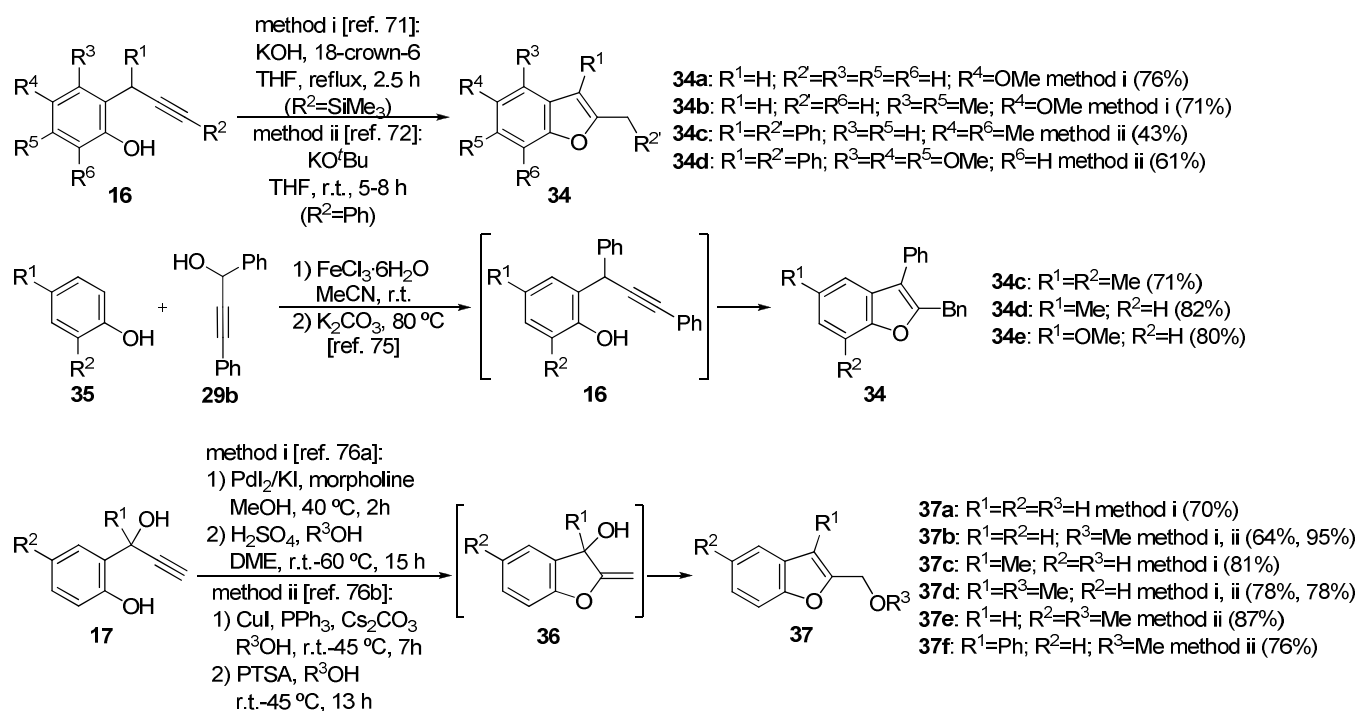
⁷² Liu, Z.; Liu, L.; Shafiq, Z.; Wu, Y.-C.; Wang, D.; Chen, Y.-J. *Synthesis* **2007**, 1961-1969

⁷³ Hu, J.; Liu, L.; Wang, X.; Hu, Y.; Yang, S.; Liang, Y. *Green Chem.* **2011**, *1*, 165-169

⁷⁴ Liu, C.-R.; Li, M.-B.; Yang, C.-F.; Tian, S.-K. *Chem. Eur. J.* **2009**, *15*, 793-797

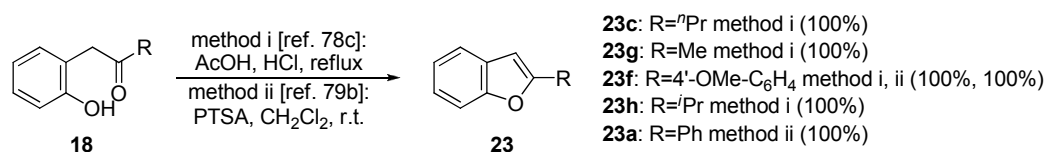
⁷⁵ Yuan, F.-Q.; Han, F.-S. *Adv. Synth. Catal.* **2013**, *355*, 537-547

⁷⁶ (a) Gabriele, B.; Mancuso, R.; Salerno, G. *J. Org. Chem.* **2008**, *73*, 7336-7341 (b) Li, X.; Xue, J.; Chen, R.; Li, Y. *Synlett* **2012**, *23*, 1043-1046 (c) Mancuso, R.; Gabriele, B. *Molecules* **2013**, *18*, 10901-10911



Scheme 1.8. Examples of benzo[*b*]furan preparation methods based on the formation of O–C₂ bond starting from 2-propargyl phenols of type **16** and **17**.

The transformation of 1-(2-hydroxyphenyl)alkan-2-ones **18** into benzo[*b*]furans can be carried out by means of an acid-promoted cyclization. Among the acids reported to successfully promote this reaction we can find phosphoric acid⁷⁷, hydrochloric acid⁷⁸, *para*-toluenesulfonic acid⁷⁹, trifluoroacetic acid⁸⁰ or acidic resin amberlyst-15⁸¹ (Scheme 1.9). Besides, the one-pot synthesis of 2-aryl benzo[*b*]furans starting from *ortho*-bromophenols via a Pd-catalyzed enolate arylation followed by the aforementioned acid-mediated cyclization was also described⁸².



Scheme 1.9. Examples of benzo[*b*]furan preparation methods based on the formation of O–C₂ bond starting from 1-(2-hydroxyphenyl)alkan-2-ones **18**.

⁷⁷ Aneja, R.; Mukerjee, S. K.; Seshadri, T. R. *Tetrahedron* **1958**, *2*, 203-210

⁷⁸ (a) Adams, R.; Whitaker, L. *J. Am. Chem. Soc.* **1956**, *78*, 658-663 (b) Koenigkramer, R. E.; Zimmer, H. *J. Org. Chem.* **1980**, *45*, 3994-3998 (c) Ledoussal, B.; Gorgues, A.; Le Coq, A. *Tetrahedron* **1987**, *43*, 5841-5852

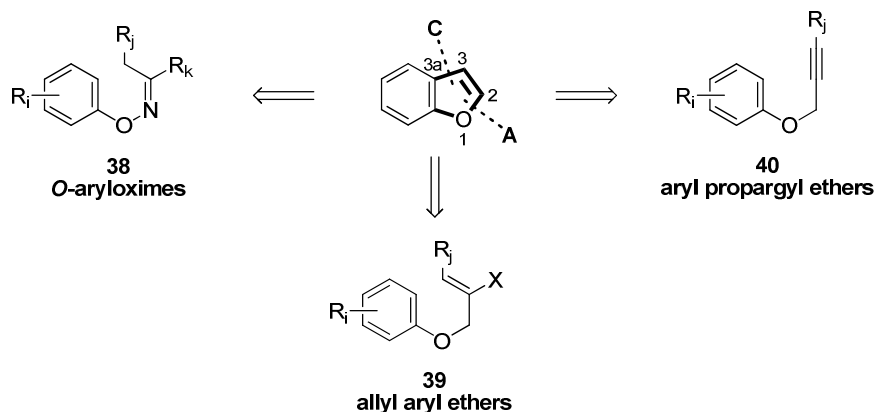
⁷⁹ (a) Waters, S. P.; Fennie, M. W.; Kozlowski, M. C. *Org. Lett.* **2006**, *8*, 3243-3246 (b) Chittimalla, S. K.; Chang, T.-C.; Liu, T.-C.; Hsieh, H.-P.; Liao, C.-C. *Tetrahedron* **2008**, *64*, 2586-2595

⁸⁰ Murphy, S. K.; Petrone, D. A.; Coulter, M. M.; Dong, V. M. *Org. Lett.* **2011**, *13*, 6216-6219

⁸¹ Mattson, A. E.; Scheidt, K. A. *J. Am. Chem. Soc.* **2007**, *129*, 4508-4509

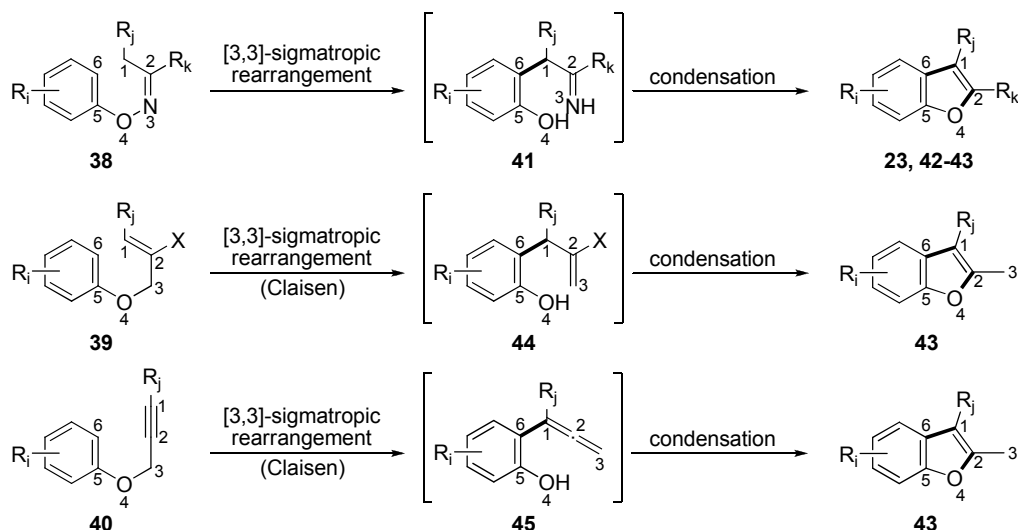
⁸² Eidamshaus, C.; Burch, J. D. *Org. Lett.* **2008**, *10*, 4211-4214

Finally, the procedures based on the sequential formation of C_3-C_{3a} and $O-C_2$ bonds in a single preparative step can also be included in this section. In addition to the countless examples in which the preparation of the 2-alkynyl phenols and their cyclization into the corresponding benzo[*b*]furan is performed in the same step, the typical starting materials of this approach are *O*-aryloximes (**38**), allyl aryl ethers (**39**) or aryl propargyl ethers (**40**) (Scheme 1.10).



Scheme 1.10. Retrosynthetic approaches having a benzenoid scaffold as starting material, based on the sequential formation of C_3-C_{3a} and $O-C_2$ bonds.

In these cases, the reactions proceed through a [3,3]-sigmatropic rearrangement, the so called Claisen rearrangement in the case of ethers, followed by a condensation leading to the benzo[*b*]furan ring. On the whole, during the process a $C-C$ bond (C_3-C_{3a} in the resulting benzo[*b*]furan) is formed, the bond between the oxygen and the non-aryl moiety of the starting material is cleaved and a new $O-C$ bond ($O-C_2$ in the resulting benzo[*b*]furan) is formed. The carbon atom involved in this last bond is different from the one initially bound to the oxygen. As a result, the obtained benzo[*b*]furan bears, at least, a substituent in position 2. In the case of allyl aryl and aryl propargyl ethers (**39** and **40**, respectively), this is typically a methyl or a methylene bridged moiety (Scheme 1.11).



Scheme 1.11. Sequential [3,3]-sigmatropic rearrangement and condensation steps of *O*-aryloximes **38**, allyl aryl ethers **39** and aryl propargyl ethers **40** leading to benzo[*b*]furan structures.

When choosing *O*-aryloximes **38** as starting materials, the transformation is analogous to the well-known Fisher 1*H*-indole synthesis. The reaction was reported both acid-catalyzed, (with hydrochloric acid⁸³, sulfuric acid⁸⁴, or formic acid / phosphoric acid mixture⁸⁵) or with borontrifluoride etherate in acetic acid⁸⁶ and under acylation conditions, using trifluoroacetyl triflate⁸⁷ (Scheme 1.12 above).

In the case of allyl aryl ethers **39**, a common reaction sequence is the Claisen rearrangement followed by an oxidative cyclization. This was described either in acid or palladium catalyzed processes^{68a,70a,88} (Scheme 1.12 middle).

The thermal rearrangement of aryl propargyl ethers **40** containing electron withdrawing groups was reported to afford 2-methyl benzo[*b*]furans (whilst aryl propargyl ethers containing electron releasing groups furnish 2*H*-benzopyrans or 2*H*-chromenes). The reaction required high temperatures and was described either in the presence of a base

⁸³ (a) Mooradian, A.; Dupont, P. E. *Tetrahedron Lett.* **1967**, 8, 859-861 (b) Kaminsky, D.; Shavel Jr., J.; Meltzer, R. I. *Tetrahedron Lett.* **1967**, 8, 2867-2870 (c) Dutov, M. D.; Vatsadze, I. A.; Vorob'ev, S. S.; Shevelev, S. A. *Mendeleev Commun.* **2005**, 202-204

⁸⁴ (a) Alemagna, A.; Baldoli, C.; Del Buttero, P.; Licandro, E.; Maiorana, S. *J. Chem. Soc., Chem Commun.* **1985**, 417-418 (b) Alemagna, A.; Baldoli, C.; Del Buttero, P.; Licandro, E.; Maiorana, S. *Synthesis* **1987**, 192-196

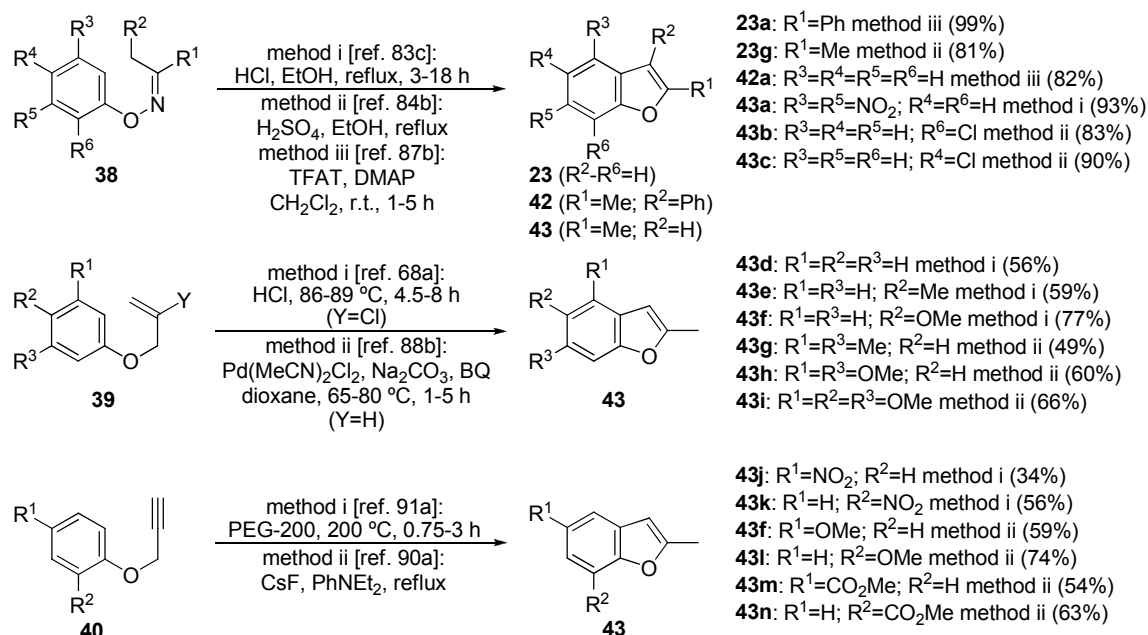
⁸⁵ Castellino, A. J.; Rapoport, H. *J. Org. Chem.* **1984**, 49, 4399-4404

⁸⁶ Sheradsky, T. *Tetrahedron Lett.* **1966**, 7, 5225-5227

⁸⁷ (a) Miyata, O.; Takeda, N.; Morikami, Y.; Naito, T. *Org. Biomol. Chem.* **2003**, 1, 254-256 (b) Miyata, O.; Takeda, N.; Naito, T. *Org. Lett.* **2004**, 6, 1761-1763 (c) Takeda, N.; Miyata, O.; Naito, T. *Eur. J. Org. Chem.* **2007**, 1491-1509

⁸⁸ (a) Sekizaki, H.; Itoh, K.; Toyota, E.; Tanizawa, K. *Heterocycles* **2003**, 59, 237-243 (b) Youn, S. W.; Eom, J. I. *Org. Lett.* **2005**, 7, 3355-3358

(such as potassium carbonate⁸⁹ or cesium fluoride⁹⁰) or simply in polyethyleneglycol⁹¹ (Scheme 1.12 below).



Scheme 1.12. Examples of benzo[*b*]furan preparation methods based on the sequential formation of C₃–C_{3a} and O–C₂ bonds, starting from *O*-aryl oximes **38**, allyl aryl ethers **39** and aryl propargyl ethers **40**.

In a similar vein, one step synthesis of 2-methyl-3-(thiomethyl)benzofuran derivatives **47** by Pummerer-type reaction (alkyl sulfoxide to α -acyloxythioether rearrangement) of β -ketosulfoxides (such as **46a**) with phenols **35** were reported. The transformation proceeds via the intermolecular nucleophilic attack of an aromatic ring on the 1-acyl-1-thiocarbocation derived from the β -ketosulfoxide in the presence of *para*-toluenesulfonic acid and successive dehydrocyclization⁹². Analogous products were obtained starting from phenols **35** and α -chlorosulfides (such as **46b**) under Friedel-Crafts reaction conditions, employing for example zinc chloride⁹³ or tin chloride⁹⁴ as Lewis acids (Scheme 1.13 methods i and ii).

⁸⁹ Šarčević, N.; Zsindely, J.; Schmid, H. *Helv. Chim. Acta* **1973**, *56*, 1457-1476

⁹⁰ (a) Ishikawa, T.; Nagai, K.; Ohkubo, N.; Ishii, H. *Heterocycles* **1994**, *39*, 371-380 (b) Lingam, V. S. P. R.; Vinodkumar, R.; Mukkanti K.; Thomas, A.; Gopalan, B. *Tetrahedron Lett.* **2008**, *49*, 4260-4261

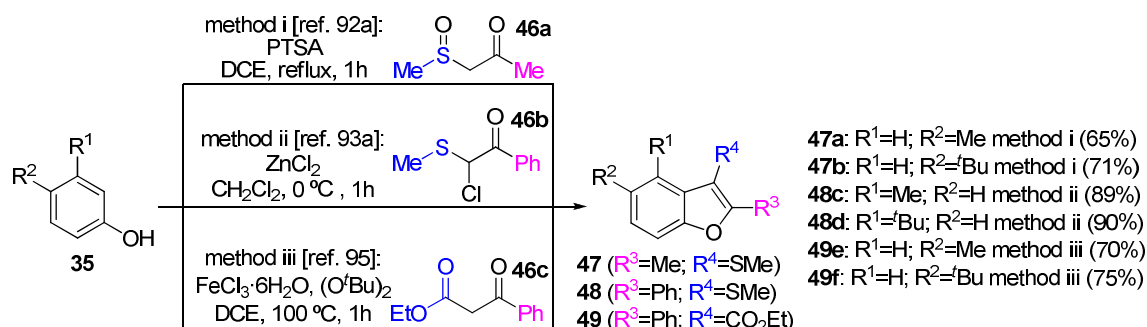
⁹¹ (a) Roa, U.; Balasubramanian, K. K. *Tetrahedron Lett.* **1983**, *24*, 5023-5024 (b) Durand, T.; Diouf, O.; Lemeune, S.; Marcoux, J.-F.; Henryon, V.; Monbrun, J.; Delamare, M. *Patent* **2008**, WO 2008152217 A2

⁹² (a) Choi, H.-D.; Seo, P.-J. *J. Korean. Chem. Soc.* **2001**, *45*, 274-276 (b) Kim, Y.-W.; Lee, S.-J.; Seo, P.-J.; Choi, H.-D.; Son, B.-W. *J. Korean. Chem. Soc.* **2001**, *45*, 377-381 (c) Chung, C.-L.; Han, C.-H.; Wang, H.-M.; Houc, R.-S.; Chena, L.-C. *J. Chin. Chem. Soc.* **2011**, *58*, 90-93 (d) Kobatake, T.; Fujino, D.; Yoshida, S.; Yorimitsu, H.; Oshima, K. *J. Am. Chem. Soc.* **2010**, *132*, 11838-11840

⁹³ (a) Choi, H.-D.; Seo, P.-J.; Son, B.-W. *J. Korean. Chem. Soc.* **1999**, *43*, 606-608 (b) Seo, P.-J.; Ha, M.-C.; Choi, H.-D.; Son, B.-W. *J. Korean. Chem. Soc.* **2000**, *44*, 391-394

⁹⁴ (a) Choi, H.-D.; Seo, P.-J.; Son, B.-W. *J. Korean. Chem. Soc.* **2001**, *45*, 500-504 (b) Seo, P.-J.; Choi, H.-D.; Son, B.-W. *J. Korean. Chem. Soc.* **2002**, *46*, 384-388

Besides these approaches, the iron-catalyzed oxidative Pechmann-type condensation can be included in this C₃–C_{3a} and O–C₂ bonds formation category. This procedure allows to prepare 2,3-disubstituted benzo[*b*]furans from phenols **35** and β -ketoesters (such as **46c**) taking advantage of the dichotomous behavior of the iron catalyst (FeCl₃ in the example), which acts as a transition metal catalyst in the oxidative coupling step and as a Lewis acid in the condensation step⁹⁵ (Scheme 1.13 method iii).

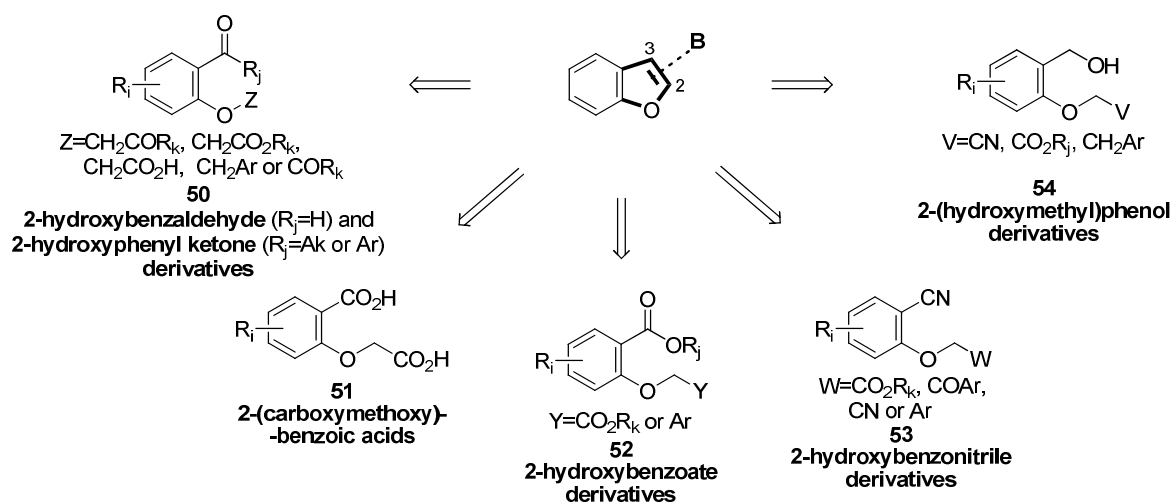


Scheme 1.13. Examples of benzo[*b*]furan preparation methods based on the sequential formation of C₃–C_{3a} and O–C₂ bonds, starting from phenols **35** and a β -ketosulfoxide **46a**, an α -chlorosulfide **46b** and a β -ketoester **46c**.

1.1.3.1.2. Methods based on the C₂–C₃ bond formation (B)

The retrosynthetic approaches having a benzenoid scaffold as starting material based on the C₂–C₃ bond discussed below are presented in Scheme 1.14. On looking at the starting material for the reactions based on this disconnection, they are mainly *ortho*-substituted phenyl methyl ether derivatives (typically coming from *ortho*-substituted phenols that have been subject to a Williamson etherification, being the attached moiety in most of the cases a methylene bridged electron withdrawing group). The *ortho* functionalities include: aldehydes (formyl) and ketones (**50**), acids (**51**), esters (**52**), nitriles (**53**) and hydroxymethyl derivatives (**54**).

⁹⁵ Guo, X.; Yu, R.; Li, H.; Li, Z. *J. Am. Chem. Soc.* **2009**, *131*, 17387-17393



Scheme 1.14. Retrosynthetic approaches having a benzenoid scaffold as starting material, based on the construction of the $\text{C}_2\text{--C}_3$ bond.

Bearing all this in mind, the transformations based on this disconnection are mainly base-mediated intramolecular cyclizations. The choice of the one or another of these precursors is made according to the substituents sought in position 2 and 3 of the benzo[*b*]furan to be formed. Most of these reactions are found as the key benzo[*b*]furan ring formation step in synthetic routes towards more complex (and often bioactive) compounds.

On looking at substituted 2-hydroxybenzaldehyde and 2-hydroxyphenyl ketone derivatives as starting materials, varied possibilities can be found in the group attached to the oxygen in *ortho* position (Z in scheme 1.14). In this vein, we could consider the compounds $50^{\text{i-v}}$ shown in figure 1.7.

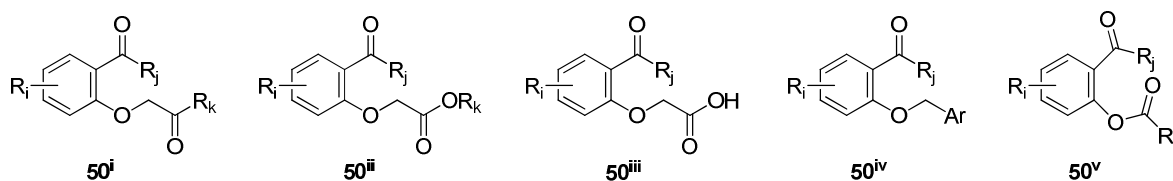
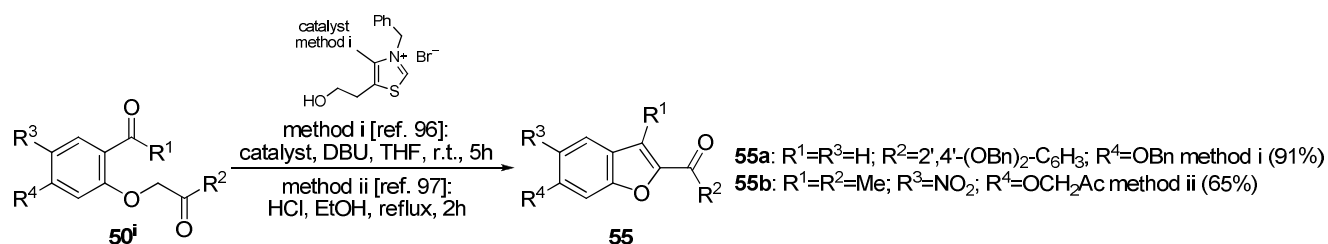


Figure 1.7. Different 2-hydroxybenzaldehyde and 2-hydroxyphenyl ketone derivatives $50^{\text{i-v}}$, depending on the attached Z substituent.

In the case of 2-(2-oxoalkoxy)aryl aldehydes or ketones 50^{i} as starting materials, examples of their transformation into benzofuran-2-yl ketones **55** via catalyzed⁹⁶ or acid-mediated intramolecular cyclizations⁹⁷ were described in literature (Scheme 1.15).

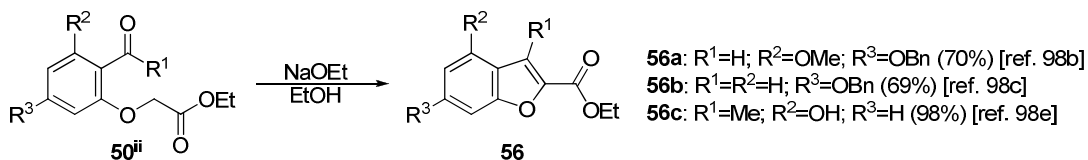
⁹⁶ Malik, N.; Erhardt, P. *Tetrahedron Lett.* **2013**, *54*, 4121-4124

⁹⁷ Hill, J.; Ramage, G. R. *J. Chem. Soc. (C)* **1967**, 783-784



Scheme 1.15. Examples of benzo[*b*]furan preparation methods based on the C₂–C₃ bond formation starting from benzaldehydes and phenyl ketones **50ⁱ**.

Alkyl 2-formylaryloxy or 2-(1-oxoalkylaryloxy) acetates **50ⁱⁱ** were reported to undergo base-mediated intramolecular cyclization to afford the corresponding 3-unsubstituted (in the case of aldehydes) or 3-substituted (in the case of ketones) benzo[*b*]furans with an ester group in position 2. The classic base employed to perform these cyclization was sodium (or potassium) ethoxide (or even methoxide and *tert*-butoxide)⁹⁸ (Scheme 1.16), though some others have also proven effective such as potassium⁹⁹ or cesium¹⁰⁰ carbonate and potassium hydroxide¹⁰¹. Particular phosphorus catalysts showed superiority over typically employed bases in certain reactions of synthesis of substituted ethyl benzofuran-2-carboxylates¹⁰².



Scheme 1.16. Examples of benzo[*b*]furan preparation methods based on the C₂–C₃ bond formation starting from benzaldehydes and phenyl ketones **50ⁱⁱ**.

2-Formylaryloxy or 2-(1-oxoalkylaryloxy) acetic acids **50ⁱⁱⁱ** were reported to undergo intramolecular decarboxylative cyclodehydration to afford the corresponding 3-unsubstituted (in the case of aldehydes) or 3-substituted (in the case of ketones) benzo[*b*]furans. The classic procedure to perform this reaction employs sodium acetate

⁹⁸ (a) Foster, R. T.; Robertson, A. *J. Chem. Soc.* **1939**, 921-925 (b) Foster, R. T.; Howell, W. N.; Robertson, A. *J. Chem. Soc.* **1939**, 930-933 (c) Foster, R. T.; Robertson, A.; Bushra, A. *J. Chem. Soc.* **1948**, 2254-2260 (d) Li, J.; Rush III, T. S.; Li, W.; DeVincentis, D.; Du, X.; Hu, Y.; Thomason, J. R.; Xiang, J. S.; Skotnicki, J. S.; Tam, S.; Cunningham, K. M.; Chockalingam, P. S.; Morris, E. A.; Levin, J. I. *Bioorg. Med. Chem. Lett.* **2005**, *15*, 4961-4966 (e) Bélanger, P. C.; Dufresne, C.; Lau, C. K.; Scheigetz, J. *Org. Prep. Proc. Int.* **1988**, *20*, 299-302 (f) Pawar, M. J.; Karale, B. K. *Synth. Commun.* **2010**, *40*, 3603-3608 (g) Deng, H.; Fang, Y. *ACS Med. Chem. Lett.* **2012**, *3*, 550-554

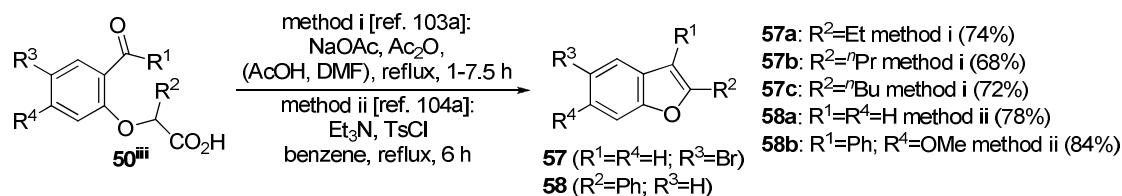
⁹⁹ Kowalewska, M.; Kwiecień, H.; Śmist, M.; Wrześniewska, A. *J. Chem.* **2013**, ID 813717, 7p

¹⁰⁰ Bazin, M.-A.; Boderio, L.; Tomasoni, C.; Rousseau, B.; Roussakis, C.; Marchand, P. *Eur. J. Med. Chem.* **2013**, *69*, 823-832

¹⁰¹ Suzuki, T.; Tanemura, K.; Horaguchi, T.; Shimizu, T.; Sakakibara, T. *J. Heterocycl. Chem.* **1992**, *29*, 423-429

¹⁰² D'Sa, B. A.; Kisanga, P.; Verkade, J. G. *Synlett* **2001**, 670-672

and acetic anhydride¹⁰³ (Scheme 1.17). Besides, compounds **50ⁱⁱⁱ** were reported to yield the same benzo[*b*]furans via intramolecular [2+2] cycloadditions of ketenes to carbonyl compounds¹⁰⁴.



Scheme 1.17. Examples of benzo[*b*]furan preparation methods based on the C₂–C₃ bond formation starting from benzaldehydes and phenyl ketones **50ⁱⁱⁱ**.

2-Alkoxyaryl aldehydes or ketones **50^{iv}** were reported to undergo base-mediated intramolecular cyclization to afford the corresponding 2-aryl 3-unsubstituted (in the case of aldehydes) or 2-aryl 3-substituted (in the case of ketones) benzo[*b*]furans. Among the bases employed to perform this cyclization we can find potassium carbonate¹⁰⁵, potassium hydroxide¹⁰⁶, potassium *tert*-butoxide¹⁰⁷, a metal (potassium or cesium) fluoride-alumina base system¹⁰⁸ or the hindered non-ionic base ^tBuN=P[N=P(NMe₂)₃]₃¹⁰⁹ (Scheme 1.18).

¹⁰³ (a) Kwiecień, K.; Szychowska, M. *Chem. Heterocycl. Compd.* **2006**, *42*, 1002-1009 (b) Ando, K.; Kawamura, Y.; Akai, Y.; Kunitomo, J.-i.; Yokomizo, T.; Yamashita, M.; Ohta, S.; Ohishid, T.; Ohishi, Y. *Org. Biomol. Chem.* **2008**, *6*, 296-307 (c) Johnson, P. C.; Robertson, A. *J. Chem. Soc.* **1950**, 2381-2389 (d) Montfort, B.; Laude, B.; Vebrel, J.; Cerutti, E. *Bull. Soc. Chim. Fr.* **1987**, 848-854 (e) Mylari, B. L.; Armento, S. J.; Beebe, D. A.; Conn, E. L.; Coutcher, J. B.; Dina, M. S.; O'Gorman, M. T.; Linhares, M. C.; Martin, W. H.; Oates, P. J.; Tess, D. A.; Withbroe, G. J.; Zembrowski, W. J. *J. Med. Chem.* **2005**, *48*, 6326-6339 (f) Beaulieu, P. L.; Gillard, J.; Bykowski, D.; Brochu, C.; Dansereau, N.; Duceppe, J.-S.; Haché, B.; Jakalian, A.; Lagacé, L.; LaPlante, S.; McKercher, G.; Moreau, E.; Perreault, S.; Stammers, T.; Thauvette, L.; Warrington, J.; Kukulj, G. *Bioorg. Med. Chem. Lett.* **2006**, *16*, 4987-4993 (g) Krueger, A. C.; Randolph, J. T.; DeGoey, D. A.; Donner, P. L.; Flentge, C. A.; Hutchinson, D. K.; Liu, D.; Motter, C. E.; Rockway, T. W.; Wagner, R.; Beno, D. W. A.; Koev, G.; Lim, H. B.; Beyer, J. M.; Mondal, R.; Liu, Y.; Kati, W. M.; Longenecker, K. L.; Molla, A.; Stewart, K. D.; Maring, C. J. *Bioorg. Med. Chem. Lett.* **2013**, *23*, 3487-3490

¹⁰⁴ (a) Brady, W. T.; Giang, Y. F.; Marchand, A. P.; Wu, A.-H. *Synthesis* **1987**, 395-396 (b) Brady, W. T.; Giang, Y. F.; Marchand, A. P.; Wu, A.-H. *J. Org. Chem.* **1987**, *52*, 3457-3461

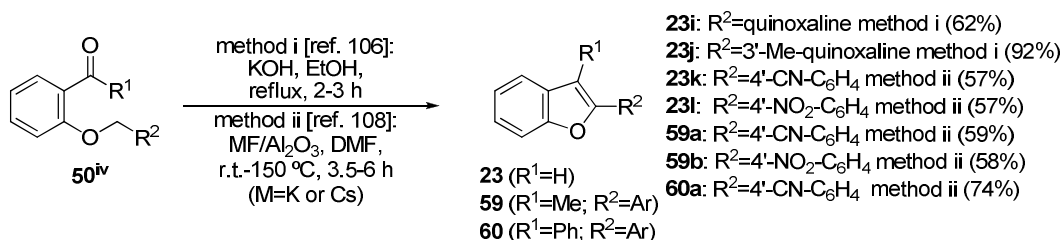
¹⁰⁵ (a) Guillaumel, J.; Boccara, N.; Demerseman, P.; Royer, R.; Bideau, J. P.; Cotrait, M.; Platzer, N. *J. Heterocycl. Chem.* **1990**, *27*, 605-614 (b) Ghate, M.; Manohar, D.; Kulkarni, V.; Shobha, R.; Kattimani, S. Y. *Eur. J. Med. Chem.* **2003**, *38*, 297-302

¹⁰⁶ Starke, I.; Sarodnick, G.; Ovcharenko, V. V.; Pihlaja, K.; Kleinpeter, E. *Tetrahedron* **2004**, *60*, 6063-6078

¹⁰⁷ Chen, W.; Deng, X.-Y.; Li, Y.; Yang, L.-J.; Wana, W.-C.; Wang, X.-Q.; Zhang, H.-B.; Yang, X.-D. *Bioorg. Med. Chem. Lett.* **2013**, *23*, 4297-4302

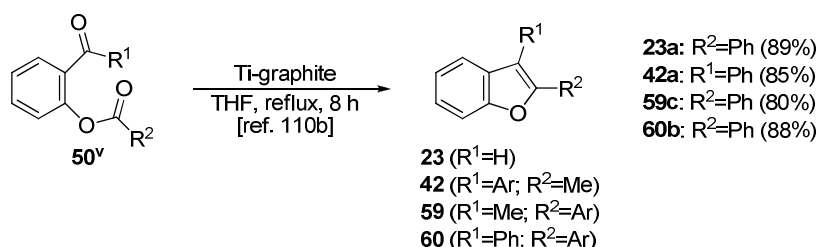
¹⁰⁸ Hellwinkel, D.; Göke, K. *Synthesis* **1995**, 1135-1141

¹⁰⁹ Kraus, G. A.; Zhang, N.; Verkade, J. G.; Nagarajan, M.; Kisanga, P. B. *Org. Lett.* **2000**, *2*, 2409-2410



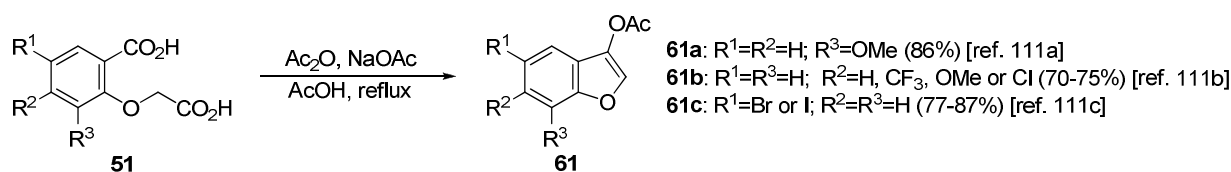
Scheme 1.18. Examples of benzo[*b*]furan preparation methods based on the C₂–C₃ bond formation starting from benzaldehydes and phenyl ketones **50^{iv}**.

Benzo[*b*]furans could also be formed starting from 2-(1-oxoalkoxy)aryl aldehydes and ketones **50^v** via McMurry type reactions (Scheme 1.19), i. e. by intramolecular reductive carbonyl coupling into an alkene using a titanium chloride compound and a reducing agent¹¹⁰.



Scheme 1.19. Examples of benzo[*b*]furan preparation methods based on the C₂–C₃ bond formation starting from benzaldehydes and phenyl ketones **50^v**.

Cyclization of 2-(carboxymethyl)benzoic acids **51** under reflux conditions with acetic anhydride, sodium acetate and acetic acid yielded benzofuran-3-yl acetates (or 3-acetoxybenzofurans)¹¹¹ **61** (Scheme 1.20).



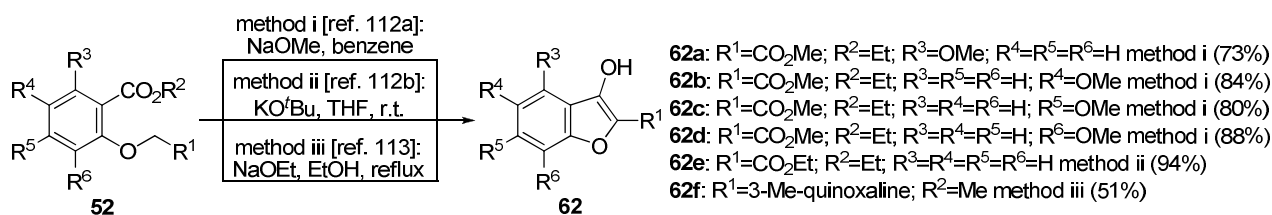
Scheme 1.20. Examples of benzo[*b*]furan preparation methods based on the C₂–C₃ bond formation starting from benzoic acids **51**.

Transformations of 2-(2-alkoxy-2-oxoethoxy)benzoates¹¹² and 2-(arylmethoxy)benzoates¹¹³ **52** into 3-hydroxybenzo[*b*]furans **62** via base-mediated

¹¹⁰ (a) Banerji, A.; Nayak, S. K. *J. Chem. Soc., Chem. Commun.* **1990**, 150-151 (b) Fürstner, A.; Jumbman, D. N. *Tetrahedron* **1992**, *48*, 5991-6010 (c) Fürstner, A.; Hupperts, A.; Ptock, A.; Janssen, E. *J. Org. Chem.* **1994**, *59*, 5215-5229 (d) Rele, S.; Talukdar, S.; Banerji, A.; Chattopadhyay, S. *J. Org. Chem.* **2001**, *66*, 2990-2994 (e) Jumbam, N. D.; Yedwa, M. P. I.; Masamba, W. *Bull. Chem. Soc. Ethiop.* **2011**, *25*, 157-160

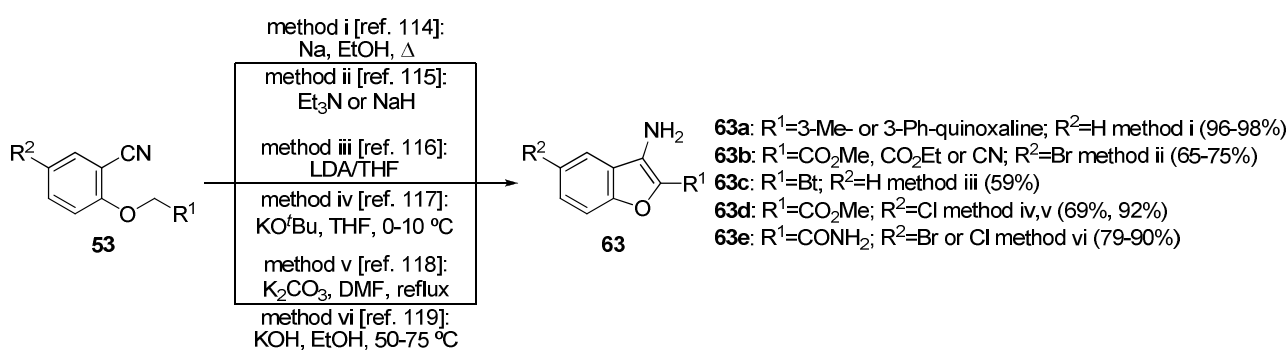
¹¹¹ (a) Bryant III, W. M.; Huhn, G. F. *Synth. Commun.* **1995**, *25*, 915-920 (b) Gormemis, A. E.; Ha, T. S.; Im, I.; Jung, K.-Y.; Lee, J. Y.; Park, C.-S.; Kim, Y.-C. *ChemBioChem* **2005**, *6*, 1745-1748 (c) Maya, Y.; Ono, M.; Watanabe, H.; Haratake, M.; Saji, H.; Nakayama, M. *Bioconjugate Chem.* **2009**, *20*, 95-101

intramolecular cyclizations were reported. The bases used for these reactions included, for example, sodium methoxide or ethoxide and potassium *tert*-butoxide (Scheme 1.21).



Scheme 1.21. Examples of benzo[*b*]furan preparation methods based on the C₂–C₃ bond formation starting from benzoates **52**.

Base-mediated intramolecular cyclization of 2-hydroxybenzoxazole derivatives **53** afforded 3-aminobenzo[*b*]furans **63**. Some of the bases employed for this purpose were sodium ethoxide¹¹⁴, triethylamine or sodium hydride¹¹⁵, lithium diisopropylamide¹¹⁶, potassium *tert*-butoxide¹¹⁷, potassium carbonate¹¹⁸ and potassium hydroxide¹¹⁹ (Scheme 1.22).



Scheme 1.22. Examples of benzo[*b*]furan preparation methods based on the C₂–C₃ bond formation starting from benzonitriles **53**.

Though less widespread than the previous procedures, an iridium catalyzed hydrogen transfer was developed in the presence of *para*-benzoquinone, allowing the synthesis of substituted benzo[*b*]furans from 2-(hydroxymethyl)phenol derivatives **54**¹²⁰ (Scheme 1.23).

¹¹² (a) Lamotte, G.; Demerseman, P.; Royer, R.; Gayral, P.; Fourniat, J. *Eur. J. Med. Chem.* **1986**, *21*, 379–383 (b) Rackham, M. D.; Brannigan, J. A.; Moss, D. K.; Yu, Z.; Wilkinson, A. J.; Holder, A. A.; Tate, E. W.; Leatherbarrow, R. J. *J. Med. Chem.* **2013**, *56*, 371–375

¹¹³ Sarodnick, G.; Kempter, G.; Jumar, A. *Patent* **1990**, DD 276479 A1

¹¹⁴ Sarodnick, G.; Kempter, G. *Patent* **1983**, DD 292001 A5

¹¹⁵ Tsuji, E.; Ando, K.; Kunitomo, J.-i.; Yamashita, M.; Ohta, S.; Kohno, S.; Ohishi, Y. *Org. Biomol. Chem.* **2003**, *1*, 3139–3141

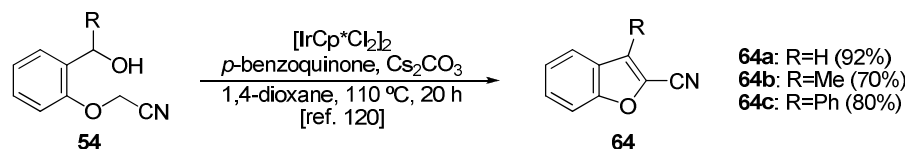
¹¹⁶ Rádl, S.; Obadalová, I. *Arkivoc* **2005**, xv, 4–11

¹¹⁷ Jones, A.; Wilson, F.; Dyke, H.; Price, S.; Cramp, S.; Szabó, A.; Repasi, J. *Patent* **2008**, EP 1925619 A1

¹¹⁸ Chavez, F.; Curtis, M. P.; Edwards, J. P.; Gomez, L.; Grice, C. A.; Kearney, A. M.; Savall, B. M. Fitzgerald, A. E.; Liu, J.; Mani, N. S. *Patent* **2008**, WO 2008008359 A2

¹¹⁹ Brown, S. D.; Du, H.; Franzini, M.; Galan, A. A.; Huang, P.; Kearney, P.; Kim, M. H.; Koltun, E. S.; Richards, S. J.; Tshako, A. L.; Zaharia, C. A. *Patent* **2009**, WO 2009086264

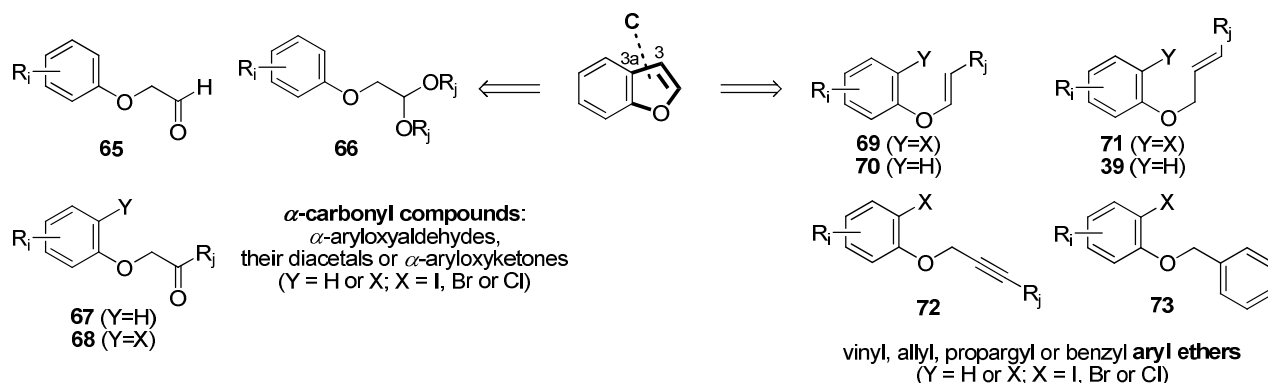
¹²⁰ Anxionnat, B.; Gomez-Pardo, D.; Ricci, G.; Rossen, K.; Cossy, J. *Org. Lett.* **2013**, *15*, 3876–3879



Scheme 1.23. Examples of benzo[*b*]furan preparation methods based on the C₂–C₃ bond formation starting from benzyl alcohols **54**.

1.1.3.1.3. Methods based on the C₃–C_{3a} bond formation (C)

The retrosynthetic approaches having a benzenoid scaffold as starting material based on the C₃–C_{3a} bond discussed below are presented in Scheme 1.24. On looking at the starting material for the reactions based on this disconnection, two big groups can be differentiated: the α -aryloxy carbonyl compounds (i.e. aldehydes **65**, as well as their corresponding diacetals **66** and ketones **67**) and the aryl vinyl (**69,70**), aryl allyl (**71,39**), aryl propargyl (**72**) and aryl benzyl (**73**) ethers. Some of these phenol derivatives can, in turn, be *ortho* unsubstituted or bear a halogen (X = Br, Cl or I) at this position.



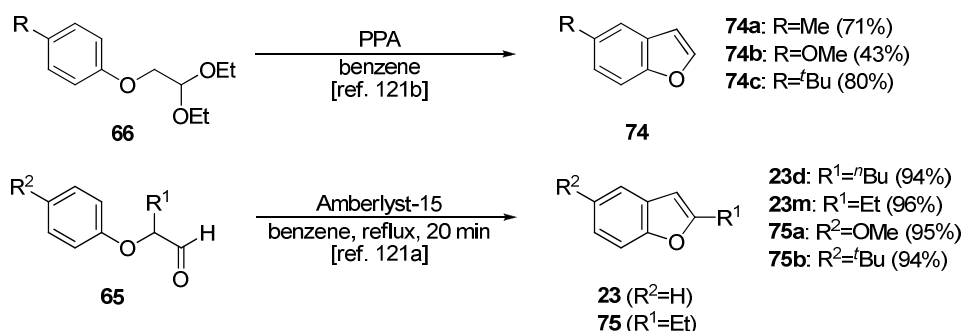
Scheme 1.24. Retrosynthetic approaches having a benzenoid scaffold as starting material, based on the construction of the C₃–C_{3a} bond.

α -Aryloxy carbonyl compounds

As far as α -aryloxyaldehydes **65** and their corresponding diacetals **66** are concerned, different methods for their acid-catalyzed cyclizations leading to benzo[*b*]furans were reported. These acidic conditions included the employment of (poly)phosphoric acid¹²¹ or Amberlyst-15 (a strongly acidic cation exchanging resin)¹²² (Scheme 1.25).

¹²¹ (a) Best, D. J.; Bruton, G.; Orlek, B. S.; Rana, K.; Walker, G. *Patent* **2001**, WO 0190100 A1 (b) Barker, P.; Finke, P.; Thompson, K. *Synth. Commun.* **1989**, *19*, 257-265

¹²² (a) Witczak, M.; Kwiecień, H. *Synth. Commun.* **2005**, *35*, 2223-2230 (b) Goel, A.; Dixit, M. *Synlett* **2004**, 1990-1994



Scheme 1.25. Examples of benzo[*b*]furan preparation methods based on the C₃–C_{3a} bond formation starting from α -aryloxyaldehydes **65** and diacetals **66**.

Starting from α -aryloxyketones **67**, several acid-promoted cyclizations to benzo[*b*]furans were reported. Among the acidic components protic acids (such as (poly)phosphoric acid¹²³, trifluoroacetic acid¹²⁴, or methanesulfonic acid¹²⁵), Lewis acids (like zinc bromide¹²⁶ and boron trichloride¹²⁷) or acidic resins or clays (as Amberlyst-15¹²⁸ and Montmorillonite KSF clay¹²⁹) can be found (Scheme 1.26 above). Besides, iridium-catalyzed cyclodehydrations (C–H bond activation, intramolecular 1,2-addition and dehydration) of α -aryloxyketones bearing an acetyl (directing) group in *meta* position also proved to effectively afford substituted benzo[*b*]furans¹³⁰ (Scheme 1.26 middle). When the α -aryloxyketones bore a halogen in *ortho* position (**68**), the corresponding benzo[*b*]furans could also be obtained by intramolecular cyclization initiated by metal-halogen exchange using methyllithium¹³¹ (Scheme 1.26 below).

¹²³ Guy, A.; Guetté, J.-P.; Lang, G. *Synthesis* **1980**, 222-223

¹²⁴ Black, D. St. C.; Craig, D. C.; Kumar, N.; Rezaie, R. *Tetrahedron* **1999**, *55*, 4803-4814

¹²⁵ Santini, C.; Berger, G. D.; Han, W.; Mosley, R.; MacNaul, K.; Berger, J.; Doebber, T.; Wu, M.; Moller, D. E.; Tolmana, R. L.; Sahoo, S. P. *Bioorg. Med. Chem. Lett.* **2003**, *13*, 1277-1280

¹²⁶ Katritzky, A. R.; Serdyuk, L.; Xie, L. *J. Chem. Soc., Perkin Trans. 1* **1998**, 1059-1064

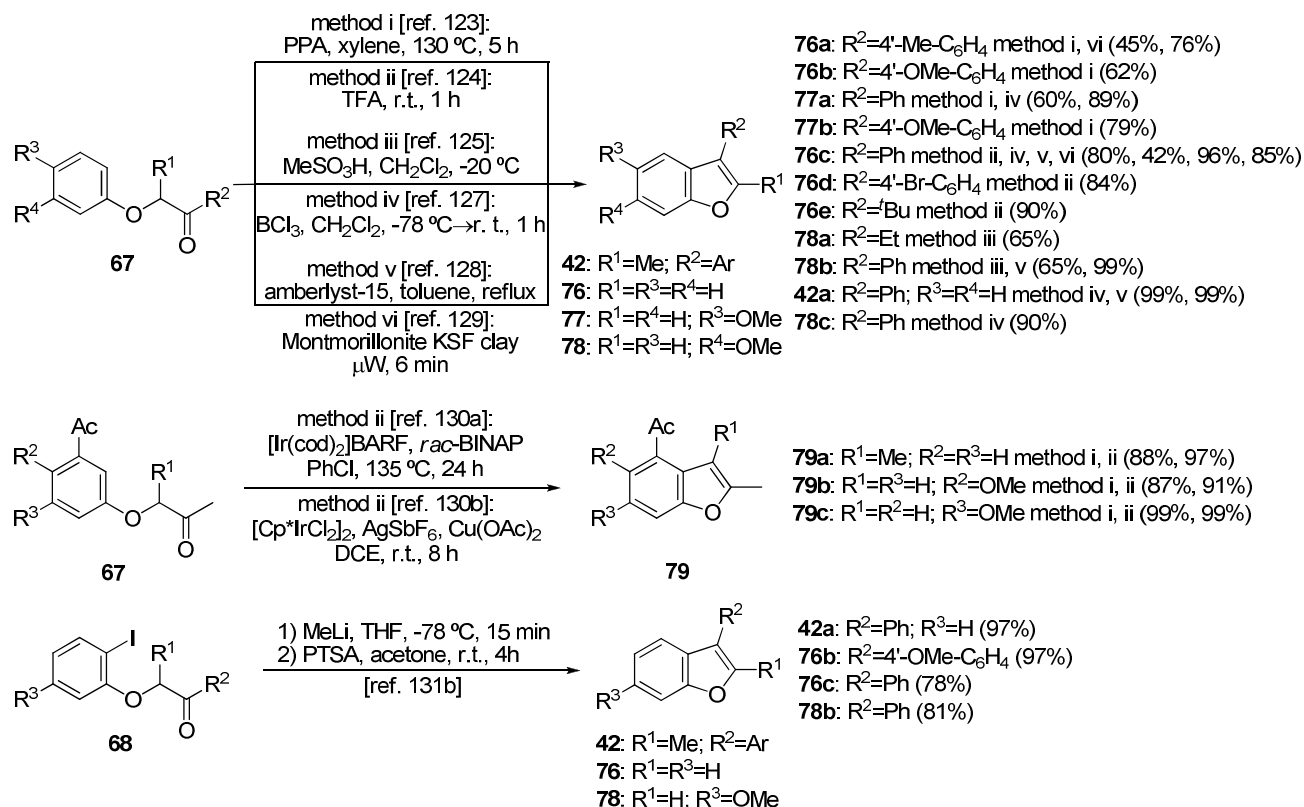
¹²⁷ Kim, I.; Lee, S.-H.; Lee, S. *Tetrahedron Lett.* **2008**, *49*, 6579-6584

¹²⁸ Habermann, J.; Ley, S. V.; Smits, R. *J. Chem. Soc., Perkin Trans. 1* **1999**, 2421-2423

¹²⁹ Meshram, H. M.; Chandra Sekhar, K.; Ganesh, Y. S. S.; Yadav, J. S. *Synlett* **2000**, 1273-1274

¹³⁰ (a) Tsuchikama, K.; Hashimoto, Y.-K.; Endo, K.; Shibata, T. *Adv. Synth. Catal.* **2009**, *351*, 2850-2854 (b) Shibata, T.; Hashimoto, Y.-K.; Otsuka, M.; Tsuchikama, K.; Endo, K. *Synlett* **2011**, 2075-2079

¹³¹ (a) Kraus, G. A.; Kim, I. *Org. Lett.* **2003**, *5*, 1191-1192 (b) Kraus, G. A.; Schroeder, J. D. *Synlett* **2005**, 2504-2506



Scheme 1.26. Examples of benzo[*b*]furan preparation methods based on the C₃–C_{3a} bond formation starting from α -aryloxyketones **67** and **68**.

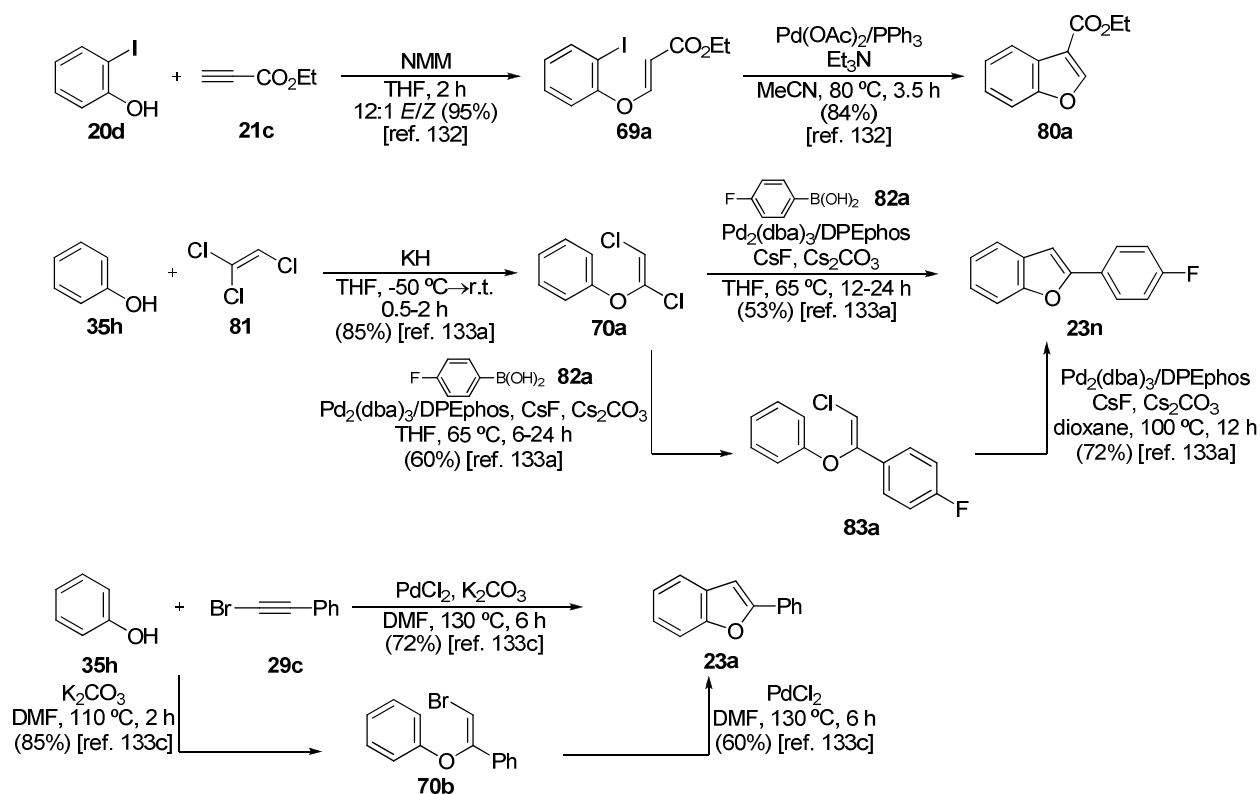
Unsaturated (vinyl, allyl, propargyl or benzyl) ethers

When the aryloxy moiety bore a halogen in the *ortho* position (**69**), its intramolecular Heck (or Mirozoki-Heck) reaction into the corresponding benzo[*b*]furan was reported. This was the case of the *E*-vinyl ester **69a**, which could in turn be obtained as the major product of the Michael addition of *o*-iodophenol **20d** to ethyl propiolate **21c**¹³² (Scheme 1.27 above).

When the aryl vinyl ethers did not bear a halogen in *ortho* position (**70**), intramolecular cyclizations to afford the benzo[*b*]furans proceeded through palladium-catalyzed C–H bond activations. Moreover, many of the reactions described following this strategy could be successfully carried out in one pot fashion (tandem procedures), starting from suitable phenols (**35**) and trichloroethene (**81**) or alkynes (**29**). These reactants underwent addition reactions or Sonogashira couplings (and even Suzuki-Miyaura couplings when a boronic acid was also added) in a first step before the cyclization took place¹³³ (Scheme 1.27 middle and below).

¹³² Malona, J. A.; Colbourne, J. M.; Frontier, A. J. *Org. Lett.* **2006**, *8*, 5661-5664

¹³³ (a) Geary, L. M.; Hultin, P. G. *Org. Lett.* **2009**, *11*, 5478-5481 (b) Geary, L. M.; Hultin, P. G. *Eur. J. Org. Chem.* **2010**, 5563-5573 (c) Wang, S.; Li, P.; Yu, L.; Wang, L. *Org. Lett.* **2011**, *13*, 5968-5971 (d) Li, C.;



Scheme 1.27. Examples of benzo[*b*]furan preparation methods based on the C₃–C_{3a} bond formation starting from aryl vinyl ethers **70**.

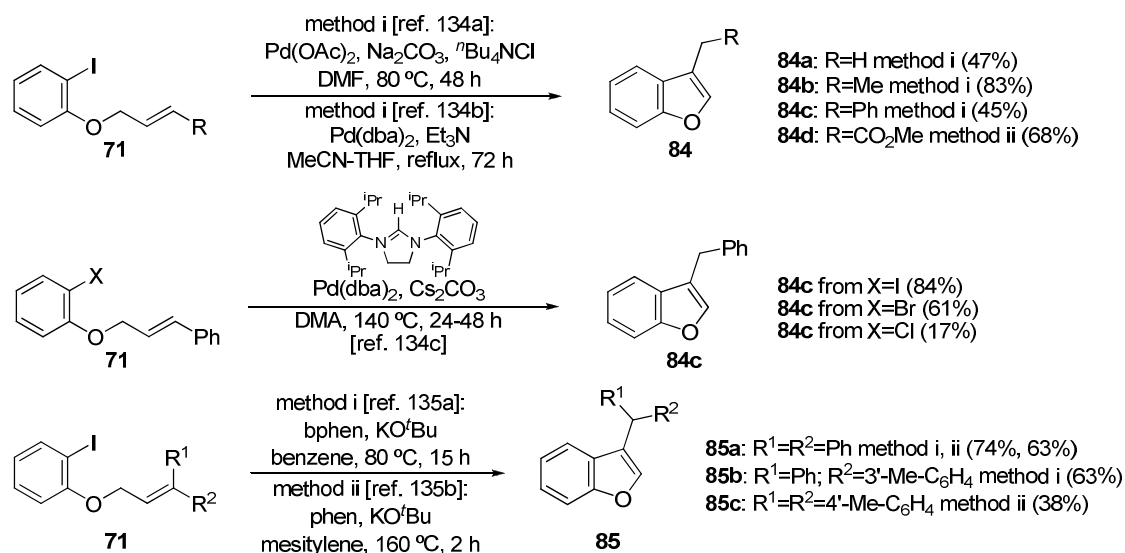
Out of the mentioned ethers, allyl aryl ones are the most widely used for the benzo[*b*]furan preparation based on the C₃–C_{3a} disconnection. When the aryl moiety is *ortho* halogenated (**71**), the typical procedures consisted of intramolecular Heck (or Mirozoki-Heck) reactions, i.e. cyclic carbopalladation of olefins containing aryl halides followed by dehydropalladation¹³⁴. Alternatively, arylations of the same type of compounds into 3-substituted benzo[*b*]furans promoted by potassium *tert*-butoxide and phenantroline (or analogous heterocyclic compounds) were also reported. These reactions were thought to proceed through an organocatalytic radical process¹³⁵ (Scheme 1.28). Moreover, intramolecular Heck-Matsuda reaction (intramolecular Heck reaction with arenediazonium salts) also proved effective for the 3-substituted benzo[*b*]furan synthesis¹³⁶.

Zhang, Y.; Li, P.; Wang, L. *J. Org. Chem.* **2011**, *76*, 4692-4694 (e) Zhou, W.; Zhang, Y.; Li, P.; Wang, L. *Org. Biomol. Chem.* **2012**, *10*, 7184-7196

¹³⁴ (a) Larock, R. C.; Stinn, D. E. *Tetrahedron Lett.* **1988**, *29*, 4687-4890 (b) Negishi, E.; Nguyen, T.; O'Connor, B.; Evans, J. M.; Silveira, A. J. *Heterocycles* **1989**, *28*, 55-58 (c) Caddick, S.; Kofie, W. *Tetrahedron Lett.* **2002**, *43*, 9347-9350 (d) Xie, X.; Chen, B.; Lu, J.; Han, J.; She, X.; Pan, X. *Tetrahedron Lett.* **2004**, *45*, 6235-6237

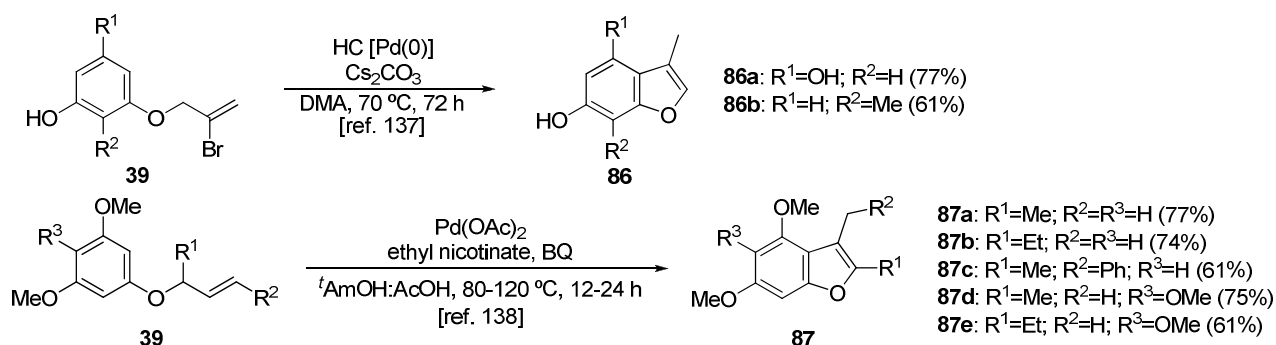
¹³⁵ (a) Sun, C.-L.; Gu, Y.-F.; Wang, G.; Shi, Z.-J. *Chem Eur. J.* **2011**, *17*, 10844-10847 (b) Rueping, M.; Leiendecker, M.; Das, A.; Poisson, T.; Bui, L. *Chem. Commun.* **2011**, *47*, 10629-10631

¹³⁶ Siqueira, F. A.; Taylor, J. G.; Correia, C. R. D. *Tetrahedron Lett.* **2010**, *51*, 2102-2105



Scheme 1.28. Examples of benzo[*b*]furan preparation methods based on the C₃–C_{3a} bond formation starting from *ortho*-halogenated aryl allyl ethers **71**.

The cyclization was also reported to occur at an *ortho* unsubstituted carbon of the aryl moiety of the allyl aryl ether. Palladium species proved useful to afford benzo[*b*]furans through intramolecular cross-DMA couplings of aryl allyl ethers **39**¹³⁷. Besides, a direct method for the synthesis of benzo[*b*]furans by palladium-catalyzed intramolecular Fujiwara-Moritani/oxidative Heck reaction starting from allyl aryl ethers **39** was reported¹³⁸. In the last stage of these last two reaction models an isomerization of the resulting exocyclic double bond took place (Scheme 1.29).



Scheme 1.29. Examples of benzo[*b*]furan preparation methods based on the C₃–C_{3a} bond formation starting from *ortho*-unsubstituted aryl allyl ethers **72**.

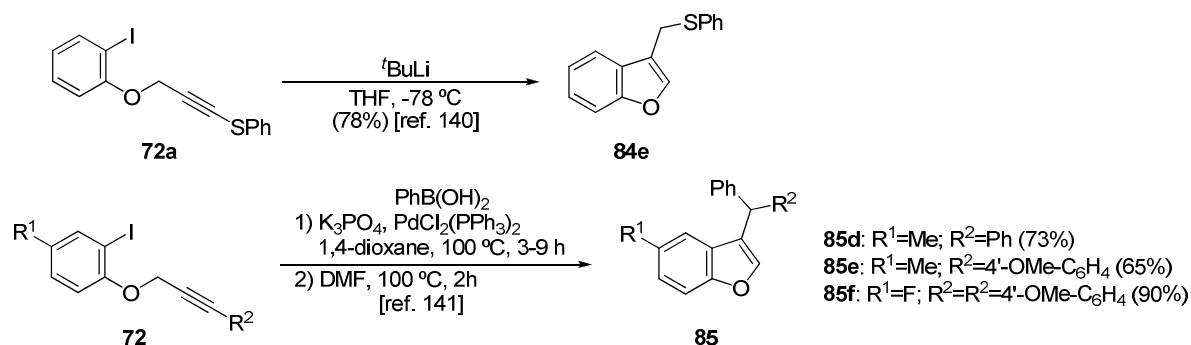
With regard to 2-haloaryl propargyl ethers **73**, they were reported to undergo intramolecular cyclization via carbolithiation performed in classical conditions with an excess of *n*-butyllithium¹³⁹ or *tert*-butyllithium¹⁴⁰. The double bond, which was originally

¹³⁷ Hennings, D. D.; Iwasa, S.; Rawal, V. H. *Tetrahedron Lett.* **1997**, *38*, 6379-6382

¹³⁸ Zhang, H.; Ferreira, E. M.; Stoltz, B. M. *Angew. Chem. Int. Ed.* **2004**, *43*, 6144-6148

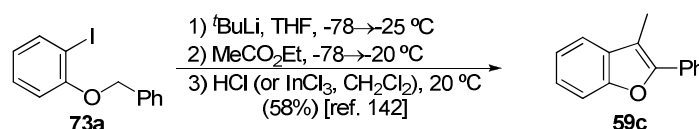
¹³⁹ Le Strat, F.; Maddaluno, J. *Org. Lett.* **2002**, *4*, 2791-2793

recovered in exocyclic position, tended to rearrange yielding the corresponding 3-substituted benzo[*b*]furans. The same starting ethers and arylboronic acids proved useful in cascade cyclocarbopalladation / Suzuki-Miyaura cross-coupling / aromatization process, leading to 3-functionalized 2-unsubstituted benzo[*b*]furans¹⁴¹ (Scheme 1.30).



Scheme 1.30. Examples of benzo[*b*]furan preparation methods based on the C₃–C_{3a} bond formation starting from aryl propargyl ethers **72**.

Finally, examples of benzo[*b*]furan construction from 2-haloaryl benzyl ethers **73** were also found in literature. The key step of this procedure was the selective double lithiation of the benzylic and *ortho* positions of the starting ethers and further trapping of the resulting dianions with carboxylic esters. Then the dehydration process (carried out with hydrochloric acid or alternatively with Lewis acid indium (III) chloride) provided the corresponding 2-aryl-3-substituted benzo[*b*]furans¹⁴² (Scheme 1.31).



Scheme 1.31. Examples of benzo[*b*]furan preparation methods based on the C₃–C_{3a} bond formation starting from aryl phenyl ethers **73**.

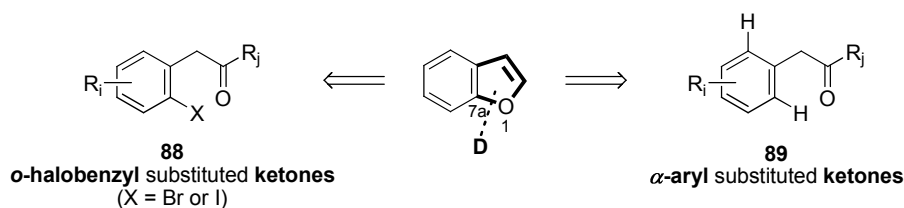
¹⁴⁰ Girard, A.-L.; Lhermet, R.; Fressigné, C.; Durandetti, M.; Maddaluno, J. *Eur. J. Org. Chem.* **2012**, 2895-2905

¹⁴¹ Arcadi, A.; Blesi, F.; Cacchi, S.; Fabrizi, G.; Goggiani, A.; Marinelli, F. *J. Org. Chem.* **2013**, *78*, 4490-4498

¹⁴² Sanz, R.; Miguel, D.; Martínez, A.; Pérez, A. *J. Org. Chem.* **2006**, *71*, 4024-4027

1.1.3.1.4. Methods based on the O–C_{7a} bond formation (D)

The retrosynthetic approaches having a benzenoid scaffold as starting material based on the O–C_{7a} bond discussed below are presented in Scheme 1.32. The starting material for the reactions based on this disconnection is typically a substituted alkyl or aryl benzyl ketone which undergoes an intramolecular O-arylation (ring closure reaction). At this point we differentiate two kinds of substrates, depending on their having or not a halogen (bromine or iodine) in the *ortho* position of the benzyl moiety.



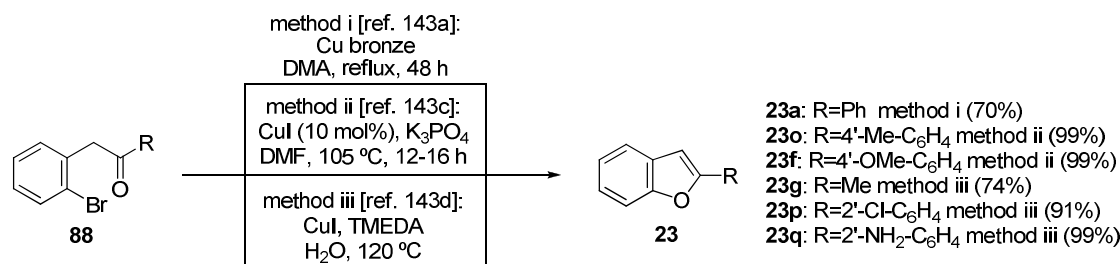
Scheme 1.32. Retrosynthetic approaches having a benzenoid scaffold as starting material, based on the construction of the O–C_{7a} bond.

Starting with the *o*-halobenzyl substituted ketones **88**, they were reported to furnish the corresponding benzo[*b*]furans via transition metal-catalyzed ring closure reactions. Most of the described reactions used *o*-halobenzyl aryl ketones, although examples with *o*-halobenzyl methyl ketones were also reported. Once more, the typical transition metals used to perform these transformations were copper¹⁴³ (Scheme 1.33), palladium¹⁴⁴ (Scheme 1.34) and to a lesser extent iron¹⁴⁵ (Scheme 1.35). The key cyclization reaction involved the coupling of the enolate oxygen to the transition metal-activated aryl halide. Therefore, the presence of a base, to generate the enolate, was also a common feature of these synthetic protocols.

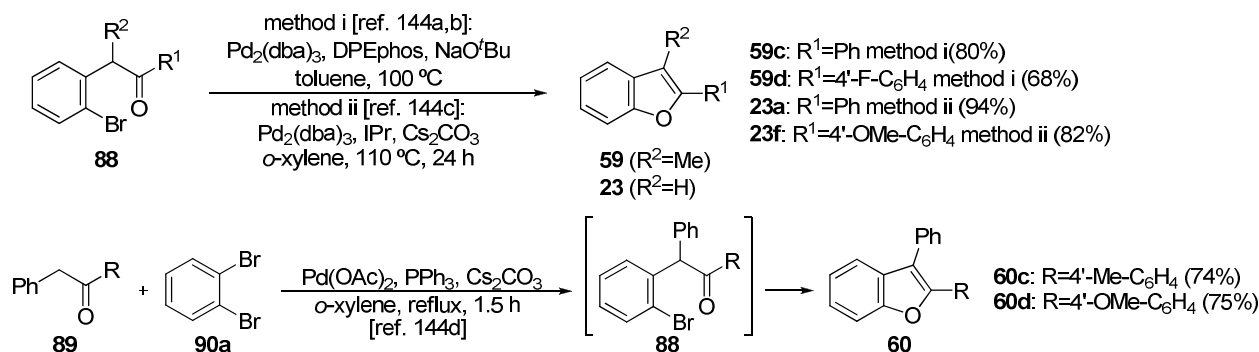
¹⁴³ (a) Grimshaw, J.; Thompson, N. *J. Chem. Soc., Chem. Commun.* **1987**, 240-241 (b) Lamas, C.; García, A.; Castedo, L.; Domínguez, D. *Tetrahedron Lett.* **1989**, 30, 6927-6928 (c) Chen, C.-Y.; Dormer, P. G. *J. Org. Chem.* **2005**, 70, 6964-6967 (d) Carril, M.; SanMartín, R.; Tellitu, I.; Domínguez, E. *Org. Lett.* **2006**, 8, 1467-1470

¹⁴⁴ (a) Willis, M. C.; Taylor, D.; Gillmore, A. T. *Org. Lett.* **2004**, 6, 4755-4757 (b) Willis, M. C.; Taylor, D.; Gillmore, A. T. *Tetrahedron* **2006**, 62, 11513-11520 (c) Faragó, J.; Kotschy, A. *Synthesis* **2009**, 85-90 (d) Terao, Y.; Satoh, T.; Masahiro, M.; Nomura, M. *Bull. Chem. Soc. Jpn.* **1999**, 72, 2345-2350

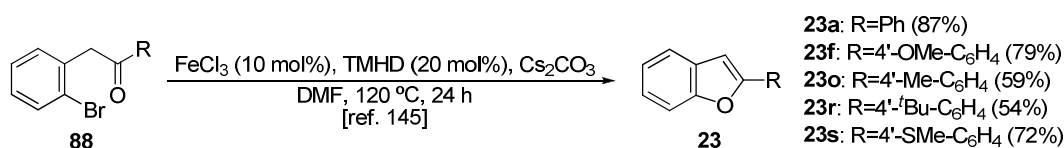
¹⁴⁵ Bonnamour, J.; Piedrafita, M.; Bolma, C. *Adv. Synth. Catal.* **2010**, 352, 1577-1581



Scheme 1.33. Examples of Cu-catalyzed benzo[*b*]furan preparation methods based on the O–C_{7a} bond formation.

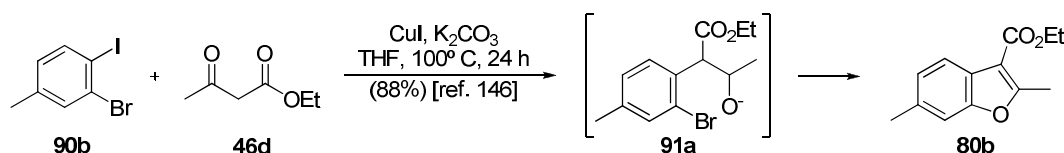


Scheme 1.34. Examples of Pd-catalyzed benzo[*b*]furan preparation methods based on the O–C_{7a} bond formation.



Scheme 1.35. Examples of a Fe-catalyzed benzo[*b*]furan preparation method based on the O–C_{7a} bond formation.

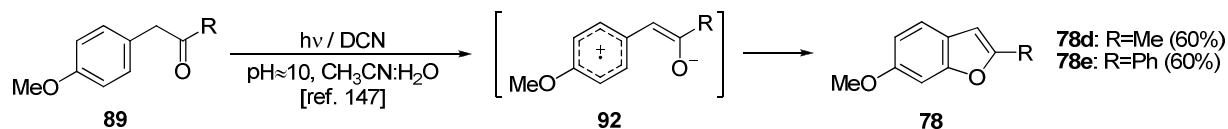
Considering the reaction at a previous step, intermolecular C–C bond formation between 1-bromo-2-iodobenzenes **90b** and β -ketoesters **46d** followed by an intramolecular C–O bond formation process (of the resulting 2-bromoketones **91a**) was also reported to yield benzo[*b*]furan **80b** when using copper iodide as catalyst and potassium carbonate as base¹⁴⁶ (Scheme 1.36).



Scheme 1.36. Example of a Cu-catalyzed benzo[*b*]furan preparation method based on the domino intermolecular C₃–C_{3a} bond formation / intramolecular O–C_{7a} bond formation.

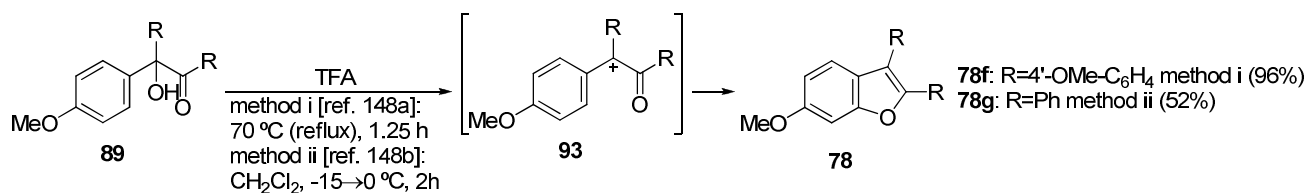
¹⁴⁶ Lu, B.; Bang, B.; Zhang, Y.; Ma, D. *J. Org. Chem.* **2007**, *72*, 5337-5341

In regard to non-*ortho*-halogenated benzyl ketones **89**, one-step synthesis of 2-substituted benzo[*b*]furans from the enolate of benzyl aryl (or methyl) ketones by photoinduced SET reactions were described¹⁴⁷ (Scheme 1.37).



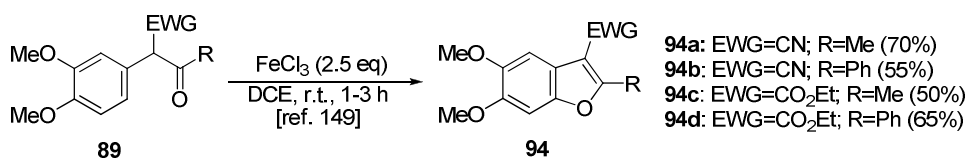
Scheme 1.37. Example of photoinduced benzo[*b*]furan preparation method based on the O–C_{7a} bond formation.

Substituted β -phenylbenzoins **89** in the presence of trifluoroacetic acid were also alternative starting materials for the preparation of 2,3-diarylbenzofurans **78**. The reaction proceeded via the cationic electrocyclization of the generated α -benzoyldiphenyl cations **93**¹⁴⁸ (Scheme 1.38).



Scheme 1.38. Example of TFA-promoted benzo[*b*]furan preparation method based on the O–C_{7a} bond formation.

Transition metals also proved useful in this approach. FeCl₃-mediated ring closure of electron-rich α -aryl ketones **89** into a variety of 3-functionalized benzo[*b*]furans **94** has been described. In this strategy, the presence of an electron withdrawing group in the benzylic position (to promote the loss of the acidic proton in benzylic position during the process) and electron-donating alkoxy substituents (for the oxidative intramolecular cyclization to occur) in the starting benzene ring **89** were crucial¹⁴⁹ (Scheme 1.39).



Scheme 1.39. Example of FeCl₃-mediated benzo[*b*]furan preparation method based on the O–C_{7a} bond formation.

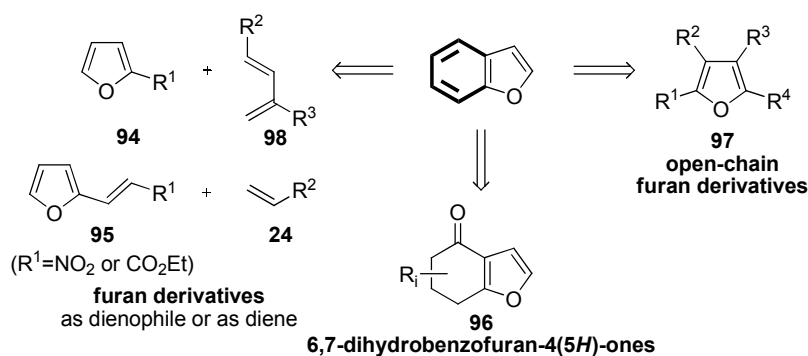
¹⁴⁷ Pandey, G.; Krishna, A.; Bhalerao, U. T. *Tetrahedron Lett.* **1989**, *30*, 1867-1870

¹⁴⁸ (a) Ohwada, T.; Shudo, K. *J. Org. Chem.* **1989**, *54*, 5227-5237 (b) Yoshida, N.; Ohwada, T. *Synthesis* **2001**, 1487-1494

¹⁴⁹ Liang, Z.; Hou, W.; Du, Y.; Zhang, Y.; Pan, Y.; Mao, D.; Zhao, K. *Org. Lett.* **2009**, *11*, 4978-4981

1.1.3.1.5. Methods based on the construction of the benzene ring (E)

As mentioned at the beginning of this section, though scarce in comparison, there also exist synthetic strategies for the benzo[*b*]furan preparation not based on the furan ring construction. They are available from suitably substituted furans by cyclization and generation of the benzene ring. The retrosynthetic approaches having a furanoid scaffold as starting material discussed below are presented in Scheme 1.40.

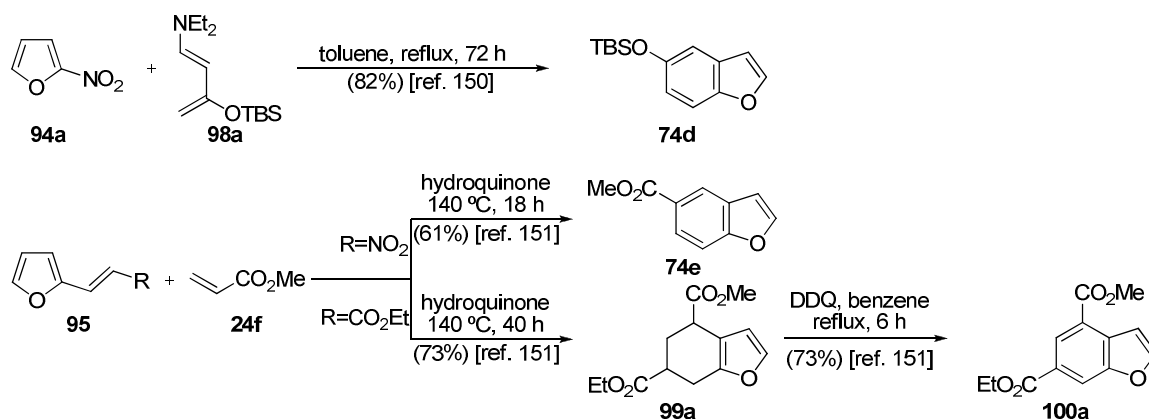


Scheme 1.40. Retrosynthetic approaches having a furanoid scaffold as starting material, based on the construction of the benzene ring.

To start with, different Diels-Alder reactions were exploited with this purpose using conveniently substituted furans, which can act both as dienes and as dienophiles, as starting materials. 2-Nitrobenzofuran **94a** for example, proved to efficiently react as dienophile in Diels-Alder reactions with several dienes, such as the so-called Rawal's diene (1-diethylamino-3-tert-butyl-dimethyl-siloxy-1,3-butadiene **98a**). The reaction selectively yielded the benzo[*b*]furan product **74d**, being the nitro substituent extruded under the thermal conditions of the reaction¹⁵⁰ (Scheme 1.41 above). 2-Vinylfurans, such as 2-(2-nitrovinyl)furan and ethyl-3-(furan-2-yl)acrylate **95** in turn, were used as dienes in Diels-Alder reactions with methyl acrylate **24f** affording benzo[*b*]furan products or their immediate 4,5,6,7-tetrahydrobenzofuran precursors **99a**, which were further converted into benzo[*b*]furans by DDQ dehydrogenation¹⁵¹ (Scheme 1.41 below).

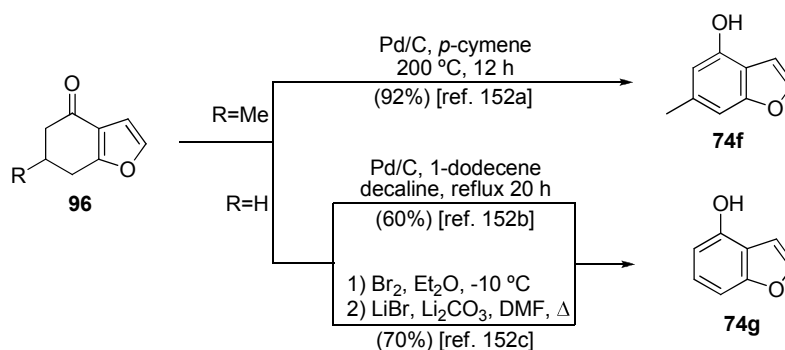
¹⁵⁰ Della Rosa, C.; Kneeteman, M. N.; Mancini, P. M. E. *Tetrahedron Lett.* **2005**, *46*, 8711-8714

¹⁵¹ Kusurkar, R. S.; Bhosale, D. K. *Synth. Commun.* **1990**, *20*, 101-109



Scheme 1.41. Examples of benzo[*b*]furan preparation methods based on the benzene ring construction via Diels-Alder reactions, using a furan as dienophile (above) or as diene (below).

Indeed, dehydrogenation strategy using palladium charcoal (Pd/C) resulted useful to obtain 4-hydroxybenzofurans **74f-g** from 6,7-dihydrobenzofuran-4(5*H*)-ones **96**, as well as the bromination-dehydrobromination sequence employing bromine and the combination of lithium bromine and lithium carbonate¹⁵² (Scheme 1.42).



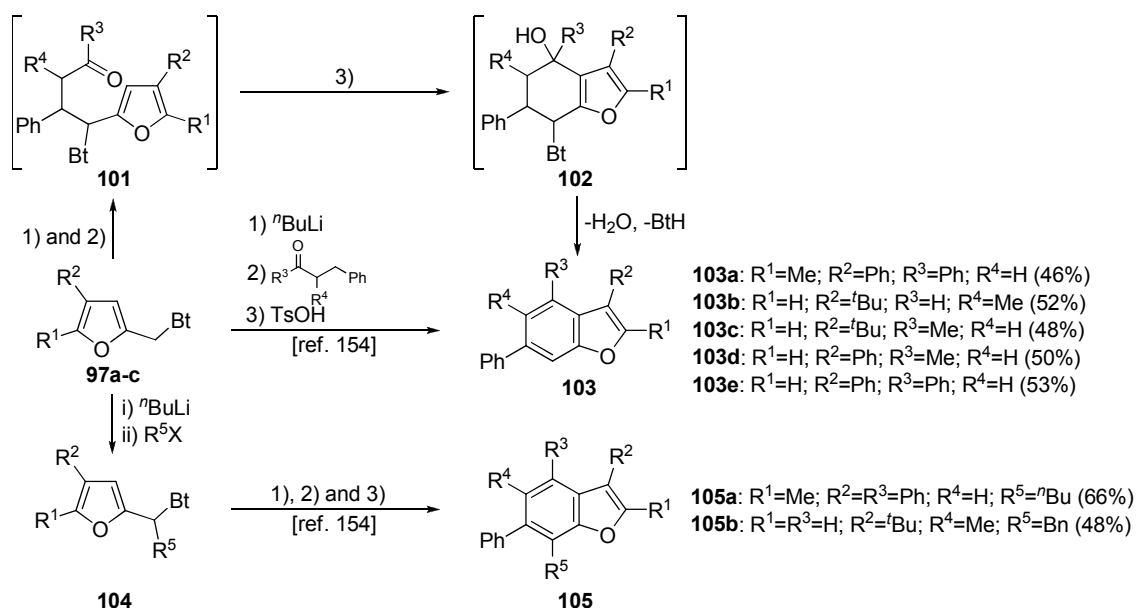
Scheme 1.42. Examples of benzo[*b*]furan preparation method based on the benzene ring construction via dehydrogenation reactions.

As a first example of cyclization of open-chain furan derivatives we found 2-(benzotriazol-1-ylmethyl)furans **97** (available from alkynyloxiranes, themselves derived from 1-propargylbenzotriazole and α -bromoketones¹⁵³). Their reaction with *n*-butyllithium and α,β -unsaturated ketones or aldehydes **100** gave the 1,4-addition intermediates **101** which, treated with *para*-toluenesulfonic acid, underwent intramolecular cyclization to **102** followed by spontaneous elimination of benzotriazole and water to give the benzo[*b*]furans **103**¹⁵⁴ (Scheme 1.43).

¹⁵² (a) Aso, M.; Ojida, A.; Yang, G.; Cha, O.-J.; Osawa, E.; Kanematsu, K. *J. Org. Chem.* **1993**, *58*, 3960-3968 (b) Kitamura, T.; Otsubo, K. *J. Org. Chem.* **2012**, *77*, 2978-2982 (c) Bonini, C.; Cristiani, G.; Funicello, M.; Viggiani, L. *Synth. Commun.* **2006**, *36*, 1983-1990

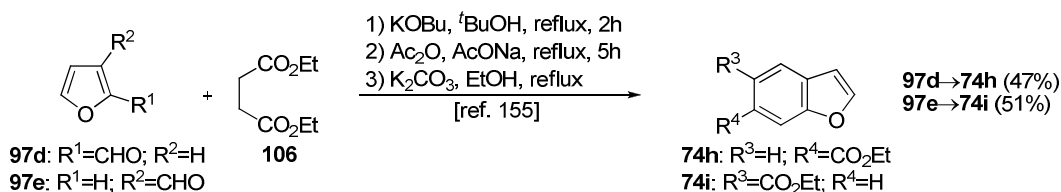
¹⁵³ Katritzky, A. R.; Li, J. *J. Org. Chem.* **1995**, *60*, 638-643

¹⁵⁴ Katritzky, A. R.; Fali, C.N.; Li, J. *J. Org. Chem.* **1997**, *62*, 8205-8209



Scheme 1.43. Examples of benzo[*b*]furan preparation methods based on the benzene ring construction via cyclization of open chain furan derivatives 2-(benzotriazol-1-ylmethyl)furans **97a-c**.

2- and 3-furaldehydes **97d-e** were also reported to yield benzo[*b*]furans via a sequence of reactions: Stobbe condensation with diethyl succinate, Friedel-Crafts acylation of the resulting product with acetic anhydride and cyclization¹⁵⁵ (Scheme 1.44).



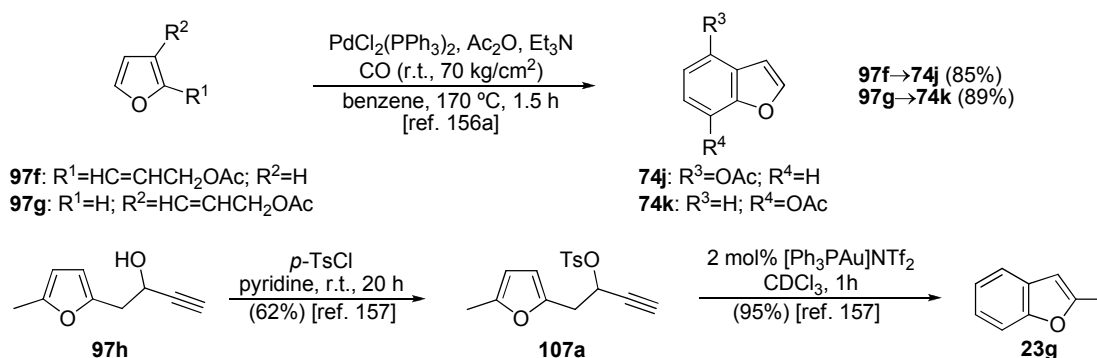
Scheme 1.44. Examples of benzo[*b*]furan preparation methods based on the benzene ring construction via cyclization of open chain furan derivatives furaldehydes **97d-e**.

Besides, transition metal-catalyzed cyclizations were described in literature to prepare benzo[*b*]furans from previously synthesized conveniently substituted furan derivatives (open-chain precursors). In this vein, palladium-catalyzed cyclocarbonylation of 2- or 3-furallyl acetates **97f-g**¹⁵⁶ (Scheme 1.45 above and middle) and gold-catalyzed cyclization of furan-yl-ol **97h** (prior transformation of the hydroxy substituent into a better leaving group) were reported¹⁵⁷ (Scheme 1.45 below).

¹⁵⁵ Simoni, D.; Romagnoli, R.; Baruchello, R.; Rondanin, R.; Rizzi, M.; Pavani, M. G.; Alloatti, D.; Giannini, G.; Marcellini, M.; Riccioni, T.; Castorina, M.; Guglielmi, M. B.; Bucci, F.; Carminati, P.; Pisano, C. *J. Med. Chem.* **2006**, *49*, 3143-3152

¹⁵⁶ (a) Iwasaki, M.; Li, J.-P.; Kobayashi, Y.; Matsuzaka, H.; Ishii, Y.; Hidai, M. *Tetrahedron Lett.* **1989**, *30*, 95-98 (b) Iwasaki, M.; Kobayashi, Y.; Li, J.-P.; Matsuzaka, H.; Ishii, Y.; Hidai, M. *J. Org. Chem.* **1991**, *56*, 1922-1927

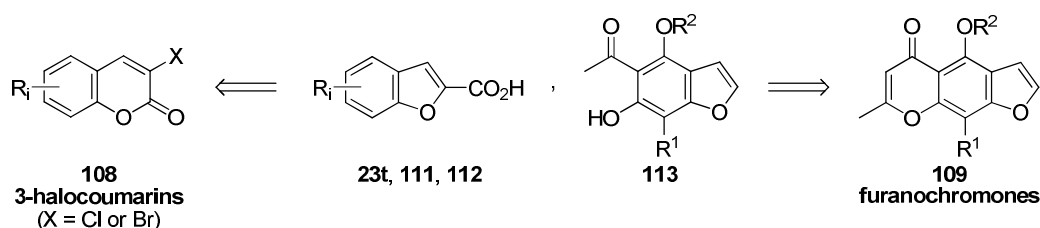
¹⁵⁷ Hashmi, A. S. K.; Wölflle, M. *Tetrahedron* **2009**, *65*, 9021-9029



Scheme 1.45. Examples of benzo[*b*]furan preparation methods based on the benzene ring construction via cyclization of open chain furan derivatives furallyl acetates **97f-g** and furan-yl-ol **97h**.

1.1.3.1.6. Methods based on the transformation of bi- or tricyclic oxygen-containing ring systems (F)

The retrosynthetic approaches available for this category are quite restricted and only a couple of representative examples will be discussed below. These are presented in Scheme 1.46.



Scheme 1.46. Some representative retrosynthetic approaches based on transformation of bi- or tricyclic oxygen-containing ring systems.

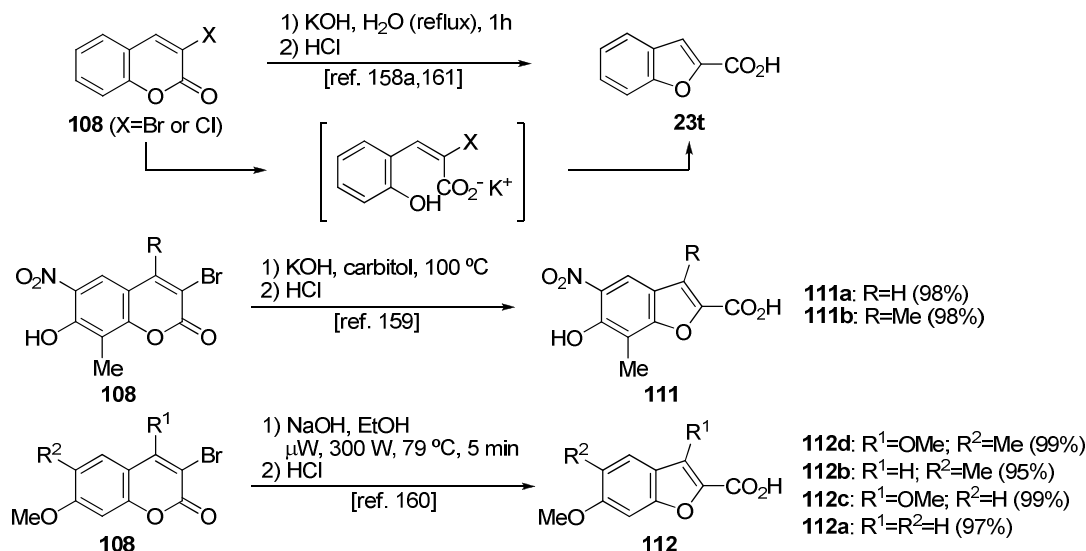
On the one hand, starting from bicyclic structures, we find ring contraction reactions. The most representative transformation of this group is the Perkin rearrangement (coumarin-benzofuran ring contraction), first reported by Perkin himself in 1870¹⁵⁸. This transformation consisted of the conversion of 3-halocoumarins **108** into benzofuran-2-carboxylic acids in the presence of a base (typically potassium or sodium hydroxide) under heating (traditionally conventional heating¹⁵⁹, but more recently also under microwave irradiation¹⁶⁰). The proposed mechanism entailed an initial base-catalyzed ring fission followed by a cyclization process leading to the benzo[*b*]furan moiety, as a result of the

¹⁵⁸ (a) Perkin, W. H. *J. Chem. Soc.* **1870**, 8, 368-371 (b) Perkin, W. H. *J. Chem. Soc.* **1871**, 9, 37-52

¹⁵⁹ Chilini, A.; Confente, A.; Pastorini, G.; Guiotto, A. *Eur. J. Org. Chem.* **2002**, 1937-1940

¹⁶⁰ Marriott, K.-S. C.; Barte, R.; Morrison, A. Z.; Stewart, L.; Wesby, J. *Tetrahedron Lett.* **2012**, 53, 3319-3321

attack of the resulting anion over the vinyl halide¹⁶¹ (Scheme 1.47). The halogenated starting materials can be readily prepared from the corresponding non-halogenated products by treatment with molecular halogens or the *N*-halosuccinimides.



Scheme 1.47. Examples of benzo[*b*]furan preparation methods based on the base-catalysed Perkin rearrangement, coumarin-benzofuran ring contraction.

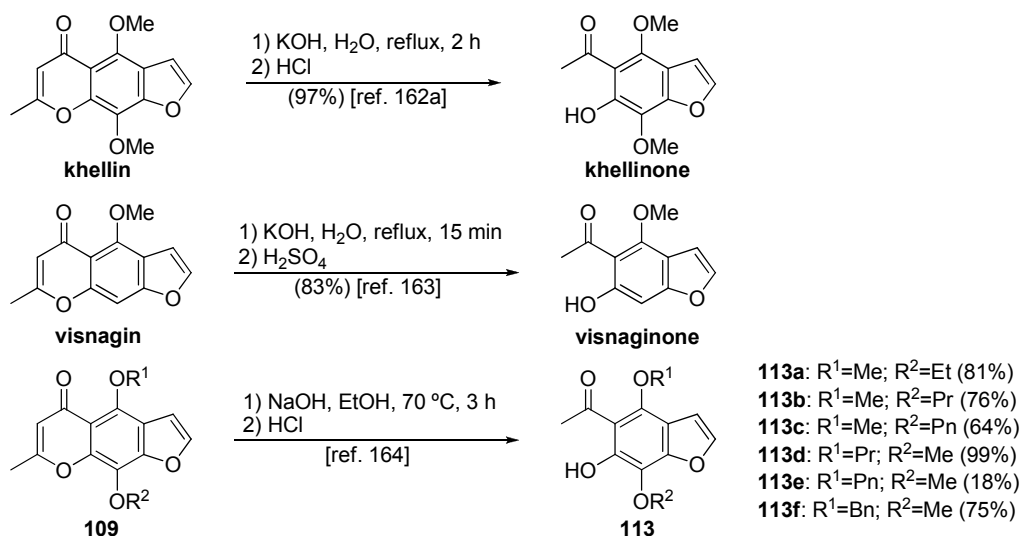
On the other hand, starting from tricyclic structures, we find cleavage reactions. It is noteworthy that these are not strictly speaking methods for the construction of the benzo[*b*]furan core, since it is already present in the starting material. However they proved useful to obtain certain compounds. Furanochromenes, for example, gave access to 1-(6-hydroxybenzofuran-5-yl)ethanones, by their cleavage under basic conditions. Khellinone, visagninone and some of their derivatives, were obtained by ring opening reactions in alkaline solution (aqueous potassium or sodium hydroxide) of natural khellin¹⁶², visnagin¹⁶³ or synthetic derivatives of them¹⁶⁴ (Scheme 1.48).

¹⁶¹ Bowden, K.; Battah, S. *J. Chem. Soc. Perkin Trans. 2* **1998**, 1603-1606

¹⁶² (a) Geissman, T. A. *J. Am. Chem. Soc.* **1949**, *71*, 1498-1498 (b) Bisagnin, M.; Buu-Hoi, Ng. Ph.; Royer, R. *J. Chem. Soc.* **1955**, 3693-3695

¹⁶³ Bodendiek, S. B.; Mahieux, C.; Hänsel, W.; Wulff, H. *Eur. J. Med. Chem.* **2009**, *44*, 1838-1852

¹⁶⁴ Harvey, A. J.; Baell, J. B.; Toovey, N.; Homerick, D.; Wulff, H. *J. Med. Chem.* **2006**, *49*, 1433-1441



Scheme 1.48. Examples of benzo[*b*]furan preparation methods based on the cleavage of furanochromones in basic conditions.

It is also worth mentioning that many of the methods presented all along this section have also been successfully applied to the preparation of naphthofurans.

1.1.3.2. Substituents in the benzo[*b*]furan structure

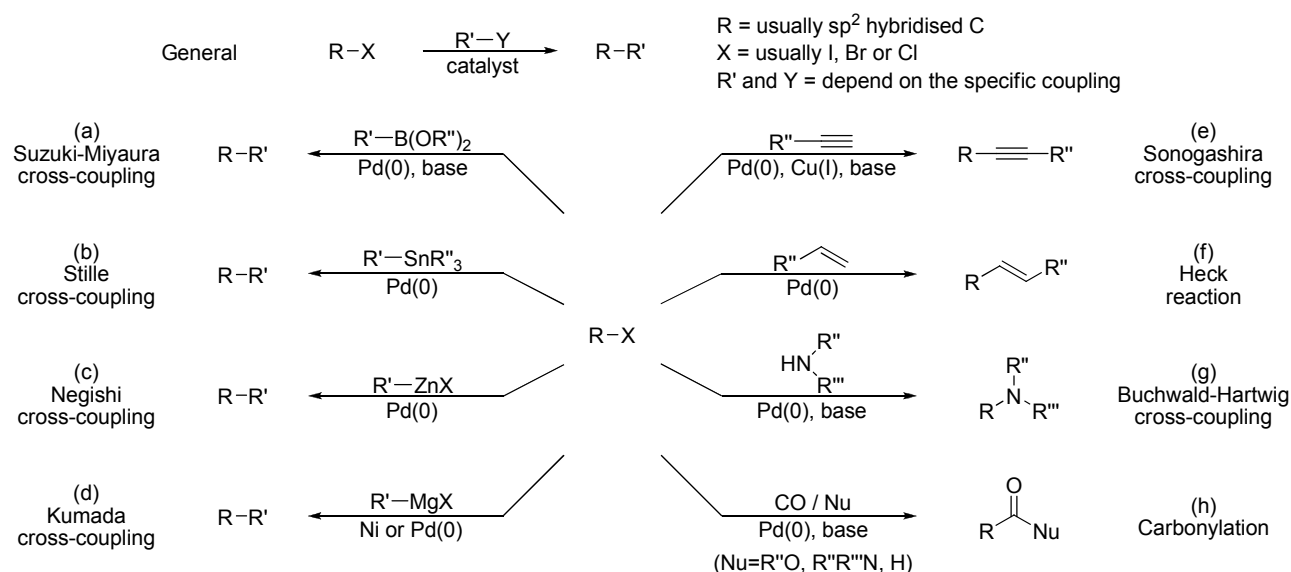
Among the collection of different substituents that can decorate the benzo[*b*]furan structure, our attention was drawn to two in particular: the halogens and the hydroxy groups.

1.1.3.2.1. Halogens

Starting with the halogen substituents, aryl chlorides, bromides, and iodides are present in a wide range of biologically active molecules. Indeed, some of the benzo[*b*]furans shown in the previous section (e.g. amiodarone, beclonazole or brofaromine) bear halogens in their structure. Nevertheless, generally one of the most relevant feature of the halogenated heterocycles (considering mainly Cl, Br, and I as halogen) is surely that they have become of significant value as building blocks in the synthesis of more complex (natural or unnatural) products, due to their reactivity and ease of derivatization.

Classically, aryl halides have been used as precursors to organolithium and Grignard reagents as well as in benzyne generation and nucleophilic aromatic substitution. More recently, these compounds have found widespread utility as substrates for transition metal (typically palladium and/or copper) catalyzed cross-coupling reactions. The most general

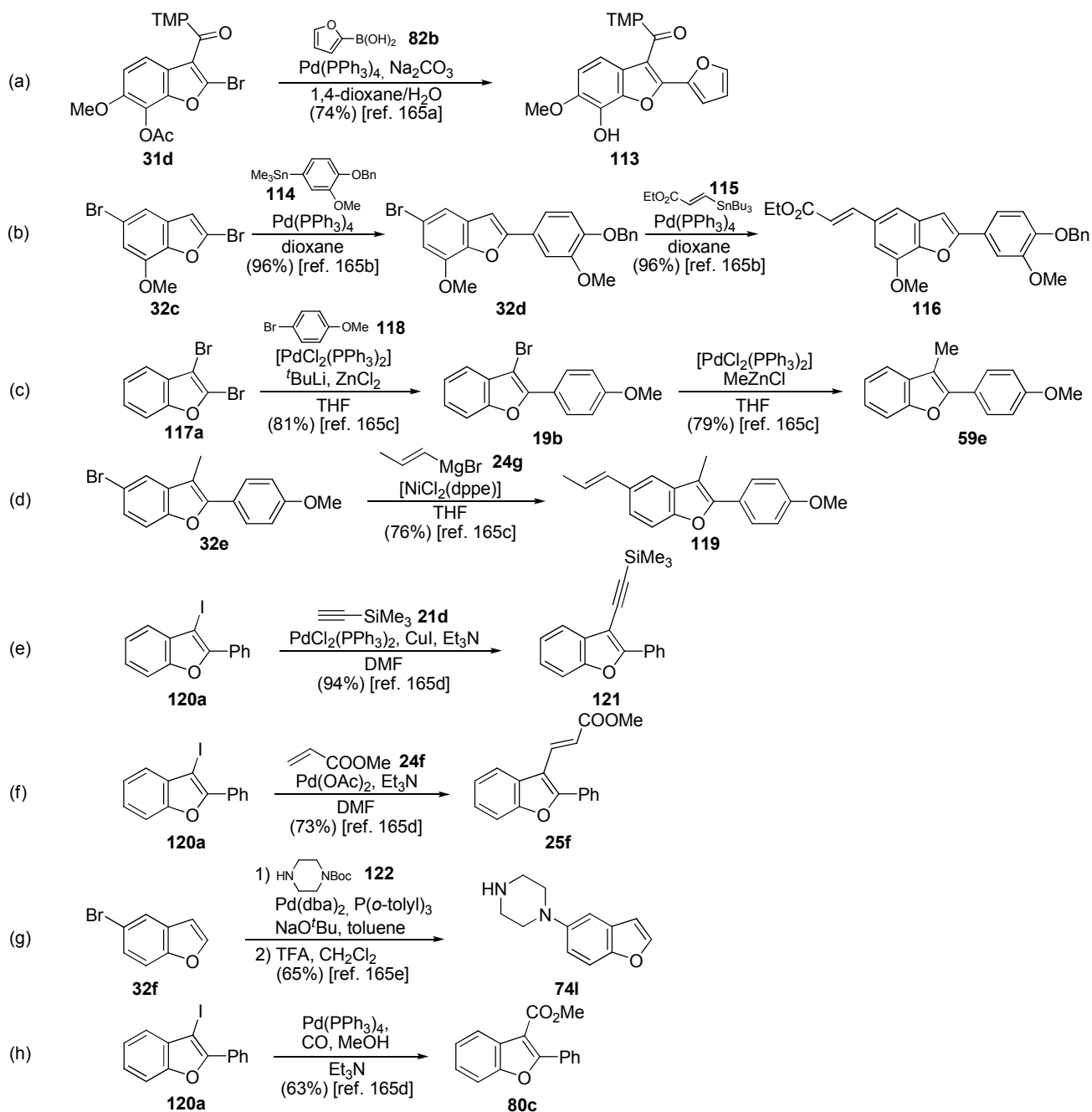
reaction scheme for a cross-coupling reaction is the one shown below, which adopts different names depending on the particular substrates employed (Scheme 1.49).



Scheme 1.49. General scheme and main types of cross-coupling reactions: (a) Suzuki (or Suzuki–Miyaura) cross-coupling: cross-coupling of organoboron compounds (typically boronic acids or esters) and carbon electrophiles (organohalides and their equivalents); (b) Stille cross-coupling: reaction of organostannanes with aryl halides (and other electrophiles); (c) Negishi cross-coupling: Pd-catalysed reactions of organozinc reagents with organohalides (and equivalents); (d) Kumada cross-coupling: cross coupling of organohalides with Grignard reagents (organomagnesium compounds); (e) Sonogashira cross-coupling: alkynylation of an aryl halide in which the alkyne moiety is usually introduced via its copper salt (generated *in situ*); (f) Heck (or Mirozoki-Heck) reaction: reaction of an unsaturated halide with an alkene and a base (typically Et_3N) in the presence of a palladium catalyst (usually $Pd(OAc)_2$) to form a substituted alkene; (g) Buchwald-Hartwig coupling: palladium catalysed coupling of aryl halides with amine nucleophiles in the presence of stoichiometric amounts of base to form a C–N bond; (h) Carbonylation: Palladium catalysed carbonylation, as an alternative to standard organolithium and Grignard chemistry for the formation of C–C bonds in the synthesis of aryl aldehydes, acids, esters and amides.

These displacements of halogen atoms, which can take place at almost all relevant carbon atoms of the benzofuran skeleton (being the substitution position unambiguously determined by the location of the halogen atom), have gained widespread use in both industrial and academic synthetic chemistry laboratories as a powerful methodology for the formation of diverse C–C and C–heteroatom bonds. Indeed, examples of all the main coupling reactions using benzo[*b*]furan halides were reported¹⁶⁵, which gives an idea of the great current and potential usefulness of these heterocyclic compounds bearing a halogen in their structure (Scheme 1.50).

¹⁶⁵ (a) Gill, G. S.; Grobelny, D. W.; Chaplin, J. H.; Flynn, B. L. *J. Org. Chem.* **2008**, *73*, 1131-1134 (b) Lin, S.-L.; Chen, C.-L.; Lee, Y.-J. *J. Org. Chem.* **2003**, *68*, 2968-2971 (c) Bach, T.; Bartels, M. *Synthesis* **2003**, *6*, 925-939 (d) Arcadi, A.; Cacchi, S.; Fabrizi, G.; Marinelli, F.; Moro, L. *Synlett* **1999**, *9*, 1432-1434 (e) Kerrigan, F.; Martin, C.; Thomas, G. H. *Tetrahedron Lett.* **1998**, *39*, 2219-2222



Scheme 1.50. Examples of halogenated benzo[*b*]furans participating in the main types of cross-coupling reactions: (a) Suzuki (or Suzuki–Miyaura) cross-coupling, (b) Stille cross-coupling, (c) Negishi cross-coupling, (d) Kumada cross-coupling, (e) Sonogashira cross-coupling, (f) Heck (or Mirozoki–Heck) reaction, (g) Buchwald–Hartwig coupling and (h) Carbonylation.

1.1.3.2.2. Hydroxy groups

The presence of hydroxy groups in certain positions confers on benzo[*b*]furans properties analogous in many ways to those of phenols. This makes them interesting starting materials and/or intermediates for transformations previously studied for phenols, which might have a similar or a different outcome, with the possible additional advantage (in terms of size and structural and/or configurational rigidity) of rendering bicyclic products.

However, the hydroxylated benzo[*b*]furans are often more interesting as such, due to the regular presence of hydroxy substituents in bioactive compounds (like the aforementioned cicerfuran or moracins). Indeed, many of these products resemble motifs present in naturally occurring plant (poly)phenols which usually play an important role in the natural defense mechanism of the plant¹⁶⁶.

Moreover, plant polyphenols have also been reported to be potentially useful in chemoprevention and/or chemotherapy of cancer, cardiovascular and metabolic disorders (like diabetes, obesity or high blood pressure) and neurological diseases (e.g. Alzheimer disease)¹⁶⁷. Not surprisingly, these compounds became promising structures in drug discovery. Among all of them (Figure 1.8), resveratrol (which will be considered more in depth in chapter 4) stands out as probably the best known (and most studied) compound of this kind in the last decades.

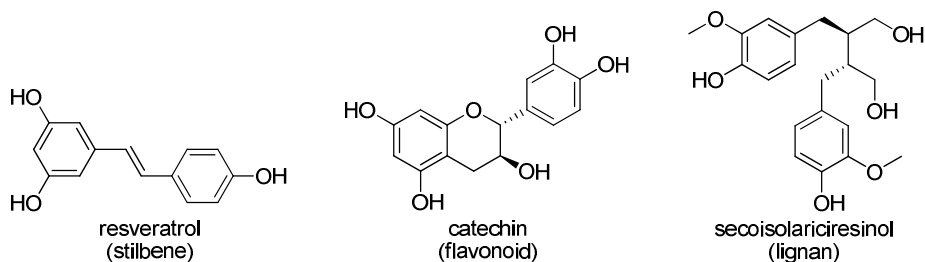


Figure 1.8. Examples of plant polyphenols belonging to different classes, indicated in brackets.

¹⁶⁶ Quideau, S.; Deffieux, D.; Douat-Casassus, C. and Pouységou, L. *Angew. Chem. Int. Ed.* **2011**, *50*, 586-621

¹⁶⁷ (a) Duthie, G. G.; Duthie, S. J.; Kyle, J. A. M. *Nutr. Res. Rev.* **2000**, *13*, 79-106 (b) Ferguson, L. R. *Mutat. Res.* **2001**, *475*, 89-111 (c) Stoclet, J.-C.; Chataigneau, T.; Ndiaye, M.; Oak, M.-H.; Schini-Kerth, V. B. *Eur. J. Pharmacol.* **2004**, *500*, 299-313 (d) Rivière, C.; Richard, T.; Vitrac, X.; Mérillon, J.-M.; Valls, J.; Monti, J.-P. *Bioorg. Med. Chem. Lett.* **2008**, *18*, 828-831 (e) Hwang, J.-T.; Kwon, D. Y.; Yoon, S. H. *N. Biotechnol.* **2009**, *26*, 17-22 (f) Ramos, S. *Mol. Nutr. Food Res.* **2008**, *52*, 507-526 (g) Pandley, K. B.; Rizvi, S. I. *Oxid. Med. Cell. Longev.*, **2009**, *2*, 270-278

1.2. OBJECTIVES

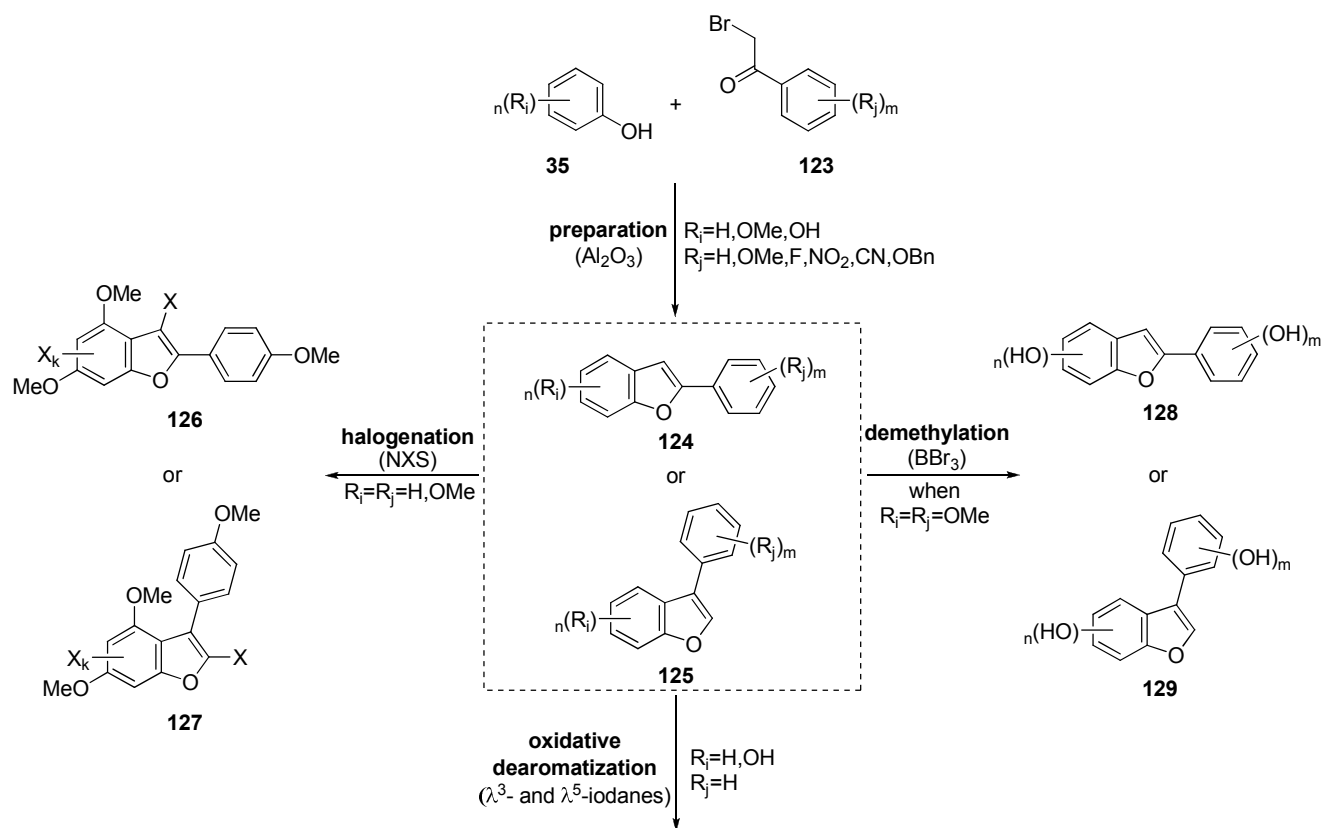
The objectives of the present Thesis work are aimed at the synthesis, functionalization and evaluation of some of the possible biological activities of 2-aryl and 3-aryl benzo[*b*]furan regioisomer families of compounds.

The first and foremost line of research is focused on the development of a synthesis procedure for the regioselective preparation of the two families of compounds. The second line gathers our efforts to assay different types of transformations with the preformed benzo[*b*]furans both to afford halogenated or polyhydroxylated derivatives and to explore their performance in hypervalent iodine-mediated oxidative dearomatization reactions. Finally, the last line of research consists of the evaluation of some biological activities of a selection of the synthesized products.

More specifically, the general objectives of this manuscript can be enumerated as follows:

1. Experimental and computational study of the alumina-mediated regioselective preparation of 2- or 3-aryl benzo[*b*]furan from phenols and α -bromoacetophenones.
2. Experimental and computational study of the *N*-halosuccinimide-mediated regioselective halogenation of the lead compounds of the prepared 2- and 3-aryl benzo[*b*]furan families.
3. Experimental study of the hypervalent iodine-based reagents-mediated oxidative dearomatization of 2- or 3-aryl benzo[*b*]furans hydroxylated in position 6 model compounds.
4. Preparation of polyhydroxylated 2- and 3-aryl benzo[*b*]furans as resveratrol analogues, via boron tribromide promoted demethylation reactions.
5. Evaluation of synthesized resveratrol analogues as SIRT-1 modulators (enzymatic assays).
6. Evaluation of synthesized resveratrol analogues as anticancer agents (cell-based assays).

A summary of the reactions studied in the present work is presented in Scheme 1.51.



Scheme 1.51. Summary of the reactions studied in the present Thesis work.

Each of these objectives and reactions will be considered more in depth in the opening section of the corresponding chapter.

Chapter 2:

Regioselective Preparation of 2- and 3-Aryl Benzo[*b*]furans

2.1. Short introduction and objectives

2.2. Experimental study: reaction conditions and products

2.2.1. General considerations

2.2.2. Optimization of the reaction conditions

2.2.3. Two families of compounds: 2-aryl and 3-aryl benzo[*b*]furans

2.2.4. Characterization: NMR spectroscopy study and X-ray diffraction analysis

2.2.5. Graphical overview

2.3. Computational study: mechanisms

2.3.1. General considerations

2.3.2. Reaction path in the absence of alumina

2.3.3. Reaction path in the presence of alumina

2.3.4. Graphical overview

2.4. Broadening the scope of the reaction: naphthofuran synthesis

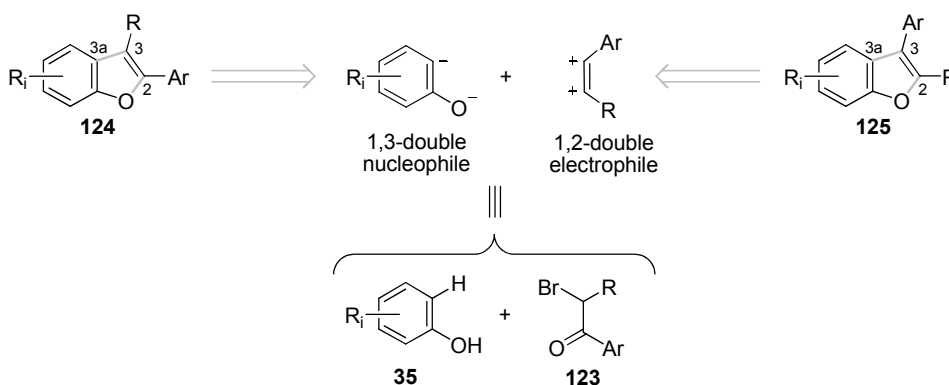
2.4.1. Experimental study

2.4.2. Insight into the reaction mechanism

2.5. Conclusions

2.1. SHORT INTRODUCTION and OBJECTIVES

The benzo[*b*]furan synthesis method described in this chapter relies on the double nucleophilic/electrophilic character of the reactants coming from the double disconnection of the O₁–C₂ and C₃–C_{3a} bonds, which is of special relevance in terms of convergence. The corresponding synthetic equivalents are an *ortho*-unsubstituted phenol **35** and an α -bromoacetophenone **123**, commercially available or very easily accessible (Scheme 2.1). The main issue associated with this approach is the control of the regioselectivity of the process in order to obtain either 2- or 3- substituted benzo[*b*]furans using the same reactants as starting materials.



Scheme 2.1. Proposed retrosynthetic analysis for 2-aryl and 3-aryl benzo[*b*]furans, based on the disconnection of O₁–C₂ and C₃–C_{3a} bonds.

Bearing this general scheme in mind, the objectives of this chapter are:

- First, to explore the reaction conditions to regioselectively obtain both 2-aryl and 3-aryl benzo[*b*]furans starting from phenols **35** and 2-bromoacetophenones **123**. This issue is covered in section **2.2. Experimental study: reaction conditions and products**.
- Next, to provide reasonable reaction paths to understand the formation of these compounds, based on DFT calculations. This matter is raised in section **2.3. Computational study: mechanisms**.
- And finally, to study the suitability of the developed synthesis methods for the preparation of naphthofurans. This subject is addressed in section **2.4. Broadening the scope of the reaction: naphthofuran synthesis**.

2.2. EXPERIMENTAL STUDY: REACTION CONDITIONS and PRODUCTS

2.2.1. General considerations

When the issue of under which reaction conditions the synthesis of benzo[*b*]furans should be carried out was first considered, our initial approach was to try to combine two features that had already shown significant advantages in organic synthesis: the use of microwave irradiation and the employment of alumina.

Microwave Irradiation

Microwave assisted heating under controlled conditions has proved to drastically reduce reaction times and, in many cases, to provide higher yields, lower cost, easy workups, greater purity and less side reactions compared to conventional thermal methods. Therefore, many academic and industrial research groups have been and are using microwave assisted organic synthesis (MAOS) for rapid optimization of reactions, for the efficient synthesis of new chemical scaffolds and for discovering and probing new chemical reactivity¹⁶⁸.

Microwave irradiation is electromagnetic irradiation in the frequency range of 0.3 to 300 GHz, being 2.45 GHz (12.24 cm wavelength) the operation frequency of all domestic ovens and dedicated reactors for chemical synthesis. Microwave enhanced chemistry is based on the efficient heating of materials by “microwave dielectric heating”. The electric component of an electromagnetic field causes heating by two main mechanisms: dipolar polarization and ionic conduction. When a sample is irradiated at microwave frequencies, its dipoles or ions align themselves with the applied field. As this field oscillates, the dipole or ion field attempts to realign itself with the alternating electric field. The amount of heat generated by this process is directly related to the ability of the solvent, reagent or catalyst to align itself with the frequency of the applied field, as the reaction vessels employed are usually made out of nearly microwave-transparent materials (borosilicate glass, quartz, or teflon).

¹⁶⁸ (a) Srinivasan, K. V.; Chaskar, P. K.; Dighe, S. N.; Rane, D. S.; Khade, P. V.; Jain, K. S. *Heterocycles* **2011**, *83*, 2451-2488; (b) Kappe, C. O. *Angew. Chem. Int. Ed.* **2004**, *43*, 6250-6284 (c) Appukkuttan, P.; Mehta, V. P.; Van der Eycken, E. V. *Chem. Soc. Rev.* **2010**, *39*, 1467-1477; (d) Suna, E.; Mutule, I. *Top Curr. Chem.* **2006**, *266*, 49-101; (e) Hayes, B. L. *Aldrichimica Acta* **2004**, *37*, 66-77

Therefore, making use of this internal heating method, the wall effects are minimized as a result of the inverted temperature gradient compared to conventional conductive thermal heating (with an external heat source), which depends on the thermal conductivity of the various materials that must be penetrated (Figure 2.1)^{168b,169}. Although microwave effects are not truly in-depth understood yet (and are still subject of considerable debate and controversy), most scientists agree that in the majority of cases the reason for the observed rate enhancements is a purely thermal/kinetic effect, that is to say, a consequence of the high reaction temperatures that can rapidly be reached irradiating polar materials in a microwave field^{168b, 169b-f}.

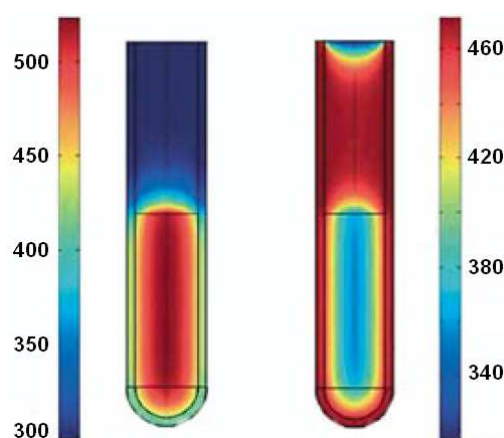


Figure 2.1. Inverted temperature gradients in microwave versus oil-bath heating: Difference in the temperature profiles after 1 min of microwave irradiation (left) and treatment in an oil bath (right). Temperature scale is in Kelvin. Figure taken from reference 169.

Microwave irradiation has been successfully applied to synthesize a wide range of organic compounds in recent years¹⁶⁸. In particular, the formation of heterocyclic rings by cycloaddition or cyclocondensation reactions is typically a process well-suited for microwave technology. Many of these reactions require high temperatures (conventional reaction conditions very often involve heating the reactants in an oil, metal, or sand bath for many hours) or are strongly favored when carried out under relatively high pressure. In our research group, for example, this source of energy has lately given access to several families of compounds¹⁷⁰.

¹⁶⁹ (a) Dal Santo, V.; Liguori, F.; Pirovano, C.; Guidotti, M. *Mol. Diversity* **2003**, *7*, 293-300 (b) Herrero, M. A.; Kremsner, J.M.; Kappe, C.O. *J. Org. Chem.* **2008**, *73*, 36-47; (c) de la Hoz, A.; Díaz-Ortiz, A.; Moreno, A. *Chem. Soc. Rev.* **2005**, *34*, 164-178; (d) Leadbeater, N.E.; Pillsbury, S. J.; Shanahan, E.; Williams, V. A. *Tetrahedron* **2005**, *61*, 3565-3585; (e) Kuhnert, N. *Angew. Chem. Int. Ed.* **2002**, *41*, 1863-1866; (f) Perreux, L.; Loupy, A. *Tetrahedron* **2001**, *57*, 9199-9223

¹⁷⁰ (a) Aginagalde, M.; Bello, T.; Masdeu, C.; Vara, Y.; Arrieta, A.; Cossío, F. P. *J. Org. Chem.* **2010**, *75*, 7435-7438; (b) Aginagalde, M.; Vara, Y.; Arrieta, A.; Zangi, R.; Cebolla, V. L.; Delgado-Camón, A.; Cossío, F. P. *J. Org. Chem.* **2010**, *75*, 2776-2784; (c) Vara, Y.; Aldaba, E.; Arrieta, A.; Pizarro, J. L.; Arriortua, M. I.; Cossío, F. P. *Org. Biomol. Chem.* **2008**, *6*, 1763-1772; (d) Arrieta, A.; Otaegui, D.; Zubia, A.; Cossío, F. P.;

Alumina

Alumina (aluminium oxide, Al_2O_3) has a rich chemistry as solid support possessing a Lewis acid character on the aluminium. Like heterogeneous catalysts, solid supports offer some complications (mainly uncertainties in active site structures and in the percentages of surface structures which are relevant for chemical transformations) but many contrasting attractions: extraordinary degrees of coordinative unsaturation, high reactivity, thermal robustness and ease of handling, separation and recycling¹⁷¹.

Solvent-free approaches that involve microwave exposure of neat reactants catalyzed by the surface of mineral supports (including alumina, silica gel, clay or “doped” surfaces), have been applied to a wide range of organic reactions. In addition, the limitations of the microwave-assisted reactions in solution, namely the development of high pressure and need for specialized sealed vessels, have been partly avoided via this solid support strategy¹⁷².

Among the different aluminas known, γ -alumina ($\gamma\text{-Al}_2\text{O}_3$) is perhaps the most important with direct applications as a catalyst and support. It is obtained by thermal dehydration (calcination) of aluminium hydroxides. The structure of $\gamma\text{-Al}_2\text{O}_3$ is considered as a cubic defect spinel type where the oxygen lattice is built up by a cubic close-packed stacking of oxygen layers, with Al atoms occupying the octahedral (cubic) and tetrahedral sites. To satisfy the $\gamma\text{-Al}_2\text{O}_3$ stoichiometry, some of the lattice positions remain empty (vacancies).

Removal of OH groups during high temperature treatments creates coordinatively unsaturated surface cations where tetrahedral (T, Al_{IV}) and octahedral or cubic (C, Al_{VI}) aluminium coordinations are the most widely accepted (Figure 2.2). The partly uncoordinated metal cations that lie at the surface of $\gamma\text{-Al}_2\text{O}_3$ can act as acids, according to the Lewis definition (electron pair acceptors).

Díaz-Ortiz, A.; de la Hoz, A.; Herrero, M. A.; Prieto, P.; Foces-Foces, C.; Pizarro, J. L.; Arriortua, M. I. *J. Org. Chem.* **2007**, *72*, 4313-4322

¹⁷¹ (a) Motta, A.; Fragalà, I. L.; Marks, T. J. *J. Am. Chem. Soc.* **2008**, *130*, 16533-16546; (b) Joubert, J.; Delbecq, F.; Sautet, P.; Le Roux, E.; Taoufik, M.; Thieuleux, C.; Blanc, F.; Copéret, C.; Thivolle-Cazat, J.; Basset, J. M. *J. Am. Chem. Soc.* **2006**, *128*, 9157-9169 (c) Sautet, P.; Delbecq, F. *Chem. Rev.* **2010**, *110*, 1788-1806

¹⁷² (a) Dandia, A.; Singh, R.; Khaturia, S. *Bioorg. Med. Chem.* **2006**, *14*, 1303-1308; (b) Kidwai, M.; Ruby; Venkataramanan, R. *Chem. Heterocycl. Compd.* **2004**, *40*, 631-634; (c) Suarez, M.; Loupy, A.; Perez, E.; Moran, L.; Gerona, G.; Morales, A.; Autie, M. *Heterocycl. Commun.* **1996**, *2*, 275-280; (d) Varma, R. S. *Green. Chem.* **1999**, *6*, 43-55

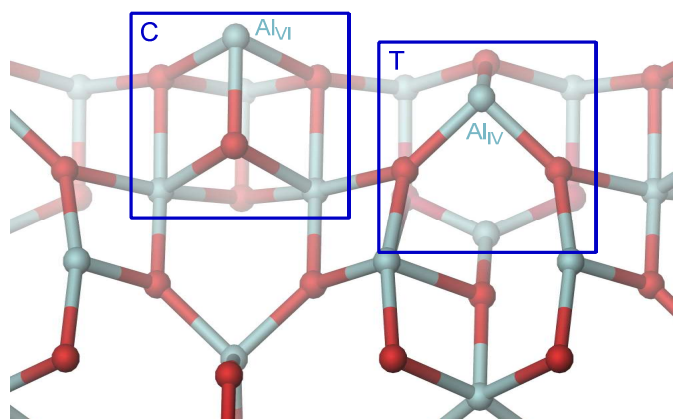


Figure 2.2. Tetrahedral (T) and cubic (C) environments for aluminium in $\gamma\text{-Al}_2\text{O}_3$ surface. Aluminium and oxygen atoms are represented in light blue and red respectively. Structural data taken from reference 171a.

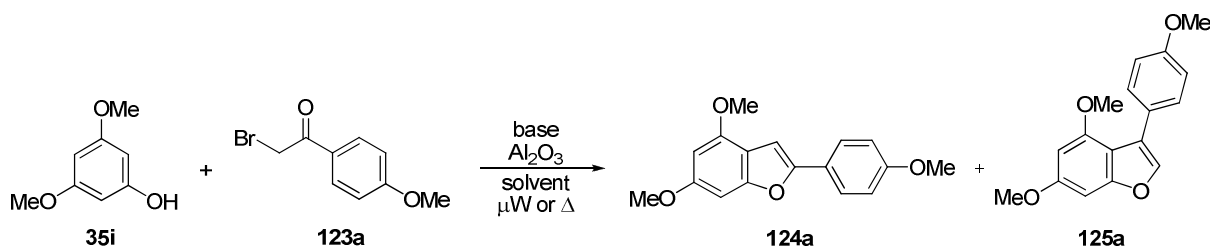
Taking into account the different transformations organic functional groups undergo with nucleophilic reagents in the presence of acid as catalysts, the fact that alumina shows Lewis acid sites makes it even a more interesting support since it might promote nucleophilic addition reactions towards heterocycle synthesis¹⁷³.

¹⁷³ (a) Trueba, M.; Trasatti, S. P. *Eur. J. Inorg. Chem.* **2005**, 3393-3403 (b) Corma, A.; García, H. *Chem. Rev.* **2003**, *103*, 4307-4365; (c) Lin, J. R.; Gubaidullin, A. T.; Mamedovb, V. A.; Tsuboi, S. *Tetrahedron* **2003**, *59*, 1781-1790

2.2.2. Optimization of the reaction conditions

Prompted by the encouraging precedents just reported and within our interest on the synthesis of benzo[*b*]furans as privileged structures in Medicinal Chemistry, an attempt was made to prepare these compounds under microwave irradiation and employing alumina as solid support and activating Lewis acid by varying different parameters reported below.

In the case of the phenols **35**, the position(s) at which electron-releasing group(s) is(are) installed on the reacting aromatic system may have an influence on the activation of the corresponding *ortho*-centers. Taking this into account, to start with 3,5-dimethoxyphenol **35i** and 2-bromo-4'-methoxyacetophenone **123a** were selected as reactants (starting materials, SM) to look for the best reaction conditions. In principle, the formation of both regioisomers could be expected by this means (Scheme 2.2).



Scheme 2.2. Optimization reaction for the synthesis of 2- and 3-aryl benzo[*b*]furans, expected reaction products mixture.

The optimization was carried out attending different parameters: the use of an organic base and alumina; the proportion of reactants; the temperature and time of the reaction; the use and choice of a convenient solvent; the heating method, thermal heating or microwave irradiation; the use of different Lewis acids and the addition of potassium carbonate (inorganic base).

Firstly, the reaction was carried out without any additive, next incorporating an organic base, such as triethylamine or pyridine and then replacing the base with alumina. The best result was obtained when only alumina was added (Table 2.1).

Table 2.1. Optimization parameter: use of an organic base and alumina. (General reaction conditions: microwave irradiation, solvent-free, 150 °C, 10 min, 100 W, 2 eq **35i**, 1 eq **123a**, 1 mmol scale)

entry	base	Al ₂ O ₃ (eq)	yield (%)
1	-	-	<5
2	Et ₃ N	-	<5
3	pyr	-	<10
4	-	5	15

The following step was to decide the appropriate amount of alumina with respect to the reactants. In a preliminary scan, 0.5, 5 and 10 equivalents were tried and it was concluded that the most suitable proportion was 5 equivalents of alumina per mol of bromoacetophenone, since exceeding this amount of alumina did not result in a higher yield (Table 2.2).

Table 2.2. Optimization parameter: equivalents of alumina. (General reaction conditions: microwave irradiation, solvent-free, 150 °C, 10 min, 100 W, 2 eq **35i**, 1 eq **123a**, 1 mmol scale)

entry	Al ₂ O ₃ (eq)	yield (%)
1	0.5	<5
2	5	15
3	10	15

With regard to the proportion of phenol and bromoacetophenone (**35i:123a**), neither the excess of phenol employed in the initial trials (2:1) nor the excess of bromoacetophenone tested later (1:2) proved to significantly improve the yield of the reaction over the use of equimolecular amounts of reactants (1:1) (Table 2.3).

Table 2.3. Optimization parameter: proportion of reactants. (General reaction conditions: microwave irradiation, solvent-free, 150 °C, 10 min, 100 W, 5 eq of Al₂O₃, 1 mmol scale)

entry	35i (eq)	123a (eq)	yield (%)
1	2	1	15
2	1	1	15
3	1	2	15

Then temperature was taken into consideration and the reaction was performed at three different temperatures. 120 °C turned out to be the optimum one amongst the conducted experiments (Table 2.4).

Table 2.4. Optimization parameter: temperature. (General reaction conditions: microwave irradiation, solvent-free, 10 min, 100 W, 5 eq of Al₂O₃, 1 eq **35i**, 1 eq **123a**, 1 mmol scale)

entry	T (°C)	yield (%)
1	150	15
2	120	25
3	100	20

On looking at the time parameter, the results obtained in 10 minutes, in 20 minutes and in four pulses of 2.5 minutes were compared. It was observed that neither longer reaction times nor pulse strategy led to a better outcome and 10 minutes irradiation stood out as the best option (Table 2.5).

Table 2.5. Optimization parameter: time. (General reaction conditions: microwave irradiation, solvent-free, 100 W, 5 eq of Al₂O₃, 1 eq **35i**, 1 eq **123a**, 1 mmol scale)

entry	T (°C)	time (min)	yield (%)
1	100	10	20
2	100	20	20
3	120	10	25
4	120	4x2.5	17

The suitability of introducing a solvent was then weighted up. To this end, xylene was selected due to its convenient boiling point, 138 °C, and ability to dissolve both reactants. The reaction was carried out with and without this solvent at different temperatures and in all the cases the introduction of xylene resulted in higher yields (Table 2.6).

Table 2.6. Optimization parameter: use of solvent. (General reaction conditions: microwave irradiation, 10 min, 100 W, 5 eq of Al₂O₃, 1 eq **35i**, 1 eq **123a**, 1 mmol scale)

entry	solvent	T (°C)	yield (%)
1	-	150	15
2	xylene	150	33
3	-	120	25
4	xylene	130	35

The heating method was also assessed. The best results obtained so far under microwave irradiation, both without solvent and with xylene, were assayed under thermal heating for that purpose. It was observed that in the absence of solvent thermal heating led to a lower yield whilst in the presence of xylene it made the reaction work better, giving the highest yield obtained so far (Table 2.7).

Table 2.7. Optimization parameter: heating method. (General reaction conditions: 5 eq of Al₂O₃, 1 eq **35i**, 1 eq **123a**, 1 mmol scale)

entry	heating method	solvent	T (°C)	time (min)	yield (%)
1	μW (100 W)	-	120	10	25
2	Δ	-	120	180	16
3	μW (100 W)	xylene	130	10	35
4	Δ	xylene	138	180	40

In view of the higher yield obtained in the thermal heating reaction in xylene, the reaction was tried in other solvents reflux in order to evaluate the effect of a different polarity (E_T^N) and/or temperature (boiling point). The tested solvents were ethanol and diglyme (diethylene glycol dimethyl ether) but, regrettably, none of them yielded the product under these reaction conditions (Table 2.8).

Table 2.8. Optimization parameter: choice of solvent. E_T^N data from ref 174. (General reaction conditions: thermal heating, 180 min, 5 eq of Al₂O₃, 1 eq **35i**, 1 eq **123a**, 1 mmol scale)

entry	solvent	E_T^N	T (°C)	yield (%)
1	xylene	0.074	138	40
2	EtOH	0.654	78	-
3	diglyme	0.244	162	-

Bearing in mind the theoretical reasons behind adding alumina to this reaction (explained in section 2.2.1) and the experimental step forward that it had meant, the possibility of replacing it with other Lewis acids was explored. With the hitherto optimized conditions, several Lewis acids were assayed but, unfortunately, they did not lead to the desired product(s). Then the amount of alumina was readjusted and 7 equivalents turned out to be the optimum (Table 2.9).

¹⁷⁴ Reichardt, C. *Chem Rev.* **1994**, *94*, 2319-2358

Table 2.9. Optimization parameter: Lewis acid. (General reaction conditions: thermal heating, xylene, 138 °C reflux, 180 min, 1 eq **35i**, 1 eq **123a**, 3 mmol scale)

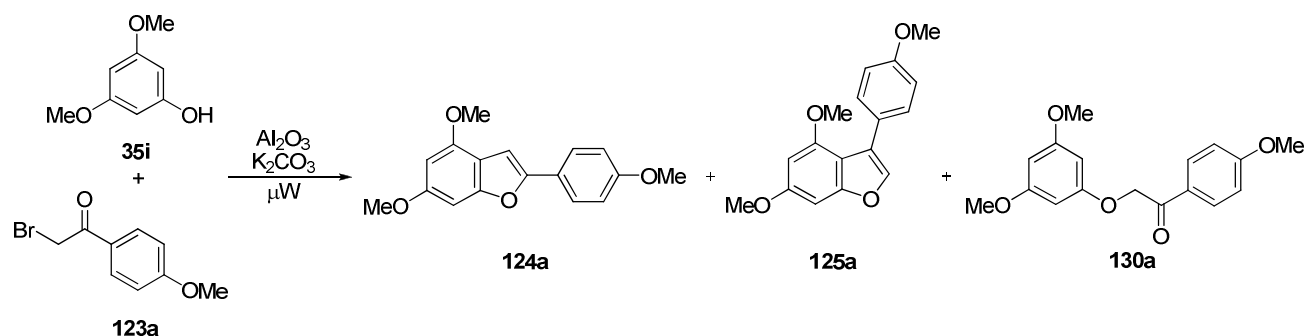
entry	Lewis acid	Lewis acid (eq)	yield (%)
1	TsOH·H ₂ O	5	-
2	AlCl ₃	5	-
3	MgBr ₂	5	polimerization
4	Al ₂ O ₃	5	40
5	Al ₂ O ₃	3	37
6	Al ₂ O ₃	7	42

Quite surprisingly, all the experiments described so far, when successful, led to the exclusive formation of 2-aryl benzo[*b*]furans, the possible 3-substituted regioisomers were not detected in the crude reaction mixtures. Having achieved this complete regiocontrol towards the formation of the 2-aryl benzo[*b*]furans, our attention was drawn to the moderate yields of the reaction.

Assuming that in the first step a nucleophilic attack from the phenolic oxygen took place, a further bibliographical research was conducted, in an attempt to find a reactant that could favor this step. The inorganic base potassium carbonate stood out as the most promising additive, since it promoted the synthesis of α -phenoxyketones starting from phenols and α -bromacetophenones with quantitative yields in most cases. So in the next trials potassium carbonate was incorporated, both in the presence and in the absence of alumina, following the optimized microwave irradiation solvent-free procedure.

On looking at the products of the different experiments it was observed that, under the same conditions, when only alumina was added, the 2-substituted benzofuran (**124a**) was obtained exclusively. The addition of both alumina and potassium carbonate yielded a mixture of 2-substituted benzofuran (**124a**), 3-substituted benzofuran (**125a**) and α -phenoxyketone (**130a**). And when only potassium carbonate was added, α -phenoxyketone (**130a**) was the only observed product, in agreement with procedures already reported in literature¹⁷⁵ (Scheme 2.3, Table 2.10).

¹⁷⁵ Leadbeter, N. E.; Schmink, J. R. *Tetrahedron* **2007**, 63, 6764-6773

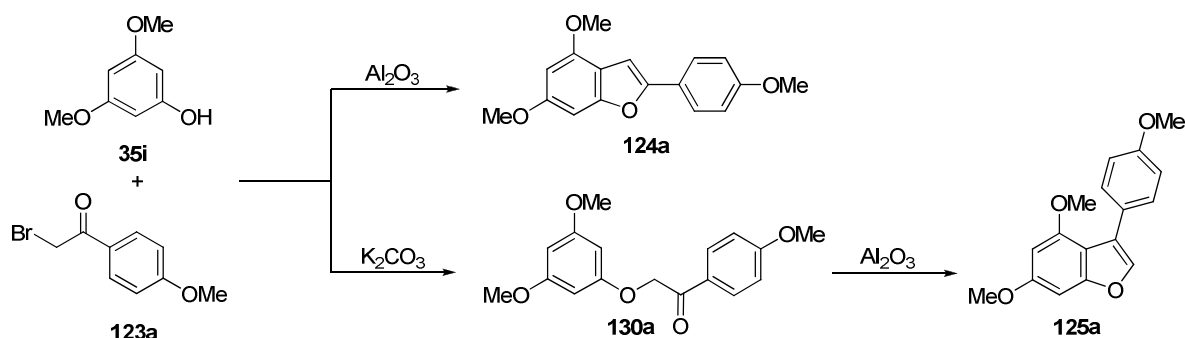


Scheme 2.3. Al₂O₃ and K₂CO₃ promoted synthesis of 2- and 3-aryl benzo[*b*]furans: experimentally obtained mixture of products.

Table 2.10. Optimization parameter: use of potassium carbonate. (General reaction conditions: microwave irradiation, 120 °C, 10 min, 100 W, 1 eq **35i**, 1 eq **123a**, 1 mmol scale)

entry	Al ₂ O ₃ (eq)	K ₂ CO ₃ (eq)	124a yield (%)	125a yield (%)	130a yield (%)
1	7	-	25	-	-
2	7	2	8	22	44
3	-	2	-	-	60

During the development of this project, Jing et al. reported a one-pot reaction between phenols and 2-bromoacetophenones for the synthesis of 3-substituted benzo[*b*]furans combining potassium carbonate and alumina under microwave irradiation¹⁷⁶. Our results suggested that alumina promotes the synthesis of 2-substituted benzofuran (**124a**) and the cyclization of α -phenoxyketone (**130a**) into 3-substituted benzofuran (**125a**), once the ether **130a** is formed with the aid of potassium carbonate (Scheme 2.4).



Scheme 2.4. Al₂O₃ and K₂CO₃ promoted synthesis of 2- and 3-aryl benzo[*b*]furans: reaction scheme proposal.

¹⁷⁶ Wang, Z.; Gu, J.; Jing, H.; Liang, Y. *Synth. Commun.* **2009**, *39*, 4079-4087

Encouraged by this finding, we decided to assay the reactions with other bromoacetophenones and/or other phenols in order to synthesize compounds of both 2-aryl and 3-aryl benzo[*b*]furan families.

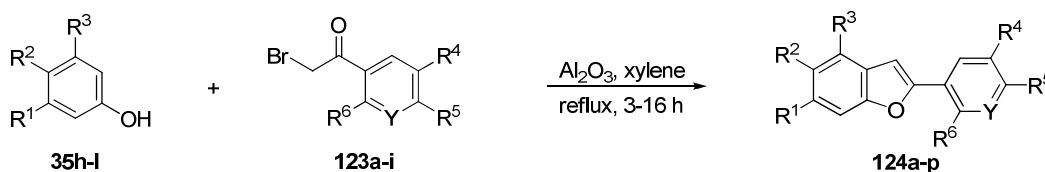
In the last experiments for the synthesis of 2-aryl benzofurans **124** it had been observed that the reaction was not complete as some unreacted phenol remained in the crude mixture along with some acetophenone, as degradation product of bromoacetophenone. In order to improve this result, one last optimization consisted of carrying out the reaction adding a slight excess of bromoacetophenone. 1.2, 1.4 and 1.6 equivalents were tried and 1.4 stood out as the best option (Table 2.11, entry 3).

Table 2.11. Optimization parameter: equivalents of bromoacetophenone **123a**. (General reaction conditions: thermal heating, xylene, 138 °C reflux, 180 min, 7 eq of Al₂O₃, 1 eq **35i**, 3 mmol scale)

entry	123a (eq)	yield (%)
1	1.0	42
2	1.2	45
3	1.4	50
4	1.6	50

2.2.3. Two families of compounds: 2-aryl and 3-aryl benzo[*b*]furans

Starting with the 2-aryl benzofurans **124**, the yields were in general moderate but acceptable given the availability of the starting materials (Scheme 2.5, Table 2.12). In some cases, depending on the starting materials, it was observed that the reaction was not complete within 3 hours: some unreacted phenol and bromoacetophenone remained in the crude mixture. In order to overcome this drawback, reactions were monitored by TLC and refluxed for longer time (up to 16 hours), when necessary.



Scheme 2.5. Preparation of 2-aryl benzo[*b*]furans **124a-p** from phenols **35h-l** and 2-bromoacetophenones **123a-i** in the presence of neutral alumina.

Table 2.12. Synthesis of 2-aryl benzo[*b*]furans **124a-p** from phenol **35h-l** and 2-bromoacetophenones **123a-i**. (Optimized reaction conditions: thermal heating, xylene, 138 °C reflux, 180 min, 7 eq of Al₂O₃, 1 eq **35h-l**, 1.4 eq **123a-i**, 3 mmol scale)

entry	reaction	R ¹	R ²	R ³	Y	R ⁴	R ⁵	R ⁶	yield ^a (%)
1	35i + 123a → 124a	OMe	H	OMe	CH	H	OMe	H	50
2	35i + 123b → 124b	OMe	H	OMe	COMe	OMe	H	H	86
3	35i + 123c → 124c	OMe	H	OMe	COMe	OMe	OMe	H	75
4	35j + 123b → 124d	OH	H	H	COMe	OMe	H	H	26
5	35j + 123a → 124e	OH	H	H	CH	H	OMe	H	32
6	35i + 123d → 124f	OMe	H	OMe	CH	OMe	H	OMe	25
7	35i + 123e → 124g	OMe	H	OMe	CH	H	NO ₂	H	44
8	35i + 123f → 124h	OMe	H	OMe	CH	H	CN	H	24
9	35i + 123g → 124i	OMe	H	OMe	CH	H	F	H	49
10	35i + 123h → 124j	OMe	H	OMe	CF	F	H	H	46
11	35i + 123i → 124k	OMe	H	OMe	N	H	OMe	OMe	53
12	35k + 123b → 124l	OMe	OMe	OMe	COMe	OMe	H	H	9
13	35k + 123c → 124m	OMe	OMe	OMe	COMe	OMe	OMe	H	11
14	35k + 123a → 124n	OMe	OMe	OMe	CH	H	OMe	H	10
15	35h + 123a → 124o	H	H	H	CH	H	OMe	H	-
16	35l + 123a → 124p	Cl	H	Cl	CH	H	OMe	H	-

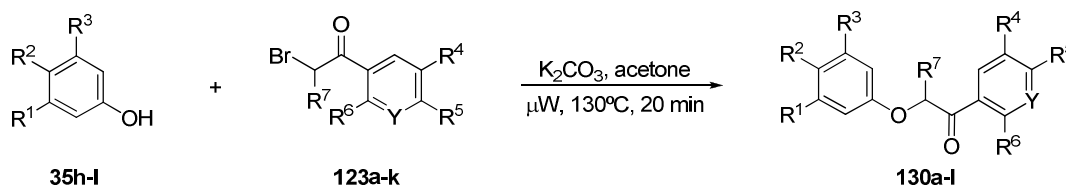
^aYield of isolated pure product after column chromatography.

Phenol itself and phenols incorporating electron-withdrawing groups did not react under these conditions (Table 2.12, entries 15-16). On the contrary, the best results were obtained when electron-releasing methoxy groups were present in the starting phenol **35**. The aryl group of reactant **123** tolerates both electron-releasing and electron-withdrawing groups (Table 2.12, entries 7-10, compounds **124g-j**). A pyridyl group can also be incorporated in the reaction product (Table 2.12, entry 11, compound **124k**).

Resorcinol **35j** reacts under these conditions to yield only products resulting from the reaction with 1 equivalent of **123a,b** (Table 2.12, entries 4 and 5, compounds **124d-e**). Attempts to obtain the products associated with the double condensation met with no success. Moreover, analysis of the reaction mixtures did not permit the detection of the regioisomer in which the furan ring is fused at the *ortho* position in between the two oxygen atoms of resorcinol.

The reaction was then performed using potassium carbonate as additive instead of alumina, employing 2 equivalents of base and acetone as solvent. In contrast with the preceding reaction, microwave irradiation gave the same (or slightly better) yields and lower reaction times with respect to thermal heating. Thus, the reaction in acetone in a sealed vessel with an external bath at 130°C required 3 h to complete whereas microwave irradiation under the same conditions required only 20 min.

Under these moderately basic optimized conditions, the corresponding ethers **130** were obtained in good to excellent yields (Scheme 2.6, Table 2.13), with the exception of compounds **130i** and **130j** (Table 2.13, entries 9-10). When the reaction involved α -methyl bromoacetophenone **123k**, the corresponding ether **130h** was obtained in good yield (Table 2.13, entry 8).



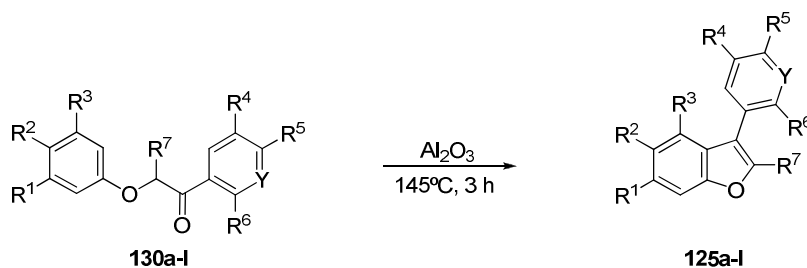
Scheme 2.6. Preparation of ethers **130a-l** from phenols **35h-l** and 2-bromoacetophenones **123a-k** in the presence of potassium carbonate.

Table 2.13. Synthesis of ethers **130a-l** from phenols **35h-l** and 2-bromoacetophenones **123a-k**. (Reaction conditions¹⁷⁵: microwave irradiation, acetone, 130 °C, 100-400 W, 20 min, 2 eq of K₂CO₃, 1 eq **35h-l**, 1 eq **123a-k**, 2 mmol scale)

entry	reaction	R ¹	R ²	R ³	Y	R ⁴	R ⁵	R ⁶	R ⁷	yield ^a (%)
1	35i + 123a → 130a	OMe	H	OMe	CH	H	OMe	H	H	99
2	35i + 123b → 130b	OMe	H	OMe	COMe	OMe	H	H	H	93
3	35i + 123c → 130c	OMe	H	OMe	COMe	OMe	OMe	H	H	99
4	35i + 123g → 130d	OMe	H	OMe	CH	H	F	H	H	97
5	35i + 123j → 130e	OMe	H	OMe	COBn	OBn	H	H	H	99
6	35i + 123f → 130f	OMe	H	OMe	CH	H	CN	H	H	99
7	35i + 123i → 130g	OMe	H	OMe	N	H	OMe	OMe	H	73
8	35i + 123k → 130h	OMe	H	OMe	CH	H	H	H	Me	84
9	35i + 123h → 130i	OMe	H	OMe	CF	F	H	H	H	24
10	35k + 123j → 130j	OMe	OMe	OMe	COBn	OBn	H	H	H	20
11	35h + 123a → 130k	H	H	H	CH	H	OMe	H	H	99
12	35l + 123a → 130l	Cl	H	Cl	CH	H	OMe	H	H	99

^aYield of isolated pure product after filtration, precipitation and/or column chromatography.

Next the cyclization of these ethers was carried out. Thermal heating of a dispersion of α -alkoxy ethers **130** in alumina (after optimization, 17 equivalents per equivalent of ether) yielded the corresponding 3-aryl benzo[*b*]furans **125** (Scheme 2.7, Table 2.14). When this cyclization was performed under microwave irradiation or in refluxing xylene, lower yields were obtained. Using the best reaction conditions, the observed yields of pure compounds **125** were, in general, moderate with the exception of densely substituted compound **125g** (Table 2.14, entry 7) and compound **125e** including two bulky benzyloxy groups (Table 2.14, entry 5). In the case of 2,3-disubstituted benzo[*b*]furan **125h** (Table 2.14, entry 8), the yield was also moderate but acceptable given the availability of the starting materials. Bulky benzyloxy groups including ether **130j**, unsubstituted phenol derivative **130k** and chlorinated ether **130l** did not react under these reaction conditions (Table 2.14, entries 10-12).



Scheme 2.7. Preparation of 3-aryl benzo[*b*]furans **125a-l** from ethers **130a-l** in the presence of neutral alumina.

Table 2.14. Synthesis of 3-aryl benzo[*b*]furans **125a-l** from ethers **130a-l**. (Optimized reaction conditions: thermal heating, 150 °C, 180 min, 17 eq of Al₂O₃, 1 eq **130a-l**, 2 mmol scale)

entry	reaction	R ¹	R ²	R ³	Y	R ⁴	R ⁵	R ⁶	R ⁷	yield ^a (%)
1	130a → 125a	OMe	H	OMe	CH	H	OMe	H	H	78
2	130b → 125b	OMe	H	OMe	COMe	OMe	H	H	H	54
3	130c → 125c	OMe	H	OMe	COMe	OMe	OMe	H	H	50
4	130d → 125d	OMe	H	OMe	CH	H	F	H	H	72
5	130e → 125e	OMe	H	OMe	COBn	OBn	H	H	H	26
6	130f → 125f	OMe	H	OMe	CH	H	CN	H	H	42
7	130g → 125g	OMe	H	OMe	N	H	OMe	OMe	H	12
8	130h → 125h	OMe	H	OMe	CH	H	H	H	Me	40
9	130i → 125i	OMe	H	OMe	CF	F	H	H	H	68
10	130j → 125j	OMe	OMe	OMe	COBn	OBn	H	H	H	-
11	130k → 125k	H	H	H	CH	H	OMe	H	H	-
12	130l → 125l	Cl	H	Cl	CH	H	OMe	H	H	-

^aYield of isolated pure product after column chromatography.

2.2.4. Characterization: NMR spectroscopy study and X-ray diffraction analysis

NMR spectroscopy study

Analysis of the ^1H -NMR spectra of the lead known compounds **124a**¹⁷⁷ and **125a**¹⁷⁵ of both series revealed that the two regioisomers could be easily differentiated by the chemical shift of the characteristic signal of the proton H^3 for the 2-aryl benzofuran series **124a-n** and the proton H^2 for the 3-aryl benzofuran series **125a-i**.

The spectroscopic study towards the identification of the aromatic proton signals consisted of the analysis of the 1D proton (^1H -NMR) (Figure 2.3) and carbon (^{13}C -NMR) (Figure 2.5) spectra; through-bond 2D homonuclear correlation (COSY) (Figure 2.4) and heteronuclear single-quantum correlation (HSQC) (Figure 2.6) as well as multiple-bond correlation (HMBC) (Figure 2.7) spectra; and through-space correlation 1D selective nuclear overhauser effect (NOE) spectra of **124a** and **125a** (Figures 2.8 and 2.9)¹⁷⁸.

Bearing all this in mind, first, our efforts were driven towards assigning the signals of hydrogens in the benzofuran ring H^2 , H^3 , H^5 and H^7 , leaving aside:

- the methoxy protons (H^a , H^b , H^c), with a chemical shift of 3.7–4.1 ppm in the ^1H -NMR spectrum (Figure 2.3), and an area that integrates to a relative value of 3 H atoms each, and
- the four hydrogens in the *para*-methoxyphenyl group (H^8 , H^9), which appear as an easily identifiable pair of doublets with an area that integrates to a relative value of 2 H atoms each and with a coupling constant of 8.8 and 8.7 for compounds **124a** and **125a**, respectively, (*ortho*-coupling in aromatic compounds) in the ^1H -NMR spectra; and as strongly coupled to each other signals in COSY spectra (Figures 2.3 and 2.4).

¹⁷⁷ Bokhari, S. A. N. N.; Whalley, W. B. *J. Chem. Soc.* **1963**, 5322-5327

¹⁷⁸ (a) Homonuclear through-bond correlation experiment (COSY) is used to identify spins, most commonly hydrogen, which are coupled to each other. Diagonal signals correspond to the peaks in a 1D-NMR experiment, while cross signals indicate couplings between pairs of nuclei, the same as multiplet splitting in 1D-NMR. (b) Heteronuclear through-bond correlation methods detect correlations between nuclei of two different type, typically hydrogen and carbon, which are separated by one bond (HSQC) or by over longer ranges of about 2-4 bonds (HMBC). They give one signal per pair of correlated nuclei, whose two coordinates are the chemical shifts of the two correlated atoms. (c) Through-space correlation methods, such as 1D selective NOE, establish correlations between nuclei, most commonly hydrogens, which are physically close to each other (within about 5 Å), regardless there is a bond between them.

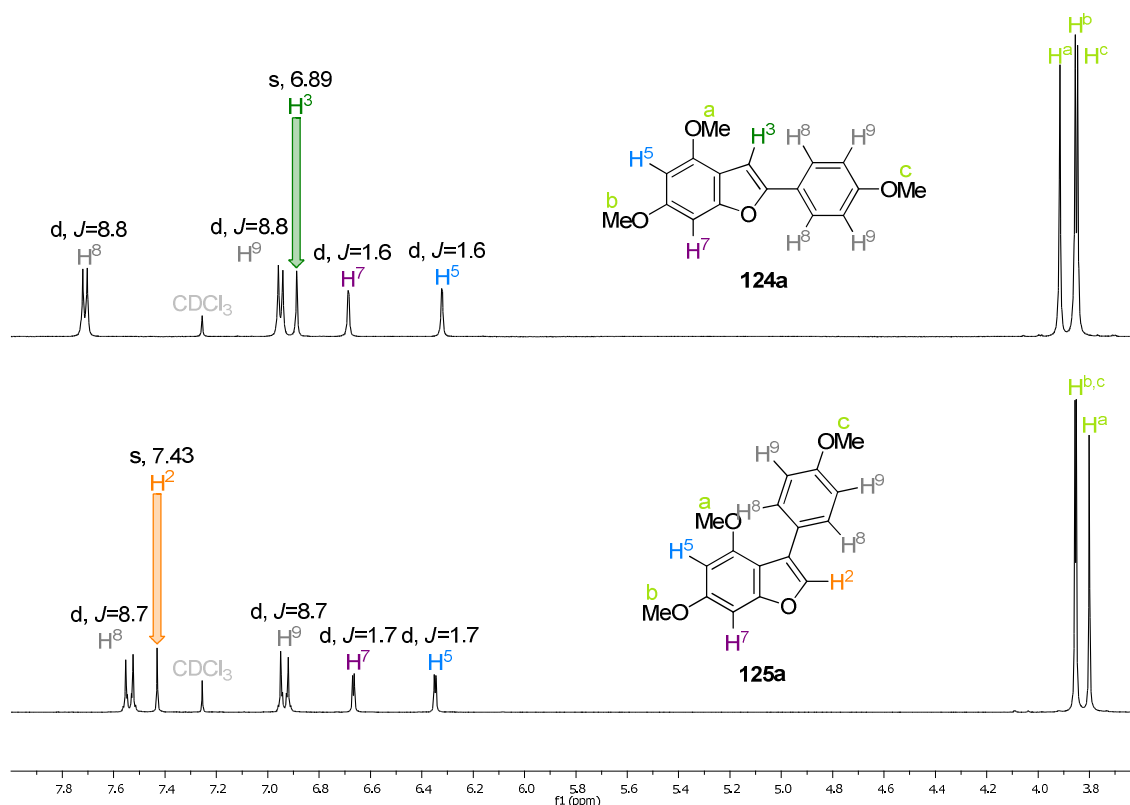


Figure 2.3. $^1\text{H-NMR}$ (500 MHz, CDCl_3) of **124a** (above) and **125a** (below). Chemical shift given in ppm and coupling constants J in Hertz; s = singlet, d = doublet.

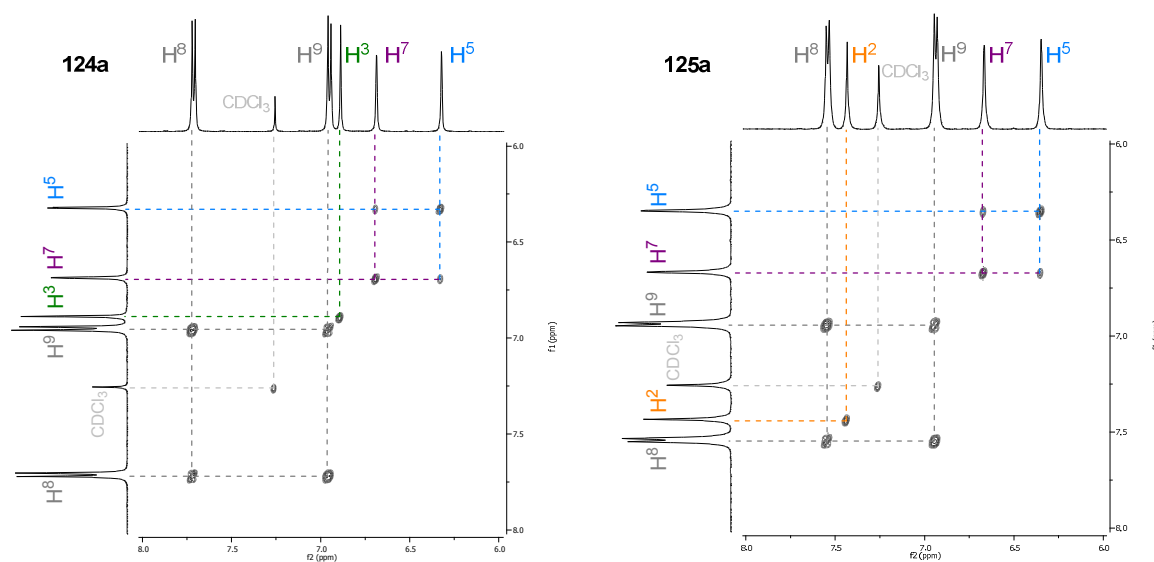


Figure 2.4. COSY (500 MHz, CDCl_3) of **124a** (left) and **125a** (right). Chemical shift given in ppm.

On looking at the other three signals in the $^1\text{H-NMR}$ (with an area that integrates to a relative value of 1 H atom each) and COSY spectra of both compounds (Figures 2.3 and 2.4), a slight coupling between two of the protons was observed, with a coupling constant of 1.6 for **124a** and of 1.7 for **125a**. This suggests that these signals correspond to H^5 and H^7 , which are at 4 bonds distance (*meta*-coupling in aromatic compounds). Between them,

the one at higher chemical shift was thought to be H⁷, due to the larger deshielding effect of the benzofuran oxygen over that of the methoxy substituent.

Then, the only signal left in each spectrum corresponded to H² or H³. The peak in the ¹H-NMR spectrum was a singlet (the closest hydrogen is at 5 bonds distance) at 6.89 ppm for **124a** and at 7.43 ppm for **125a**. Again, the larger deshielding effect of the benzofuran oxygen over that of other carbons in the bicyclic structure suggests that **124a** is the 2-aryl benzofuran and **125a** the 3-aryl one (Figure 2.3).

This tendency was kept in all the experiments conducted, obtaining singlets at 7.05 ppm on average (6.89–7.37 ppm) for the 2-aryl benzofuran series (**124a-n**) and at 7.50 ppm on average (7.43–7.60 ppm) for the 3-aryl benzofuran series (**125a-i**).

The assignment of the remaining proton signals (H⁸ and H⁹ from the *para*-methoxy substituent and the majority of methoxy proton signals H^a, H^b and H^c) was completed analyzing the ¹³C-NMR, HSQC and HMBC spectra of **124a** and **125a**, in the light of the information obtained from ¹H-MNR and COSY spectra.

On the one hand, in the ¹³C-NMR (Figure 2.5) spectra, the carbon signals were assigned according to the type (primary, secondary, tertiary or quaternary) of carbon and the chemical shift that could be expected for it, taking into account its environment.

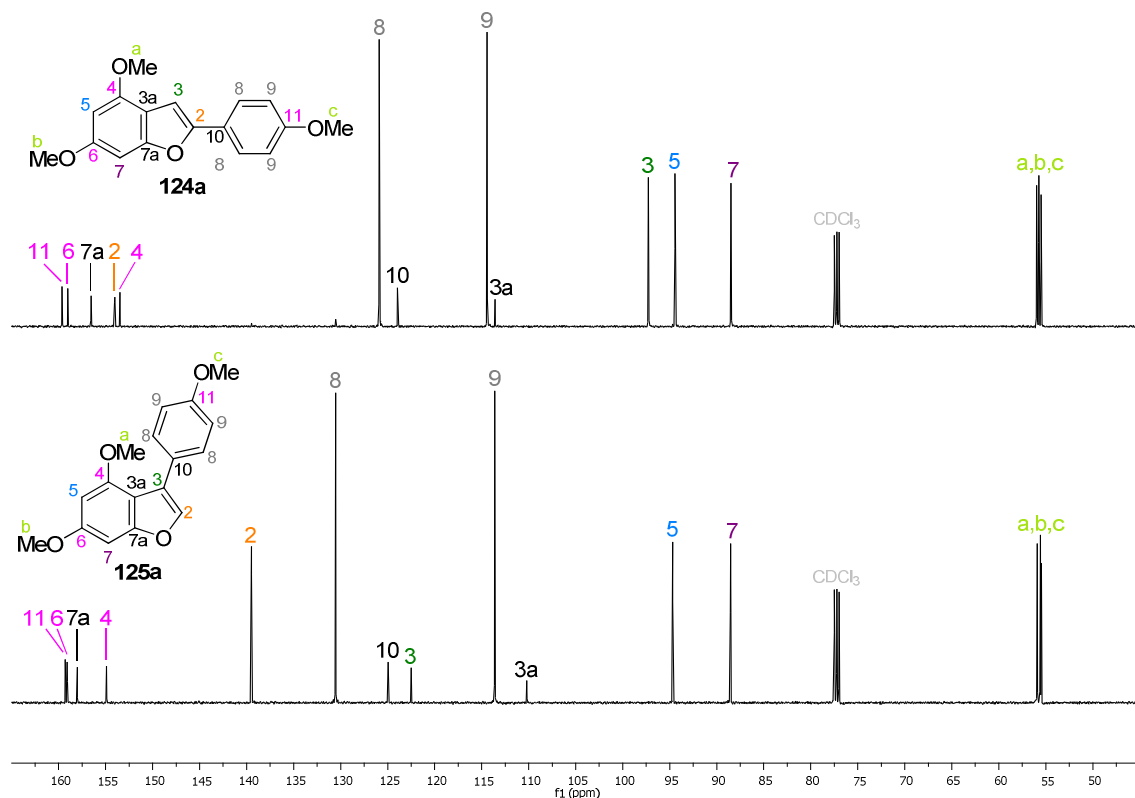


Figure 2.5. ^{13}C -NMR (500 MHz, CDCl_3) of **124a** (above) and **125a** (below). Chemical shifts given in ppm.

On the other hand, all the proton and carbon assignments were validated by analysing the proton-carbon correlations shown in the HSQC (1 bond distance) and HMBC (2-4 bond distance), (Figures 2.6 and 2.7).

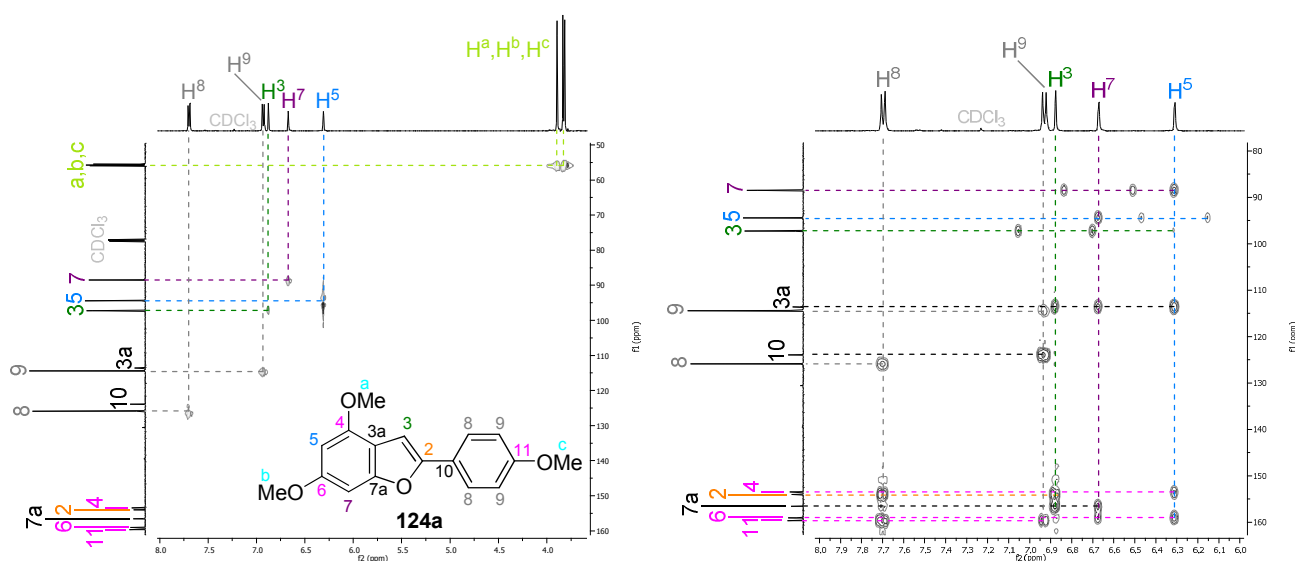


Figure 2.6. HSQC (left) and HMBC (right) (500 MHz, CDCl_3) of **124a**. Chemical shift given in ppm.

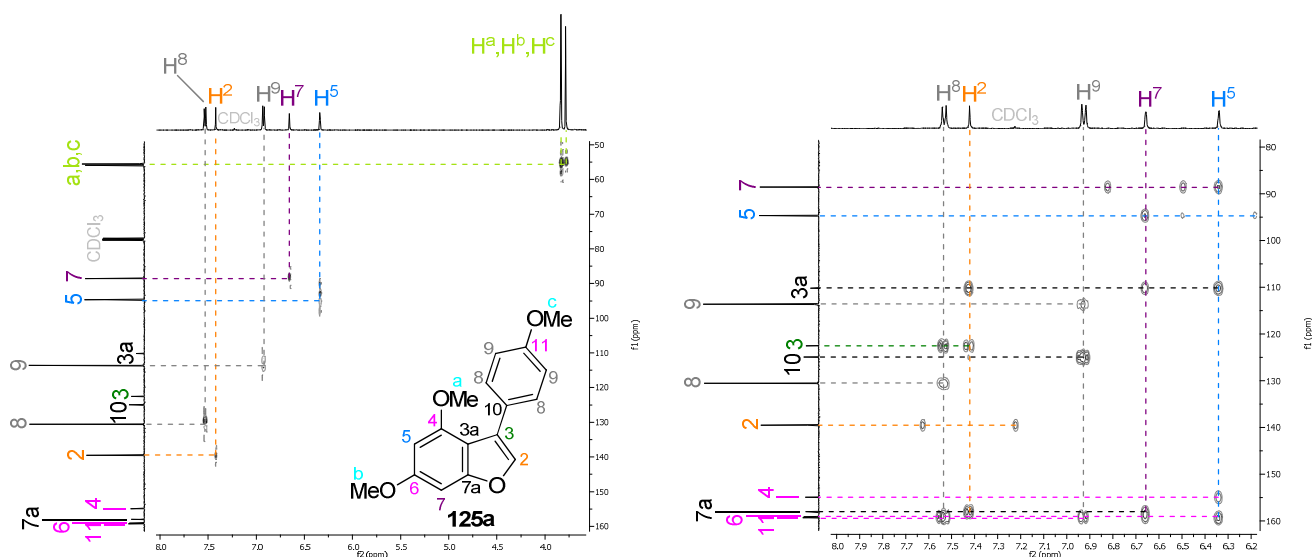


Figure 2.7. HSQC (left) and HMBC (right) (500 MHz, CDCl₃) of **125a**. Chemical shift given in ppm.

Finally, in order to reinforce the aromatic proton assignments, selective NOE spectra resulting from the selective irradiation of protons H^{2/3}, H⁵, H⁷ and H⁸ of both **124a** and **125a** compounds were registered, obtaining in each case signals in agreement with our proposal.

Starting with compound **124a** (Figure 2.8), the signal assigned to H⁵ was first selectively irradiated, giving rise to two signals in the methoxy region, associated with H^a and H^b (*¹ and *², respectively). This confirmed the correct assignment of H⁵, since it was the only proton in the molecule close enough to two methoxy groups. Then the signal assigned to H⁷ was selectively irradiated, which brought about a single signal, again in the methoxy region, which was associated in this case with H^b (*³). The signal assigned to H³ was next selectively irradiated. This time it provoked the appearance of a single signal associated to H⁸ protons (*⁴), but no signal corresponding to a possible H³–H^a through-space correlation, thus indicating that the H^a protons of the methoxy group are not oriented in the furan ring direction. Finally, the signal assigned to H⁸ was also selectively irradiated and it showed through-space correlation with H³ and H⁹ protons (*⁵ and *⁶, respectively) and with no methoxy protons, excluding a possible exchanged assignment of protons H⁸ and H⁹ (no correlation observed with H^c).

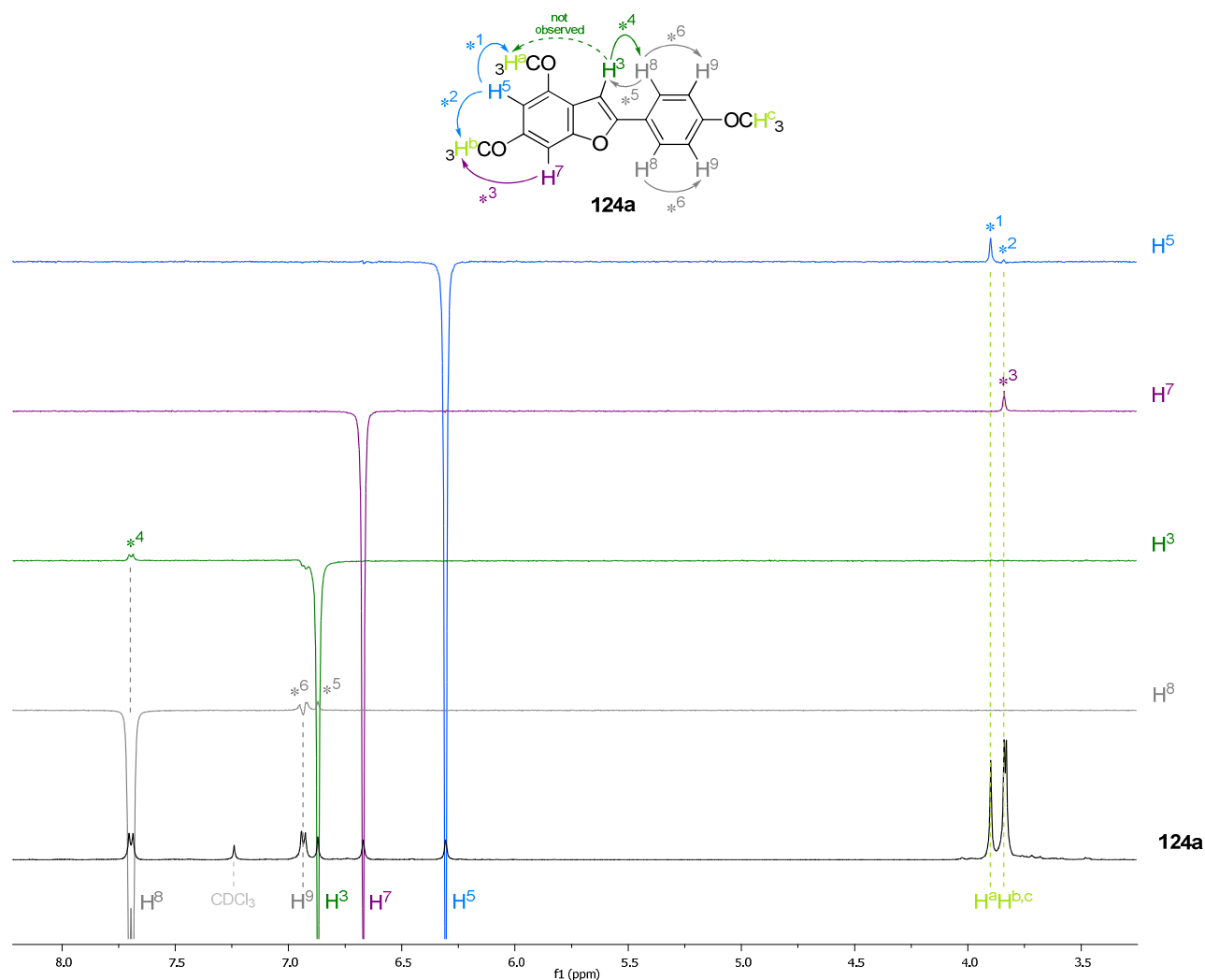


Figure 2.8. Stacked selective NOE spectra (with the proton assigned to the selectively irradiated signal indicated in the right) and ^1H -NMR spectrum of compound **124a** (500 MHz, CDCl_3). NOE signals associated with the different irradiations are indicated with numbered stars.

Following with compound **125a** (Figure 2.9), the same series of selective irradiations was performed. The selective irradiation of signal assigned to H^5 gave again raise to two signals in the methoxy region, associated with H^a and H^b (* 1 and * 2 , respectively). Selective irradiation of the signal assigned to H^7 brought about a single signal in the methoxy region, which was again associated with H^b (* 3). The selective irradiation of signal assigned to H^2 provoked the appearance of a single signal associated to H^8 protons (* 4). And finally, the selective irradiation of the signal assigned to H^8 showed through-space correlation with H^2 and H^9 protons (* 5 and * 6 , respectively) and, as in the previous case, with no methoxy protons, thus excluding a possible exchanged assignment of protons H^8 and H^9 (no correlation observed with H^c) and suggesting that the H^a protons of the methoxy group are not oriented in the furan ring direction and/or that the *para*-

methoxyphenyl substituent could be twisted from the plane defined by the benzofuran bicycle (no correlation observed with H^a).

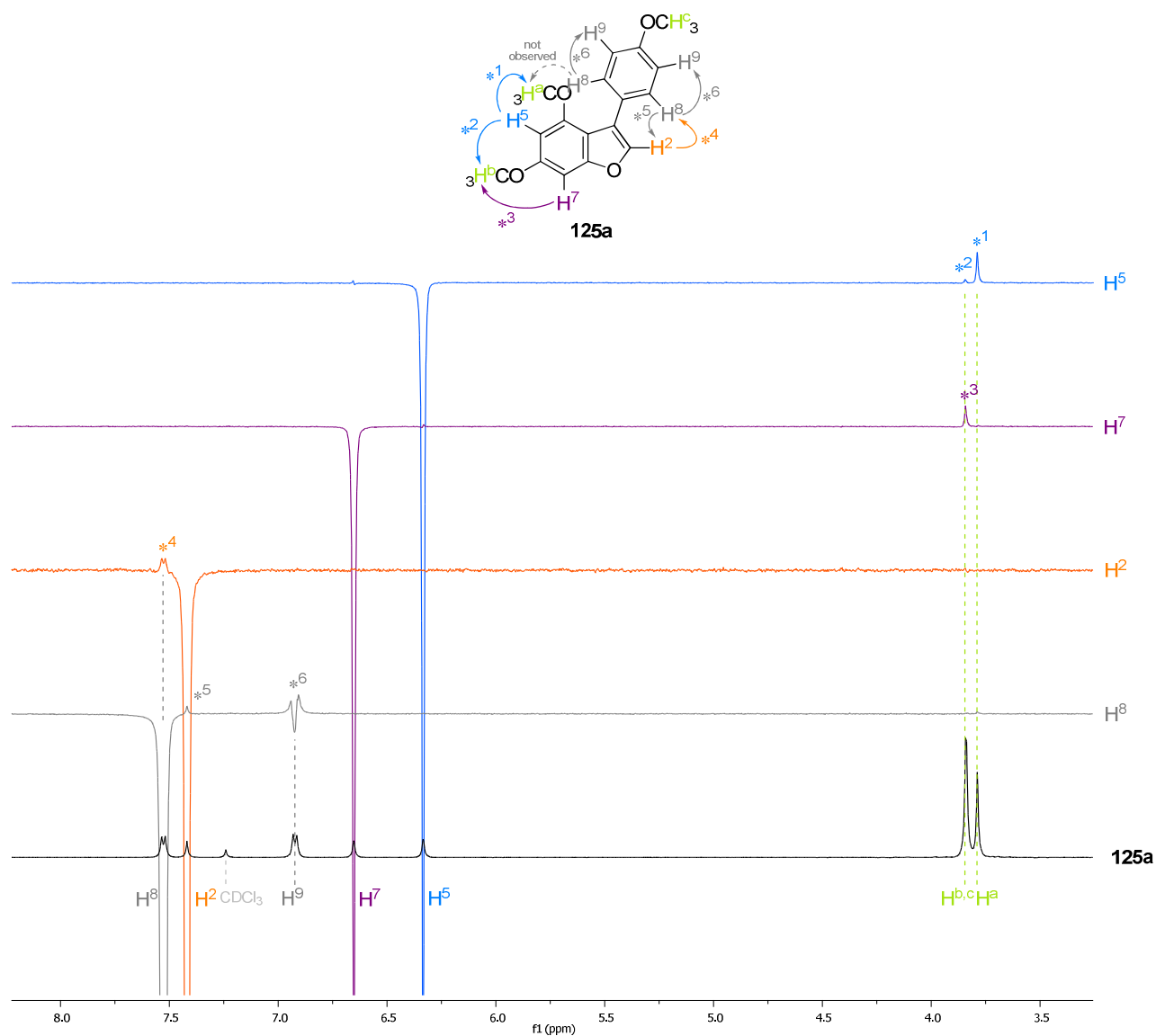


Figure 2.9. Stacked selective NOE spectra (with the proton assigned to the selectively irradiated signal indicated in the right) and ¹H-NMR spectrum of compound **125a** (500 MHz, CDCl₃). NOE signals associated with the different irradiations are indicated with numbered stars.

All the NMR experiments shown in this section were registered on a spectrometer operating at 500 MHz and using deuterated chloroform as solvent.

X-ray diffraction analysis

Besides, in order to secure the regiochemistry of these compounds, the structure of both lead compounds **124a** and **125a** were unambiguously determined by X-ray diffraction analysis (Figures 2.10 and 2.11). This study also revealed that:

- There are two molecules in the asymmetric unit of compound **124a** (in Figure 2.10, only one of them is shown in order to simplify the picture). Both of them are almost plane and identical, except for the direction of rotation of the methoxyphenyl group with respect to the rest of the molecule, being this rotation of 19.54° on average.

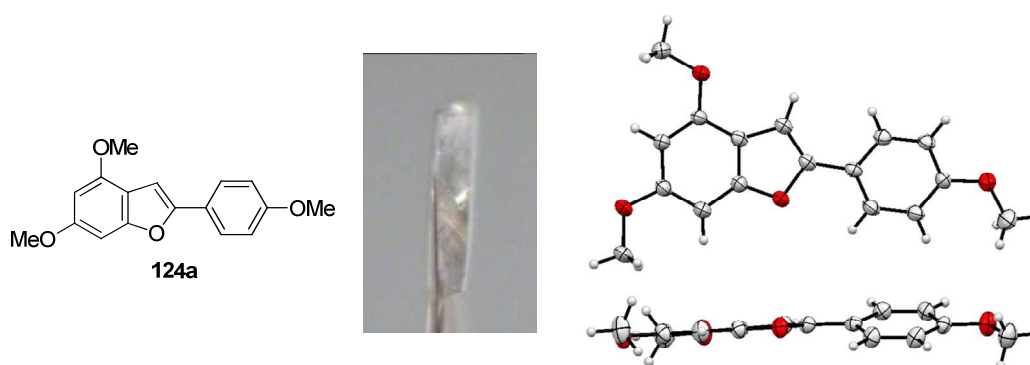


Figure 2.10. Picture of the crystal and ORTEP diagram (top and front views) of **124a**.

- In compound **125a**, the 4,6-dimethoxyphenylbenzofuran is almost plane and the methoxyphenyl group is rotated 43.37° with respect to it (Figure 2.11).

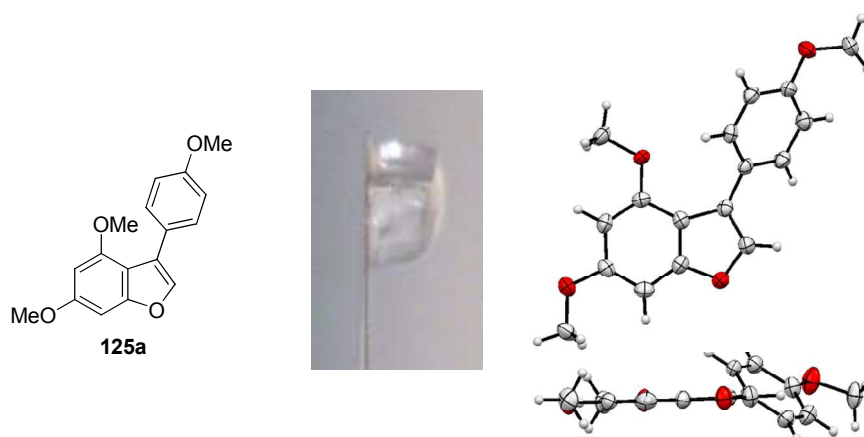
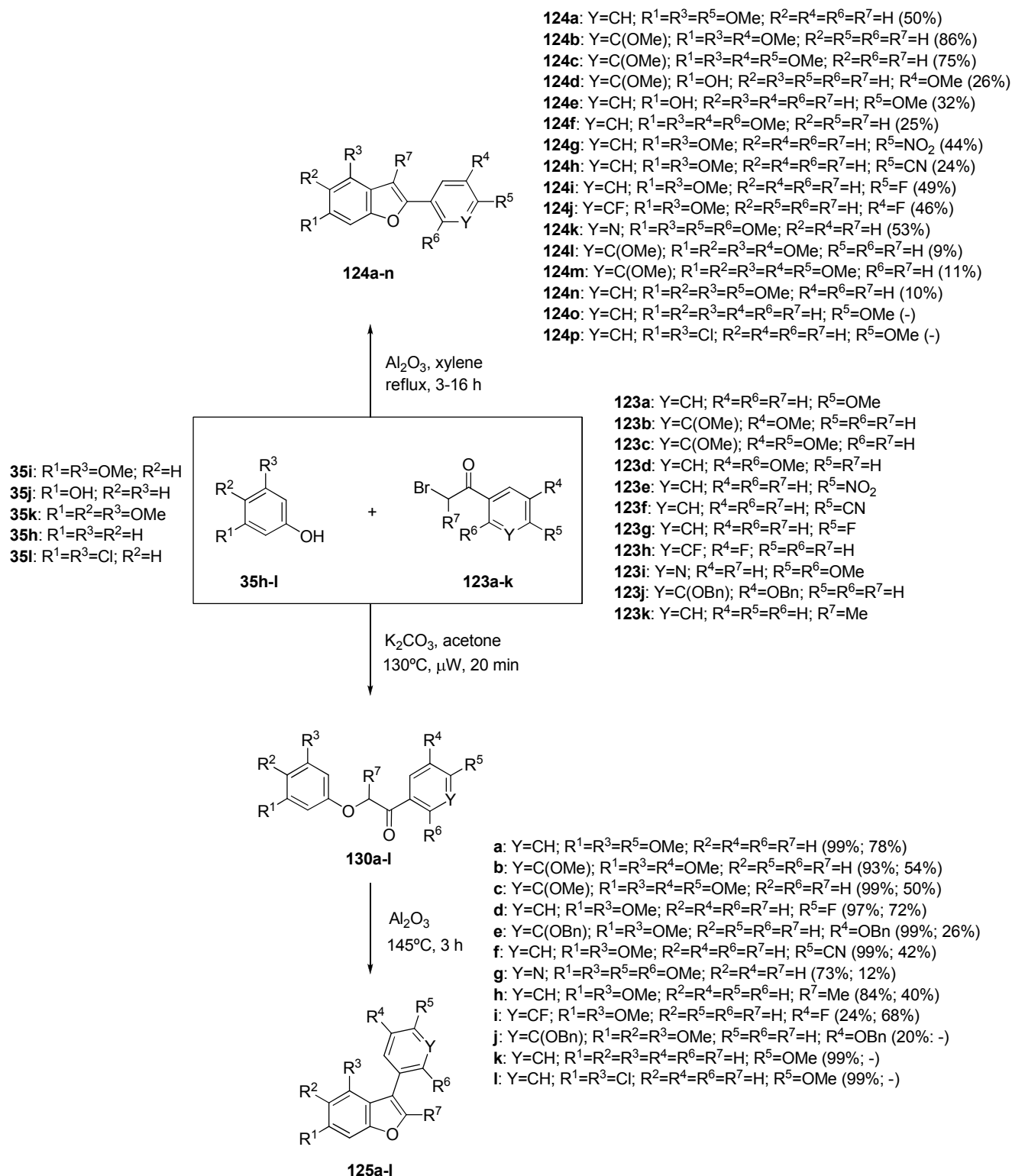


Figure 2.11. Picture of the crystal and ORTEP diagram (top and front views) of **125a**.

- No significant interaction is observed among the molecules in either of these crystalline structures, which form layers with parallel molecular planes.

2.2.5. Graphical overview



Scheme 2.8. Graphical overview of the experimental study of the synthesis of 2-aryl and 3-aryl benzo[*b*]furans **124** and **125**, respectively. Reaction yield of each step is given in brackets.

2.3. COMPUTATIONAL STUDY: MECHANISMS

2.3.1. General considerations

In order to get a better understanding of the reaction paths these reactions leading to the two different regioisomers go through, computational studies were performed to assess the electrophilicity of the 2-bromoacetophenone in the absence and in the presence of alumina to evaluate its distinct behavior in both cases.

First, the electrostatic potentials of the fully optimized structures were calculated, in an attempt to localize the preferential sites for a charge driven nucleophilic attack.

Next, a possible orbital control of the reaction was considered and the study also involved computing the LUMO orbitals, with the same purpose. The two possibilities studied involve the attack of the nucleophile over the 2-bromoacetophenone (**123I**) (a) on the methylene (*alpha*) carbon, a process involving the σ^* (C–Br) molecular orbital, or (b) on the carbonyl (*ipso*) carbon, which should involve the π^* (C=O) molecular orbital (Figure 2.12).

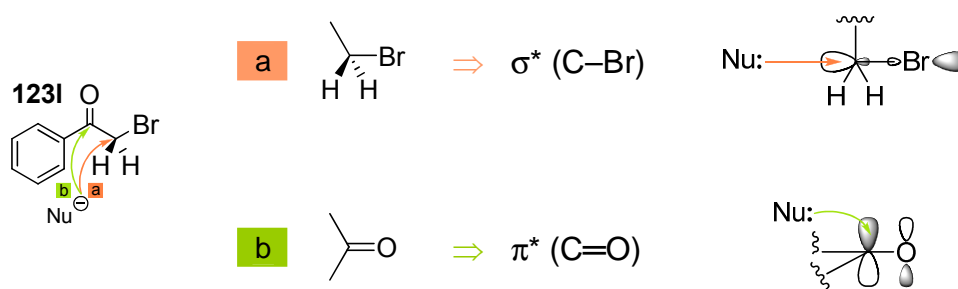


Figure 2.12. Possible nucleophilic attacks over the 2-bromoacetophenone (**123I**).

Then, the NBO charges of both carbons were calculated and finally the transition structures (TS) and the activation energies (E_a) of the different possible reaction paths were analyzed.

The calculations presented in this section were carried out in our research group and consisted of DFT studies computed at the B3LYP/6-31+G* level of theory¹⁷⁹ to get the fully

¹⁷⁹ (a) Parr, R. G.; Yang, W. *Density-Functional Theory of Atoms and Molecules*; Oxford: New York, **1989** (b) Frisch, M. J.; Trucks, G. W.; Schlegel, H. B.; Scuseria, G. E.; Robb, M. A.; Cheeseman, J. R.; Scalmani, G.; Barone, V.; Mennucci, B.; Petersson, G. A.; Nakatsuji, H.; Caricato, M.; Li, X.; Hratchian, H. P.; Izmaylov, A.

optimized structures of reactants, transition structures (TS), intermediates and products. The corresponding reaction (ΔE_{rxn}), activation (E_a) and relative energies, which are given in kcal/mol, were computed at the B3LYP/6-31+G*+ Δ ZPVE level of theory. Unsubstituted phenol and 2-bromoacetophenone were used as reactants to simplify the model.

2.3.2. Reaction path in the absence of alumina

The structure of 2-bromoacetophenone (**123I**) was optimized and its electrostatic potential, which in Figure 2.13 is projected onto the electron density, calculated. It was observed that the positive region (given in blue) was extended mainly over the *alpha* (methylene) carbon, suggesting a slight preference for this site towards a nucleophilic attack from a Coulombic standpoint. When the aluminium oxide is not present in the reaction medium, the parameters considered to measure the electrophilicity of the 2-bromoacetophenone like the LUMO of the compound, give inconclusive results since the free rotation of the molecule under these conditions results in a linear combination of the sigma and pi antibonding (σ^* and π^*) molecular orbitals and the calculations considering a fixed conformation of **123I** are not a sufficiently reliable model of the system.

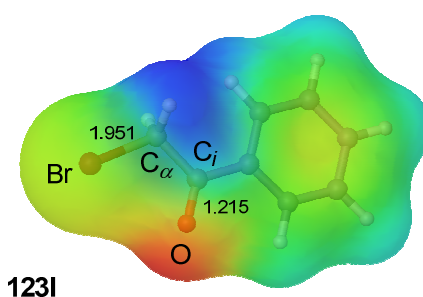


Figure 2.13. Fully optimized (B3LYP/6-31+G* level of theory) structure of 2-bromoacetophenone (**123I**) showing the electrostatic potential projected onto the electron density. Negative and positive potentials are given in red and blue, respectively.

F.; Bloino, J.; Zheng, G.; Sonnenberg, J. L.; Hada, M.; Ehara, M.; Toyota, K.; Fukuda, R.; Hasegawa, J.; Ishida, M.; Nakajima, T.; Honda, Y.; Kitao, O.; Nakai, H.; Vreven, T.; Montgomery, Jr., J. A.; Peralta, J. E.; Ogliaro, F.; Bearpark, M.; Heyd, J. J.; Brothers, E.; Kudin, K. N.; Staroverov, V. N.; Kobayashi, R.; Normand, J.; Raghavachari, K.; Rendell, A.; Burant, J. C.; Iyengar, S. S.; Tomasi, J.; Cossi, M.; Rega, N.; Millam, N. J.; Klene, M.; Knox, J. E.; Cross, J. B.; Bakken, V.; Adamo, C.; Jaramillo, J.; Gomperts, R.; Stratmann, R. E.; Yazyev, O.; Austin, A. J.; Cammi, R.; Pomelli, C.; Ochterski, J. W.; Martin, R. L.; Morokuma, K.; Zakrzewski, V. G.; Voth, G. A.; Salvador, P.; Dannenberg, J. J.; Dapprich, S.; Daniels, A. D.; Farkas, O.; Foresman, J. B.; Ortiz, J. V.; Cioslowski, J.; Fox, D. J. *Gaussian 09*, Revision A.02; Gaussian, Inc.: Wallingford, CT, **2009** (c) Becke, A. D. *J. Chem. Phys.* **1983**, *98*, 5648-5652 (d) Becke, A. D. *Phys. Rev. A: At., Mol., Opt. Phys.* **1998**, *38*, 3098-3100 (e) Kohn, W.; Becke, A. D.; Parr, R. G. *J. Phys. Chem.* **1996**, *100*, 12974-12980 (f) Lee, C.; Yang, W.; Parr, R. G. *Phys. Rev. B: Condens. Matter Mater. Phys.* **1998**, *37*, 785-789

DFT studies on the reaction paths associated with the interaction between 2-bromoacetophenone **123I** and phenoxide anion **[35h]⁻** (Figure 2.14), generated in the presence of a base such as potassium carbonate, showed a low activation barrier for the bimolecular nucleophilic substitution (S_N2) process ($E_a = 4.5$ kcal/mol), whereas the nucleophilic addition (Ad_{N2}) reaction resulted to be an uphill process with no detectable transition structure. All our attempts to locate saddle point **TS2** were unfruitful and spontaneously converged to **TS1** instead.

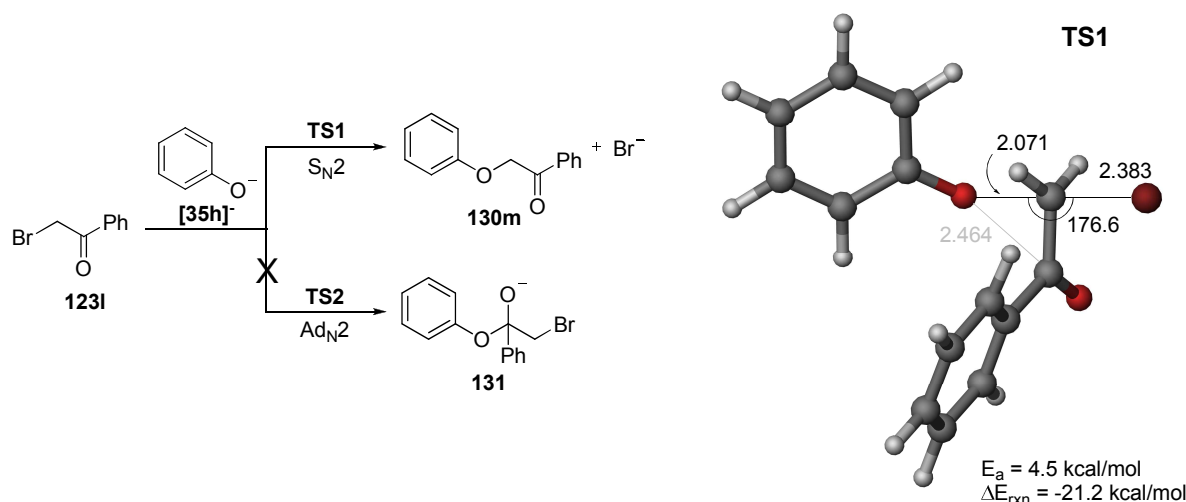


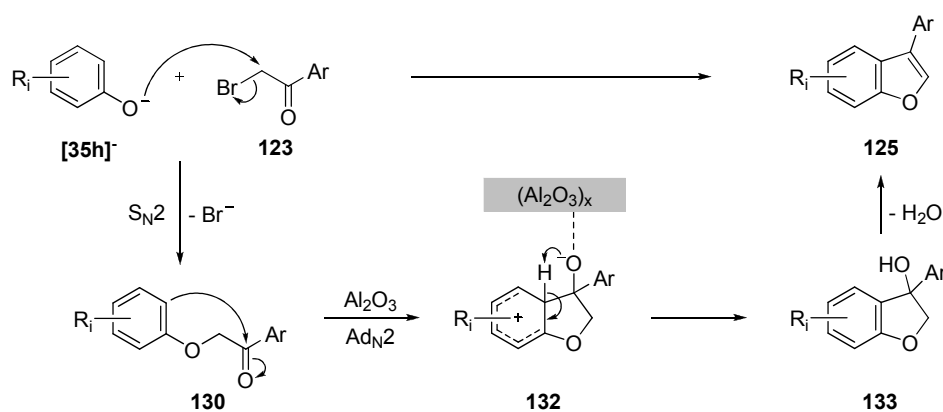
Figure 2.14. Model S_N2 and Ad_{N2} reactions between phenoxide anion (**[35h]⁻**) and α -bromoacetophenone (**123I**). Fully optimized structure of **TS1**, computed at the B3LYP/6-31+G* level of theory. Bond distances and angle are given in Å and degrees, respectively. Activation and reaction energies are given in kcal/mol and were computed at the B3LYP/6-31+G*+ Δ ZPVE level of theory.

Although in this latter stationary point the bond distance between the nucleophilic oxygen atom and the carbon atom of the carbonyl group of **123I** is quite short (2.464 Å), and almost comparable to the distance between oxygen atom and methylene carbon atom (2.071 Å) (Figure 2.14), harmonic analysis revealed that **TS1** corresponds to a true S_N2 transition structure, as its imaginary frequency is only related to the formation of that bond. This confirms that the calculated saddle point is associated with the reaction between the oxygen atom of phenoxide anion, the hardest nucleophilic center, and the electrophilic methylene moiety of **123I**.

This result is in agreement with our experimental findings since they suggest that, in the absence of alumina, only the S_N2 process is energetically available, thus resulting in the formation of ethers **130** which, after further transformation, lead to the formation of the

corresponding 3-aryl benzo[*b*]furans **125**. However, the presence of alumina is needed to promote the cyclization step via carbonyl activation of compounds **130**.

Taking all this into account, the mechanism we propose for this reaction could be summed up as follows: first a S_N2 takes place as the phenoxide anion (generated in the presence of potassium carbonate) attacks the *alpha* carbon of the 2-bromoacetophenone yielding the phenoxyketone **130**; once this ether is formed, in the presence of alumina (which enhances the electrophilicity of the carbonyl carbon), a nucleophilic addition occurs on the carbonyl carbon from the *ortho* unsubstituted position of the aromatic ring leading to a loss of aromaticity; the resulting species neutralizes and dehydrates regaining aromaticity to yield the 3-aryl benzofuran **125** (Scheme 2.9).



Scheme 2.9. Proposed mechanism for the formation of 3-aryl benzo[*b*]furans **125**.

2.3.3. Reaction path in the presence of alumina

To study the behavior of the α -bromoacetophenone in the presence of alumina, previous computational studies on the reactivity of alumina¹⁷¹, which reveal tetrahedral and cubic reactive sites for aluminium (Section 2.2.1, Figure 2.2, T and C, respectively), were taken into account. First, tetrahedral environment for aluminium oxide dimer (Al_4O_6) was considered in our calculations as a simplified computational model for the alumina surface.

To start with, the interaction of **123** with alumina dimer according to the tetrahedral pattern T shown in Figure 2.2 was computationally analyzed. The structure of this complex was optimized and its electrostatic potential, which in Figure 2.15 A is projected onto the electron density, calculated. It was observed that the positive region (given in blue) was extended over both *ipso* (carbonyl) and *alpha* (methylene) carbons. This reveals a general activation of the molecule toward a nucleophilic attack but does not permit apparent selectivity prediction. On looking at the optimized structure, the complex showed an

enlargement of both the C–O and the C–Br bond distances (Figure 2.15, A) with respect to those of isolated **123I**, together with a significant CO–Al interaction.

In addition, further calculations displayed that the Kohn-Sham LUMO of this complex is localized mainly on the carbonyl group, thus suggesting that this will be the preferred electrophilic centre for the interaction with a nucleophile (Figure 2.15, B).

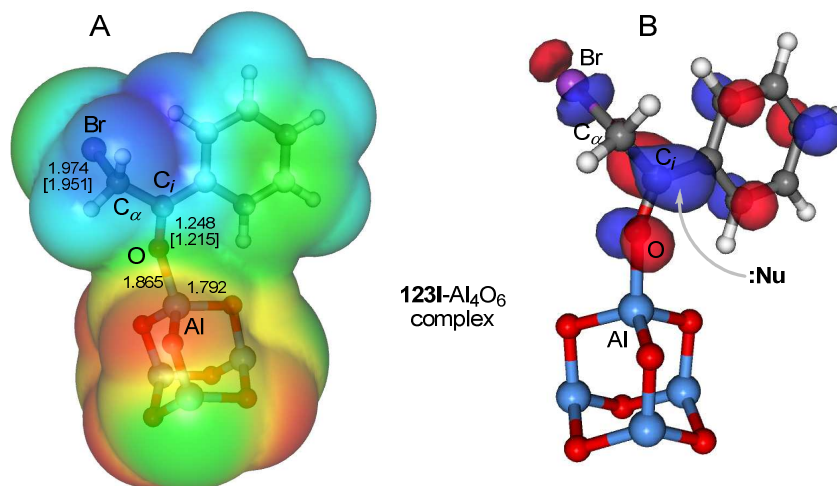


Figure 2.15. (A) Fully optimized (B3LYP/6-31+G* level of theory) structure of 2-bromoacetophenone **123I** bound to Al_4O_6 , showing the electrostatic potential projected onto the electron density. Negative and positive potentials are given in red and blue, respectively. Bond distances are in Å, values in square brackets correspond to those of isolated **123I**. (B) Kohn-Sham LUMO of the **123I**- Al_4O_6 complex. The preferential site of a nucleophilic attack is shown. Aluminium and oxygen atoms are represented in light blue and red respectively.

The NBO charges were also calculated and they let us conclude that the enhancement of the electrophilicity of the **123I**- Al_4O_6 complex is localized at the carbonyl group, since the charge of the corresponding carbon atom (besides being greater than that of the methylene carbon) is increased with respect to isolated **123I** (Table 2.15).

Table 2.15. The NBO charges of the *ipso*-carbonyl and the *alpha*-methylene groups (C_i and $C_{\alpha}H_2$, respectively), in a.u. in **123I** and **123I**- Al_4O_6 complex.

entry	compound	$q(C_i)$	$q(C_{\alpha}H_2)$
1	123I	+0.55	+0.00
2	123I - Al_4O_6	+0.63	+0.00

Next a similar analysis of the interaction between phenol and alumina dimer was conducted. This led to two possible structures: phenol moiety $\text{PhOH}-\text{Al}_4\text{O}_6$ (or **35h**- Al_4O_6) and phenoxide anion moiety $\text{PhO}^- - \text{Al}_4\text{O}_6$ (or [**35h**]- Al_4O_6) (Figure 2.16, structures A and B

respectively). The neutral hydroxyl structure A is computed to be significantly less stable (20.7 kcal/mol) than structure B, associated with a proton transfer from phenol to the alumina surface. Therefore, formation of phenoxide anion in the reaction medium can occur in a significant extent. In the following part of this study, only phenoxide nucleophile will be considered.

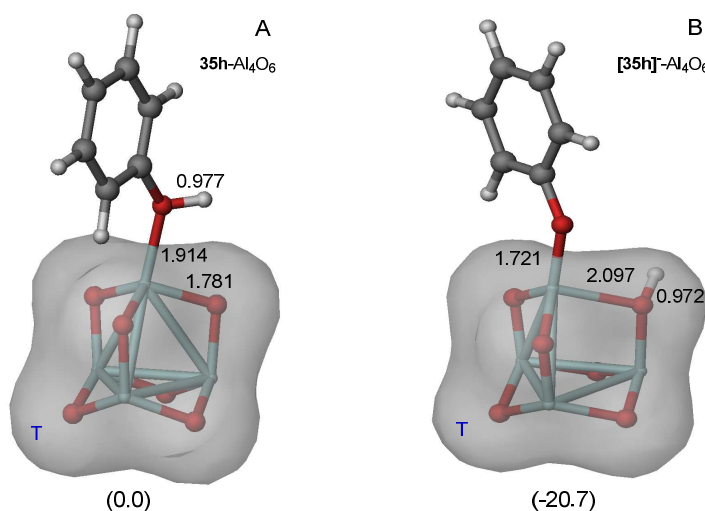


Figure 2.16. Fully optimized (B3LYP/6-31+G* level of theory) structures for phenol (**35h**, A) and phenoxide anion (**[35h]⁻**, B) on tetrahedral Al_4O_6 , together with solvent accessible surfaces (probe radius: 1.4 Å). Aluminium and oxygen atoms are represented in light blue and red respectively. Bond distances are given in Å. Numbers in brackets are the corresponding relative energies, calculated at the B3LYP/6-31+G*+ Δ ZPVE level of theory.

DFT exploration of the reaction paths between phenoxide anion and **123i** on Al_4O_6 led to two possible situations. When pattern T for the alumina (Figure 2.2, T) was considered, only transition structure **TS3** could be located, associated with a $\text{S}_{\text{N}}2$ process (Figure 2.17), with an activation energy of 35.8 kcal/mol. In contrast, when the C environment for the alumina (Figure 2.2, C) was considered, another saddle point, denoted as **TS4** in the figure, was located and characterized. This latter transition structure is associated with an addition reaction ($\text{Ad}_{\text{N}}2$) on the carbonyl group of benzophenone and has an activation energy of 29.4 kcal/mol, 6.4 kcal/mol lower than that associated with **TS3**. Therefore, we concluded that, in the presence of alumina, formation of the $\text{Ad}_{\text{N}}2$ product **136a** is strongly favored (Figure 2.17).

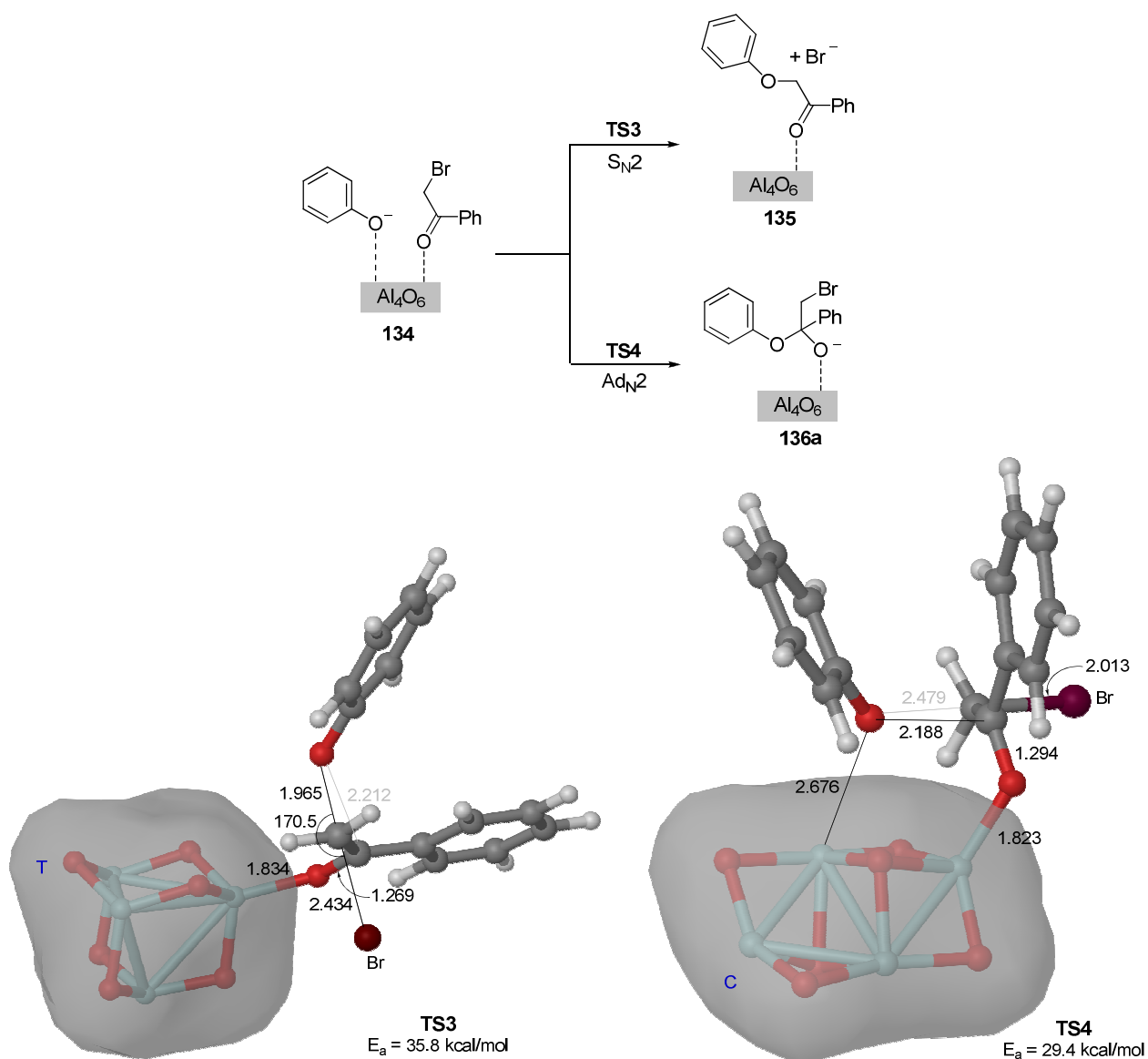


Figure 2.17. Possible reaction paths for the interaction between phenoxide and 2-bromoacetophenone **123I** in Al_4O_6 . Fully optimized (B3LYP/6-31+G* level of theory) structures of transition structures leading to intermediates **135** and **136a**. The Al_4O_6 clusters are represented in configurations T (tetrahedral) and C (cubic), together with solvent accessible surfaces (probe radius: 1.4 Å). Aluminium and oxygen atoms are represented in light blue and red respectively. Bond distances and angle are given in Å and degrees, respectively. Activation energies are given in kcal/mol and were computed at the B3LYP/6-31+G*+ΔZPVE level of theory.

Next, the cyclization step leading to the precursors of benzo[*b*]furans **124** was studied. It was found that the $\text{S}_{\text{N}}2$ transition structure **TS5a** leads to intermediate **137a** with a calculated activation energy of 45.6 kcal/mol (Figure 2.18). This value is quite large and agrees with our experimental finding that reaction between unsubstituted phenol and bromoacetophenone in the presence of alumina does not lead to the formation of 2-phenyl benzo[*b*]furan.

However, adequately located methoxy or hydroxy groups in the starting phenol can promote the formation of the corresponding aromatic bicyclic compounds **124**. Bearing this in mind, the S_N2 process associated with the transformation of intermediate **136b**, with two methoxy groups in *ortho* and *para* disposition with respect to the reacting carbon atom, was evaluated. It was observed that it led to the formation of bicyclic intermediate **137b** via **TS5b**, with an activation energy of 39.9 kcal/mol, 6.3 kcal/mol lower than that associated with the reaction of nonactivated intermediate **136a** (Figure 2.18).

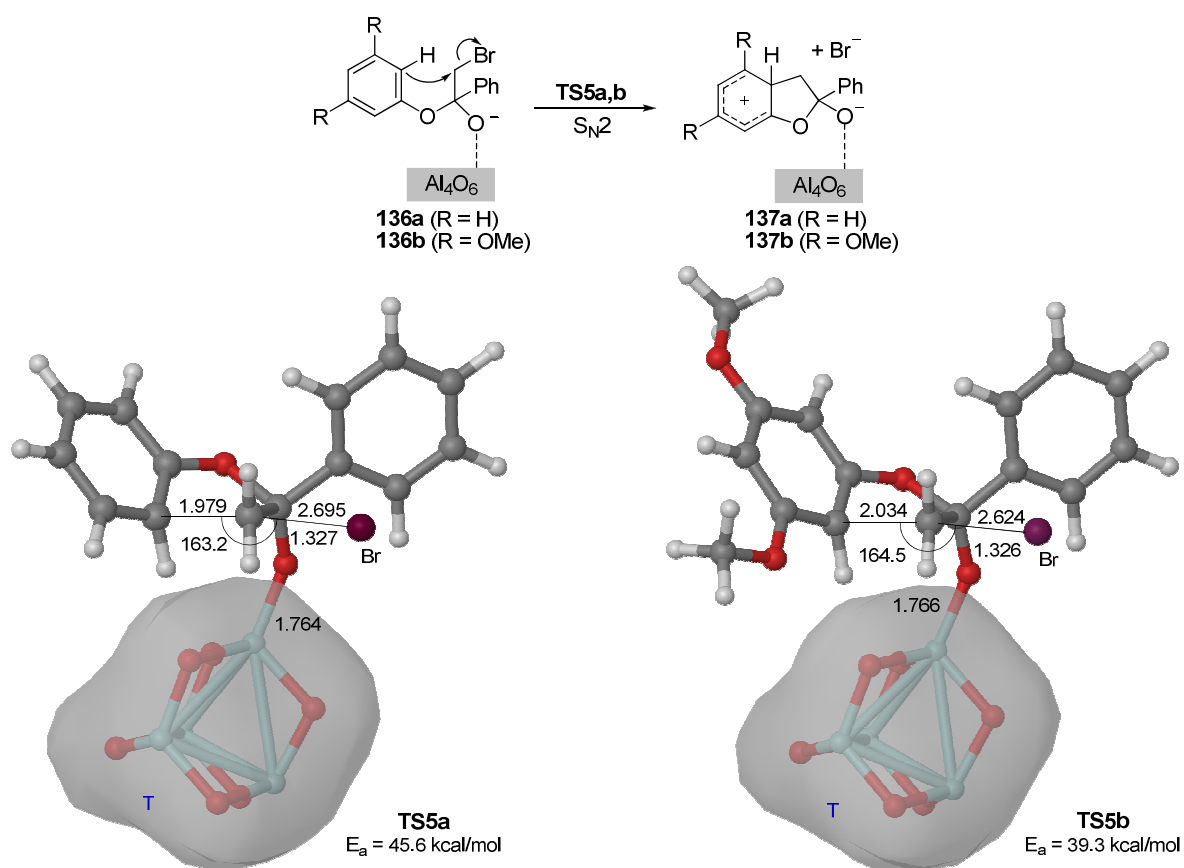
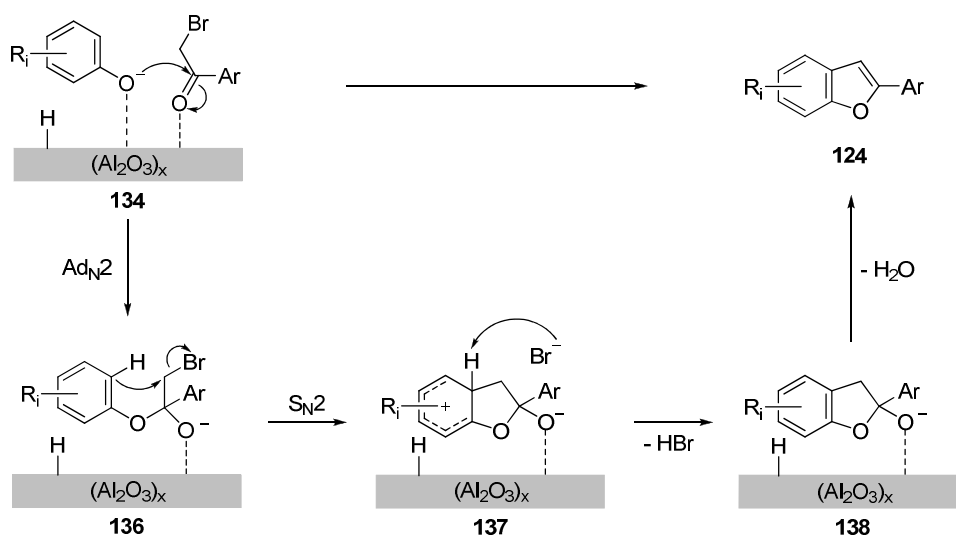


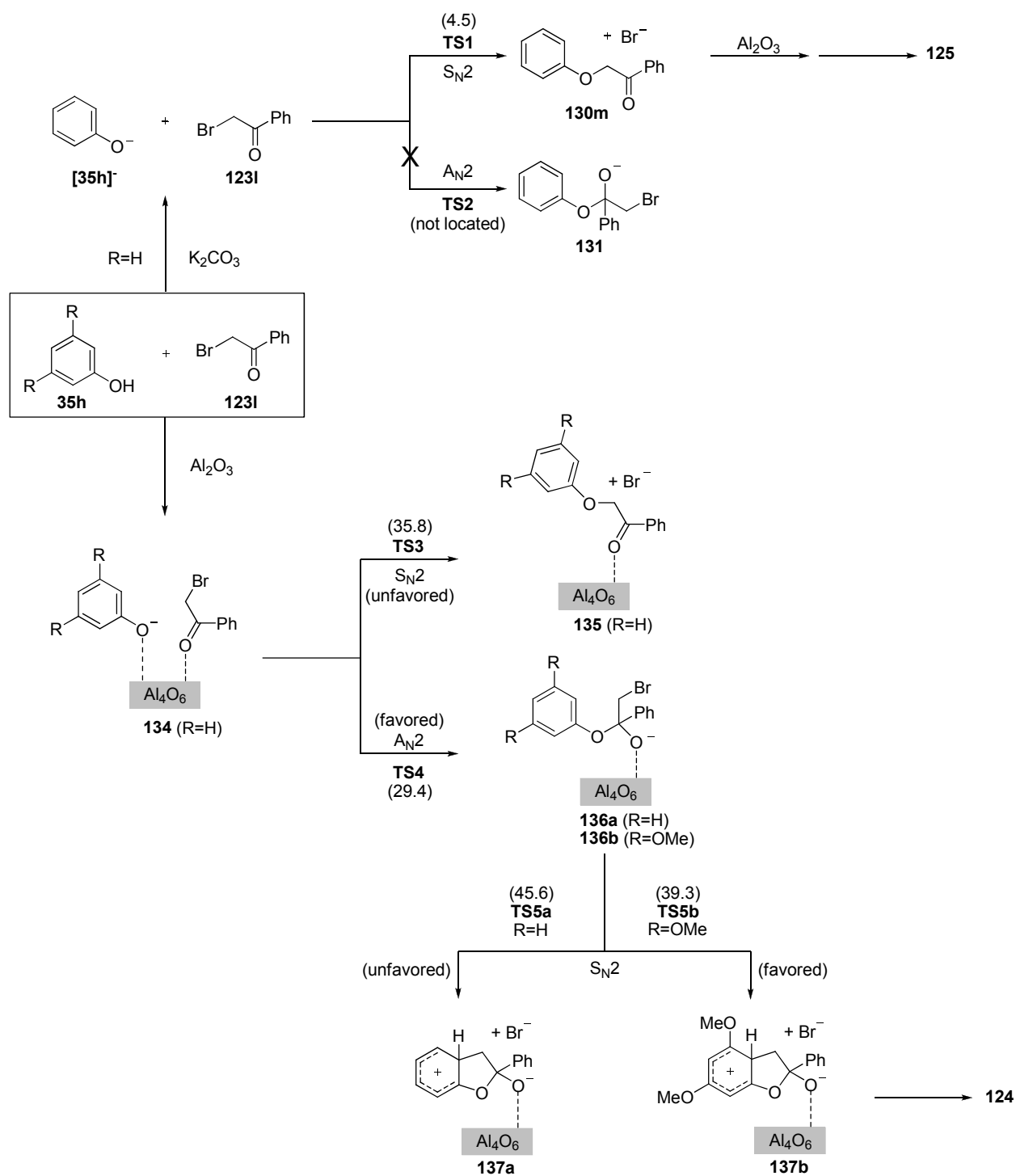
Figure 2.18. Chief geometry features of transition structures **TS5a,b**, associated with conversion of intermediates **136a,b** into bicyclic structures **137a,b**, respectively. The Al_4O_6 clusters are represented in tetrahedral configuration (T) together with solvent accessible surface (probe radius: 1.4 Å). Aluminium and oxygen atoms are represented in light blue and red respectively. Bond distances are given in Å. Activation energies are given in kcal/mol and were computed at the B3LYP/6-31+G*+ Δ ZPVE level of theory.

Therefore, on the basis of our DFT calculations, we propose the mechanism outlined in Scheme 2.10 to explain the exclusive formation of 2-aryl benzo[*b*]furans **124**: the reaction consists of a stepwise process, in which the first step is a nucleophilic addition (Ad_{N2}) of the phenol **35** on the carbonyl group of bromoacetophenone **123**. The second step consists of an intramolecular S_N2 process, where elimination of HBr and dehydration leads to the formation of the corresponding product **124** (Scheme 2.10).



Scheme 2.10. Proposed mechanism for the formation of 2-aryl benzo[*b*]furans **124**.

2.3.4. Graphical overview



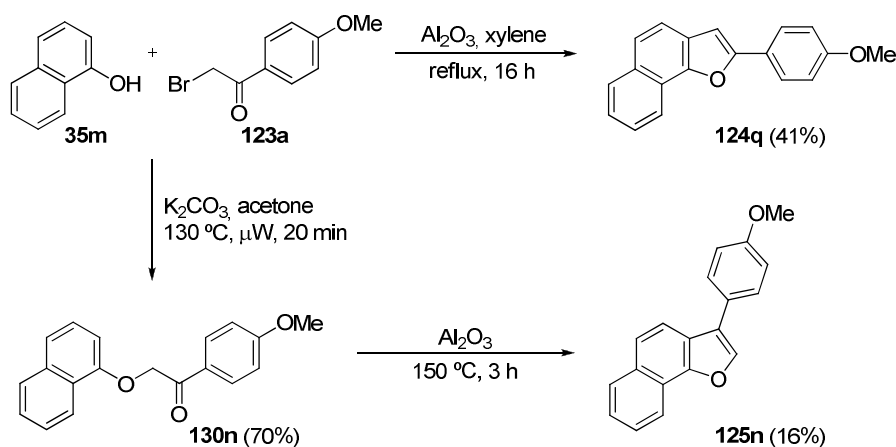
Scheme 2.11. Graphical overview of the computational study of the synthesis of 2-aryl and 3-aryl benzo[*b*]furans **124** and **125**, respectively. Activation energies are given in kcal/mol in brackets and were computed at the B3LYP/6-31+G*+ Δ ZPVE level of theory.

2.4. BROADENING the SCOPE of the REACTION: SYNTHESIS of NAPHTHOFURANS

In the light of the results obtained so far, it was decided to broaden the scope of these reactions by applying the developed synthetic methods to the preparation of the tricyclic analogues of benzofurans, i.e. naphthofurans, starting from naphthols instead of phenols.

2.4.1. Experimental study

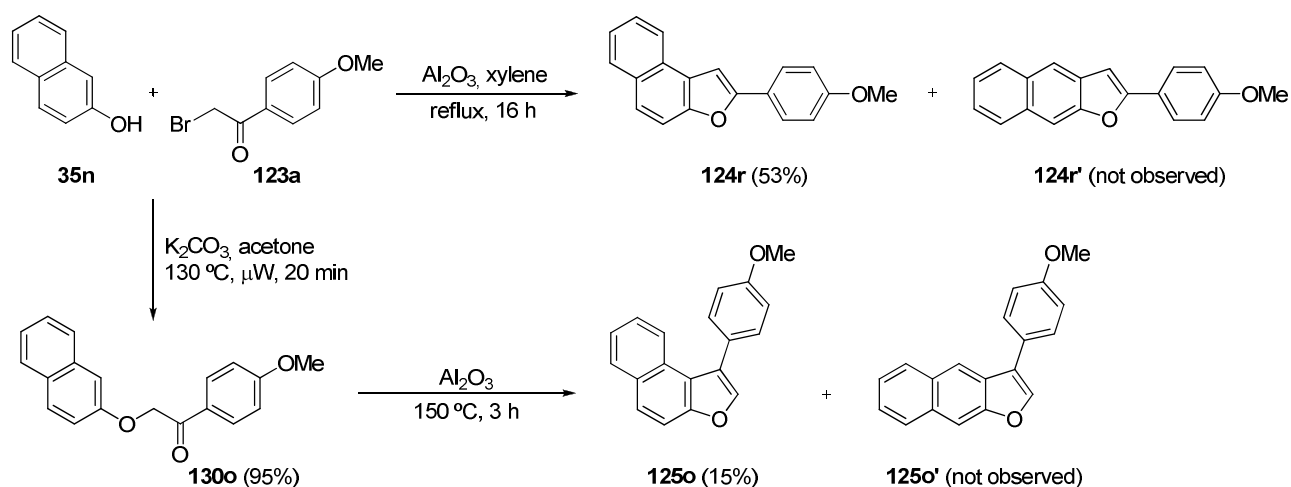
In the case of 1-naphthol **35m** (α -naphthol) and 2-naphthol **35n** (β -naphthol), no additional activation of the aryl moiety is required. Thus, reaction between 1-naphthol **35m** and **123a** in the presence of alumina yields **124q**, whereas microwave irradiation in the presence of K_2CO_3 leads to the formation of ether **130n**. Cyclization of this latter compound yields **125n**, the 3-substituted analogue of **124q**. In this case, only one possibility exists to form the naphtho[1,2-*b*]-furan scaffold, and both 2- and 3-(4-methoxyphenyl) derivatives can be prepared from **35m** and **123a** (Scheme 2.12).



Scheme 2.12. Reactions between 1-naphthol **35m** and 2-bromo-4'-methoxyacetophenone **123a** for the synthesis of 2-aryl and 3-aryl naphthofurans **124q** and **125n**, respectively.

However, in the case of 2-naphthol **35n** (β -naphthol), two possible adducts can be envisaged in its reaction with **123a** in the presence of alumina. Under these conditions, however, only compound **124r** was obtained in moderate yield, whereas the corresponding naphtho[2,3-*b*]furan analogue **124r'** was not observed. Like in the previous example, microwave irradiation of a mixture of 2-naphthol **35n** and **123a** in the presence of K_2CO_3 leads to the formation of ether **130o**. Again, in the cyclization of this ether two possible adducts can be envisaged. Under these conditions, however, only compound **125o** was

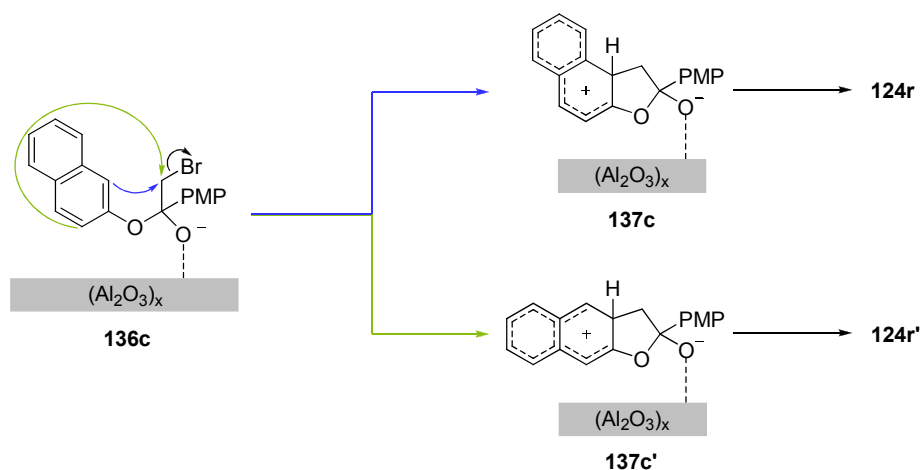
obtained, whereas the corresponding naphtho[2,3-*b*]furan analogue **125o'** was not observed (Scheme 2.13).



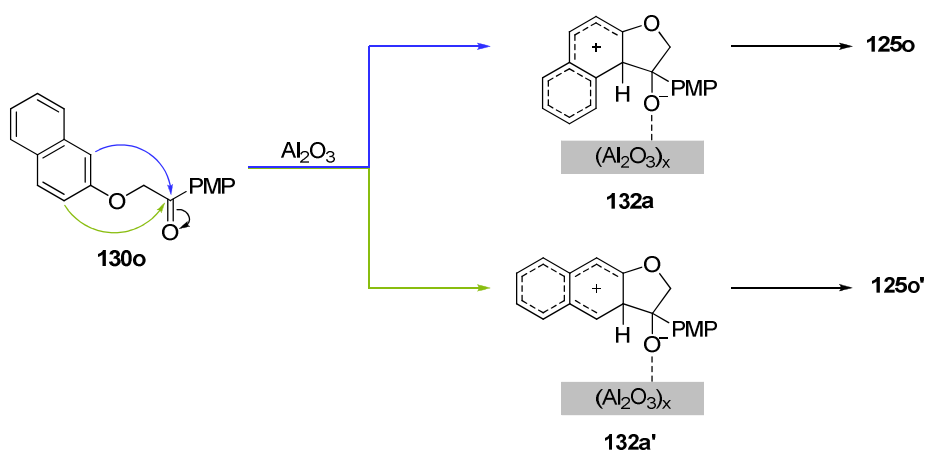
Scheme 2.13. Reaction between 2-naphthol **35n** and 2-bromo-4'-methoxyacetophenone **123a** for the synthesis of 2-aryl and 3-aryl naphthofurans **124r,r'** and **125o,o'**, respectively.

2.4.2. Insight into the reaction mechanism

In order to get a better understanding of the total regioselectivity of these reactions towards the formation of compounds **124r** and **125o** (over compounds **124r'** and **125o'**), the canonical forms corresponding to the resonance hybrids of the cyclic intermediates leading to compounds **124r** and **124r'** (Scheme 2.14) and compounds **125o** and **125o'** (Scheme 2.15) were studied. The proposed resonance hybrids are similar to those showed in the mechanisms proposed in Schemes 2.10 and 2.9 for 2-aryl and 3-aryl benzo[*b*]furans **124a-p** and **125a-l**, respectively.



Scheme 2.14. Resonance hybrids of the proposed cyclic intermediates leading to compounds **124r** and **124r'**. PMP = *para*-methoxyphenyl.

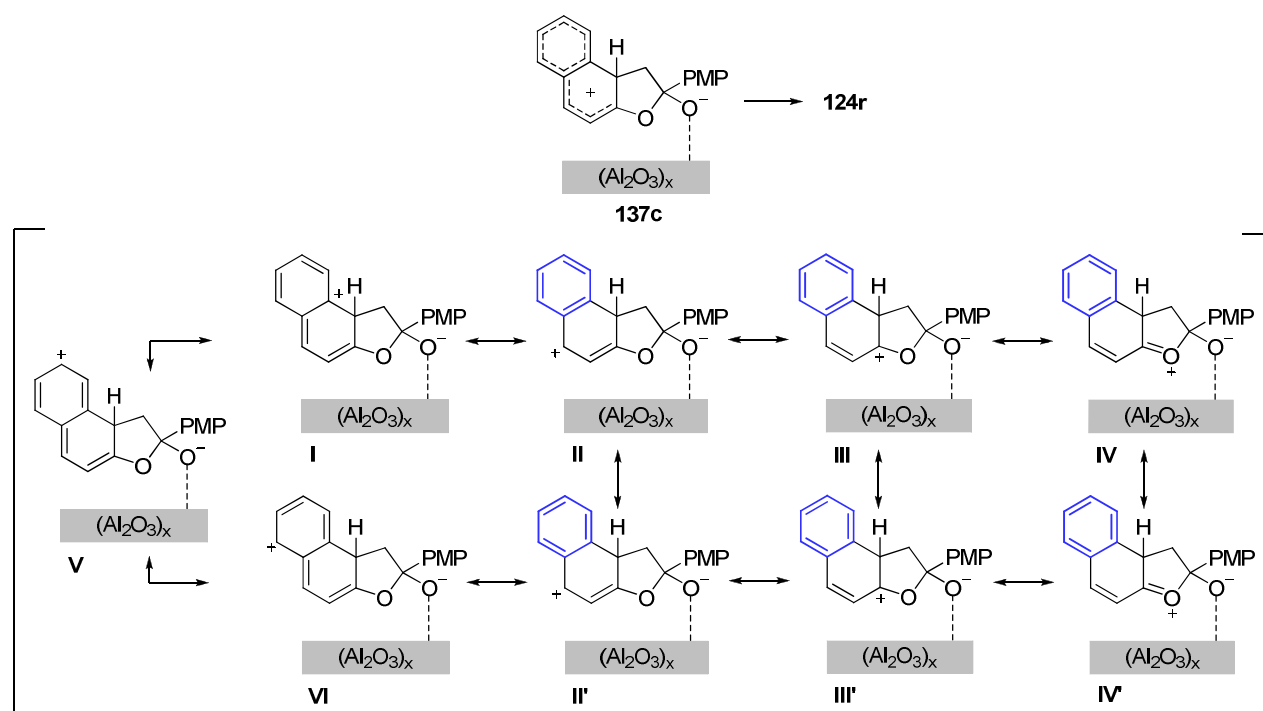


Scheme 2.15. Resonance hybrids of the proposed cyclic intermediates leading to compounds **125o** and **125o'**. PMP = *para*-methoxyphenyl.

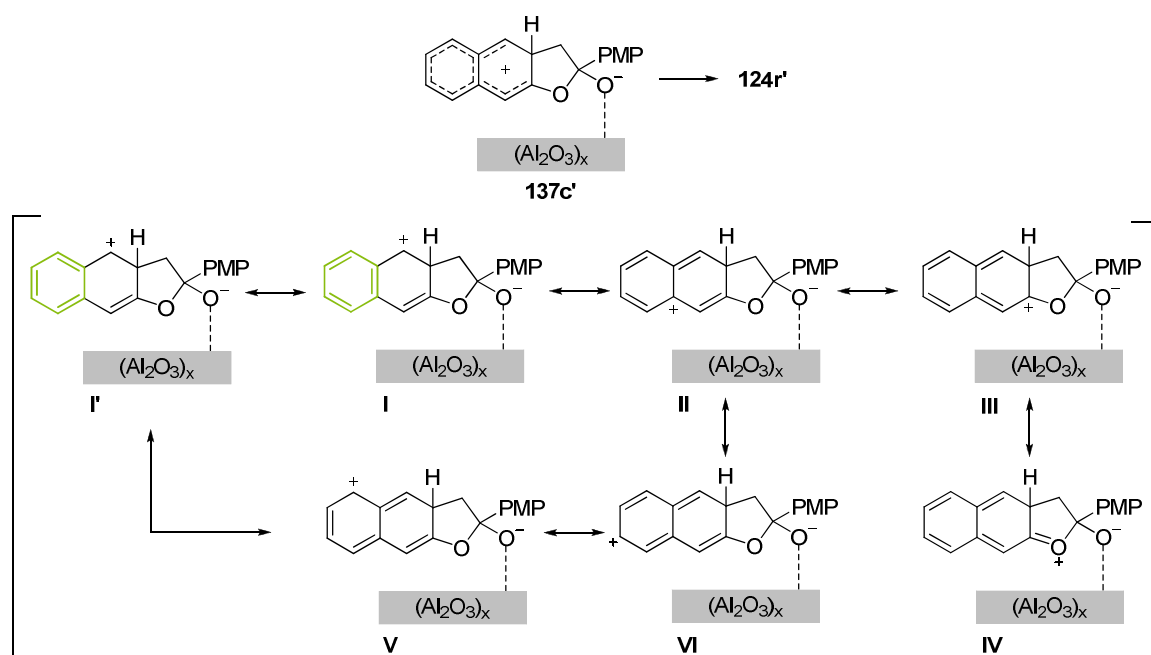
When assessing the intermediates from this standpoint, it must be taken into account that the greater the number of resonance structures, the more stable (less energetic, more thermally accessible) the intermediate. In other words, the more likely for the reaction to follow that particular path. Besides, high values of resonance energy (high stabilization) are found in hybrids with aromatic resonance structures.

In the case of the intermediate leading to **124r** (**137c**), it was observed that nine resonance structures can be envisaged, six of which preserve the aromaticity of one phenyl group in the aryl moiety. For the intermediate leading to **124r'** (**137c'**), on the other hand, seven canonical forms were proposed and only two of them preserved the aromaticity of one phenyl group in the aryl moiety. This suggests a preference for the formation of **124r** over **124r'** (Schemes 2.16 and 2.17).

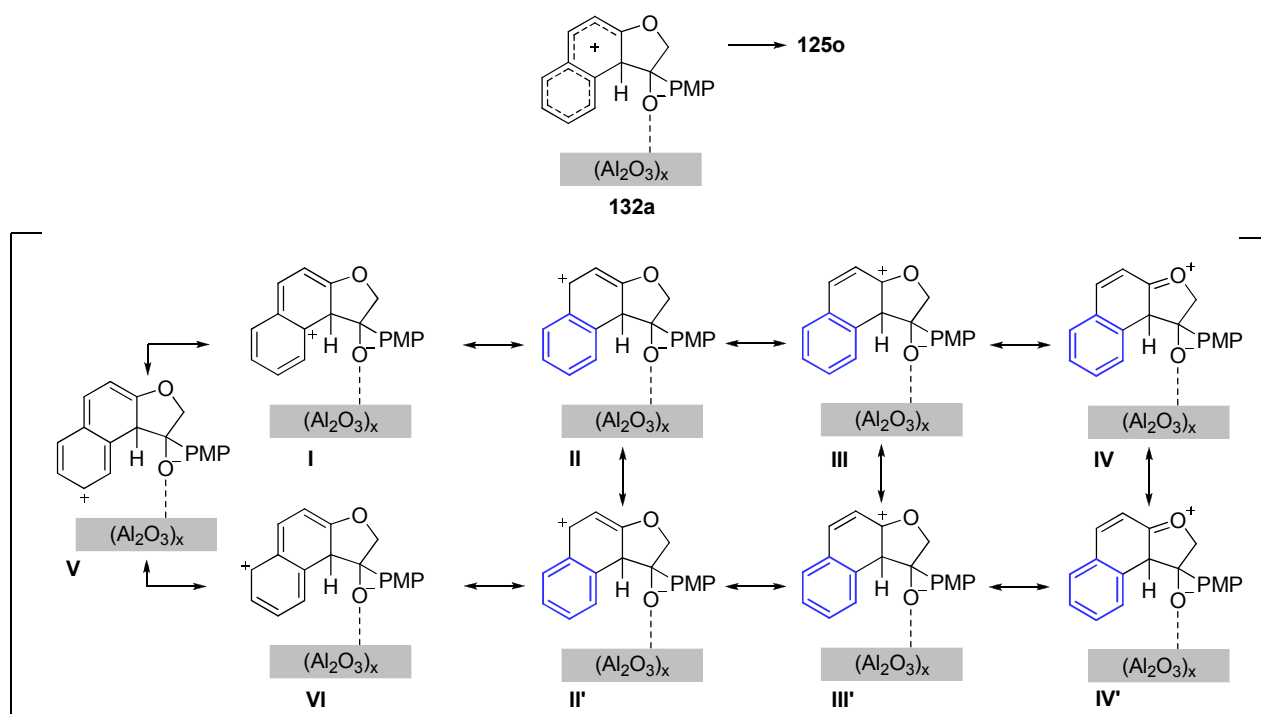
The study of the resonance structures of the intermediates leading to compounds **125o** and **125o'** (**132a** and **132a'**, respectively) was exactly the same as the one shown above for compounds **124r** and **124r'** and also concluded that there is a preference for the formation of **125o** over **125o'** (Schemes 2.18 and 2.19). Thus, both of these models are compatible with the experimental results.



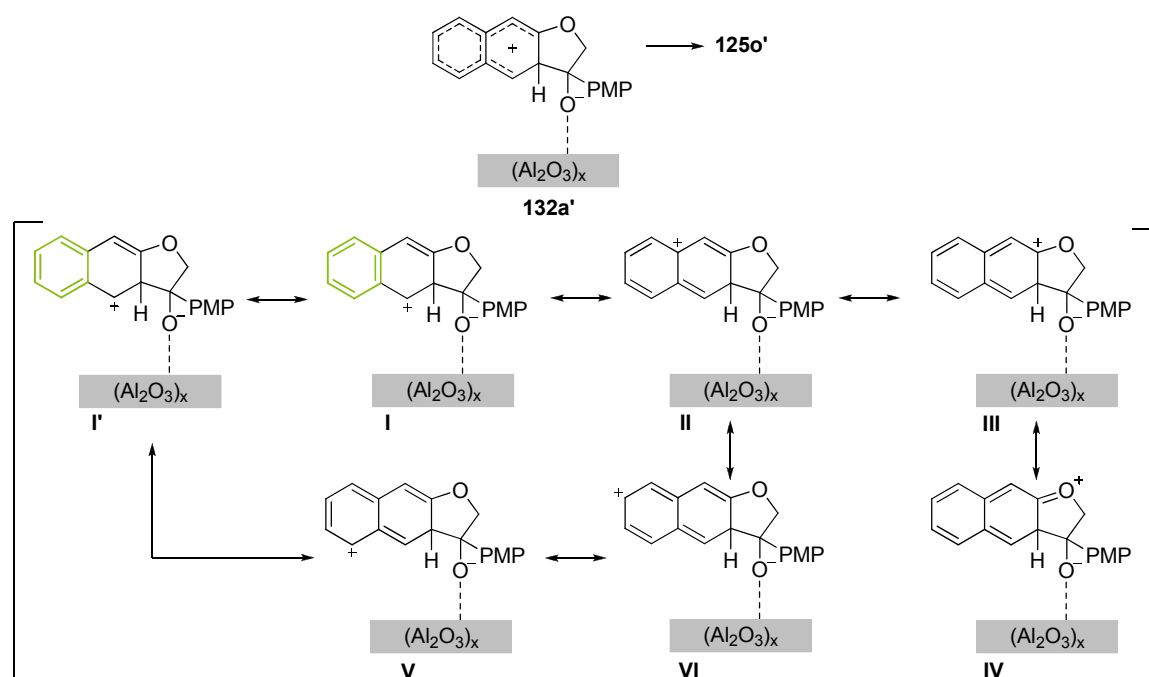
Scheme 2.16. Resonance hybrid and resonance structures of the proposed cyclic intermediate leading to compound **124r**. The benzene rings (which preserve the aromaticity) are highlighted in blue. PMP = *para*-methoxyphenyl.



Scheme 2.17. Resonance hybrid and resonance structures of the proposed cyclic intermediate leading to compound **124r'**. The benzene rings (which preserve the aromaticity) are highlighted in light green. PMP = *para*-methoxyphenyl.



Scheme 2.18. Resonance hybrid and resonance structures of the proposed cyclic intermediate leading to compound **125o**. The benzene rings (which preserve the aromaticity) are highlighted in blue. PMP = *para*-methoxyphenyl.



Scheme 2.19. Resonance hybrid and resonance structures of the proposed cyclic intermediate leading to compound **125o'**. The benzene rings (which preserve the aromaticity) are highlighted in light green. PMP = *para*-methoxyphenyl.

2.5. CONCLUSIONS

From this chapter, in which a new method for the preparation of benzo[*b*]furans from 2-bromoacetophenones and activated phenols is described, the following conclusions can be drawn:

- Under the optimized procedures, both 2-aryl and 3-aryl benzo[*b*]furans can be obtained with complete regiocontrol, from the same readily available reactants (*ortho* unsubstituted phenols and 2-bromoacetophenones) and with moderate yields.
- Alumina plays a vital role in both synthesis methods; without it the cyclization step does not take place.
- The reaction between phenols and 2-bromoacetophenones in the presence of neutral alumina yields exclusively 2-substituted benzo[*b*]furans **124**.
- The corresponding 3-aryl derivatives can be obtained via a two-step Williamson-cyclization sequence: when a basic salt such as potassium carbonate is used, the corresponding 2-oxoethers **130** are obtained; cyclization of these latter compounds promoted by neutral alumina yields the corresponding 3-substituted benzo[*b*]furans **125**.
- A model based on DFT calculations has been presented and the possible reaction mechanisms have been proposed, which provide a better understanding of the experimentally observed results. According to them, the first step towards the synthesis of 2-aryl benzo[*b*]furans **124** consists of a nucleophilic addition (A_{N2}) on the carbonyl carbon whilst the preparation of the 3-aryl derivatives **125** starts with a nucleophilic substitution (S_{N2}) on the methylene carbon.
- Under the same optimized reaction conditions but starting from 1- or 2-naphthols, bicyclic analogues of phenols (the corresponding naphthofurans) can be prepared also with complete regiocontrol and with moderate yields for the direct reaction promoted by alumina and for the oxoether formation in the presence of K_2CO_3 .

Chapter 3:

Chemical Transformations on 2- and 3-Aryl Benzo[*b*]furans

3.1. Short introduction and objectives

3.2. *N*-halosuccinimides-mediated aromaticity driven regioselective halogenation of substituted benzo[*b*]furans

- 3.2.1. Preparation of halogenated benzofurans overview
- 3.2.2. Experimental study: *N*-halosuccinimides (NXS)
- 3.2.3. Computational study
- 3.2.4. Conclusions

3.3. Hypervalent iodine-mediated oxidative dearomatization of monohydroxylated benzo[*b*]furans

- 3.3.1. Oxidative dearomatization of phenols overview
- 3.3.2. Experimental study: λ^3 -Iodanes
- 3.3.3. Experimental study: λ^5 -Iodanes (preliminary results)
- 3.3.4. Conclusions

3.4. Boron tribromide-mediated demethylation of methoxy groups in benzo[*b*]furans

- 3.4.1. Preparation of hydroxylated benzofurans overview
 - 3.4.2. Experimental study: boron tribromide (BBr₃)
 - 3.4.3. Conclusions
-

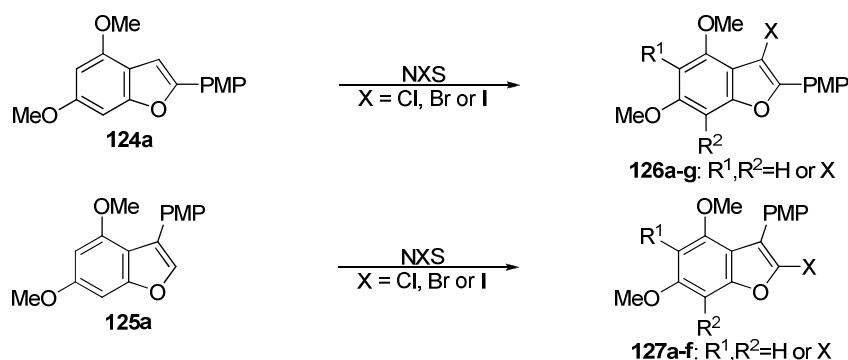
3.1. SHORT INTRODUCTION and OBJECTIVES

The benzo[*b*]furan structure is common to many bioactive molecules and natural products and therefore, efficient methods for the synthesis of substituted derivatives (that could be useful both as such and/or as intermediates for longer syntheses) are highly desirable. These derivatives include, for example, halogenated benzofurans (which have well-documented utility in organic synthesis for the formation of new C–C, C–N, C–S or C–O bonds, as previously seen in section 1.1.3.2.1) or hydroxylated ones (which can act as starting materials for further transformations and have also been extensively used in traditional medicine).

Having a fast and effective access to the benzo[*b*]furan scaffold (by means of the synthesis methods described in chapter 2) and bearing in mind the wide range of potential fields of action of these compounds, in this chapter our efforts driven towards the introduction of new substituents or the derivatization of existing functional groups (starting from compounds **124** and **125**) are described, along with the study of the application of a well documented reaction for phenols to (mono)hydroxylated benzofurans.

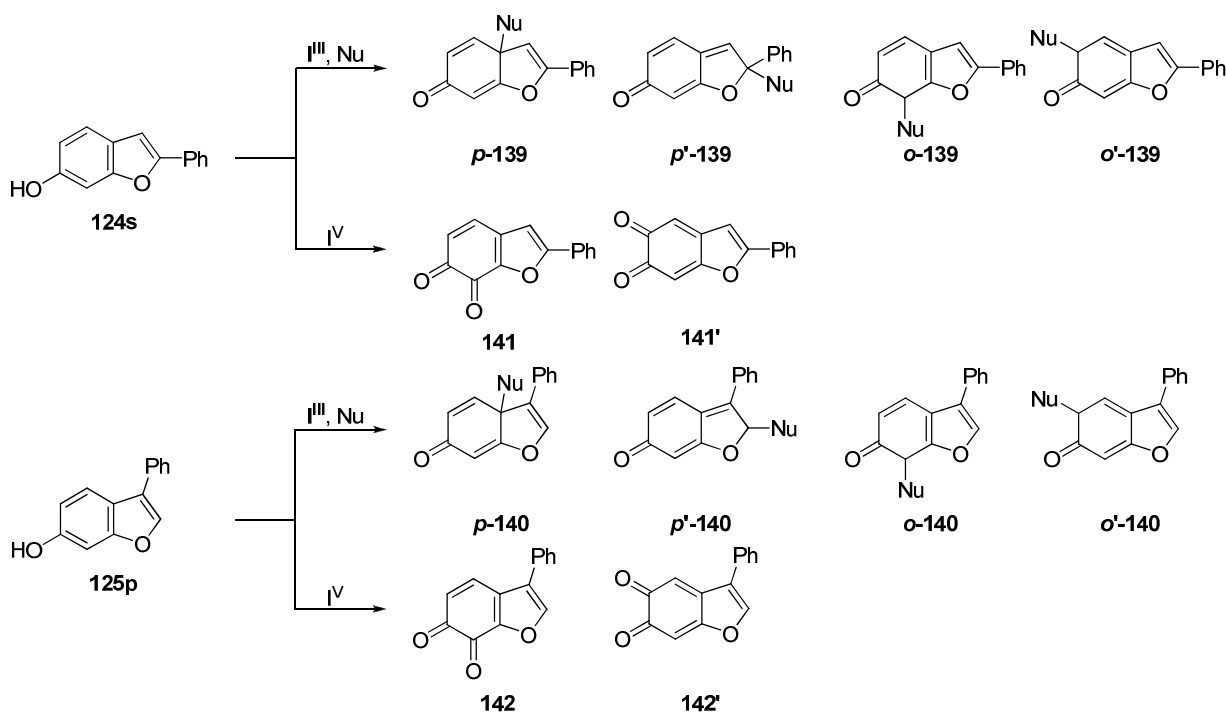
The chemical transformations showed here are the halogenation of substituted benzo[*b*]furans on the one hand, the oxidative dearomatization of monohydroxylated benzo[*b*]furans on the other hand and last but not least the demethylation of the methoxy groups present in some of the already prepared benzo[*b*]furans.

The main issue associated with the halogenation was the control of the regioselectivity and possible polyhalogenation of the process, as well as the unambiguous determination of the resulting reaction products (Scheme 3.1).



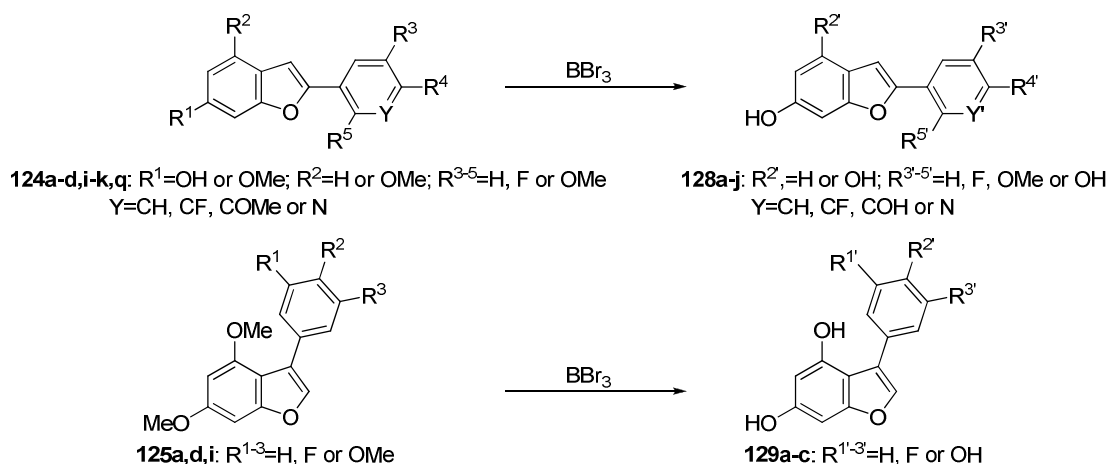
Scheme 3.1. General scheme of the halogenation reactions of benzo[*b*]furans.

The oxidative dearomatization, in turn, constituted a challenge since the aromatic bicyclic structure of benzo[*b*]furan presented more possible reaction sites than phenol, greatly complicating the prediction of the outcome of the reaction (Scheme 3.2). Besides, it required, as a starting point, the preparation of 2- and 3-phenylbenzofuran-6-ols (**124s** and **125p**, respectively).



Scheme 3.2. Predicted products of the λ^3 - and λ^5 -iodine-mediated (I^{III} and I^V , respectively) dearomatization of 2- and 3-phenylbenzofuran-6-ols (**124s** and **125p**, respectively).

The demethylation of methoxy groups, for its part, yielded interesting polyhydroxylated compounds (Scheme 3.3), which can be considered as conformationally restricted polyhydroxylated stilbene analogues (see section 1.1.3.2.2).



Scheme 3.3. General scheme of the demethylation of methoxy groups of benzo[*b*]furans.

Bearing this general scheme in mind, the objectives of this chapter are:

- i) First, to explore the reaction conditions to regioselectively obtain mono-, di-, or even trihalogenated 2-aryl and 3-aryl benzo[*b*]furans starting from compounds **124a** and **125a** and determining the preferential reaction site(s) in each case using *N*-halosuccinimides (NXS). This matter is raised in section **3.2. *N*-halosuccinimides-mediated aromaticity driven regioselective halogenation of substituted benzo[*b*]furans.**
- ii) Next, to explore the application of the reaction conditions for the λ^3 and λ^5 -iodane-mediated oxidative dearomatization of phenols to 2- and 3-phenylbenzofuran-6-ols (**124s** and **125p**, respectively). This subject is addressed in section **3.3. Hypervalent iodine-mediated oxidative dearomatization of monohydroxylated benzo[*b*]furans.**
- iii) Finally, to obtain the (poly)hydroxylated compounds resulting from the demethylation of methoxy groups present in some of the benzo[*b*]furans already prepared in chapter 2. This issue is covered in section **3.4. Boron tribromide-mediated demethylation of methoxy groups in benzo[*b*]furans.**

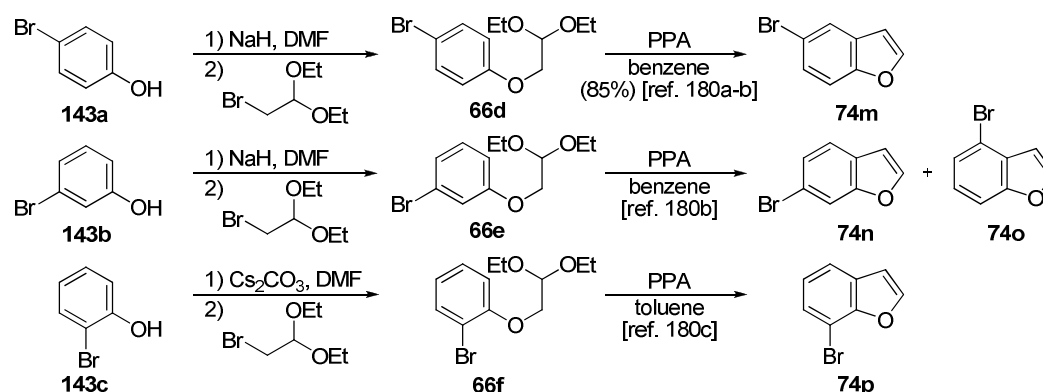
3.2. N-HALOSUCCINIMIDES-MEDIATED AROMATICITY DRIVEN REGIOSELECTIVE HALOGENATION of SUBSTITUTED BENZO[*b*]FURANS

3.2.1. Preparation of halogenated benzofurans overview

In this section the most conventional strategies used for the preparation of halogenated benzofurans will be reviewed. These include the two approaches mentioned in chapter 1 for the synthesis of (multiply) substituted benzofurans: on the one hand, the strategies based on formation of the heterocyclic framework after the introduction of the substituents and, on the other hand, those introducing the substituents to the preformed heterocycle.

3.2.1.1. Formation of the heterocyclic framework after the introduction of the halogen(s)

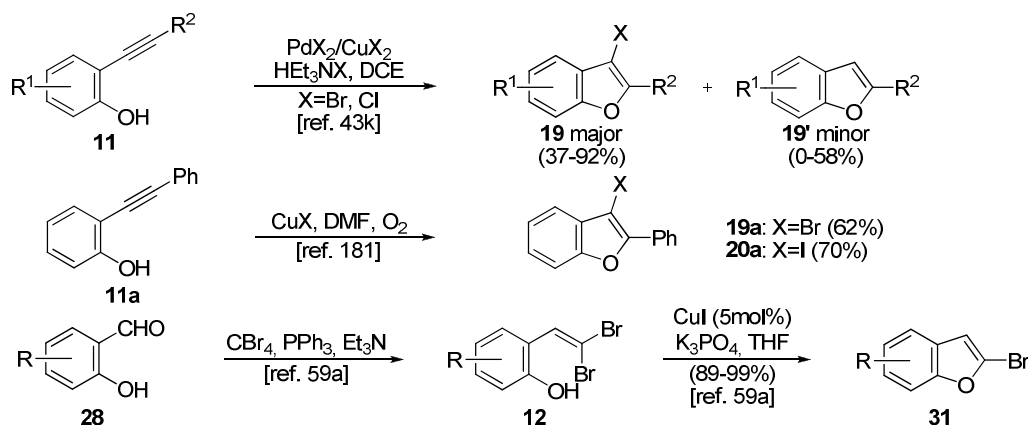
One of the more practical syntheses of bromobenzofurans, with the halogen substituent located at any position of the benzene ring (4, 5, 6 or 7), consists of the etherification of the corresponding bromophenol with bromoacetaldehyde diethyl acetal using NaH (or Cs₂CO₃) in DMF followed by a cyclocondensation (intramolecular Friedel-Crafts) by treatment of the resulting aryloxyacetal with polyphosphoric acid (PPA) (Scheme 3.4)¹⁸⁰.



Scheme 3.4. Examples of two-step preparation of 4, 5, 6 or 7-bromobenzofurans from the corresponding bromophenols.

¹⁸⁰ (a) Tasker, A. S.; Sorensen, B. K.; Jae, H.-S.; Winn, M.; von Geldern, T. W.; Dixon, D. B.; Chiou, W. J.; Dayton, B. D.; Calzadilla, S.; Hernandez, L.; Marsh, K. C.; WuWong, J. R.; Opgenorth, T. J. *J. Med. Chem.* **1997**, *40*, 322-330 (b) Taveras, A. G.; Aki, C. J.; Bond, R. W.; Chao, J.; Dwyer, M.; Ferreira, J. A.; Chao, J.; Yu, Y.; Baldwin, J. J.; Kaiser, B.; Li, G.; Merritt, J. R.; Nelson, K. H.; Rokosz, L. L. *Patent* WO 02/083624 A1, PCT/US02/12681 (c) Venkatraman, S.; Velazquez, F.; Gavalas, S.; Wu, W.; Chen, K. X.; Nair, A. G.; Bennett, F.; Huang, Y.; Pinto, P.; Jiang, Y.; Selyutin, O.; Vibulbhan, B.; Zeng, Q.; Lesburg, C.; Duca, J.; Huang, H.-C.; Agrawal, S.; Jiang, C.-K.; Ferrari, E.; Li, C.; Kozlowski, J.; Rosenblum, S.; Shih, N.-Y.; Njoroge, F. G. *Bioorg. Med. Chem.* **2013**, *21*, 2007-2017

When considering the 2- or 3-halogenated benzofuran preparation, transition metal-mediated reactions are the methodologies of choice. As examples of this, the synthesis of 2-substituted 3-halobenzo[*b*]furans via Pd-catalyzed^{43k} or Cu-mediated¹⁸¹ cyclization-halogenation of the corresponding 2-alkynylphenols have been described in literature. The CuI catalyzed intramolecular Ullmann-type cross-coupling of *gem*-dibromoolefins^{59a,182} has also been reported to be an entry to 2-halobenzofurans (Scheme 3.5).



Scheme 3.5. Examples of transition-metal mediated preparation of 2 or 3-halobenzofurans.

3.2.1.2. Introduction of the halogen(s) to the preformed heterocycle

There are many known methods for the preparation of haloarenes from aromatics, especially from electron-rich systems. The most straightforward method for the synthesis of halogenated heterocycles is the treatment of the unsubstituted parent substrate with an electrophilic halogen source. General halogenation procedures could be summed up as follows¹⁸³.

Chlorination. Apart from conventional Friedel-Crafts chlorination of aromatics, the use of hypochlorites (or hypochlorous acid), calcium hypochlorite, *tert*-butyl hypochlorite, benzoyl hypochlorite or sodium chlorate-chlorotrimethylsilane have also been extensively studied.

¹⁸¹ Swamy, N. K.; Yazici, A.; Pyne, S. G. *J. Org. Chem.* **2010**, *75*, 3412-3419

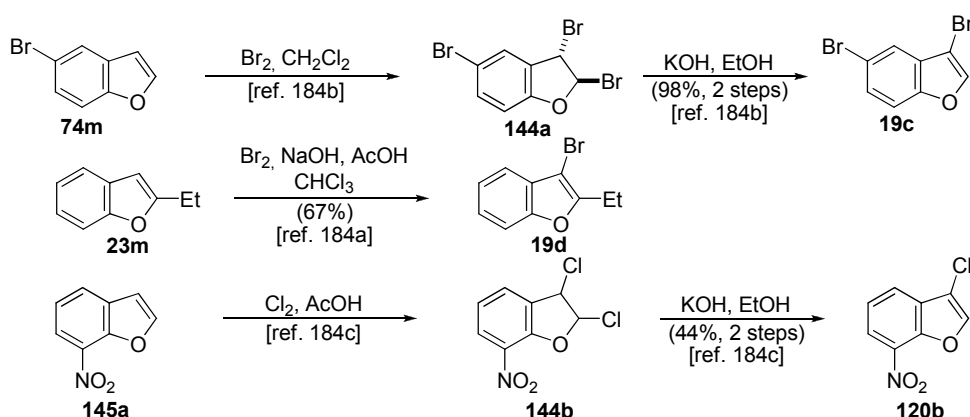
¹⁸² (a) Newman, S. G.; Aureggi, V.; Bryan, C. S.; Lautens, M. *Chem. Commun.* **2009**, 5236-5238 (b) The "classic" Ullmann reaction is the synthesis of symmetric biaryls via copper-catalyzed coupling. The "Ullmann-type" reactions include copper-catalyzed nucleophilic aromatic substitution between various nucleophiles (e.g. substituted phenoxides) with aryl halides. The most common of these is the Ullmann ether synthesis.

¹⁸³ Prakash, G. K. S.; Mathew, T.; Hoole, D.; Esteves, P. M.; Wang, Q.; Rasul, G.; Olah, G. A. *J. Am. Chem. Soc.* **2004**, *126*, 15770-15776

Bromination. Molecular bromine is the most widely used brominating agent. Many Lewis acids are effective catalysts for the reaction, although it works even without them with highly electron-rich substrates. Other reported reagents suitable for bromination are elemental bromine, dibromoisocyanuric acid in sulfuric acid, BrNO_3 in sulphuric acid, elemental bromine with mercurous oxide or HF and SbF_5 , and a mixture of benzoyl peroxide and lithium bromide.

Iodination. Incorporation of iodine into the aromatic ring is achieved by indirect methods, being the Sandmeyer reaction, substitution of an aromatic amino group via preparation of its diazonium salt followed by its displacement with a nucleophile (halide anions, cyanide, thiols, water, and others) often catalyzed by copper (I) salts, the most popular one.

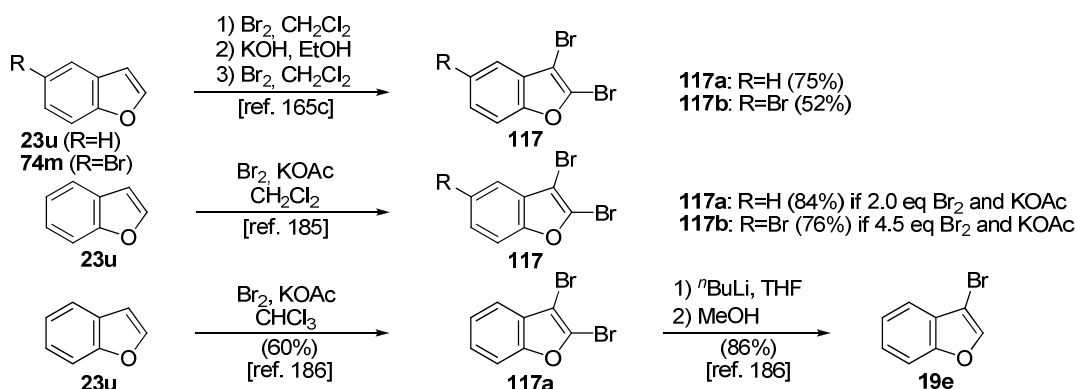
For the benzofused heterocycles such as indoles, benzofurans and benzotiofenenes, halogenation reaction typically provides access to 3-halogenated substrates. A common strategy for the synthesis of 3-halobenzofurans involves a 2-step procedure of halogenation and elimination. In the first step the addition product (2,3-dihalogenated-2,3-dihydrobenzofuran) is obtained by treatment of the starting benzofuran with molecular halogen. In the second, elimination with ethanolic KOH takes place, yielding the 3-halobenzofuran. Bromination and chlorination reactions following this procedure have been reported¹⁸⁴ (Scheme 3.6).



Scheme 3.6. Examples of the two-step (halogenation and elimination) preparation of 3-halobenzofurans.

¹⁸⁴ (a) Katritzky, A. R.; He, H.-Y.; Long, Q.; Cui, X.; Level, J.; Wilcox, A. L. *Arkivoc* **2000**, *iii*, 240-251 (b) Hamilton, C. J.; Saravanamuthu, A.; Fairlamb, A. H.; Eggleston, I. M. *Bioorg. Med. Chem.* **2003**, *11*, 3683-3693 (c) Plé, P. A.; Green, T. P.; Hennequin, L. F.; Curwen, J.; Fennell, M.; Allen, J.; Lambert-van der Brempt, C.; Costello, G. *J. Med. Chem.* **2004**, *47*, 871-887

In addition, in the case of bromine, further halogenation of the 3-bromobenzofuran following the same procedure was reported to give access to the 2,3-dihalobenzofuran^{165c}. However, this is not the only way to obtain this product since treatment of benzofuran with bromine under basic conditions yields 2,3-dibromobenzofuran¹⁸⁵. This can, at the same time, act as an intermediate towards the 3-bromobenzofuran, via regioselective halogen/metal exchange at the C(2) position with ^tBuLi followed by quenching with methanol¹⁸⁶ (Scheme 3.7).



Scheme 3.7. Examples of the preparation of 2,3-dibromobenzofurans from 2,3-unsubstituted benzofurans.

In contrast, 2-halogenated (3-unsubstituted) benzofused heterocycles are less accessible, typically requiring transition metals to catalyze the reaction. The most widely used method consists of deprotonative (*ortho*) metalation of the aromatic heterocycle followed by electrophilic trapping of the resulting species with iodine. Different lithium compounds proved useful for this transformation such as lithium magnesates (Bu₄MgLi₂)¹⁸⁷, aluminates (*i*-Bu₃Al(TMP)Li)¹⁸⁸, cuprates (MeCu(TMP)(CN)Li₂)¹⁸⁹, or mixed lithium-zinc or lithium-cadmium species (ZnCl₂TMDEA or CdCl₂TMDEA with LiTMP)¹⁹⁰ (Scheme 3.8).

¹⁸⁵ Hussain, M.; Hung, N. T.; Langer, P. *Tetrahedron Lett.* **2009**, *50*, 3929-3932

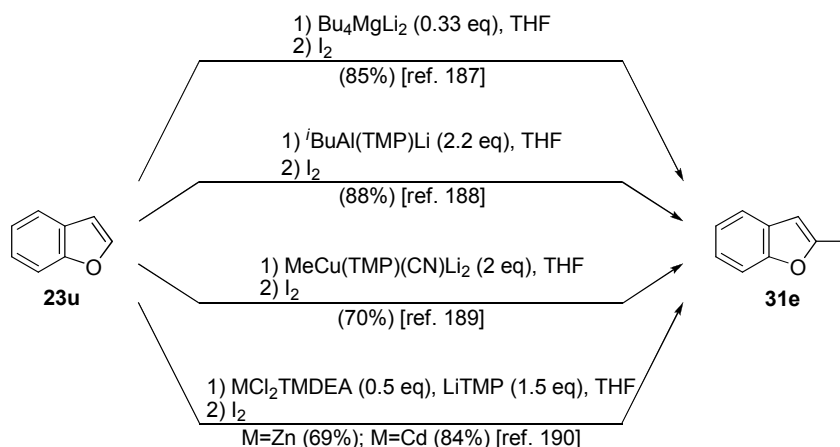
¹⁸⁶ Benincori, T.; Brenna, E.; Sannicolò, F.; Trimarco, L.; Antognazza, P.; Cesarotti, E.; Demartin, F.; Pilati, T. *J. Org. Chem.* **1996**, *61*, 6244-6251

¹⁸⁷ Mongin, M.; Bucher, A.; Bazureau, J. P.; Bayh, O.; Awadb, H.; Trécourt, F. *Tetrahedron Lett.* **2005**, *46*, 7989-7992

¹⁸⁸ Naka, H.; Uchiyama, M.; Matsumoto, Y.; Wheatley, A. E. H.; McPartlin, M.; Morey, J. V. *J. Am. Chem. Soc.* **2007**, *129*, 1921-1930

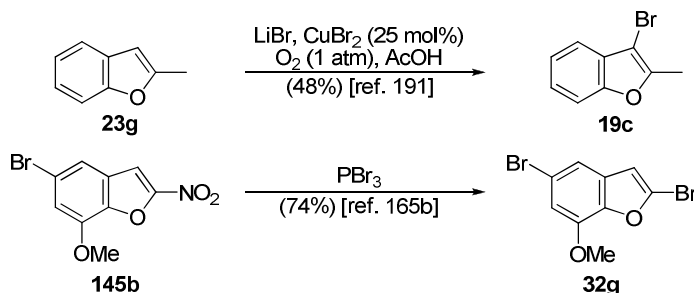
¹⁸⁹ Usui, S.; Hashimoto, Y.; Morey, J. V.; Wheatley, A. E. H.; Uchiyama, M. *J. Am. Chem. Soc.* **2007**, *129*, 15102-15103

¹⁹⁰ (a) L'Helgoual'ch, J.-L.; Bentabed-Ababsa, G.; Chevallier, F.; Yonehara, M.; Uchiyama, M.; Dourdour, A.; Mongin, F. *Chem. Commun.* **2008**, 5375-5377 (b) L'Helgoual'ch, J.-L.; Seggio, A.; Chevallier, F.; Yonehara, M.; Jeanneau, E.; Uchiyama, M.; Mongin, F. *J. Org. Chem.* **2008**, *73*, 177-183 (c) Snégaroff, K.; L'Helgoual'ch, J.-L.; Bentabed-Ababsa, G.; Nguyen, T. T.; Chevallier, F.; Yonehara, M.; Uchiyama, M.; Dourdour, A.; Mongin, F. *Chem. Eur. J.* **2009**, *15*, 10280-10290 (d) Snégaroff, K.; Komagawa, S.; Chevallier, F.; Gros, P. C.; Golhen, S.; Roisnel, T.; Uchiyama, M.; Mongin, F. *Chem. Eur. J.* **2010**, *16*, 8191-8201



Scheme 3.8. Examples of transition-metal mediated preparation of 2-iodobenzofuran from unsubstituted benzofuran.

Other atypical strategies to obtain these isomers have also been described, the regioselective oxidative bromination of electron-rich arenes in the presence of CuBr_2 , LiBr and molecular oxygen¹⁹¹ and the conversion of nitrobenzofurans to bromobenzofurans by phosphorus tribromide^{165b} being suitable examples (Scheme 3.9).



Scheme 3.9. Examples of other strategies for the preparation of 2- or 3-bromobenzofurans from benzofurans unsubstituted at these positions.

At this point we found interesting to recall the *N*-halosuccinimides (NXS) which, to our surprise, had not been extensively used as halogen source in the halogenation of benzo[*b*]furans. However, taking into account their general features and the fact that these reagents have been reported to be excellent to perform halogenation reactions in aromatic compounds (see section 3.2.2.1), we decided to explore their employment in the halogenation of both 2- and 3-aryl benzo[*b*]furans.

¹⁹¹ Yang, L.; Lub, Z.; Stahl, S. S. *Chem. Commun.* **2009**, 6460-6462

3.2.2. Experimental study: *N*-halosuccinimides (NXS)

3.2.2.1. General considerations

N-halosuccinimides: general features

The so-called *N*-halo reagents constitute a large group of substances which have extensively been used in organic synthesis and in the chemistry of natural compounds. These include *N*-halo amines, *N*-halo amides, *N*-halo carbamates, *N*-halo ureas, etc. In particular, the wide application of *N*-halosuccinimides (NXS) in organic synthesis is justified by some of their specific features.

To start with, the high lability of the N–X (X=halogen) bond and its diverse modes of splitting. Various highly reactive intermediates can be formed depending on the conditions, such as halogen radicals, halogen cations, halogen anions, N-radicals, N-cations, N-anions, etc.

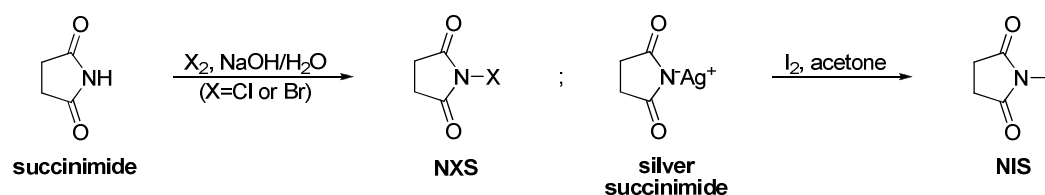
This gives rise to their second major virtue, their ability to promote different and very important reactions ranging from halogenation to oxidation, including imidation and other processes resulting in the formation of compounds with a C–X, C–O, C=O, S–X, P–X, C–N, P–N, S–N, S=N bond, etc. Besides, in the chemistry of natural compounds, they are widely used as halogenating, hydroxyhalogenating, oxidizing, and condensing agents.

Thirdly, and enhancing the previous feature, the high selectivity of the processes with participation of *N*-halosuccinimides, which cannot usually be achieved through the use of other reagents.

Another interesting advantage of these reactants is their ease of handling as well as the generation of relative inert succinimide as by-product, which can be easily recovered and reconverted to *N*-halosuccinimide to be used in subsequent reactions.

And last but not least, *N*-halosuccinimides are accessible and relatively stable compounds, compared to other *N*-halo reagents. The most commonly used ones are *N*-chlorosuccinimide (NCS), *N*-bromosuccinimide (NBS) and *N*-iodosuccinimide (NIS). All

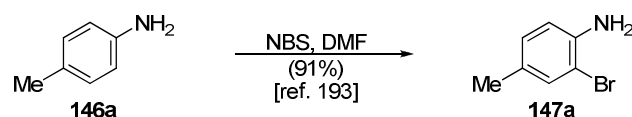
these NXS reagents are usually prepared from succinimide by the action of molecular halogens (Scheme 3.10)¹⁹².



Scheme 3.10. Preparation of *N*-halosuccinimides NXS: X = Cl (NCS), Br (NBS) and I (NIS).

N-halosuccinimides and C-halogenations (background)

Among all the reactions in which *N*-halosuccinimides can take part, we focused our attention on the C-halogenations, especially those involving aromatic and/or heterocyclic compounds. Replacement of hydrogen by halogen in an aromatic ring using *N*-halosuccinimides follows an electrophilic substitution pattern, holding in general the same relations as in the halogenation of aromatic compounds by halogens. For example, *p*-toluidine reacts with NBS leading to the formation of 91% of 2-bromo-4-methylaniline (Scheme 3.11)¹⁹³.



Scheme 3.11. Bromination of *p*-toluidine with NBS.

However, the reaction often requires some kind of activation or catalyst to work out. In this line, ZrCl_4 Lewis acid was reported to catalyze selective halogenation of aromatic compounds¹⁹⁴ and trifluoromethanesulfonic acid and $\text{BF}_3\text{-H}_2\text{O}$ activation combination also proved useful in the halogenation of deactivated aromatics via *N*-halosuccinimides¹⁸³. In addition, these reactants were used as halogen source in Pd-catalyzed halogenation of carbon-hydrogen bonds in biaryl systems¹⁹⁵ or gold-catalyzed halogenation of aromatics¹⁹⁶ and aromatic boronates¹⁹⁷ (Scheme 3.12).

¹⁹² Koval', I. V. *Russ. J. Org. Chem.* **2002**, *38*, 301-337

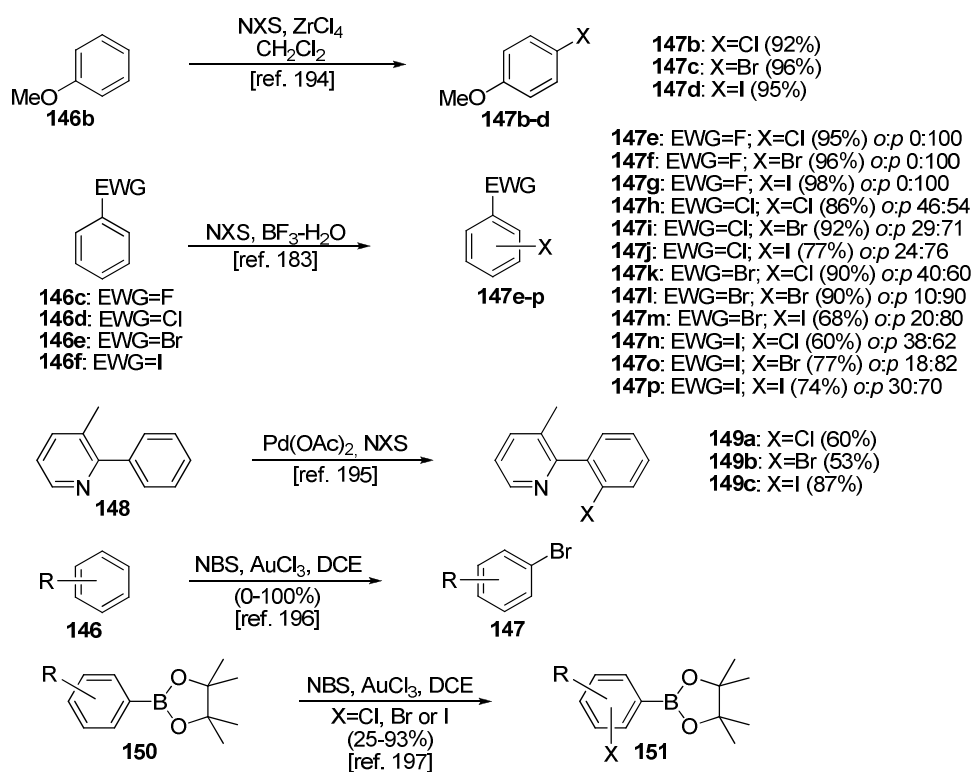
¹⁹³ Lai, Y. H.; Peck, T. G. *Aust. J. Chem.* **1992**, *45*, 2067-2071

¹⁹⁴ Zhang, Y.; Shibatomi, K.; Yamamoto, H. *Synlett* **2005**, *18*, 2837-2842

¹⁹⁵ Kalyani, D.; Dick, A. R.; Anani, W. Q.; Sanford, M. S. *Org. Lett.* **2006**, *8*, 2523-2526

¹⁹⁶ Mo, F.; Yan, J. M.; Qiu, D.; Li, F.; Zhang, Y.; Wang, J. *Angew. Chem. Int. Ed.* **2010**, *49*, 2028-2032

¹⁹⁷ Qiu, D.; Mo, F.; Zheng, Z.; Zhang, Y.; Wang, J. *Org. Lett.* **2010**, *12*, 5474-5477



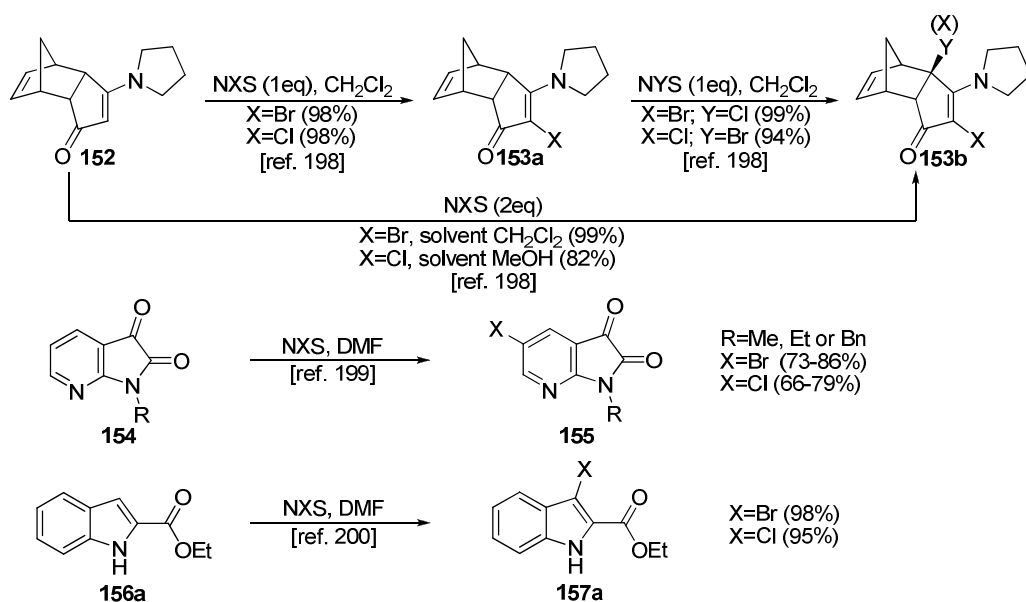
Scheme 3.12. Examples of conveniently catalyzed or activated halogenation of aromatics with NXS.

The C-halogenation reaction also occurs with fused cycles. An example of this is the halogenation of enaminones **152** to obtain α -halo enaminones **153** with *N*-halosuccinimides in dichloromethane¹⁹⁸. Following with the reactions involving heterocycles, a regioselective protocol for the halogenation of 1-alkyl-7-azaisatins **154** with *N*-halosuccinimides to synthesize 1-alkyl-5-halo-7-azaisatins **155** was reported¹⁹⁹. In the same vein, reaction of *N*-halosuccinimides with 2-substituted (3-unsubstituted) 1*H*-indoles **156a** was also described²⁰⁰ (Scheme 3.13).

¹⁹⁸ Ramesh, N. G.; Heijne, E. H.; Klunder, A. J. H. Zwanenburg, B. *Tetrahedron Lett.* **1998**, 39, 3295-3298

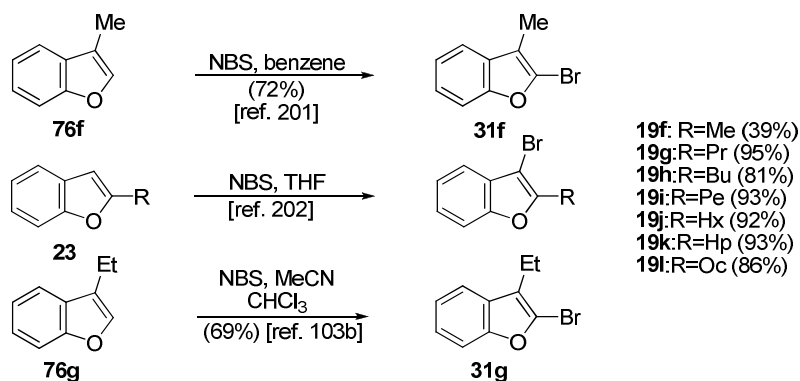
¹⁹⁹ Tatsugi, J.; Zhiwei, T.; Tsuchiya, Y.; Ito, T. *Arkivoc* **2009**, ii, 132-137

²⁰⁰ Wang, Z.; Vince, R. *Bioorg. Med. Chem.* **2008**, 16, 3587-3595



Scheme 3.13. Examples of halogenation of fused (hetero)cycles with NXS.

Examples of the particular case of C-halogenation reactions of benzofurans (on carbons in the bicyclic structure) are quite scarce, although bromination of 3-methyl benzofuran **76f**²⁰¹, 2-alkyl benzofurans **23**²⁰² or 3-ethyl benzofurans **76g**^{103b} using NBS have already been reported (Scheme 3.14).



Scheme 3.14. Examples of reported C-bromination reactions of benzofurans with NBS.

²⁰¹ Cugnon de Sevrécourt, M.; Robba, M. *Bull. Soc. Chim. Fr.* **1977**, 1-2, 139-141

²⁰² (a) Yamaguchi, T.; Irie, M. *J. Org. Chem.* **2005**, *70*, 10323-10328 (b) Yamaguchi, T.; Irie, M. *Eur. J. Org. Chem.* **2006**, 3105-3111

3.2.2.2. Two families of compounds: 2-aryl and 3-aryl halobenzofurans

Encouraged by these precedents in C-halogenation reactions of heterocycles with *N*-halosuccinimides, our work was driven towards conducting a study on the employment of NBS as brominating agent for the halogenation of the benzofurans synthesized in the previous chapter.

Having revised previous reactions in this field (sections 3.2.1 and 3.2.2.1), the conditions chosen for the trials were the dropwise addition of a solution of the corresponding benzofuran in dichloromethane over a solution of NBS (also in dichloromethane) followed by stirring at room temperature. The equivalents of NBS and the reaction time were adjusted depending on the number of positions to be brominated and the progress of the reaction, monitored by TLC. Room temperature was kept in all experiments, since uncontrolled multihalogenations were reported at higher temperatures¹⁹⁷.

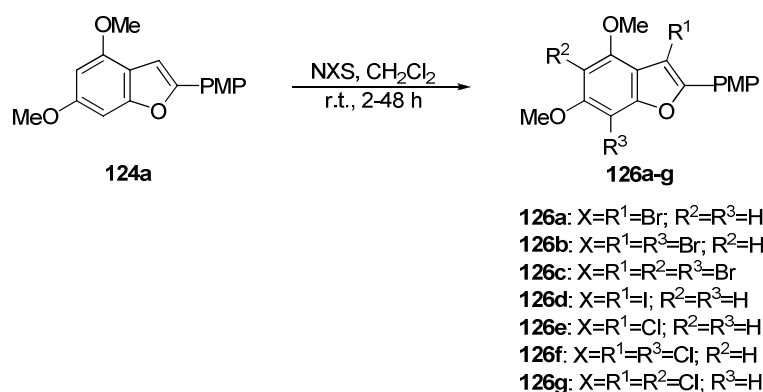
The benzofurans selected for the trials were the lead compounds of both 2-aryl and 3-aryl series, **124a** and **125a**, respectively. These were expected to be adequate starting materials since the oxygen in the five membered heterocyclic fused ring and the electron-releasing methoxy groups contained in their structure should collaborate in the stabilization of the cationic intermediate formed during the electrophilic substitution, highly activating these electron-rich aromatics towards this transformation. The reactions were in general, when successful, clean and yielded the halogenated product along with succinimide as major (or even only) byproduct. The main issue associated with these transformations was to unambiguously determine the halogenation position(s) in each case (Scheme 3.15).



Scheme 3.15. Possible halogenation positions of benzofurans **124a** and **125a**. PMP = *para*-methoxyphenyl.

2-aryl halobenzofurans

Starting with the 2-aryl benzofuran **124a** (Scheme 3.2.16), monobromination was first carried out, employing one equivalent of NBS. The reaction yielded the benzofuran **126a** halogenated in position 3 (81%) (Table 3.1, entry 1), as expected bearing in mind that this is the most reactive site towards an electrophilic substitution. The reason for this behavior is that the unshared pair of electrons of the oxygen contained in the furan substantially increases the stability of the cationic intermediate formed in this five membered ring, highly activating 2 and 3 positions compared with the ones in benzene ring²⁰³. This was in agreement with the analysis of the signals of the ¹H-NMR (Figures 3.1 and 3.7) and COSY (Figure 3.6 left) spectra registered for compound **126a**.



Scheme 3.16. Preparation of halobenzofurans **126a-g** from benzofuran **124a** via halogenation with *N*-halosuccinimide (NXS). PMP = *para*-methoxyphenyl.

Table 3.1. Synthesis of halobenzofurans **126a-g** from benzofuran **124a** via halogenation with *N*-halosuccinimide (NXS).

entry	eq of NXS	time (h)	product	yield ^a (%)
1	1 NBS	2	126a	81
2	2 NBS	4	126b	89
3	3 NBS	48	126b^b	89
4	6 NBS	48	126c	30
5	1 NIS	2	126d	- (degrad.)
6	1 NCS	48	126e	-
7	2 NCS	16	126f	57
			126g	14

^aYield of isolated pure product after column chromatography.

^bTribrominated compound was not obtained, the reaction was stopped at dibromination; the yield was estimated (same aspect as entry 2).

When two equivalents of NBS were used, dibromination of **124a** took place (Table 3.1, entry 2). In this case the regioselectivity of the reaction was more difficult to predict. The extra electron density delivered into the ring by the methoxy groups is concentrated on the carbon atoms in *ortho* and *para* positions with respect to these substituents. Both 5 and 7 positions are [*ortho*, *ortho*] and [*para*, *ortho*] with respect to the electron releasing groups and, therefore, equally activated by them in principle.

At this point the steric hindrance between the electrophile (bromine) and the substituents (methoxy groups) was considered, as it might offset the increased reactivity of one position to a greater extent than that of the other. Taking this into account, position 7 seemed more easily accessible for the electrophile than methoxy surrounded position 5, suggesting that this could be the preferential site for the second bromination and **126b** the obtained product (89%) (Table 3.1, entry 2). Again, this prediction was in agreement with the analysis of the signals of the ¹H-NMR (Figure 3.1) and other NMR (see section 3.2.2.3, Figures 3.8, 3.9 and 3.12) spectra registered for compound **126b**. In any case, the regioselectivity of the bromination reactions was examined more in depth in the computational study in section 3.2.3.

Tribromination of **124a** was next attempted employing three equivalents of NBS. It was observed that the reaction was stopped at the dibromination and did not further progress stirring it for longer time (up to 48 h) (Table 3.1, entry 3). The same transformation was then tried doubling the equivalents of NBS and stirring it for 48 h, obtaining the desired tribrominated benzofuran **126c** (Table 3.1, entry 4), again in agreement with the analysis of the signals of the ¹H-NMR spectrum (Figure 3.1), although in lower yield (30%) than its mono- and dibrominated analogues (81 and 89%).

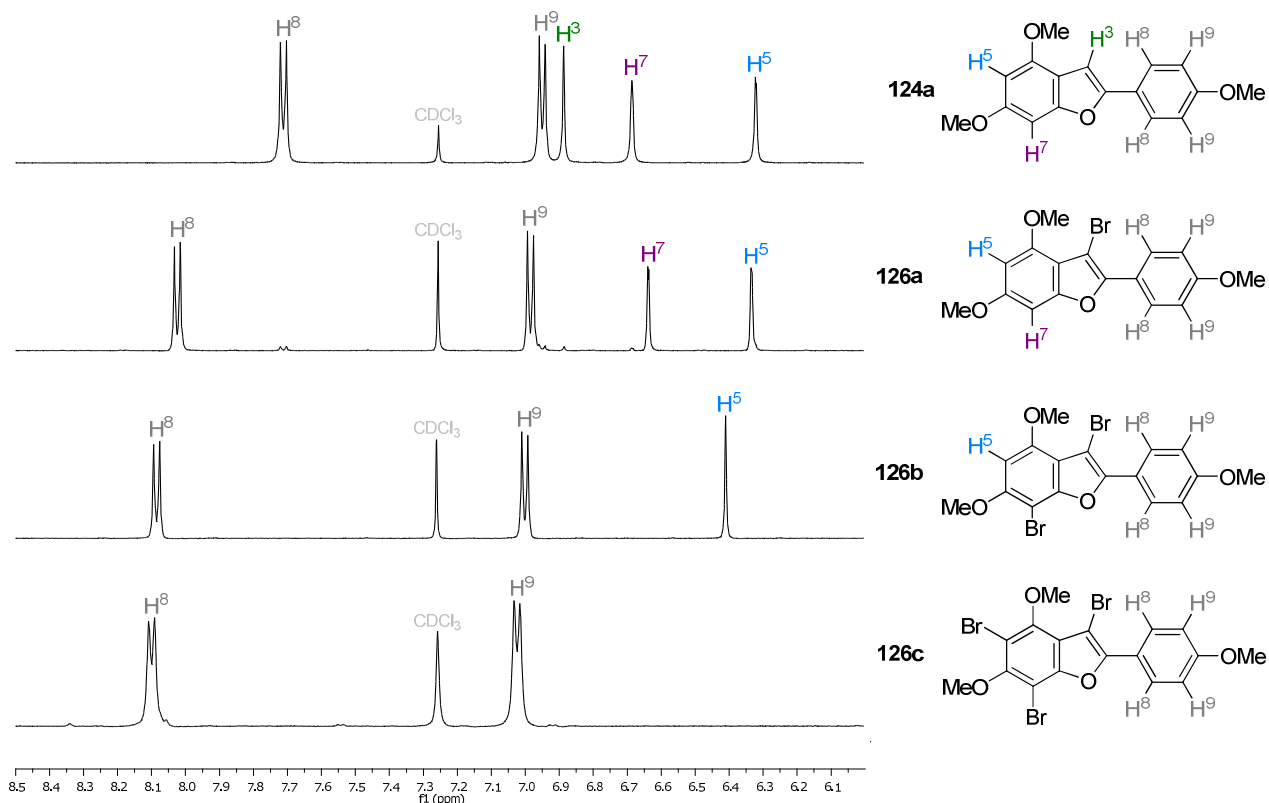


Figure 3.1. Enlarged aromatic region of $^1\text{H-NMR}$ spectra (500 MHz, CDCl_3) of compounds **124a**, monobrominated **126a**, dibrominated **126b** and tribrominated **126c**. Signals corresponding to protons H^3 , H^5 and H^7 in **124a** and **126a-b** were assigned according to the characterization study in section 2.2.4 and 3.2.2.3, respectively.

The difficulty of the bromination of the third position of the benzofuran might be attributed to the deactivating effect the two bromine atoms previously introduced exert over the aromatic system since halogens, in spite of having an unshared pair of electrons, are substantially more electronegative than carbon and, as a result, withdraw electron density away from the π cyclic array.

The following step in our study consisted of trying to extend the procedure to the use of other *N*-halosuccinimides, i.e. NIS and NCS.

Iodination was not achieved as the diverse attempts resulted always in complex mixtures of degraded products, which were not tried to be identified (Table 3.1, entry 5).

On the other hand, even after longer stirring, chlorination was not considerable (most of the reaction crude corresponded to the starting material **124a**) when one equivalent of NCS was employed (Table 3.1, entry 6) but yielded a 4:1 mixture of two dichlorinated isomers when two equivalents were added. This result was not surprising, since chlorination is reported to be relatively slower than bromination in many cases (and

iodination faster), typically requiring longer reaction times and/or higher temperatures^{183,194}.

According to the analysis of the signals in the ¹H-NMR (Figures 3.2 and 3.14) and other NMR (see section 3.2.2.3, Figures 3.15-3.20) spectra of the isolated compounds, the major product was the 3,7-dichlorobenzofuran derivative **126f** (57%), whilst the minor one would correspond to the 3,5-dichlorinated isomer **126g** (14%) (Table 3.1, entry 7). This suggests that position 3 is the preferential site for the first halogenation followed by position 7 and position 5, although the difference between the last two is not large enough to obtain exclusively one of the isomers, as happened in the bromination of the same compound.

In fact, the equivalent brominated minor regioisomer was never detected during the bromination assays and its presence, together with the lower overall yield of the reaction (with respect to the dibromination), was in agreement with the lower selectivity and reactivity of chlorination over bromination (and even iodination) already reported in literature^{43k,183,194}.

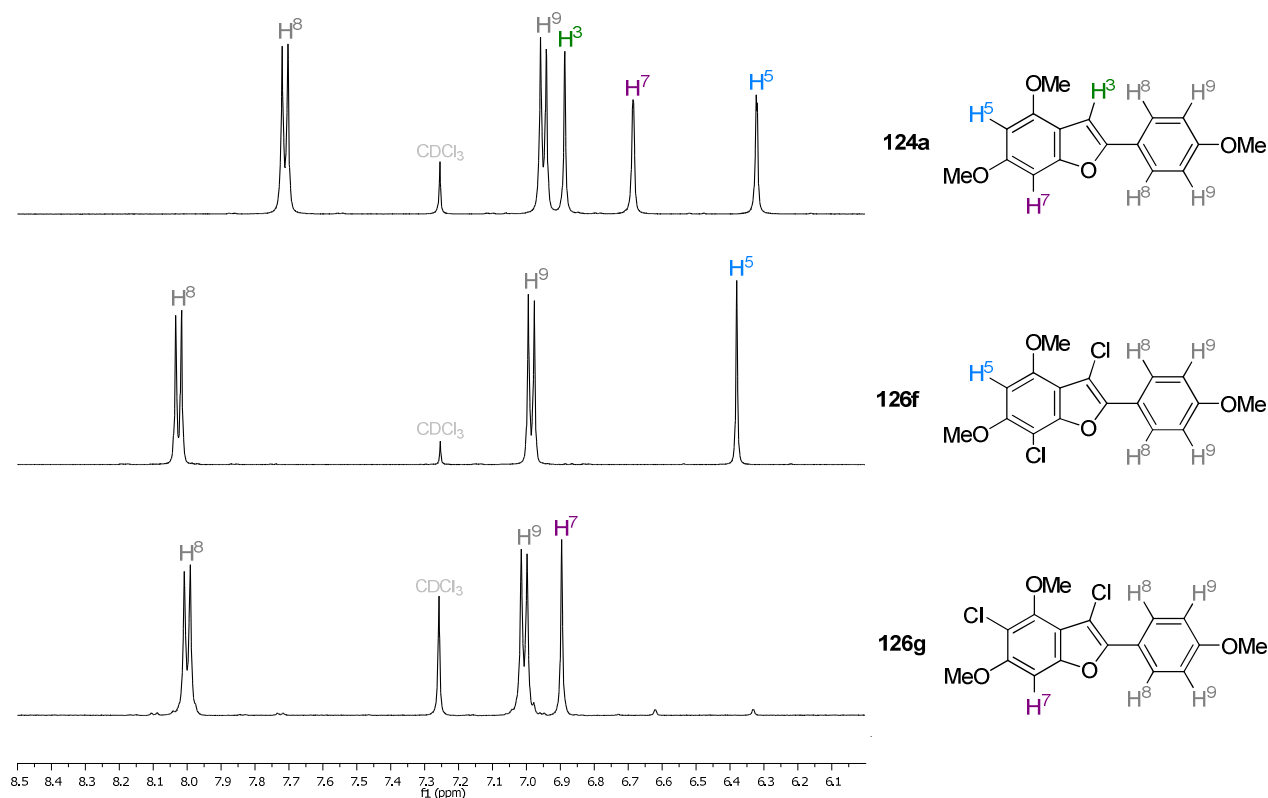
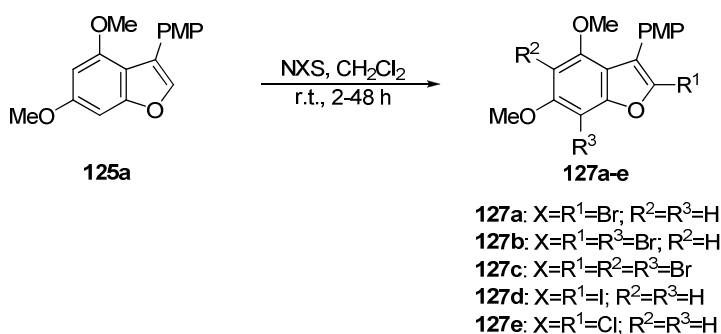


Figure 3.2. Enlarged aromatic region of ¹H-NMR spectra (500 MHz, CDCl₃) of compounds **124a**, dichlorinated major isomer **126f** and dichlorinated minor isomer **126g**. Signals corresponding to protons H³, H⁵ and H⁷ in **124a** and **126f-g** were assigned according to the characterization study in section 2.2.4 and 3.2.2.3, respectively.

3-aryl halobenzofurans

Next, the same ensemble of experiments was carried out with the 3-aryl series lead compound **125a** (Scheme 3.17). One equivalent of NBS led to the monobromination of the position 2 of the benzofuran, the vacant site in the five membered furan ring, furnishing product **127a** (81%) (Table 3.2, entry 1), according to the signals recorded in the $^1\text{H-NMR}$ (Figures 3.3 and 3.7) and COSY (Figure 3.6 middle) spectra registered for compound **127a**.



Scheme 3.17. Preparation of halobenzofurans **127a-e** from benzofuran **125a** via halogenation with *N*-halosuccinimide (NXS). PMP = *para*-methoxyphenyl.

Table 3.2. Synthesis of halobenzofurans **127a-e** from benzofuran **125a** via halogenation with *N*-halosuccinimide (NXS).

entry	eq of NXS	time (h)	product	yield ^a (%)
1	1 NBS	2	127a	81
2	2 NBS	4-16	127b	68
3	3 NBS	48	127b^b	68
4	6-15 NBS	16	127c	- (degrad.)
5	1 NIS	4	127d^c	41
6	1 NCS	2	127e	86

^aYield of isolated pure product after column chromatography.

^bTribrominated compound was not obtained, the reaction was stopped at dibromination; the yield was estimated (same aspect as entry 2).

^cUnstable, fast degradation.

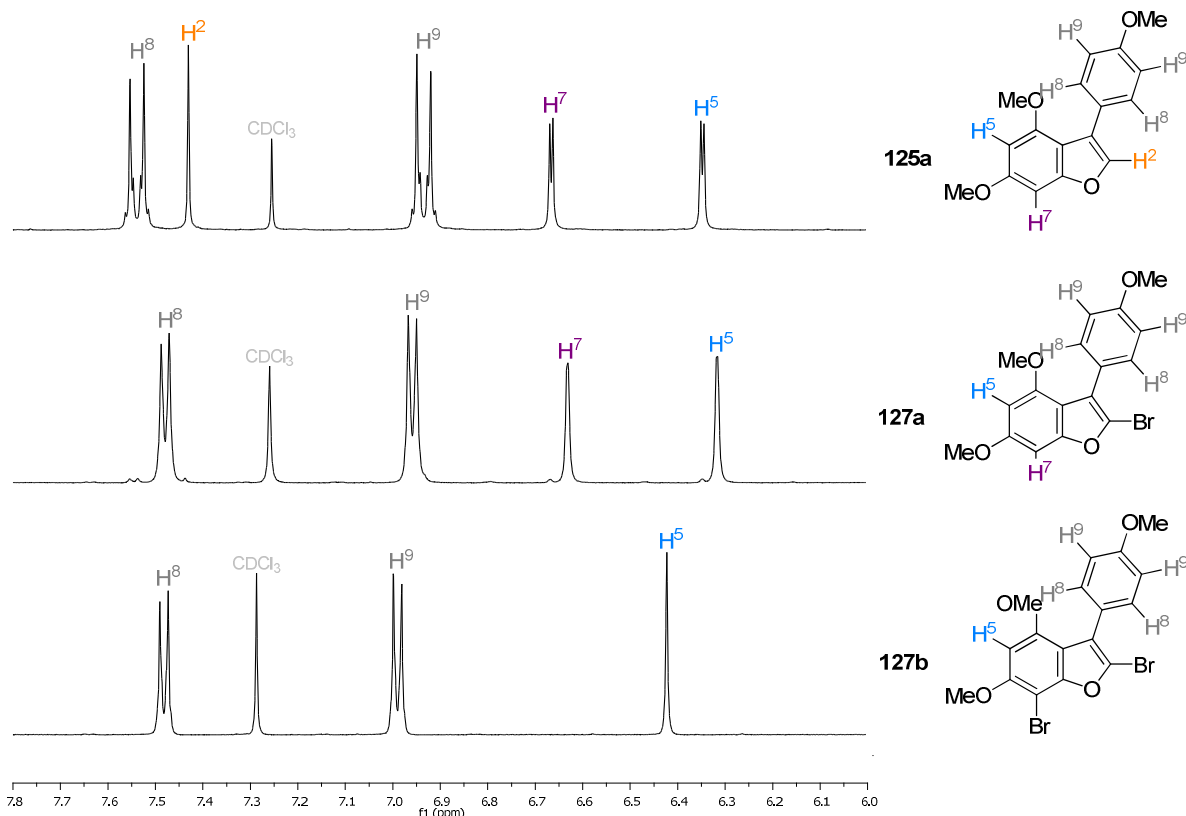


Figure 3.3. Enlarged aromatic region of ¹H-NMR spectra (500 MHz, CDCl₃) of compounds **125a**, monobrominated **127a**, and dibrominated **127b**. Signals corresponding to protons H², H⁵ and H⁷ in **125a** and **127a-b** were assigned according to the characterization study in section 2.2.4 and 3.2.2.3, respectively.

Dibromination with two equivalents of NBS was also possible, although with lower yield (68%) than in the corresponding 2-aryl series (89%), probably due to a higher deactivation of the molecule towards an electrophilic substitution, as a result of the incorporation of the first bromine atom. As in the previous assays, the second bromination site corresponded to position 7 and the obtained product was **127b** (Table 3.2, entry 2), once more according to the signals in the ¹H-NMR (Figure 3.3) and other NMR (see section 3.2.2.3, Figures 3.10, 3.11 and 3.13) spectra registered for compound **127b**. The mentioned deactivation became more pronounced with the presence of the second bromine in the benzofuran structure, so much so that tribromination did not take place even keeping the stirring for longer time and/or increasing the equivalents of NBS up to fifteen, leading this latter measure to the degradation of the products in reaction mixture (Table 3.2, entries 3 and 4).

The scope of the reaction was then widened to the use of NIS and NCS. This time iodination with one equivalent of NIS permitted the preparation of 2-iodinated species **127d** (Table 3.2, entry 5), according to the signals observed in the ¹H-NMR (Figure 3.4 and 3.7). Unfortunately, the product turned out not to be very stable and was only purified

in a 41% yield, despite the almost complete conversion observed in the crude reaction mixture, and for no much longer than the $^1\text{H-NMR}$ running time (the sample was degraded during $^{13}\text{C-NMR}$ spectrum registration).

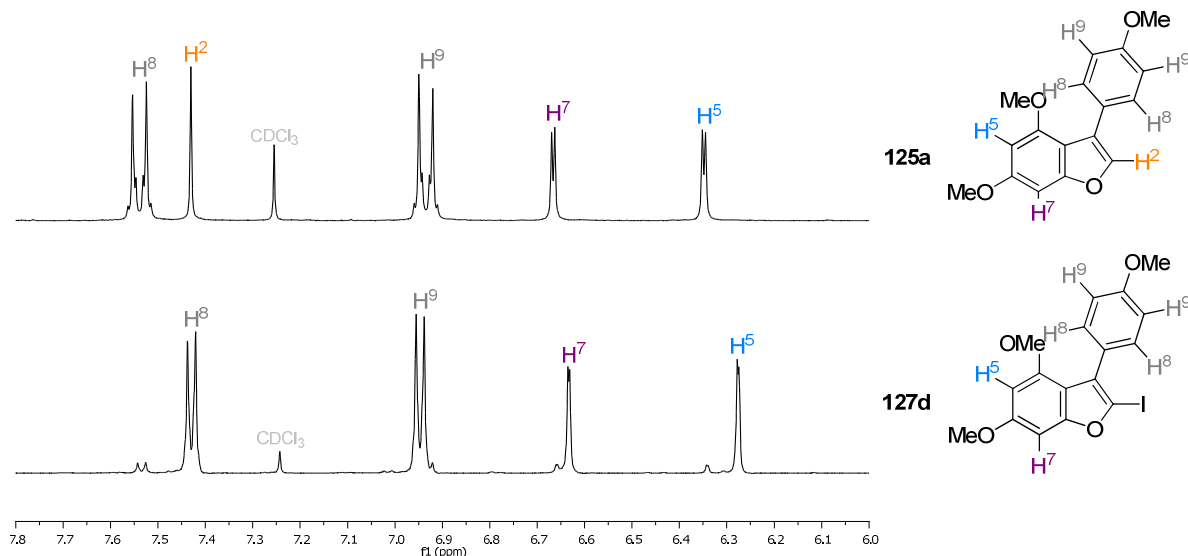
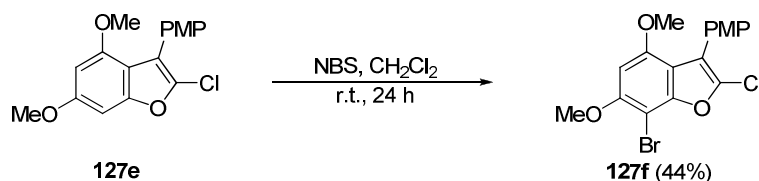


Figure 3.4. Enlarged aromatic region of $^1\text{H-NMR}$ spectra (500 MHz, CDCl_3) of compounds **125a** and monoiodinated **127d**. Signals corresponding to protons H^2 , H^5 and H^7 in **125a** and **127d** were assigned according to the characterization study in section 2.2.4 and 3.2.2.3, respectively.

Chlorination with one equivalent of NCS, in turn, gave the 2-chlorinated compound **127e** (Table 3.2, entry 6), again according to the signals in the NMR experiments ($^1\text{H-NMR}$ Figures 3.5 and 3.7 and COSY Figure 3.6 right), in the same reaction time and slightly higher yield (86%) than the corresponding bromination (81%).

Finally, one last experiment was carried out to get a combined dihalogenated derivative. It was to brominate the 3-chlorinated compound **127e** with NBS, following the same procedure as in the previous trials. The reaction performed with moderate yield (44%) when two equivalents of NBS were used and compound **127f** was obtained (Scheme 3.18), brominated in position 7 according to NMR experiments (Figure 3.5 and section 3.2.2.3, Figures 3.21-3.24), as could had been anticipated.



Scheme 3.18. Preparation of combined 7-bromo-2-chlorobenzofuran **127f** from benzofuran **127e** via bromination with NBS. PMP = *para*-methoxyphenyl.

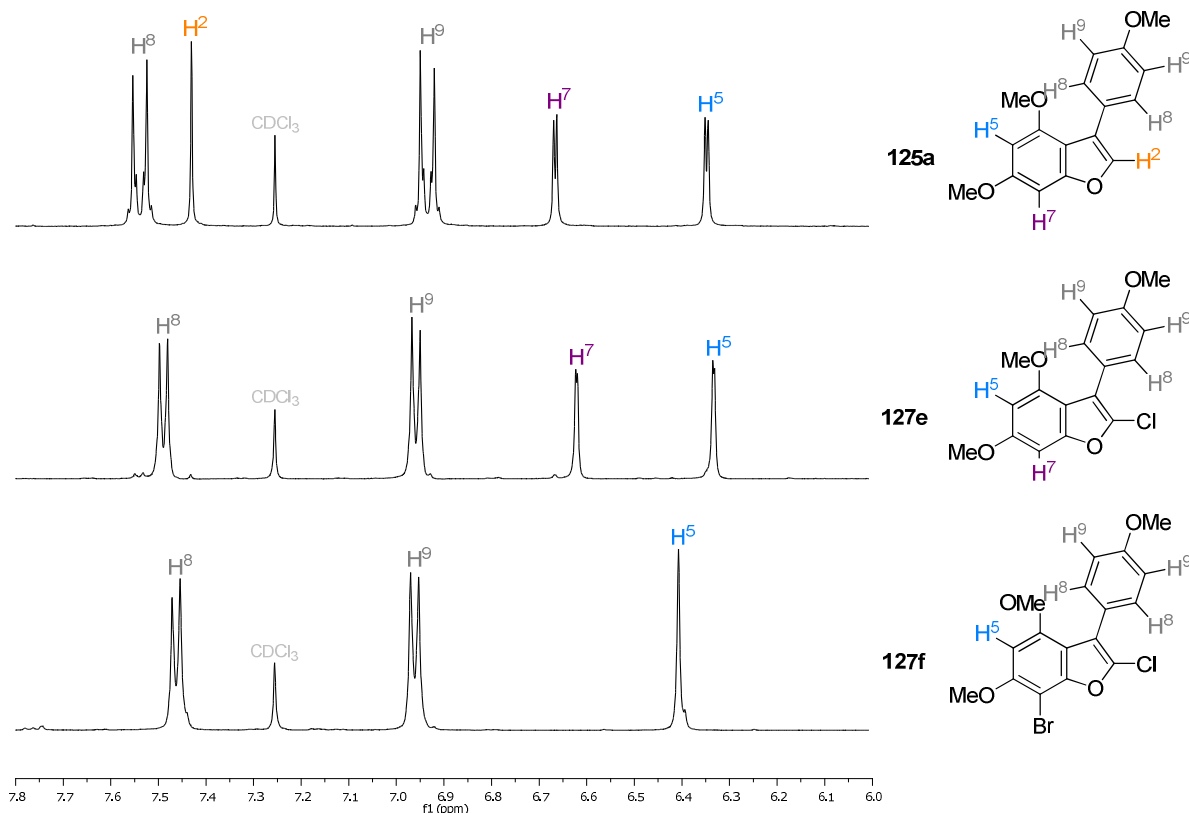


Figure 3.5. Enlarged aromatic region of ¹H-NMR spectra (500 MHz, CDCl₃) of compounds **125a**, monochlorinated **127e** and combined dihalogenated (chlorinated and brominated) **127f**. Signals corresponding to protons H², H⁵ and H⁷ in **125a** and **127e-f** were assigned according to the characterization study in section 2.2.4 and 3.2.2.3, respectively.

3.2.2.3. Structural elucidation: NMR spectroscopy study

The elucidation of the structures of the different **126** and **127** compounds, that is to determine the halogenated position(s) in each case, was carried out making use of the suitable NMR experiments from the series: ^1H -NMR, ^{13}C -NMR, COSY, HSQC, HMBC and selective NOEs¹⁷⁸, as already presented in section 2.2.4 for the now starting compounds **124a** and **125a**. In this study only stable mono- and dihalogenated compounds were analysed. All the experiments shown in this section were registered on a spectrometer operating at 500 MHz, except for some NOE experiments which were registered on a spectrometer operating at 400 MHz, and using deuterated chloroform as solvent.

Monohalogenation of **124a** (**126a**) and **125a** (**127a,d-e**)

Starting with the monohalogenated compounds **126a** and **127a** and **127e**, besides ^1H and ^{13}C NMRs, only COSY experiment was considered, since it made it clear that the first halogenation position in each case was the unsubstituted one in the furan ring, position 3 for **126a** and position 2 for **127a** and **127e**, respectively.

The COSY spectra (Figure 3.6) evidenced the persistence of the $\text{H}^5\text{--H}^7$ coupling, in agreement with signals corresponding to H^5 and H^7 in ^1H -NMR spectrum being doublets with a coupling constant of 1.1–1.7 Hz (*meta*-coupling in aromatic compounds, 4 bonds distance) (Figure 3.7). Due to degradation problems, for product **127d** only ^1H -NMR was considered. As for compounds **124a** and **125a**, the signal at higher chemical shift was assigned to H^7 (see section 2.2.4), due to the larger deshielding effect of the benzofuran oxygen over that of the methoxy substituent.

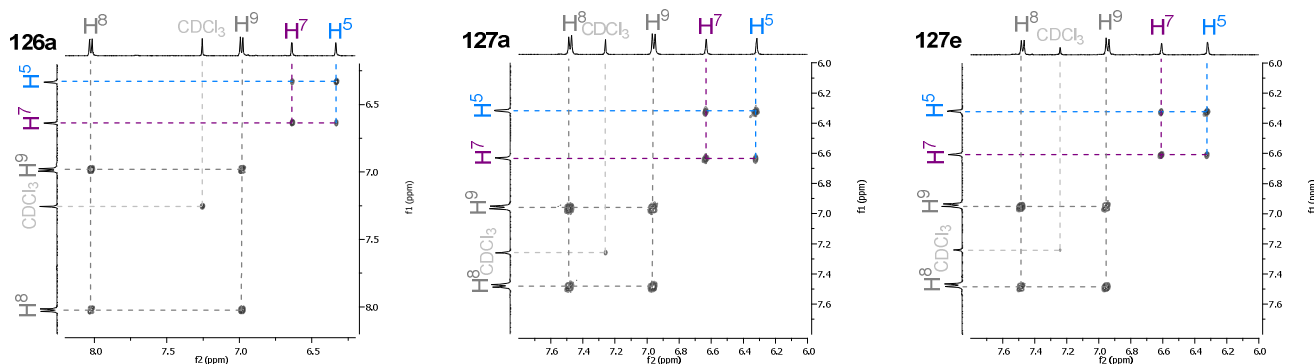


Figure 3.6. COSY (500 MHz, CDCl_3) of **126a** (left), **127a** (middle) and **127e** (right). Chemical shift given in ppm.

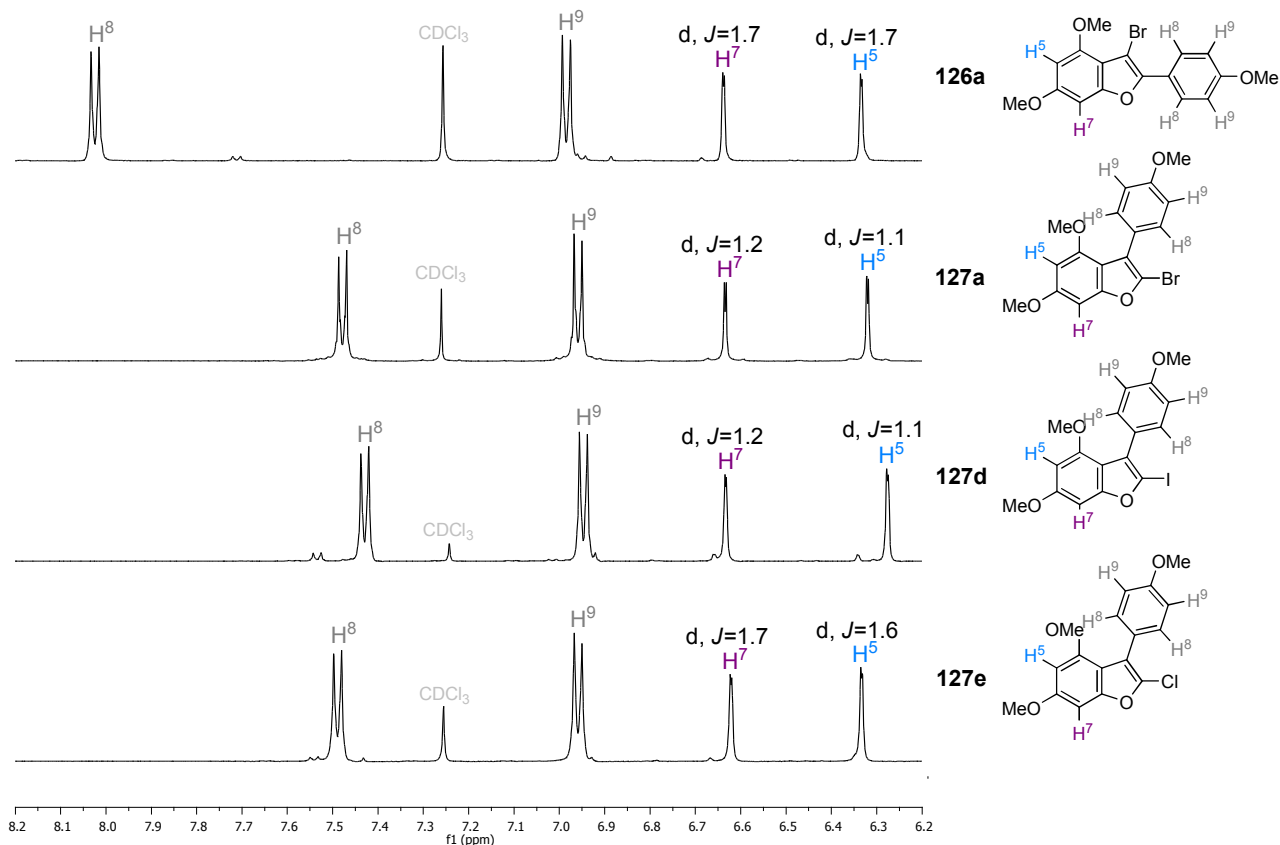


Figure 3.7. Enlarged aromatic region of $^1\text{H-NMR}$ spectra (500 MHz, CDCl_3) of monohalogenated compounds **126a**, **127a**, **127d** and **127e**. Chemical shift given in ppm and coupling constants J in Hertz. d = doublet.

Dibromination of **124a** (**126b**) and **125a** (**127b**)

Next dibromination products were analysed. This time the presence of a single aromatic proton, besides the *para*-methoxy $\text{H}^8\text{--H}^9$ system, made it not possible to assign it using COSY experiments. Then, besides ^1H and ^{13}C NMR experiments (Figures 3.8 and 3.10), HSQC and HMBC experiments were registered (Figures 3.9 and 3.11).

Based on these experiments, the signal assignment depicted in the different figures was proposed, in which the aromatic proton not belonging to the *para* system would be in position 5 (H^5). The following aspects/parameters were taken into account: the multiplicity and relative integration area of the signals in the $^1\text{H-NMR}$, the type of carbon in the $^{13}\text{C-NMR}$, the chemical shifts that could be expected for both H and C signals according to their environment in both 1D experiments and the couplings showed in the 2D-heteronuclear through-bond correlation HSQC and HMBC spectra.

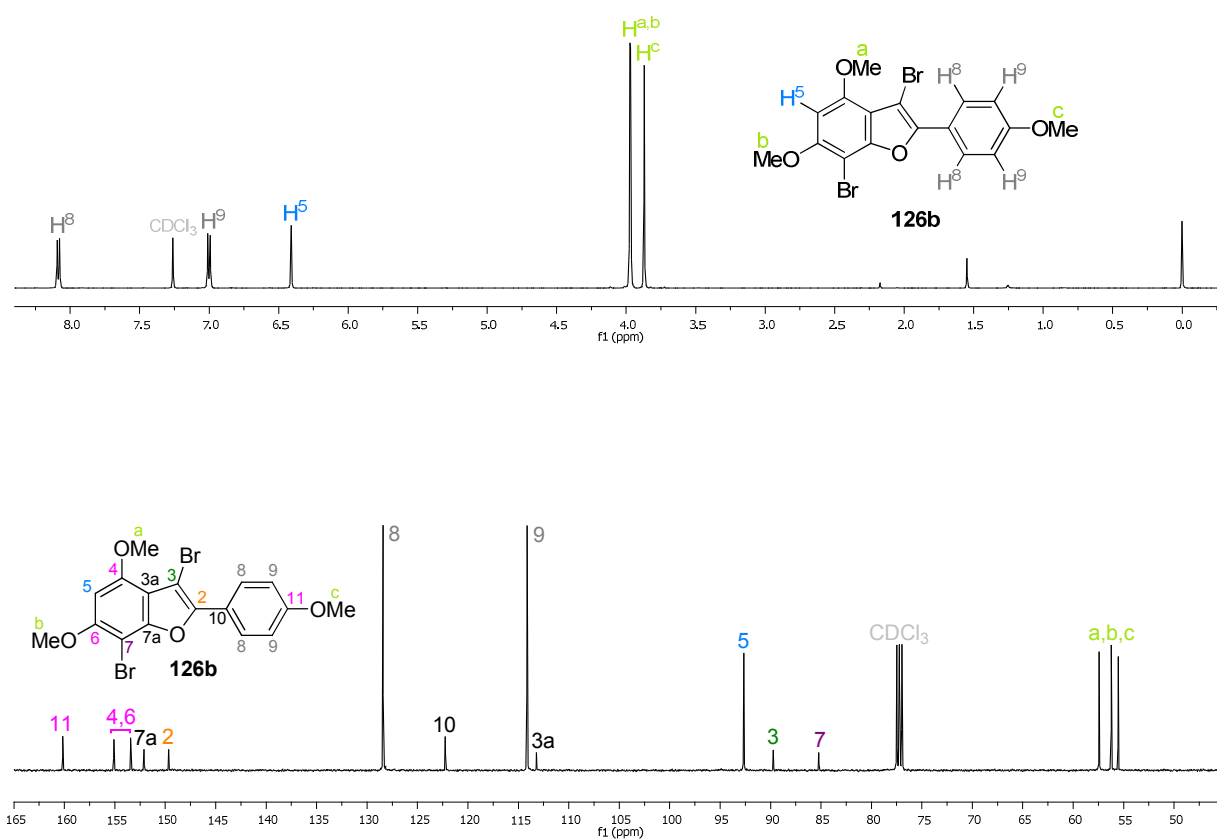


Figure 3.8. ^1H -NMR (above) and ^{13}C -NMR (below) (500 MHz, CDCl_3) of **126b**. Chemical shift given in ppm.

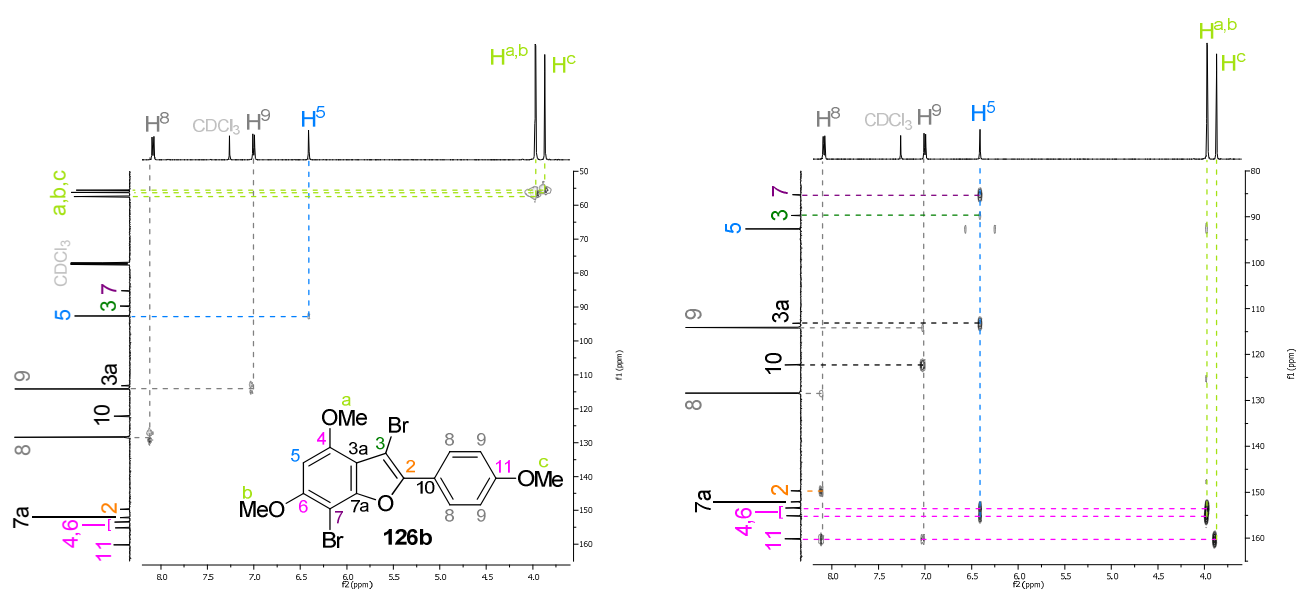


Figure 3.9. HSQC (left) and HMBC (right) (500 MHz, CDCl_3) of **126b**. Chemical shift given in ppm.

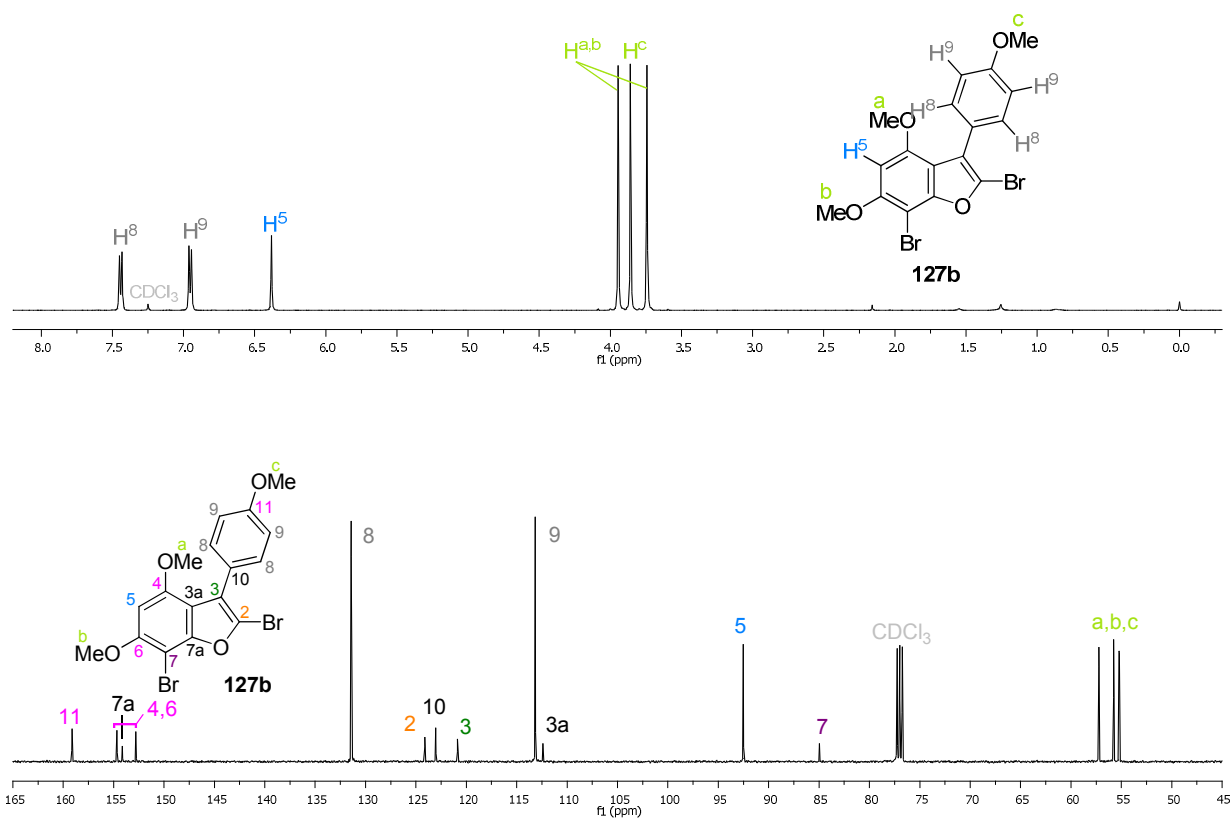


Figure 3.10. ^1H -NMR (above) and ^{13}C -NMR (below) (500 MHz, CDCl₃) of **127b**. Chemical shift given in ppm.

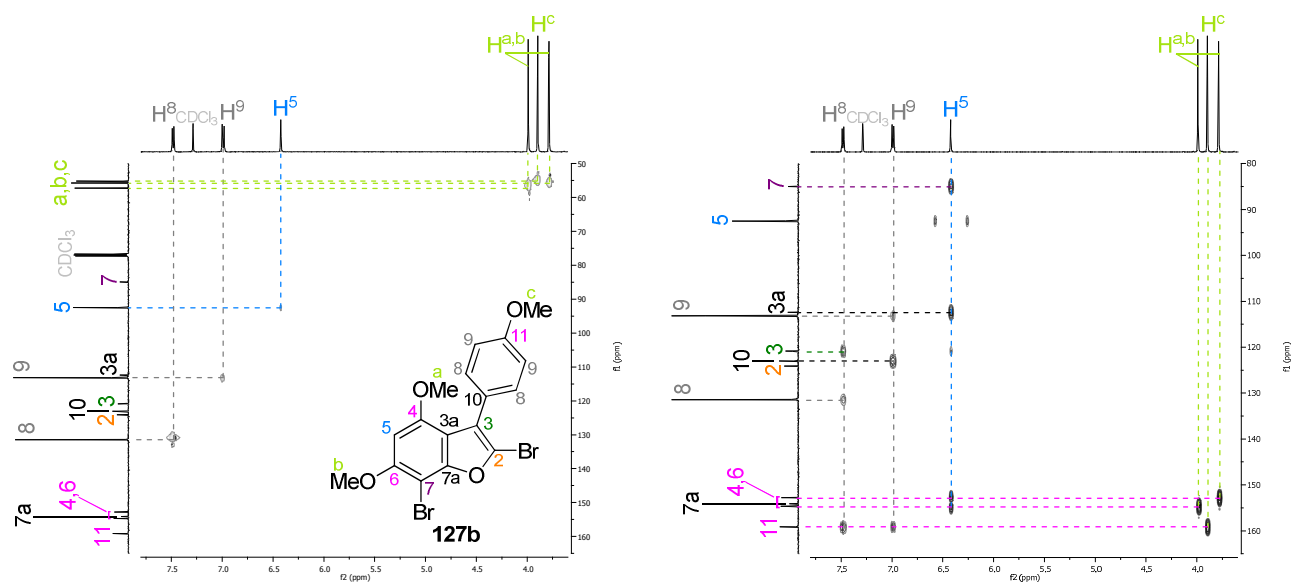


Figure 3.11. HSQC (left) and HMBC (right) (500 MHz, CDCl₃) of **127b**. Chemical shift given in ppm.

In order to double-check the aromatic signal assignment, selective NOE spectra resulting from the selective irradiation of protons H^5 and H^8 for compound **126b** and protons H^5 , H^8 and H^9 for compound **127b** were also registered.

Starting with compound **126b** (Figure 3.12), the signal assigned to H^5 was first selectively irradiated, giving rise to one doublet-like signal in the methoxy region, associated with H^a and H^b (*¹ and *², respectively). This confirmed the correct assignment of H^5 , since it was the only proton in the molecule close enough to two methoxy groups. Then, the signal assigned to H^9 was also selectively irradiated and it showed through-space correlation with H^8 and H^c protons (*³ and *⁴, respectively), excluding a possible exchanged assignment of protons H^8 and H^9 (correlation observed with H^c).

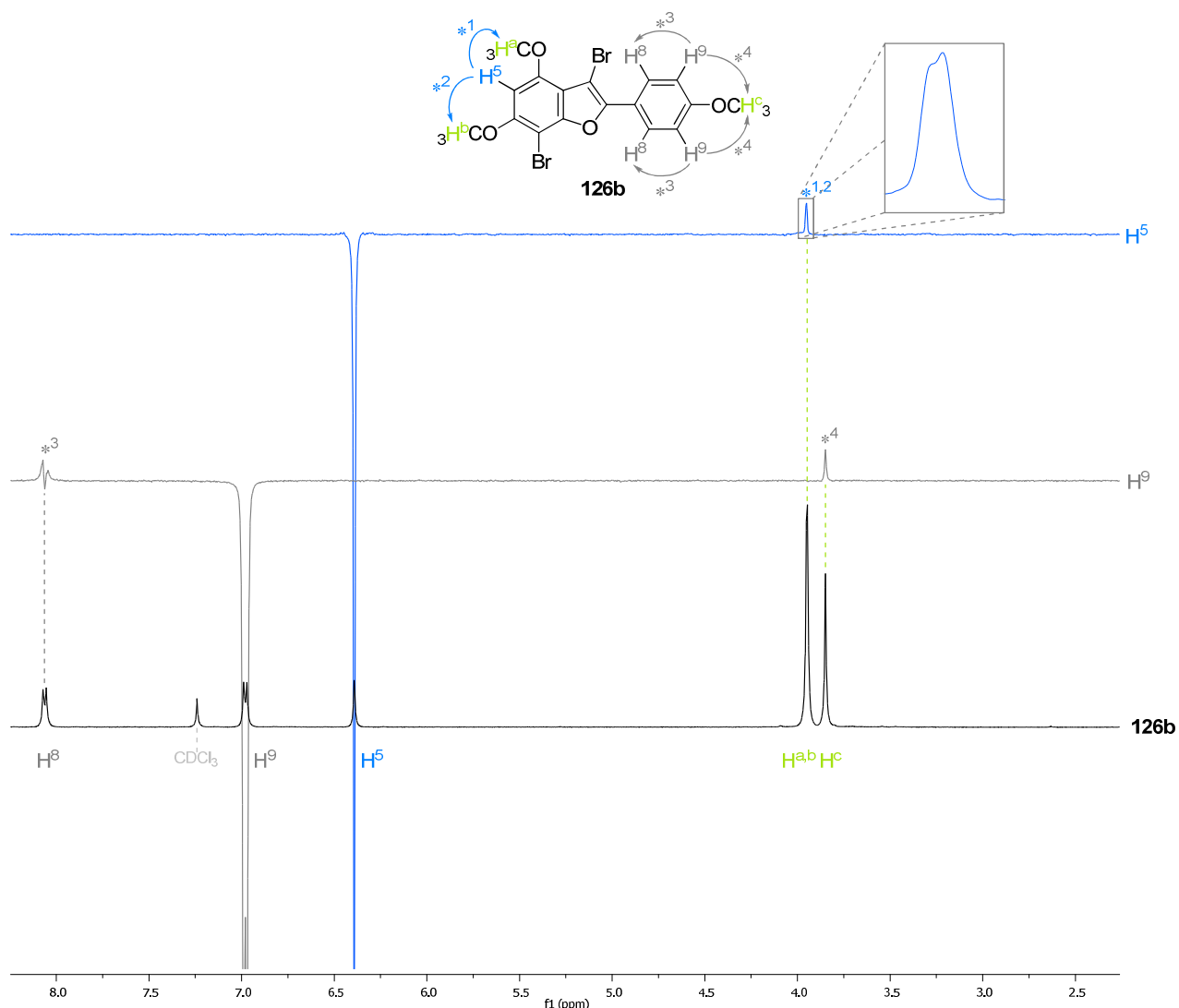


Figure 3.12. Stacked selective NOE spectra (with the proton assigned to the selectively irradiated signal indicated in the right) and $^1\text{H-NMR}$ spectrum of compound **126b**, (500 MHz, CDCl_3). NOE signals associated with the different irradiations are indicated with numbered stars.

Following with compound **127b** (Figure 3.13), the selective irradiation of signal assigned to H^5 gave again rise to two signals in the methoxy region, associated with H^a and H^b ($*^1$ and $*^2$, respectively), confirming once again the correct assignment of H^5 . Then, the selective irradiation of the signal assigned to H^8 showed through-space correlation with H^9 protons ($*^3$) and with no methoxy protons whilst the selective irradiation of the signal assigned to H^9 showed through-space correlation with H^8 and H^c protons ($*^4$ and $*^5$, respectively), excluding a possible exchanged assignment of protons H^8 and H^9 .

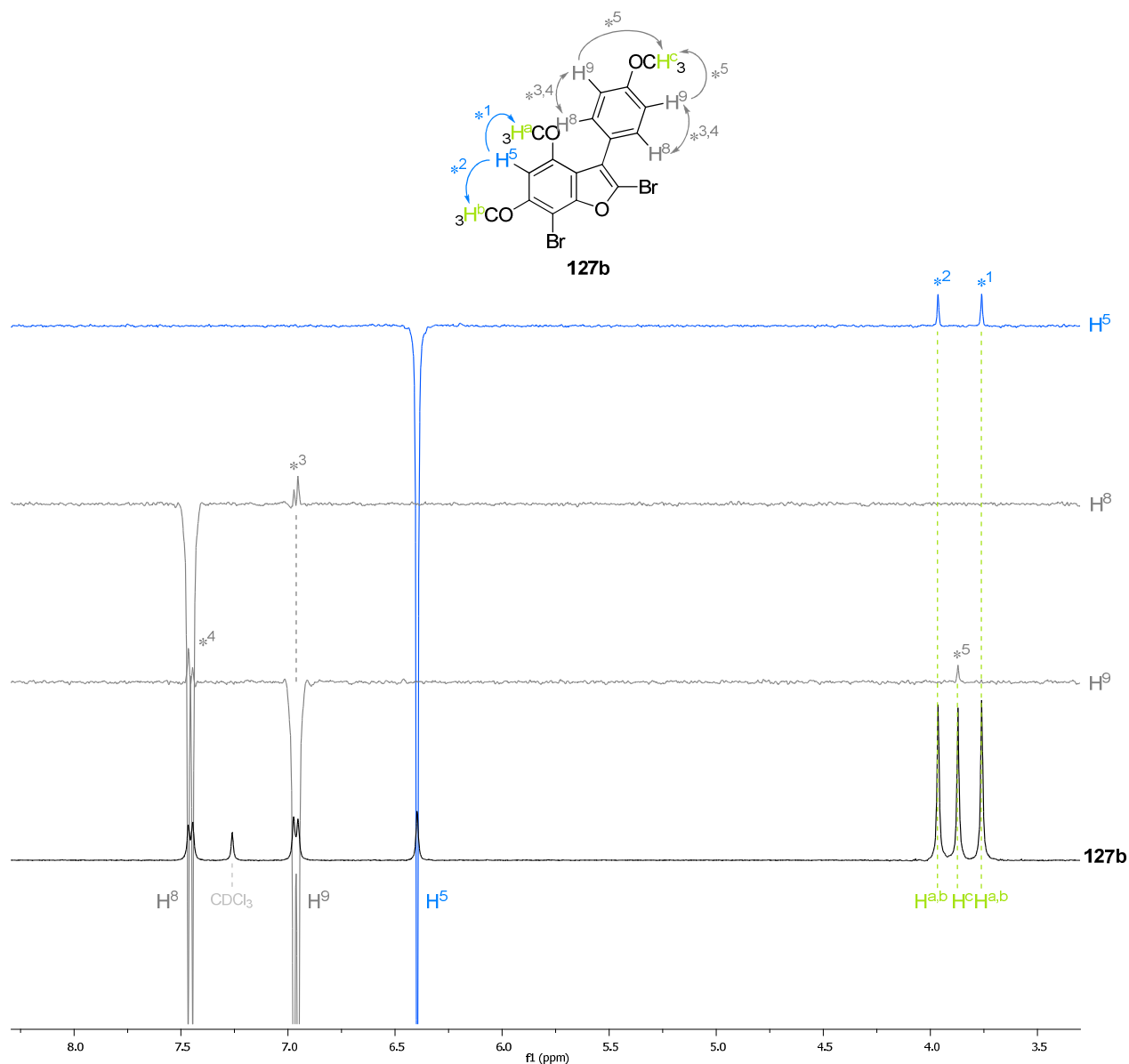


Figure 3.13. Stacked selective NOE spectra (with the proton assigned to the selectively irradiated signal indicated in the right) and $^1\text{H-NMR}$ spectrum of compound **127b**, (400 MHz, CDCl_3). NOE signals associated with the different irradiations are indicated with numbered stars.

Dichlorination of **124a**: major (**126f**) and minor (**126g**) isomers

Our attention was then drawn to dichlorination experiments. The reaction had this time led to the formation of two isomers, being the major one **126f**. This compound is analogous to dibrominated **126b**, thus suggesting that the only aromatic proton of its $^1\text{H-NMR}$ spectrum, besides the *para*-methoxy $\text{H}^8\text{--H}^9$ system, was H^5 . Assuming that the first halogenation of compound **124a** occurs preferentially at position 3, the corresponding aromatic signal in the $^1\text{H-NMR}$ spectrum of the minor isomer **126g** was thought to be H^7 (Figure 3.14).

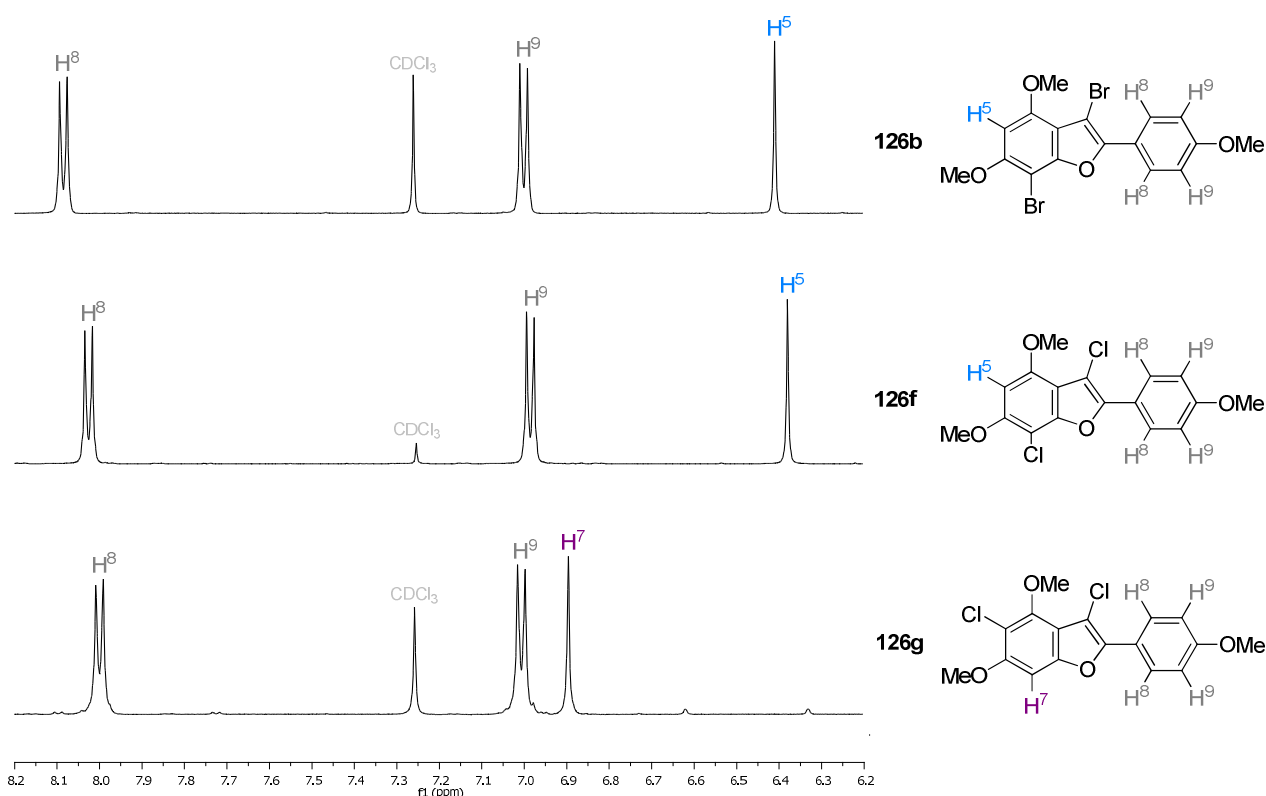


Figure 3.14. Enlarged aromatic region of $^1\text{H-NMR}$ spectra (500 MHz, CDCl_3) of dihalogenated 2-aryl compounds **126b** and **126f-g**. Chemical shift given in ppm.

As in previous structural elucidations, the study was performed first by analysing the multiplicity and relative integration area of the signals in the $^1\text{H-NMR}$. Then, the type of carbon in the $^{13}\text{C-NMR}$ was considered. The chemical shifts that could be expected for both H and C signals according to their environment in both 1D experiments (Figures 3.15 and 3.17 for **126f** and **126g**, respectively) were also born in mind. Besides, the couplings showed in the 2D-heteronuclear through-bond correlation HSQC and HMBC spectra (Figures 3.16 and 3.18 for **126f** and **126g**, respectively) were taken into consideration.

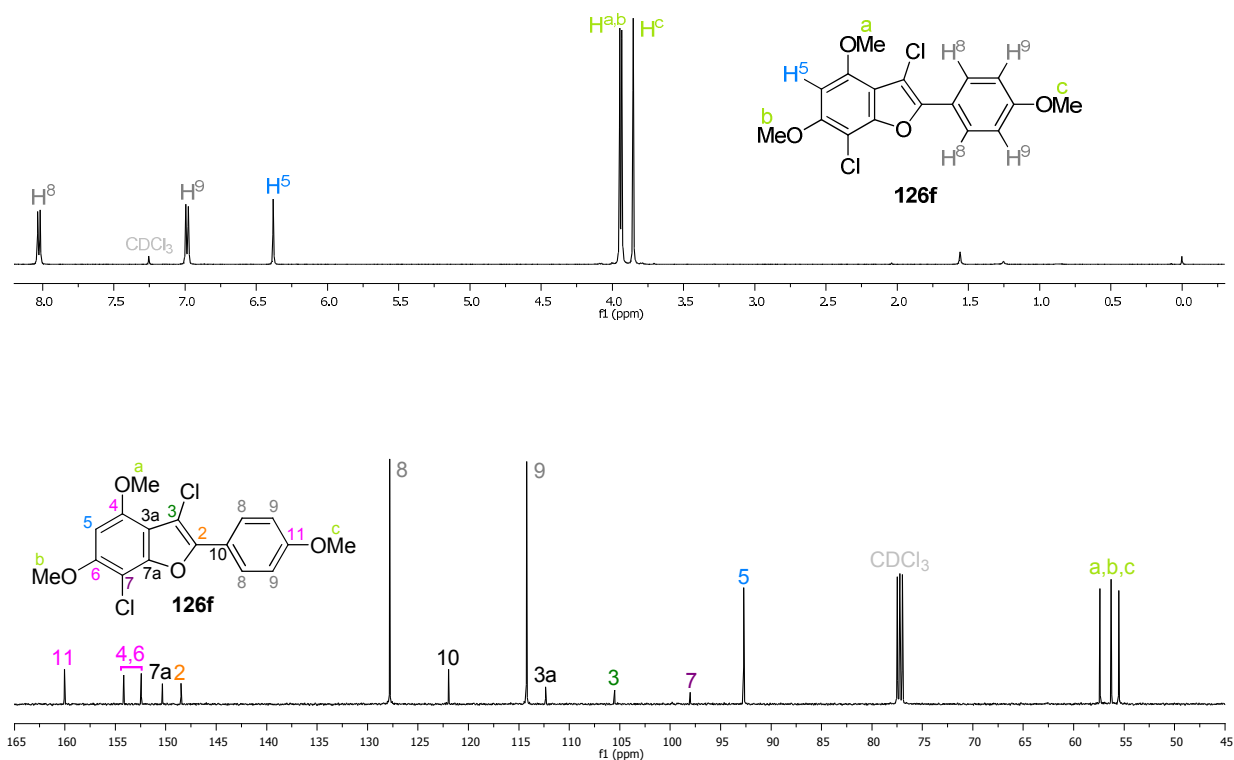


Figure 3.15. ^1H -NMR (above) and ^{13}C -NMR (below) (500 MHz, CDCl_3) of **126f**. Chemical shift given in ppm.

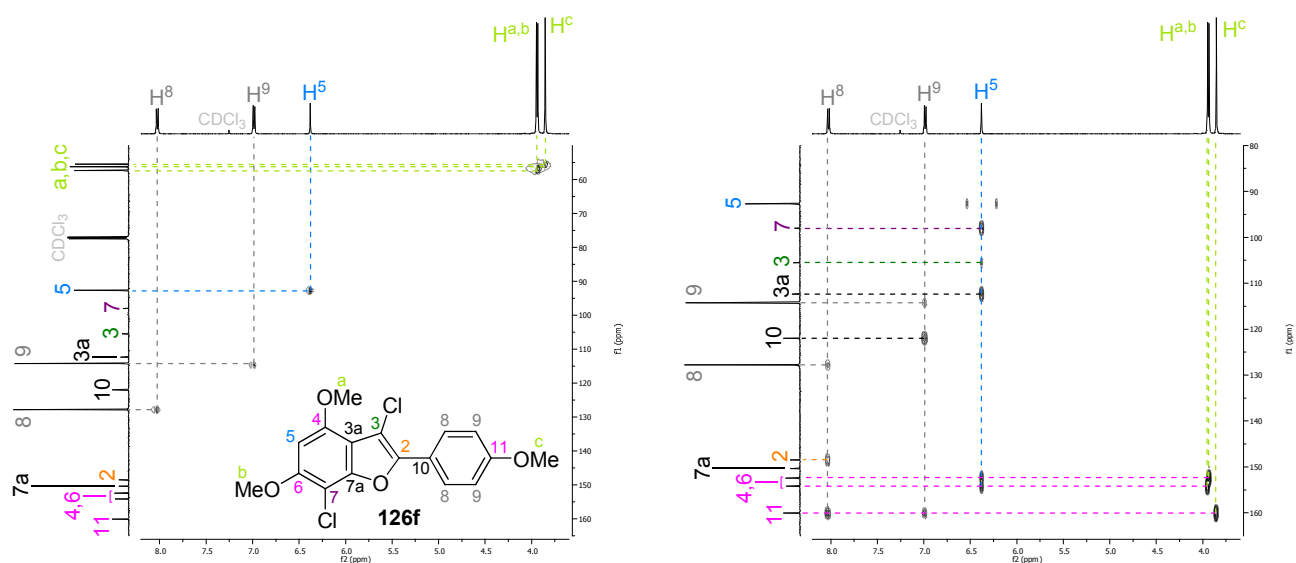


Figure 3.16. HSQC (left) and HMBC (right) (500 MHz, CDCl_3) of **126f**. Chemical shift given in ppm.

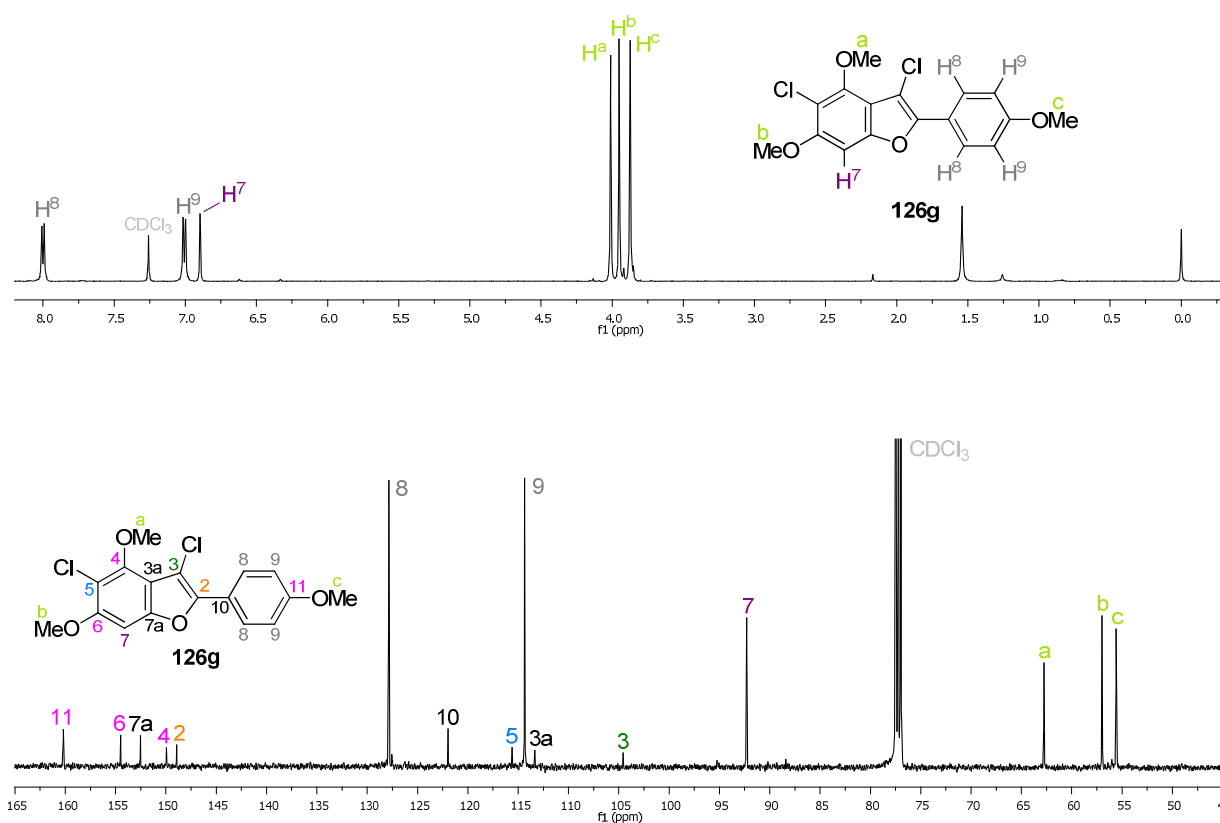


Figure 3.17. ^1H -NMR (above) and ^{13}C -NMR (below) (500 MHz, CDCl_3) of **126g**. Chemical shift given in ppm.

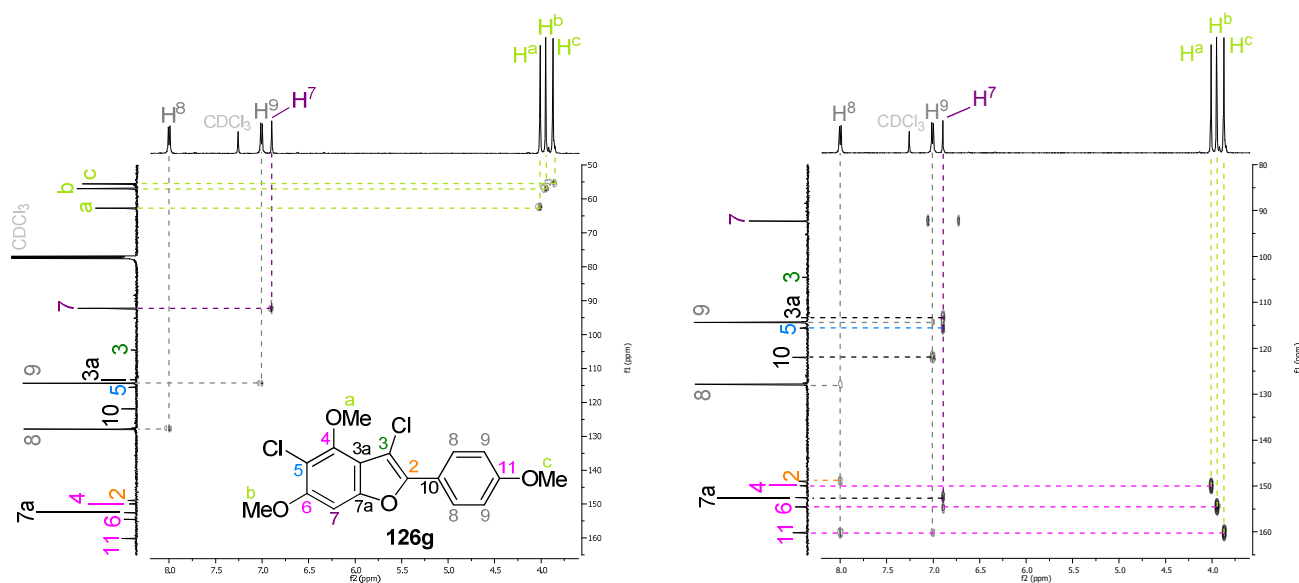


Figure 3.18. HSQC (left) and HMBC (right) (500 MHz, CDCl_3) of **126g**. Chemical shift given in ppm.

Once more, the aromatic signal assignments were reassessed making use of selective NOE spectra resulting from the selective irradiation of protons H⁵ and H⁸ for compound **126f** and protons H⁸, H⁹, H^a and H^b for compound **126g**.

Starting with compound **126f** (Figure 3.19), the signal assigned to H⁵ was first selectively irradiated, giving rise to one doublet signal in the methoxy region, associated with H^a and H^b (*¹ and *², respectively), thus confirming the correct assignment of H⁵. Then, the signal assigned to H⁸ was also selectively irradiated and it showed through-space correlation with H⁹ (*³) and with no methoxy group. Therefore, a possible exchanged assignment of protons H⁸ and H⁹ (no correlation observed with H^c) was excluded.

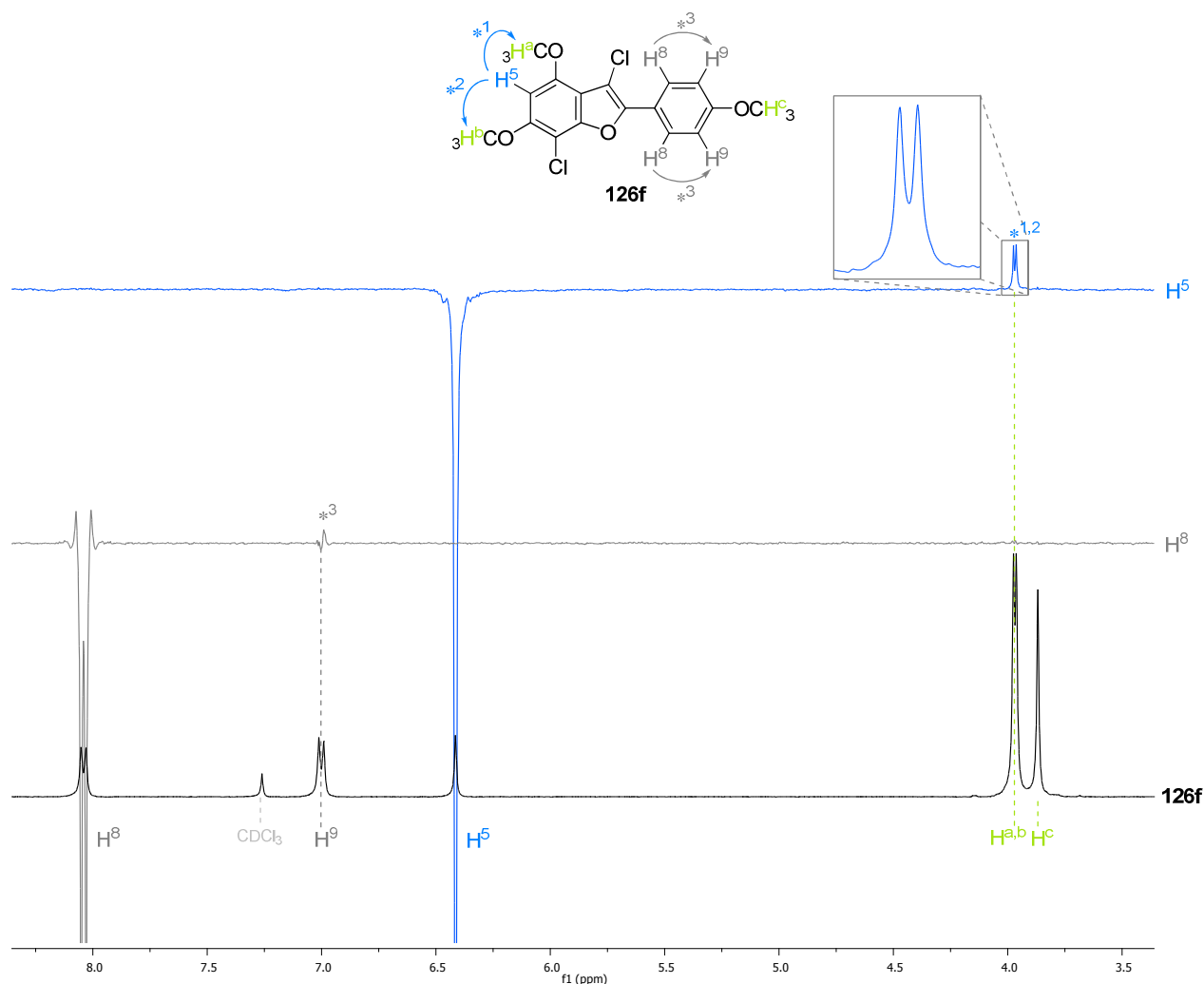


Figure 3.19. Stacked selective NOE spectra (with the proton assigned to the selectively irradiated signal indicated in the right) and ¹H-NMR spectrum of compound **126f**, (500 MHz, CDCl₃). NOE signals associated with the different irradiations are indicated with numbered stars.

For compound **126g**, a slightly different series of selective irradiations was performed (Figure 3.20). To start with, the selective irradiation of the signal assigned to H⁸ showed through-space correlation with H⁹ protons (*¹) and with no methoxy protons whilst the selective irradiation of the signal assigned to H⁹ showed through-space correlation with H⁸ and H^c protons (*² and *³, respectively). These observations excluded a possible exchanged assignment of protons H⁸ and H⁹ and let us determine the signal corresponding to the H^c methoxy protons. Then the methoxy protons in the benzofuran scaffold (i.e. H^a and H^b) were considered. The selective irradiation of H^a resulted in no correlation signals, in agreement with positions 3 and 5 of the benzofuran structure being chlorinated, whilst the selective irradiation of H^b gave rise to a single signal associated with H⁷ proton (*⁴).

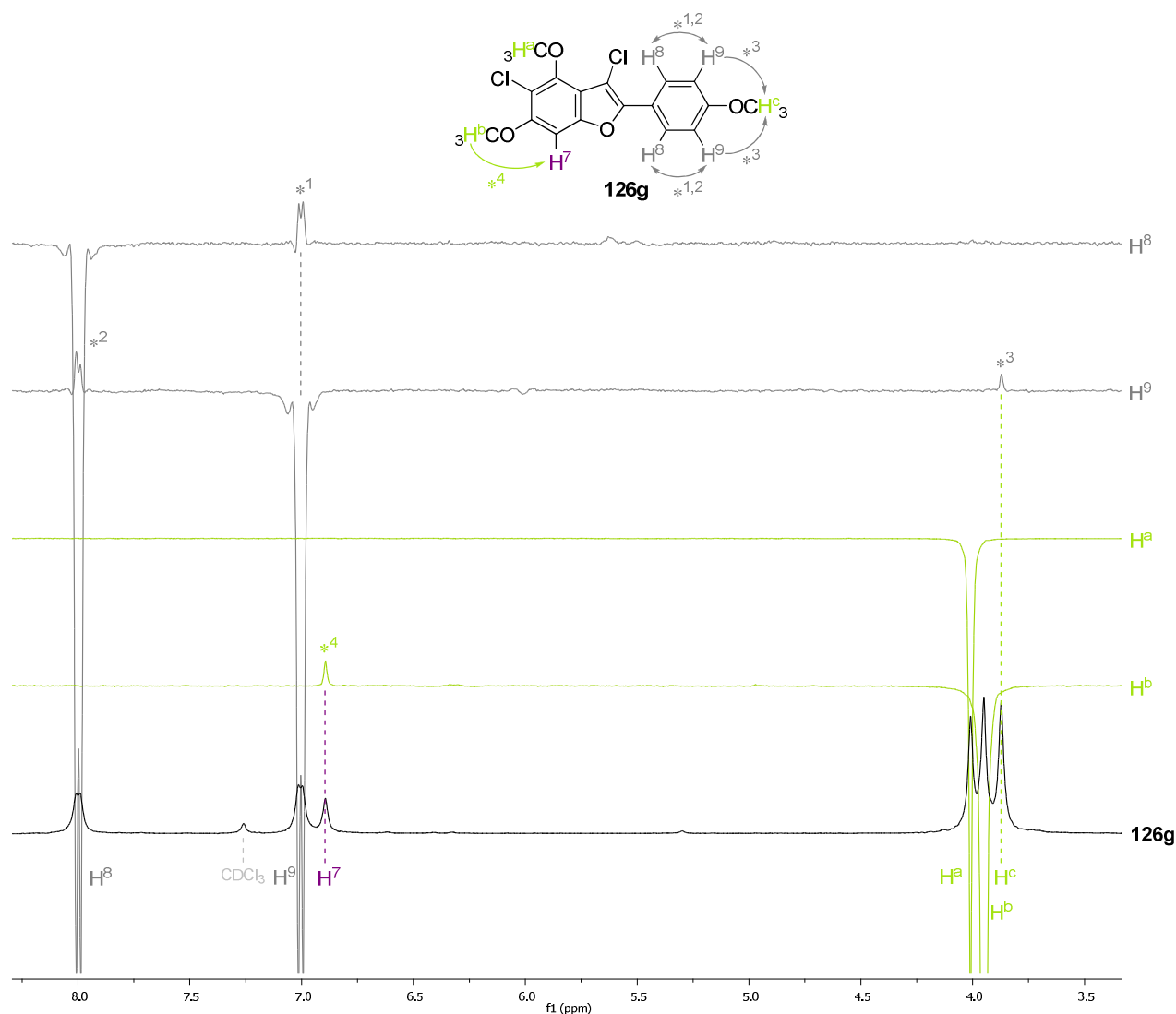


Figure 3.20. Stacked selective NOE spectra (with the proton assigned to the selectively irradiated signal indicated in the right) and ¹H-NMR spectrum of compound **126g**, (400 MHz for H⁸ and 500 MHz for the others, CDCl₃). NOE signals associated with the different irradiations are indicated with numbered stars.

Combined dihalogenation: monobromination of **127e** (**127f**)

The last compound to be analysed was the dihalogenated benzo[*b*]furan **127f**. Coming from **127e**, chlorinated in position 2, the second substituted position (by bromine this time) was proposed to be position 7, due to the analogy between the $^1\text{H-NMR}$ spectra of **127f** and **127b** (Figure 3.21).

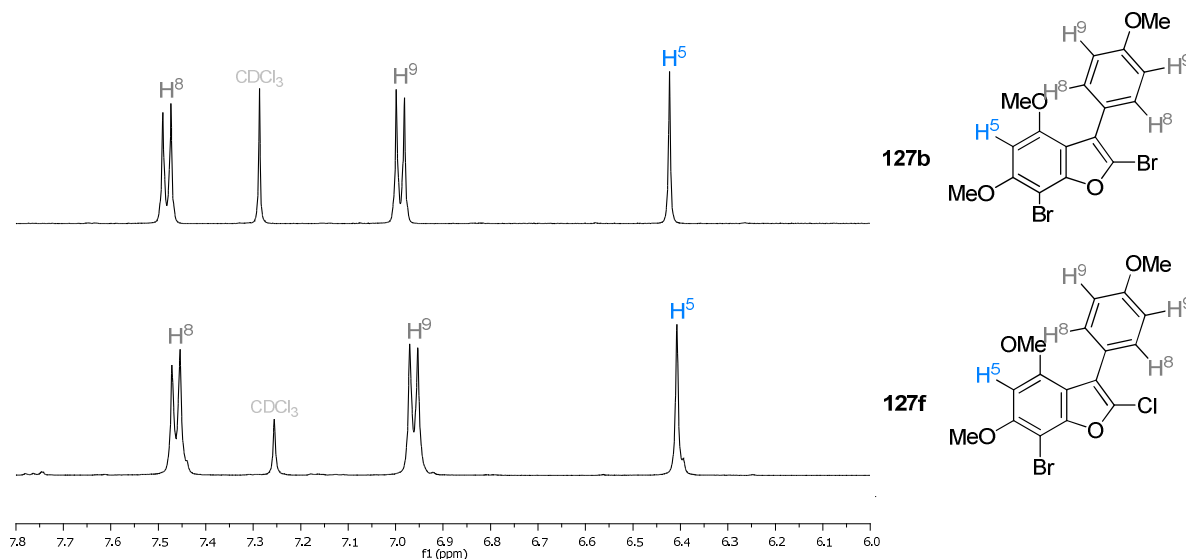


Figure 3.21. Enlarged aromatic region of $^1\text{H-NMR}$ spectra (500 MHz, CDCl_3) of dihalogenated 3-aryl compounds **127b** and **127f**. Chemical shift given in ppm.

Nevertheless, as in previous cases of dihalogenation, besides ^1H and ^{13}C NMR experiments (Figure 3.22), HSQC and HMBC experiments were registered (Figure 3.23). Again, the multiplicity and relative integration area of the signals in the $^1\text{H-NMR}$ were first analysed. Then, the type of carbon in the $^{13}\text{C-NMR}$ was considered. The chemical shifts that could be expected for both H and C signals according to their environment in both 1D experiments were also born in mind. Besides, the couplings showed in the 2D-heteronuclear through-bond correlation HSQC and HMBC spectra were taken into consideration. With all this information, the signal assignment depicted in the different figures was proposed, in which the aromatic proton not belonging to the *para* system would be in position 5 (H^5).

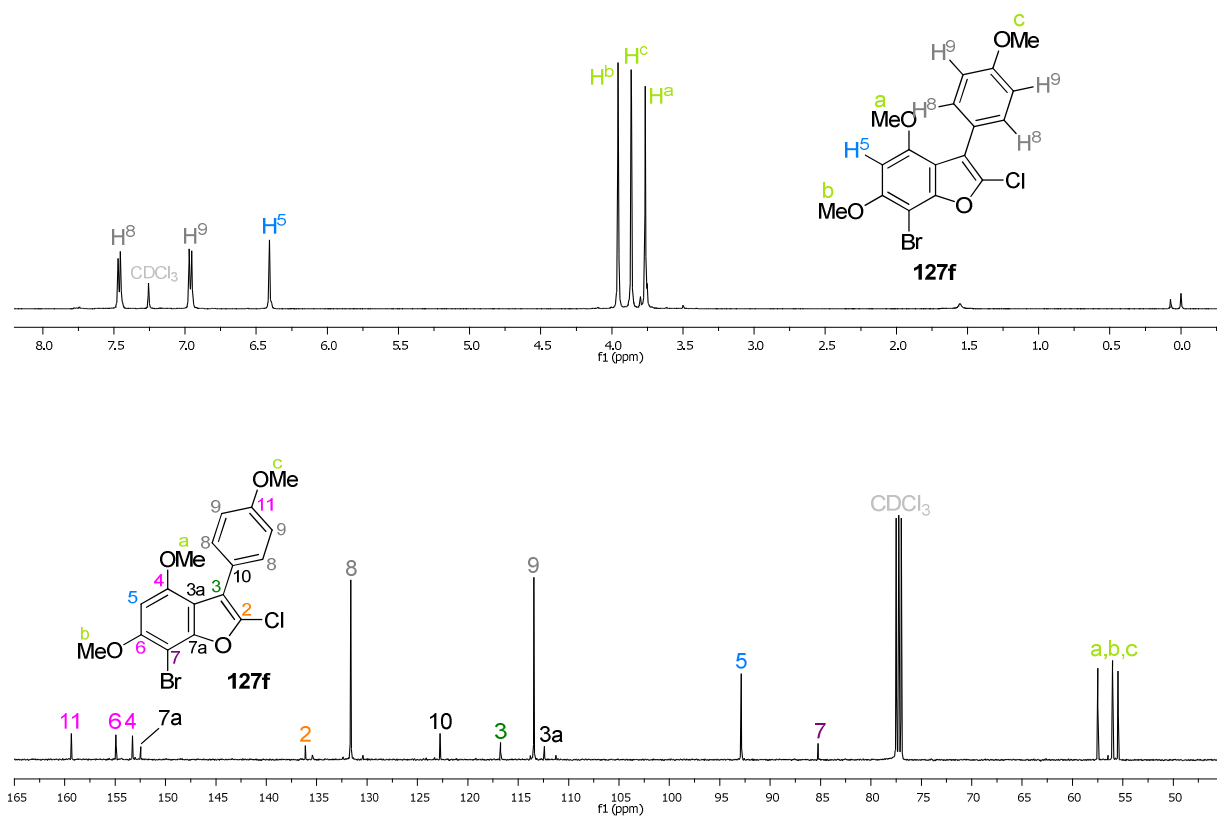


Figure 3.22. ^1H -NMR (above) and ^{13}C -NMR (below) (500 MHz, CDCl_3) of **127f**. Chemical shift given in ppm.

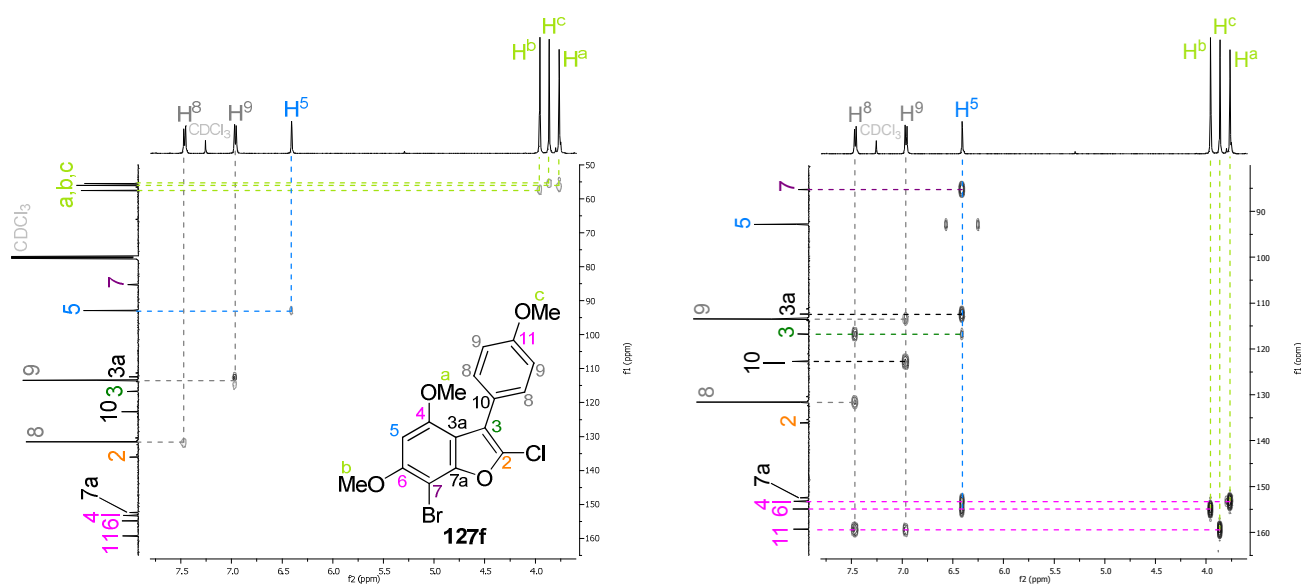


Figure 3.23. HSQC (left) and HMBC (right) (500 MHz, CDCl_3) of **127f**. Chemical shift given in ppm.

Again, in order to double-check the aromatic signal assignment, selective NOE spectra resulting from the selective irradiation of protons H⁵, H⁸ and H⁹ of compound **127f** were also registered (Figure 3.24). The selective irradiation of signal assigned to H⁵ gave again rise to two signals in the methoxy region, associated with H^a and H^b (*¹ and *², respectively), confirming the correct assignment of H⁵. Then, selective irradiation of the signal assigned to H⁸ showed through-space correlation with H⁹ protons (*³) and with no methoxy protons whilst the selective irradiation of the signal assigned to H⁹ showed through-space correlation with H⁸ and H^c protons (*⁴ and *⁵, respectively), excluding a possible exchanged assignment of protons H⁸ and H⁹.

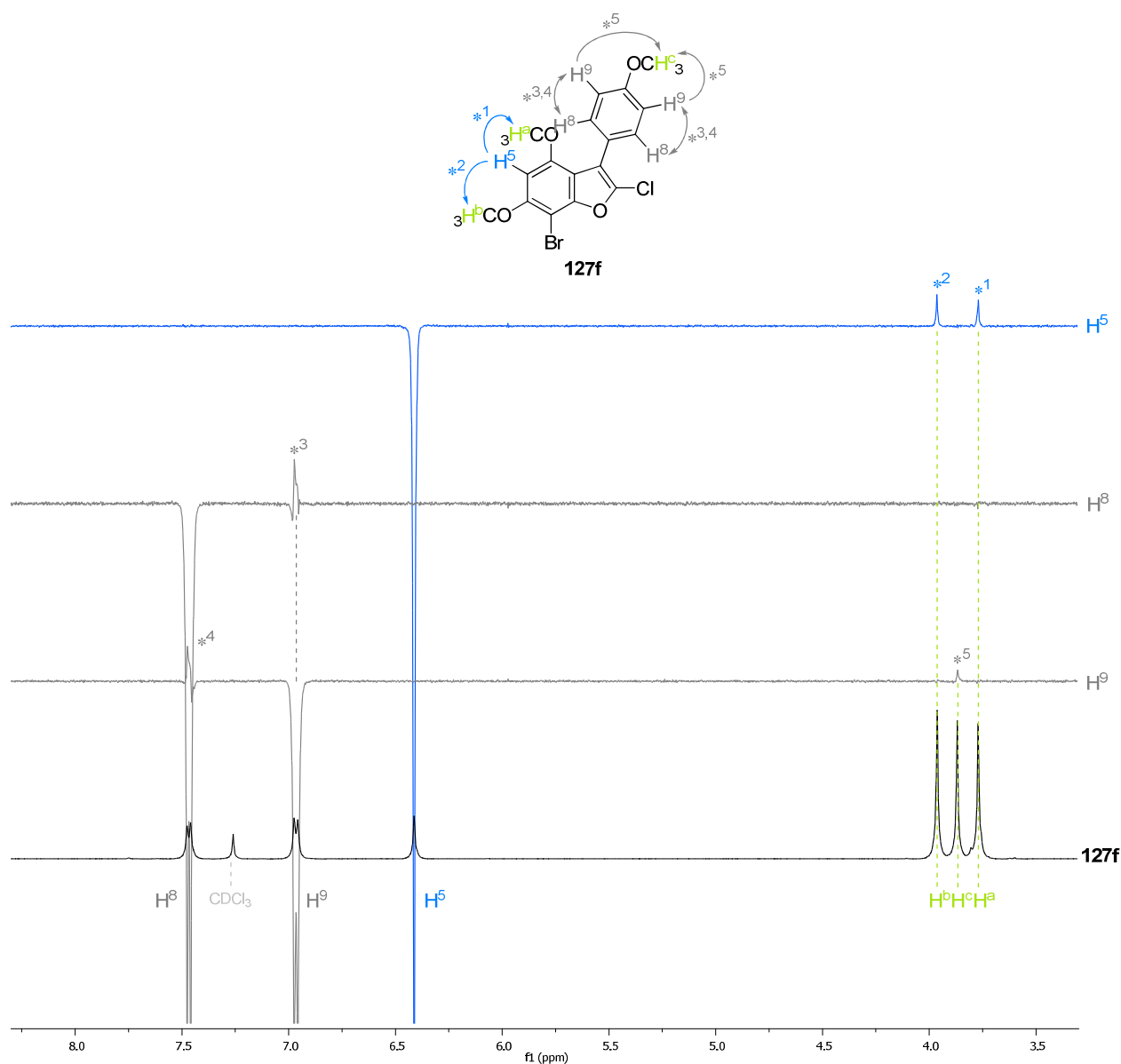
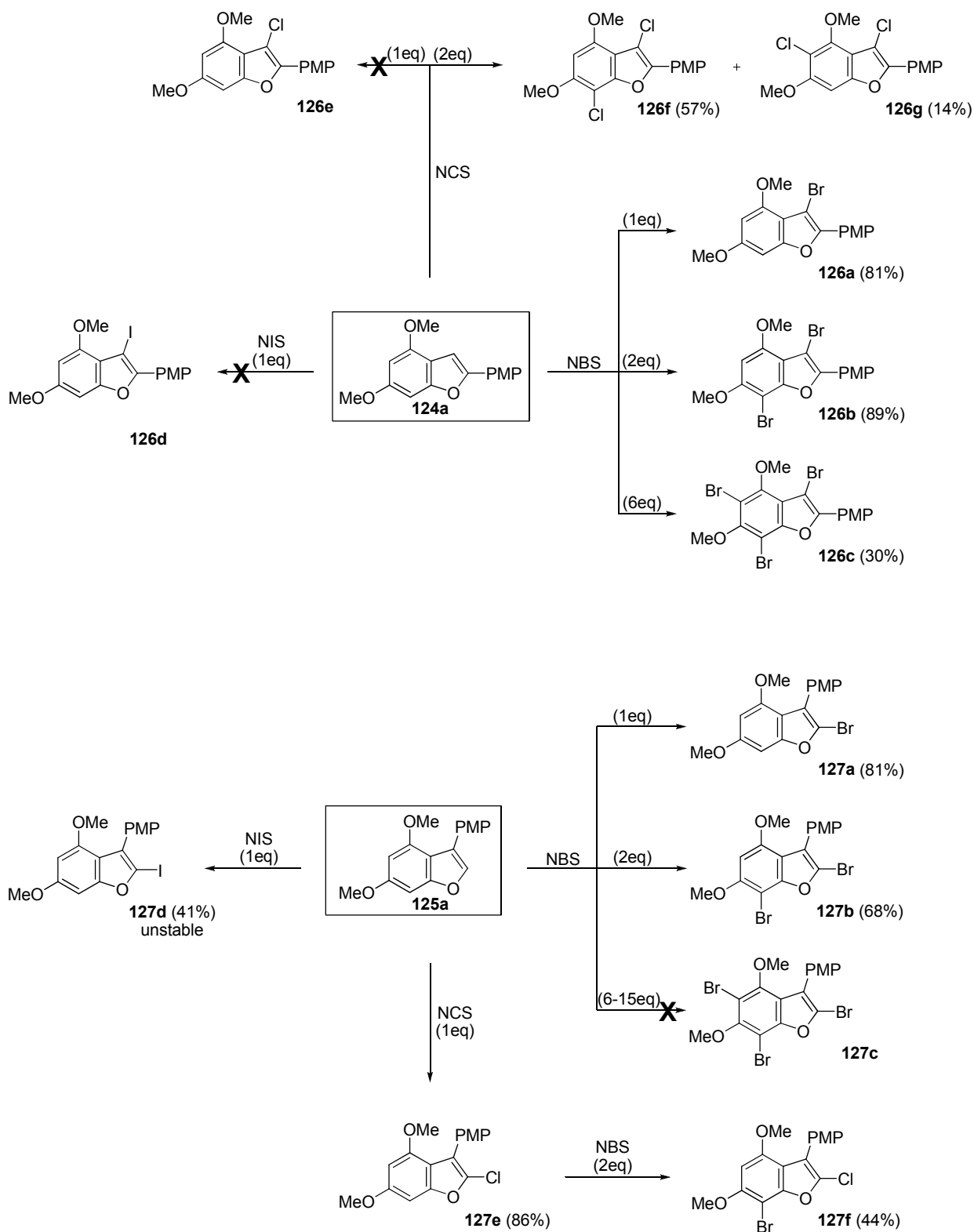


Figure 3.24. Stacked selective NOE spectra (with the proton assigned to the selectively irradiated signal indicated in the right) and ¹H-NMR spectrum of compound **127f**, (500 MHz, CDCl₃). NOE signals associated with the different irradiations are indicated with numbered stars.

3.2.2.4. Graphical overview



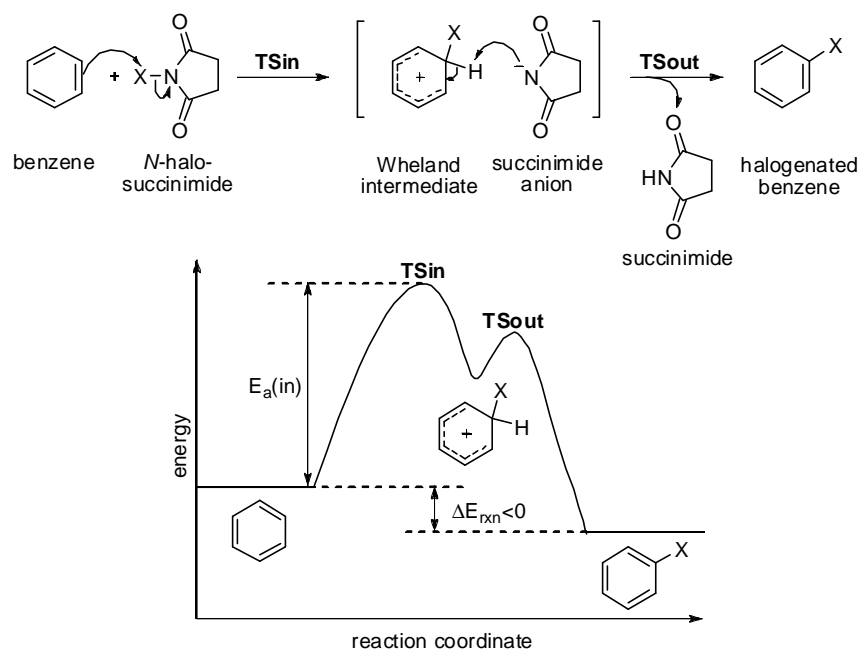
Scheme 3.19. Graphical overview of the experimental study of the preparation of 2-aryl and 3-aryl halobenzofurans **126** and **127** respectively, via halogenation with NXS. In all the reactions dichloromethane was used as solvent and the reaction mixture was stirred for 2-48 hours at room temperature. Reaction yields are given in brackets. PMP = *para*-methoxyphenyl.

3.2.3. Computational study

3.2.3.1. General considerations

In order to get a better understanding of the regioselectivity of the halogenation reactions, computational studies were performed to assess the preferential substitution site(s) in 2- and 3-(4'-methoxyphenyl)-4,6-dimethoxybenzo[*b*]furans, **124a** and **125a** respectively, employed as starting materials in the experimental study.

For so doing, firstly general features of electrophilic aromatic substitutions (S_{EAr} or EAS) are worth recalling. The generally accepted mechanism of this reaction, in which an atom attached to the aromatic system (usually hydrogen) is replaced by an electrophile (a halogen in our case), consists of two steps. As a model, the scheme of the mechanism of the halogenation reaction of benzene with *N*-halosuccinimide (NXS) is depicted in Scheme 3.20 together with its proposed energy profile.



Scheme 3.20. Proposed mechanism and energy profile of the halogenation of benzene with *N*-halosuccinimide.

The first step is the entry of the halogen, an addition resulting from the reaction of the aromatic system with the electrophilic *N*-halosuccinimide. It leads to a cyclohexadienyl carbocation (Wheland intermediate) in which aromaticity is lost. The second step consists of the withdrawal of the hydrogen by the negatively charged succinimide anion. Thus, the conjugate base of the electrophile withdraws the hydrogen atom at the carbon which has

suffered the electrophilic attack, leading to the recovery of the aromaticity of the system. This deprotonation is faster and affords a product more stable than the starting materials (exothermic reaction $\Delta E_{\text{rxn}} < 0$ in Scheme 3.20).

On looking at the process as a whole, the first step is the limiting one, that is to say, the rate of the reaction is determined by the activation energy of the first step ($E_a(\text{in})$ in Scheme 3.20). This barrier is usually considerably high due to the aromaticity loss and charge separation that it implies.

Going back to the substituted benzo[*b*]furans **124a** and **125a**, different halogenation positions in different rings of the molecules could be envisaged (Scheme 3.15). Taking this into account, the computational study carried out in our research group focused first on the calculation and evaluation of the aromaticity of each ring in the starting materials. The nucleus-independent chemical shifts (NICS) aromaticity probe was selected with this purpose. Then, the energy profile of the possible reaction paths was assessed. Besides, the study was completed with the analysis of the frontier molecular orbitals (FMO) of the reacting benzo[*b*]furan, i.e. the HOMO orbital participating in the electrophilic aromatic substitution.



Scheme 3.15. (duplicate) Possible halogenation positions of benzo[*b*]furans **124a** and **125a**. PMP = *para*-methoxyphenyl.

All the optimizations of stationary points along the reaction coordinates were carried out by means of Gaussian 09 suite of programs. The calculations were performed within the density functional theory (DFT) framework. The different stationary points were optimized using B3LYP hybrid functional with standard 6-311++G** split valence basis-set¹⁷⁹. All stationary points were characterized by harmonic analysis. Reactants, intermediates and products have positive definite Hessian matrices. Transition structures show a single negative eigenvalue in their diagonalized force constant matrices, and their associated eigenvectors were confirmed to correspond to motion along the reaction coordinate under consideration.

Solvent effects were estimated by using the polarization continuum model (PCM)²⁰⁴ method within the self-consistent reaction field (SCRF)²⁰⁵ approach. All SCRF-PCM calculations were performed using dichloromethane ($\epsilon = 8.93$). The relative activation energies (E_a) and the relative Gibbs free energies (ΔG^\ddagger), which are given in kcal/mol, were computed at the B3LYP(PCM)/6-311++G**// B3LYP/6-311++G** level of theory.

The nucleus-independent chemical shifts NICS²⁰⁶ were calculated by means of the gauge-independent atomic orbitals (GIAO) method²⁰⁷ and were computed at the B3LYP/6-311+G** level of theory.

3.2.3.2. Assessment of the aromaticity of the starting benzofurans 124a and 125a

The nucleus-independent chemical shift (NICS) was used as an aromaticity criterion. NICS uses absolute magnetic shieldings computed at characteristic ring points (the non-weighted geometrical ring center of the ring, NICS(0); the ring critical point of electronic density, NICS(0)^{rcp}; the NICS values computed 1 Å above the ring center where the π orbitals have their maximum density, NICS(1); etc.). The NICS values measured in the ring plane are associated with σ aromaticity and NICS values 1 Å above the ring plane with π aromaticity²⁰⁸. To follow the familiar NMR chemical shift convention, NICS values are expressed in ppm, denoting negative NICSs diamagnetic ring currents and positive NICSs antiaromaticity. Therefore, in principle, the more negative the NICS value of a ring, the more aromatic it is. This parameter allows the evaluation of the aromaticity contribution of individual rings in polycyclic systems.

Considering the whole substitution process (Scheme 3.20), the positive charge in the reaction intermediate might be better stabilized in the fused bicyclic system (A-B) rather than in the substituent benzene moiety (C). For this reason, only six- and five-membered rings of benzo[*b*]furan scaffold (rings A and B, respectively) were considered in our NICS evaluation.

²⁰⁴ Cammi, R.; Mennucci, B.; Tomasi, J. *J. Phys. Chem. A* **2000**, *104*, 5631-5637

²⁰⁵ Tomasi, J.; Mennucci, B.; Cammi, R. *Chem. Rev.* **2005**, *105*, 2999-3093

²⁰⁶ Schleyer, P. v. R.; Maerker, C.; Dransfeld, A.; Jiao, H.; Hommes, N. J. R. v. E. *J. Am. Chem. Soc.* **1996**, *118*, 6317-6318

²⁰⁷ Wolinski, K.; Hinton, J. F.; Pulay, P. *J. Am. Chem. Soc.* **1990**, *112*, 8251-8260

²⁰⁸ (a) Bader, R. F. W. *Atoms in Molecules: A Quantum Theory* Clarendon Press, Oxford 1990; pp 13-52 (b) Morao, I.; Lecea, B.; Cossío, F. P. *J. Org. Chem.* **1997**, *62*, 7033-7036 (c) Morao, I.; Cossío, F. P. *J. Org. Chem.* **1999**, *64*, 1868-1874 (d) Foroutan-Nejad, C.; Shahbazian, S.; Rashidi-Ranjbar, P. *Phys. Chem. Chem. Phys.* **2010**, *12*, 12630-12637 (e) Foroutan-Nejad, C.; Shahbazian, S.; Feixas, F.; Rashidi-Ranjbar, P.; Solà, M. *J. Comp. Chem.* **2011**, *32*, 2422-2431

The NICS values of the rings A and B in compounds **124a** and **125a** were studied at the ring critical point of electron density $\text{NICS}(0)^{\text{rcp}}$ ²⁰⁹ and 1 Å above it $\text{NICS}(1)^{\text{rcp}}$. They were calculated at the B3LYP/6-311+G** level of theory and compared with each other and with the literature values for unsubstituted benzo[*b*]furan at the ring center²¹⁰ (Table 3.3).

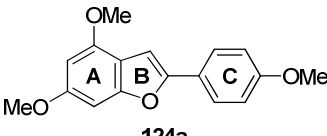
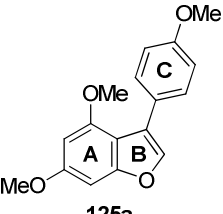

compound							
entry	ring	$\text{NICS}(0)^{\text{rcp}}$	$\text{NICS}(1)^{\text{rcp}}$	$\text{NICS}(0)^{\text{rcp}}$	$\text{NICS}(1)^{\text{rcp}}$	$\text{NICS}(0)$	$\text{NICS}(1)$
1	A	-11.09	-9.82	-11.56	-9.94	-9.96	-10.99
2	B	-8.50	-7.17	-9.58	-7.22	-9.56	-8.26

Table 3.3. NICSs values (ppm) for rings A and B in compounds **124a**, **125a** and benzo[*b*]furan computed at the B3LYP/6-311+G** level of theory. Values for unsubstituted benzo[*b*]furan are taken from reference 205.

The computed values show that the aromaticity of ring B is significantly lower than that of ring A in both **124a** and **125a**. This suggests a higher reactivity of the furan ring B over benzene ring A towards $\text{S}_{\text{E}}\text{Ar}$, that is to say a preference of available positions of the five membered ring to be first substituted. This result is in agreement with our experimental observations which showed that the first halogenation site was the one available in the furan ring B (position 3 when starting from 2-arylbenzo[*b*]furan **124a** and position 2 when starting from 3-arylbenzo[*b*]furan **125a**), whilst the second and third halogenations took place at benzene ring A (positions 5 and 7).

Besides, the difference of aromaticity between rings A and B in **124a**, **125a** and in benzo[*b*]furan were compared. Although the difference of π aromaticity is almost the same in the three cases, the difference of σ aromaticity is considerably higher in compounds **124a** and **125a**. This suggests a higher selectivity for the reactions of **124a** and **125a** than that expected for unsubstituted benzo[*b*]furan.

²⁰⁹ We considered the (3,+1) ring critical point of the electron density as defined by Bader 208a, i.e. the only point at which the electron density is a minimum with respect to motion on the plane of the ring and maximum with respect to motion perpendicular to the plane defined by the ring. We argue that it constitutes an unambiguous choice for the calculation of the NICSs, which is especially interesting given the unsymmetrical character of our cyclic systems.

²¹⁰ Chen, Z.; Wannere, C. S.; Corminboeuf, C.; Puchta, R.; Schleyer, P. v. R. *Chem. Rev.* **2005**, *105*, 3842-3888

3.2.3.3. Energy profiles of the bromination reactions of **124a** and **125a** using NBS

The halogenation reactions studied here were the experimentally performed mono-, di- and tribrominations of compounds **124a** and **125a** with NBS. Compounds **124a** and **125a** are separately assessed below.

Considering **124a** as starting material, three possible halogenation positions could be envisaged: positions 3, 5 and 7. DFT calculations were performed to obtain the transition structures associated with the addition of a bromine atom in each of these positions (**TS6in**, **TS7in** and **TS8in**, respectively), along with the activation (E_a) and relative Gibbs free (ΔG^\ddagger) energies associated with these processes. The results showed the lowest activation barrier for the entry of the bromine atom in position 3. This activation energy was 0.4 kcal/mol lower than that of the addition in position 7 and 4.9 kcal/mol lower than that of the addition in position 5. The same trend is observed when relative Gibbs free energies were considered, being the energy associated with the addition at position 3 1.0 kcal/mol lower than that of position 7, and 3.9 kcal/mol lower than that of position 5 (Figure 3.25 A and C).

The Kohn-Sham HOMO of **124a** is gathered in Figure 3.25 B. According to it, the expansion coefficient on C5 is negligible, suggesting a preference for substitution at positions 3 or 7, but allowing no apparent selectivity prediction between them on its own.

The combination of all these results, together with the higher reactivity of furan ring predicted by the NICS-based aromaticity evaluation, is in agreement with the experimentally obtained regioselectivity, i.e. preferential formation of compound **126a**.

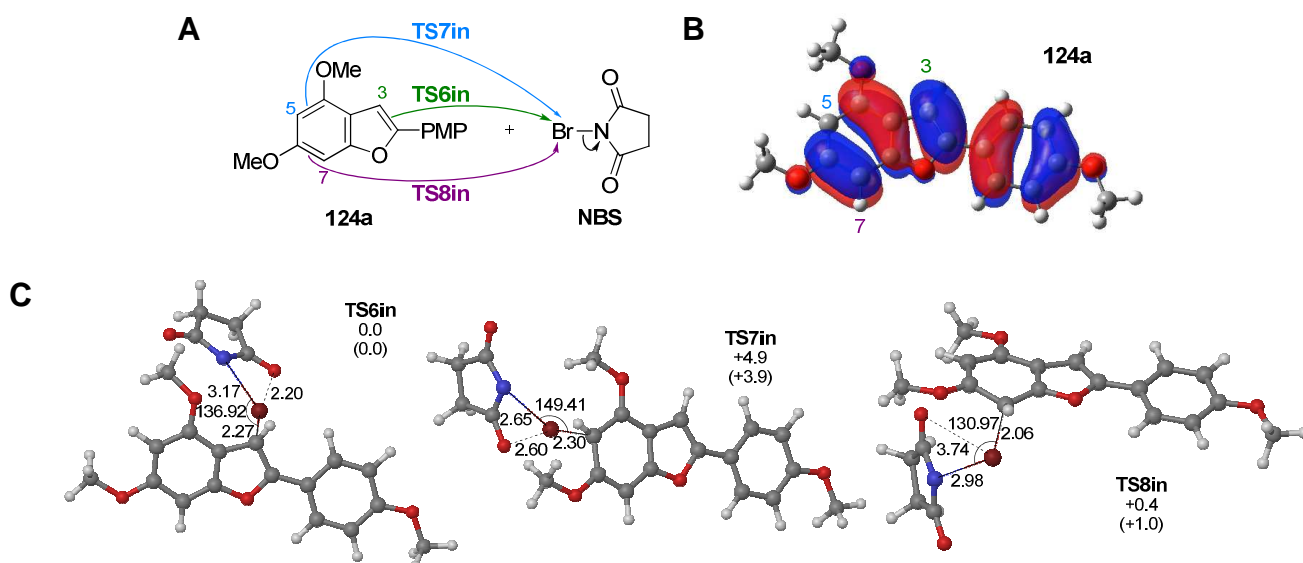


Figure 3.25. (A) Possible reaction paths for the interaction between 2-arylbenzo[*b*]furan **124a** and NBS. (B) Kohn-Sham HOMO of **124a**. (C) Fully optimized structures of the corresponding transition structures **TS6in**, **TS7in** and **TS8in**. Bond distances and angles are given in Å and degrees, respectively. Plain numbers correspond to the relative activation energies and numbers in brackets correspond to the relative Gibbs free energies, both with respect to **TS6in**, given in kcal/mol and computed at the B3LYP(PCM)/6-311++G**// B3LYP/6-311++G** level of theory.

As bromine was preferentially added in position 3, only that path was considered in the rest of the reaction coordinate. The next step was the withdrawal of hydrogen in position 3 via saddle point **TS6out** leading to monobrominated compound **126a**. Calculations predicted a favored process (with low or even without energy barrier) for this deprotonation step in which aromaticity is regained (Figure 3.26).

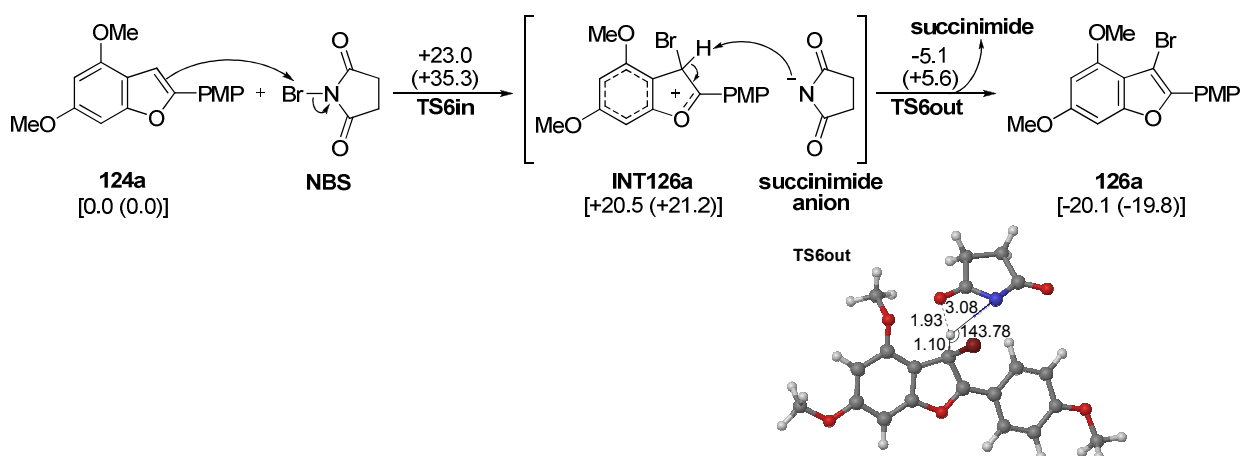


Figure 3.26. Mechanism of the bromination reaction of 2-arylbenzo[*b*]furan **124a** with NBS leading to monobrominated product **126a** and fully optimized structure of transition structure associated with the withdrawal of the hydrogen **TS6out**. Bond distances and angles are given in Å and degrees, respectively. Plain numbers correspond to the relative activation energies and numbers in brackets correspond to the relative Gibbs free energies of the two steps considered. Numbers in square brackets correspond to the relative energies associated with compounds and intermediates with respect to **124a** [internal energy (Gibbs free energy)]. All the energies are given in kcal/mol and were computed at the B3LYP(PCM)/6-311++G**// B3LYP/6-311++G** level of theory.

Once the monobrominated compound **126a** was obtained, the addition of a second bromine atom was assessed. The two available positions in the benzene moiety of benzo[*b*]furan, positions 5 and 7, were then possible. The transition structures associated with the addition of bromine at these two positions were located (**TS9in** and **TS10in**, respectively) and their activation and relative Gibbs free energies calculated. The activation energy computed for the entry of the bromine in position 7 was 4.7 kcal/mol lower than that corresponding to the addition of bromine in position 5. When relative Gibbs free energies were regarded, this difference was of 3.5 kcal/mol (Figure 3.27 A and C). The Kohn-Sham HOMO of **126a** is displayed in Figure 3.27 B. As happened for compound **124a**, the expansion coefficient on C5 is close to zero, suggesting a preference for substitution at position 7 over position 5. Both results are in agreement with the experimentally obtained regioselectivity, i.e. exclusive formation of compound **126b**.

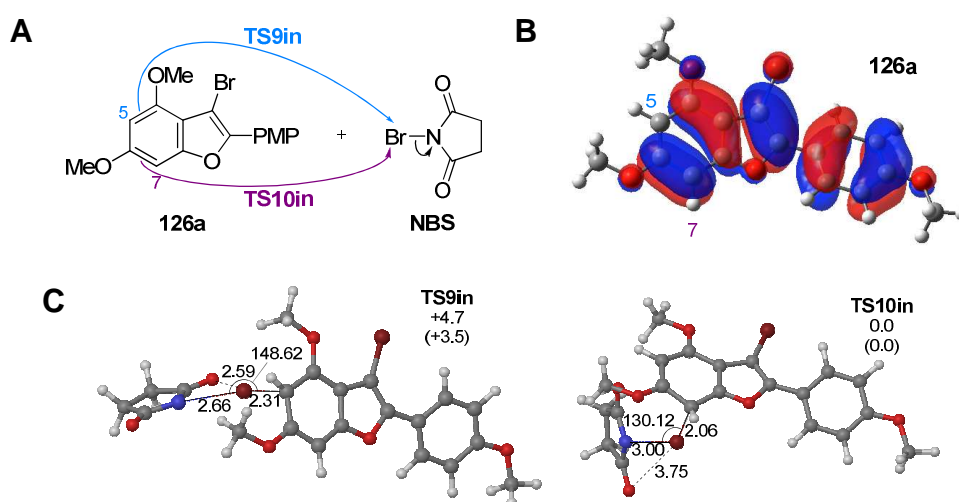


Figure 3.27. (A) Possible reaction paths for the interaction between **126a** and NBS. (B) Kohn-Sham HOMO of **126a**. (C) Fully optimized structures of the corresponding transition structures **TS9in** and **TS10in**. Bond distances and angles are given in Å and degrees, respectively. Plain numbers correspond to the relative activation energies and numbers in brackets correspond to the relative Gibbs free energies, both with respect to **TS10in**, given in kcal/mol and computed at the B3LYP(PCM)/6-311++G**// B3LYP/6-311++G** level of theory.

As in the previous addition-elimination process, the next step was the withdrawal of hydrogen in position 7 leading to dibrominated compound **126b** via transition structure **TS10out**. Again, calculations predicted a favored process (with low or even without energy barrier) for this deprotonation step in which aromaticity is regained and neutral species are formed (Figure 3.28).

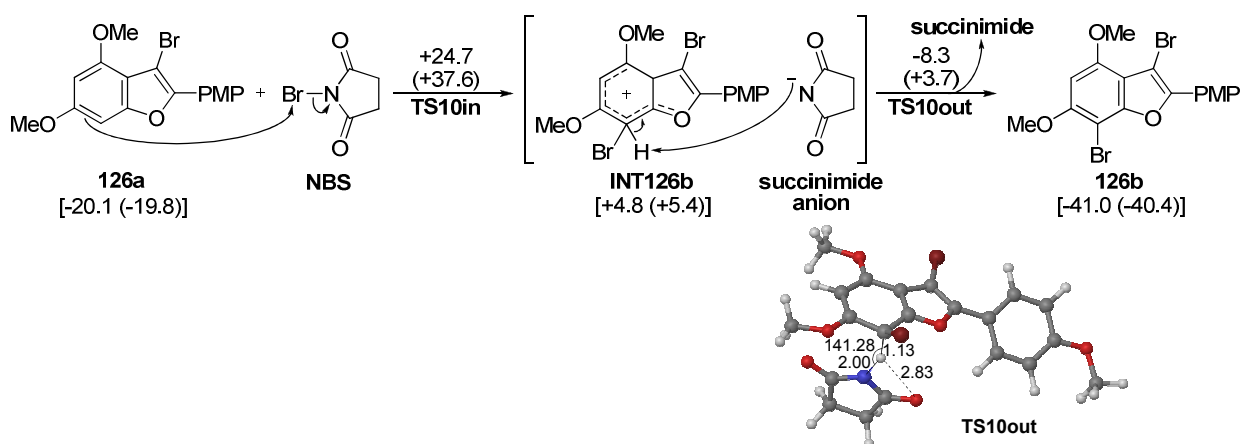


Figure 3.28. Mechanism of the bromination reaction of **126a** with NBS leading to dibrominated product **126b** and fully optimized structure of transition structure associated with the withdrawal of the hydrogen **TS10out**. Bond distances and angles are given in Å and degrees, respectively. Plain numbers correspond to the relative activation energies and numbers in brackets correspond to the relative Gibbs free energies of the two steps considered. Numbers in square brackets correspond to the relative energies associated with compounds and intermediates with respect to **124a** [internal energy (Gibbs free energy)]. All the energies are given in kcal/mol and were computed at the B3LYP(PCM)/6-311++G**// B3LYP/6-311++G** level of theory.

Once the dibrominated compound **126b** was obtained, the addition of the third bromine at the single available position 5 of the benzo[*b*]furan was evaluated. The transition structures associated with the addition of bromine at position 5 (**TS11in**) and elimination of hydrogen (**TS11out**) were located and the activation and relative Gibbs free energies associated with both processes calculated. Once again, calculations predicted a downhill process (without energy barrier) for the deprotonation step in which aromaticity is regained (Figure 3.29 A and C). The Kohn-Sham HOMO of **126b** (Figure 3.29 B) showed that the participation of C5 in the HOMO makes it plausible the substitution at this position (formation of compound **126c**), in agreement with the experimentally obtained result.

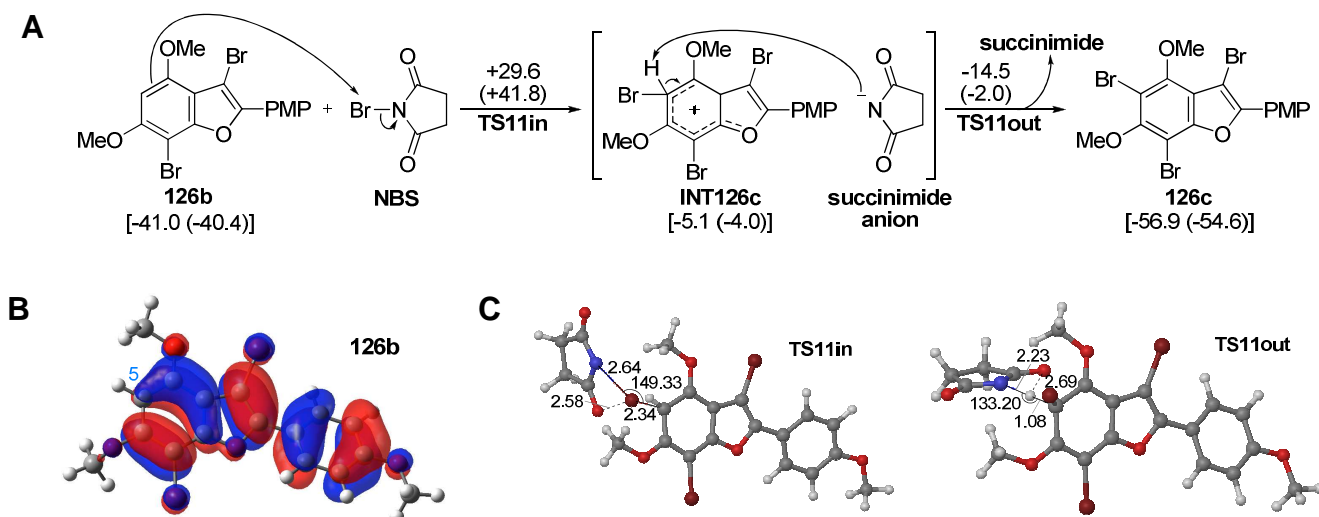
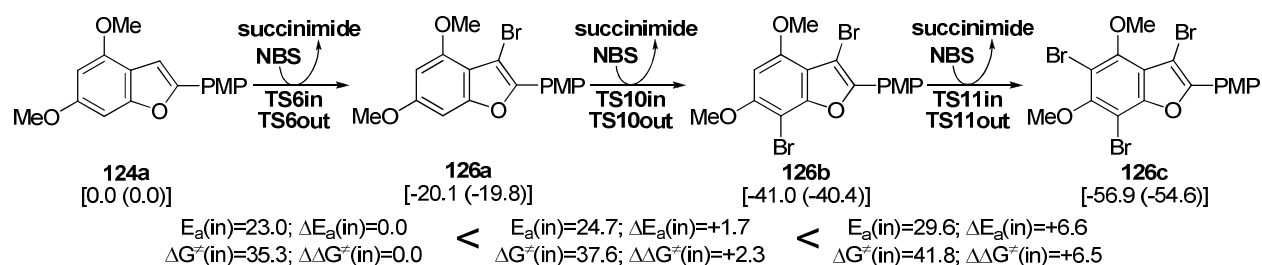


Figure 3.29. (A) Mechanism of the bromination reaction of **126b** with NBS leading to tribrominated product **126c**. Plain numbers correspond to the relative activation energies and numbers in

brackets correspond to the relative Gibbs free energies of the two steps considered. Numbers in square brackets correspond to the relative energies associated with compounds and intermediates with respect to **124a** [internal energy (Gibbs free energy)]. All the energies are given in kcal/mol and were computed at the B3LYP(PCM)/6-311++G**// B3LYP/6-311++G** level of theory. (B) Kohn-Sham HOMO of **126b**. (C) Fully optimized structures of transition structures associated with the addition of bromine **TS11in** and the withdrawal of the hydrogen **TS11out**. Bond distances and angles are given in Å and degrees, respectively.

The relative activation Gibbs energies associated with the successive introduction of bromine atoms progressively increase, being the differences among them of, at least, 1.7 kcal/mol (Scheme 3.21). This means that the addition of the first bromine in **124a** is favored over the addition of the second bromine in **126a** which is, in turn, favored over the addition of the third bromine in **126b**. This result suggested that it is possible to control the number of halogenated positions by adjusting the equivalents of bromine source, in agreement with experimentally obtained results. This also backed the fact that halogen substituents in aromatics deactivate the compound towards electrophilic aromatic substitutions, as they withdraw charge from the aromatic system rendering it less reactive.



Scheme 3.21. Reaction scheme for the successive bromination of **124a** with NBS. Activation energies ($E_a(\text{in})$) and relative Gibbs free energies ($\Delta G^\ddagger(\text{in})$) of the addition steps and their relative value with respect to **TS6in** ($\Delta E_a(\text{in})$ and $\Delta\Delta G^\ddagger(\text{in})$) are given. Numbers in square brackets correspond to the relative energies with respect to **124a** [internal energy (Gibbs free energy)]. All the energies are given in kcal/mol and were computed at the B3LYP(PCM)/6-311++G**// B3LYP/6-311++G** level of theory.

The theoretical study considering **125a** as starting material was analogous to that of starting from **124a**. The only difference is found in the first attack, which takes place at position 2 rather than position 3 of the benzo[*b*]furan, since it is the available position of the furan ring of the starting benzofused system.

The three possible halogenation sites for the first attack were then position 2, 5, and 7. DFT calculations were performed to obtain the transition structures associated with the entry of a bromine in each of these positions (**TS12in**, **TS13in** and **TS14in**, respectively) together with their associated activation and relative Gibbs free energies. According to

these results, the activation barrier of the addition in position 2 was 8.6 kcal/mol lower than that of the addition in position 7 and 13.3 kcal/mol lower than that of the addition in position 5. The same tendency was observed when relative Gibbs free energies were considered, being the energy associated with the addition at position 2 8.3 kcal/mol lower than that of position 7, and 12.6 kcal/mol lower than that of position 5 (Figure 3.30 A and C).

The Kohn-Sham HOMO of **125a** is shown in Figure 3.30 B. As happened with **124a**, the expansion coefficient on C5 is almost zero, suggesting a preference for substitution at positions 3 or 7, but allowing no apparent selectivity prediction between them on its own.

The combination of all these results (together with the higher reactivity of furan ring predicted by the NICS-based aromaticity evaluation) is in agreement with the experimentally obtained regioselectivity, i.e. exclusive formation of compound **127a**.

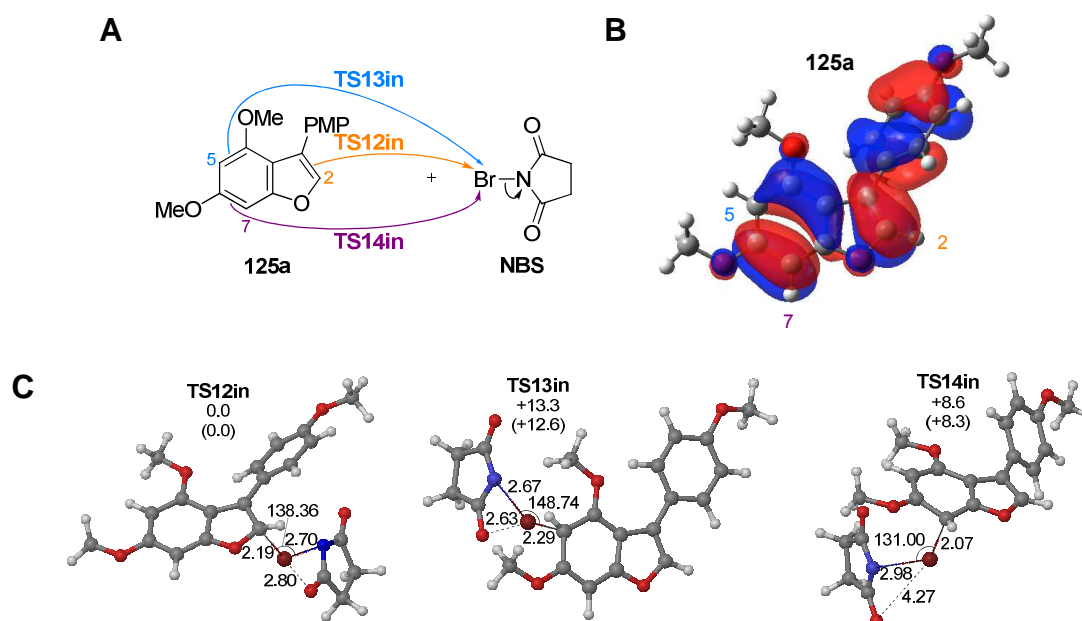


Figure 3.30. (A) Possible reaction paths for the interaction between 3-arylbenzo[*b*]furan **125a** and NBS. (B) Kohn-Sham HOMO of **125a**. (C) Fully optimized structures of the corresponding transition structures **TS12in**, **TS13in** and **TS14in**. Bond distances and angles are given in Å and degrees, respectively. Plain numbers correspond to the relative activation energies and numbers in brackets correspond to the relative Gibbs free energies, both with respect to **TS12in**, given in kcal/mol and computed at the B3LYP(PCM)/6-311++G**// B3LYP/6-311++G** level of theory.

As bromine was preferentially added in position 2, only that path was considered in the rest of study. The next step was the withdrawal of hydrogen from position 2 via **TS12out** (Figure 3.31) leading to monobrominated compound **127a**. As happened for 2-aryl benzo[*b*]furan series, calculations predicted a kinetically favored process with a very low energy barrier.

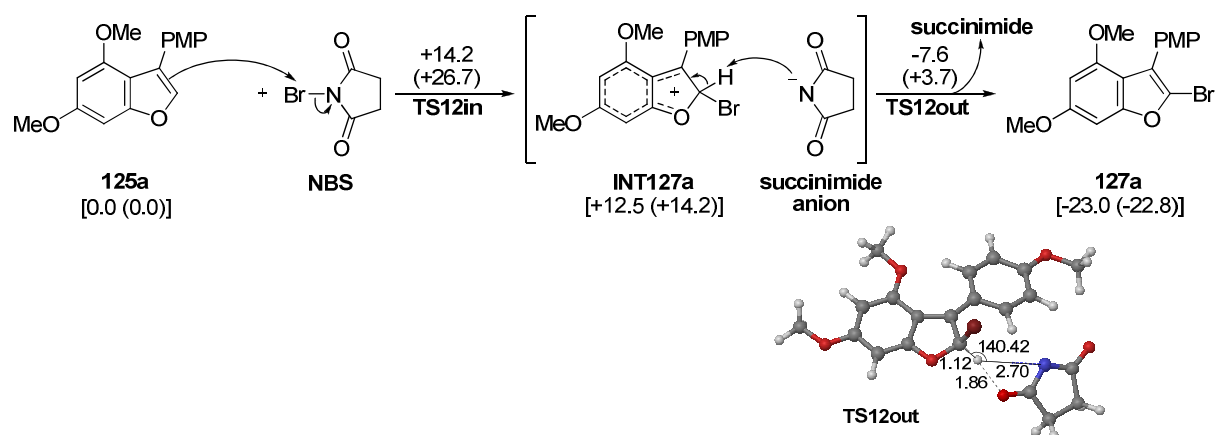


Figure 3.31. Mechanism of the bromination reaction of 3-arylbenzo[*b*]furan **125a** with NBS leading to monobrominated product **127a** and fully optimized structure of transition structure associated with the withdrawal of the hydrogen **TS12out**. Bond distances and angles are given in Å and degrees, respectively. Plain numbers correspond to the relative activation energies and numbers in brackets correspond to the relative Gibbs free energies of the two steps considered. Numbers in square brackets correspond to the relative energies associated with compounds and intermediates with respect to **125a** [internal energy (Gibbs free energy)]. All the energies are given in kcal/mol and were computed at the B3LYP(PCM)/6-311++G**// B3LYP/6-311++G** level of theory.

Once the monobrominated compound **127a** was obtained, the assessment of the entry of the second and third bromines was equivalent to that of the 2-aryl benzo[*b*]furan series. The two available positions in the benzene moiety of benzo[*b*]furan were positions 5 and 7 (Figure 3.32) and the calculations showed the same order of preferential substitution for the successive brominations.

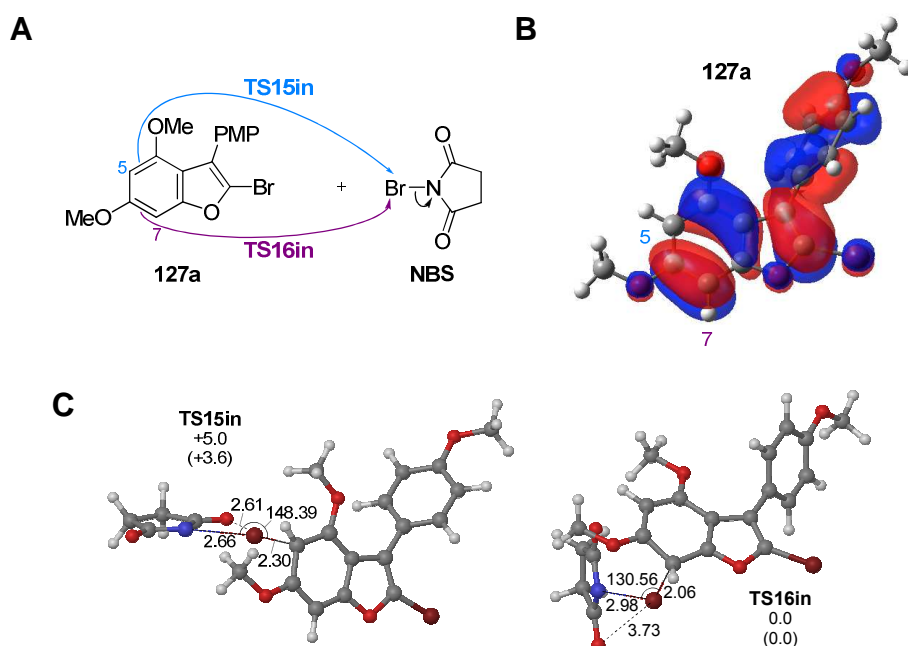


Figure 3.32. (A) Possible reaction paths for the interaction between **127a** and NBS. (B) Kohn-Sham HOMO of **127a**. (C) Fully optimized structures of the corresponding transition structures **TS15in** and **TS16in**. Bond distances and angles are given in Å and degrees, respectively. Plain numbers correspond to the relative activation energies and numbers in brackets correspond to the relative Gibbs free energies, both with respect to **TS16in**, given in kcal/mol and computed at the B3LYP(PCM)/6-311++G**// B3LYP/6-311++G** level of theory.

Thus, computational studies predicted the formation of dibrominated product **127b** (Figure 3.33), i.e. the addition of the second bromine in position 7.

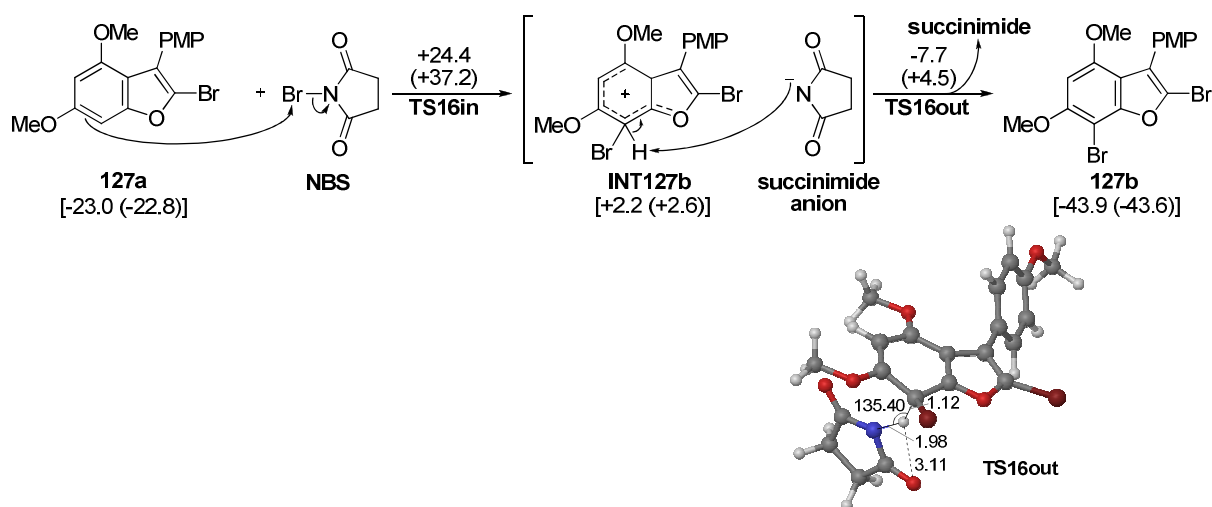


Figure 3.33. Mechanism of the bromination reaction of **127a** with NBS leading to dibrominated product **127b** and fully optimized structure of transition structure associated with the withdrawal of the hydrogen **TS16out**. Bond distances and angles are given in Å and degrees, respectively. Plain numbers correspond to the relative activation energies and numbers in brackets correspond to the relative Gibbs free energies of the two steps considered. Numbers in square brackets correspond to the relative energies with respect to **125a** [internal energy (Gibbs free energy)]. All the energies are given in kcal/mol and were computed at the B3LYP(PCM)/6-311++G**// B3LYP/6-311++G** level of theory.

The formation of tribrominated product **127c** (Figure 3.34), i.e. the addition of the third bromine in position 5, was studied in a similar manner.

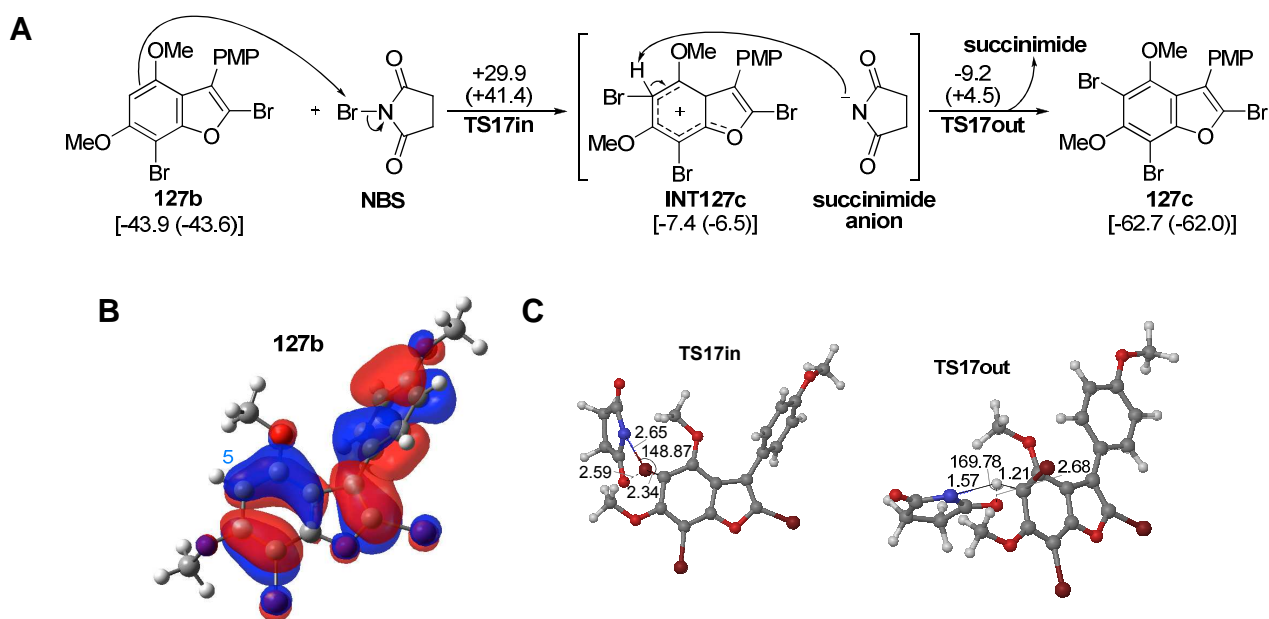
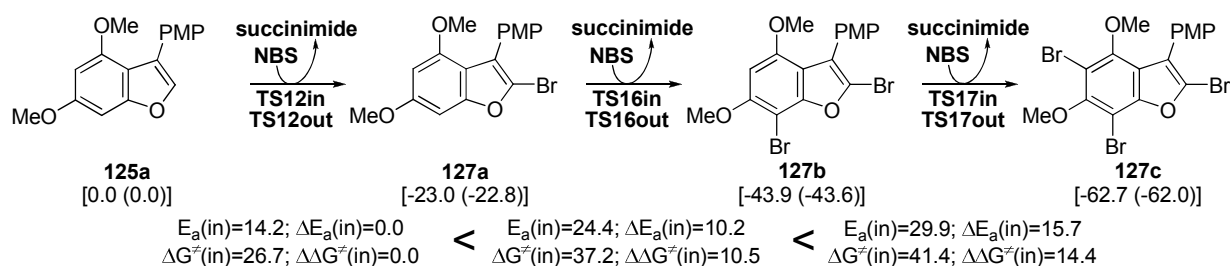


Figure 3.34. (A) Mechanism of the bromination reaction of **127b** with NBS leading to tribrominated product **127c**. Plain numbers correspond to the relative activation energies and numbers in brackets correspond to the relative Gibbs free energies of the two steps considered. Numbers in square brackets correspond to the relative energies associated with compounds and intermediates

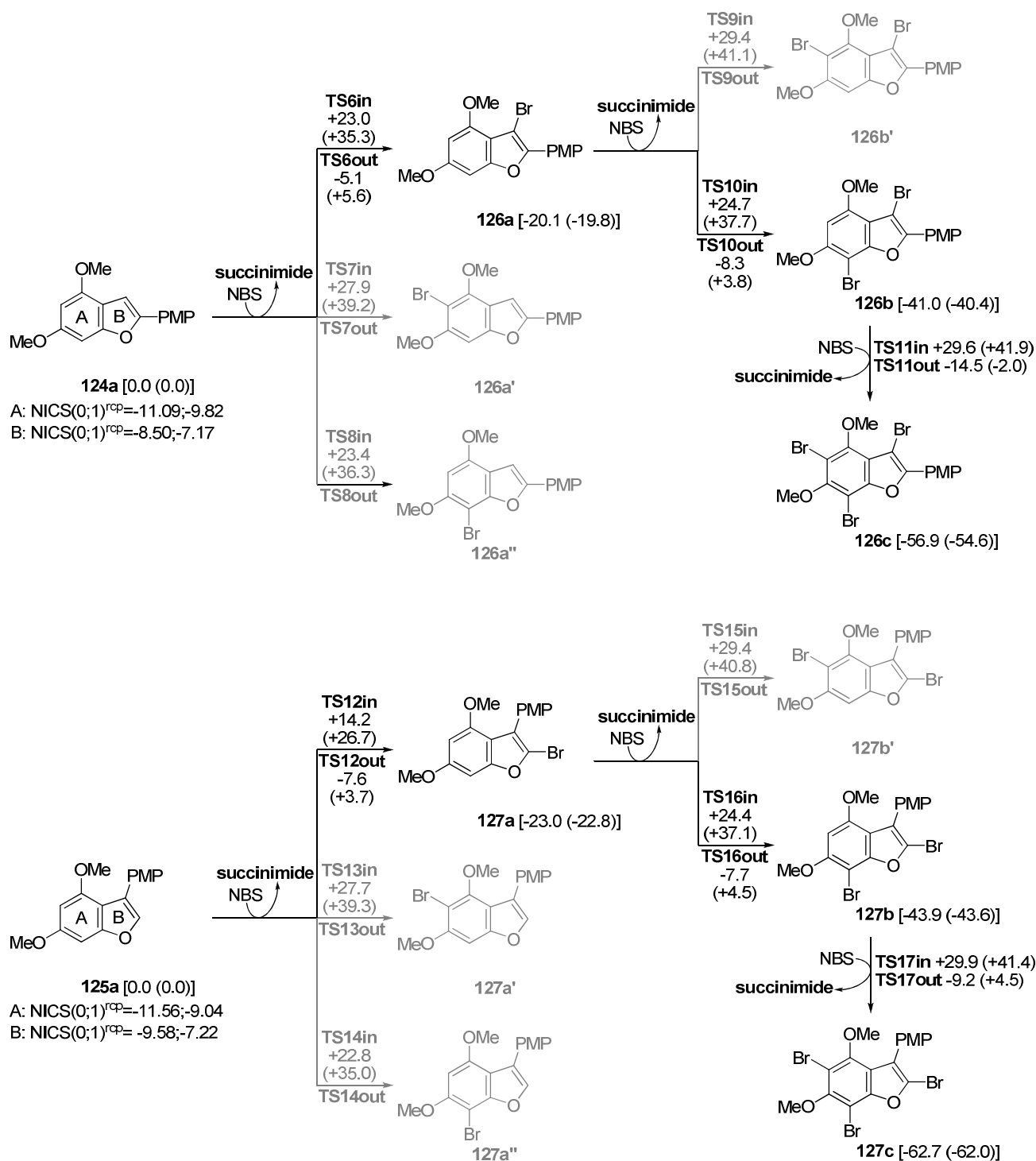
with respect to **125a** [internal energy (Gibbs free energy)]. All the energies are given in kcal/mol and were computed at the B3LYP(PCM)/6-311++G**// B3LYP/6-311++G** level of theory. (B) Kohn-Sham HOMO of **127b**. (C) Fully optimized structures of transition structures associated with the addition of bromine **TS17in** and the withdrawal of the hydrogen **TS17out**. Bond distances and angles are given in Å and degrees, respectively.

Again, the activation and relative Gibbs free energies of the processes of successive introduction of a halogen substituent progressively increase, being the differences among them of, at least, 3.9 kcal/mol (Scheme 3.22). This means that the addition of the first bromine in **125a** is faster than the addition of the second bromine in **127a** which is, in turn, favored over the addition of the third bromine in **127b**. It also suggests the possibility of isolating the mono- and dihalogenated compounds, in nice agreement with the experimental results.



Scheme 3.22. Reaction scheme for the successive bromination of **125a** with NBS. Activation energies ($E_a(\text{in})$) and relative Gibbs free energies ($\Delta G^\ddagger(\text{in})$) of the addition steps and their relative value with respect to **TS12in** ($\Delta E_a(\text{in})$ and $\Delta\Delta G^\ddagger(\text{in})$) are given. Numbers in square brackets correspond to the relative energies with respect to **125a** [internal energy (Gibbs free energy)]. All the energies are given in kcal/mol and were computed at the B3LYP(PCM)/6-311++G**// B3LYP/6-311++G** level of theory.

3.2.3.4. Graphical overview



Scheme 3.23. General overview of the computational study of the bromination of 2-aryl and 3-aryl benzo[*b*]furans **124a** and **125a**, respectively. NICS values of rings A and B in starting **124a** and **125a** are given in ppm and were computed at the B3LYP/6-311+G** level of theory. Activation energies (plain numbers) and relative Gibbs free energies (numbers in brackets) are given in kcal/mol and were computed at the B3LYP(PCM)/6-311++G**// B3LYP/6-311++G** level of theory. Numbers in square brackets correspond to the relative energies [internal energy (Gibbs free energy)] with respect to **124a** in the 2-aryl series and to **125a** in the 3-aryl series. They are given in kcal/mol and were computed at the same level of theory.

Having gathered all the data obtained in the computational study in scheme 3.23, a last comparison was made between these results and the experimentally obtained ones. Considering the activation and relative Gibbs free energies of the first bromination of both series, it was observed that the entry of the first substituent is more favored in the 3-arylbenzo[*b*]furan **125a** than in the 2-arylbenzo[*b*]furan **124a**. Nevertheless, this difference was not reflected in the results of the experimental study, as compounds **126a** and **127a** were obtained in the same yield (table 3.4, monobromination).

Indeed, calculations provide no significant differences between the two series in the activation energies associated with the entry of the second and the third bromine. Unfortunately, these values did not let us explain the different yields of the reactions leading to dibrominated **126b** and **127b** (table 3.4, dibromination) and the fact that tribrominated **126c** was experimentally obtained whilst **127c** was not afforded (table 3.4, tribromination) under the same conditions.

Table 3.4. Calculated activation energies ($E_a(\text{in})$ and $\Delta G^\ddagger(\text{in})$, kcal/mol) and experimentally obtained reaction yields (%) of the indicated bromination reactions.

entry	monobromination			dibromination				tribromination			
	reaction	comp.	exp.	comp.		exp.		comp.		exp.	
		$E_a(\text{in})$ $\Delta G^\ddagger(\text{in})^a$	yield ^b	reaction	$E_a(\text{in})$ $\Delta G^\ddagger(\text{in})^a$	reaction	yield ^b	reaction	$E_a(\text{in})$ $\Delta G^\ddagger(\text{in})^a$	reaction	yield ^b
1	124a → 126a	23.0 35.3	81	126a → 126b	24.7 37.6	124a → 126b	89	126b → 126c	29.6 41.8	124a → 126c	30
2	125a → 127a	14.2 26.7	81	127a → 127b	24.4 37.2	125a → 127b	68	127b → 127c	29.9 41.4	125a → 127b	–

^a Activation and relative Gibbs free energies (kcal/mol) calculated at the B3LYP(PCM)/6-311++G**// B3LYP/6-311++G** level of theory, from the computational study (comp.)

^b Yields (%) from the experimental study (exp.)

Therefore, the computational study presented in this section resulted useful to qualitatively evaluate the regioselectivity of the bromination reactions of compounds **124a** and **125a** but allowed not straightforward correlation to quantitative experimental results.

3.2.4. Conclusions

From this section, in which the *N*-halosuccinimides-mediated aromaticity driven regioselective halogenation of substituted benzofurans is developed, the following conclusions can be drawn:

- In general, *N*-halosuccinimides (NXS) are appropriate reagents for the halogenation of benzofurans. Bromination (using *N*-bromosuccinimide, NBS) worked better than chlorination (using *N*-chlorosuccinimide, NCS) which, in turn, performed better than iodination (using *N*-iodosuccinimide, NIS).
- 3-Aryl benzofuran **125a** is more reactive than its 2-aryl congener **124a** towards the halogenation of the five-membered ring, although this tendency is inverted for further halogenations since the resulting 3-aryl-2-halo-benzofuran is more deactivated. The halogenation of the third position of **125a** was not achieved.
- Bromination is selective and, when using one equivalent of NBS, out of the three possible sites, it occurs first in the unsubstituted position of the furan ring (i.e. position 3 and 2 for compounds **124a** and **125a**, respectively). When a second equivalent of NBS is introduced position 7 is exclusively halogenated, whilst halogenation of position 5 required a large excess of NBS to proceed.
- Iodination resulted in unstable reaction products that progressively degrade.
- In the case of 2-aryl benzofuran **124a** chlorination is less selective, not being possible to isolate any monochlorination product. A mixture of two dichlorinated products was obtained when two equivalents of NCS were employed. Both isomers are chlorinated in position 3 and the major one also in position 7, the minor one being chlorinated in position 5.
- The developed procedure permits the preparation of combined dihalogenated products such as 7-bromo-2-chloro-4,6-dimethoxy-3-(4-methoxyphenyl)benzofuran **127f** by successive halogenations using different *N*-halosuccinimides.

- The computational study, based on DFT calculations, successfully predicts the regioselectivity of the electrophilic aromatic substitutions studied and provide interesting additional information. Both the global process and each substitution step are exothermic processes. In both 2-aryl and 3-aryl series, the first substitution is kinetically more accessible than the second and the third ones, which is in agreement with the NICS prediction of a higher reactivity of the five-membered ring over six-membered one. The selectivity between the two available positions in the benzene moiety (positions 5 and 7) could be attributed to the different expansion coefficient of the HOMO of the corresponding products on carbon atoms 5 and 7.

3.3. HYPERVALENT IODINE-MEDIATED OXIDATIVE DEAROMATIZATION of MONOHYDROXYLATED BENZO[*b*]FURANS

3.3.1. Oxidative dearomatization of phenols overview

3.3.1.1. Basic concepts

Oxidation of phenols is an essential biochemical process in oxidative phosphorylation²¹¹. Furthermore, controlled oxidative transformations of substituted phenols are included in many organic synthetic sequences.

The oxidative dearomatization of phenols (**35**) can be understood as a two step process²¹²: an oxidation followed by a nucleophilic attack, which yields cyclohexadienones. In principle two cyclohexadienone regioisomers can be obtained, depending mainly on the substitution pattern of the starting phenol and the reaction conditions²¹³. In general, in the presence of an appropriate nucleophile, the reaction yields 6,6-disubstituted cyclohexa-2,4-dienones (**158**) in a regiocontrolled manner when the starting phenol is *ortho* substituted (electron-releasing group, *para* unsubstituted)²¹⁴ and 4,4-disubstituted cyclohexa-2,5-dienone (**159**) when the starting phenol is *para* substituted (electron releasing group, *ortho* unsubstituted)²¹⁵ (Scheme 3.24 and 3.25). When the substitution pattern is more complex each case should be analysed²¹⁶, although a preference for the

²¹¹ Oxidative phosphorylation is the metabolic pathway which uses the energy released in the oxidation of nutrients to produce adenosine-5'-triphosphate (ATP), the molecule that supplies energy to metabolism.

²¹² (a) Arzeno, H.; Barton, D. H. R.; Bergé-Lurion, R.-M.; Lusinchi, X.; Pinto, B. M. *J. Chem. Soc. Perkin Trans. 1* **1984**, 2069-2076 (b) Barton, D. H. R.; Bergé-Lurion, R.-M.; Lusinchi, X.; Pinto, B. M. *J. Chem. Soc. Perkin Trans. 1* **1984**, 2077-2080

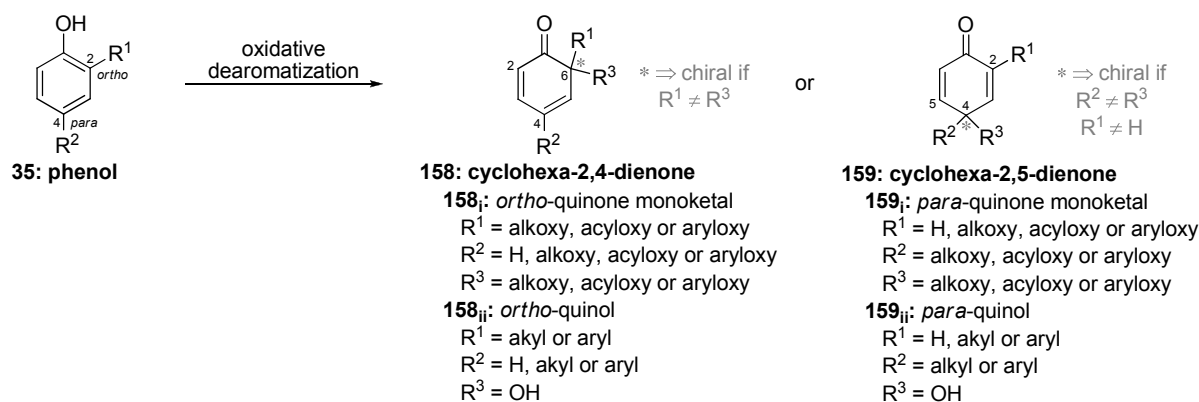
²¹³ Roy, H. N.; Sarkar, M. S.; Mal, D. *Synth. Commun.* **2005**, *35*, 2183-2188

²¹⁴ (a) Quideau, S.; Pouységu, L. *Org. Prep. Proc. Int.* **1999**, *31*, 617-680 (b) Magdziak, D.; Rodriguez, A. A.; Van De Water, R. W.; Pettus, T. R. R. *Org. Lett.* **2002**, *4*, 285-288 (c) Lebrasseur, N.; Gagnepain, J.; Ozanne-Beaudenon, A.; Léger, J.-M.; Quideau, S. *J. Org. Chem.* **2007**, *72*, 6280-6283 (d) Quideau, S.; Pouységu, L.; Deffieux, D. *Synlett* **2008**, *4*, 467-495 (e) Pouységu, L.; Chassaing, S.; Dejugnac, D.; Lamidey, A.-M.; Miqueu, K.; Sotiropoulos, J.-M.; Quideau, S. *Angew. Chem. Int. Ed.* **2008**, *47*, 3552-3555 (f) Pouységu, L.; Sylla, T.; Garnier, T.; Rojas, L. B.; Charris, J.; Deffieux, D.; Quideau, S. *Tetrahedron* **2010**, *66*, 5908-5917

²¹⁵ (a) McKillop, A.; Perry, D. H.; Edwards, M.; Antus, S.; Farkas, L.; Nógrádi, M.; Taylor, E. C. *J. Org. Chem.* **1976**, *41*, 282-287 (b) Tamura, Y.; Yakura, T.; Haruta, J.-I.; Kita, Y. *J. Org. Chem.* **1987**, *52*, 3927-3930 (c) Fleck, A. E.; Hobart, J. A.; Morrow, G. W. *Synth. Commun.* **1992**, *22*, 179-187 (d) Pelter, A.; Elgendy, S. M. A. *J. Chem. Soc. Perkin Trans 1* **1993**, 1891-1896 (e) Omura, K. *Synth. Commun.* **2000**, *30*, 877-885 (f) Van De Water, R. W.; Hoarau, C.; Pettus, T. R. R. *Tetrahedron Lett.* **2003**, *44*, 5109-5113 (g) Hammill, J. T.; Contreras-García, J.; Virshup, A. M.; Beratan, D. N.; Yang, W.; Wipf, P. *Tetrahedron* **2010**, *66*, 5852-5862

²¹⁶ (a) Mal, D.; Roy, H. N.; Hazra, N. K.; Adhikari, S. *Tetrahedron* **1997**, *53*, 2177-2184 (b) Kürti, L.; Herczegh, P.; Visy, J.; Simonyi, M.; Antus, S.; Pelter, A. *J. Chem. Soc. Perkin Trans 1*, **1999**, 379-380 (c) Kraus, G. A.; Cui, W. *J. Org. Chem.* **2002**, *67*, 9475-9476

2,5-regioisomer is observed under equal terms (in the absence of an orientating group or an *ortho* selective reagent)²¹⁷.



Scheme 3.24. Access to cyclohexa-2,4- and -2,5-dienones through oxidative dearomatization of 2- and/or 4-substituted phenols.

Cyclohexadienones are very interesting intermediates in various complex organic syntheses^{214a,218}. In fact, these compounds have successfully been applied to the total synthesis of several natural products²¹⁹. They are good electrophilic substrates for various reactions including [4+2] Diels-Alder cycloadditions and cyclodimerizations^{214c,220} or nucleophilic additions, but tend also to undergo acid-catalyzed rearrangements, reductive eliminations or prototropic events resulting in rearomatization²²¹. This implicit reactivity of cyclohexadienones has on the one hand been exploited with preparative purposes but, on the other hand, it has prevented their widespread use in total synthesis, since many of these processes are difficult to control or avoid.

In this line, bearing in mind that one of the best added values of the oxidative dearomatization of phenols is the possibility of creating a stereogenic center at the *ortho* or *para* aromatic carbon undergoing the $sp^2 \rightarrow sp^3$ hybridization change (Scheme 3.24),

²¹⁷ (a) Pelter, A.; Elgandy, S. *Tetrahedron Lett.* **1988**, 29, 677-680 (b) Mitchell, A. S.; Russell, R. A. *Tetrahedron* **1997**, 53, 4387-4410 (c) Sels, B. F.; De Vos, D. E.; Jacobs, P. A. *Angew. Chem. Int. Ed.* **2005**, 44, 310-313 (d) Omura, K. *Synthesis* **2010**, 208-210

²¹⁸ Magdziak, D.; Meek, S. J.; Pettus, T. R. R. *Chem. Rev.* **2004**, 104, 1383-1430

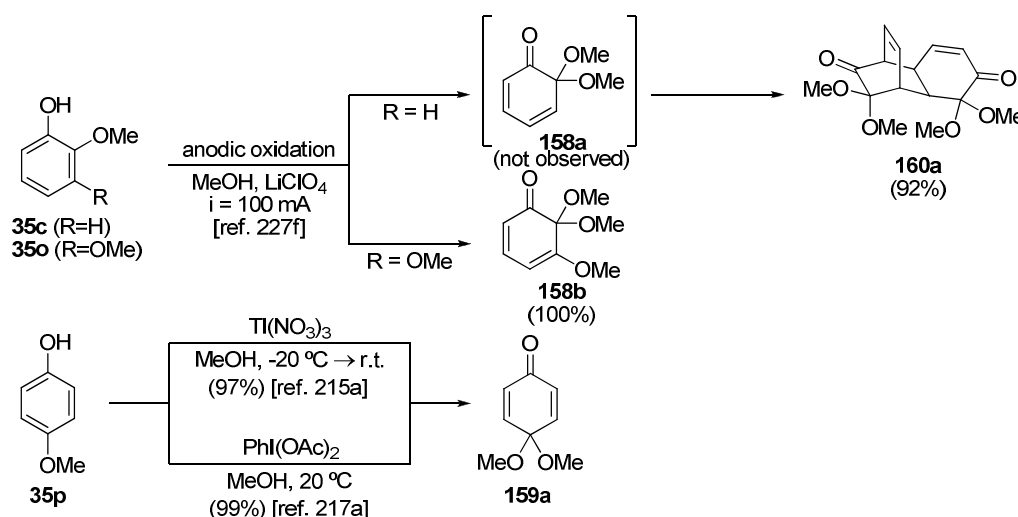
²¹⁹ Pouységu, L.; Deffieux, D.; Quideau, S. *Tetrahedron* **2010**, 66, 2235-2261

²²⁰ (a) Kürti, L.; Szilágyi, L.; Antus, S.; Nógrádi, M. *Eur. J. Org. Chem.* **1999**, 2579-2581 (b) Liao, C.-C.; Chu, C.-S.; Lee, T.-H.; Rao, P. D.; Ko, S.; Song, L.-D.; Shiao, H.-C. *J. Org. Chem.* **1999**, 64, 4102-4110 (c) Chittimalla, S. K.; Shiao, H.-Y.; Liao, C.-C. *Org. Biomol. Chem.* **2006**, 4, 2267-2277 (d) Gagnepain, J.; Méreau, R.; Dejugnac, D.; Léger, J.-M.; Castet, F.; Deffieux, D.; Pouységu, L.; Quideau, S. *Tetrahedron* **2007**, 63, 6493-6505

²²¹ (a) Miller, B. *J. Am. Chem. Soc.* **1965**, 87, 5115-5120 (b) Waring, A. J.; Zaidi, J. H.; Pilkington, J. W. *J. Chem. Soc. Perkin Trans. 1* **1981**, 5, 1454-1459 (c) Hong, F.-T.; Lee, K.-S.; Liao, C.-C. *Tetrahedron Lett.* **1992**, 33, 2155-2158 (d) Dohi, T.; Kamitanaka, T.; Watanabe, S.; Hu, Y.; Washimi, N.; Kita, Y. *Chem. Eur. J.* **2012**, 18, 13614-13618 (e) Ratnikov, M. O.; Farkas, L. E.; Doyle, M. P. *J. Org. Chem.* **2012**, 77, 10294-10303

another reason behind the underuse of cyclohexadienones in the field of organic synthesis has been, for a long time, the absence of general methods for the enantioselective preparation of these structures. Nevertheless, this matter is being increasingly overcome, constituting an ongoing research line of several groups²²².

As a consequence of its great proven and potential utility, a large number of agents and methods have been developed for phenol oxidation. These can be divided into four broad categories: redox (heavy) metal-based oxidants such as Pb(IV), typically lead tetraacetate (Pb(OAc)₄ or LTA)²²³, and Tl(III), most commonly thallium trinitrate (Tl(NO₃)₃ or TTN)^{215a,224}, among many others; non-metallic neutral organic oxidants including, for example, 2,3-dichloro-5,6-dicyano-1,4-benzoquinone (DDQ)^{212,225}; methods based in electrochemical oxidation²²⁶, like anodic oxidation using LiOCl₄ as supporting electrolyte; and last but not least hypervalent iodine-based reagents^{227,214b,c,f,215b-d,f,217,219} (Scheme 3.25).



Scheme 3.25. Examples of methods and/or reagents for the oxidative dearomatization of substituted phenols leading to *ortho*- or *para*-quinone monoketals and a Diels-Alder [4+2] cycloaddition product.

²²² (a) Ding, Q.; Ye, Y.; Fan, R. *Synthesis* **2013**, *45*, 1-16 (b) Dohi, T.; Maruyama, A.; Takenaga, N.; Senami, K.; Minamitsuji, Y.; Fujioka, H.; Caemmerer, S. B.; Kita, Y. *Angew. Chem. Int. Ed.* **2008**, *47*, 3787-3790

²²³ (a) Wessely, F.; Lauterbachkeil, G.; Sinwel, F. *Monatsh. Chem.* **1950**, *81*, 811-818 (b) Harrison, M. J.; Norman, R. O. C. *J. Chem. Soc. C* **1970**, 728-730 (c) Perumal, P. T.; Bhatt, M. V. *Synthesis* **1980**, *11*, 943-945

²²⁴ Horie, T.; Yamada, T.; Kawamura, Y.; Tsukayama, M.; Kuramoto, M. *J. Org. Chem.* **1992**, *57*, 1038-1042

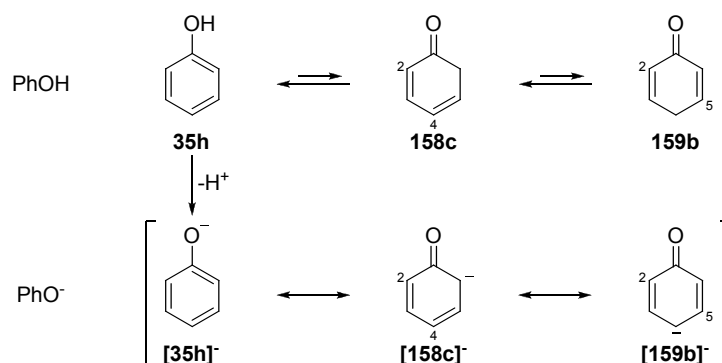
²²⁵ Kasturi, T. R.; Rajasekhar, B.; Raju, G. J.; Reddy, G. M.; Sivaramakrishnan, R.; Ramasubbu, N.; Venkatesan, K. *J. Chem. Soc. Perkin Trans. 1* **1984**, 2375-2382

²²⁶ (a) Henton, D. R.; Anderson, K.; Manning, M. J.; Swenton, J. S. *J. Org. Chem.* **1980**, *45*, 3422-3433 (b) Dolson, M. G.; Swenton, J. S. *J. Am. Chem. Soc.* **1981**, *103*, 2361-2371 (c) Yamamura, S.; Shizuri, Y.; Shigemori, H.; Okuno, Y.; Ohkubo, M. *Tetrahedron* **1991**, *47*, 635-644 (d) Yamamura, S.; Nishiyama, S. *Synlett* **2002**, 533-543 (e) Quideau, S.; Pouységu, L.; Deffieux, D.; Ozanne, A.; Gagnepain, J.; Fabre, I.; Oxoby, M. *Arkivoc* **2003**, *vi*, 106-119 (f) Deffieux, D.; Fabre, I.; Titz, A.; Léger, J.-M.; Quideau, S. *J. Org. Chem.* **2004**, *69*, 8731-8738

²²⁷ Pelter, A.; Ward, R. S. *Tetrahedron* **2001**, *57*, 273-282

3.3.1.2. The reaction of oxidative dearomatization of phenols

At this point it is interesting to examine the transformation itself more in depth²¹⁹. For so doing, the reactivity of phenol **35h** will be first analysed. When considering ionic reactions, phenols are included in the nucleophile list. In principle, they need no special activation to express their nucleophilic character, although the acidity of the phenolic O–H bond can be exploited under (mild) basic conditions to generate phenolate anions (PhO⁻, [**35h**]⁻), with an enhanced (harder) nucleophilic power. Besides, by appropriately choosing reaction conditions, this nucleophilicity can be modulated to selectively direct reactions at either their oxygen or one of the *ortho* or *para* carbon centers (Scheme 3.26).

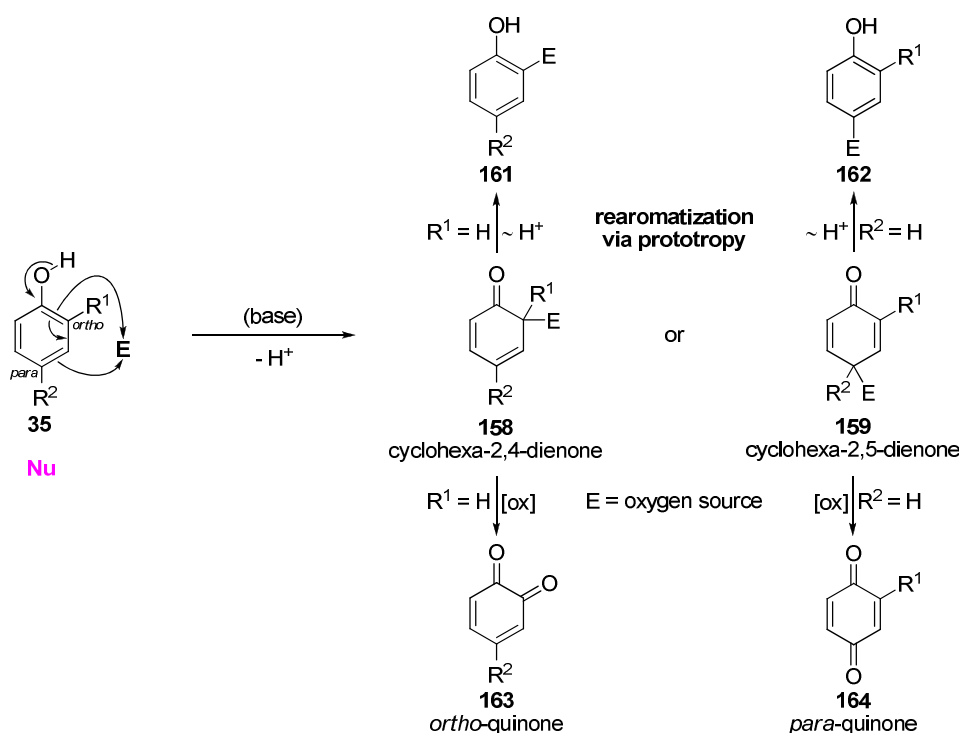


Scheme 3.26. Resonance structures of phenol (PhOH, **35h**) and phenolate anion (PhO⁻, [**35h**]⁻)²¹⁹.

The critical difference between these reaction pathways is that any bond-forming event taking place at one of the *ortho/para* carbon centers does imply a thermodynamically unfavored dearomatized species (Scheme 3.27).

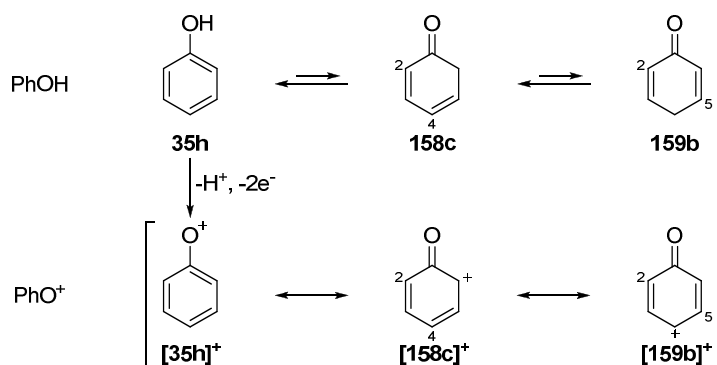
If the targeted carbon is unsubstituted, the dearomatized species can be limited to an intermediate which will readily rearomatize via prototropy ($\sim\text{H}^+$) or which can lead, under appropriate oxidative reaction conditions, to a product (e.g. *ortho*- or *para*-quinone **163** or **164**, respectively) that can be isolated as such (provided it is stable and its reactivity is moderate), via the formation of a carbon-heteroatom (e.g. oxygen) bond at the *ortho/para* position.

If the targeted carbon already bears a substituent of moderate or poor nucleofugality, the dearomatized product can usually be isolated as such. This leads to the useful aforementioned cyclohexa-2,4- or -2,5-dienones **158** or **159**, respectively.



Scheme 3.27. Phenol dearomatization process via “nucleophilic” phenol pathway²¹⁹. [ox] = oxidant.

Despite the marked nucleophilic character of phenols, their susceptibility toward oxidation by electron transfer processes can be exploited to, under appropriate reaction conditions, generate an phenoxenium cation (PhO^+ , **[35h]⁺**) intermediate (Scheme 3.28).

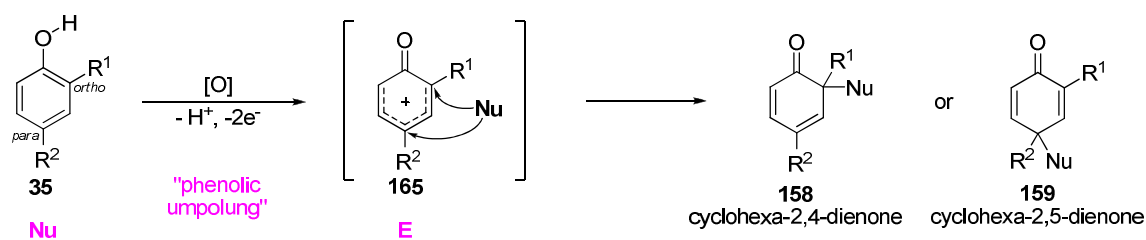


Scheme 3.28. Resonance structures of phenol (PhOH , **35h**) and phenoxenium cation (PhO^+ , **[35h]⁺**)²¹⁹.

This phenoxenium cation can be trapped by a nucleophilic species at substituted *ortho/para* carbons, in a regioselective manner by adequately choosing the substitution pattern of the starting phenol and the reaction conditions, yielding the cyclohexadienone products. This switch of reactivity of phenols from being nucleophiles into becoming electrophiles is known as “phenolic umpolung”²²⁸ and is the underlying event in the

²²⁸ (a) Sabot, C.; Bérard, D.; Canesi, S. *Org. Lett.* **2008**, *10*, 4629-4632 (b) Bérard, D.; Giroux, M.-A.; Racicot, L.; Sabot, C.; Canesi, S. *Tetrahedron* **2008**, *64*, 7537-7544

presented oxidative phenol dearomatizations (using metal-based two-electron oxidants, anodic oxidations or hypervalent iodine-based reagents) (Scheme 3.29).



Scheme 3.29. Phenol dearomatization process via phenolic “umpolung” pathway²¹⁹.

Indeed, any reagent combining the dual reactivity criteria of electrophilicity and nucleofugality will be a good candidate to perform the desired transformation. It is precisely due to these considerations that hypervalent iodine-based reagents have gained ground in this field in the last decades. Besides meeting the electrophilicity and nucleofugality requirements just mentioned, their ease of handling, their low toxicity (they are considered environmentally benign), their excellent performance under mild conditions (they generally reproduce, and even improve, the effectiveness of other oxidizing reagents and/or methods) and the fact that they are increasingly commercially available or accessible from inexpensive products have made them the most used alternative to carry out the phenol oxidation reactions. These reasons led us to choose them as oxidizing agents and, therefore, hypervalent iodine-based compounds and their role in phenol oxidation reactions are studied in more detail below.

3.3.1.3. Hypervalent iodine-based reagents

Iodine was discovered in 1811 by French chemist B. Courtois and named by J. L. Gay-Lussac in 1813 (because of the Greek word *ιώδης* for violet, alluding the color of both iodine vapor and resublimed crystalline iodine)²²⁹. From a physicochemical standpoint, it is the chemical element of atomic number 53 (group VII and period 5) and the largest, the least electronegative and the most polarizable of the common halogens. Its electronic configuration confers on it a monovalent character, with an oxidation state of -1, although it is capable of forming stable compounds in which iodine has an oxidation state of +3, +5 and even +7, being the most common hypervalent (or polyvalent)²³⁰ organic iodine

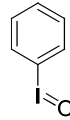
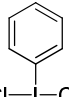
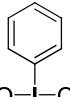
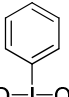
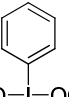
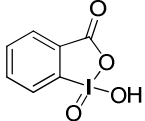
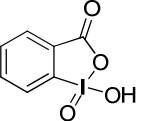
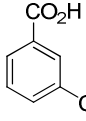
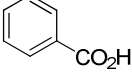
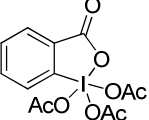
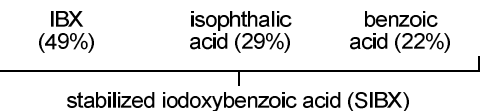
²²⁹ (a) Courtois, B. *Ann. Chim.* **1813**, 88, 304-310 (b) Gay-Lussac, J. L. *Ann. Chim.* **1813**, 88, 311-318

²³⁰ The molecules with a Lewis structure in which the central atom bears more than eight electrons are called hypervalent; hypervalence constitutes therefore an exception to the octet rule. To learn more about the chemistry of hypervalent molecules see: Musher, J. I. *Angew. Chem. Int. Ed.* **1969**, 8, 54-68

compounds I(III) and I(V) species. The first reported hypervalent iodine compound, dichloriodobenzene (PhICl_2), was first synthesized by Willgerodt in 1886²³¹. Soon after that, many other compounds were prepared²³². Nevertheless, the extensive development of their use in organic synthesis, which continues today, did not start until the mid-twentieth century²³³.

According to the IUPAC notation, compounds bearing a non-standard valence are denoted with the Greek letter lambda (λ) followed by the corresponding valence indicated as a superscript. Therefore, hypervalent iodine families of compounds of valence 3 (III), 5 (V) and 7 (VII) are referred to as λ^3 -, λ^5 - and λ^7 -iodanes, respectively. The λ^7 -iodane family includes compounds such as NaIO_4 and HIO_4 and will not be further considered in this study; the main λ^3 - and λ^5 -iodanes are shown in Table 3.5. λ^3 -iodanes will be addressed straightaway (section 3.3.3.1) and λ^5 -iodanes further on in this chapter (section 3.3.5.1).

Table 3.5. Main λ^3 - and λ^5 -iodanes classified according to their Martin-Arduengo designation²³⁴.

	8-I-2	10-I-3			
λ^3 -iodanes	 iodosylbenzene	 Cl-I-Cl dichloro-iodobenzene	 HO-I-OTs hydroxy(tosyloxy)-iodobenzene (Koser reactive)	 AcO-I-OAc diacetoxy-iodobenzene (DIB or PIDA)	 $\text{F}_3\text{COCO-I-OCOCF}_3$ bis(trifluoroacetoxy)-iodobenzene (BTI or PIFA)
λ^5 -iodanes	10-I-4				12-I-5
	 iodoxybenzoic acid (IBX)	 IBX (49%)	 isophthalic acid (29%)	 benzoic acid (22%)	 Dess-Martin periodinane (DMP)
		 stabilized iodoxybenzoic acid (SIBX)			

²³¹ Willgerodt, C. *J. Prakt. Chem.* **1886**, 33, 154-160

²³² (a) Sandin, R. B. *Chem. Rev.* **1943**, 32, 249-276 (b) Banks, D. F. *Chem. Rev.* **1966**, 66, 243-266

²³³ (a) Varvoglis, A. *Synthesis* **1984**, 709-726 (b) Moriarty, R. M.; Vaid, R. K. *Synthesis* **1990**, 431-447 (c) Varvoglis, A.; Spyroudis, S. *Synlett* **1998**, 221-232 (d) Wirth, T.; Hirt, U. H. *Synthesis* **1999**, 1271-1287 (e) Stang, P. J. *J. Org. Chem.* **2003**, 68, 2997-3008 (f) Wirth, T. *Angew. Chem. Int. Ed.* **2005**, 44, 3656-3665 (g) Moriarty, R. M. *J. Org. Chem.* **2005**, 70, 2893-2903

²³⁴ The Martin-Arduengo designation N-X-L, which expresses the number of valence electrons (N), the central atom (X) and the number of ligands (L), is a very useful nomenclature adopted for the three-dimensional structure of hypervalent iodine compounds, reported in: Perkins, C. W.; Martin, J. C.; Arduengo, A. J.; Lau, W.; Alegria, A.; Kochi, J. K. *J. Am. Chem. Soc.* **1980**, 102, 7753-7759

3.3.2. Experimental Study: λ^3 -Iodanes

3.3.2.1. General considerations

λ^3 -iodanes are of common use in organic synthesis. Among the different types of them, the ones comprising one aromatic cycle (Ar) and two monovalent heteroaromatic ligands (L) ArIL_2 , like diacetoxyiodobenzene (DIB) and bis(trifluoroacetoxy)iodobenzene (BTI), are the most suitable ones for oxidation reactions.

Molecular orbital theory describes hypervalent binding in the ArIL_2 compounds as 3 centers (3c) – 4 electrons (4e) systems. Two electrons stem from a doubly occupied $5p$ orbital of iodine and one electron from each L ligand. The 3 atoms or centers (3c) are iodine and the two atoms of the L ligands bound to it, that is to say one hypervalent bond (3c-4e) (Figure 3.35 A). As only one orbital of iodine participates in the two bonds, the three centers (L-I-L) are aligned. With regard to their geometry, these iodine derivatives present a trigonal bipyramid structure: the central iodine atom is the donor; the covalent aromatic C–I bond together with the two lone pairs of electrons of iodine are in the same plane in equatorial position; and the hypervalent bond formed between the iodine and the two L ligands, the (3c-4e) bond, is in axial position. This distribution confers on these molecules a characteristic “T” structure (Figure 3.35 B). The hypervalent bond is highly polarized, longer and weaker than a covalent bond, which justifies the high electrophilicity of these compounds.

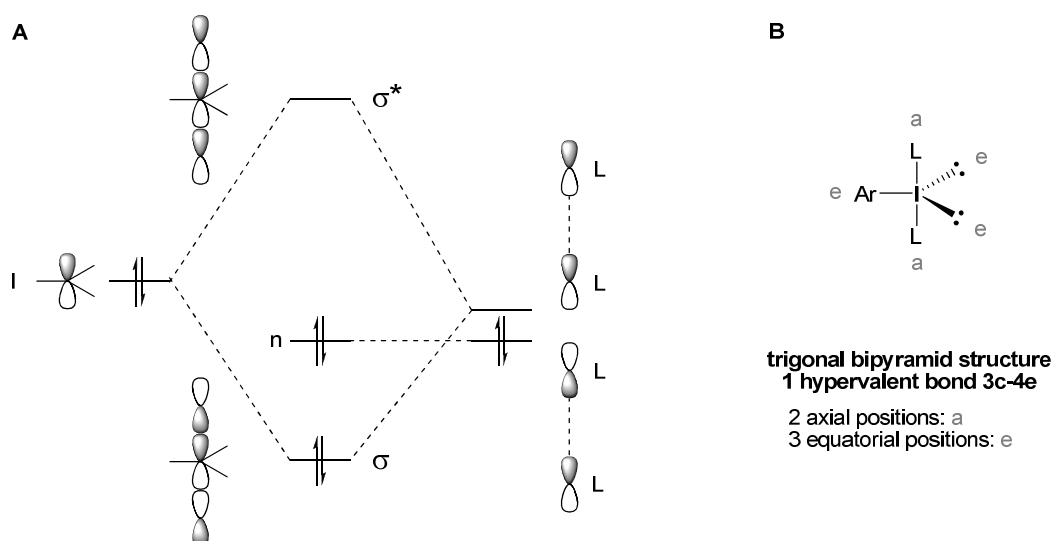
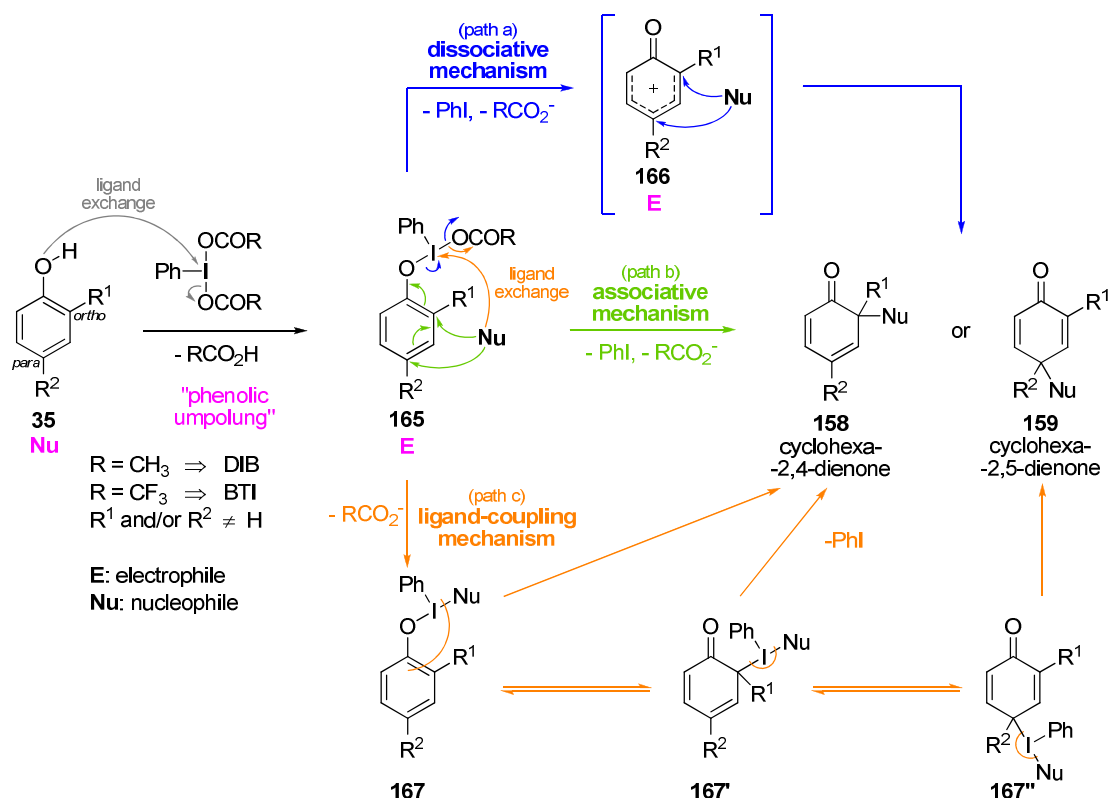


Figure 3.35. (A) Qualitative MO diagram of a hypervalent (3c-4e) binding scheme (σ^* = bonding; n = non-bonding; σ^* = antibonding). (B) Geometry of λ^3 -iodanes of type ArIL_2 .

Being iodine an electrophilic center susceptible of suffering nucleophilic attacks and being the PhI an excellent leaving group²³⁵, ligand exchange over iodine atom and ligand transfer by reductive elimination are the two principal reactivities of these reagents. The different mechanisms proposed for these λ^3 -iodanes-mediated oxidative dearomatization of phenolic compounds resulting from these properties are presented in Scheme 3.30^{214d},
219



Scheme 3.30. Proposed mechanistic paths for the oxidative dearomatization of phenols by λ^3 -iodanes of type ArI₂ (DIB and BTI)²¹⁹.

First I(III) atom plays the role of electrophilic center in a ligand exchange step in which, as a result of a nucleophilic attack, a carboxylate ligand is replaced by the phenol. Once the phenoxy group is bound to the I(III) center, the development of the reaction is essentially determined by the nucleofugality of the λ^3 -phenyliodanyl group. Indeed, this is the driving force of the reaction: the reduction of two electrons of the I(III) center and the elimination of the I(I) compound, i.e. iodobenzene (PhI). Three alternative pathways are proposed for the development of the reaction after the starting ligand exchange.

²³⁵ Okuyama, T.; Takino, T.; Sueda, T.; Ochiai, M. *J. Am. Chem. Soc.* **1995**, *117*, 3360-3367

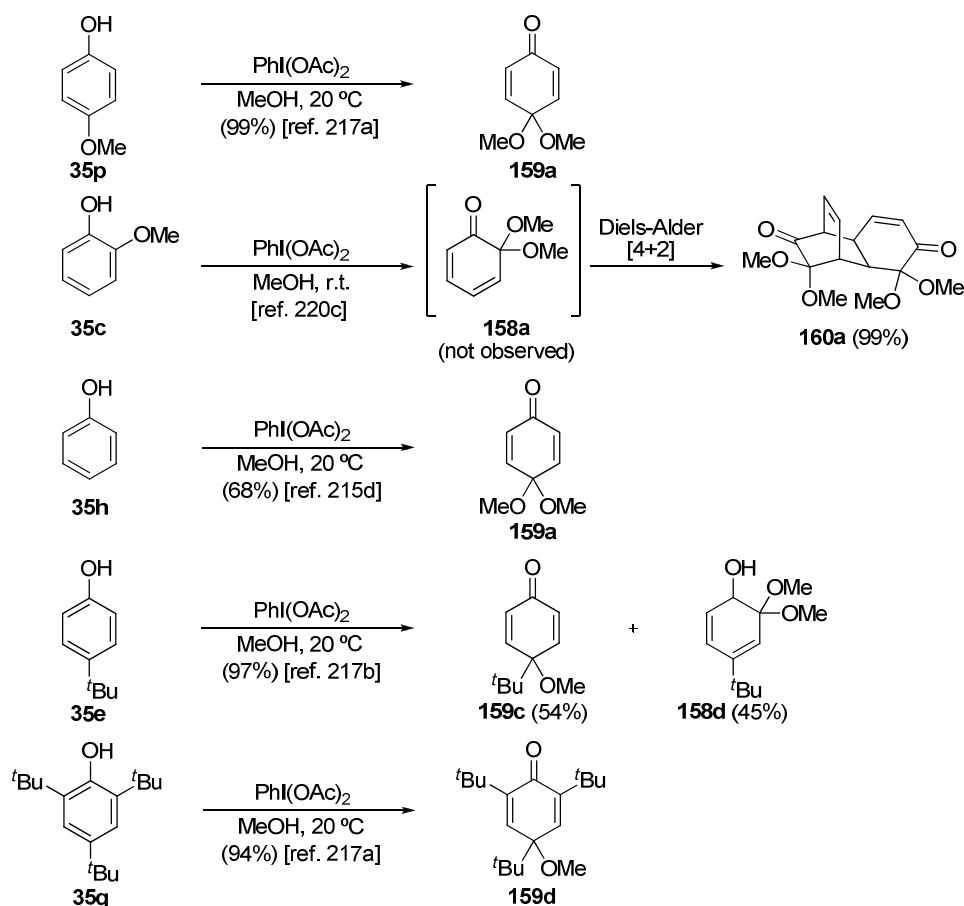
The first one, which goes through a phenoxenium intermediate (**166**), is known as dissociative mechanism (Scheme 3.30, path a) and is supported by the great nucleofugality of the λ^3 -phenyliodane just mentioned. Although it is not strictly necessary, the employment of coordinative polar solvents, such as alcohols, contributes to the stabilization of these cationic intermediates.

An alternative option consists of the bimolecular associative mechanism (Scheme 3.30, path b) in which the withdrawal of the λ^3 -phenyliodanyl group and the entry of the nucleophile takes place in a concerted manner (**165**), no needing the intervention of the phenoxenium cation as intermediate.

Another possibility (Scheme 3.30, path c) assumes that the initially formed λ^3 -phenyliodane species undergoes a second ligand exchange with other nucleophile (**167**, **167'**, **167''**), leading to a reductive elimination of iodobenzene (PhI), with simultaneous formation of a bond between the other two ligands (i.e. phenoxy unity and the new nucleophilic ligand), analogously to the coupling mechanism by transition metals.

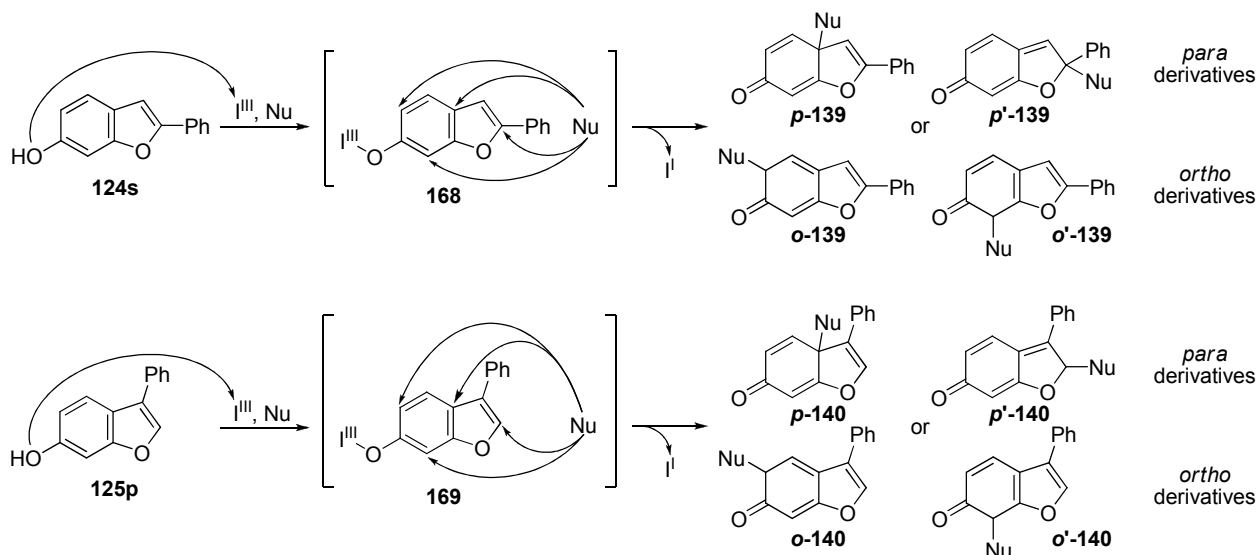
These mechanistic explanations are still subject to debate in literature. As in many chemical reactions, the mechanistic path and the success of a particular reaction will depend on the reaction conditions, understood not only as the type of solvent used but also as the nature of the ligands of the selected iodane and the regiochemical and stereoelectronic nature of the substitution pattern of the starting phenolic compound.

In this line, as already mentioned, there is evidence in literature that when methanol is used as nucleophile, the presence of an electron-releasing group (like methoxy group) favors the nucleophilic attack over the already substituted carbon atom, making it possible to control the formation of cyclohexa-2,4-dienones (*ortho* orientation) or cyclohexa-2,5-dienones (*para* orientation). In the absence of any directing group, the nucleophilic attack takes place preferentially in *para* position, although a big enough steric hindrance can also play a role in some cases^{213, 214a,d-e, 215b-d,f-e, 216, 217a-b} (Scheme 3.31).



Scheme 3.31. Examples of λ^3 -iodane DIB-mediated oxidative dearomatization of phenols.

Taking into account the results obtained for the differently substituted phenols, we wondered what we could expect if 2- or 3-phenylbenzofuran-6-ols (**124s** or **125p**) were used as starting materials. Considering the oxidation reaction using λ^3 -iodanes [I(III)] in the presence of an appropriate nucleophile, the formation of four possible cyclohexadienone-type compounds could be envisaged, two *para* and two *ortho* derivatives, which could in turn undergo further transformations (Scheme 3.32).



Scheme 3.32. λ^3 -iodane-mediated dearomatization of 2- and 3-phenylbenzofuran-6-ols **124s** and **125p** preview.

3.3.2.2. Preparation of the starting 2- and 3- phenylbenzofuran-6-ols **124a** and **125p**

First, the choice of the starting monohydroxylated benzo[*b*]furans was tackled. As a starting point, and in order to simplify as much as possible the reaction to be studied, we considered that the compound should bear a single hydroxy group, that it should be located in its benzofuran part and that no other substituent should be present in the molecule. With these requirements in mind and recalling that resorcinol **35j** had already given access to 2-arylbenzofuran-6-ols (compounds **124d-e** in chapter 2, table 2.12, entries 4 and 5), we selected 2- and 3-phenylbenzofuran-6-ols (**124s** and **125p**, respectively) as starting compounds (Figure 3.36).

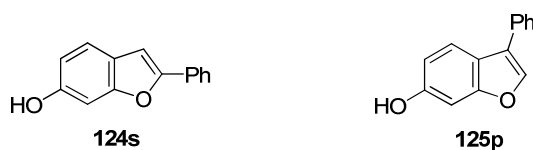
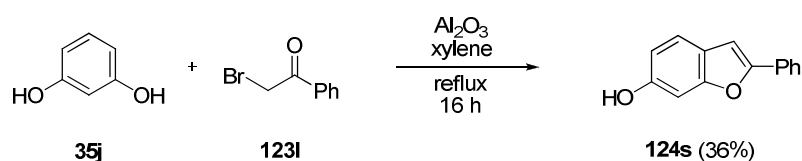


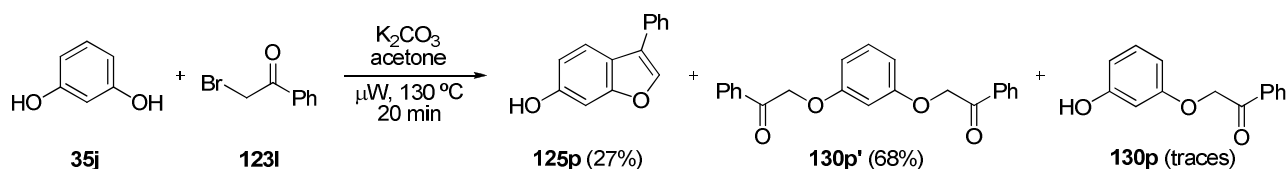
Figure 3.36. Structures of 2- and 3-phenylbenzofuran-6-ols (**124s** and **125p**, respectively).

Reaction between resorcinol **35j** and 2-bromoacetophenone **123i**, in the presence of alumina and in refluxing xylene (under optimized conditions, see section 2.2.2 and 2.2.3) yielded the desired benzofuran **124s** in a 36% yield (Scheme 3.33). As happened when carrying out the reaction with resorcinol **35j** and 2-bromoacetophenones **123a,b**, no product associated neither with the furan ring fused at the *ortho* position in between the two hydroxy groups nor with the double condensation was detected in the crude reaction mixture.



Scheme 3.33. Preparation of 2-phenylbenzofuran-6-ol **124s** from resorcinol **35j** and 2-bromoacetophenone **123I**.

When the same starting materials **35j** and **123I** in the presence of potassium carbonate and using acetone as solvent were subjected to microwave irradiation (under optimized conditions, see section 2.2.3) the reaction furnished a mixture of three major compounds. On the one hand, the targeted benzofuran **125p** in a 27% yield, although in a single step and not needing the alumina to promote the cyclization. On the other hand, the product of the double Williamson etherification **130p'** in a 68% yield (with respect to starting 2-bromoacetophenone **123I**, the limiting reactant in this case) along with unreacted starting resorcinol **35j** (the reactant in excess), and traces of the single Williamson etherification product **130p** (Scheme 3.34). Again, no product associated either with the furan ring fused at the *ortho* position in between the two hydroxy groups or with the double cyclization was detected in the crude reaction mixture.



Scheme 3.34. Preparation of 3-phenylbenzofuran-6-ol **125p** from resorcinol **35j** and 2-bromoacetophenone **123I**.

Taking into account that the reaction was set on a 1:1 equivalent proportion of **35j**:**123I** and that the formation of **130p'** requires 2 equivalents of **123I** per equivalent of **35j**, the result means an almost complete conversion for the reaction transforming **35j** and **123I** into either **125p** or **130p'**, together with the subsequent excess of **35j**. Although with low yield, this reaction afforded the desired product **125p** in a single preparative step and in an easy-to-purify manner. Therefore, this time the synthetic procedure was not optimized.

3.3.2.3. Reaction of 2- and 3-phenylbenzofuran-6-ols **124s** and **125p** with λ^3 -iodanes

As mentioned before (section 3.3.2.1), the most convenient and widely used λ^3 -iodanes in organic synthesis with oxidative purposes are diacetoxyiodobenzene (DIB) and bis(trifluoroacetoxy)iodobenzene (BTI). Therefore, these reactants will be the only ones considered in this study.

At this point it is also worth remembering that one of the hallmarks of the oxidative dearomatization reaction of phenols, and by extension of hydroxylated benzofurans, is that the oxidation step is followed by a nucleophilic attack. This being the case, for the first assays and the optimization of the reaction conditions we chose methanol, which can play both the role of nucleophile and solvent.

2-phenylbenzofuran-6-ol (**124s**) as starting material

Methanol

Using the two substituted benzofuran **124s** as starting material and methanol as nucleophile and solvent, the optimization of the reaction conditions for the oxidative dearomatization was carried out attending different parameters: solvent and the λ^3 -iodane used (DIB/BTI), the order of addition and proportion of the reactants, the temperature and time of reaction, and the workup conditions. Besides, all the experiments were conducted under inert argon atmosphere. The greater convenience of some reaction conditions over others was determined evaluating the results obtained by $^1\text{H-NMR}$. The first experiments were performed at small scale (0.143 mmol of benzofuran) and were not further purified.

Firstly the λ^3 -iodane reagent was pondered. The reaction was carried out by dropwise adding a solution of 1.1 equivalent (to ensure that the benzofuran is the limiting reactant) of the corresponding λ^3 -iodane reagent in methanol to a solution of benzofuran **124s** also in methanol at 0 °C. The mixture was left stirring until TLC revealed the complete consumption of starting benzofuran (0.5 h for DIB and 1.2 h for BTI). Then the reaction was quenched with saturated NaHCO_3 aqueous solution, extracted with EtOAc, washed with brine, dried over Na_2SO_4 , filtered, and evaporated to furnish the crude reaction mixture to be analysed. BTI was then discarded, since both reagents provided almost the

same result and the DIB is cheaper. In addition, this latter reagent yielded a reaction mixture that presented a cleaner (with less byproducts) $^1\text{H-NMR}$ spectrum.

Interestingly, the reaction yielded a mixture of two products (apparently a major and a minor isomer), bearing each of them, to our surprise, two methoxy groups in its structure according to their $^1\text{H-NMR}$ spectra. After isolation of both compounds it was also noticed the presence of one hydroxy group in the structure of both of them (Figure 3.37). The hydroxy group was assumed to be the original one in position 6 (which in principle could be recovered following prototropic events), but the assignment of the position of the new methoxy substituents was not straightforward. However, after a thorough NMR study (including ^1H , ^{13}C , DEPT-135, COSY and HSQC experiments) and registration of the IR spectrum of the major product, we reached the conclusion that the compounds corresponded to the *cis* and *trans* isomers of 2,3-dimethoxy-2-phenyl-2,3-dihydrobenzofuran-6-ol, ***cis*-170a** and ***trans*-170a** (Scheme 3.35). This structural elucidation was confirmed by X-ray diffraction analysis of both major (*cis*) and minor (*trans*) products (for more detail see section 3.3.2.4).

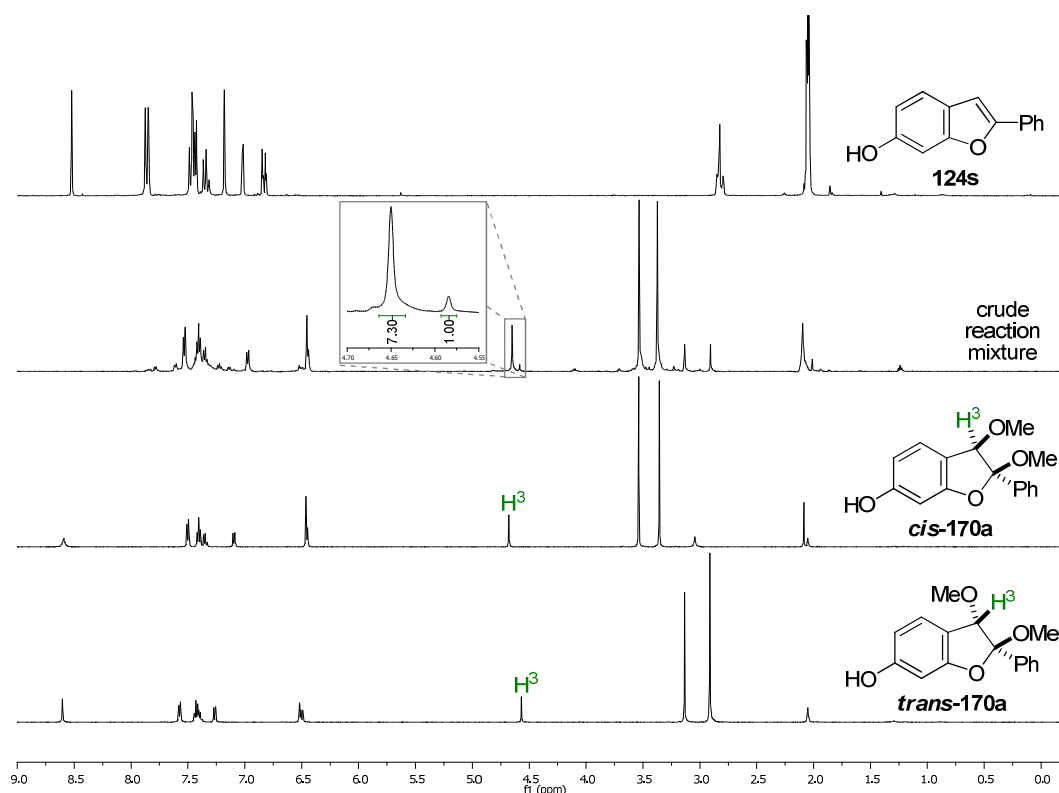
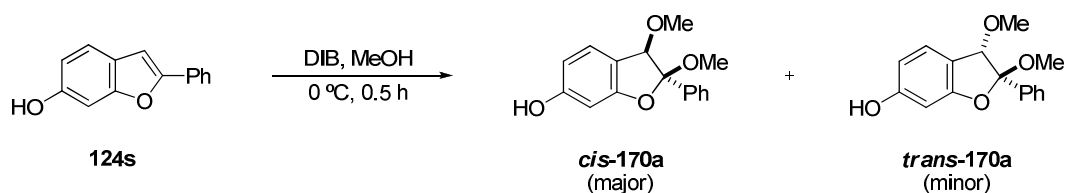


Figure 3.37. $^1\text{H-NMR}$ (500 MHz, acetone- d_6) spectra of, arranged from top to bottom, the starting 2-phenylbenzofuran-6-ol **124s**, the crude reaction mixture, the isolated major product ***cis*-170a** and the isolated minor product ***trans*-170a**.



Scheme 3.35. First attempt of the oxidative dearomatization reaction of 2-phenylbenzofuran-6-ol **124s** with DIB in the presence of methanol.

The order of addition of the reactants was next considered. For so doing, the solution of benzofuran **124s** in methanol was dropwise added to the solution of 1.1 equivalent of DIB in methanol at 0 °C. It was observed that the crude reaction was the same regardless of which solution was dropwise added over which. Then, it was decided to keep the initial addition order to avoid, to the full extent, any possible loss of benzofuran upon handling.

Given the mixture of products obtained, and seeking a higher selectivity, temperature and time of reaction were also taken into account. The reaction was repeated and monitored by TLC at -78, -40 and -10 °C, stirring it for longer time (up to 16 h). It was observed that at -78 °C the reaction did not proceed, at -40 °C the reaction was very slow and most of the starting material remained unreacted and the results at -10 °C did not improve those at 0 °C. So the reaction was kept at 0 °C.

Then the workup was assessed and a non-aqueous workup already reported in literature for this kind of reactions was tried^{214f}. It consisted of the addition of dry NaHCO₃ powder to the reaction mixture to quench it and to left it stirring for 15 minutes before filtering and evaporating it. Once more, the results were almost identical to those obtained with the previous workup and, therefore, this latter procedure was adopted because of its greater simplicity.

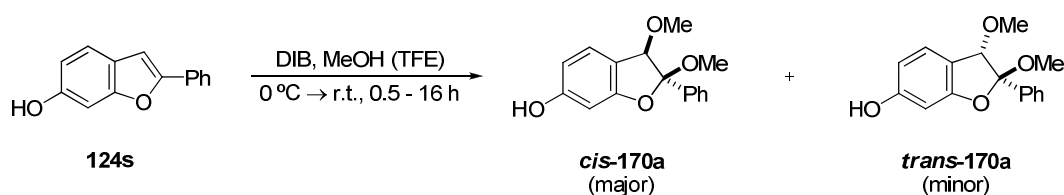
Lastly, we drew our attention to the proportion of benzofuran, DIB and MeOH. In order to vary the equivalents of methanol keeping the reaction in a solution of approximately the same concentration, the introduction of another solvent was necessary. At this stage, 2,2,2-trifluoroethanol (TFE) was chosen, since it is a polar solvent of little nucleophilic character which had already proven useful with phenols in these transformations^{236,214f}.

The reaction was then assayed using 1.1, 12.5, 25, 50 and 100 equivalents of methanol, besides the 700 corresponding to our initial assays using methanol as the only solvent

²³⁶ Kita, Y.; Tohma, H.; Kikuchi, K.; Inagaki, M.; Yakura, T. *J. Org. Chem.* **1991**, *56*, 435-438

(Table 3.6, entries 1-7), and using 100 equivalents of methanol but doubling the equivalents of DIB (2.2 equivalents per equivalent of benzofuran) (Table 3.6, entry 8). Finally, the reaction was also tried using TFE only to prepare the DIB solution, which was dropwise added to the benzofuran solution, meaning a proportion of approximately 520 equivalents of MeOH per equivalent of benzofuran for this case (Table 3.6, entry 9).

Table 3.6. Optimization of the reaction conditions for the preparation of 2,3-dimethoxy-2-phenyl-2,3-dihydrobenzofuran-6-ols **cis-170a** and **trans-170a** from oxidative dearomatization of 2-phenylbenzofuran-6-ol **124s** with DIB in the presence of methanol.



entry	eq of DIB	eq of MeOH	solvent	conversion (%) ^a	product ^a	yield (%) ^b
1	1.1	700	-	99	170a cis:trans 7:1	43
2	1.1	1.1	TFE	0	starting material	-
3	1.1	12.5	TFE	0	starting material	-
4	1.1	25	TFE	61	starting material + 170a cis:trans 15:1	n.d.
5	1.1	50	TFE	99	170a cis:trans 14:1	n.d.
6	1.1	75	TFE	99	170a cis:trans 13:1	n.d.
7	1.1	100	TFE	99	170a cis:trans 11:1	30
8	2.2	100	TFE	-	- (degradation)	-
7	1.1	520	TFE	99	170a cis:trans 7:1	30

^a Estimated from the ¹H-NMR spectrum of the crude reaction mixture.

^b Yield of isolated combined pure products after column chromatography.

n.d. = not determined

The results of these experiments are summarized in table 3.6, where it can be observed that at least 50 equivalents of methanol are necessary for the complete conversion of the starting benzofuran. Interestingly, when a large excess of nucleophile is used, the *cis/trans* selectivity of the reaction decreases. Finally, we observed that the increase of the equivalents of DIB resulted in the degradation of the products in the reaction mixture. Both conversion and proportion of isomers were determined by analysis of the ¹H-NMR spectra of the crude reaction mixtures. In all these experiments the addition of the DIB solution was carried out at 0 °C and then the mixture was allowed to reach room temperature and stirred overnight.

Only reactions showing complete conversion (except for the ones adding 50 and 75 equivalents of methanol) were scaled up and purified by column chromatography. The yields, which decreased with the introduction of the TFE as cosolvent, were moderate and lower than expected considering the weight and $^1\text{H-NMR}$ spectra of the crude reaction mixtures, suggesting that the products could decompose during purification (Figure 3.37). Despite this possibility, no alternative purification was searched, although the precaution of having the product both in column and in solution the shortest necessary period of time was taken. The best result obtained this way was the 43% yield of combined *cis* and *trans* isomers (in 7:1 ratio) of the reaction using only methanol as both nucleophile and solvent (table 3.6, entry 1).

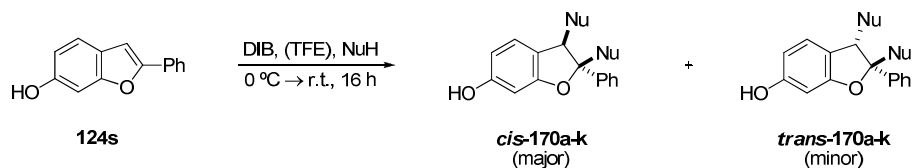
Other nucleophiles

The next step was to try to introduce other nucleophiles besides methanol. The first attempt in this line was to perform the reaction in the absence of an external nucleophile which would compete with the carboxylate ligand released from the λ^3 -iodane during the initial ligand exchange event, provided this ligand bears the appropriate reactivity. This could be, for example, the case of the acetate when using DIB in TFE or in dichloromethane (CH_2Cl_2)²³⁷. Unfortunately the trials with these combinations met with no success. In the case of the TFE, unchanged starting material was recovered. In the case of the dichloromethane, in turn, the reaction led to a mixture of products (in which the desired product was not even identified) that degraded in chromatographic column.

Then a series of alcohols was assayed. This included EtOH, $^n\text{PrOH}$, $^n\text{BuOH}$, $^i\text{PrOH}$, $^t\text{BuOH}$ and PhOH (Table 3.7).

²³⁷ Quideau, S.; Pouységu, L.; Looney, M. A. *J. Org. Chem.* **1998**, 63, 9597-9600

Table 3.7. Preparation of 2,3-disubstituted-2-phenyl-2,3-dihydrobenzofuran-6-ols **cis-170a-k** and **trans-170a-k** from oxidative dearomatization of 2-phenylbenzofuran-6-ol **124s** with DIB in the presence of various nucleophiles.



entry	nucleophile (NuH)	Nu	solvent	product	yield (%) ^a	<i>cis:trans</i> ^b
1	MeOH	OMe	-	170a	43	7:1
2	MeOH	OMe	TFE ^c	170a	30	7:1
3	EtOH	OEt	-	170b	42	4:1
4	EtOH	OEt	TFE ^c	170b	23	4:1
5	ⁿ PrOH	O ⁿ Pr	TFE ^c	170c	38	4:1
6	ⁿ BuOH	O ⁿ Bu	TFE ^c	170d	24	4:1
7	ⁱ PrOH	O ⁱ Pr	- / TFE ^c	170e	-	-
8	^t BuOH	O ^t Bu	- / TFE ^c	170f	-	-
9	PhOH (50 eq)	OPh	TFE	170g	-	-
10	HOEtOH	OEtO ^d	-	170h	-	-
11	EtSH (50 eq)	SEt	TFE	170i	-	-
12	PhSH (50 eq)	SPh	TFE	170j	-	-
13	Et ₂ NH (50 eq)	NEt ₂	TFE	170k	-	-

^a Yield of isolated combined pure products after column chromatography.

^b Estimated from the ¹H-NMR spectrum of the crude reaction mixture.

^c Reaction in which TFE was used only as solvent to prepare the solution of DIB.

^d Double nucleophile for an intramolecular second attack

Starting with the linear alcohols (EtOH, ⁿPrOH, ⁿBuOH), the reaction furnished crude mixtures analogous to the one obtained for methanol, but in which the two isomers were indistinguishable from each other by TLC and, therefore, much more difficult to separate into the corresponding *cis* and *trans* products. In these cases we resorted to semipreparative HPLC to try to isolate the compounds. The purification technique was successful with the products derived from EtOH but failed to separate the ones derived from ⁿPrOH and ⁿBuOH, which were left as a mixture and were characterized as an inseparable mixture of *cis* and *trans* isomers. It was observed that DIB is not completely soluble in propanol and butanol. Therefore, in these cases the DIB solution was only prepared in TFE, despite the fact it had resulted in lower yields with MeOH and EtOH (Table 3.7, entries 1-6).

In regard to the branched alcohols ⁱPrOH and ^tBuOH, the reaction proceeded neither using them as nucleophile and solvent nor adding DIB in TFE solution, not even leaving them stir for longer hours or increasing the reaction temperature up to refluxing the reaction mixtures. These results were thought to be a consequence of the steric hindrance between these bulky alcohols and the phenyl group in position 2 of the benzofuran (Table 3.7, entries 7-8). In the same vein, phenol (PhOH) did not work either (Table 3.7, entry 9). Given the outcome of the reactions with linear alcohols, i.e. the double entry of the nucleophiles, diols were envisaged as possible “bidentate” nucleophiles and ethylene glycol (HOEtOH) was tried. Unfortunately, the reaction did not proceed and starting materials were recovered unchanged after workup (Table 3.7, entry 10).

Then our attention was drawn to non-oxygenated nucleophiles like thiols and amines. Being softer nucleophiles, we thought that thiols might stop the reaction in the benzofuran-6-one derivative, or at least avoid the entry of the second nucleophile to some extent. However, under the optimized reaction conditions of carrying out the experiments in TFE with the minimal nucleophile for complete conversion (50 eq), neither EtSH nor PhSH were able to transform the initial benzofuran (Table 3.7, entries 11-12). To complete the nucleophile screening Et₂NH was assayed, both using it as nucleophile and solvent and in a 50 eq proportion in TFE. None of these trials resulted successful (Table 3.7, entry 13).

3-phenylbenzofuran-6-ol (**125p**) as starting material

Methanol

The reaction conditions just optimized (methanol as nucleophile and solvent, dropwise addition of the 1.1 eq DIB solution, 0 °C → r.t., overnight stirring and non-aqueous workup) were applied to the 3-substituted benzofuran **125p**. This time, the reaction yielded a product which, according to the analysis of the ¹H-NMR spectrum of the crude reaction mixture, seemed to correspond with the rearomatized 2-methoxy benzofuran derivative **171a** (Figure 3.38 and Scheme 3.36).

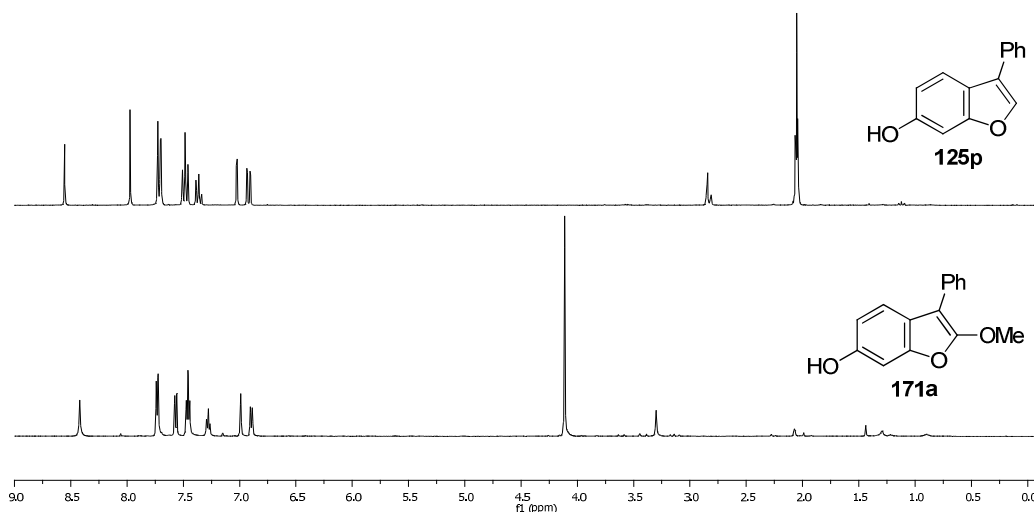
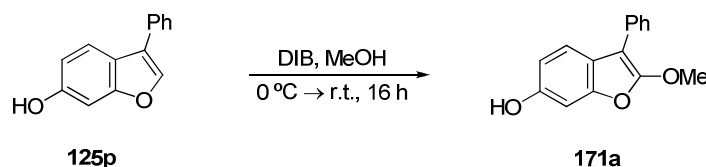


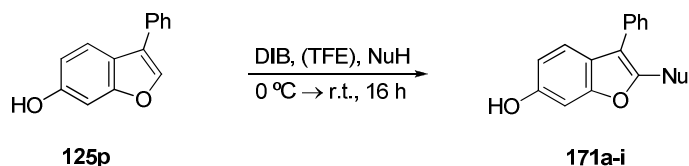
Figure 3.38. $^1\text{H-NMR}$ (500 MHz, acetone- d_6) spectra of the starting 3-phenylbenzofuran-6-ol **125p** (above) and the isolated product **171a** (below).



Scheme 3.36. Oxidative dearomatization reaction of 3-phenylbenzofuran-6-ol **125p** with DIB in the presence of methanol.

Other nucleophiles

Again, our next step was to try to introduce other nucleophiles besides methanol. The previously chosen series of alcohols (EtOH, n PrOH, n BuOH, i PrOH, t BuOH, and PhOH), as well as a thiol (EtSH) and an amine (Et $_2$ NH) were assayed (Table 3.8). As it had been observed in previous assays, out of all the liquid nucleophiles tried, DIB is completely soluble only in methanol and ethanol, providing better yields when the reaction was carried out using them as the only solvents in the reaction. Thus, DIB solution was prepared in MeOH and EtOH when these nucleophiles were to be tested and in TFE in all other cases.

Table 3.8. Preparation of 2-substituted 3-phenylbenzofuran-6-ols **171a-i** from oxidative dearomatization of 3-phenylbenzofuran-6-ol **125p** with DIB in the presence of various nucleophiles.

entry	nucleophile (NuH)	Nu	solvent	product	yield (%) ^a
1	MeOH	OMe	-	171a	61
2	EtOH	OEt	-	171b	57
3	ⁿ PrOH	O ⁿ Pr	TFE ^b	171c	37
4	ⁿ BuOH	O ⁿ Bu	TFE ^b	171d	42
5	ⁱ PrOH	O ⁱ Pr	TFE ^b	171e	52
6	^t BuOH	O ^t Bu	TFE ^b	171f	49
7	PhOH (50 eq)	OPh	TFE	171g	-
8	EtSH (50eq)	SEt	TFE	171h	-
9	Et ₂ NH	NEt ₂	TFE ^b	171i	-

^a Yield of isolated pure product after column chromatography.

^b Reaction in which TFE was used only as solvent to prepare the solution of DIB.

Starting with the linear alcohols (EtOH, ⁿPrOH, ⁿBuOH), the reaction furnished crude mixtures similar to the one obtained for methanol, with slightly better yields than those obtained with the 2-phenyl benzofuran isomer (Table 3.8, entries 2-4).

Following with the branched alcohols (ⁱPrOH, ^tBuOH), the reaction proceeded this time, furnishing the corresponding products with better yields than those of their equivalent linear isomers (Table 3.8, entries 5-6). This different reactivity from one isomer to the other was attributed to the lower steric hindrance of the position 2, the one to be first substituted, of the starting benzofuran. Unfortunately, in this case phenol (PhOH) also failed to transform the benzofuran into the expected corresponding **171g** product (Table 3.8, entry 7).

Finally non-oxygenated nucleophiles thiol EtSH and amine Et₂NH were tried, recovering in both cases the unchanged starting material (Table 3.8, entries 8-9).

3.3.2.4. Structural elucidation and characterization

In this study only the lead compound of both series, the ones resulting from the reaction using methanol as solvent, are analysed: compounds **cis-170a** and **trans-170a** of the experiments using 2-phenylbenzofuran-6-ol **124s** as starting material and compound **171a** of the experiments using 3-phenylbenzofuran-6-ol **125p** as starting material.

Compounds **cis-170a** and **trans-170a**

Although the structure of the products of the oxidative dearomatization reaction of the 2-phenylbenzofuran-6-ol **124s** had already been revealed, their determination was not so straightforward.

The $^1\text{H-NMR}$ spectrum of the crude reaction mixture showed the presence of two products, apparently isomers with signals slightly shifted, which bore one hydroxy and two methoxy groups each, substituents that did not fit with our initial proposal for the outcome of the reaction (Scheme 3.32). As aforementioned, these two compounds were separated (Figure 3.37) and the major one was analysed more in depth.

Our new structure proposal (Figure 3.39) implied a *cis/trans* isomerism describing the two possible orientations of the two methoxy groups in positions 2 and 3 of the benzofuran relative to the average plane of the ring. According to this notation, the diastereomer where the vicinal methoxy groups are closer to each other is referred as *cis* (**cis-170a**) and the one where they are oriented in opposing sides as *trans* (**trans-170a**).

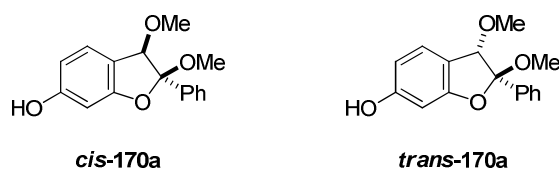


Figure 3.39. Structure of the diastereomeric products **cis-170a** and **trans-170a**.

The absolute configuration of these compounds was not even considered since both are expected to be racemic mixtures of the two possible *cis* and the two possible *trans* products respectively, as no chirality induction has been introduced in the reactions.

Anyway, the fact that compound **170a** presented two diastereomeric forms perfectly matched with the mixture of products obtained in all of our oxidative dearomatization reactions, meaning that the outcome of the reaction led to formation of the two possible diastereomers.

First the $^1\text{H-NMR}$ and $^{13}\text{C-NMR}$ spectra of **cis-170a** were registered, together with DEPT-135²³⁸ spectrum (Figure 3.40). From these three spectra the following information can be extracted: the molecule has 16 H and 16 C (provided H^8 and H^9 from the phenyl group in position 2 are equivalent); two $-\text{OMe}$ and one $-\text{OH}$ substituents; and neither carbonyl ($\text{C}=\text{O}$) nor methylene (CH_2) carbons in its structure (the absence of the carbonyl group was also confirmed by IR spectroscopy, Figure 3.41). Besides, the hydroxy group was assumed to be the original one in position 6 and the chemical shifts of the proton signal assigned to H^3 suggested the loss of aromaticity of the furan ring.

²³⁸ DEPT-135 is the acronym for Distortionless Enhancement by Polarization Transfer with a flip angle of 135° . It is a ^{13}C NMR experiment that allows to determine multiplicity of carbon atoms substituted with hydrogens, showing signals from CH_2 in a phase opposite to those from CH and CH_3 ones. Signals from carbons with no attached protons are always absent.

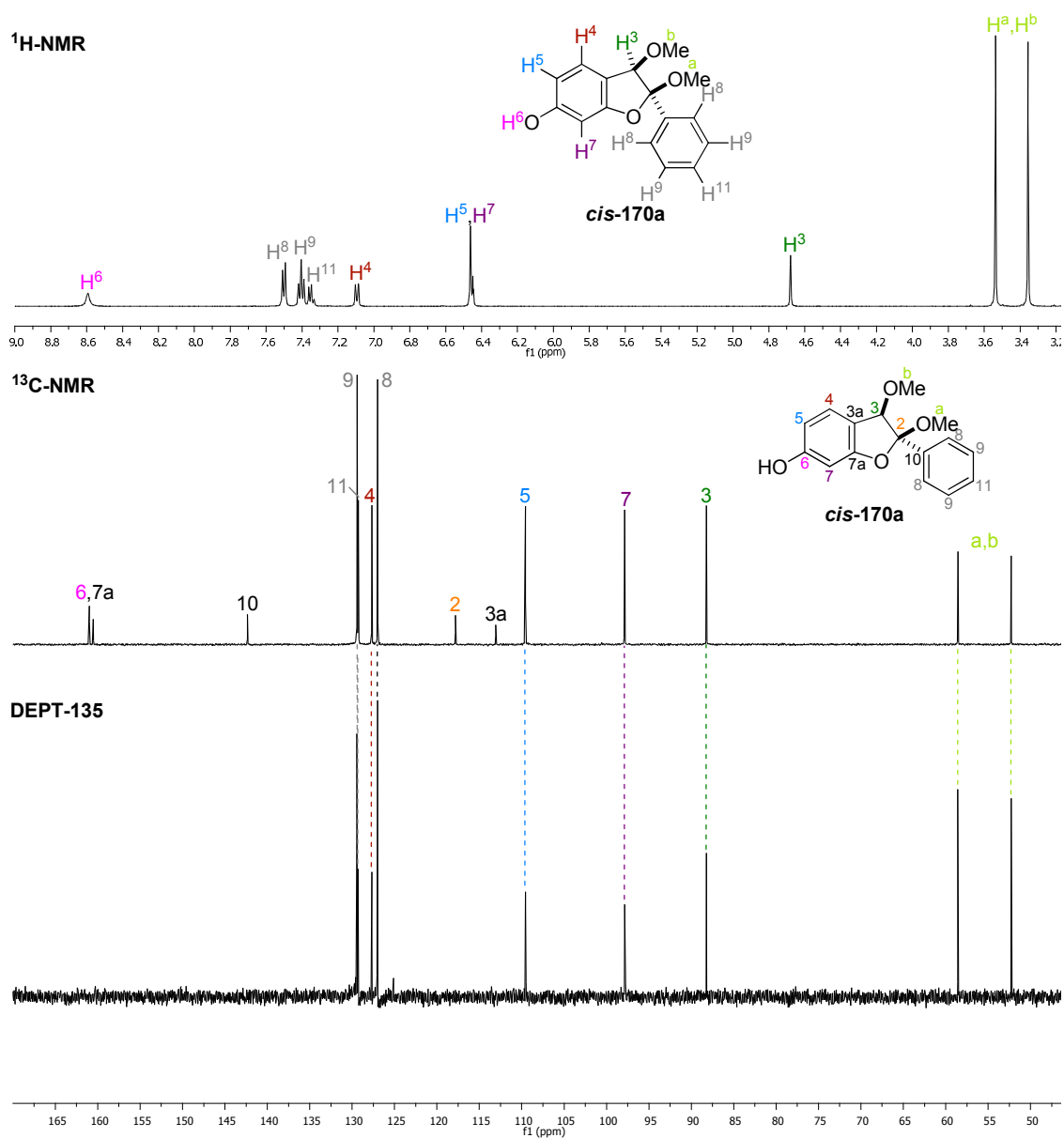


Figure 3.40. ¹H-NMR (500 MHz, acetone-d₆) (above), ¹³C-NMR (500 MHz, acetone-d₆) (middle) and DEPT-135 (300 MHz, acetone-d₆) (below) spectra of *cis*-170a.

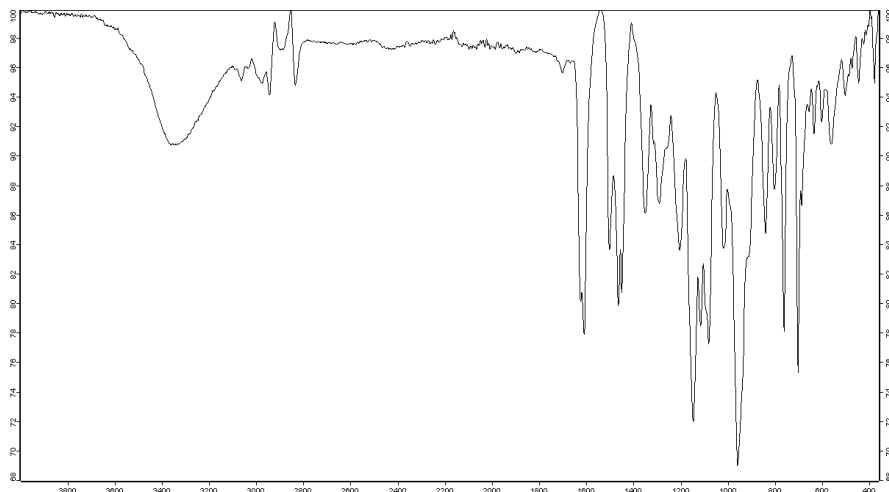


Figure 3.41. IR spectrum of *cis*-170a.

Then we turned to 2D-NMR spectroscopy and COSY and HSQC experiments¹⁷⁸ of *cis*-**170a** were registered (Figure 3.42). The COSY spectrum showed two groups of strongly coupled signals: on the one hand the ones corresponding to the phenyl protons H⁸, H⁹ and H¹¹ (at 7.37-7.52 ppm) and, on the other hand, the signals assigned to H⁴ and H⁵ (at 7.12 and 6.47 ppm, respectively) (*ortho* coupling in aromatic compounds). From this last correlation it can be inferred that neither position 4 nor 5 of the benzofuran bear any substituent (methoxy or hydroxy). The HSQC spectrum, in turn, allowed us to confirm the assignment of the carbon signals, showing which ones do bear protons and which ones do not.

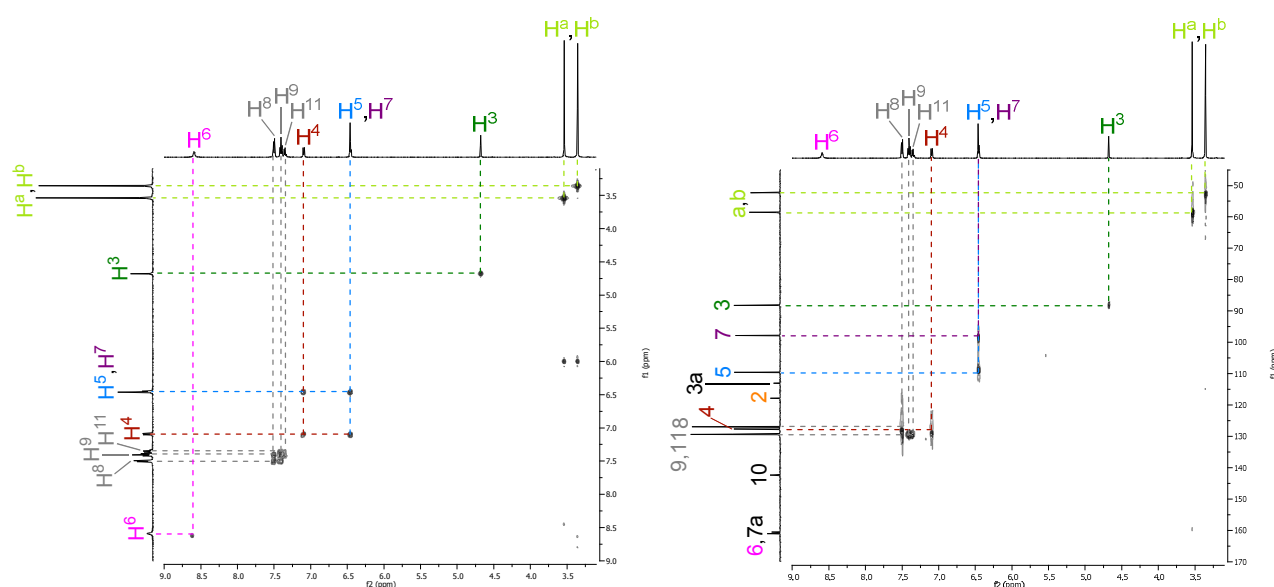


Figure 3.42. COSY (500 MHz, acetone-*d*₆) (left) and HSQC (500 MHz, acetone-*d*₆) (right) spectra of *cis*-**170a**.

Then, the time had come to consider which diastereomer could be expected to be the major one and why. At this point the reaction mechanism (which will be assessed in section 3.3.2.6, Scheme 3.38) was taken into account, more precisely the stage in which the second methoxy group is introduced, i.e. the one in position 3. According to our proposal, the reaction is likely to proceed through intermediate **173**, in which the entry of the second methanol moiety can in principle occur from both sides of the plane defined by the 6-hydroxy-2,3-dihydrobenzofuran-3-ylum ring/bicycle. The bulkiness of the phenyl group in position 2 and/or a possible formation of a hydrogen bond between the entering methanol and the methoxy group already present in position 2 should favor the entry of the second methanol moiety from the same side as the methoxy substituent in position 2 (Figure 3.43). This way, both steric (–Ph > –OMe) and electronic (possible MeOH ⋯ O –

OMe hydrogen bond) requirements just described would lead to the preferential formation of **cis-170a** over **trans-170a**.

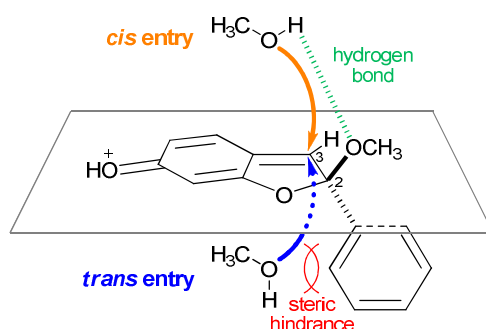


Figure 3.43. Representation of the possible steric (steric hindrance, red) and electronic (hydrogen bond, green) factors governing the *cis* (orange) and *trans* (blue) entries of the second methanol moiety in intermediate **173**.

Finally, in order to secure the stereoisomerism of these compounds, the structure of both major and minor products was unambiguously determined by X-ray diffraction analysis. By this means, **cis-170a** was confirmed as the major product of the reaction, and **trans-170a** as the minor one, in agreement with our previous reasoning. The study of the crystal samples also revealed that:

- They are racemic mixtures, with the presence of both enantiomers.
- In compound **cis-170a**, the 2,3-dihydrobenzofuran-6-ol ring is almost plane (with the largest deviations from average molecular plane smaller in absolute value than 0.06 Å) (Figure 3.44).

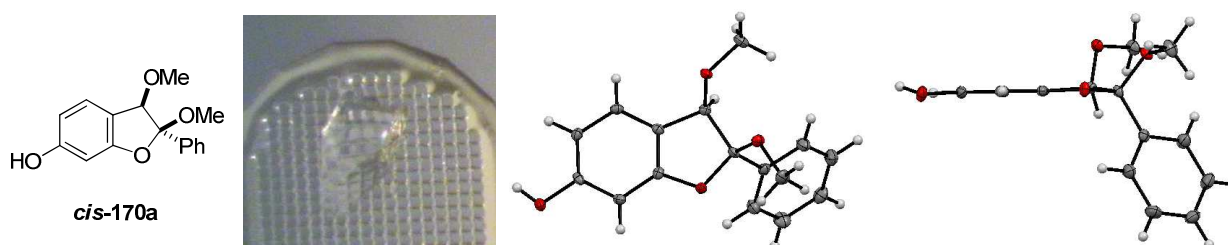


Figure 3.44. Picture of the crystal and ORTEP diagram (top and front views) of **cis-170a**.

- In compound **trans-170a**, the five-membered ring adopts an envelope geometry, in which atom C2 which is deviated a distance of 0.447 Å with respect to the average molecular plane (Figure 3.45).

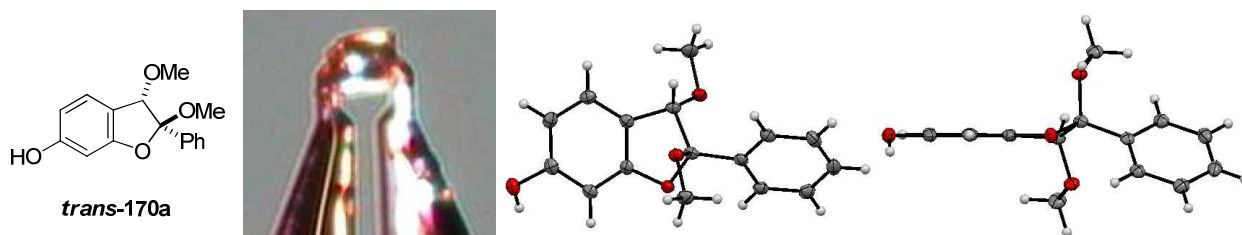


Figure 3.45. Picture of the crystal and ORTEP diagram (top and front views) of ***trans*-170a**.

- In both isomers, the only significant intermolecular interaction is a hydrogen bond between the proton of the hydroxy group in position 6 and the oxygen of the methoxy group in position 3 (the methoxy group in position 2 is slightly farther, resulting in a weaker interaction). Hydrogen bonds give rise to chains of molecules along crystallographic *y* (*b*) axis in the case of ***cis*-170a** and along crystallographic *z* (*c*) axis in the case of ***trans*-170a** (Figure 3.46).

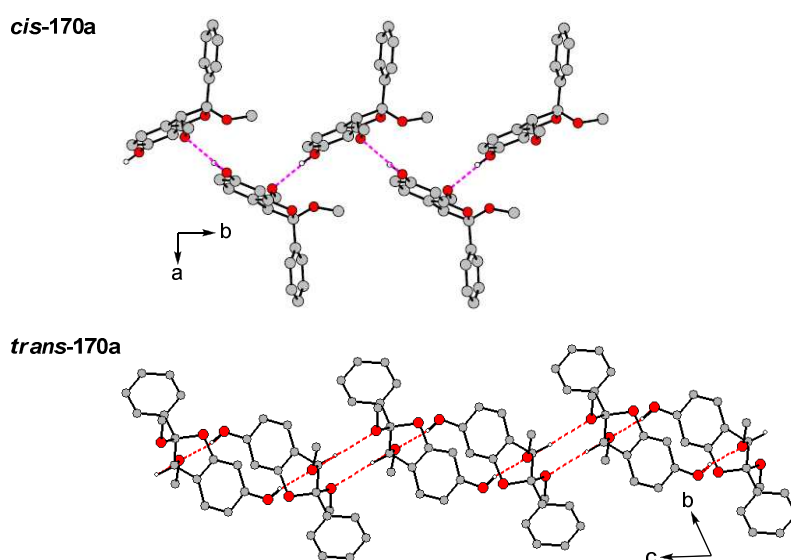


Figure 3.46. View of the hydrogen bond-formed chains present in the crystalline structure of ***cis*-170a** (above) and ***trans*-170a** (below).

Compound 171a

Taking into account all the information learnt from the structural study of the 2-substituted regioisomer, the determination of the structure of the product of the reaction using 3-phenylbenzofuran-6-ol **125p** as starting material was straightforward from the $^1\text{H-NMR}$ spectrum analysis (Figure 3.38), and in agreement with its corresponding $^{13}\text{C-NMR}$ spectrum (Figure 3.47). Nevertheless, we found it impossible to get a crystal of the product

this time, as in all our attempts compound **171a** progressively degraded when left in solution for medium-long term.

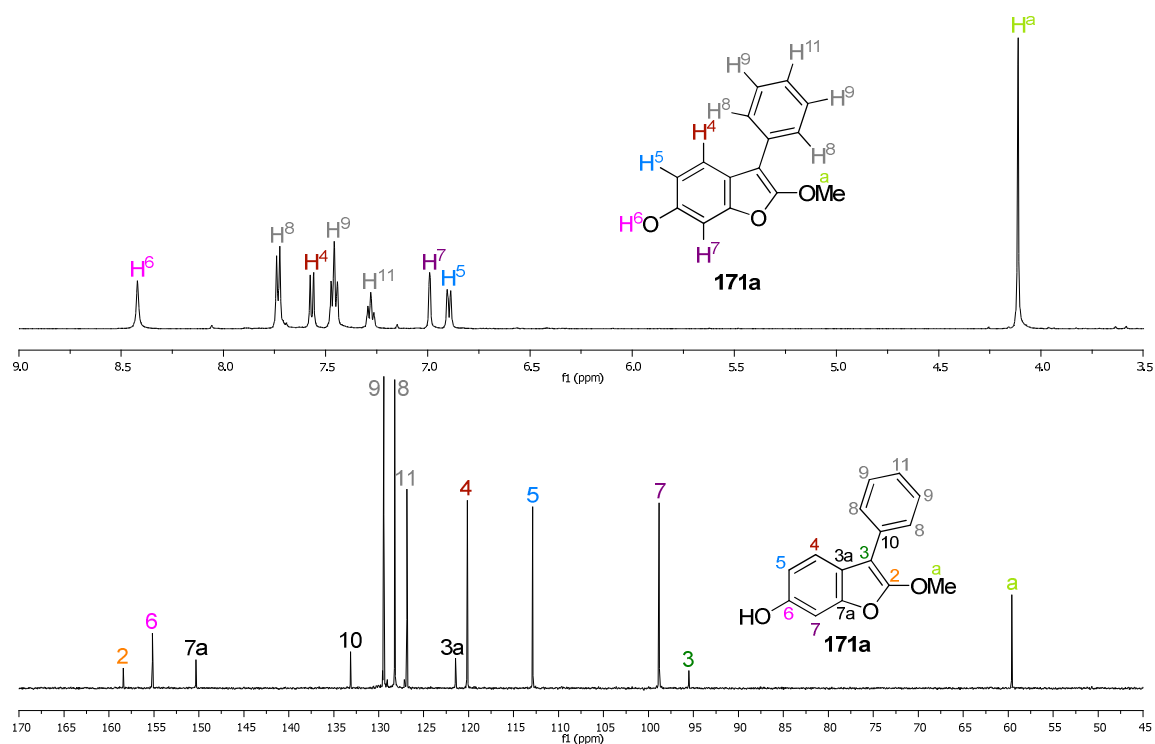
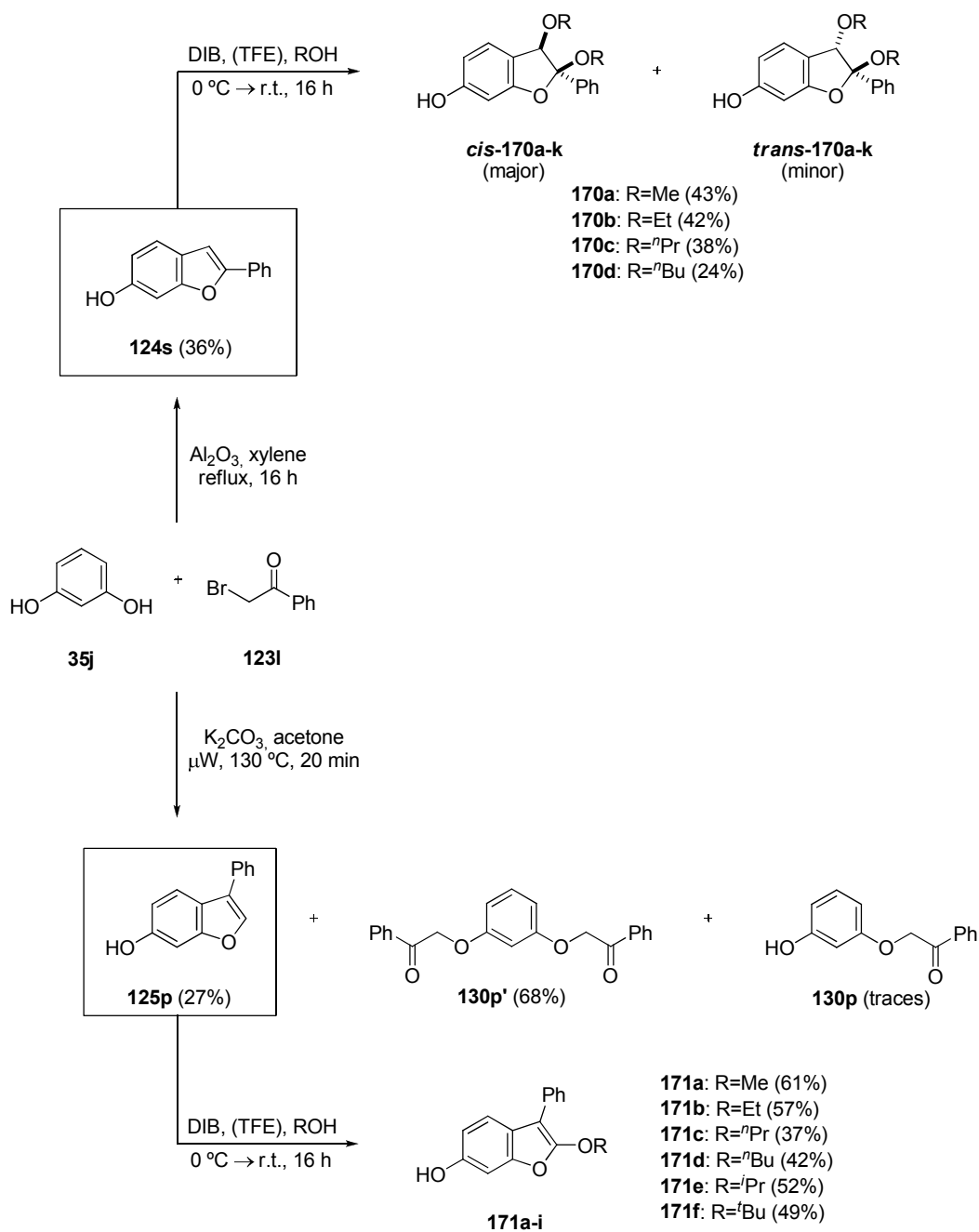


Figure 3.47. $^1\text{H-NMR}$ (500 MHz, acetone- d_6) (above) and $^{13}\text{C-NMR}$ (500 MHz, acetone- d_6) (below) spectra of **171a**.

All the NMR experiments shown in this section were registered on a spectrometer operating at 500 MHz (except for the DEPT-135 experiment which was registered on a spectrometer operating at 300 MHz) and using deuterated acetone as solvent, since the deuterated chloroform used in the initial assays proved to progressively degrade the samples.

3.3.2.5. Graphical overview



Scheme 3.37. Graphical overview of the experimental study of the oxidative dearomatization reaction of 2-phenylbenzofuran-6-ol **124s** and 3-phenylbenzofuran-6-ol **125p** using λ^3 -iodane DIB. Reaction yields are given in brackets.

3.3.2.6. Insight into the reaction mechanism

In order to get a better understanding of the reaction of the monohydroxylated benzofurans **124s** and **125p** with DIB in the presence of alcohols, the mechanism that these transformations might go through was considered and a proposal is made in this section. For this purpose, the generally accepted mechanism for the λ^3 -iodanes-mediated oxidative dearomatization of phenols (Scheme 3.30) was kept in mind together with the experimentally obtained reaction products (alkoxylated compounds **170** and **171**, summarized in Tables 3.7 and 3.8).

2-phenylbenzofuran-6-ol (**124s**) as starting material

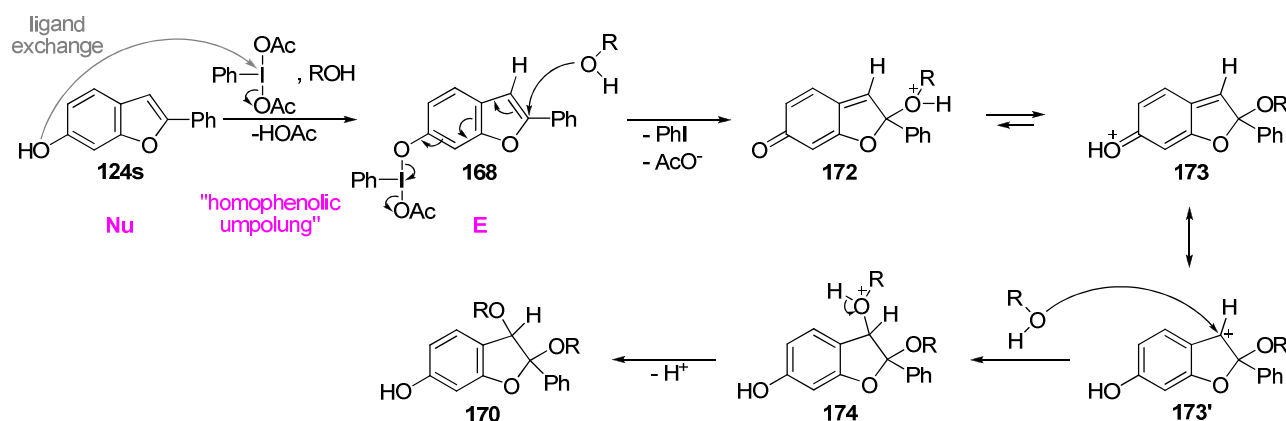
Considering the 2-substituted benzofurans, the mechanism depicted in Scheme 3.38 was proposed. In it, as in the case of phenols, I(III) atoms play the role of electrophilic center in a starting ligand exchange step. As a result of the nucleophilic attack (from the hydroxylic oxygen of the benzofuranol over the iodine atom of the DIB), an acetoxy ligand is replaced by the benzofuranolic moiety. This way the species **168**, in which the benzofuranoxy group is bound to the I(III) center, is generated.

Intermediate **168** shows an electrophilic character and will therefore be susceptible to suffer a nucleophilic attack in the presence of the appropriate nucleophile, i.e. a linear alcohol. The reactivity switch of benzofuranol from being nucleophile into becoming electrophile is referred to as “homophenolic umpolung” in scheme 3.38, by analogy to the “phenolic umpolung” previously described in section 3.3.1.2 (Scheme 3.29). The driving force of the nucleophilic attack just mentioned is the reduction of two electrons of the I(III) center and the elimination of the I(I) compound, i. e. iodobenzene (PhI).

The main issue associated with this step is to determine the regioselectivity of the attack, since different *ortho* and *para* positions are in principle available giving raise to various plausible options (remember reaction preview in Scheme 3.32). Attending to the obtained reaction products **170**, out of the four suggested sites for the attack, the carbon at position 2 of the benzofuran stood out as the preferred one. For this reason, from now on, our study follows only that pathway.

The nucleophilic attack over the carbon 2 leads to the positively charged monoalkoxylated intermediate **172**, in equilibrium with **173** and thus **173'**, which is thought to be strongly favored since in it the aromaticity of the benzene moiety is regained.

Moreover, in the presence of an appropriate nucleophile, the still positively charged intermediate **173'** is prone to undergo a second nucleophilic attack, this time on the carbon at position 3 of the benzofuran, furnishing species **174** which readily neutralizes to yield the dialkoxyated product **170** (Scheme 3.38).

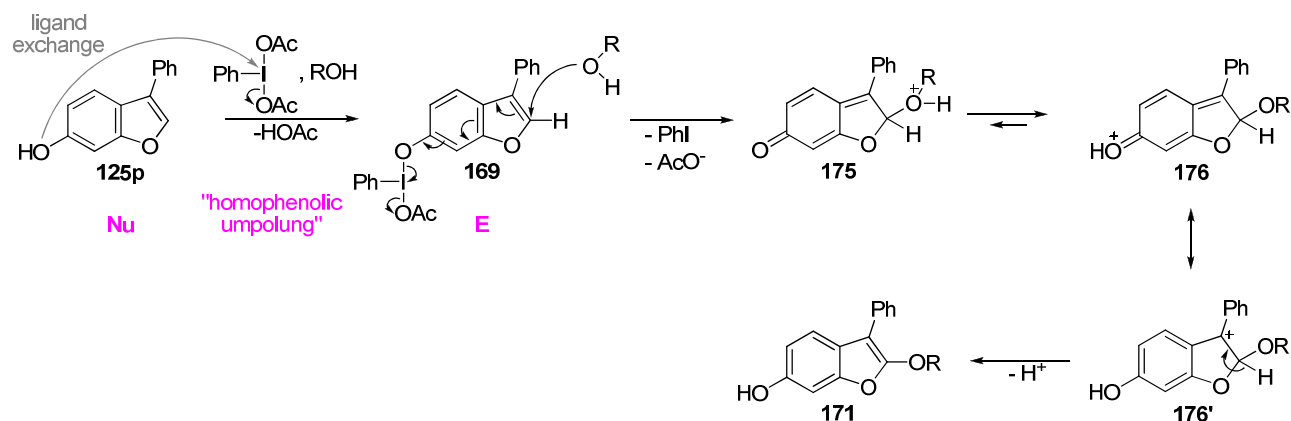


Scheme 3.38. Proposed mechanism for the DIB-mediated oxidative dearomatization of 2-phenylbenzofuran-6-ol **124s** in the presence of alcohols (ROH).

The diastereoisomerism of the resulting compound **170** (coming from the two possible entries of the second alkoxy moiety with respect to the plane defined by the bicyclic structure of **173'**, which already bears an alkoxy group) was considered in section 3.3.2.4 (Figure 3.43).

3-phenylbenzofuran-6-ol (**4p**) as starting material

On looking at the 3-substituted benzofurans, the mechanism depicted in Scheme 3.39 was proposed. It is essentially the equivalent to the one just postulated for the 2-substituted analogue up to intermediate **176'**. However, in this case, intermediate **176'** neutralizes to yield monoalkoxylated product **171**, regaining the aromaticity of the whole benzofuran moiety.



Scheme 3.39. Proposed mechanism for the DIB-mediated oxidative dearomatization of 3-phenylbenzofuran-6-ol **125p** in the presence of alcohols (ROH).

Interestingly, the outcome of the reaction starting from 2-phenyl and 3-phenylbenzofuran-6-ol is different (dialkoxylation and monoalkoxylation, respectively). This was attributed to the impossibility of intermediate **173'** to rearomatize into a benzofuran structure (position 2 is already disubstituted), and to the greater stability regained by intermediate **176'** developing into products **171** rather than undergoing a second nucleophilic attack leading to products **177** (Figure 3.48).

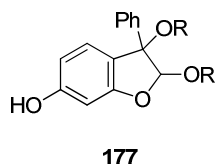
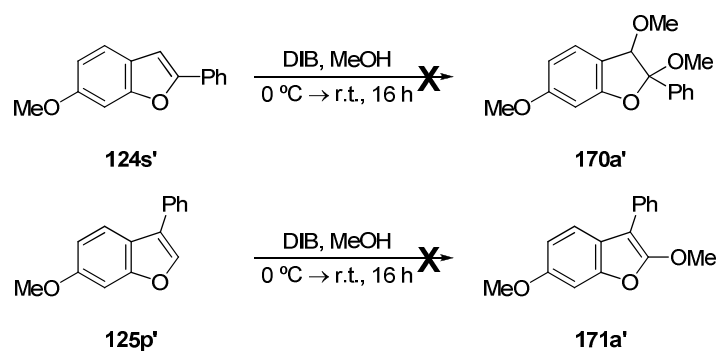


Figure 3.48. Structure of products **177**, which might result of a second nucleophilic attack on **176**.

One last test was performed in order to assess the necessity of the hydroxy group in the starting material to make the first nucleophilic attack (the initial ligand exchange step) possible. It consisted of trying the reaction under the same conditions but using the methoxylated compounds **124s'** and **125p'** as starting material, instead of hydroxylated **124s** and **125p**. These two products (which were prepared by methylation of **124s** and **125p** following a procedure described in literature²³⁹) did not lead to any product and were recovered unchanged after workup (Scheme 3.40).

²³⁹ Riant, O.; Samuel, O.; Flessner, T.; Taudien, S.; Kagan, H. B. *J. Org. Chem.* **1997**, *62*, 6733-6745

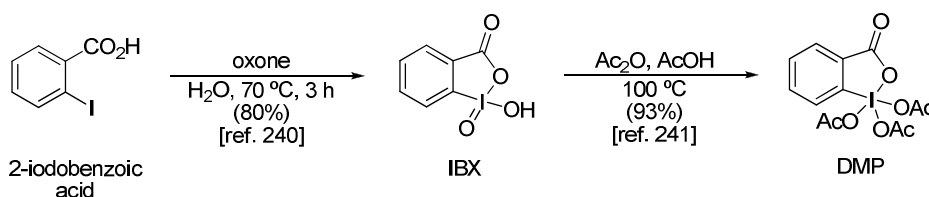


Scheme 3.40. DIB-mediated oxidative dearomatization reaction of 6-methoxy-2-phenylbenzofuran **124s'** (above) and 6-methoxy-3-phenylbenzofuran **125p'** (below) in the presence of methanol. No reaction was observed in both cases.

3.3.3. Experimental study: λ^5 -iodanes (preliminary results)

3.3.3.1. General considerations

λ^5 -iodanes, compared to λ^3 -iodanes, have been less and later studied. As mentioned before, Dess-Martin periodinane (DMP), *o*-iodoxybenzoic acid (IBX) and more recently its stabilized version SIBX are the main reagents of this family (Table 3.5). 2-iodobenzoic acid furnishes the majority of λ^5 -iodane heterocycles, such as IBX²⁴⁰ which has, in turn, proven useful in the synthesis of DMP²⁴¹ (Scheme 3.41).



Scheme 3.41. Preparation of IBX and DMP from 2-iodobenzoic acid.

IBX comprises one aromatic cycle (Ar) and two monovalent and one divalent heteroaromatic ligands (L), being therefore formally considered as a compound of type ArIL₄. It is an explosive reagent under impact or heating over 200 °C and insoluble in almost any organic solvent, except for DMSO. Due to its insolubility problem, IBX was transformed into DMP, which is soluble in most of the organic solvents and not impact-sensitive, but is humidity-sensitive and violently explodes at high temperature. In order to overcome the major safety concerns related to the violent decomposition under impact and/or heating of these environmentally benign and *ortho*-selective mild oxidants, a stabilized version of IBX called SIBX (which consist of IBX itself together with isophthalic and benzoic acids, table 3.5) was developed²⁴².

Molecular orbital theory describes hypervalent binding in the ArIL₄ compounds as two hypervalent bonds (3c-4e), as the ones described before for ArIL₂ λ^3 -iodanes (section 3.3.2.1). In this case, two *p* atomic orbitals of iodine participate in four bonds. Therefore, the two sets of three centers (L-I-L) are aligned in a cross-like structure with the iodine atom at its center. With regard to their geometry, these iodine derivatives present an octahedral structure: the central iodine atom is the donor; the covalent aromatic C-I bond,

²⁴⁰ Frigeiro, M.; Santagostino, M.; Sputore, S. *J. Org. Chem.* **1999**, *64*, 4537-4538

²⁴¹ Dess, D. B.; Martin, J. C. *J. Org. Chem.* **1983**, *48*, 4155-4156

²⁴² (a) Ozanne, A.; Pouységu, L.; Depernet, D.; François, B.; Quideau, S. *Org. Lett.* **2003**, *5*, 2903-2906 (b) Depernet, D.; François, B. *Patent* WO 02/057210 A1

together with the lone pair of electrons of iodine are in the same plane in axial position; and the two hypervalent bonds formed between the iodine and the four L ligands, two (3c-4e) bonds, are in equatorial position. The presence of two hypervalent bonds (highly polarized, longer and weaker than covalent bonds) gives them a strong electrophilic character (Figure 3.49).

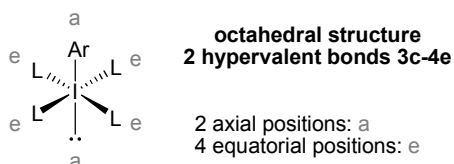
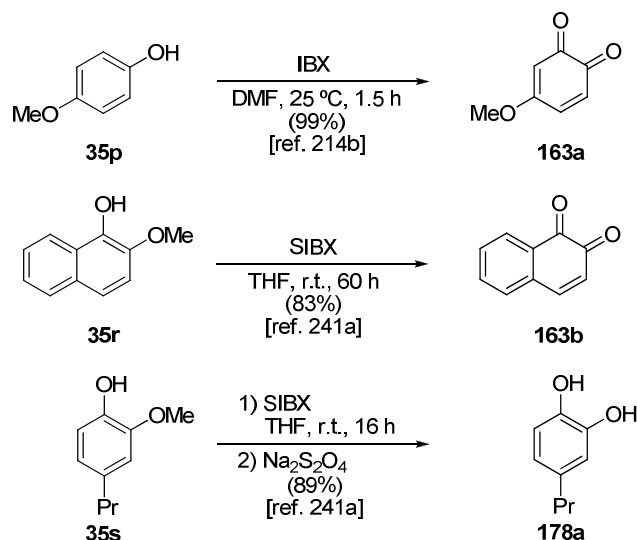


Figure 3.49. Geometry of λ^5 -iodanes of type ArIL_4 .

The IBX, as such and as its stabilized version (SIBX), is being increasingly used in organic synthesis due to its ability to mediate a wide range of reactions²⁴³. On looking at the oxidative dearomatization of phenols, it has been identified as a powerful reagent for promoting this reaction in a strictly *ortho*-selective manner, transforming phenols into *ortho*-quinones, or the corresponding catechols if a reductive workup is carried out^{214b,242a} (Scheme 3.42).



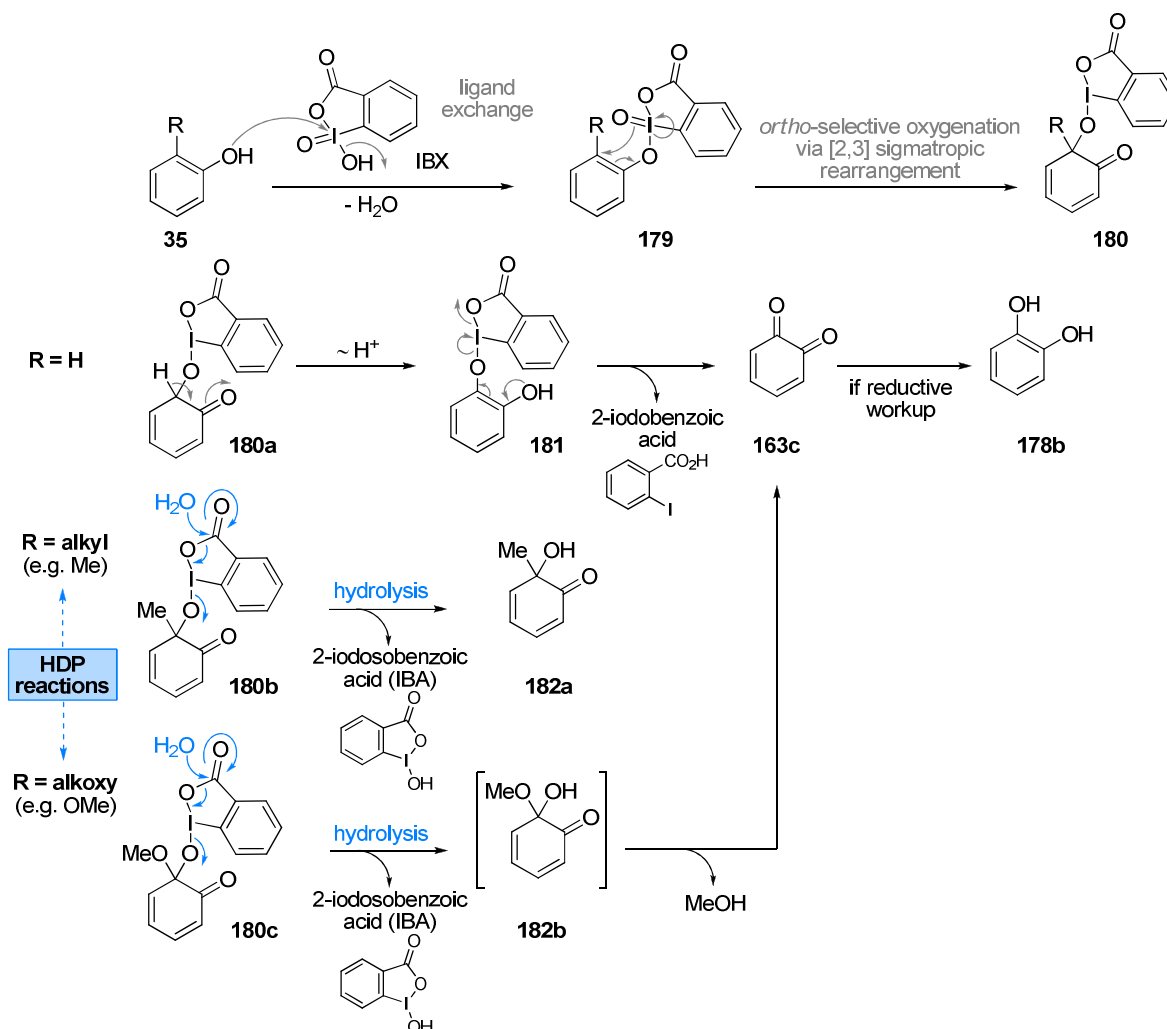
Scheme 3.42. Examples of λ^5 -iodane (S)IBX-mediated oxidative dearomatization of phenols.

The mechanism proposed for these λ^5 -iodanes-mediated *ortho*-selective oxidative dearomatization of phenolic compounds is presented in Scheme 3.43^{214d, 219}.

The phenol can react with IBX, probably via a ligand exchange step (nucleophilic attack of the non-bonding pair of electrons of oxygen over electropositive iodine) with elimination of a molecule of water to furnish a phenyloxyiodane- λ^5 type of **179**. This species can then

²⁴³ (a) Chaudhari, S. S. *Synlett* **2000**, 278-278 (b) Wirth, T. *Angew. Chem. Int. Ed.* **2001**, *40*, 2812-2814

undergo a [2,3] sigmatropic rearrangement, regioselectively forming a single carbon-oxygen bond on one of the *ortho*-carbon centers of phenyloxy moiety. This intramolecular oxygenation explains the *ortho*-selectivity of this reaction and releases two electrons to I(V) atom, leading to iodanyl- λ^3 species of type **180**. This species can then differently evolve depending on the substitution of the starting phenol.



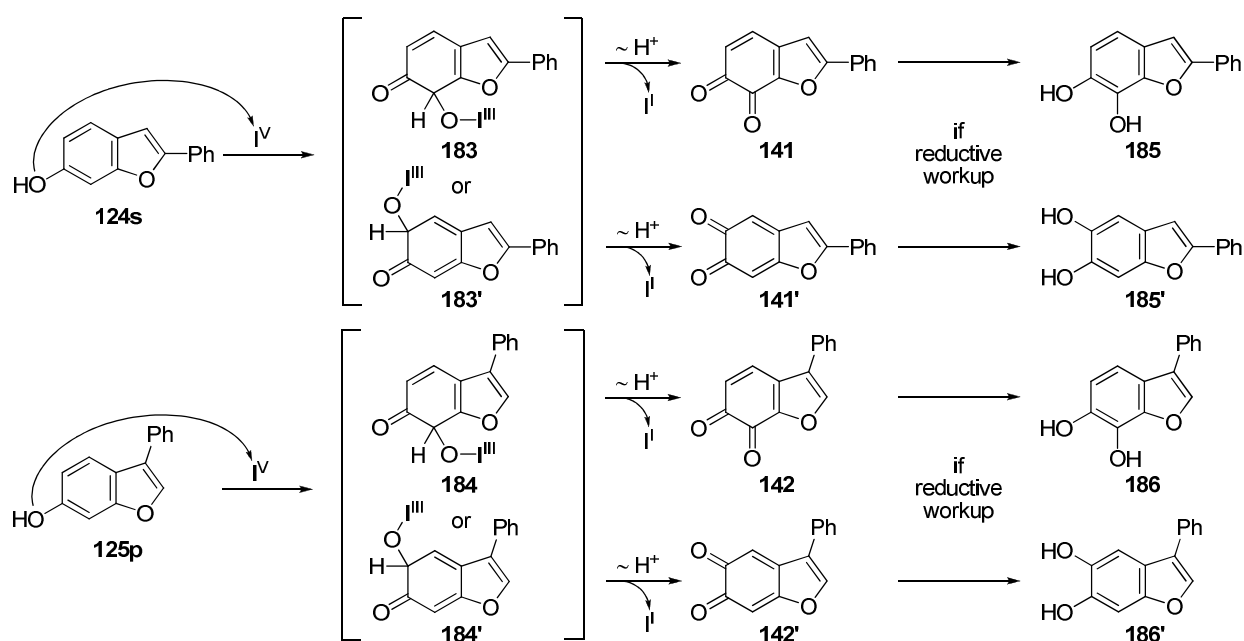
Scheme 3.43. Proposed mechanism for the *ortho*-selective oxidative dearomatization of phenols by λ^5 -iodanes of type ArIL_4 IBX²¹⁹.

If the *ortho* position is unsubstituted (i.e. R=H), the rearomatization of **180a** via 1,3-prototropy before the reductive elimination of λ^3 -iodanyl species leading to generation of *ortho*-quinone **163c** can be envisaged. Moreover, this species can be transformed into the corresponding catechol derivative **178b**, if a reductive workup is carried out.

If the *ortho* position was occupied by an alkyl substituent (e.g. R=Me), λ^3 -iodanyl species **180b** can be hydrolysed giving 2-iodosobenzoic acid (IBA) and the *ortho*-quinol **182a**. This transformation is called hydroxylative dearomatization of phenols (HDP reaction).

If the *ortho* position is occupied by an alkoxy group (e.g. R=OMe), the result of HDP reaction is different. The hemiketal **182b** (resulting from the hydrolysis of **180c**) eliminates a molecule of methanol to furnish the *ortho*-quinone **163c**.

Again, taking into account the results obtained for the differently substituted phenols, we wondered what we could expect if 2- or 3-phenylbenzofuran-6-ols (**124s** or **125p**) were used as starting materials. On looking at the oxidation reactions using λ^5 -iodanes [I(V)], the formation of two possible *ortho*-quinone-like compounds could be envisaged, or even the corresponding catechol-like compounds if a reductive workup is carried out (Scheme 3.44).



Scheme 3.44. λ^5 -iodane-mediated dearomatization of 2- and 3-phenylbenzofuran-6-ols **124s** and **125p** preview.

3.3.3.2. Reaction of 2- and 3- phenylbenzofuran-6-ols **124s** and **125p** with λ^5 -iodanes

As mentioned before (section 3.3.4.1), the main and most widely used λ^5 -iodanes in organic synthesis are the DMP and the IBX. However, being DMP much more sensitive to reaction conditions, IBX and its stabilized formulation SIBX were the only reagents considered in this study.

2-phenylbenzofuran-6-ol (124s) as starting material

Starting with the 2-substituted benzofuran **124s**, the reaction was attempted using conditions similar to those previously reported in literature for phenols^{214f, 242a}, together with some extra precautions: inert argon atmosphere, protection from light with aluminium foil (due to the well-known light sensitivity of *ortho*-quinones), THF as solvent, portionwise addition of the (S)IBX and room temperature stirring. Besides, the experiments were monitored by TLC and were left to stir until complete consumption of starting benzofuran, progressively adding 0.5 equivalents of the λ^5 -iodane every 8-12 hours (up to 3 equivalents). In addition, three different workups were tried.

The first one was a reductive workup, trying to make the reaction progress to the benzofurandiol (catechol-like derivative), in principle more stable and therefore easier to purify. This procedure consisted of the addition of an aqueous solution of sodium dithionite followed by 30 minutes stirring. The reaction mixture was then filtered and evaporated. Next it was dissolved in ethyl acetate, washed with sodium bicarbonate and brine, dried over magnesium sulphate and filtered and evaporated again. Unfortunately, this handling led to the degradation of the reaction mixture.

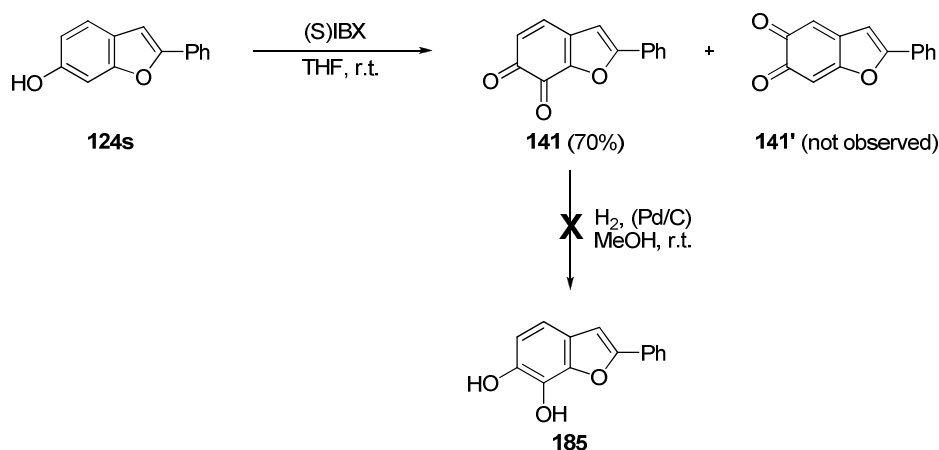
Secondly, with the aim of isolating the benzofurandione (*ortho*-quinone-like compound) instead of reaching up to the catechol-like derivative, a reported workup for this kind of compounds was tried^{242a}. This proceeded as follows: the reaction mixture was first evaporated to dryness and dissolved in dichloromethane; then it was washed with water and sodium bicarbonate, dried over sodium sulphate, filtered and evaporated. As in the previous option, this led to the apparent degradation of the reaction crude resulting in a complex mixture in which no product could be identified.

Finally, bearing in mind that according to TLC the assayed workups had ruined the original outcome of the experiment, a “no-workup” strategy was adopted and the reaction mixture was simply filtered and evaporated. The crude obtained this way resulted apparently in a mixture of only one benzofurandione derivative (out of the two *ortho* possibilities **141** and **141'**) and byproducts presumably coming from (S)IBX, according to its ¹H-NMR spectrum analysis (Scheme 3.45 and Figure 3.50). From the comparison of the ¹H-NMR spectra of the crudes resulting from the reaction with SIBX and IBX, it was concluded that the SIBX

generated more byproducts and, given the problems of purification that we found (detailed in next paragraph), IBX was chosen as preferential reagent for the experiments.

Then our efforts were driven towards the purification of the benzofurandione. Unfortunately, chromatographic column in silica, alumina semi-preparative TLC, precipitation in diethyl ether or dichloromethane and crystallization in dichloromethane, ethanol, isopropanol, *n*-pentane or some mixtures of them met with no success. In fact, our best result, which was a 70% yield of product, arose from the overnight precipitation of the reaction crude in a mixture of THF and cold *n*-pentane. Although the ¹H-NMR and IR spectra of this precipitate were registered, the product was unstable (progressively degraded) and was not further characterized. The analysis of this ¹H-NMR spectrum showed benzofurandione **141** as the single product of the reaction (**141'** was not observed), taking into account the multiplicity of the signals at 6.24 and 7.54 ppm (Figure 3.50).

As an alternative that allowed us to skip the purification step of the benzofurandione, we thought of transforming it into the corresponding benzofurandiol **185** by means of a catalytic (Pd/C) hydrogenation using methanol (MeOH) as solvent. Nevertheless, this trial was again unsuccessful.



Scheme 3.45. λ^5 -iodanes (S)IBX-mediated oxidative dearomatization reaction of 2-phenylbenzofuran-6-ol **124s** and hydrogenation of the resulting benzofurandione **141**.

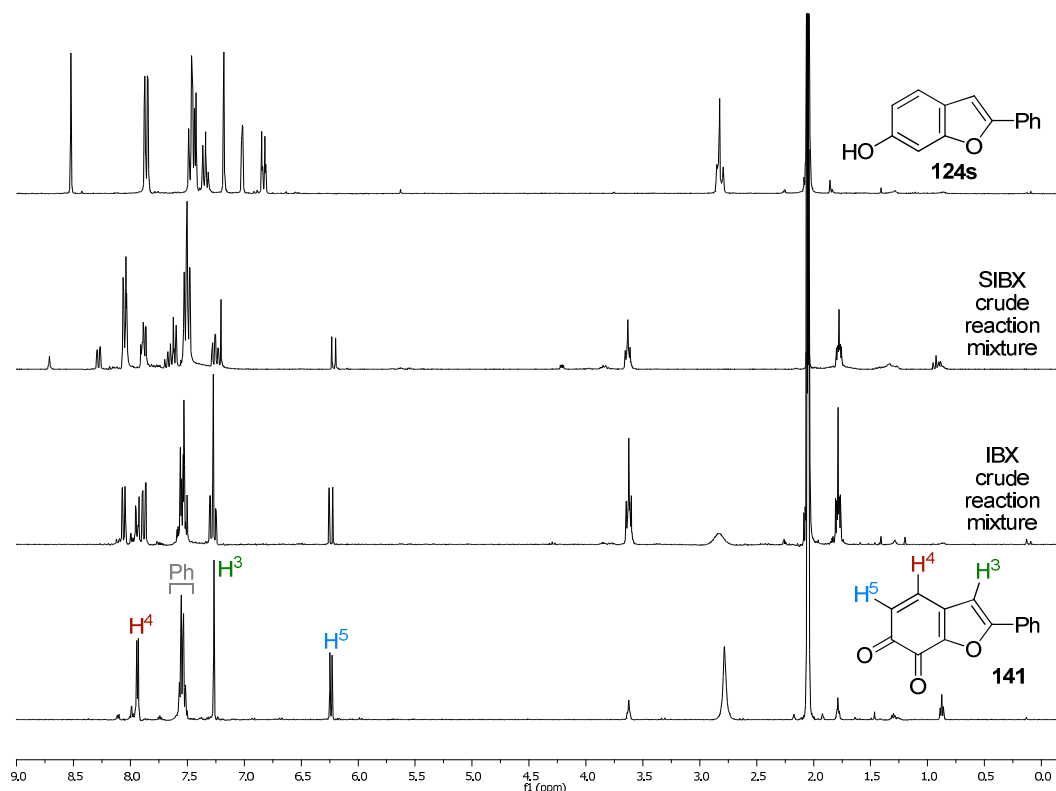
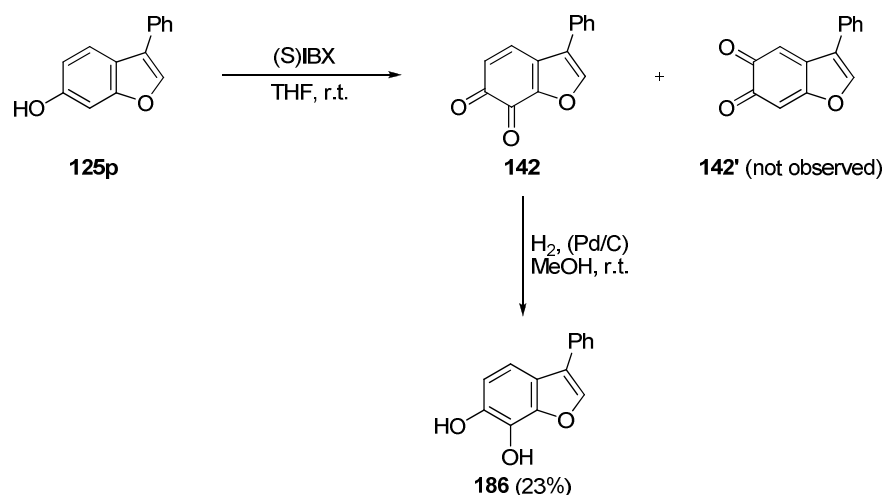


Figure 3.50. ¹H-NMR (500 MHz, acetone-d₆) spectra of, arranged from top to bottom, the starting 2-phenylbenzofuran-6-ol **124s**, the crude reaction mixture using SIBX, the crude reaction mixture using IBX and the isolated product **141**.

3-phenylbenzofuran-6-ol (**125p**) as starting material

The same set of experiments was repeated with the 3-substituted benzofuran-6-ol **125p**, with practically parallel results in terms of obtained crude reaction mixtures and selectivity of the reaction product (**142** is the only observed regioisomer, according to the analysis of the signals in the ¹H-NMR spectra).

Nevertheless, some differences showed up during purification attempts. This time even the overnight precipitation of the reaction crude in a mixture of THF and cold *n*-pentane failed to provide a precipitate enriched in product **142**. The catalytic hydrogenation, in turn, resulted in a partial success, furnishing the benzofurandiols **186**, although in low yield (23% overall yield) after column chromatography (Scheme 3.46 and Figure 3.51).



Scheme 3.46. λ^5 -iodanes (S)IBX-mediated oxidative dearomatization reaction of 3-phenylbenzofuran-6-ol **125p** and hydrogenation of the resulting benzofurandione **142**.

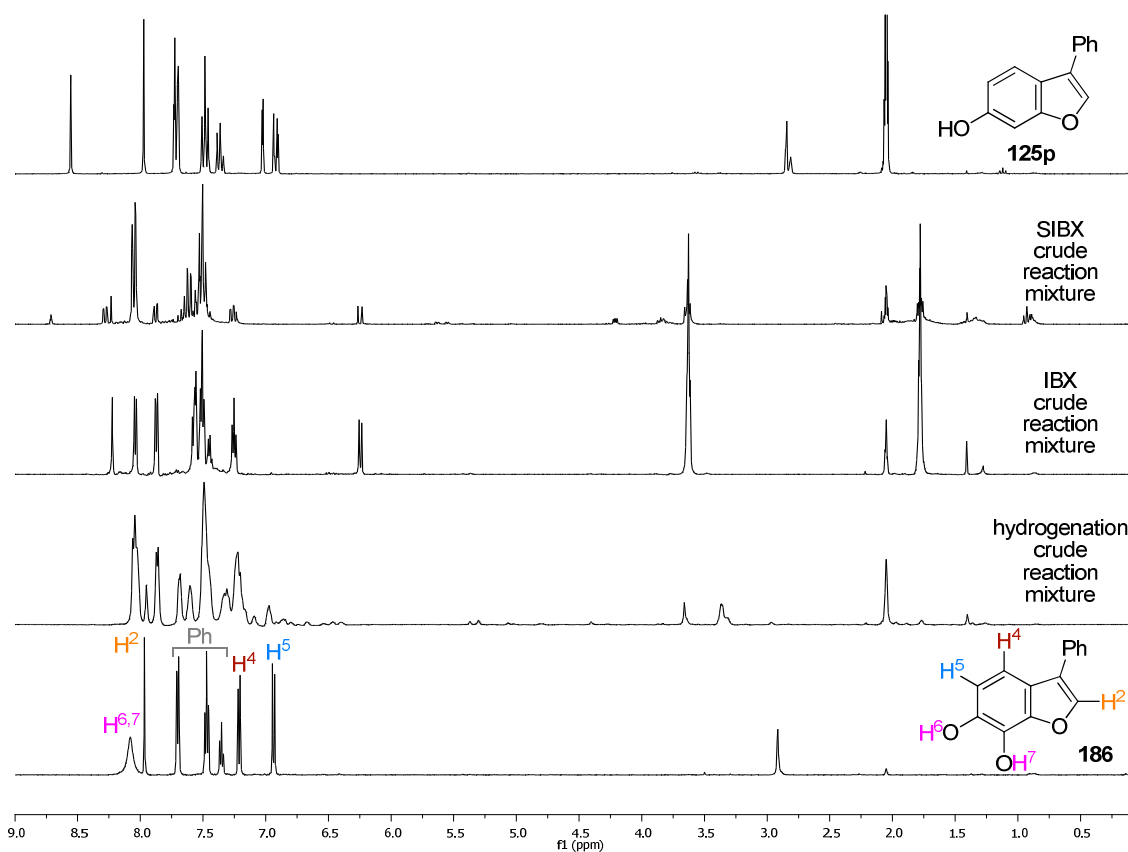


Figure 3.51. $^1\text{H-NMR}$ (500 MHz, acetone- d_6) spectra of, arranged from top to bottom, the starting 3-phenylbenzofuran-6-ol **125p**, the crude reaction mixture using SIBX, the crude reaction mixture using IBX, the crude reaction mixture of the hydrogenation and the isolated hydrogenated product **186**.

3.3.4. Conclusions

From this chapter, in which reaction conditions for hypervalent iodine-mediated oxidative dearomatization of phenols are applied to 2- and 3-phenylbenzofuran-6-ols, **124s** and **125p**, the following conclusions can be drawn:

- Under the optimized procedure, the oxidative dearomatization of 2-phenylbenzofuran-6-ol **124s** with diacetoxyiodobenzene (DIB) λ^3 -iodane, in the presence of the appropriate nucleophile, results in *cis:trans* mixtures of the corresponding 2,3-dialkoxy-2-phenyl-2,3-dihydrobenzofuran-6-ols **170a-d** with moderate yields. *Cis* is the major isomer of these mixtures.
- Under the same conditions, the oxidative dearomatization of 3-phenylbenzofuran-6-ol **125p** with diacetoxyiodobenzene (DIB) λ^3 -iodane, in the presence of the appropriate nucleophile, furnishes the corresponding 2-alkoxy-3-phenylbenzofuran-6-ols **171a-f** with moderate yields.
- Although different kinds of nucleophiles were assayed, only alcohols succeeded at transforming the starting benzofuranols into the mentioned products.
- Among the tested alcohols, linear MeOH, EtOH, ⁿPrOH and ⁿBuOH worked when starting from both **124s** and **125p**, whilst branched ⁱPrOH and ^tBuOH were only effective when 3-phenylbenzofuran-6-ol **125p** was used as starting material.
- Mechanisms for the reactions of both **124s** and **125p** with DIB in the presence of alcohols were proposed, taking into account the equivalent reaction for phenols and the experimentally obtained products. They provide a better understanding of the different outcome of the reaction starting from 2- and 3-substituted benzofurans based on the possibilities of intermediates **174'** and **177'** to render the most favorable product in each case: by suffering a second nucleophilic attack (2-substituted **124s** → **174'** → **170**) or preferably by regaining aromaticity when possible (3-substituted **125p** → **177'** → **171**).

- Preliminary studies of the reaction of 2- and 3-phenylbenzofuran-6-ols, **124s** and **125p** with (stabilized) *o*-iodoxybenzoic acid [(S)IBX] λ^5 -iodanes resulted in promising crude reaction mixtures with 2- and 3-phenylbenzofuran-6,7-diones **141** and **142** as major products, which turned out to be unstable products.

3.4. BORON TRIBROMIDE-MEDIATED DEMETHYLATION of METHOXY GROUPS in BENZO[*b*]FURANS

3.4.1. Preparation of hydroxylated benzofurans overview

As mentioned earlier in the introduction (poly)hydroxylated benzofurans are highly interesting compounds. Therefore, preparing them was one of our targets from the very beginning of this project. From the two possible approaches towards substituted heterocycle synthesis (previously presented in section 3.2.1), the introduction of the substituents to the performed heterocycle presented in this case two main problems: the formation of the benzofuran from the unsubstituted phenol following our optimized procedure did not work (Table 2.12, entry 15, compound **124o** and Table 2.14, entry 11, compound **125k**), and the reported regioselective and efficient hydroxylations of benzofurans (or similar aromatics) were quite scarce²⁴⁴.

The alternative strategy, formation of the heterocyclic framework after the introduction of the substituents, for its part, had the problem of having to work in the presence of hydroxy group(s). The principal (and well known) issue with the hydroxy group is that it can participate in a wide range of transformations, even under mild conditions, due to its nucleophilic character, its acidity (pK_a of 10 for phenols) and the fact that it can be easily oxidized by numerous reagents.

The synthetic procedure optimized in chapter 2 for the preparation of benzofurans was not an exception. In fact, the reaction of phenols with hydroxylated bromoacetophenones led to complex mixtures (as bromoacetophenone polymerizes) and to lower reaction yields when hydroxylated phenols were tried (Table 2.12, entries 4 and 5, compounds **124d-e**), although products associated with the double condensation were not detected.

Therefore, in order to overcome this functional group incompatibility in the synthesis of the benzofuran scaffold, a hydroxy protecting group had to be envisaged. Among all the

²⁴⁴ (a) Oliveira, A. M. A. G.; Raposo, M. M. M.; Oliveira-Campos, A. M. F.; Griffiths, J.; Machado, A. E. H. *Helv. Chim. Acta* **2003**, *86*, 2900-2907 (b) Maharoo, U. S. M.; Sulikowski, G. A. *Tetrahedron Lett.* **2003**, *44*, 9021-9023 (c) Shultz, D. A.; Sloop, J. C.; Washington, G. *J. Org. Chem.* **2006**, *71*, 9104-9113 (d) Cano, C.; Barbeau, O. R.; Bailey, C.; Cockcroft, X.-L.; Curtin, N. J.; Duggan, H.; Frigerio, M.; Golding, B. T.; Hardcastle, I. R.; Hummersone, M. G.; Knights, C.; Menear, K. A.; Newell, D. R.; Richardson, C. J.; Smith, G. C. M.; Spittle, B.; Griffin, R. J. *J. Med. Chem.* **2010**, *53*, 8498-8507 (e) Kantevari, S.; Yempala, T.; Yogeeswari, P.; Sriram, D.; Sridhar, B. *Bioorg. Med. Chem. Lett.* **2011**, *21*, 4316-4319

reported strategies²⁴⁵, protection as methyl ether was selected, although an attempt was made with benzyl group (bearing in mind its easy deprotection via catalytic hydrogenolysis), which resulted unsuccessful at the benzofuran cyclization stage (Table 2.14, entry 10, compound **125j**).

The main reasons behind the choice of the methyl group were that it was simple and small enough not to difficult the cyclization step. In addition, the resulting electron-releasing methoxy substituent(s) favored the reaction and furnished the also interesting methoxylated products. Finally, aryl methyl ethers can be cleaved under conditions that do not to endanger the benzofuran scaffold or other substituents present in the molecule.

Demethylation of aryl methyl ethers can be effected by a wide range of reagents, usually requiring harsh reaction conditions (especially, fairly high temperatures). Many of them suffer from one or more drawbacks (besides the harsh reaction conditions), such as long reaction times, difficulty of manipulation, employment of exotic reagents, use of large excess amounts of demethylating agent and low reaction yields. These methods involve strong acids (concentrated hydroiodic, hydrobromic or hydrochloric acids) or bases^{163, 244d,246}, or sources of them²⁴⁷; oxidizing or reducing agents (like L-Selectride and superhydride)²⁴⁸; or the assistance of highly polar solvents (like ionic liquids such as [BMIM]BF₄)²⁴⁹ or even microwave irradiation²⁵⁰ (Scheme 3.47).

²⁴⁵ Kociensky, P. J. *Protecting groups* **2005**, 3rd edition Georg Thieme Verlag, chapter 4, 187-364

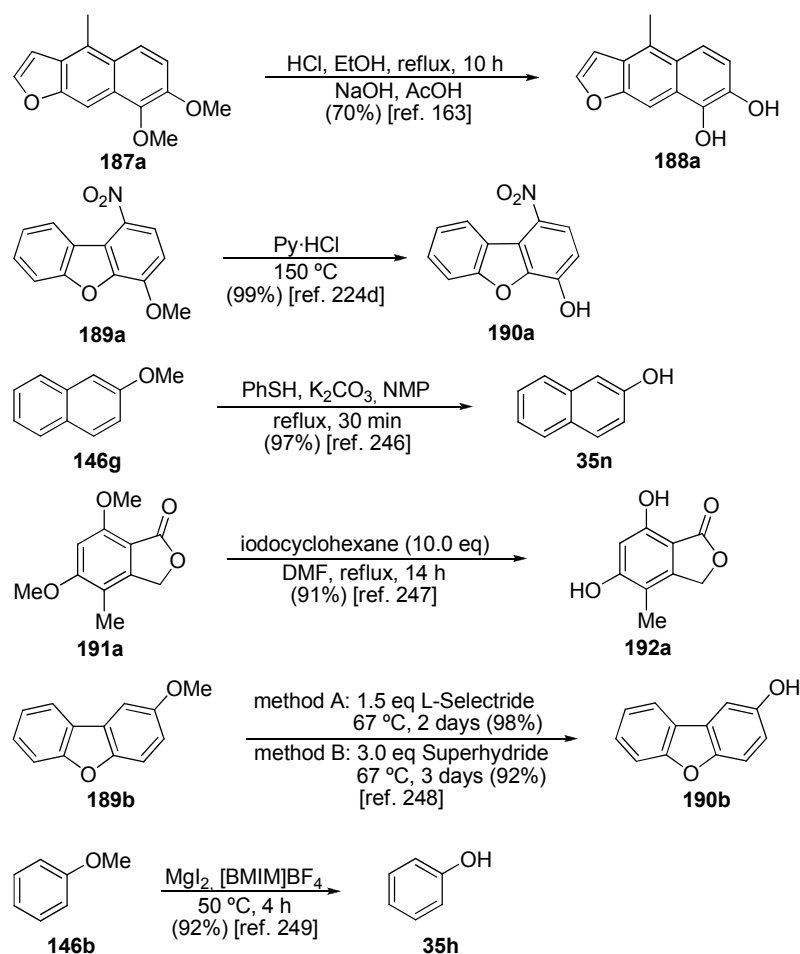
²⁴⁶ Chakraborti, A. K.; Sharma, L.; Nayak, M. K. *J. Org. Chem.* **2002**, *67*, 6406-6414

²⁴⁷ Zuo, L.; Yao, S.; Wang, W.; Duan, W. *Tetrahedron Lett.* **2008**, *49*, 4054-4056

²⁴⁸ Majetich, G.; Zhang, Y.; Wheless, K. *Tetrahedron Lett.* **1994**, *35*, 8727-8730

²⁴⁹ Lee, K. S.; Kim, K. D. *Bull. Korean Chem. Soc.* **2010**, *31*, 3842-3843

²⁵⁰ Fredriksson, A.; Stone-Elander, S. *J. Label. Compd. Radiopharm.* **2002**, *45*, 529-538

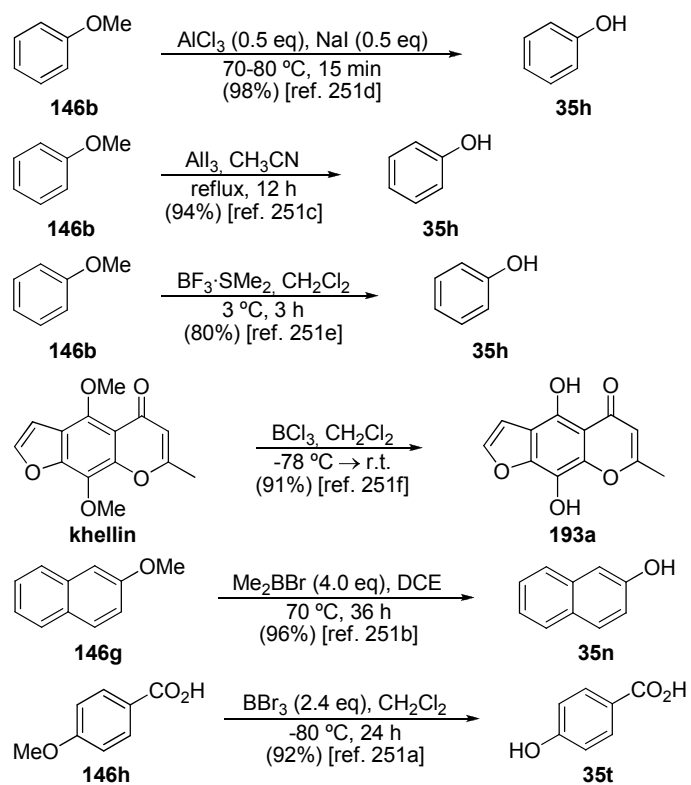


Scheme 3.47. Aryl methyl ether cleavage by various reagents.

However, aromatic ethers can also be cleaved under less drastic conditions by means of aluminium and boron halides²⁵¹ (Scheme 3.48). Due to the empty *p*-orbital on boron, boron halides (BX_3) and organoboron halides (RBX_2 , R_2BX) are Lewis acids. Generally, stoichiometric amounts of boron halide are required to complete the cleavage. These reactions have demonstrated high chemoselectivity, regioselectivity and compatibility with a variety of functional groups. Overall, the reaction produces a phenol and an alkyl halide²⁵².

²⁵¹ (a) McOmie, J. F. W.; Watts, M. L.; West, D. E. *Tetrahedron* **1968**, *24*, 2289-2292 (b) Guindon, Y.; Yoakim, C.; Morton, H. E. *Tetrahedron Lett.* **1983**, *29*, 2969-2972 (c) Bhatt, M. V.; Babu, J. R. *Tetrahedron Lett.* **1984**, *25*, 3497-3500 (d) Ghiaci, M.; Asghari, J. *Synthetic Commun.* **1999**, *29*, 973-979 (e) Konieczny, M. T.; Maciejewski, G.; Konieczny, W. *Synthesis* **2005**, *10*, 1575-1577 (f) Cianci, J.; Baell, J. B.; Flynn, B. L.; Gable, R. W.; Mould, J. A.; Paul, D.; Harvey, A. *J. Biorg. Med. Chem.* **2008**, *18*, 2055-2061

²⁵² Yao, M.-L.; Kabalka, G. W. *Boron Science* **2012**, 579-621



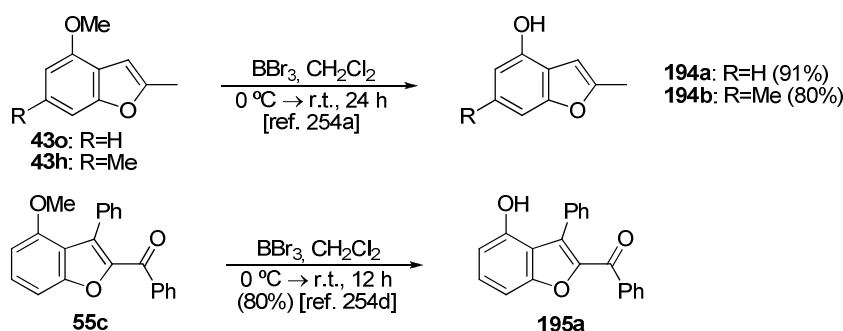
Scheme 3.48. Aryl methyl ether cleavage by some aluminium and boron halides.

3.4.2. Experimental study: boron tribromide (BBr₃)

3.4.2.1. General considerations

Although all BX₃ reagents cleave ethers, boron tribromide (BBr₃) is most widely used because these deprotection reactions proceed under very mild reaction conditions, at room temperature or below. This reagent is a colorless fuming liquid, commercially available neat or in solution in dichloromethane or hexanes. It is highly moisture-sensitive and decomposes in air with evolution of HBr. It must be stored under a dry inert atmosphere and reacts violently with protic solvents, such as water and alcohols²⁵³.

In fact, it has already been successfully applied to the demethylation of methoxy groups in benzofurans (and very similar compounds)^{163, 254} (Scheme 3.49), even when simultaneous deprotection of multiple methoxy groups had to be performed^{164, 255} (Scheme 3.50).

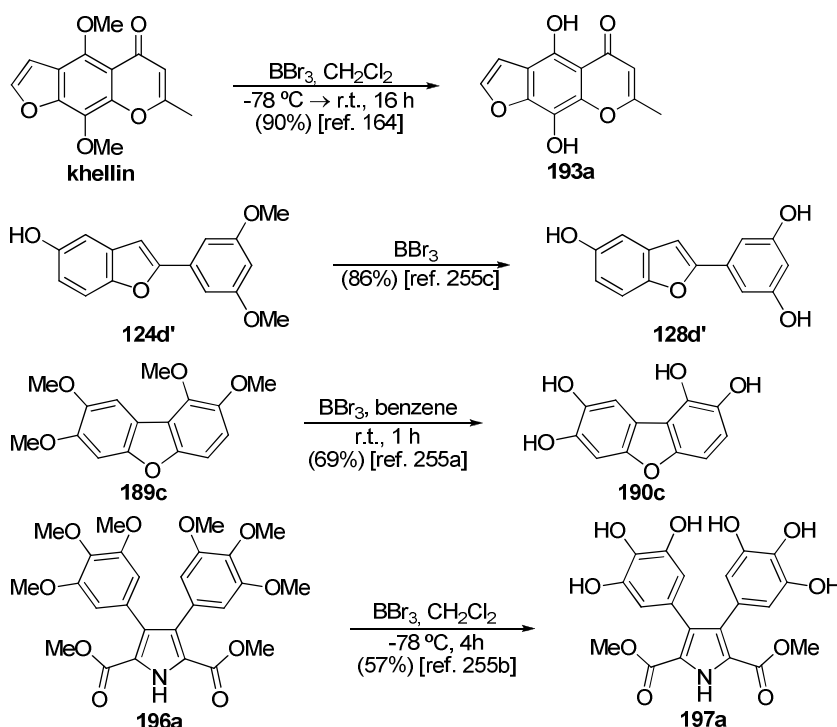


Scheme 3.49. Examples of aryl methyl ether cleavage by BBr₃ in benzofurans.

²⁵³ García, E. *Synlett* **2005**, 10, 1636-1637

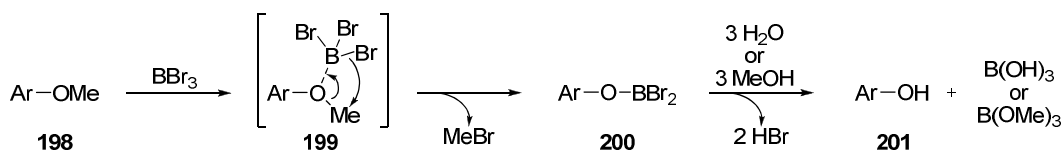
²⁵⁴ (a) Mphahlele, M. J.; Moekwa, T. B. *Org. Biomol. Chem.* **2005**, 3, 2469-2475 (b) Fardis, M.; Mertzman, M.; Thomas, W.; Kirschberg, T.; Collins, N.; Polniaszek, R.; Watkins, W. J. *J. Org. Chem.* **2006**, 71, 4835-4839 (c) Row, E. C.; Brown, S. A.; Stachulski, A. V.; Lennard, M. S. *Org. Biomol. Chem.* **2006**, 4, 1604-1610 (d) Yeh, J.-Y.; Coumar, M. S.; Horng, J.-T.; Shiao, H.-Y.; Kuo, F.-M.; Lee, H.-L.; Chen, I.-C.; Chang, C.-W.; Tang, W.-F.; Tseng, S.-N.; Chen, C.-J.; Shih, S.-R.; Hsu, J. T.-A.; Liao, C.-C.; Chao, Y.-S.; Hsieh, H.-P. *J. Med. Chem.* **2010**, 53, 1519-1533

²⁵⁵ (a) Tashiro, M.; Yoshiya, H. *Heterocycles* **1982**, 19, 2349-2354 (b) Fürstner, A.; Krause, H.; Thiel, O. R. *Tetrahedron* **2002**, 58, 6373-6380 (c) Kim, I.; Kim, K.; Choi, J. *J. Org. Chem.* **2009**, 74, 8492-8495



Scheme 3.50. Multiple aryl methyl ether cleavage by BBr_3 .

The generally accepted mechanism for this reaction proceeds via the formation of a complex between the boron and the ether oxygen atom followed by the elimination of methyl bromide to yield a dibromoorganoborane. It is therefore advisable to use at least one equivalent of BBr_3 per methoxy group to be deprotected, together with an extra equivalent for each group containing potentially basic N or O atoms. The dibromoorganoborane can then undergo hydrolysis to give a hydroxy group, boric acid (or borate esters, as alcohols behave analogously), and hydrogen bromide as products^{246, 256} (Scheme 3.51).



Scheme 3.51. Proposed mechanism for aryl methyl ethers cleavage by BBr_3 (from references 246 and 256).

3.4.2.2. Synthesis of 2-aryl and 3-aryl hydroxybenzofurans

Literature review (section 3.4.1) suggested that boron tribromide was the most appropriate reagent to perform the demethylation reaction of the methoxylated benzofurans. The

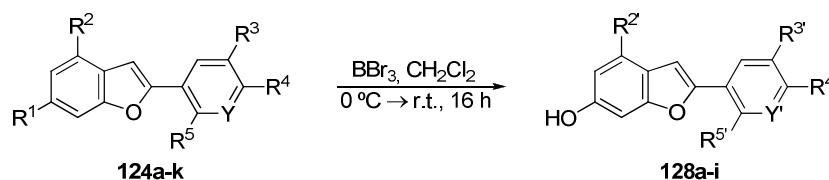
²⁵⁶ (a) Kemperman, G. J.; Roeters, T. A.; Hilberink, P. W. *Eur. J. Org. Chem.* **2003**, 1681-1686 (b) Punna, S.; Meunier, S.; Finn, M. G. *Org. Lett.* **2004**, 6, 2777-2779

reaction conditions selected to carry out this transformation were the dropwise addition of the boron tribromide solution in dichloromethane over a solution of the corresponding benzofuran (also in dichloromethane) at 0 °C followed by overnight (about 16 hours) room temperature stirring under inert atmosphere. The equivalents of BBr₃ were adjusted depending on the number of methoxy groups to be deprotected, adding an excess of two equivalents for each methoxy group. All the experiments performed were, in principle, aimed at exhaustive demethylation.

2-aryl hydroxybenzofurans (128)

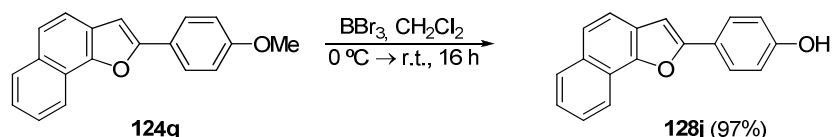
The benzofurans and naphthofuran chosen from the 2-aryl series (**124a-r**) were the compounds bearing only methoxy substituents **124a-c,q**, hydroxylated benzofurans **124d-e**, fluorinated compounds **124i-j** and pyridyl group incorporating benzofuran **124k** (Table 3.9 and Scheme 3.52).

Table 3.9. Synthesis of 2-aryl hydroxybenzofurans **128a-i** from benzofurans **124a-k** via demethylation with BBr₃.



entry	reaction	Y	R ¹	R ²	R ³	R ⁴	R ⁵	Y'	R ^{2'}	R ^{3'}	R ^{4'}	R ^{5'}	yield ^a (%)
1	124a → 128a	CH	OMe	OMe	H	OMe	H	CH	OH	H	OH	H	93
2	124b → 128b	COMe	OMe	OMe	OMe	H	H	COH	OH	OH	H	H	74
3	124c → 128c	COMe	OMe	OMe	OMe	OMe	H	COH	OH	OH	OH	H	62
4	124d → 128d	COMe	OH	H	OMe	H	H	COH	H	OH	H	H	25
5	124i → 128e	CH	OMe	OMe	H	F	H	CH	OH	H	F	H	80
6	124j → 128f	CF	OMe	OMe	F	H	H	CF	OH	F	H	H	60
7	124k → 128g	N	OMe	OMe	H	OMe	OMe	N	OH	H	OMe	OMe	47
8	124k → 128h	N	OMe	OMe	H	OMe	OMe	N	OH	H	OH	OH	-
9	124e → 128i	CH	OH	H	H	OMe	H	CH	H	H	OH	H	71

^aYield of isolated pure product after column chromatography.



Scheme 3.52. Preparation of 2-aryl hydroxynaphthofuran **128j** from naphthofuran **124q** via demethylation with boron tribromide BBr_3 .

The reaction yields were in general good with the exception of compound **128d** (25%, Table 3.9, entry 4). The increase in the number of methoxy groups also led to the decrease in the reaction yields (93-74-62%, Table 3.9, entries 1-3). Fluorinated compounds also performed with good yields, although it was observed that the higher the number of substituents in the aryl group in position 2, the lower the reaction yield (80-60%, Table 3.9, entries 5-6).

The case of the benzofuran including the pyridyl group, **124k**, was the only experiment in which exhaustive demethylation was not achieved. From this trial, a single product, **128g**, was obtained with moderate yield (47%, Table 3.9, entry 7). This product is the result of the exclusive demethylation of the methoxy groups in the benzofuran bicycle. Indeed, the methoxy groups in the pyridyl group remained intact after the addition of 8 equivalents of boron tribromide. The corresponding completely demethylated compound, **128h**, was not even detected in the analysis of the $^1\text{H-NMR}$ spectrum of the crude reaction mixture (-, Table 3.9, entry 8).

The completion of these transformations was checked by analysing the signals in the $^1\text{H-NMR}$ spectrum registered in deuterated dimethyl sulfoxide (DMSO-d_6) for compounds **128a-j**. The solvent choice was supported by its suitability to dissolve polar (and especially hydroxy containing) compounds and, essentially, by its ability to show sharp signals for hydroxy protons (due to its slow intermolecular deuterium – labile proton exchange rate).

On looking at the spectra it was observed that, compared to those of their precursors **124a-q**, methoxy signals at 3.7–4.1 ppm disappeared and new signals appeared at chemical shifts of 8.0–11.0 ppm (mainly between 9.0 and 10.0), as correspond to phenolic hydroxy protons in dimethyl sulfoxide. As an example, in Figure 3.52 the comparison of the $^1\text{H-NMR}$ spectra of **124a** and **128a** in DMSO-d_6 is shown.

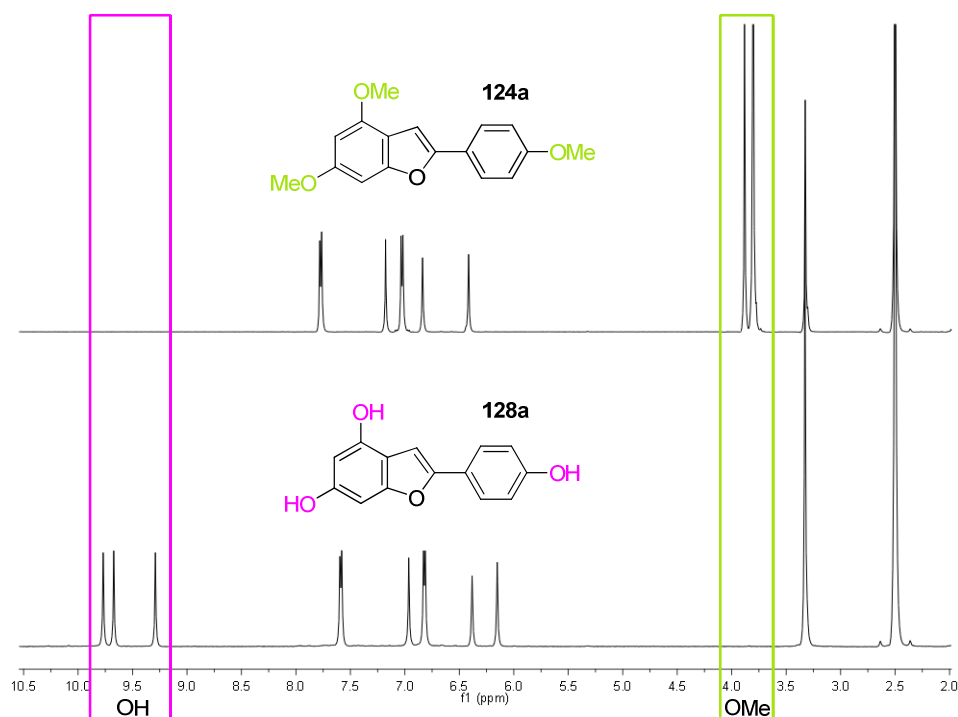
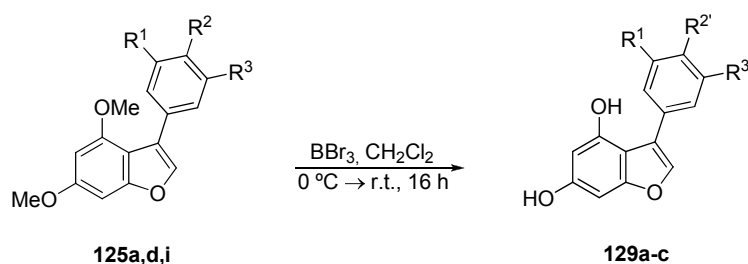


Figure 3.52. $^1\text{H-NMR}$ spectra (500 MHz, DMSO-d_6) of **124a** (above) and **128a** (below). Aromatic $-\text{OMe}$ and $-\text{OH}$ regions are highlighted in light green and pink, respectively.

3-aryl hydroxybenzofurans (129)

The benzofurans chosen from the 3-aryl series (**125a-o**) were the methoxylated lead compound **125a**, and the fluorinated benzofurans **125d** and **125i** (Table 3.10).

Table 3.10. Synthesis of 3-aryl hydroxybenzofurans **129a-c** from benzofurans **125a,d,i** via demethylation with BBr_3 .



entry	reaction	R ¹	R ²	R ³	R ^{2'}	yield ^a (%)
1	125a → 129a	H	OMe	H	OH	38
2	125d → 129b	H	F	H	F	58
3	125i → 129c	F	H	F	H	70

^aYield of isolated pure product after column chromatography.

Under the experimental conditions used for 2-substituted benzofurans, the yield of the reaction with 3-substituted lead compound **125a** was moderate (38%, Table 3.10, entry 1), noticeably lower than that of its regioisomer **125a** (93%, Table 3.9, entry 1), probably due to the larger steric hindrance created by the aryl group in position 3, close to methoxy group in position 4 in the benzofuran ring.

Fluorinated compounds performed with good yields again, although with reversed influence of the number of substituents: the higher the number of substituents in the aryl group in position 3, the higher the reaction yield (58-70%, Table 3.10, entries 2-3).

Analogously, the completion of these transformations was checked analysing the signals in the $^1\text{H-NMR}$ spectrum registered in deuterated dimethyl sulfoxide (DMSO-d_6) for compounds **129a-c**.

On looking at the spectra it was again observed that methoxy signals at 3.7–4.1 ppm disappeared and new signals appeared at chemical shifts of 8.0–11.0 ppm (mainly between 9.0 and 10.0). As an example, in Figure 3.53 the comparison of the $^1\text{H-NMR}$ spectra of **125a** and **129a** in DMSO-d_6 is shown.

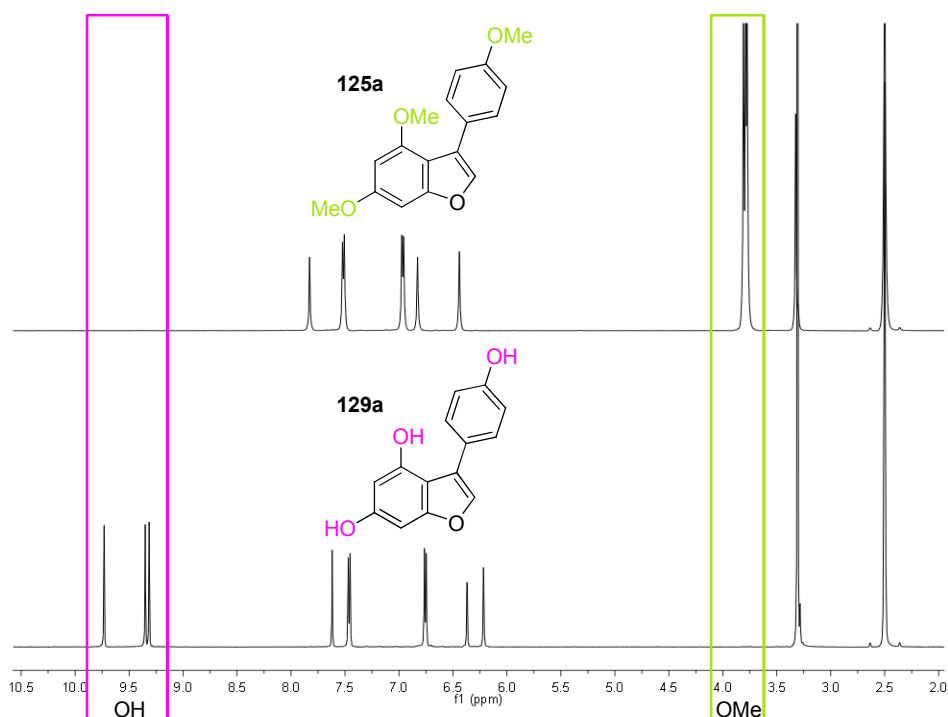


Figure 3.53. $^1\text{H-NMR}$ spectra (500 MHz, DMSO-d_6) of **125a** (above) and **129a** (below). Aromatic –OMe and –OH regions are highlighted in light green and pink, respectively.

3.4.3. Conclusions

From this section, in which the preparation of polyhydroxylated benzo[*b*]furans via BBr₃-mediated demethylation of pre-existing methoxy groups is presented, the following conclusions can be extracted:

- Hydroxylated benzofurans **128** and **129** can be obtained in moderate to good yields from methoxylated precursors via ether cleavage using BBr₃. In general, the transformation performs with higher yields for 2-aryl benzofurans (transformation of **124** into **128**) than for 3-aryl ones (transformation of **125** into **129**).
- The higher the number of methoxy groups to be demethylated, the lower the yield of the reaction.
- In these transformations, compounds bearing fluorine substituents also perform with good yields.

Chapter 4:

Benzo[*b*]furans as Resveratrol Analogues: Biological Assays

4.1. Short introduction and objectives

4.2. Resveratrol overview

4.3. Enzymatic assays: modulation of SIRT1

4.3.1. General considerations: Sirtuins

4.3.2. Experimental procedure of the enzymatic assays

4.3.3. Results and discussion of the enzymatic assays

4.3.4. Controversy: uncertain validity of the fluorescence assays

4.4. Cell-based assays: anticancer properties

4.4.1. General considerations: Cancer

4.4.2. Experimental procedures of the cell-based assays

4.4.3. Results and discussion of the cell-based assays

4.4.4. Graphical overview

4.5. Conclusions

4.1. SHORT INTRODUCTION and OBJECTIVES

In the search for resveratrol and other polyhydroxy stilbene analogues, the hydroxylated benzofurans prepared in section 3.4. constitute a new family of candidates, extending the collection of analogues previously synthesized in our research group. The project started with an iminic mimetic (called azaresveratrol) and continued with the 1*H*-pyrrole and 1*H*-indole analogues (**197b** and **156b**), in an attempt to avoid the possible *cis-trans* isomerization of the double bond present in stilbene and stilbene-like structures by using aromatic heterocyclic scaffolds. Encouraged by the positive results obtained from the biological assays carried out for these compounds²⁵⁷, the aromatic spacer proposed this time was the oxygenated heteroaromatic bicyclic version of the indole, the benzofuran (Figure 4.1).

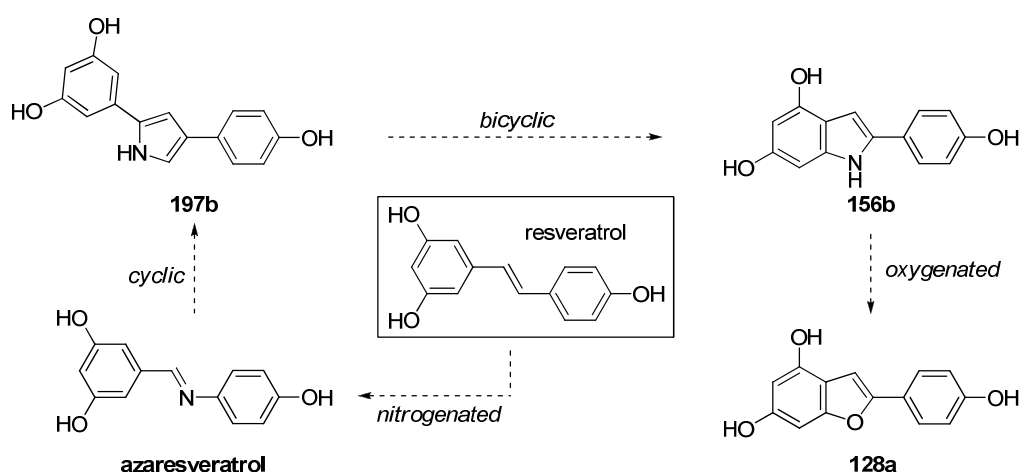


Figure 4.1. Resveratrol analogues proposed in our research group.

In figure 4.2.A the high structural analogy between *trans*-stilbene and 2-aryl benzofuran families can be observed. In order to check whether our candidates could present properties analogous to those of resveratrol, the distances between the carbons that connect the two phenyl groups and the carbons that bear hydroxy substituents were calculated, obtaining very similar values for both families (Figure 4.2.C).

Besides, electronic parameters of resveratrol and hydroxylated benzofuran series lead compound **128a** were studied, which also showed a notable resemblance between both

²⁵⁷ (a) Cossio, F. P.; Aldaba, E.; Vara, Y. I.; Zubia, A.; Vivanco, S.; Mendoza, M. L.; Salado, C.; Gallot, N.; Vidal, F. Patent WO 2006/108864 A2, PCT/EP2006/061565 (b) Aldaba, E. *Nuevas aplicaciones de las cicloadiciones [3+2] en la preparación de compuestos de interés en biomedicina y ciencias de materiales* Doctoral Thesis, Universidad del País Vasco, Donostia – San Sebastián, **2006** (c) Vara, Y.I. *Síntesis convergente y aplicaciones de nuevas familias de pirrolidinas e indoles* Doctoral Thesis, Universidad del País Vasco, Donostia – San Sebastián, **2008**

compounds when looking at the electrostatic potential projected onto the electron density (Figure 4.2.D). The benzofuran scaffold was therefore promising, with the additional advantage, over the nitrogen heterocyclic models proposed before, of avoiding the presence of acidic NH groups.

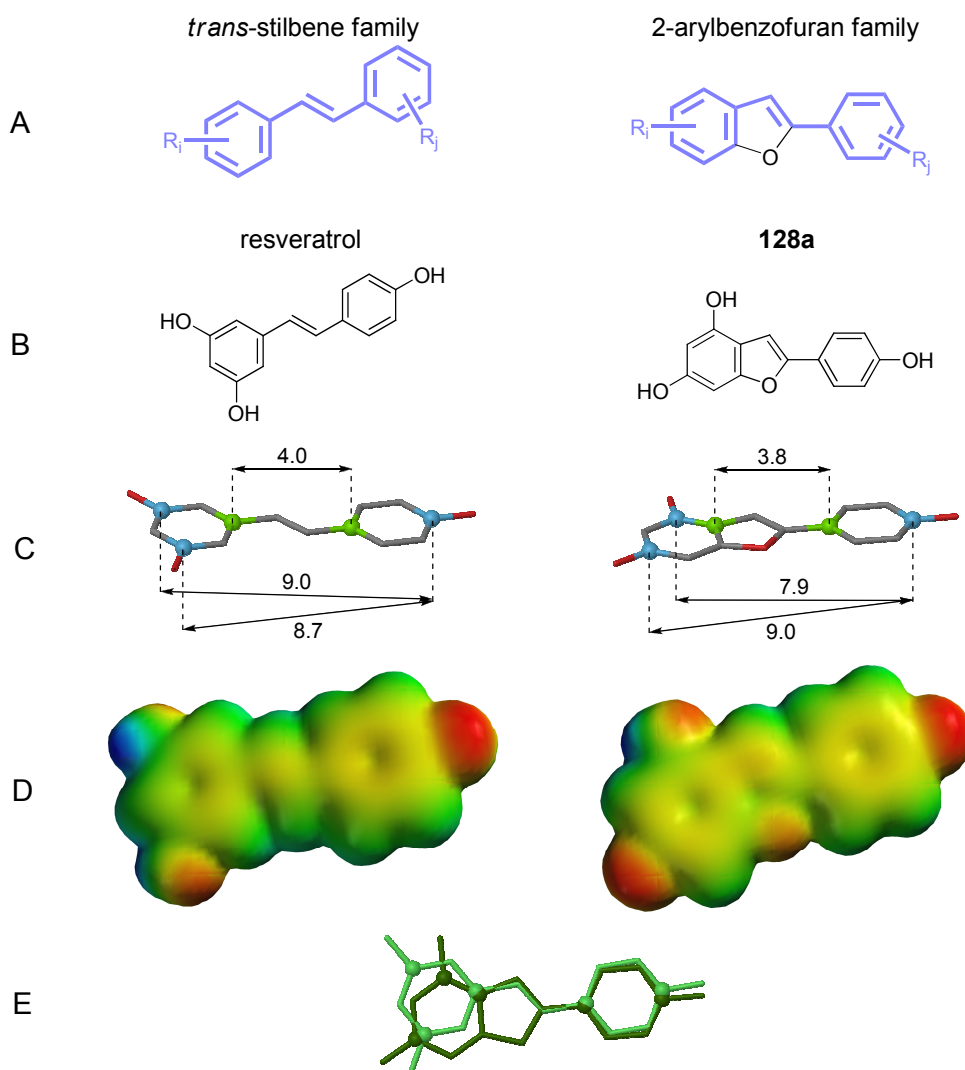


Figure 4.2. (A) Structural analogy between *trans*-stilbene and 2-aryl benzofuran families. (B) Structures of resveratrol and lead compound **128a**, 2-(4-hydroxyphenyl)benzofuran-4,6-diol. (C) Optimized (semi-empirical PM3 method) structures of resveratrol and compound **128a**; light green and blue spheres indicate the carbon atoms bound to the central structure and the ones that bear hydroxy groups, respectively; distances are given in Å. (D) Fully optimized structures of resveratrol and **128a** showing the electrostatic potential projected onto the electron density. Negative and positive potentials are given in red and blue, respectively. (E) Superposition of the optimized structures of resveratrol (light green) and compound **128a** (dark green).

Taking all this into account, the objective of this chapter is to assess whether this new family of arylbenzofurans could retain (or even improve) some of the pharmacological properties of resveratrol, which are considered straightaway (Section **4.2. Resveratrol overview**). For so doing, two type of biological assays were proposed:

- i) Enzymatic assays to test the ability of the compounds to modulate (activate or inhibit) the activity of SIRT1 (Section **4.3. Enzymatic assays: modulation of SIRT1**).
- ii) Cell-based assays to study the anticancer properties of the compounds at different stages of cancer. These included tumor cell adhesion assays, tumor cell proliferation assays and tumor cell migration assays (Section **4.4. Cell-based assays: anticancer properties**).

4.2. RESVERATROL OVERVIEW

Getting to know resveratrol

Resveratrol, 3,5,4'-trihydroxystilbene, exists as two diastereomeric forms, *cis* (*Z*) and *trans* (*E*), being the last one preferred in nature, relatively more stable and the one to which most of its biological activities are attributed²⁵⁸. For these reasons, unless otherwise specified, the term resveratrol is generally used to refer only to the *trans* isomer. This compound is classified as a phytoalexin, a substance synthesized *de novo* by plants in response to a stress, injury, ultraviolet irradiation and/or fungal infection. It was first isolated from the roots of white hellebore (*Veratrum grandiflorum* O. Loes) in 1940 and, from then on, its presence has been detected in a great variety of plants including dietary sources such as grapes (*Vitis vinifera*) and their derivatives (red wine, other wines and grape juices), peanuts (*Arachis hypogaea*) and mulberries (*Morus rubra*), to name a few (Figure 4.3)^{258,259}.

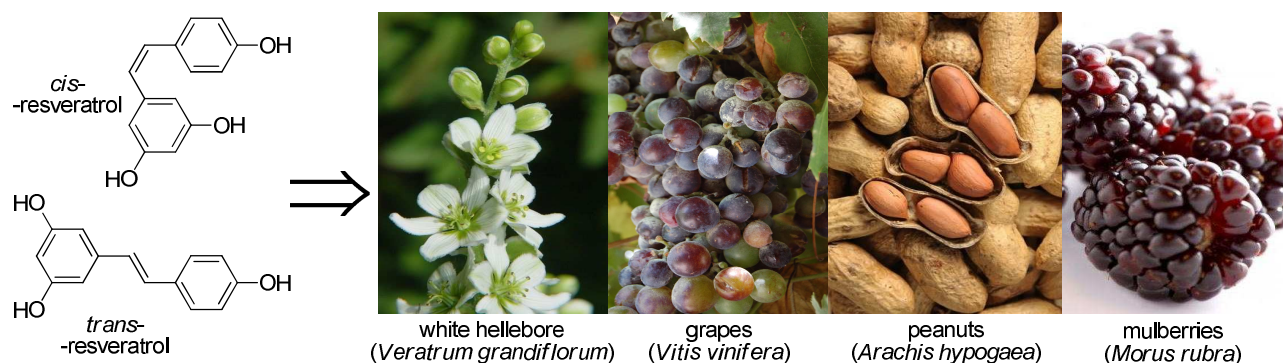


Figure 4.3. Structures of *cis* and *trans* resveratrol and some of their natural sources.

Despite being known for over half a century, it was not until the nineties that its popularity began to spectacularly grow, boosted by the publication of its metabolic effects as inhibitor of human LDL oxidation in 1993²⁶⁰, and the first report of its cancer chemopreventive activity at three major stages of carcinogenesis (initiation, progression, and proliferation, addressed in section 4.4.1) in 1997²⁶¹. From then on, the studies on resveratrol and its biological activities have increased (and are still increasing) extraordinarily, as it is shown

²⁵⁸ (a) Aggarwal, B. B.; Bhardwaj, A.; Aggarwal, R. S.; Seeram, N. P.; Shishodia, S.; Takada, Y. *Anticancer Res.* **2004**, *24*, 2783-2840 (b) Anekonda, T. S. *Brain Res. Rev.* **2006**, *52*, 316-326 (c) Quideau, S.; Defieux, D.; Pouységou, L. *Angew. Chem. Int. Ed.* **2012**, *51*, 6824-6826

²⁵⁹ (a) Borriello, A.; Cucciolla, V.; Della Ragione, F.; Galletti, P. *Nutr. Metab. Cardiovasc. Dis.* **2010**, *20*, 618-625 (b) Li, H.; Xia, N.; Förstermann, U. *Nitric Oxide* **2012**, *26*, 102-110

²⁶⁰ Frankel, E. N.; Waterhouse, A. L.; Kinsella, J. E. *Lancet* **1993**, *341*, 1103-1104

²⁶¹ Jang, M.; Cai, L.; Udeani, G. O.; Slowing, K. V.; Thomas, C. F.; Beecher, C. W. W.; Fong, H. H. S.; Farnsworth, N. R.; Kinghorn, A. D.; Mehta, R. G.; Moon, R. C.; Pezzuto, J. M. *Science* **1997**, *275*, 218-220

in the evolution of the number of publications related to “resveratrol” in scientific databases (Figure 4.4).

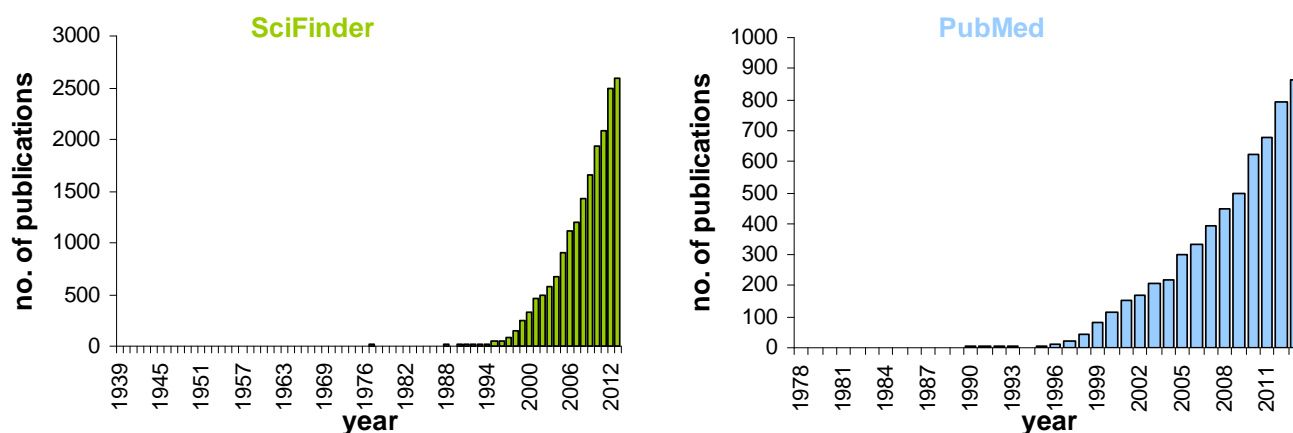


Figure 4.4. Timeline of the scientific publications related to “resveratrol” using SciFinder²⁶² and PubMed²⁶³ databases as sources.

Another milestone in this line was the finding of the ability of resveratrol to activate sirtuins (issue covered in section 4.3.1) and mimic calorie or dietary restriction regimes (CR or DR, hereafter), reported in 2003²⁶⁴. CR can be roughly defined as the reduction of caloric intake in the absence of malnutrition (maintaining essential nutrient requirements) and it has been shown to increase not only lifespan in a variety of organisms²⁶⁵ (including mammals^{265a}), but also the period of life spent in relatively good health (free of age-associated diseases)^{264,266}. In this line, resveratrol was proposed as a CR mimetic^{258b,264,266,267} due to its ability to induce lifespan extension in organisms on a regular diet but not to further increase CR-induced lifespan extension, which suggests that both resveratrol and CR may use similar pathways²⁶⁴.

²⁶² SciFinder is a Chemical Abstracts Service (CAS) database of chemical and bibliographic information from many scientific disciplines including chemistry, biomedical sciences, engineering, materials science, agricultural science and more.

²⁶³ PubMed is a free database accessing primarily the Medline database of references and abstracts on life sciences and biomedical topics, including medicine, nursing, pharmacy, dentistry, veterinary medicine, health care, biology, biochemistry and molecular evolution.

²⁶⁴ Howitz, K. T.; Bitterman, K. J.; Cohen, H. Y.; Lamming, D. W.; Lavu, S.; Wood, J. G.; Zipkin, R. E.; Chung, P.; Kisielewski, A.; Zhang, L.-L.; Scherer, B.; Sinclair, D. A. *Nature* **2003**, *425*, 191-196

²⁶⁵ (a) Sohal, R. S.; Weindruch, R. *Science* **1996**, *273*, 59-63 (b) Lin, S.-J.; Kaeberlein, M.; Andalis, A. A.; Sturtz, L. A.; Defossez, P.-A.; Culotta, V. C.; Fink, G. R.; Guarente, L. *Nature* **2002**, *418*, 344-348 (c) Koubova J.; Guarente, L. *Genes Dev.* **2003**, *17*, 312-321 (d) Cantó, C.; Auwerx, J. *Trends Endocrinol. Metab.* **2009**, *20*, 325-331

²⁶⁶ Pallàs, M.; Junyent, F.; Verdaguer, E.; Beas-Zarate, C.; Camins, A. *Drug. Discov. Today Ther. Strateg.* **2010**, *7*, 51-56

²⁶⁷ (a) Wood, J. G.; Rogina, B.; Lavu, S.; Howitz, K.; Helfand, S. L.; Tatar, M.; Sinclair, D. *Nature* **2004**, *430*, 686-689 (b) Baur, J. A.; Sinclair, D. A. *Nat. Rev. Drug Discov.* **2006**, *5*, 493-506 (c) Pallàs, M.; Casadesús, G.; Smith, M. A.; Coto-Montes, A.; Pelegri, C.; Vilaplana, J.; Camins, A. *Curr. Neurovasc. Res.* **2009**, *6*, 70-81

Biological activity of resveratrol

Since both activation of sirtuins and CR mimicking are related to beneficial effects in aging, resveratrol is a promising molecule for aging related conditions, in its widest sense (Figure 4.5).

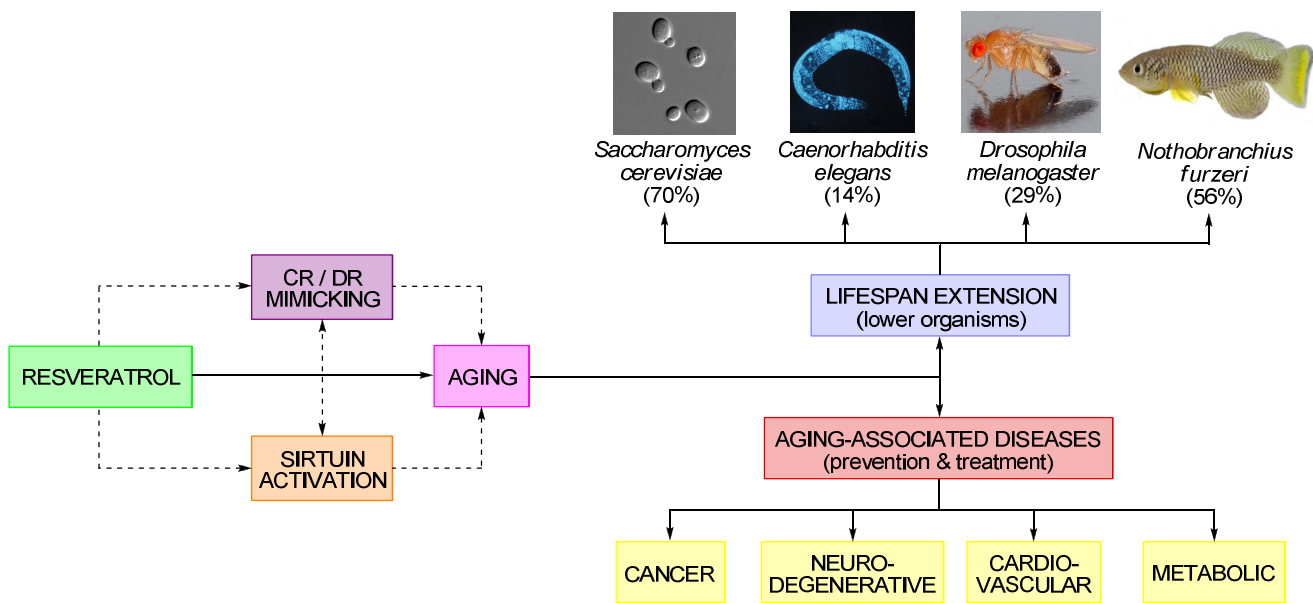


Figure 4.5. Rough scheme of the effect of resveratrol in aging: lifespan extension and aging-related diseases.

On the one hand, resveratrol has successfully been used to extend the lifespan of lower organisms in an apparently sirtuin-dependent manner. These species include *Saccharomyces cerevisiae* (yeast) with a lifespan extension of 70%²⁶⁴, *Caenorhabditis elegans* (nematode, worm) with 14%, *Drosophila melanogaster* (fruit fly) with 29%^{267a} or *Nothobranchius furzeri* (short-lived species of fish) with 56%²⁶⁸, although the implications of sirtuins in the last case was not sure.

On the other hand, it has proven effective in the prevention and treatment of important aging-associated diseases (diseases whose incidence increases rapidly with aging) such as cancer, neurodegenerative diseases, including stroke, Alzheimer's disease (AD), Parkinson's disease (PD), Huntington's disease (HD), cardiovascular dysfunctions, and metabolic disorders, such as diabetes and obesity. These results are of special relevance taking into account that ischemic heart disease, stroke and cerebrovascular disease, trachea, bronchus and lung cancers and diabetes mellitus were listed by the World Health

²⁶⁸ Valenzano, D. R.; Terzibasi, E.; Genade, T.; Cattaneo, A.; Domenici, L.; Cellerino, A. *Curr. Biol.* **2006**, *16*, 296-300

Organization (WHO) among the ten leading causes of death worldwide in 2008, with a higher incidence in middle and high-income countries²⁶⁹.

The promising anticancer properties of resveratrol include blockage of carcinogen activation by inhibiting phase I metabolic enzymes, induction of the expression of phase II carcinogen detoxifying metabolic enzymes^{270,271}, arrest of cell proliferation by modulating cell cycle regulatory machinery^{258a,267b,271} and inducing apoptosis of damaged or transformed cells^{267b,271,272}, inhibition of angiogenesis or neovascularisation in tumor tissues^{258a,271} and suppression of invasion and metastasis, among others.

On looking at its utility in neurodegenerative diseases, and bearing in mind that it can cross blood-brain barrier and reach the brain tissue rapidly²⁷³, resveratrol leads to the protection of neurons from oxidants^{267c,274}, the increase of mitochondrial number and function²⁷⁴, the prevention of apoptotic death of neurons (through different pathways)^{258b,267c}, the suppression of neuroinflammation²⁷³, the reduction in the secretion of amyloid- β peptides (A β)^{258b,273,274} and the promotion of intracellular degradation of them (relevant in AD)²⁷², the rescue of neuronal dysfunction caused by polyQ toxicity (relevant in HD)²⁷², and other features.

The beneficial effects of resveratrol in cardiovascular dysfunctions were somehow implied in the so-called “French paradox”, namely the lower incidence of coronary heart diseases among French people having a diet rich in saturated fats but drinking red wine on a regular basis^{258b-c,273}, since the favorable influence of drinking red wine has largely been attributed to its content in this polyphenol. The main of these effects could be listed as follows: inhibition or suppression of platelet aggregation^{258a,259a-b,267b,272,273,275}, prevention of atherosclerosis; vasodilatation or vasorelaxation^{258a,259a,267b,272,275}, reduction of blood

²⁶⁹ The top ten causes of death, available at WHO (World Health Organization) website, fact sheet n. 310, updated July 2013, <<http://who.int/mediacentre/factsheets/fs310/en/index.html>>

²⁷⁰ Roughly, phase I metabolic enzymes oxidize, reduce, hydrolyze foreign molecules to render them more polar and facilitate their excretion; e. g. cytochrome P450, CYP enzymes and phase II metabolic enzymes metabolically (typically glucuronic acid, sulphate and methyl conjugations) detoxify harmful molecules, including toxic products; e.g. glutathione S-transferase (GST), glutathione peroxidase (GPx), UDP glucuronosyl transferase (UGT)-1A, NADPH: quinone oxidoreductase (NQO), heme oxygenase-1 (HO-1), glutamate cysteine ligase (GCL), from ref. 271

²⁷¹ Kundu, J. K.; Surh, Y.-J. *Cancer Lett.* **2008**, *269*, 243-261

²⁷² Saiko, P.; Szakmary, A.; Jaeger, W.; Szekeres, T. *Mutat. Res.* **2008**, *658*, 68-94

²⁷³ Sun, A. Y.; Wang, Q.; Simonyi, A.; Sun, G. Y. *Mol. Neurobiol.* **2010**, *41*, 375-383

²⁷⁴ Farooqui, T.; Farooqui, A. A. *Mech. Ageing Dev.* **2009**, *130*, 203-215

²⁷⁵ Frémont, L. *Life Sci.* **2000**, *66*, 663-673

pressure (hypertension) and cardiac hypertrophy^{259b}; reduction of oxidative stress^{259a,276}, due to its antioxidant properties^{258a,c,267b,275}; inhibition of vascular inflammation^{259b}, due to its anti-inflammatory properties^{258a,267b}; protection and maintenance of intact endothelium^{259a,272}; induction of neovascularisation of infarcted myocardium^{259a}; and protection of heart against ischemia/reperfusion injury^{259b,267b,272}.

The influence of resveratrol in metabolic disorders²⁷⁷ is mainly a consequence of its antioxidant properties and its ability to modulate lipid and lipoprotein metabolism (prevention of LDL oxidation)^{267b,272,275}. In diabetes its effects involve, for example, the improvement of glucose homeostasis^{277c-d} and reduction of blood glucose^{277a,d}; the amelioration of insulin sensitivity^{277b-c,278}, and action and the preservation of β cells, whose metabolic changes result in inhibition of insulin secretion^{277d}.

Combining both lifespan extension and aging-associated diseases treatment, resveratrol has also been claimed to rescue SIRT1-dependent adult stem cell decline and alleviate progeroid features in laminopathy-based progeria, a severe form of early-onset premature aging in which affected people eventually die, mainly due to cardiovascular diseases, at an average age of 14-15 years²⁷⁹.

As a polyphenol, resveratrol bears a marked antioxidant character which might be, to a certain extent, responsible for most of its biological effects. The precise mechanisms through which resveratrol exerts its influence, however, are not completely clear and to summarize all of them and their potential applications is not an easy task. Paradoxically, at first glance, some of the beneficial effects of resveratrol seem contradictory²⁸⁰. This has been attributed to the ability of resveratrol to cause opposed effects depending on the cell

²⁷⁶ Baur, J. A. *Mech. Ageing Dev.* **2010**, *131*, 261-269

²⁷⁷ (a) Su, H.-C.; Hung, L.-M.; Chen, J.-K. *Am. J. Physiol. Endocrinol. Metab.* **2006**, *290*, e1339-e1346 (b) Lagouge, M.; Argmann, C.; Gerhart-Hines, Z.; Meziane, H.; Lerin, C.; Daussin, F.; Messadeq, N.; Milne, J.; Lambert, P.; Elliott, P.; Geny, B.; Laakso, M.; Puigserver, P.; Auwerx, J. *Cell* **2006**, *127*, 1109-1122 (c) Milne, J. C.; Lambert, P. D.; Schenk, S.; Carney, D. P.; Smith, J. J.; Gagne, D. J.; Jin, L.; Boss, O.; Perni, R. B.; Vu, C. B.; Bemis, J. E.; Xie, R.; Disch, J. S.; Ng, P. Y.; Nunes, J. J.; Lunch, A. V.; Yang, H.; Galonek, H.; Israelian, K.; Choy, W.; Iffland, A.; Lavu, S.; Medvedik, O.; Sinclair, D. A.; Olefsky, J. M.; Jirousek, M. R.; Elliott, P.; Westphal, C. H. *Nature* **2007**, *450*, 712-716 (d) Szkudelski, T.; Szkudelska, K. *Ann. N.Y. Acad. Sci.* **2011**, *1215*, 34-39

²⁷⁸ Baur, J. A.; Pearson, K. J.; Price, N. L.; Jamieson, H. A.; Lerin, C.; Kalra, A.; Prabhu, V. V.; Allard, J. S.; Lopez-Lluch, G.; Lewis, K.; Pistell, P. J.; Poosala, S.; Becker, K. G.; Boss, O.; Gwinn, D.; Wang, M.; Ramaswamy, S.; Fishbein, K. W.; Spencer, R. G.; Lakatta, E. G.; Le Couteur, D.; Shaw, R. J.; Navas, P.; Puigserver, P.; Ingram, D. K.; de Cabo, R.; Sinclair, D. A. *Nature* **2006**, *444*, 337-342

²⁷⁹ Liu, B.; Ghosh, S.; Yang, X.; Zheng, H.; Liu, X.; Wang, Z.; Jin, G.; Zheng, B.; Kennedy, B. K.; Suh, Y.; Kaeberlein, M.; Tryggvason, K.; Zhou, Z. *Cell Metab.* **2012**, *16*, 738-750

²⁸⁰ Deng, C.-X. *Int. J. Biol. Sci.* **2009**, *5*, 147-152

type (cancer cell, neural cell), the cellular conditions (normal or stress) and the concentration (dose)^{259b,272,273}.

Bioavailability of resveratrol

Despite the therapeutic potential of resveratrol presented so far, the results obtained from several pharmacokinetic studies indicate that circulating resveratrol is rapidly metabolized and has low bioavailability. As a polyphenol, it undergoes extensive phase I (oxidation, reduction and hydrolyses) and phase II (glucuronic acid, sulphate and methyl conjugations) biochemical changes immediately after ingestion^{258b}. Different analysis reveal that resveratrol itself has a short initial half life, of about 15 min in blood stream^{267b,272}, whilst its metabolites (mainly sulphated and glucorinated forms^{258b,267b,272}, converted within about 30 min in humans after oral or intravenous injection) are detectable up to 9 hours after in serum, thus suggesting that the metabolites might also be responsible for its biological activities²⁷².

In fact, some of the properties listed above have also been observed in other polyphenols present in red wine and other natural sources such as quercetin, resveratrol derivatives like piceid (resveratrol-3-O- β -D-glucoside, polydatin) or ϵ -viniferin (a dimer of resveratrol) and resveratrol metabolites resveratrol-3-sulphate, resveratrol-3-O-glucuronide and dihydroresveratrol^{267b,281} (Figure 4.6).

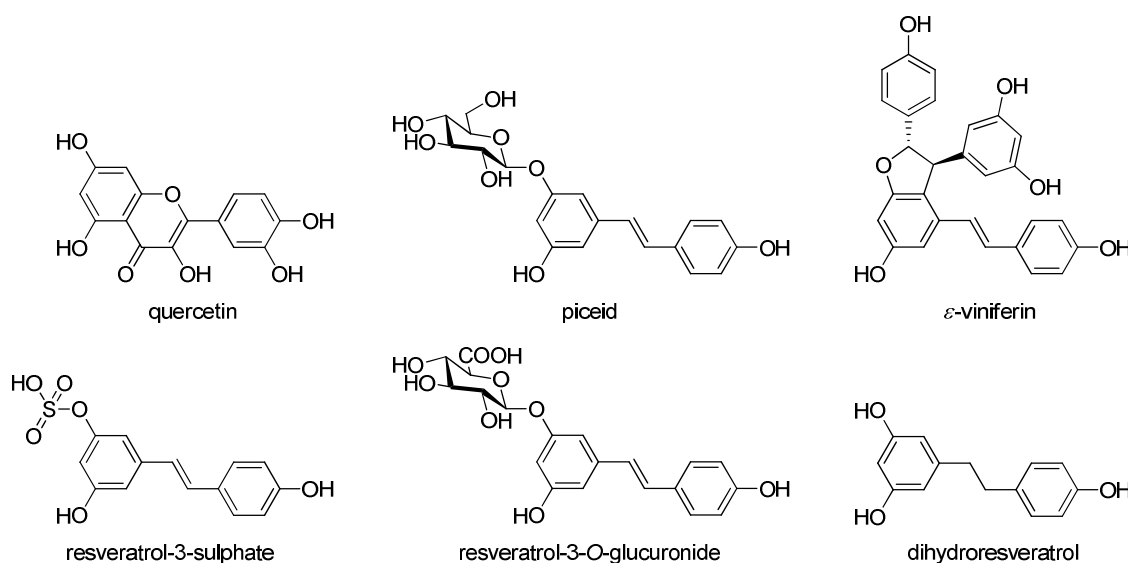


Figure 4.6. Structures of other polyphenols present in red wine and resveratrol derivatives and metabolites^{267b,281}.

²⁸¹ Piver, B.; Berthou, F.; Dreano, Y.; Lucas, D. *Life Sci.* **2003**, 73, 1199-1213

Resveratrol analogues

Prompted by these findings, there has been an extensive search for resveratrol analogues that could reproduce (or even enhance) its beneficial properties. In this line, several substituted *trans*-stilbenes (typically –OH and –OMe but also –NH₂, –SH, –F, etc.) of both natural (pterostilbene²⁸², piceatannol²⁸³ and isorhapontigenin²⁸⁴ for example) and synthetic origin²⁸⁵ and compounds with analogue frameworks (*trans*-styrylpyridines²⁸⁶, for example) have proved to be interesting candidates for the discovery of new chemopreventive and therapeutic treatments of aging-associated diseases.

In general it can be said, that most synthetic analogues of resveratrol conserve the stilbene structure, along with the problems of bioavailability and pharmacokinetic profile associated with it. Nevertheless, in order to overcome the inherent configurational instability of this scaffold, aromatic and heteroaromatic compounds have been proposed as linking structures between the two aryl moieties of resveratrol, giving rise to naphthalene²⁸⁷, pyrrole and indole²⁵⁷ analogues (Figure 4.7).

²⁸² Tolomeo, M.; Grimaudo, S.; Di Cristina, A.; Roberti, M.; Pizzirani, D.; Meli, M.; Dusonchet, L.; Gebbia, N.; Abbadessa, V.; Crosta, L.; Barucchello, R.; Grisolia, G.; Invidiata, F.; Simoni, D. *Int. J. Chem. Cell Biol.* **2005**, *37*, 1709-1726

²⁸³ (a) Hung, L.-M.; Chen, J.-K.; Lee, R.-S.; Liang, H.-C.; Su, M.-J. *Free Radical Biol. Med.* **2001**, *30*, 877-883 (b) Potter, G. A.; Patterson, L. H.; Wanogho, E.; Perry, P. J.; Butler, P. C.; Ijaz, T.; Ruparella, K. C.; Lamb, J. H.; Farmer, P. B.; Stanley, L. A.; Burke, M. D. *Brit. J. Cancer* **2002**, *86*, 774-778

²⁸⁴ Liu, Y.; Liu, G. *Biochem. Pharmacol.* **2004**, *67*, 777-785

²⁸⁵ (a) Eddarir, S.; Abdelhadib, Z.; Rolandoa, C. *Tetrahedron Lett.* **2001**, *42*, 9127-9130 (b) Kim, S.; Ko, H.; Park, J. E.; Jung, S.; Lee, S. K.; Chun, Y.-J. *J. Med. Chem.* **2002**, *45*, 160-164 (c) Roberti, M.; Pizzirani, D.; Simoni, D.; Rondanin, R.; Barucchello, R.; Bonora, C.; Buscemi, F.; Grimaudo, S.; Tolomeo, M. *J. Med. Chem.* **2003**, *46*, 3546-3554 (d) Murias, M.; Handler, N.; Erker, T.; Pleban, K.; Ecker, G.; Saiko, P.; Szekeres, T.; Jäger, W. *Bioorg. Med. Chem.* **2004**, *12*, 5571-5578 (e) Amorati, R.; Lucarini, M.; Mugnaini, V.; Pedulli, G. F.; Roberti, M.; Pizzirani, D. *J. Org. Chem.* **2004**, *69*, 7101-7107

²⁸⁶ Chen, G.; Shan, W.; Wu, Y.; Ren, L.; Dong, J.; Ji, Z. *Chem. Pharm. Bull.* **2005**, *53*, 1587-1590

²⁸⁷ Minutolo, F.; Sala, G.; Bagnacani, A.; Bertini, S.; Carboni, I.; Placanica, G.; Prota, G.; Rapposelli, S.; Sacchi, N.; Macchia, M.; Ghidoni, R. *J. Med. Chem.* **2005**, *48*, 6783-6786

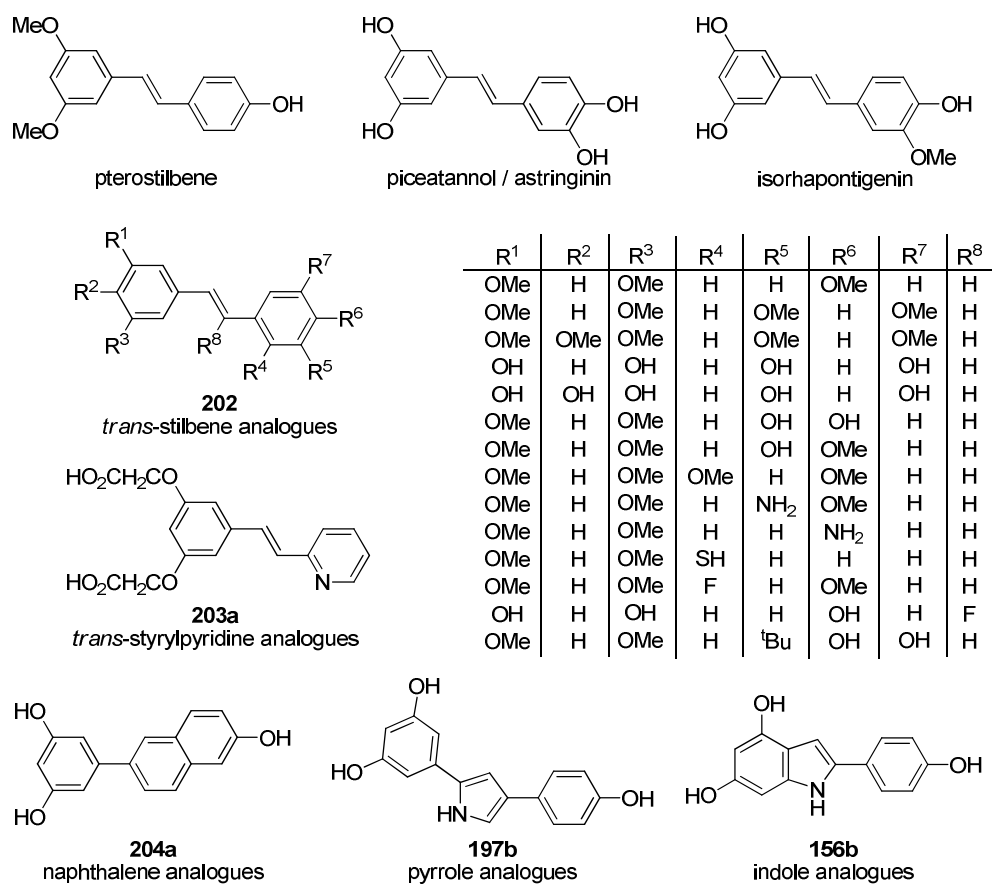


Figure 4.7. Examples of natural and synthetic analogues of resveratrol^{283-288, 257}.

4.3. ENZYMATIC ASSAYS: MODULATION OF SIRT1

4.3.1. General considerations: sirtuins

Among the different mechanisms by which CR may act, sirtuin regulation has been the most widely proposed pathway^{258b,264,266,267a-b,274} and resveratrol has been described both as a CR (calorie restriction) mimetic and as a sirtuin activator^{258b,264,266,267,273,274,277b,288}.

Getting to know sirtuins

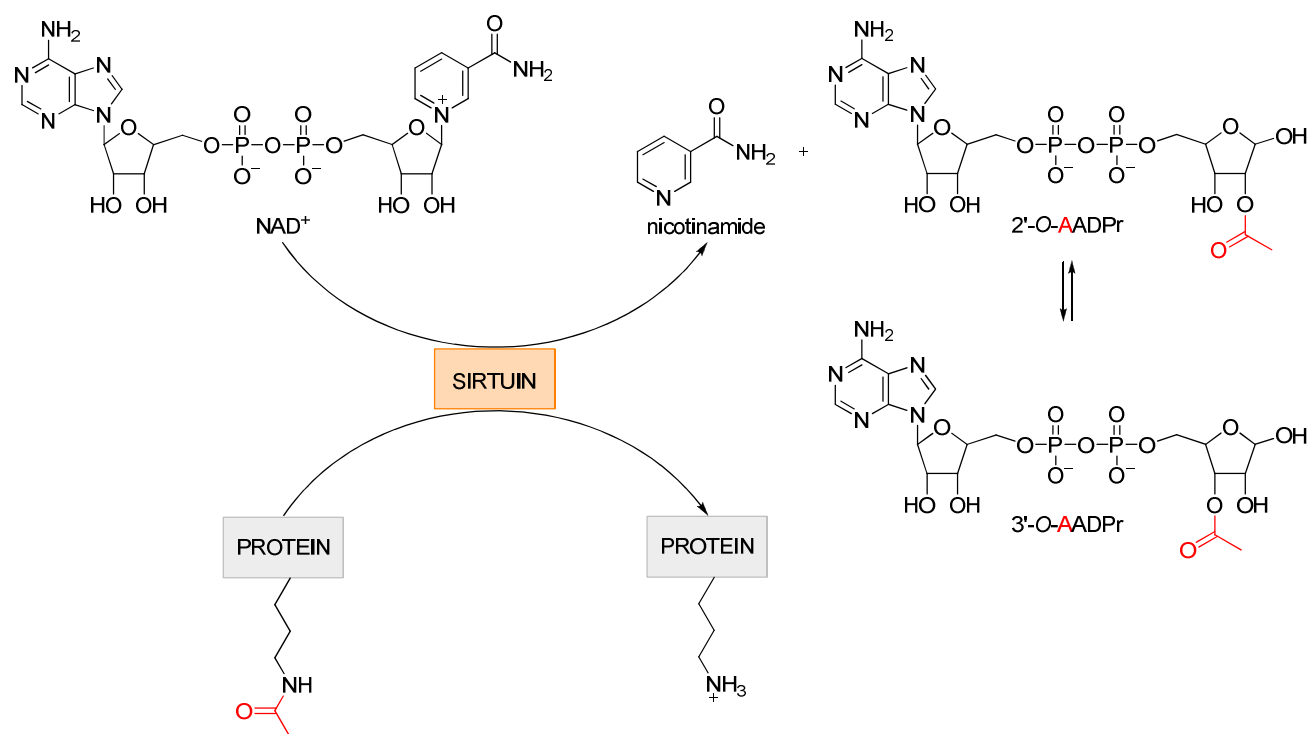
Sirtuins or Sir2 proteins constitute the class III histone deacetylases (HDACs). The protein that gives name to this family is the silent information regulator 2, Sir2 protein, which was first discovered in yeasts. They are highly phylogenetically conserved proteins from bacteria (*Escherichia coli*) to humans and up to seven mammal homologues have been described for Sir2 (SIRT1-7), being SIRT1 considered the closest Sir2 orthologue and, therefore, the most extensively studied one up to date^{258b,265b,266,267b,289}.

These HDAC enzymes cleave acetyl groups from acetylated lysine residues of histone and non-histone substrates. Unlike class I and class II HDACs, which are Zn²⁺-dependent and produce acetate, sirtuins depend on nicotinamide adenine dinucleotide (NAD⁺) for their catalytic activity and their deacetylation reaction produces deacetylated proteins, nicotinamide and the novel metabolite 2'-O-acetyl-ADP-ribose (2'-OAADPr), which spontaneously equilibrates with its regioisomer 3'-O-acetyl-ADP-ribose (3'-OAADPr) through transesterification (Scheme 4.1)^{289a,c,e-f,290}.

²⁸⁸ (a) Hou, X.; Xu, S.; Maitland-Toolan, K. A.; Sato, K.; Jiang, B.; Ido, Y.; Lan, F.; Walsh, K.; Wierzbicki, M.; Verbeuren, T. J.; Cohen, R. A.; Zang, M. *J. Biol. Chem.* **2008**, *283*, 20015-20026 (b) Ramadori, G.; Gautron, L.; Fujikawa, T.; Vianna, C. R.; Elmquist, J. K.; Coppari, R. *Endocrinology* **2009**, *150*, 5326-5333 (c) Tang, B. L. *Brain Res. Bull.* **2010**, *81*, 359-361

²⁸⁹ (a) Denu, J. M. *Curr. Opin. Chem. Biol.* **2005**, *9*, 431-440 (b) Kaeberlein, M.; McDonagh, T.; Heltweg, B.; Hixon, J.; Westman, E. A.; Caldwell, S. D.; Napper, A.; Curtis, R.; DiStefano, P. S.; Fields, S.; Bedalov, A.; Kennedy, B. K. *J. Biol. Chem.* **2005**, *280*, 17038-17045 (c) Borra, M. T.; Smith, B. C.; Denu, J. M. *J. Biol. Chem.* **2005**, *280*, 17187-17195 (d) Pallàs, M.; Verdaguer, E.; Tajés, M.; Gutierrez-Cuesta, J.; Camins, A. *Recent Pat. CNS Drug Discov.* **2008**, *3*, 61-69 (e) Lawson, M.; Uciechowska, U.; Schemies, J.; Rumpf, T.; Jung, M.; Sippl, W. *Biochim. Biophys. Acta* **2010**, *1799*, 726-739 (f) Baur, J. A. *Biochim. Biophys. Acta* **2010**, *1804*, 1626-1634

²⁹⁰ Porcu, M.; Chiarugi, M. *Trends Pharmacol. Sci.* **2005**, *26*, 94-103



Scheme 4.1. Sirtuin-operated NAD⁺-dependent protein deacetylation reaction. Acetyl group is highlighted in red color.

Biological activity of sirtuins

Promotion of survival and stress resistance in times of adversity has been claimed to be the main function of sirtuins^{267b-c}. They are implicated in several important cellular processes including genomic stability (DNA repair, rDNA recombination, transcriptional silencing), cell cycle regulation (including senescence and apoptosis, or programmed cell death) and metabolism (adipogenesis, fatty acid metabolism, lipid mobilization, glucose homeostasis, insulin secretion)^{258b,267a,289a-d,291}. For so doing, *in vivo* sirtuins (and resveratrol-induced SIRT-1 activity) deploy a complex net of biochemical events and trigger cascades which result in the modulation of the activity of many enzymes and the regulation of the expression of several nuclear factors. Some of the most widely reported targets of resveratrol (and their subsequent effects and possible applications to aging-associated diseases) are shown in figure 4.8.

²⁹¹ Beher, D.; Wu, J.; Cumine, S.; Kim, K. W.; Lu, S.-C.; Atangan, L.; Wang, M. *Chem. Biol. Drug Des.* **2009**, *74*, 619-624

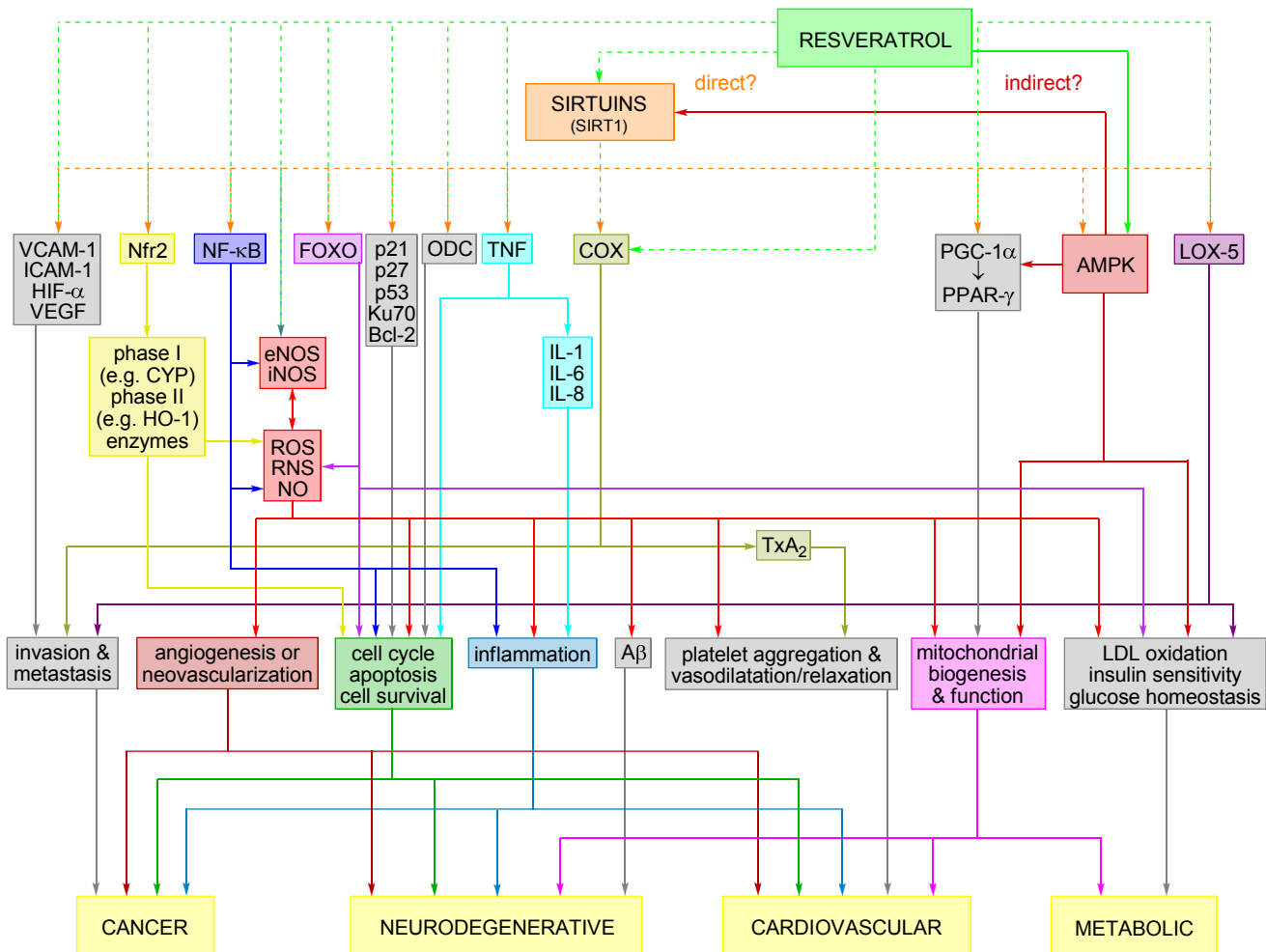


Figure 4.8. Some of the reported resveratrol and sirtuin targets (enzymes, substrates or interactors), acting pathways and diseases over which might have an effect (based on almost all the references cited so far in this chapter). Abbreviations: Sir2 = silent information regulator 2; SIRT1 = silent information regulator human homologue 1; VCAM-1 = vascular cell adhesion molecule 1; ICAM-1 = intercellular cell adhesion molecule 1; HIF- α = hypoxia inducible factor alpha; VEGF = vascular endothelial growth factor; Nfr2 = nuclear factor (erythroid-derived 2)-like factor 2; NF- κ B = nuclear factor kappa B; FOXO = FKRF = Forkhead transcription factor; p21 = cyclin-dependent kinase inhibitor 1; p27 = cyclin-dependent kinase inhibitor 1B; p53 = tumor suppressor protein 53; Ku70 = ATP-dependent DNA helicase 2 subunit 1; Bcl-2 = B-cell lymphoma 2; ODC = ornithine decarboxylase; TNF = tumor necrosis factor; COX = cyclooxygenase; PGC-1 α = PPAR- γ transcriptional coactivator; PPAR- γ = nuclear receptor peroxisome proliferator-activated receptor gamma; AMPK = AMP-activated protein kinase; AMP = 5'-adenosine monophosphate; LOX-5 = lipoxygenase 5; CYP = cytochrome P450; HO-1 = heme oxygenase 1; eNOS = endothelial nitric oxide synthase; iNOS = inducible nitric oxide synthase; ROS = reactive oxygen species; RNS = reactive nitrogen species; NO = nitric oxide; IL = interleukin; TxA₂ = thromboxane A₂; A β = amyloid beta peptide; LDL = low-density lipoprotein.

Sirtuin modulators

The major role that sirtuins may play on regulating so many important cellular processes awoke an extensive and enduring interest in understanding their regulatory mechanisms as well as in identifying natural or synthetic molecules (substrate and product analogues and small molecules) that modify their ability to deacetylate substrate proteins. Activation

and inhibition of SIRT1 may have different therapeutic applications²⁹⁴. In this line, for example, SIRT1 activation has proven useful as anti-aging²⁷⁸ strategy and in the treatment of type 2 diabetes^{277c}, whilst SIRT1 inhibition has been applied to the treatment of neurological disorders²⁹². Besides, SIRT1 modulators have also shown synergic activity with other agents²⁹³.

Reported sirtuin activators include, besides well-known resveratrol^{258b,264,266,273,274,277b-c,288,289a}, fisetin, butein and SRT1460, SRT1720 and SRT2183 members of the sirtris series^{277c}, among others (Figure 4.9).

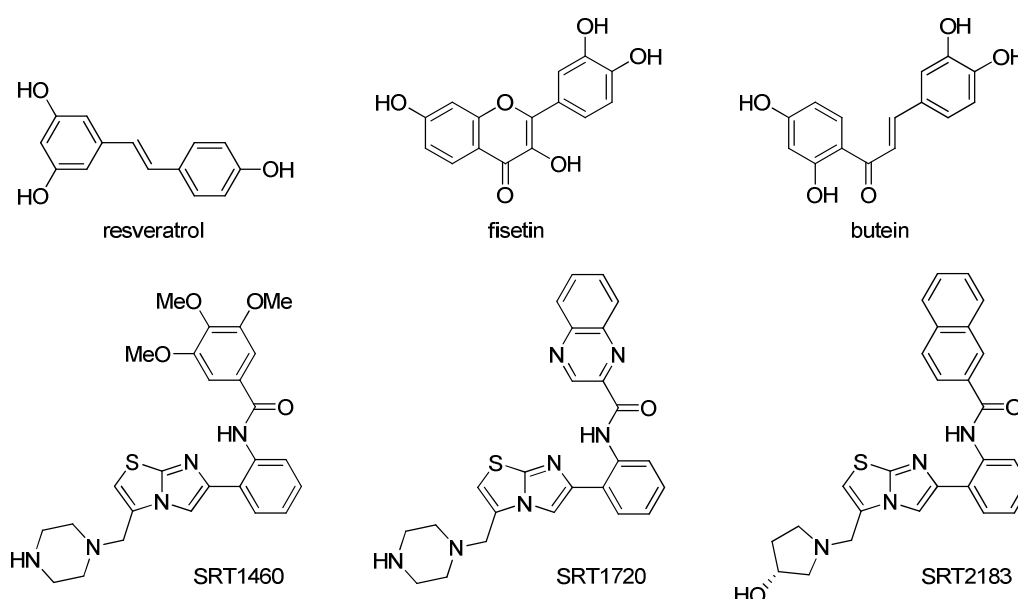


Figure 4.9. Examples of sirtuin activators.

In regard to negative modulation, nicotinamide is the endogenous inhibitor of these enzymes^{289a-c,e} although other compounds have also been described, such as splitomycin^{289a-c,e,294}, dihydrocoumarin²⁹⁵, some indole derivatives^{289e,296}, cambinol^{289e,297}, sirtinol^{289a-c,e,298}, salermide^{289e} and suramin (suramin sodium)^{289,299}, to name a few (Figure 4.10).

²⁹² Biacsi, R.; Kumari, D.; Usdin, K. *PLoS Genetics* **2008**, *4*, e1000017

²⁹³ Kojima, K.; Ohhashi, R.; Fujita, Y.; Hamada, N.; Akao, Y.; Nozawa, Y.; Deguchi, T.; Ito, M. *Biochem. Biophys. Res. Commun.* **2008**, *373*, 423-428

²⁹⁴ Bedalov, A.; Gattabont, T.; Irvine, W. P.; Gottschling, D. E.; Simon, J. A. *Proc. Natl. Acad. Sci. USA* **2001**, *98*, 15113-15118

²⁹⁵ Olaharski, A. J.; Rine, J.; Marshall, B. R.; Babiarz, J.; Zhang, L.; Verdin, E.; Smith, M. T. *PLoS Genet.* **2005**, *1*, e77

²⁹⁶ Napper, A. D.; Hixon, J.; McDonagh, T.; Keavey, K.; Pons, J.-F.; Barker, J.; Yau, W. T.; Amouzegh, P.; Flegg, A.; Hamelin, E.; Thomas, R. J.; Kates, M.; Jones, S.; Navia, M. A.; Saunders, J. O.; DiStefano, P. S.; Curtis, R. *J. Med. Chem.* **2005**, *48*, 8045-8054

²⁹⁷ Heltweg, B.; Gattabont, T.; Schuler, A. D.; Posakony, J.; Li, H.; Goehle, S.; Kollipara, R.; DePinho, R. A.; Gu, Y.; Simon, J. A.; Bedalov, A. *Cancer Res.* **2006**, *66*, 4368-4377

²⁹⁸ Grozinger, C. M.; Chao, E. D.; Blackwell, H. E.; Moazed, D.; Schreiber, S. L. *J. Biol. Chem.* **2001**, *276*, 38837-38843

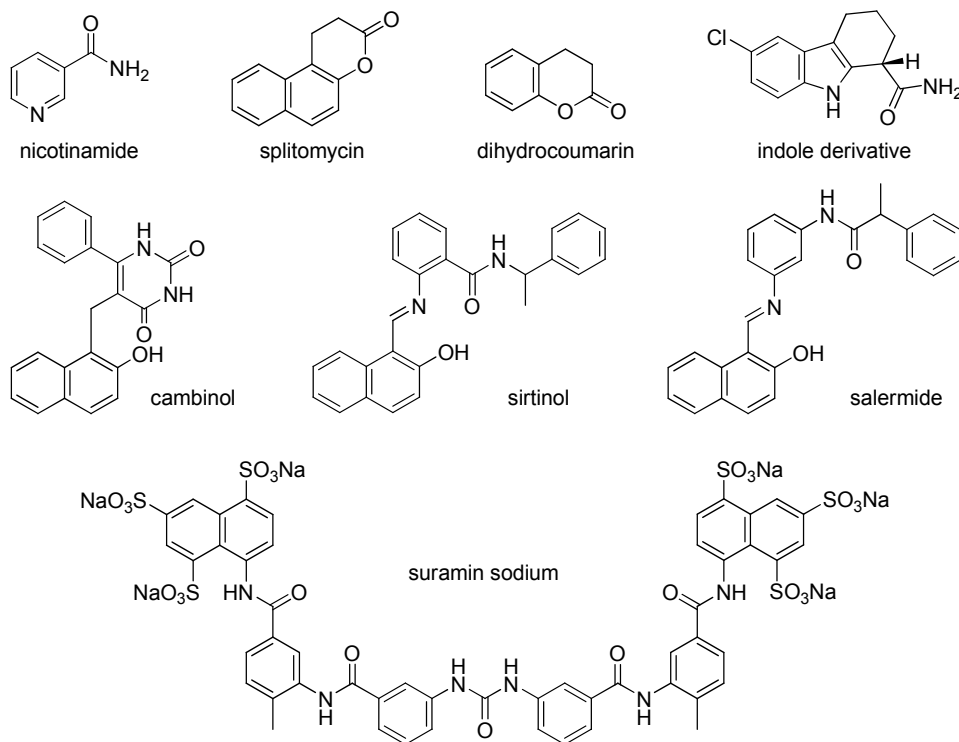


Figure 4.10. Examples of sirtuin inhibitors.

4.3.2. Experimental procedure of the enzymatic assays

The SIRT1 modulating ability of ten selected compounds was analyzed by means of the at the time commercially available fluorescent assay employing Fluor-de-Lys-Developer. Screening experiments were performed by the company Reaction Biology (Malvern, PA).

4.3.2.1. Tested compounds

The activities as SIRT1 modulators of the compounds described in section 3.4 2-substituted benzofurans **128a-g** and 3-substituted benzofurans **129a-c** (Figure 4.11) were tested.

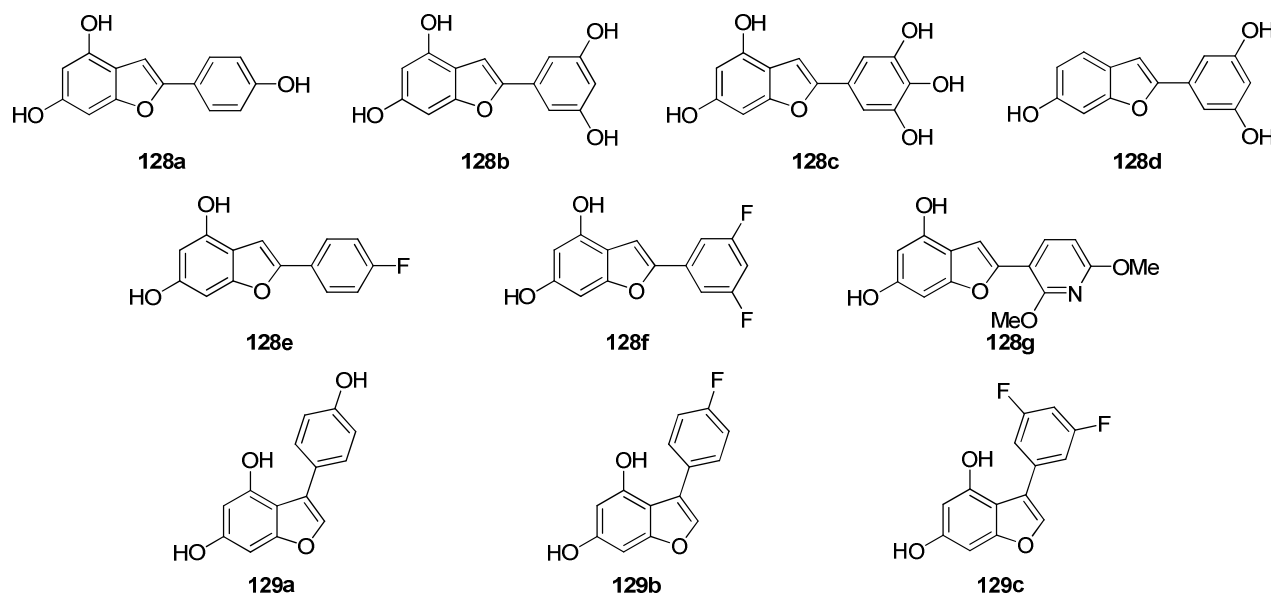


Figure 4.11. Hydroxylated benzofuran compounds tested in the enzymatic assays.

These compounds were added at various concentrations, ranging besides control from 0.05 to 1000 μM , to the assays when indicated. The corresponding concentrations were obtained from stock solutions of the compounds in DMSO, by successive dilutions.

4.3.2.2. SIRT1 modulation assay

50 μM of substrate peptide (acetylated AMC-labelled peptide from p-53 residues 379 – 382, RHKKA_c, Biomol Cat. # KI-177), 91 nM of human SIRT1 (full length human Sirtuin 1 expressed in *E. Coli*, Biomol Cat. # SE-239) and 500 μM NAD⁺ in the assay buffer (50 nM Tris-HCl, pH 8.0, 137 mM NaCl, 2.7 mM KCl, 1 mM MgCl₂ supplemented with 1 mg/ml

BSA for dilution, Biomol Cat. # KI-143) and 1% final concentration of DMSO were incubated in the presence of gradient concentrations of test compounds (10-dose with 3-fold serial dilution) at 30 °C for 2 h. The reactions were carried out in a 96-well microplate for fluorometry in a 50 µl reaction volume.

After deacetylation reaction, Fluor-de-Lys-Developer II (Biomol Cat. # KI-176) was added to each well to digest the deacetylated substrate, thus producing the fluorescent signal. The reaction was allowed to develop for 45 minutes at 30 °C with 5% CO₂; then the fluorescent signal was measured with an excitation wavelength of 360 nm and an emission wavelength of 460 nm in a microplate-reading fluorometer (GeminiXS; Molecular Devices, Sunnyvale, CA).

A curve of Deacetylated Standard (Biomol Cat. # KI-142, made from 100 µM with 1:2 dilution and 10 doses, 6 µl) allowed the conversion of fluorescent signal into micromoles of deacetylated product. All the experiments were performed in triplicate and DMSO was used as negative control.

Relative activities were calculated as the percentage of the micromoles of deacetylated product in the treated assay with respect to that in the untreated one (negative control).

4.3.3. Results and discussion of the enzymatic assays

4.3.3.1. General considerations

Some compounds were inhibitors of the enzyme SIRT1. Suramin sodium (Biomol Cat. # G-430) was used as inhibition positive control. The inhibitory activity was measured as the concentration of compound required to reduce the enzyme activity by 50% (IC_{50}) (Figure 4.12).

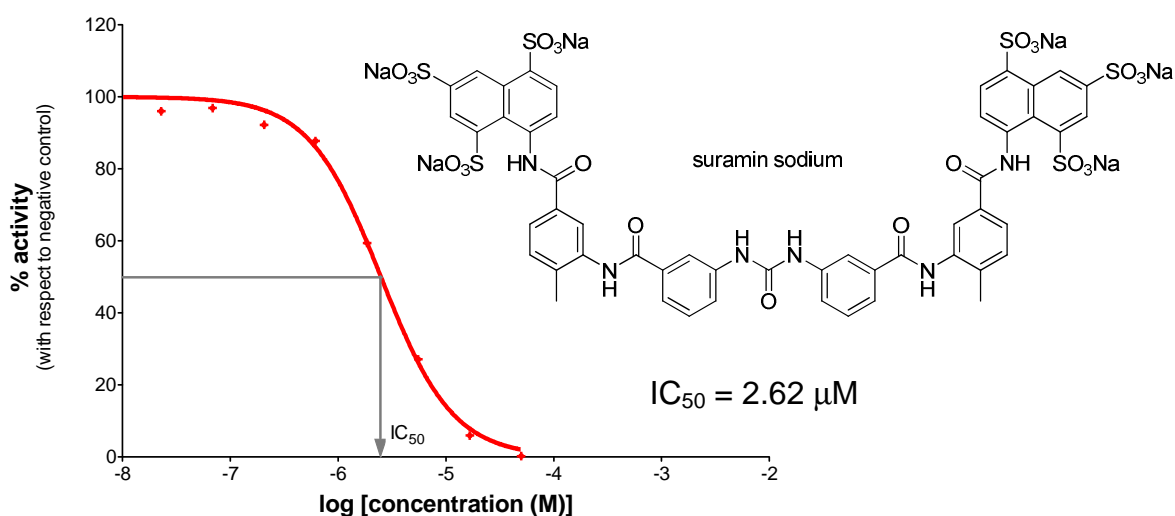


Figure 4.12. *In vitro* enzymatic assay of suramin sodium (inhibition positive control).

Some other compounds were activators of the enzyme SIRT1. Resveratrol (Biomol Cat. # FR-104) was used as activation positive control. Activation was measured both as the concentration of compound required to increase the enzyme activity by 50% ($EC_{1.5}$) as well as by the percentage of maximum activation achieved (% Max) (Figure 4.13).

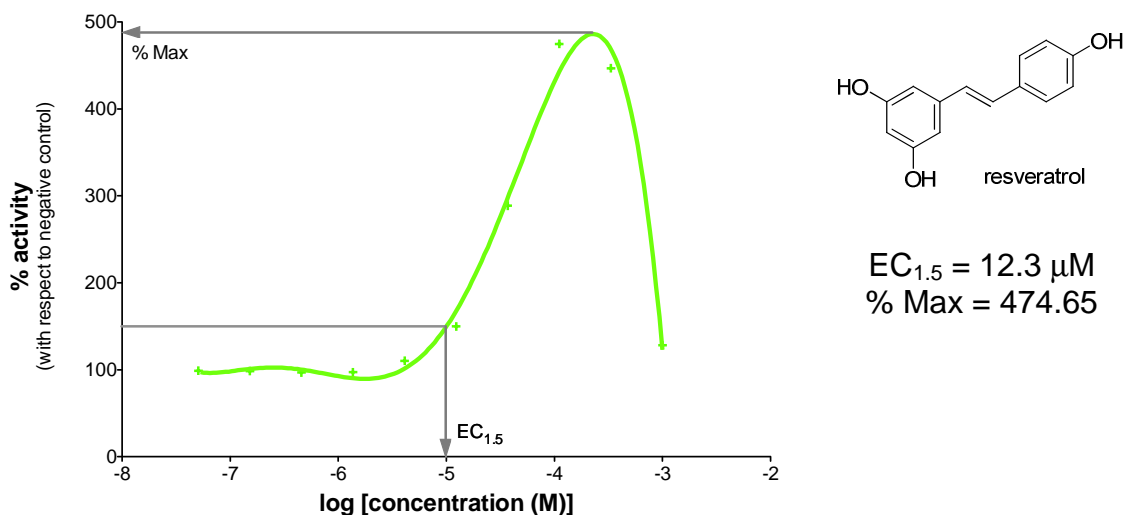


Figure 4.13. *In vitro* enzymatic assay of resveratrol (activation positive control).

4.3.3.2. SIRT1 inhibitors

Compounds **128c**, **128f** and **129a-c** showed inhibitory effect on enzyme SIRT1 activity. Data obtained from the different tested concentrations of these compounds are represented in figure 4.14. and the values of the studied inhibition parameter, IC_{50} , calculated from these graphs are given in table 4.1.

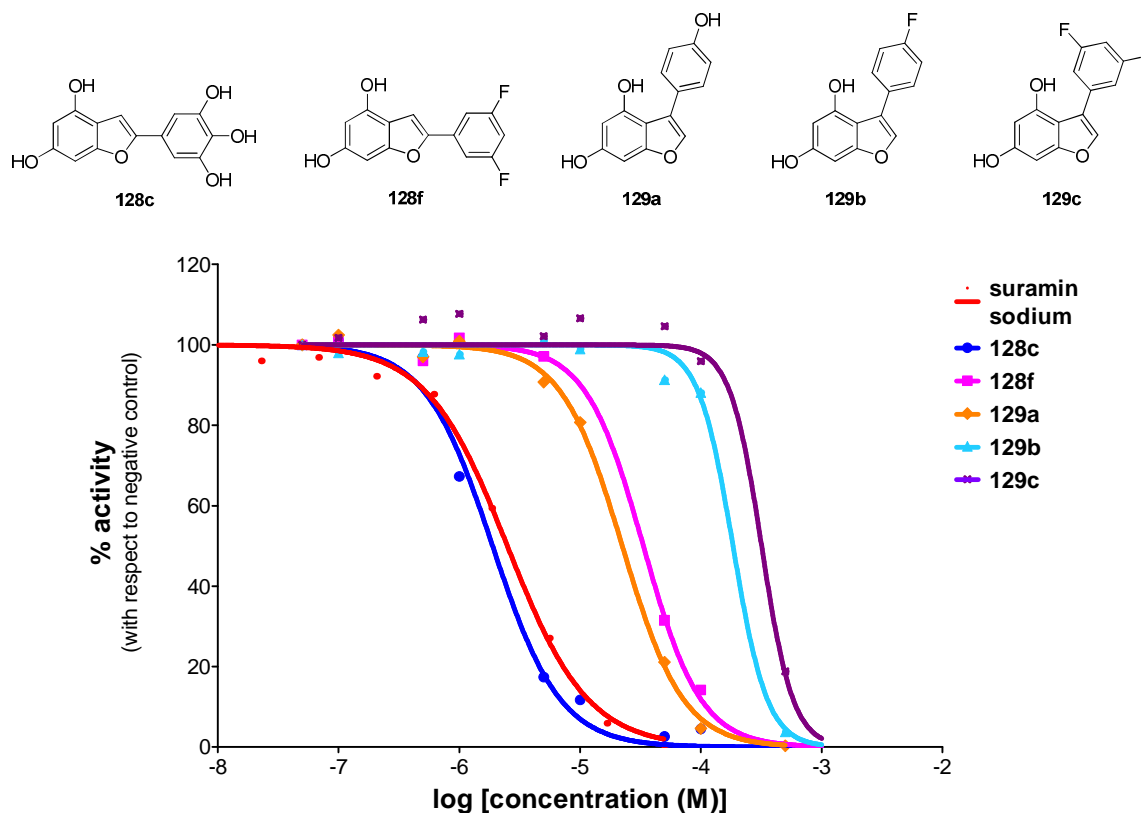


Figure 4.14. *In vitro* enzymatic assays of SIRT1 inhibitors (suramin sodium used as inhibition positive control).

Table 4.1. IC_{50} values of the SIRT1 inhibitors (suramin sodium used as inhibition positive control).

entry	compound	IC_{50} (μ M)
1	suramin sodium	2.62
2	128c	1.84
3	128f	36.7
4	129a	22.8
5	129b	192
6	129c	274

Compound **128c** emerged as the most potent inhibitor of the series with an IC_{50} of 1.84 μ M, which even improves that of the inhibition positive control suramin sodium. Among the others, compounds **129a** and **128f** also showed a significant inhibitory effect in the

micromolar range, whilst compounds **129b** and **129c** provided higher values for this parameter.

4.3.3.3. SIRT1 activators

Compounds **128a-b**, **128d-e** and **128g** proved to activate enzyme SIRT1 activity. Data obtained from the different tested concentrations of these compounds are represented in figure 4.15. and the values of the studied activation parameters, $EC_{1.5}$ and % Max, calculated from these graphs are given in table 4.2.

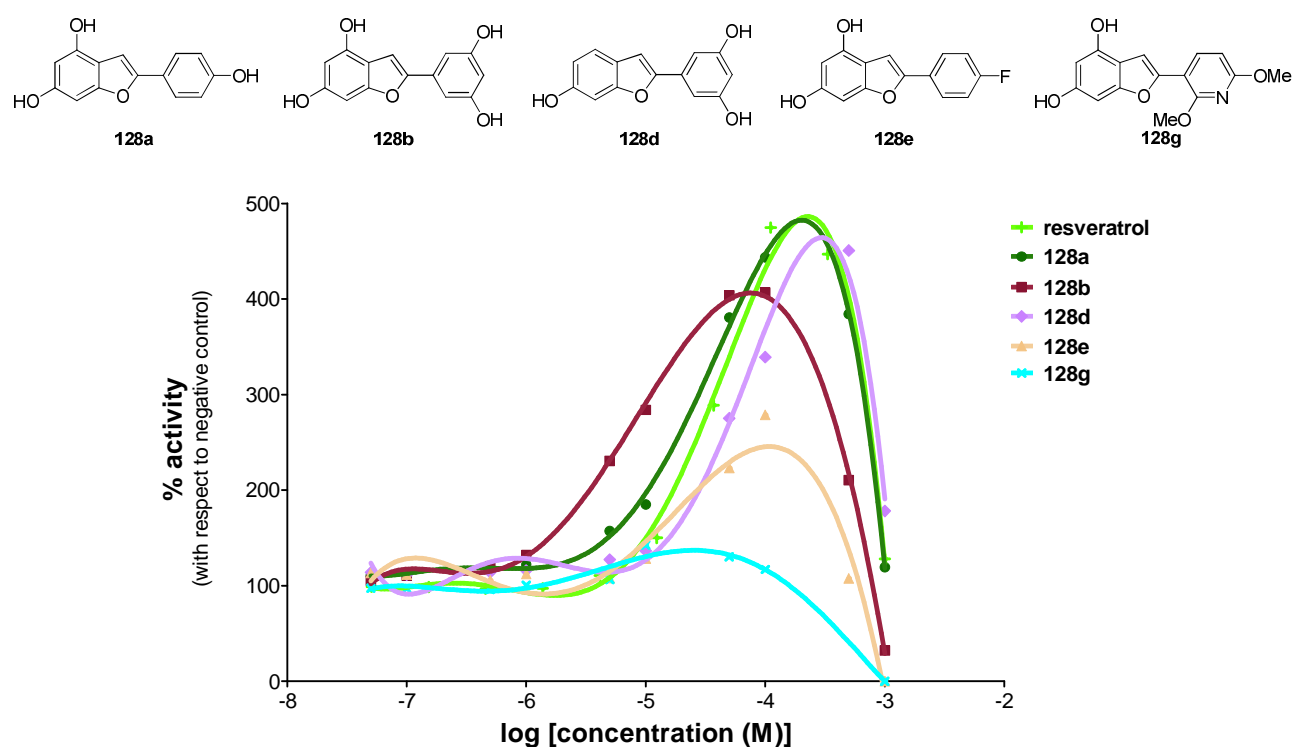


Figure 4.15. *In vitro* enzymatic assays of SIRT1 activators (resveratrol used as activation positive control).

Table 4.2. $EC_{1.5}$ and % Max values of the SIRT1 activators (resveratrol used as activation positive control).

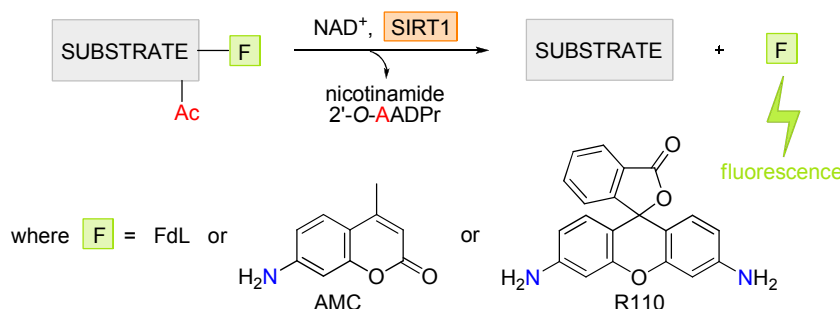
entry	compound	$EC_{1.5}$ (μ M)	% Max
1	resveratrol	12.3	474.65
2	128a	3.55	443.52
3	128b	1.32	406.85
4	128d (moracin M)	11.48	450.78
5	128e	13.49	278.80
6	128g	-	142.47

When considering activation it should be taken into account that a good activator combines both low $EC_{1.5}$ and high % Max values. In this line, both compounds **128a** and **128b** present an interesting trade off between these two parameters, resulting in promising candidates for SIRT1 activation according to this study. Compounds **128d** (natural product moracin M) and **128e**, for their part, present slightly worse values of the studied activation parameters, although still comparable to those of the resveratrol reference, in general. In contrast, the activation effect of compound **128g** was comparatively the lowest, failing to increase the enzyme activity even by 50%.

4.3.4. Controversy: uncertain validity of the fluorescence assays

During the development of this project the ability of resveratrol to directly activate sirtuins was severely called into question after the publication that, *in vitro*, the fluorescent method employed to measure it could lead to artefacts. Unfortunately, the debate is still open³⁰⁰.

The standard procedure for the *in vitro* determination of SIRT1 activity was the commercially available SIRT1 fluorescent activity assay drug discovery kit (BioMol), which utilizes the Fluor de Lys (FdL) method. The FdL assay is a biochemical method for measuring deacetylation based on fluorescence. It employs a chemically modified acetylated peptide substrate coupled to a fluorophore (F), typically the non-physiological FdL moiety, although 7-amino-4-methylcoumarin (AMC) and rhodamine 110 (R110) are also possible. Upon deacetylation, the FdL/AMC/R110 group is proteolytically cleaved resulting in fluorescence (Scheme 4.2).



Scheme 4.2. Fluorescence assay for the determination of *in vitro* deacetylation activity of SIRT1. Nitrogen atoms highlighted in blue indicate the binding site(s) of the fluorophores to the peptidic sequence, at its C terminus adjacent to the acetylated (lysine) residue.

According to the reports that arose the debate^{289b-c}, *in vitro* activation of SIRT1 by resveratrol is substrate-dependent. Specifically, resveratrol activates the enzyme against acetylated peptide containing the covalently attached fluorophore, typically residue sequence Arg³⁷⁹-His-Lys-Lys³⁸²(Ac)-F of p53, but fails to affect it on the same peptide substrate when the fluorophore is removed.

This result has been subject to, at least, three different interpretations:

³⁰⁰ Yuan, H.; Marmorstein, R. *Science* **2013**, 339, 1156-1157

The first and most radical explanation would be that resveratrol does not activate sirtuins at all and its effects follow a different pathway. However, this would be in disagreement with many of the observed *in vivo* activities aforementioned.

A second view suggests that the fluorescent assay could reproduce some important aspects of *in vivo* biology more accurately than the non-fluorescent version. Biochemical modelling studies of the reaction suggest that, binding to SIRT1, resveratrol promotes a conformational change that better accommodates the attached coumarin group of the artificial substrate p53-Ac-F and leads to a more efficient turnover of native acetylated proteins. In support of this theory, SIRT1 has a much lower K_m (Michaelis-Menten constant) for unconjugated peptide substrates: substrate competition studies indicated that, in the absence of resveratrol, the fluorophore decreased the binding affinity of the peptide whereas in the presence of resveratrol fluorescently labelled peptides bound more tightly to SIRT1.

In any case, the key of this second possibility would be unravelling whether the addition of a bulky hydrophobic molecule (like the fluorophore) to the peptide substrate could better mimic the steric constraints that SIRT1 endogenous protein targets experience *in vivo*. In this way, a first approach would be to test the effect of resveratrol using full length endogenous substrates of SIRT1. Unfortunately, challenging this argument, a study³⁰¹ revealed that neither resveratrol nor sirtris series (SRT1460, SRT1720 and SRT2183) activate SIRT1 even against native systems (full length protein substrates) p53 and acetyl-CoA synthetase 1 (AceCS1) in the absence of a fluorophore. Nevertheless, more recently hydrophobic motifs present in some SIRT1 substrates, such as PGC-1 α and FOXO3a, have been found to facilitate SIRT1 activation by sirtuin-activating compounds (STACs), supporting the hypothesis of the direct SIRT1 activation through an allosteric mechanism³⁰².

The third interpretation proposes that the activation of sirtuins by resveratrol proceeds through an indirect mechanism. There is much evidence that resveratrol has SIRT1-

³⁰¹ Pacholec, M.; Bleasdale, J. E.; Chrnyk, B.; Cunningham, D.; Flynn, D.; Garofalo, R. S.; Griffith, D.; Griffior, M.; Loulakis, P.; Pabst, B.; Qiu, X.; Stockman, B.; Thanabal, V.; Varghese, A.; Ward, J.; Withka, J.; Ahn, K. *J. Biol. Chem.* **2010**, *285*, 8340-8351

³⁰² Hubbard, B. P.; Gomes, A. P.; Dai, H.; Li, J.; Case, A. W.; Considine, T.; Riera, T. V.; Lee, J. E.; E, S. Y.; Lamming, D. W.; Pentelute, B. L.; Schuman, E. R.; Stevens, L. A.; Ling, A. J. Y.; Armour, S. M.; Michan, S.; Zhao, H.; Jiang, Y.; Sweitzer, S. M.; Blum, C. A.; Disch, J. S.; Ng, P. Y.; Howitz, K. T.; Rolo, A. P.; Hamuro, Y.; Moss, J.; Perni, R. B.; Ellis, J. L.; Vlasuk, G. P.; Sinclair, D. A. *Science* **2013**, *339*, 1216-1219

dependent effects in mammalian cells, but resolving whether this occurs through a direct or indirect mechanism is not clear and has been claimed to require further research (structural explanation or identification of the presumed upstream pathway). In this line, some reports have recently shown that resveratrol can also activate (5'-adenosine monophosphate)-activated protein kinase (AMPK). Although there is no consensus on whether resveratrol-induced AMPK activation is SIRT1 dependent or not, a conciliatory view suggests that SIRT1 may be essential for resveratrol action but as a downstream consequence of AMPK activation.

This last pathway³⁰³ points at the phosphodiesterases (PDEs), which degrade cyclic adenosine monophosphate (cAMP), as primary targets of resveratrol. The resulting inhibition of PDEs by resveratrol causes an increase in the cellular cAMP levels which triggers a signalling cascade that, by means of the activation of AMPK (a major regulator of cellular energy by modulation of NAD⁺ metabolism), leads to an enhancement of the NAD⁺-dependent sirtuin SIRT1 activity (Figure 4.16).

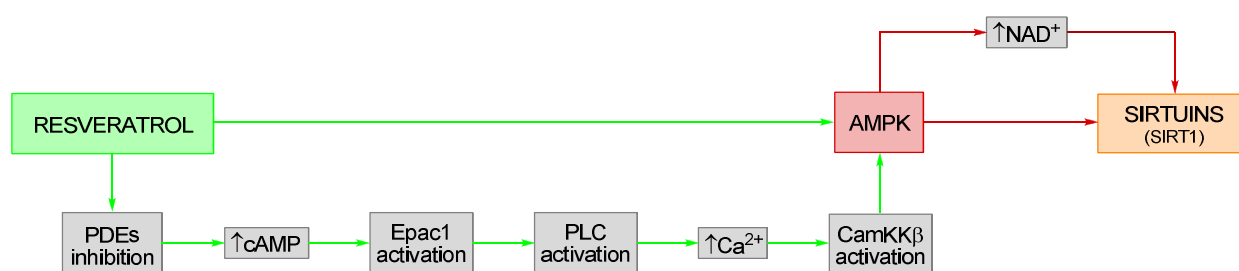


Figure 4.16. Proposed indirect mechanism for the activation of SIRT1 by resveratrol, via AMPK. Abbreviations: SIRT1 = silent information regulator human homologue 1; AMPK = (5'-adenosine monophosphate)-activated protein kinase; PDE = phosphodiesterase; cAMP = cyclic adenosine monophosphate; Epac1 = cAMP-dependent guanine nucleotide exchange factor; PLC = phospholipase C; CamKKβ = Ca²⁺/calmodulin-dependent kinase beta; NAD⁺ = nicotinamide adenine dinucleotide.

Bearing all this in mind, the validity of the presented enzymatic assays is, to say the least, uncertain. For this reason, taking into account that the benzofuran scaffold still seemed appropriate to mimic, or even improve, many structural features of resveratrol (section 4.1), we contemplated the possibility of assessing the potential biological activity of some of the synthesized benzofurans using other type of assay.

³⁰³ (a) Cantó, C.; Auwerx, J. *Cell Mol. Life Sci.* **2010**, *67*, 3407-3423 (b) Tennen, R. I.; Michishita-Kioi, E.; Chua, K. F. *Cell* **2012**, *148*, 387-389 (c) Park, S.-J.; Ahmad, F.; Philp, A.; Baar, K.; Williams, T.; Luo, H.; Ke, H.; Rehmann, H.; Taussig, R.; Brown, A. L.; Kim, M. K.; Beaven, M. A.; Burgin, A. B.; Manganiello, V.; Chung, J. H. *Cell* **2012**, *148*, 421-433

Thereupon, cell-based assays to evaluate the effect of the candidate compounds on the prometastatic potential of a particular cancer model were considered. To perform these studies a new selection of benzofurans was made. On the one hand, hydroxylated compounds **128a-c** and **129a**, the ones showing most promising activity both as inhibitors and as activators in the questionable enzymatic assays, were chosen. On the other hand, their corresponding methoxylated analogues **124a-c** and **125a** were selected, since this substituent had already proven useful in the design of resveratrol analogues and/or other bioactive compounds.

4.4. CELL-BASED ASSAYS: ANTICANCER PROPERTIES

4.4.1. General considerations: cancer

Cancer in few words

Cancer is a generic term coined to describe a large group of diseases that can affect any part of the body. One defining feature of cancer is the rapid and uncontrolled cell proliferation (creation of abnormal cells that grow beyond their usual boundaries) which can then invade adjacent parts of the body and/or spread to other organs, process referred to as metastasis. Metastases are the major cause of death from cancer, being responsible for approximately 90% of all cancer-related deaths³⁰⁴.

The beginning of cancer involves a single normal cell which is transformed into a cancer cell as a result of a genetic mutation arising spontaneously or induced by exposure to external agents: physical carcinogens (e.g. ultraviolet radiation), chemical carcinogens (e.g. asbestos) and biological carcinogens (e.g. certain viruses like hepatitis B)^{304c}. Cancer cells have defects in the regulatory circuits that govern normal cell proliferation and homeostasis. The hallmarks of cancer, alterations shared in common by most and perhaps all type of human cancers, have been listed as self-sufficiency in growth signals, insensitivity to antigrowth signals, evasion of apoptosis (programmed cell death), limitless replicative potential, sustained angiogenesis and tissue invasion and metastasis³⁰⁵.

Carcinogenesis stages and the metastatic process

Carcinogenesis (or oncogenesis or tumorigenesis), literally the creation of cancer, is a multi-step process in which three main stages are recognized³⁰⁶ (Figure 4.17):.

- I. **Initiation** refers exclusively to the initial genetic change that irreversibly alters normal cells, produced spontaneously or induced by carcinogen exposure.

³⁰⁴ (a) Mehlen, P.; Puisieux, A. *Nat. Rev. Cancer* **2006**, 6, 449-458 (b) Spano, D.; Heck, C.; De Antonellis, P.; Christofori, G.; Zollo, M. *Semin. Cancer Biol.* **2012**, 22, 234-249 (c) Cancer, available at WHO (World Health Organization) website, fact sheet n. 297, reviewed January 2013, <<http://www.who.int/mediacentre/factsheets/fs297/en/>>

³⁰⁵ Hanahan, D.; Weinberg, R. A. *Cell* **2000**, 100, 57-70

³⁰⁶ (a) Wetson, A.; Harris, C. C. *Chemical carcinogenesis (chapter 12)*, in: Bast, R. C. Jr.; Kufe, D. W.; Pollock, R. E. et al, editors. *Holland-Frei Cancer Medicine. 5th edition*. Hamilton (ON): DB Decker; **2000** (b) Devi, P. U. *Health Administrator* **2005**, XVII, 16-24

- II. **Promotion** comprises the selective proliferation of a population of initiated cells. It results in the formation of the primary tumor, in which nutrients for expanding tumor mass are initially supplied by simple diffusion. These premalignant or preneoplastic cells are at risk for transformation into cells that expresses the malignant phenotype (malignant conversion).
- III. **Progression** involves the expression of malignant phenotype, whose main characteristic is the propensity for genomic instability and uncontrolled growth. This leads to the increasing of malignant sub-populations and the tendency of already malignant cells to acquire more aggressive characteristics with time. If a tumor mass is to exceed 1-2 mm in diameter, extensive vascularization must occur (angiogenesis). As tumor progression advances, its cells lose their adherence property, detach from the tumor mass and invade the neighboring tissues or enter the blood and/or lymph circulatory system, being transported to other organs where develop into secondary tumors. This process of tumor formation away from the site of the primary growth is called metastasis and results in widely spread cancers.

The described cancer metastasis, in turn, consists of a number of steps³⁰⁷, being the following ones common to all tumors (Figure 4.17):

- a. **Detachment:** it is the beginning of metastasis, the first step in which cancer cells from the primary tumor set off for the circulatory system (blood and/or lymph streams).
- b. **Intravasation:** it is the invasion of cancer cells into blood or lymph vessels disrupting the endothelial walls and entering the circulatory system.
- c. **Migration:** once in the circulatory stream, dissemination of single tumor cells or aggregates along the body takes place. However, most circulating tumor cells are destroyed as a consequence of the environmental conditions of blood and lymph systems as well as the action of immunologic system they have to face.

³⁰⁷ (a) Poste, G.; Fidler, I. J. *Nature* **1980**, 283, 139-146 (b) Fidler, I. J. *Nature Rev. Cancer* **2003**, 3, 453-458 (c) Gupta, G. P.; Massagué, J. *Cell* **2006**, 127, 679-695

- d. **Adhesion:** the surviving tumor cells in circulation are transported until they become trapped in the capillary beds of distant organs, by adhering to endothelial cells of their vessel walls.
- e. **Extravasation:** it is the invasion of cancer cells escaping out of the endothelial vasculature into the tissue of the target organ in which they have arrested.
- f. **Proliferation:** once in the host organ, tumor cells establish their own microenvironment allowing them to evade the host defence, to progressively grow and to create a new vascular net (angiogenesis), forming a secondary tumor. When this new tumor is stable, cancer cells in it can initiate this process again and produce additional metastases.

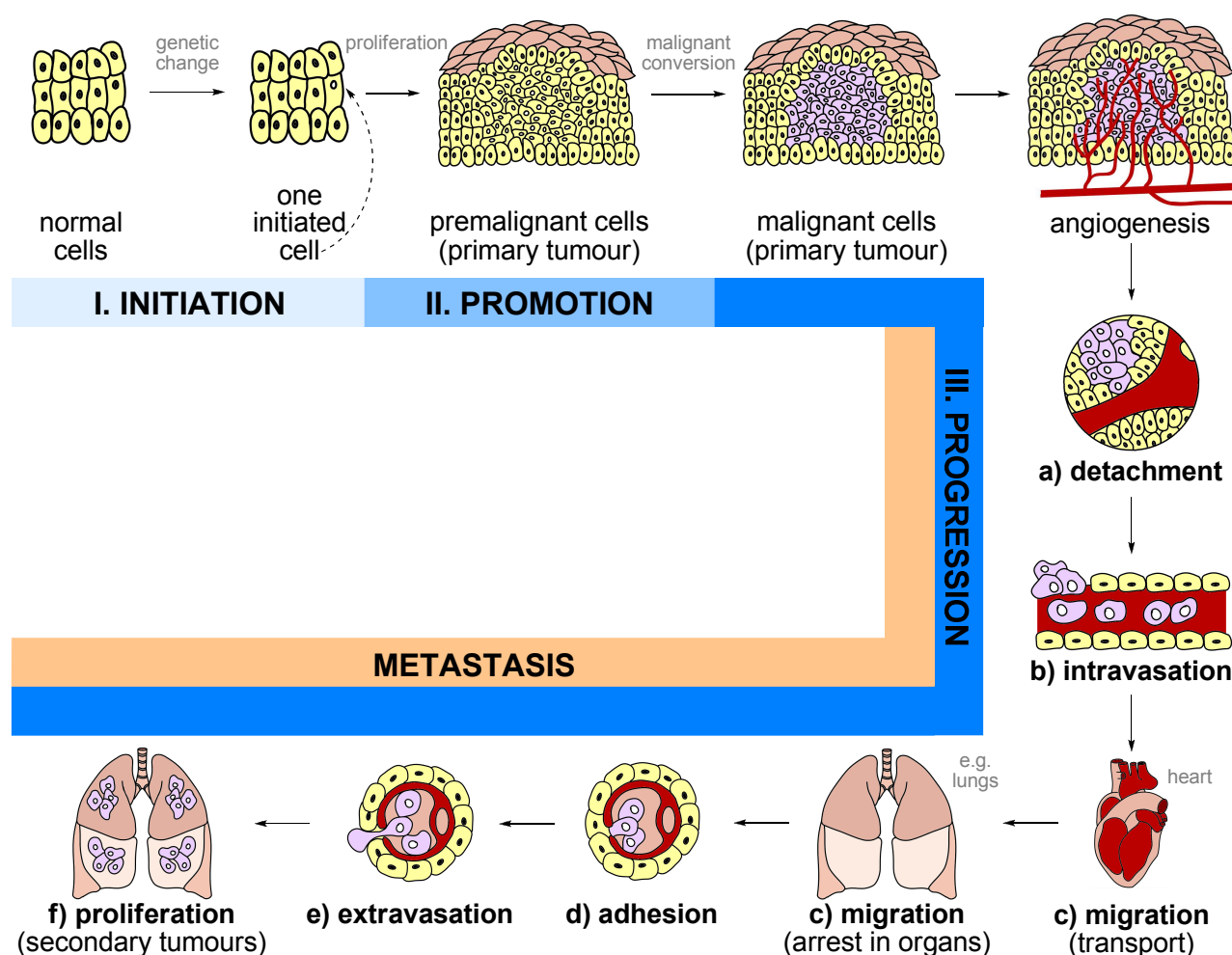


Figure 4.17. Schematic representation of carcinogenesis stages (I-III) and metastasis steps (a-f). (Adapted and expanded from reference 307b)

Each discrete step of the sequential pathogenesis of cancer metastasis is likely to be regulated by transition or permanent changes in DNA, RNA or proteins. Most cancer cells fail to undergo metastasis because of different deficiencies, meaning that cancer cell metastasis can be blocked at a variety of stages including invasion, survival in the circulation and proliferation or ability to grow at the final metastatic site. In other words, if one of the steps fails, the whole process can get to be interrupted. This makes highly interesting to study the influence that potential anticancer agents can exert on the different steps of this pathogenesis.

Colon tumor model for the evaluation of anticancer agents

In particular, the studies presented in this section will focus on evaluating our resveratrol analogues at three different steps of the metastatic process, measuring their effect on the endothelial proadhesive potential (adhesion assay), on the tumor viability (proliferation assay), and on the tumor migration (migration assay).

The study of the potential anticancer properties of chemical agents requires appropriate animal tumor models which closely correspond to human cancers. Being colorectal cancer one of the most prevalent cancers in humans, numerous chemically induced murine colon tumors have been established and described. These models accurately recapitulate the molecular and pathologic characteristics of human colorectal cancers and represent various levels of differentiation, growth rates, metastatic potentials and sensitivities to chemotherapeutic agents³⁰⁸.

Among all the reported models, murine colon carcinoma C26 was selected for the study. The main reasons behind this choice were that this model is well characterized and there is wide knowledge of its adhesive, immunologic, stromagenic and angiogenic behavior within the hepatic microenvironmental context during experimental development of metastasis. Besides, it is claimed to be reproducible, both *in vitro* and *in vivo* (parallel HT29 model), and highly dependent on initial ICAM-1/LFA-1 interaction-induced COX-2^{308,309}.

³⁰⁸ (a) Griswold, D. P.; Corbett, T. H. *Cancer* **1975**, *36*, 2441-2444 (b) Uronis, J. M.; Threadgill, D. W. *Mamm. Genome* **2009**, *20*, 261-268

³⁰⁹ (a) Chapple, K. S.; Cartwright, E. J.; Hawcroft, G.; Tisbury, A.; Bonifer, C.; Scott, N.; Windsor, A. C. J.; Guillou, P. J.; Markham, A. F.; Coletta, P. L.; Hull, M. A. *Am. J. Pathol.* **2000**, *156*, 545-553 (b) Valcarcel, M.; Arteta, B.; Jaureguibeitia, A.; Lopategi, A.; Martinez, I.; Mendoza, L.; Muruzabal, F. J.; Salado, C.; Vidal-

4.4.2. Experimental procedure of the cell-based assays

The antitumor properties of eight selected compounds were analyzed in the highly metastatic model of murine colon carcinoma C26 in the Department of Cell Biology and Histology (School of Medicine and Dentistry – University of Basque Country, UPV/EHU) by Assoc. Prof. Beatriz Arteta, PhD, and her group: Prof. Elvira Olaso, PhD, Joana Marquez, Ph.D, and Aitor Benedicto, PhD student. *In vitro* experiments were conducted to analyze the modulation of the metastatic potential by these compounds, in terms of endothelium adhesive potential to the tumor, tumor proliferation, and tumor migratory potential.

4.4.2.1. Treatments: benzofuran analogues of resveratrol at various concentrations

Hydroxylated products **128a-c** and **129a** and the corresponding methoxylated compounds **124a-c** and **125a** were chosen for the cell-based assays (Figure 4.18).

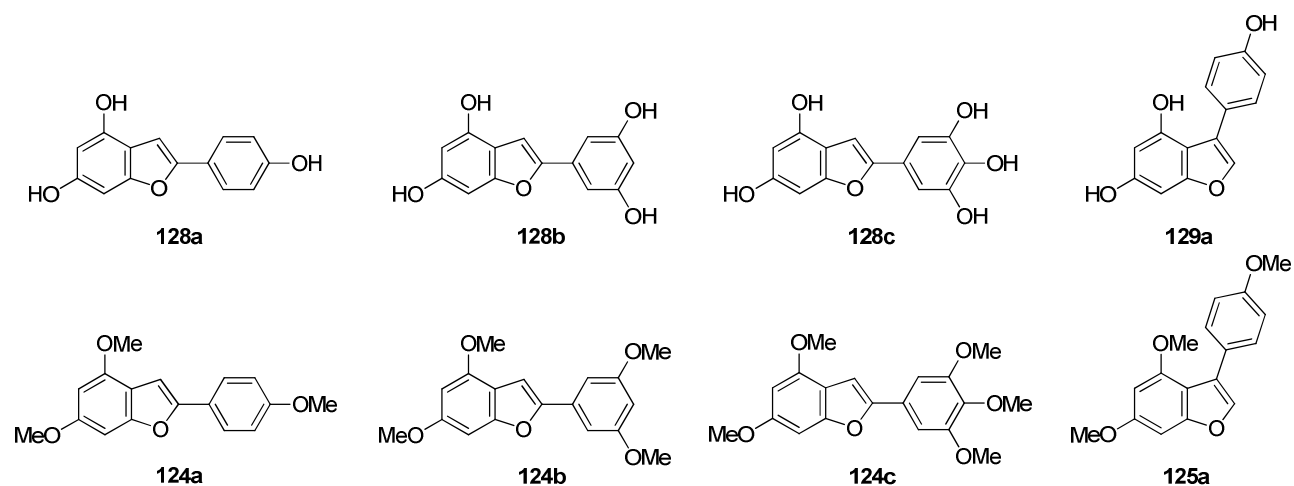


Figure 4.18. Benzofuran analogues of resveratrol tested in the cell-based assays.

These compounds were added at various concentrations, ranging besides control from 0.5 to 50 μ M, to the cultures when indicated to perform the different assays. The corresponding concentrations were obtained from 50 mM stock solutions in ethanol (in the case of hydroxylated compounds) and in DMSO (in the case of methoxylated compounds), by successive dilutions. The change of solvent owed to the solubility problems and consequent precipitation of the methoxylated products in EtOH. The treatments were carried out by addition of the analogues in RPMI-1640 medium (Roswell Park Memorial Institute cell culture medium) supplemented with antibiotics.

4.4.2.2. Cancer cell line: murine colon carcinoma C26

Murine colon carcinoma C26 cells (CT26 or MCA26) constitute a *N*-nitroso-*N*-methylurethan-induced mouse undifferentiated colon carcinoma³¹⁰ (ATCC, Manassas, VA), syngeneic with Balb/c mice. C26 cells were grown at 37°C, 5% CO₂, in RPMI-1640 medium supplemented with 10% FBS (fetal bovine serum) and antibiotics-antimycotics.

Sub-confluent C26 cells were detached by using 0.4 mM PBS-EDTA (phosphate buffered saline - ethylenediaminetetraacetic acid) solution and pelleted by centrifugation at 1500 rpm for 10 min. The supernatant was discarded and resulting pellet was diluted to a concentration of 10⁵ tumor cells/ml for further experimentation.

4.4.2.3. Tumor cell adhesion assay to primary cultured LSECs

Cultured LSECs (liver sinusoidal endothelial cells) were exposed to different concentrations of resveratrol analogues (0 as control, 0.5, 2.5 and 12.5 μM) treatment for 30 minutes before the adhesion assays.

Primary culture, isolation and purification of LSECs

LSECs were cultured, isolated and purified from mice strain Balb/c, following modified protocol by Smedsrød and Pertoft described in literature³¹¹.

Briefly, liver was perfused first with a physiological saline buffer without calcium to wash blood cells, and second with a collagenase solution of *Clostridium histolycitum* (Sigma-Aldrich, St. Louis, MO, USA) to disperse the liver cells. This single cell suspension was subjected to 2 x 2 min centrifugation at 50 G to pellet PCs (parenchymal cells), and the resulting supernatant was concentrated by centrifugation (850 g). The pellet obtained this way was subjected to an isopicnic centrifugation onto Percoll gradient, yielding a suspension enriched in NPCs (nonparenchymal cells): LSECs and KCs (Kupffer cells). This LSECs-KCs enriched layer was subjected to concentration by centrifugation (850 g) and KCs were eliminated by selective adhesion to plastic culture dish, obtaining a solution enriched in LSECs.

³¹⁰ Sato, N.; Michaelides, M. C.; Wallack, M. K. *Cancer Res.* **1981**, *41*, 2267-2272

³¹¹ (a) Smedsrød, B.; Pertoft, H. *J. Leukoc. Biol.* **1985**, *38*, 213-230 (b) Hansen, B.; Arteta, B.; Smedsrød, B. *Mol. Cell. Biochem.* **2002**, *240*, 1-8

Then, LSECs were seeded at 4×10^5 cells / 0.95 cm^2 in RPMI-1640 culture medium supplemented with 5% FBS and antibiotics [100 units/ml penicillin, $100 \text{ }\mu\text{g/ml}$ streptomycin, $0.25 \text{ }\mu\text{g/ml}$ amphotericin B (Gibco Life Technologies, Gaithersburg, MD)] onto tissue culture plates pre-coated with type I collagen solution (0.03 mg/ml) (Sigma-Aldrich, St. Louis, MO, USA) and incubated for 45 min at 37°C , 5% CO_2 . When primary cultures were used, culture medium was additionally complemented with gentamicin (0.1 mg/ml) (Sigma-Aldrich; St. Louis, MO, USA). LSECs were incubated for 2 hours in serum-free medium supplemented with antibiotics before use.

Adhesion assay

Adhesion assays were performed using a quantitative method based on fluorescence measurement system. Tumor cells were labelled with the vital fluorescent probe CFSE (carboxyfluorescein diacetate succinimidyl ester) (Invitrogen Lifer Technologies, Gaithersburg, MD) (Figure 4.19) which passively diffuses into cells, and keeps colorless until the acetate groups are cleaved by intracellular esterases to yield highly fluorescent carboxyfluorescein succinimidyl ester. Succinimidyl ester group reacts with intra-cellular amines forming fluorescent conjugates that are well retained.

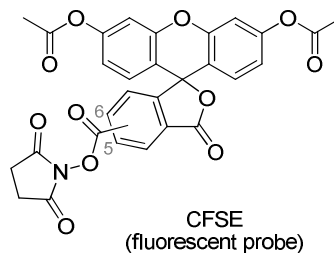


Figure 4.19. CFSE fluorescent probe (also called 5(6)-CFDA, SE; 5-(and-6)-carboxyfluorescein diacetate succinimidyl ester, mixed isomers).

After labelling (30 min incubation of the tumor C26 cells with the fluorescent probe), the excess of unconjugated reagent and byproducts passively diffuse to the extracellular medium where it is washed away twice. These labelled C26 tumor cells were added to primary LSECs cultures (untreated as control and previously treated with the selected compounds) at a concentration of 2.5×10^5 cells/ 0.95 cm^2 and allowed to adhere for 30 min, after which total added fluorescence was measured. Then, cultures were washed away with fresh media to eliminate non-adhered cells and emitted fluorescence, associated with C26 cells adhered to LSECs, was measured. The fluorescence measurements were

carried out using Fluoroskan Ascent Microplate Fluorometer (Thermo Scientific Inc. Barrington, IL).

Relative adhesion was calculated as a percentage of adhered cells with respect to adhesion to untreated LSECs (control).

4.4.2.4. Proliferation assay

Proliferation assay was conducted by incubation of tumor cells cultured in 96 well-plate (covered with collagen) at a concentration of 5×10^3 / 0.38 cm^2 first for 2 hours, to allow their adhesion and stretching, and second for 24 hours in the presence of concentrations ranging from 0 to 50 μM of resveratrol analogues, diluted in RPMI-1640 supplemented with antibiotics and 0.5% FBS.

Then, cells were incubated for 90 min with 10% Presto Blue solution (Invitrogen Lifer Technologies, Gaithersburg, MD) in RPMI-1640, and absorbance (associated with the developed color) was measured in Multiskan EX (Thermo Scientific Inc. Barrington, IL), following manufacturer instructions. Results are presented as number of cells.

Additionally, plates with initial number and decreasing concentrations (1:2 diluting factor) of C26 tumor cells were cultured in order to establish a standard curve relating absorbance with cell number.

Relative proliferation was calculated as the percentage of the number cells with respect to initial number of cells, although it was also compared with the number of cells resulted from the untreated assay (control).

4.4.2.5. *In vitro* migration assay

In vitro migration assays were conducted using modified Boyden chambers. These chambers consist of wells modified by the addition of a $8.0 \mu\text{m}$ \varnothing pore colored PET membrane, as previously described³¹² (BD Biosciences; San Jose, CA, USA), which

³¹² Olaso, E.; Salado, C.; Egilegor, E.; Gutierrez, V.; Santisteban, A.; Sancho-Bru, P.; Friedman, S. L.; Vidal-Vanaclocha, F. *Hepatology* **2003**, *37*, 674-685

allows the pass of tumor cells. These wells are placed on top of a complementary culture 24-well plate in which RPMI-1640 medium and the corresponding treatment are added.

CFSE-labelled tumor cells at a concentration of 2×10^4 / 0.3 cm^2 in RPMI-1640 in the presence of 0.5% FBS and antibiotics were incubated in the upper part of the inserts for 2 h (to allow suitable adhesion). Then the treatment was added (control and $2.5 \mu\text{M}$ concentrations of corresponding benzofurans in RPMI-1640 supplemented with antibiotics and 0.5% FBS) to both upper and lower compartments. Cells were incubated for further 18 h (to allow migration) and fluorescence of only migrated cells (those crossing the porous membrane of the inserts) was quantified in Fluoroskan Ascent Microplate Fluorometer (Thermo Scientific Inc. Barrington, IL).

Membranes in the chambers are Fluoroblock type which, due to their material, do not permit the pass of the fluorescence emitted by the cells in the upper side of the insert, resulting in the detection of the fluorescence associated only with the cells migrating through this membrane.

Relative migration was calculated as the percentage of migrating tumor cells with respect to migration of untreated tumor cells (control).

4.4.3. Results and discussion of the cell-based assays

4.4.3.1. Effect of the resveratrol analogues on the adhesion of murine colon carcinoma C26 cells to primary cultures of LSECs

LSECs were treated with increasing concentrations (0.5, 2.5 and 12.5 μM) of testing compounds in EtOH (in the case of hydroxylated products) and DMSO (in the case of methoxylated products) 30 min before the addition of the tumor cells, as previously detailed (section 4.4.2.3).

The results shown here are the average of the data obtained from three independent experiments. Differences between tumor cell adhesion to primary cultures of untreated LSECs and LSECs treated with the benzofurans were considered significant when the value of statistical parameter p is less than 0.02 ($p < 0.02$). These significant results are highlighted with a star (*) in figures 4.20 and 4.21. The following results were obtained:

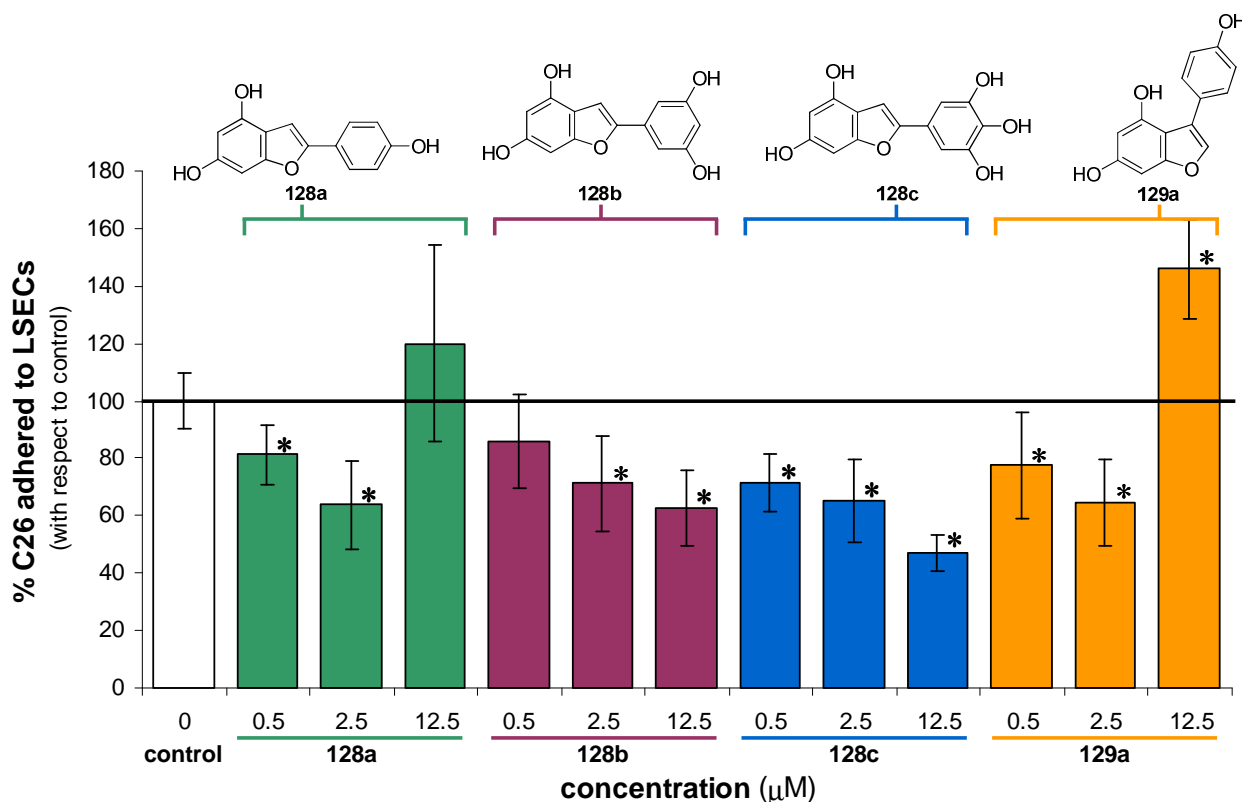


Figure 4.20. *In vitro* adhesion assays of C26 tumor cells to LSECs treated with hydroxylated benzofurans **128a-c** and **129a**. Control reference is shown by a continuous black line and significant differences with respect to it are marked with a star (*).

All the hydroxylated benzofurans showed a similar inhibitory capacity of about 30% at 2.5 μM . Among these compounds it is worth mentioning the maximum inhibition of 47%

obtained with **128c** at 12.5 μM . Besides, the behavior of this product was proved constant, being the one showing the least interexperimental variation. Compounds **128a** and **129a** induced an increase in the adhesion at the highest tested concentration (12.5 μM) (Figure 4.20).

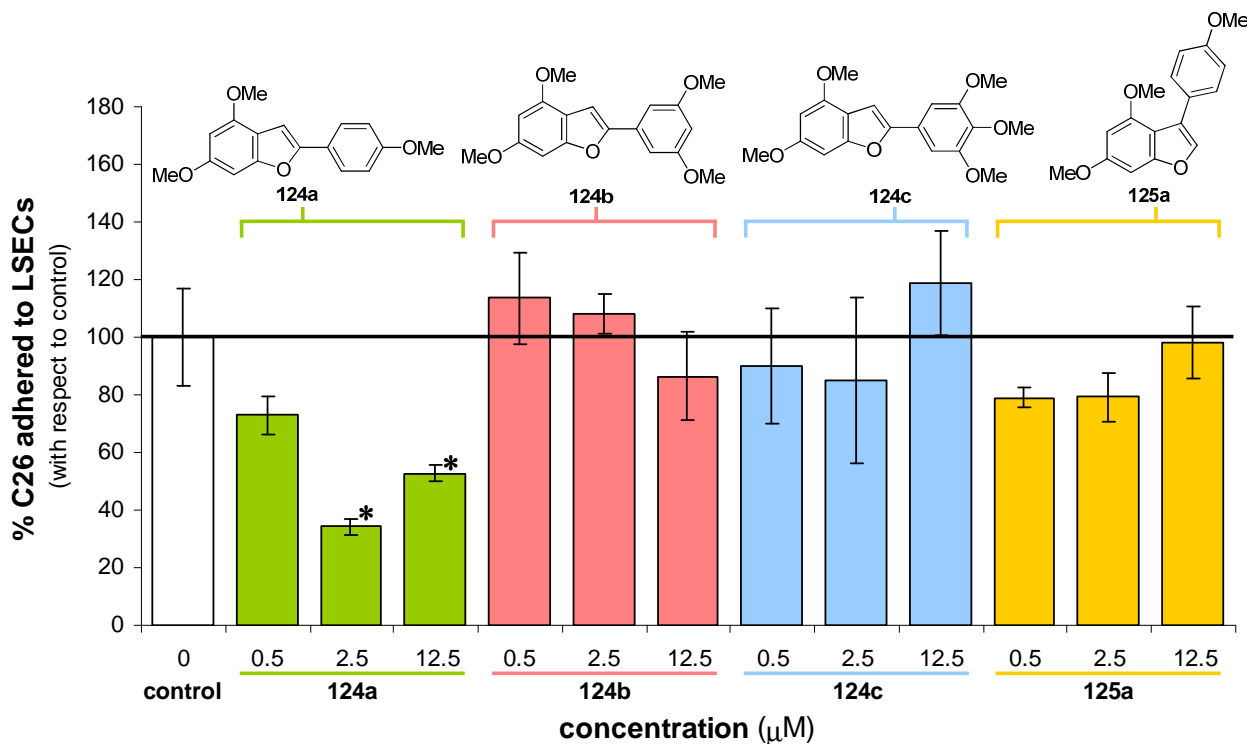


Figure 4.21. *In vitro* adhesion assays of C26 tumor cells to LSECs treated with methoxylated benzofurans **124a-c** and **125a**. Control reference is shown by a continuous black line and significant differences with respect to it are marked with a star (*).

Among the methoxylated benzofurans only **124a** showed a significant inhibition of the adhesion at the two highest tested concentrations (2.5 and 12.5 μM). On the contrary, compounds **124b-c** and **125a** showed no effect on the adhesive potential of murine colon carcinoma C26 cells to LSECs treated with them (Figure 4.21).

4.4.3.2. Effect of the resveratrol analogues on the net proliferation rate of murine colon carcinoma C26 cells

C26 tumor cells were treated with increasing concentrations (0.5, 2.5, 12.5, 25 and 50 μM) of testing compounds in EtOH (in the case of hydroxylated products) and DMSO (in the case of methoxylated products) for 24 hours in RPMI-1640 supplemented with antibiotics and 0.5% FBS before the proliferation measurement using Presto Blue assay, as previously detailed (section 4.4.2.4).

The results shown here are the average of the data obtained from three independent experiments. The effect of the compounds on tumor cell proliferation was considered significant when the value of statistical parameter p associated with the differences between the number of treated tumor cells with respect to the initial cell number or with respect to the number of untreated cells (control) was less than 0.01 ($p < 0.01$). These significant results are highlighted with a star (*) in the case of treatment vs. initial and with two stars (**) in the case of treatment vs. control in figures 4.22 and 4.23. The following results were obtained:

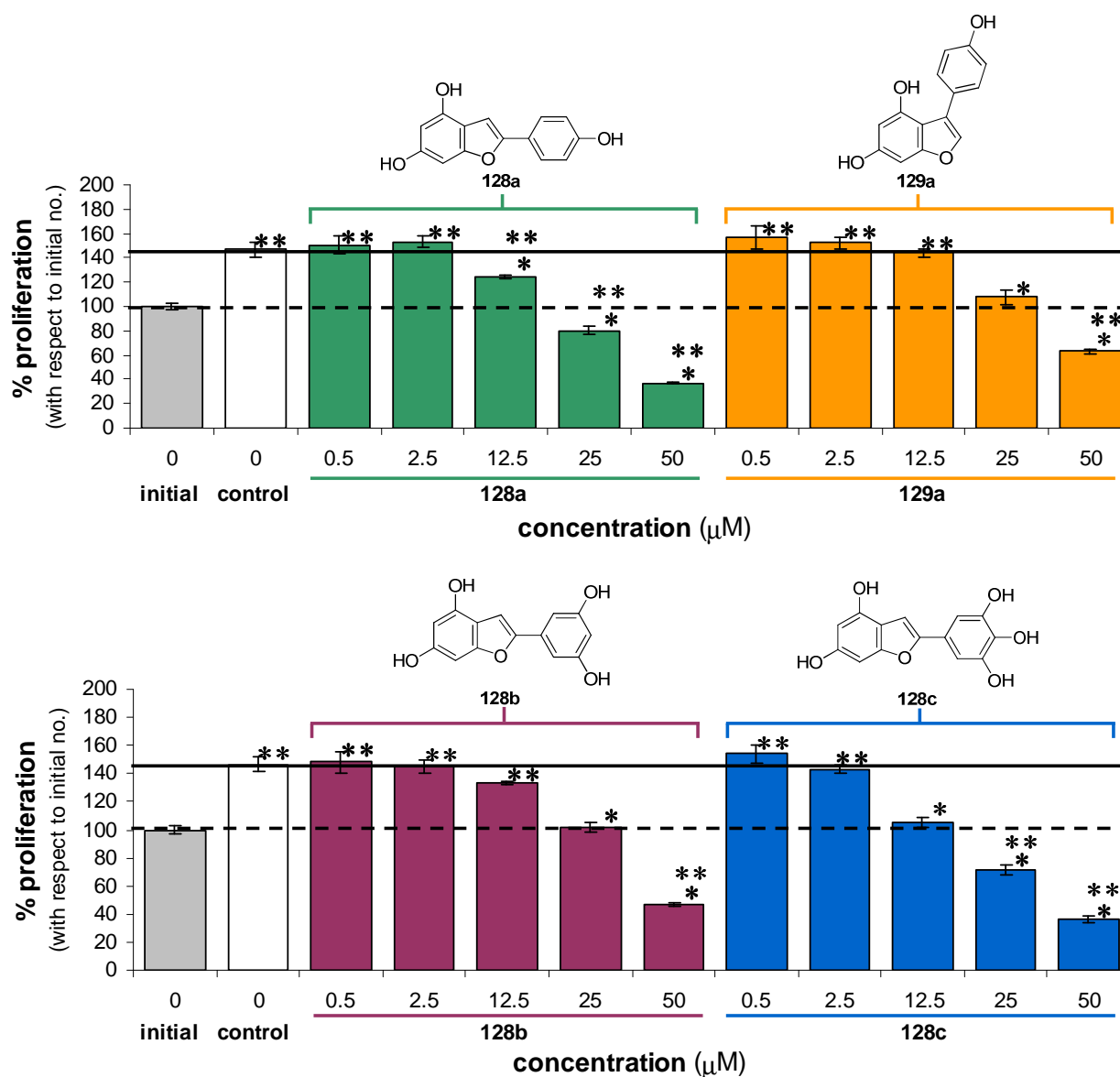


Figure 4.22. *In vitro* proliferation assays of C26 tumor cells treated with hydroxylated benzofurans **128a-c** and **129a**. Control reference is shown by a continuous black line and significant differences with respect to it are marked with a star (*). Initial reference is shown by a dashed black line and significant differences with respect to it are marked with two stars (**).

On looking at the hydroxylated benzofurans it was observed that, in general, they showed no effect on proliferation at the lowest tested concentrations (0.5 and 2.5 μM) and resulted clearly cytotoxic at the highest tested concentration (50 μM). Compounds **128a** and **128c** inhibited proliferation at 12.5 μM and were cytotoxic also at 25 μM , whilst compounds **128b** and **129a** did not affect proliferation at 12.5 μM but inhibited it at 25 μM (Figure 4.22).

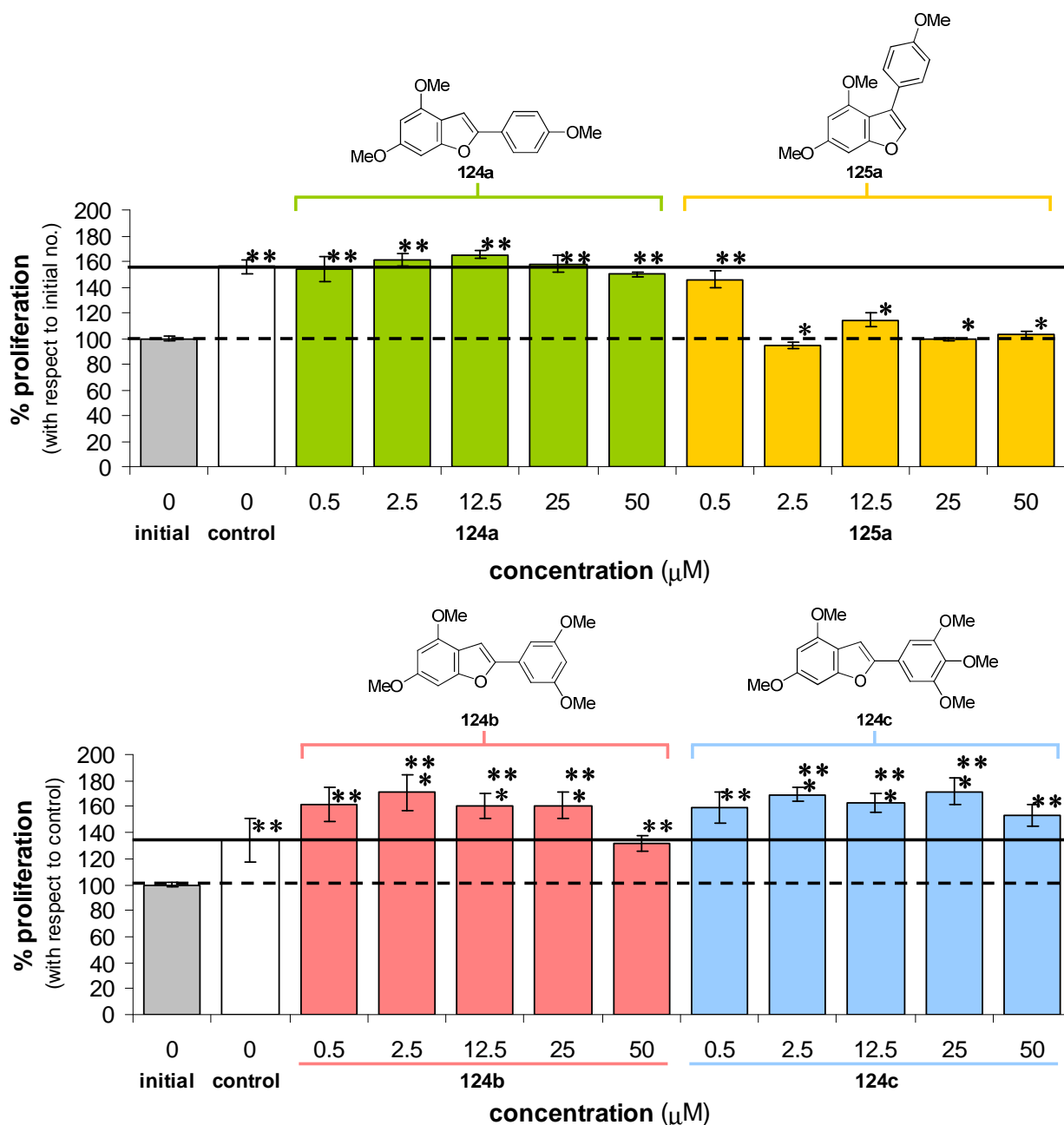


Figure 4.23. *In vitro* proliferation assays of C26 tumor cells treated with methoxylated benzofurans **124a-c** and **125a**. Control reference is shown by a continuous black line and significant differences with respect to it are marked with a star (*). Initial reference is shown by a dashed black line and significant differences with respect to it are marked with two stars (**).

Analyzing the values obtained for the methoxylated benzofurans, it was observed that 3-substituted benzofuran **125a** was the only compound giving positive results, having an inhibiting effect on proliferation at all the tested concentrations except for 0.5 μM and not resulting significantly cytotoxic at any of them. On the contrary, among the 2-substituted benzofurans, compound **124a** did not affect proliferation at any of the tested concentrations and compounds **124b** and **124c** slightly, although significantly, increased tumor cell proliferation (Figure 4.23).

An aspect that should be taken into consideration when evaluating these proliferation assays is the possible existence of subpopulations whose cell cycle or cellular death induction are differently affected by the tested compounds, resulting in no significant change in the total proliferation rate. In other words, a net zero proliferation could be the result of an inhibition of the general cycle or the result of a balance between a sub-population in cell cycle and a sub-population in apoptosis. Therefore, it would be advisable to label the treated populations to study the existence of different subpopulations and even to analyze the quiescent subpopulations (in G_0) with possibility of entering in cycle again. For so doing, some of the possible labels and tests could be Ki67, to identify cells in cycle (active phases G_1 , S, G_2 or M); fluorescently tagged annexin V, to identify apoptotic and dead cells; or DAPI (4',6-diamidino-2-phenylindole), to identify cells not showing cellular death signs.

With regard to the cytotoxicity (here associated with a decrease with respect to initial cell number), although in principle any compound toxic to the tumor cells bears potential value as anti-tumor agent, its effects must be validated in the stroma in a physiological and in a pro-tumor environment, both *in vitro* and *in vivo*.

The results presented in this section constitute then a start, but require further assays.

4.4.3.3 Effect of the resveratrol analogues on the migration of murine colon carcinoma C26 cells

After culture of CFSE labelled murine colon carcinoma C26 cells in the upper part of the inserts, they were allowed to adhere for 2 h, after which treatment were added at concentrations of 2.5 μM to both upper and lower compartments. Cells were allowed to migrate for 18 h before measuring the fluorescence emitted by only the cells passing the porous membrane, as previously detailed (section 4.4.2.5).

The results shown here are the average of the data obtained from three independent experiments. Differences between untreated and resveratrol analogues treated tumor cell migration were considered significant when the value of statistical parameter p is less than 0.05 ($p < 0.05$). These significant results are highlighted with a star (*) in figure 4.24. The following results were obtained:

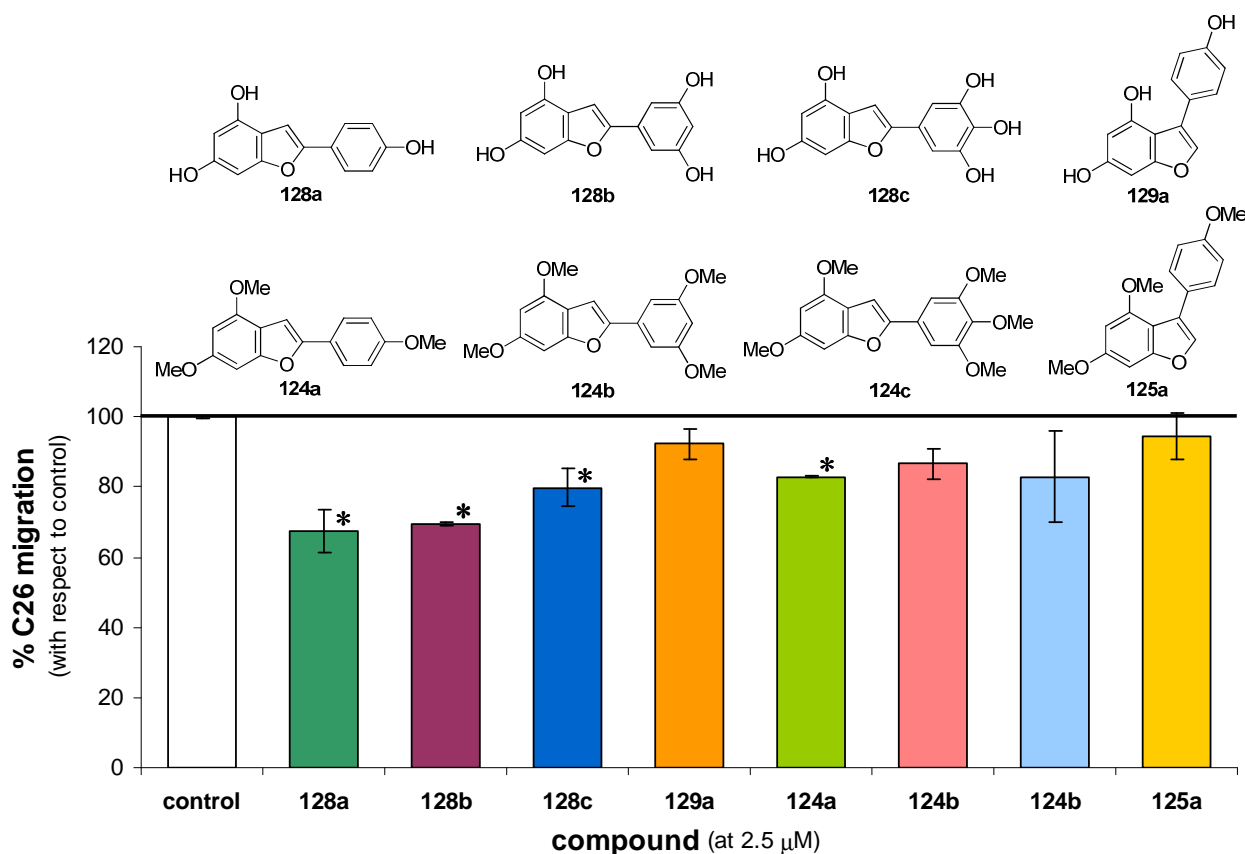


Figure 4.24. *In vitro* migration assay of C26 tumor cells treated with hydroxylated benzofurans **128a-c** and **129a** and methoxylated benzofurans **124a-c** and **124a** at 2.5 μM . Control reference is shown by a continuous black line and significant differences with respect to it are marked with a star (*).

All the hydroxylated 2-substituted benzofurans **128a-c** significantly inhibited migration at 2.5 μM concentration, whilst 3-substituted **129a** did not significantly affect this process.

Among the methoxylated benzofurans, only compound **124a** showed inhibitory activity (Figure 4.24). The concentration of 2.5 μM was selected for this assay because it did not result cytotoxic for any of the tested benzofurans, nevertheless further experiments at different concentrations would be needed to evaluate whether the effect of these compounds on the migration of tumor cells is concentration dependent and can be improved.

4.4.4. Graphical overview

The results of the three cell-based assays presented in this chapter (preliminary studies) are summarized in the table below (Table 4.3). In it, it can be observed that some of the tested compounds bear different effects on different pro-metastatic parameters.


Table 4.3. Summary table of the cell-based assays.


assay	with respect to	entry	conc. (μM)	hydroxylated (solvent: EtOH)				methoxylated (solvent: DMSO)			
				128 a	128 b	128 c	129 a	124 a	124 b	124 c	125 a
adhesion	control	1	0.5	↓	–	↓	↓	–	–	–	–
		2	2.5	↓	↓	↓	↓	↓	–	–	–
		3	12.5	–	↓	↓	↑	↓	–	–	–
proliferation	control	4	0.5	–	–	–	–	–	–	–	–
		5	2.5	–	–	–	–	–	↑	↑	↓
		6	12.5	↓	–	↓	–	–	↑	↑	↓
		7	25	↓	↓	↓	↓	–	↑	↑	↓
		8	50	↓	↓	↓	↓	–	–	–	↓
	initial no.	9	0.5	↑	↑	↑	↑	↑	↑	↑	↑
		10	2.5	↑	↑	↑	↑	↑	↑	↑	–
		11	12.5	↑	↑	–	↑	↑	↑	↑	–
		12	25	↓	–	↓	–	↑	↑	↑	–
13	50	↓	↓	↓	↓	↑	↑	↑	–		
migration	control	14	2.5	↓	↓	↓	–	↓	–	–	–


↓ = significant inhibition or decrease in number

↑ = significant activation or increase in number

– = no significant effect

 = inhibitor

 = activator

 = cytotoxic

control = 0 μM

conc. = concentration

Among hydroxylated benzofurans, **128a** and **129b** show inhibitory effect on adhesion of C26 tumor cells to LSECs, net proliferation (cycle arrest, induction of apoptosis in some subpopulations, etc.), resulting cytotoxic at high concentrations, and migration. **128c**, for its part, has a marked inhibitory effect on adhesion and net proliferation (resulting cytotoxic at 25 and 50 μM), but has only a slight inhibitory effect on migration. And 3-substituted

129a has inhibitory effects on adhesion at the lowest concentrations tested (0.5 and 2.5 μM), although activates it at 12.5 μM , inhibits net proliferation (resulting cytotoxic at 50 μM) but has no effect on migration.

Looking at the methoxylated benzofurans, **124a** has a marked inhibitory effect on adhesion but lacks inhibitory effect on net proliferation rate and shows only a slight inhibition of migration. **124b** and **124c**, for their part, show no effect either on adhesion or on migration and have a slight activation effect on net proliferation. And 3-substituted **125a** inhibits neither adhesion nor migration but has an inhibitory effect on net proliferation, not resulting cytotoxic at any of the tested concentrations.

4.5. CONCLUSIONS

From this chapter, in which the biological assays (enzymatic and cell-based assays) carried out with some hydroxylated and methoxylated benzofurans are presented, the following conclusions can be drawn:

- Computational studies showed that, adequately substituted, benzofuran scaffold holds a notable structural resemblance (distances between carbon atoms in its structure, electrostatic potential) with resveratrol. This suggests that benzofurans could potentially constitute a new family of compounds with interesting pharmacological properties and with the additional advantage of having a greater configurational stability over the *trans*-stilbene structures.
- Compound **128c** proved to improve the inhibitory effect of suramin sodium (inhibition reference compound) on SIRT1 deacetylation activity *in vitro*, presenting a lower value of the IC₅₀ parameter according to a now questioned enzymatic fluorescence assay. Other hydroxylated benzofurans, such as **129a** or **128f**, also showed significant inhibitory activity according to the same test.
- Compounds **128a** and **128b** stood out as interesting candidates for SIRT1 activation, according to a now questioned enzymatic fluorescence assay, showing a promising trade off between the values of the studied parameters (low EC_{1.5} and high %Max), comparable to those of resveratrol (activation reference compound).
- Performed preliminary cell-based assays revealed that the analyzed hydroxylated, **128a-c** and **129a**, and methoxylated, **124a-c** and **125a**, compounds bear different and significant effects on the studied pro-metastatic parameters: endothelium adhesive potential to the tumor, tumor proliferation, and tumor migratory potential. The results obtained from methoxylated compounds **124a** and **125a** are in principle more encouraging although, in any case, further biological assays would be needed.

Chapter 5:

Experimental Section

5.1. Analytical techniques and reagents

5.2. Regioselective synthesis of 2- and 3-aryl benzo[*b*]furans

- 5.2.1. General procedure for the preparation of α -bromoketones **123b-c,h-j**
- 5.2.2. Procedure for the preparation of 2-aryl benzo[*b*]furans **124a-n** and 2-aryl naphtho[1,2-*b*] and 2-aryl naphtho[2,1-*b*] furans **124q-r**
- 5.2.3. Procedure for the preparation of α -phenoxyketones **130a-l** and α -naphthoxyketones **130n-o**
- 5.2.4. Procedure for the preparation of 3-aryl benzo[*b*]furans **125a-i** and 3-aryl naphtho[1,2-*b*] and 3-aryl naphtho[2,1-*b*] furans **125n-o**

5.3. *N*-halosuccinimides (NXS)-mediated regioselective halogenation of 2- and 3-aryl benzo[*b*]furans **124a** and **125a**

- 5.3.1. Procedure for the monohalogenation of 2-aryl benzo[*b*]furan **124a** and 3-aryl benzo[*b*]furan **125a** with NXS leading to products **126a** and **127a,d-e**
- 5.3.2. Procedure for the dihalogenation of 2-aryl benzo[*b*]furan **124a** and 3-aryl benzo[*b*]furan **125a** with NXS leading to products **126b,f-g** and **127b**
- 5.3.3. Procedure for the tribromination of 2-aryl benzo[*b*]furan **124a** with NBS leading to product **126c**
- 5.3.4. Procedure for the monobromination of 2-chloro 3-aryl benzo[*b*]furan **127e** with NBS leading to product **127f**

5.4. Hypervalent iodine reagents-mediated oxidative dearomatization of 2- and 3-aryl benzo[*b*]furans 124s and 125p

- 5.4.1. Procedure for the preparation of 2-phenylbenzofuran-6-ol **124s**
- 5.4.2. Procedure for the preparation of 3-phenylbenzofuran-6-ol **125p**
- 5.4.3. Procedure for the preparation of *cis/trans*-2,3-dialkoxy-2-phenyl-2,3-dihydrobenzofuran-6-ols ***cis/trans*-170a-d**
- 5.4.4. Procedure for the preparation of 2-alkoxy-3-phenylbenzofuran-6-ols **171a-f**
- 5.4.5. Methylation of 2- and 3-phenyl benzo[*b*]furans **124s** and **125p** with methyl iodide
- 5.4.6. Synthesis of *o*-iodoxybenzoic acid IBX
- 5.4.7. Procedure for the preparation of 2-phenylbenzofuran-6,7-dione **141**
- 5.4.8. Procedure for the preparation of 3-phenylbenzofuran-6,7-diol **186**

5.5. Boron tribromide (BBr₃)-mediated demethylation of methoxy groups of 2- and 3-aryl benzo[*b*]furans 124a-e,i-k,q and 125a,d,i

5.6. Characterization reports

- 5.6.1. X-ray diffraction analysis report of compound **124a**
 - 5.6.2. X-ray diffraction analysis report of compound **125a**
 - 5.6.3. X-ray diffraction analysis report of compound ***cis*-170a**
 - 5.6.4. X-ray diffraction analysis report of compound ***trans*-170a**
 - 5.6.5. HRMS report of *cis/trans* mixtures of compounds **170c** and **170d**
-

5.1. ANALYTICAL TECHNIQUES and REAGENTS

Reagents and solvents

Reagents were purchased from different commercial suppliers (Aldrich, Fluka, Acros, Alfa Aesar, Merck, TCI, etc.), stored as specified by the manufacturer and used without previous purification. Considerably expensive or commercially unavailable (at the suppliers our laboratory works with) products were prepared following procedures reported in literature or developed by ourselves.

With respect to solvents, acetone, methanol (MeOH), dichloromethane (CH₂Cl₂), diethylether (Et₂O), ethylacetate (EtOAc), and hexane (Hx) were purified by fractional distillation at atmospheric pressure when not purchased with a synthesis or reagent grade of purity. Cyclohexane, *n*-butanol (^{*n*}BuOH), *t*-butanol (^{*t*}BuOH), diethylene glycol (HOEtOH), diglyme, ethanol (EtOH), 2,2,2-trifluoroethanol (TFE), *n*-propanol (^{*n*}PrOH), *i*-propanol (^{*i*}PrOH), tetrahydrofuran (THF) and xylene (mixture of isomers) were used without previous purification as they were purchased with a synthesis or reagent grade of purity.

When anhydrous solvents were required, they were dried following established procedures³¹³, i.e. dichloromethane was distilled over phosphorus pentoxide, methanol over calcium sulfate and acetone over potassium carbonate, and stored over molecular sieves of 4Å or immediately used. In the case of tetrahydrofuran, the Pure Solv MD3 (multi dispensing) solvent purification system from Innovative Technology company was employed to obtain the anhydrous solvent immediately before its use.

Solvent evaporation was carried out in either a Büchi R-II rotavapor (equipped with a Büchi V-710 vacuum pump and a Büchi V-850 vacuum controller) or in an IKA RV 10 Basic rotavapor (equipped with a Vacuubrand for VWR VP 2 autovac vacuum pumping unit with a CVC 3000 vacuum controller). Distillations at lowered pressure were conducted in a Büchi Glass Oven B-585 connected to a Vacuubrand rotatory vane vacuum pump RZ 5. For the complete removal of solvents a Büchi V-710 vacuum pump or a Vacuubrand rotatory vane vacuum pump RZ 5 was also employed.

³¹³ Armarego, W. L. F.; Perrin, D. D. *Purification of Laboratory Chemicals 4th Edition* Butterworth-Heinemann, Oxford 1996

Microwave and hydrogenation reactors

Microwave irradiations were conducted in a focused microwave Biotage Initiator EXP EU reactor or a CEM Discover System reactor at the temperature, at the power and for the time indicated.

Hydrogenation reactions were performed in the H-cube® hydrogenation reactor of the Thalesnano trademark.

Chromatography

Purification column chromatographies were carried out employing Merck silica gel 60 (0.040-0.063 mm) for column chromatography (230-400 mesh), and a suitable mixture of solvents (typically ethyl acetate and hexane or cyclohexane) as eluent. Alternatively, in some particular cases, the high performance flash purification system Biotage Isolera Four was employed.

Thin layer chromatographies (TLCs) were performed over Merck TLC silica gel 60 F₂₅₄ aluminium sheets. Separations by preparative thin layer chromatography (PLC) were performed over Merck PLC Silica gel 60 F₂₅₄, 1mm glass plates. Both of them were visualized with ultraviolet light (Vilber-Lourmat lamp VL-4.LC, $\lambda = 254$ and 365 nm) and/or by heating them after contact with an appropriate stain (typically a solution of phosphomolybdic acid in absolute ethanol).

Preparative high performance liquid chromatography (HPLC) purifications were conducted in a Waters Delta Prep 4000 preparative chromatography system, equipped with a Waters 2487 dual λ absorbance detector, a deuterium lamp ultraviolet detector (set at $\lambda = 254$ and 285 nm) and a Hichrom Kromasil 6-10SIL column (of 25 cm x 3.5 cm) as stationary phase. HPLC grade solvents (EtOAc and Hx) were employed as mobile phase.

Nuclear magnetic resonance (NMR)

All the NMR spectra (¹H, ¹³C, COSY, HSQC, HMBC and NOE) were registered in Varian Gemini 200 (200 MHz for ¹H), Bruker Advance DPX 300 (300 MHz for ¹H, 75 MHz for ¹³C),

or Bruker Advance Ultrashield 400 (400 MHz for ^1H , 101 MHz for ^{13}C) or 500 (500 MHz for ^1H , 126 MHz for ^{13}C) spectrometers.

Different deuterated solvents were employed, depending on the product to be analysed: deuterated chloroform (CDCl_3), deuterated dimethylsulfoxide (DMSO-d_6), deuterated methanol (CD_3OD) and deuterated acetone (acetone-d_6). Chemical shifts (δ) are given in parts per million (ppm) with respect to an internal reference of trimethylsilane (TMS) ($\delta=0.00$) for the ^1H spectra in CDCl_3 including TMS and with respect to the corresponding solvent residual peak in all other cases: CDCl_3 , ^1H ($\delta=7.24$) and ^{13}C ($\delta=77.23$); DMSO-d_6 , ^1H ($\delta=2.50$), ^{13}C ($\delta=39.51$); CD_3OD , ^1H ($\delta=3.31$) and ^{13}C ($\delta=49.15$); acetone-d_6 , ^1H ($\delta=2.05$) and ^{13}C ($\delta=29.92$).

The following abbreviations are used to indicate the multiplicity in NMR spectra: s, singlet; d, doublet; t, triplet; q, quartet; m, multiplet; dd, doublet of doublets; td, triplet of doublets; tt, triplet of triplets and bs, broad signal. Coupling constants (J) are given in Hz. MestrReNova 5.3.0-4487 program was used to process and edit the registered spectra.

Melting points (m.p.) and infrared spectroscopy (IR)

Melting points (m.p.) were determined in open capillaries on a Büchi B-450 model equipment and were uncorrected.

Infrared (IR) spectra were registered in a Bruker Alpha model system (using the neat sample as such) or in a Perkin Elmer 1600 FTIR device (employing a translucent mechanically pressed pellet of the sample ground with potassium bromide, KBr).

Elemental analysis and high resolution mass spectrometry (HRMS)

Elemental analyses were carried out in a LECO CNS-932 microanalyzer calibrated with sulfametazine. The analysis were performed in duplicate by combustion of 1-2 mg samples (oven temperature $1000\text{ }^\circ\text{C} + \text{O}_2$) using helium as carrier gas. The carbon, hydrogen, nitrogen and sulphur content of each sample was quantitatively determined by this means.

Mass spectrometry analyses were performed in the General Research Service (SGIker) of the University of the Basque Country (UPV/EHU) using an ultrafast liquid chromatograph (UPLC ACQUITY model from Waters) coupled to a photodiode detector (PDA detector model from Waters) and a QTOF type mass spectrometer (Synapt G2 model from Waters). The spectra were registered in the positive ion mode employing electrospray ionization (ESI) as ionization source.

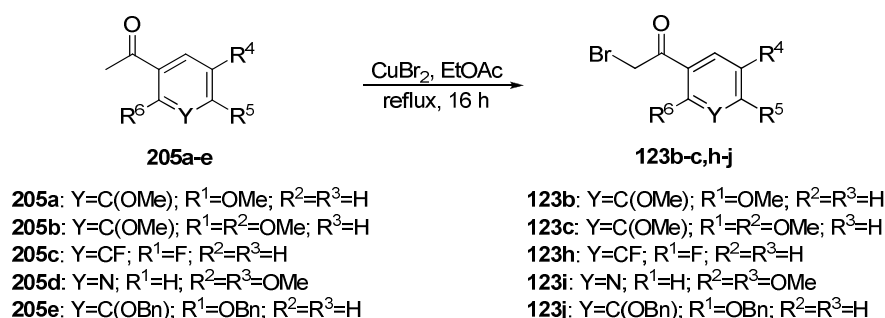
X-ray diffraction analysis

The X-ray diffraction analysis experiments were conducted in the General Research Service (SGIker) of the University of the Basque Country (UPV/EHU) using diffractometers for monocrystals: Oxford Diffraction Xcalibur 2 (equipped with a CCD type detector model Sapphire 2) or Agilent SuperNova Cu (equipped a CCD type detector model Atlas).

5.2. REGIOSELECTIVE SYNTHESIS of 2- and 3-ARYL BENZO[*b*]FURANS

5.2.1. General procedure for the preparation of α -bromoketones 123b-c,h-j

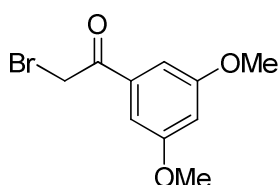
The α -bromoketones **123** not directly purchased from commercial sources were prepared following a CuBr₂-mediated bromination of the corresponding acetophenones **205** strategy reported in literature³¹⁴.



Scheme 5.1. Preparation of α -bromoacetophenones **123b-c,h-j** from the corresponding acetophenones **205**.

Accordingly, acetophenone **205** (12.8-60.0 mmol), CuBr₂ (20.5-96.0 mmol, 1.6 eq) and 26-120 ml of EtOAc (2 ml per mmol of acetophenone) were placed in a round bottom flask equipped with a reflux condenser. The mixture was heated under reflux for 16 hours. The resulting reaction mixture was left to cool until it reached room temperature. It was then filtered through a Celite pad and evaporated under reduced pressure. The crude obtained this way was purified by column chromatography on silica gel, using EtOAc/Hx mixtures as eluent to afford the corresponding pure products **123**.

2-Bromo-3',5'-dimethoxyacetophenone³¹⁵, **123b**:



Molecular formula: C₁₁H₁₀BrO₃

Molecular weight: 259.10 g/mol

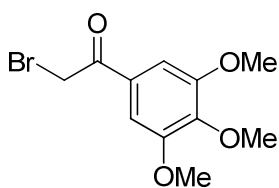
Aspect: Yellow oil

Yield: 90%

¹H-NMR (300 MHz, CDCl₃) δ = 7.11 (d, *J*=2.3 Hz, 2H), 6.69 (t, *J*=2.3 Hz, 1H), 4.41 (s, 2H), 3.84 (s, 6H).

³¹⁴ (a) King, L. C.; Ostrum, G. K. *J. Org. Chem.* **1964**, 29, 3459-3461 (b) Diwu, Z.; Beachdel, C.; Klaubert, D. H. *Tetrahedron Lett.* **1998**, 39, 4987-4990 (c) Chen, L.; Ding, Q.; Gillespie, P.; Kim, K.; Lovey, A. J.; McComas, W. W.; Mullin, J. G.; Perrota, A. *Patent* **2002** WO 2002057261 (d) Bakke, B. A.; McIntosh, M. C.; Turnbull, K. D. *J. Org. Chem.* **2005**, 70, 4338-4345

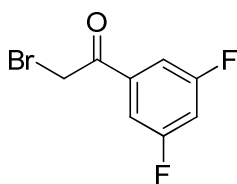
³¹⁵ Commercial product, CAS: 50841-50-4

2-Bromo-3',4',5'-trimethoxyacetophenone³¹⁶, 123c:Molecular formula: C₁₁H₁₃BrO₄

Molecular weight: 289.12 g/mol

Aspect: Pale yellow solid

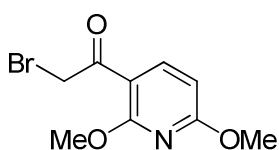
Yield: 56%

¹H-NMR (300 MHz, CDCl₃) δ = 7.25 (s, 2H), 4.40 (s, 2H), 3.94 (s, 3H), 3.93 (s, 6H).**2-Bromo-3',5'-difluoroacetophenone³¹⁷, 123h:**Molecular formula: C₈H₅BrF₂O

Molecular weight: 235.03 g/mol

Aspect: Yellow oil

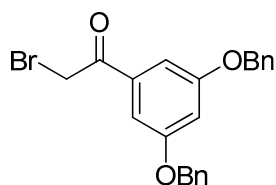
Yield: 95%

¹H-NMR (300 MHz, CDCl₃) δ = 7.52–7.48 (m, 2H), 7.07 (tt, *J*=8.4, 2.3 Hz, 1H), 4.37 (s, 2H).**2-Bromo-1-(2',6'-dimethoxy-pyridin-3-yl)ethanone³¹⁸, 123i:**Molecular formula: C₉H₁₀BrNO₃

Molecular weight: 260.08 g/mol

Aspect: White solid

Yield: 81%

¹H-NMR (500 MHz, CDCl₃) δ = 8.20 (d, *J*=8.6 Hz, 1H), 6.41 (d, *J*=8.6 Hz, 1H), 4.57 (s, 2H), 4.09 (s, 3H), 4.00 (s, 3H).**2-Bromo-3',5'-dibenzyloxyacetophenone³¹⁹, 123j:**Molecular formula: C₂₂H₁₉BrO₃

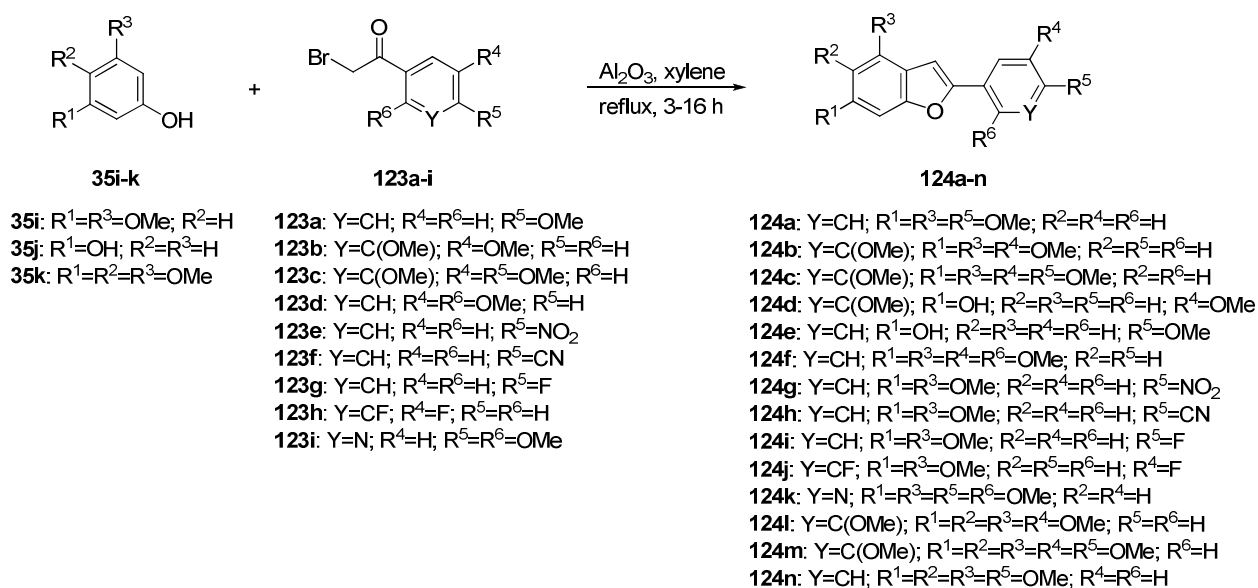
Molecular weight: 411.29 g/mol

Aspect: White solid

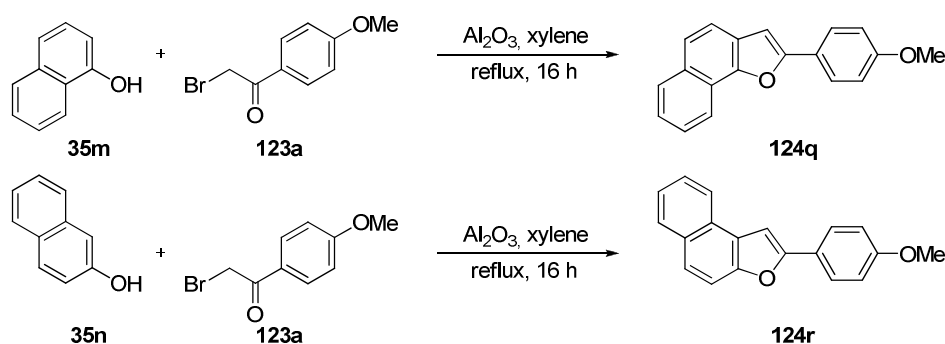
Yield: 49%

¹H-NMR (300 MHz, CDCl₃) δ = 7.31–7.44 (m, 10H), 7.20 (d, *J*=2.4 Hz, 2H), 6.85 (t, *J*=2.1 Hz, 1H), 5.08 (s, 4H), 4.39 (s, 2H).³¹⁶ Commercial product, CAS: 51490-01-8³¹⁷ Commercial product, CAS: 22607-75-0³¹⁸ Dickson, J. K. Jr.; Hodge, C. N.; Mendoza, J. S.; Chen, K. *Patent* **2006**, WO 2006020767 A2³¹⁹ Commercial product, CAS: 28924-18-7

5.2.2. Procedure for the preparation of 2-aryl benzo[*b*]furans **124a-n** and 2-aryl naphtho[1,2-*b*] and 2-aryl naphtho[2,1-*b*] furans **124q-r**

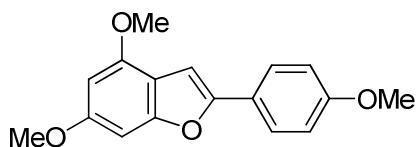


Scheme 5.2. Preparation of 2-aryl benzo[*b*]furans **124a-n** from phenols **35i-k** and α -bromoacetophenones **123a-i**.



Scheme 5.3. Preparation of 2-aryl naphtho[*b*]furans **124q-r** from naphthols **35m-n** and α -bromoacetophenone **123a**.

Phenol or naphthol **35** (3.0 mmol), α -bromoacetophenone **123** (4.2 mmol, 1.4 eq), alumina (21.0 mmol, 7 eq) and 12 ml of xylene were placed in a round bottom flask equipped with a reflux condenser. The mixture was heated under reflux for 16 hours. The resulting reaction mixture was left to cool until it reached room temperature. It was then filtered through a Celite pad and evaporated under reduced pressure. The crude obtained this way was purified by column chromatography on silica gel, using EtOAc/Hx mixtures as eluent to afford the corresponding pure products **124**. The alumina (aluminium oxide) employed was neutral (activated, Brockmann I, STD grade, approx. 150 mesh, 58 Å) and the xylene, a mixture of isomers.

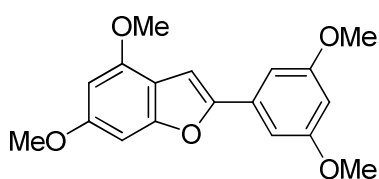
4,6-dimethoxy-2-(4'-methoxyphenyl)benzofuran¹⁷⁷, 124a:Molecular formula: C₁₇H₁₆O₄

Molecular weight: 284.31 g/mol

Aspect: White solid

Yield: 50%

¹H-NMR (500 MHz, CDCl₃) δ = 7.71 (d, *J*=8.8 Hz, 2H), 6.95 (d, *J*=8.8 Hz, 2H), 6.89 (s, 1H), 6.69 (s, 1H), 6.32 (d, *J*=1.6 Hz, 1H), 3.91 (s, 3H), 3.86 (s, 3H), 3.85 (s, 3H).

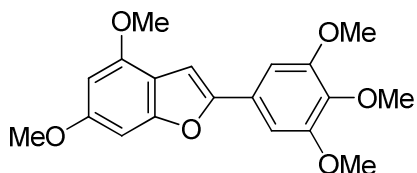
2-(3',5'-dimethoxyphenyl)-4,6-dimethoxybenzofuran³²⁰, 124b:Molecular formula: C₁₈H₁₈O₅

Molecular weight: 314.33 g/mol

Aspect: White solid

Yield: 86%

¹H-NMR (500 MHz, CDCl₃) δ = 7.02 (s, 1H), 6.95 (s, 2H), 6.70 (s, 1H), 6.43 (s, 1H), 6.33 (s, 1H), 3.92 (s, 3H), 3.86 (s, 3H), 3.85 (s, 6H).

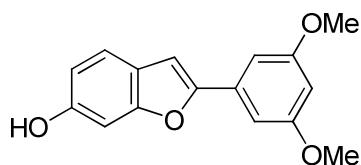
4,6-dimethoxy-2-(3',4',5'-trimethoxyphenyl)benzofuran, 124c:Molecular formula: C₁₉H₂₀O₆

Molecular weight: 344.36 g/mol

Aspect: White solid

Yield: 75%

m.p.: 131-132 °C. IR (KBr): 2960, 1619, 1497, 1227, 1203, 1134, 1110 cm⁻¹. ¹H-NMR (500 MHz, CDCl₃) δ = 7.04 (s, 2H), 7.00 (s, 1H), 6.74 (s, 1H), 6.36 (d, *J*=1.8 Hz, 1H), 3.97 (s, 6H), 3.95 (s, 3H), 3.91 (s, 3H), 3.89 (s, 3H). ¹³C-NMR (126 MHz, CDCl₃) δ = 159.4, 156.7, 153.8, 153.7, 153.7, 138.4, 126.6, 113.5, 101.9, 98.7, 94.6, 88.5, 61.2, 56.4, 56.0, 55.8. Elemental analysis calculated for C₁₉H₂₀O₆: C, 66.3; H, 5.8. Found: C, 66.0; H, 6.0.

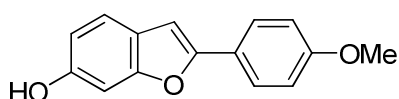
2-(3',5'-dimethoxyphenyl)benzofuran-6-ol³²¹, 124d:Molecular formula: C₁₆H₁₄O₄

Molecular weight: 270.28 g/mol

Aspect: Brown solid

Yield: 26%

¹H-NMR (500 MHz, CDCl₃) δ = 7.39 (d, *J*=8.0 Hz, 1H), 7.01 (s, 1H), 6.97 (s, 2H), 6.92 (s, 1H), 6.77 (d, *J*=7.9 Hz, 1H), 6.45 (s, 1H), 5.02 (s, 1H), 3.86 (s, 6H).

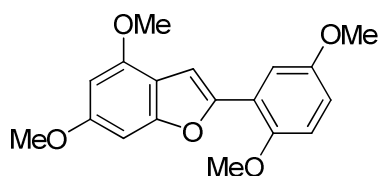
2-(4'-methoxyphenyl)benzofuran-6-ol³²⁰, 124e:Molecular formula: C₁₅H₁₂O₃

Molecular weight: 240.25 g/mol

Aspect: White solid

Yield: 32%

¹H-NMR (500 MHz, DMSO-*d*₆) δ = 9.49 (s, 1H), 7.76 (d, *J*=8.7 Hz, 2H), 7.37 (d, *J*=8.3 Hz, 1H), 7.09 (s, 1H), 7.03 (d, *J*=8.8 Hz, 2H), 6.93 (s, 1H), 6.73 (dd, *J*=8.3, 1.9 Hz, 1H), 3.81 (s, 3H).

2-(2',5'-dimethoxyphenyl)-4,6-dimethoxybenzofuran, 124f:Molecular formula: C₁₈H₁₈O₅

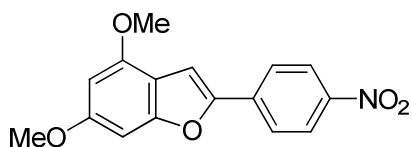
Molecular weight: 314.33 g/mol

Aspect: Pale pink solid

Yield: 25%

m.p.: 82-83°C. IR (KBr): 2896, 1604, 1503, 1212, 1130 cm⁻¹. ¹H-NMR (500 MHz, CDCl₃) δ = 7.54 (d, *J*=3.0 Hz, 1H), 7.37 (s, 1H), 6.89 (d, *J*=8.9 Hz, 1H), 6.80 (dd, *J*=8.9, 3.0 Hz, 1H), 6.69 (s, 1H), 6.31 (d, *J*=1.6 Hz, 1H), 3.92 (s, 3H), 3.91 (s, 3H), 3.85 (s, 3H), 3.84 (s, 3H). ¹³C-NMR (126 MHz, CDCl₃) δ = 159.5, 155.9, 153.9, 150.7, 150.0, 120.5, 114.1, 114.0, 112.5, 111.7, 104.2, 94.4, 88.3, 56.2, 56.1, 56.0, 55.8. Elemental analysis calculated for C₁₈H₁₈O₅: C, 68.8; H, 5.8. Found: C, 68.9; H, 5.7.

³²¹ Watanabe, M.; Kawanishi, K.; Furukawa, S. *Chem. Pharm. Bull.* **1991**, *39*, 579-583

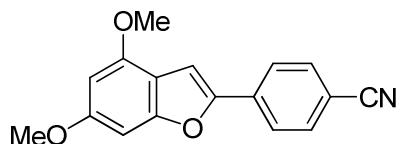
4,6-dimethoxy-2-(4'-nitrophenyl)benzofuran, 124g:Molecular formula: C₁₆H₁₃NO₅

Molecular weight: 299.28 g/mol

Aspect: Orange solid

Yield: 44%

m.p.: 192-193 °C. IR (KBr): 2943, 2914, 1594, 1504, 1319, 1145, 1104 cm⁻¹. ¹H-NMR (500 MHz, CDCl₃) δ = 8.26 (d, *J*=8.8 Hz, 2H), 7.88 (d, *J*=8.8 Hz, 2H), 7.24 (s, 1H), 6.69 (s, 1H), 6.34 (s, 1H), 3.93 (s, 3H), 3.88 (s, 3H). ¹³C-NMR (75 MHz, DMSO-d₆) δ = 160.3, 156.7, 153.6, 150.6, 146.1, 135.9, 124.5, 124.4, 112.4, 104.0, 95.0, 88.5, 55.8, 55.7. Elemental analysis calculated for C₁₆H₁₃NO₅: C, 64.2; H, 4.4; N, 4.7. Found: C, 64.2; H, 4.3; N, 4.6.

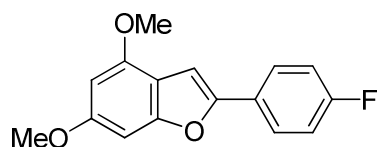
4-(4',6'-dimethoxybenzofuran-2-yl)benzonitrile, 124h:Molecular formula: C₁₇H₁₃NO₃

Molecular weight: 279.29 g/mol

Aspect: Yellow solid

Yield: 24%

m.p.: 220-221 °C. IR (KBr): 3042, 2955, 2223, 1600, 1507, 1217, 1145, 1104 cm⁻¹. ¹H-NMR (500 MHz, CDCl₃) δ = 7.84 (d, *J*=8.2 Hz, 2H), 7.67 (d, *J*=8.3 Hz, 2H), 7.18 (s, 1H), 6.68 (s, 1H), 6.34 (s, 1H), 3.92 (s, 3H), 3.87 (s, 3H). ¹³C-NMR (126 MHz, CDCl₃) δ = 160.5, 157.4, 154.2, 151.6, 135.0, 132.8, 124.5, 119.1, 113.4, 110.8, 102.4, 95.0, 88.4, 56.1, 55.9. Elemental analysis calculated for C₁₇H₁₃NO₃: C, 73.1; H, 4.7; N, 5.0. Found: C, 73.3; H, 5.0; N, 5.1.

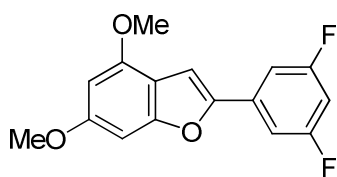
2-(4'-fluorophenyl)-4,6-dimethoxybenzofuran, 124i:Molecular formula: C₁₆H₁₃FO₃

Molecular weight: 272.27 g/mol

Aspect: White solid

Yield: 49%

m.p.: 142-143 °C. IR (KBr): 2914, 1614, 1496, 1220, 1145, 1116, 1043 cm⁻¹. ¹H-NMR (200 MHz, CDCl₃) δ = 7.74 (dd, *J*=8.8, 5.4 Hz, 2H), 7.10 (t, *J*=8.7 Hz, 2H), 6.96 (s, 1H), 6.68 (s, 1H), 6.33 (d, *J*=1.7 Hz, 1H), 3.92 (s, 3H), 3.86 (s, 3H). ¹³C-NMR (126 MHz, CDCl₃) δ = 162.6 (d, *J*=247.7 Hz), 159.5, 156.8, 153.7, 153.0, 127.4 (d, *J*=3.0 Hz), 126.2 (d, *J*=8.0 Hz), 116.0 (d, *J*=22.0 Hz), 113.5, 98.7, 94.6, 88.5, 56.0, 55.8. Elemental analysis calculated for C₁₆H₁₃FO₃: C, 70.6; H, 4.8. Found: C, 70.3; H, 4.9.

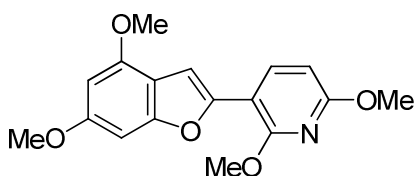
2-(3',5'-difluorophenyl)-4,6-dimethoxybenzofuran, 124j:Molecular formula: C₁₆H₁₂F₂O₃

Molecular weight: 290.26 g/mol

Aspect: Pale pink solid

Yield: 46%

m.p.: 124-125 °C. IR (neat): 3084, 2884, 1598, 1466, 1338, 1224, 1145 cm⁻¹. ¹H-NMR (500 MHz, CDCl₃) δ = 7.26 (d, *J*=8.6 Hz, 2H), 7.06 (s, 1H), 6.71 (t, *J*=8.8 Hz, 1H), 6.67 (s, 1H), 6.33 (s, 1H), 3.92 (s, 3H), 3.86 (s, 3H). ¹³C-NMR (126 MHz, CDCl₃) δ = 163.6 (dd, *J*=247.6, 13.1 Hz), 160.2, 157.0, 154.0, 151.5, 133.9 (t, *J*=10.5 Hz), 113.2, 107.1 (dd, *J*=20.7, 6.7 Hz), 103.0 (t, *J*=25.6 Hz), 101.2, 94.9, 88.3, 56.0, 55.8. Elemental analysis calculated for C₁₆H₁₂F₂O₃: C, 66.2; H, 4.2. Found: C, 66.2; H, 4.1.

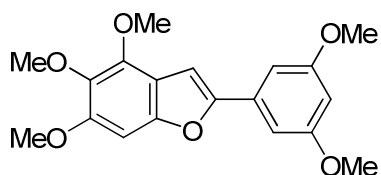
3-(4',6'-dimethoxybenzofuran-2-yl)-2,6-dimethoxypyridine, 124k:Molecular formula: C₁₇H₁₇NO₅

Molecular weight: 315.32 g/mol

Aspect: Pale pink solid

Yield: 53%

m.p.: 155-156 °C. IR (KBr): 2937, 2961, 1605, 1504, 1475, 1460, 1272, 1107, 1011 cm⁻¹. ¹H-NMR (500 MHz, CDCl₃) δ = 8.12 (d, *J*=8.2 Hz, 1H), 7.18 (s, 1H), 6.66 (s, 1H), 6.41 (d, *J*=8.2 Hz, 1H), 6.32 (s, 1H), 4.10 (s, 3H), 3.96 (s, 3H), 3.93 (s, 3H), 3.85 (s, 3H). ¹³C-NMR (126 MHz, CDCl₃) δ = 162.0, 159.1, 158.7, 156.0, 153.7, 149.5, 137.4, 113.9, 106.7, 101.7, 101.5, 94.4, 88.4, 56.0, 55.8, 53.8, 53.7. Elemental analysis calculated for C₁₇H₁₇NO₅: C, 64.8; H, 5.4; N, 4.4. Found: C, 64.9; H, 5.2; N, 4.3.

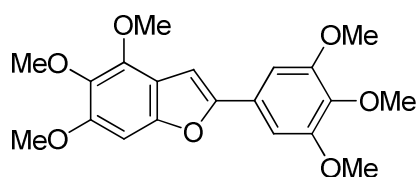
2-(3',5'-dimethoxyphenyl)-4,5,6-trimethoxybenzofuran, 124l:Molecular formula: C₁₉H₂₀O₆

Molecular weight: 344.36 g/mol

Aspect: Brown solid

Yield: 9%

m.p.: 82-84 °C. IR (neat): 2938, 2836, 1594, 1414, 1125 cm⁻¹. ¹H-NMR (500 MHz, CDCl₃) δ = 7.05 (s, 1H), 6.94 (s, 2H), 6.83 (s, 1H), 6.43 (s, 1H), 4.12 (s, 3H), 3.91 (s, 3H), 3.86 (s, 3H), 3.85 (s, 6H). ¹³C-NMR (126 MHz, CDCl₃) δ = 161.3, 154.2, 152.7, 152.0, 146.1, 137.5, 132.4, 115.0, 102.7, 100.8, 100.1, 90.8, 61.6, 60.8, 56.6, 55.6. Elemental analysis calculated for C₁₉H₂₀O₆: C, 66.3; H, 5.8. Found: C, 66.4; H, 5.8.

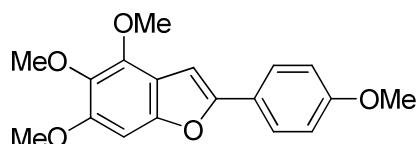
4,5,6-trimethoxy-2-(3',4',5'-trimethoxyphenyl)benzofuran, 124m:Molecular formula: C₂₀H₂₂O₇

Molecular weight: 374.38 g/mol

Aspect: White solid

Yield: 11%

m.p.: 172-173 °C. IR (neat): 2940, 2836, 1415, 1203, 1121 cm⁻¹. ¹H-NMR (500 MHz, CDCl₃) δ = 7.01 (s, 2H), 6.99 (s, 1H), 6.85 (s, 1H), 4.13 (s, 3H), 3.95 (s, 6H), 3.92 (s, 3H), 3.89 (s, 3H), 3.88 (s, 3H). ¹³C-NMR (126 MHz, CDCl₃) δ = 154.3, 153.9, 152.6, 152.0, 146.1, 138.7, 137.7, 126.3, 115.3, 102.1, 99.3, 90.8, 61.6, 61.2, 60.9, 56.6, 56.5. Elemental analysis calculated for C₂₀H₂₂O₇: C, 64.1; H, 5.9. Found: C, 64.0; H, 5.8.

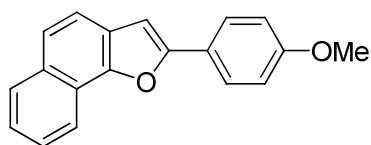
4,5,6-trimethoxy-2-(4'-methoxyphenyl)benzofuran, 124n:Molecular formula: C₁₈H₁₈O₅

Molecular weight: 314.33 g/mol

Aspect: White solid

Yield: 10%

m.p.: 120-121 °C. IR (neat): 2937, 2836, 1587, 1467, 1247, 1127 cm⁻¹. ¹H-NMR (500 MHz, CDCl₃) δ = 7.72 (d, *J*=8.7 Hz, 2H), 6.96 (d, *J*=8.7 Hz, 2H), 6.92 (s, 1H), 6.83 (s, 1H), 4.12 (s, 3H), 3.91 (s, 3H), 3.87 (s, 3H), 3.85 (s, 3H). ¹³C-NMR (126 MHz, CDCl₃) δ = 159.9, 154.6, 152.1, 151.9, 145.9, 137.5, 126.1, 123.7, 115.4, 114.5, 97.9, 90.9, 61.6, 60.8, 56.6, 55.6. Elemental analysis calculated for C₁₈H₁₈O₅: C, 68.8; H, 5.8. Found: C, 68.5; H, 5.8.

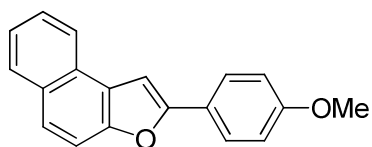
2-(4'-methoxyphenyl)naphtho[1,2-*b*]furan³²², 124q:Molecular formula: C₁₉H₁₄O₂

Molecular weight: 274.31 g/mol

Aspect: Light brown solid

Yield: 41%

¹H-NMR (500 MHz, CDCl₃) δ = 8.37 (d, *J*=8.2 Hz, 1H), 7.92 (d, *J*=8.2 Hz, 1H), 7.88 (d, *J*=8.8 Hz, 2H), 7.64 (s, 2H), 7.59 (t, *J*=7.6 Hz, 1H), 7.47 (t, *J*=7.5 Hz, 1H), 7.02 (d, *J*=8.8 Hz, 2H), 7.00 (s, 1H), 3.88 (s, 3H).

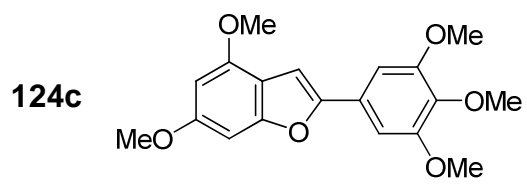
2-(4'-methoxyphenyl)naphtho[2,1-b]furan^{63a}, 124r:Molecular formula: C₁₉H₁₄O₂

Molecular weight: 274.31 g/mol

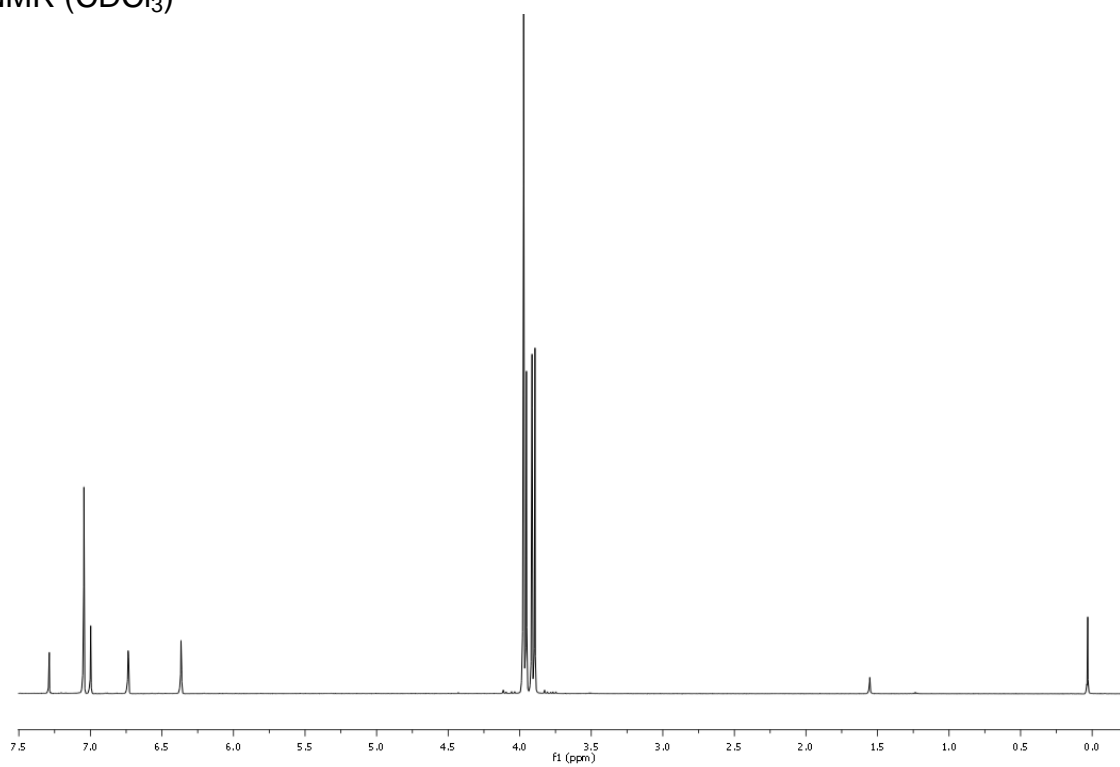
Aspect: White solid

Yield: 53%

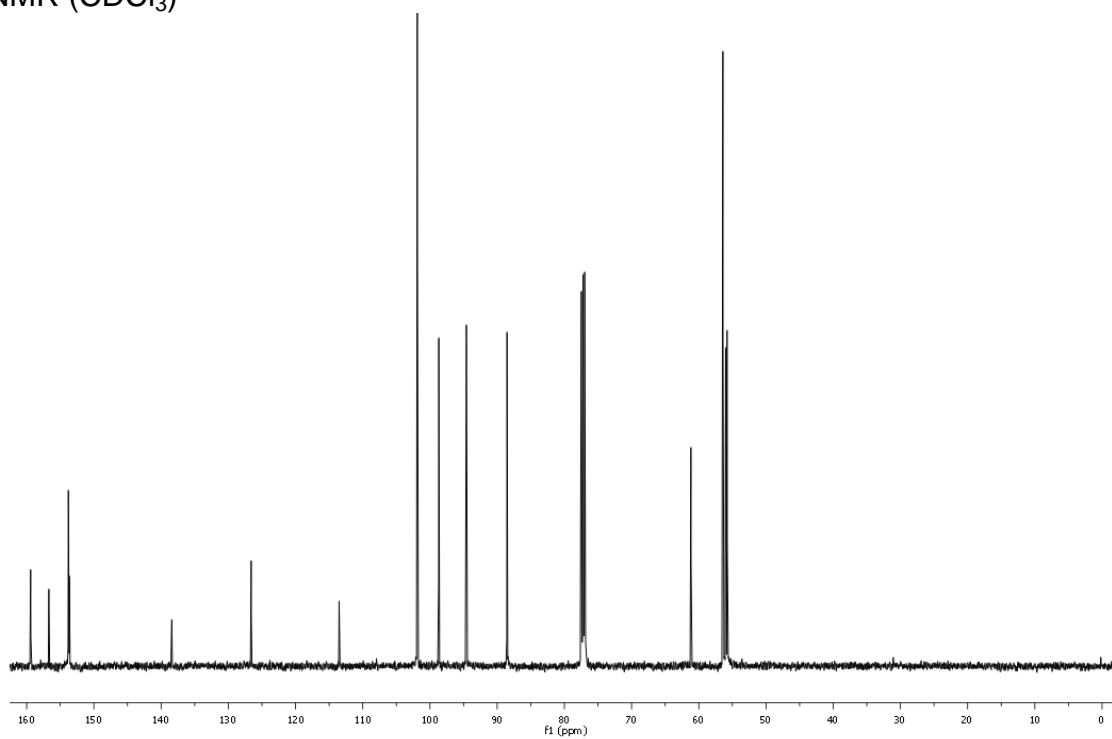
¹H-NMR (500 MHz, CDCl₃) δ = 8.14 (d, *J*=8.2 Hz, 1H), 7.93 (d, *J*=8.1 Hz, 1H), 7.84 (d, *J*=8.9 Hz, 2H), 7.67 (d, *J*=2.6 Hz, 2H), 7.57 (t, *J*=7.0 Hz, 1H), 7.47 (t, *J*=7.0 Hz, 1H), 7.37 (s, 1H), 6.99 (d, *J*=8.8 Hz, 2H), 3.86 (s, 3H).

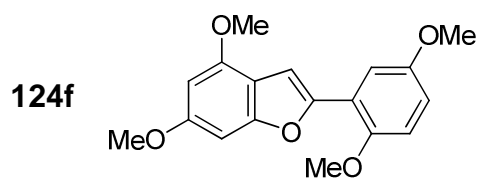


$^1\text{H-NMR}$ (CDCl_3)

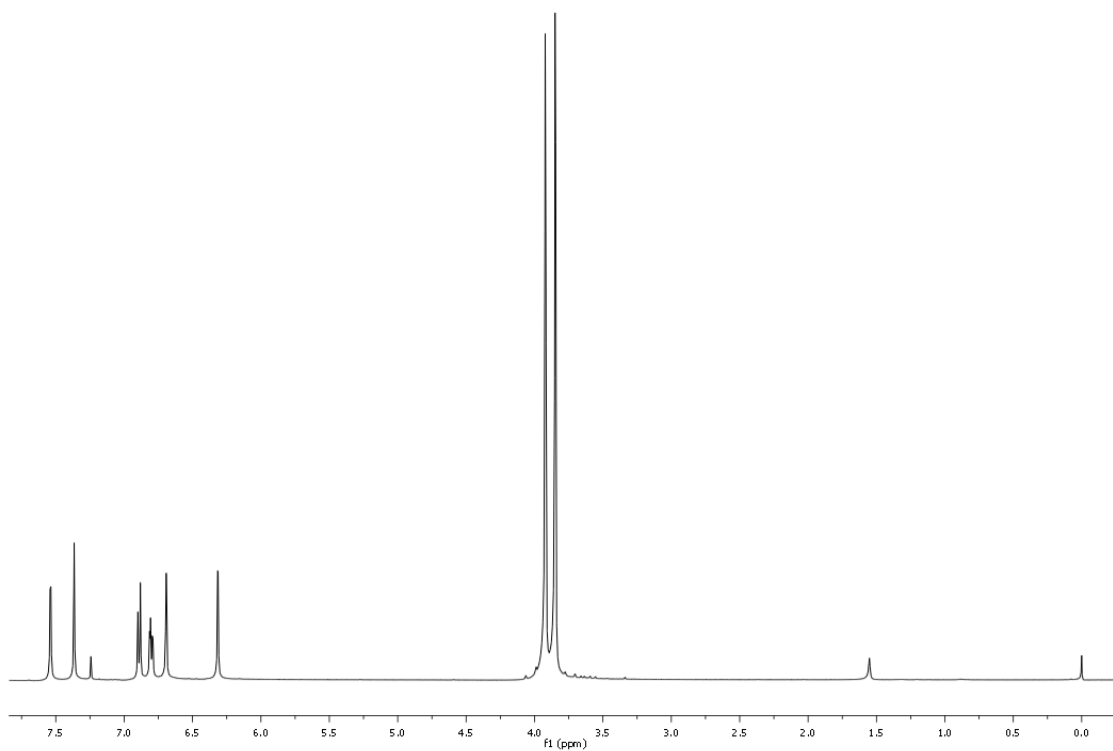


$^{13}\text{C-NMR}$ (CDCl_3)

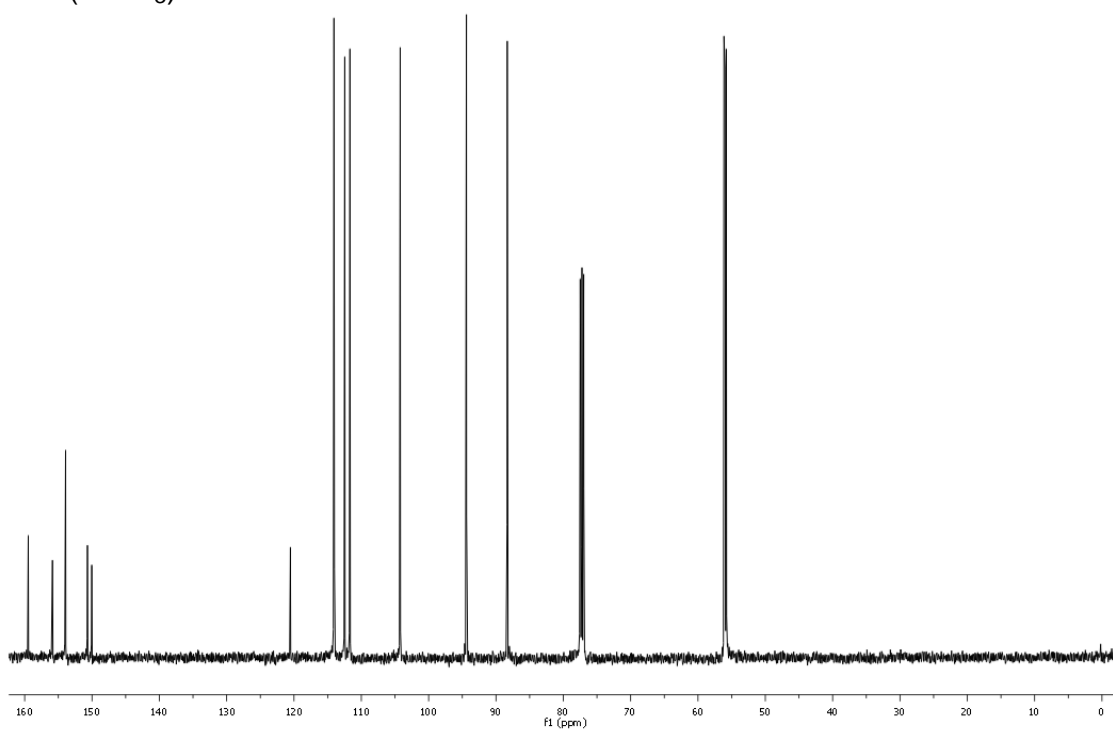


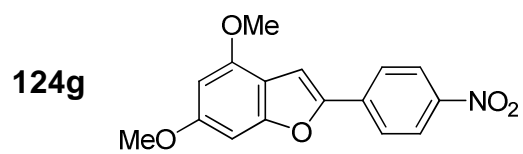


$^1\text{H-NMR}$ (CDCl_3)

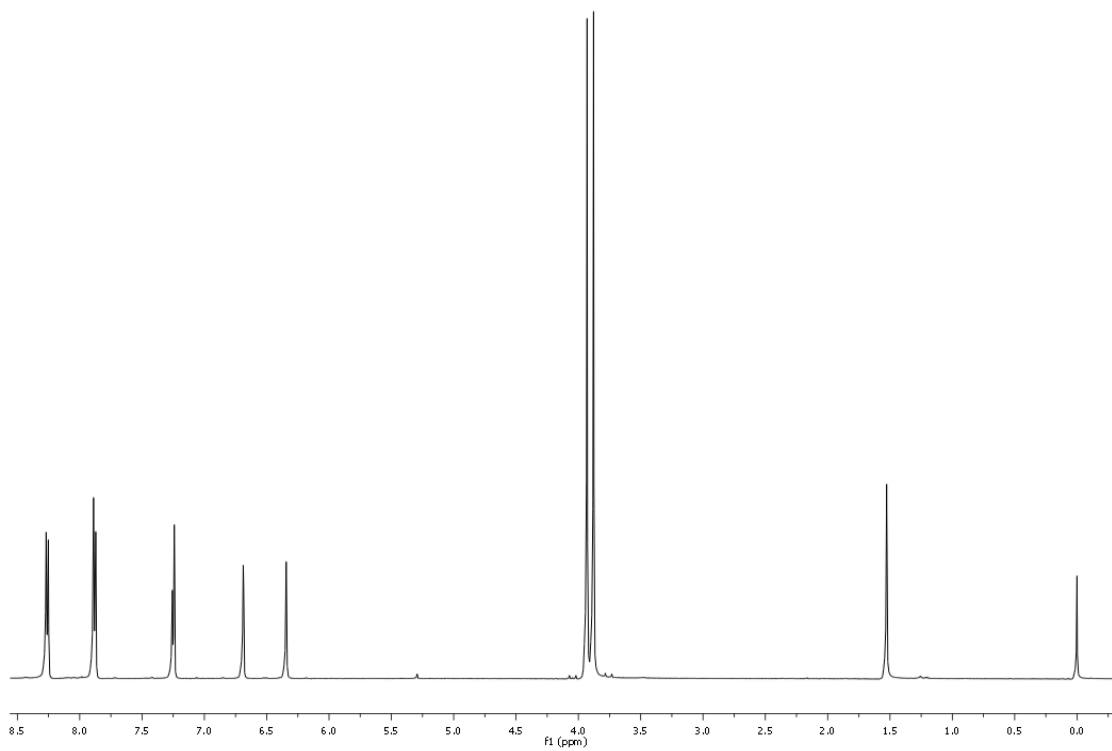


$^{13}\text{C-NMR}$ (CDCl_3)

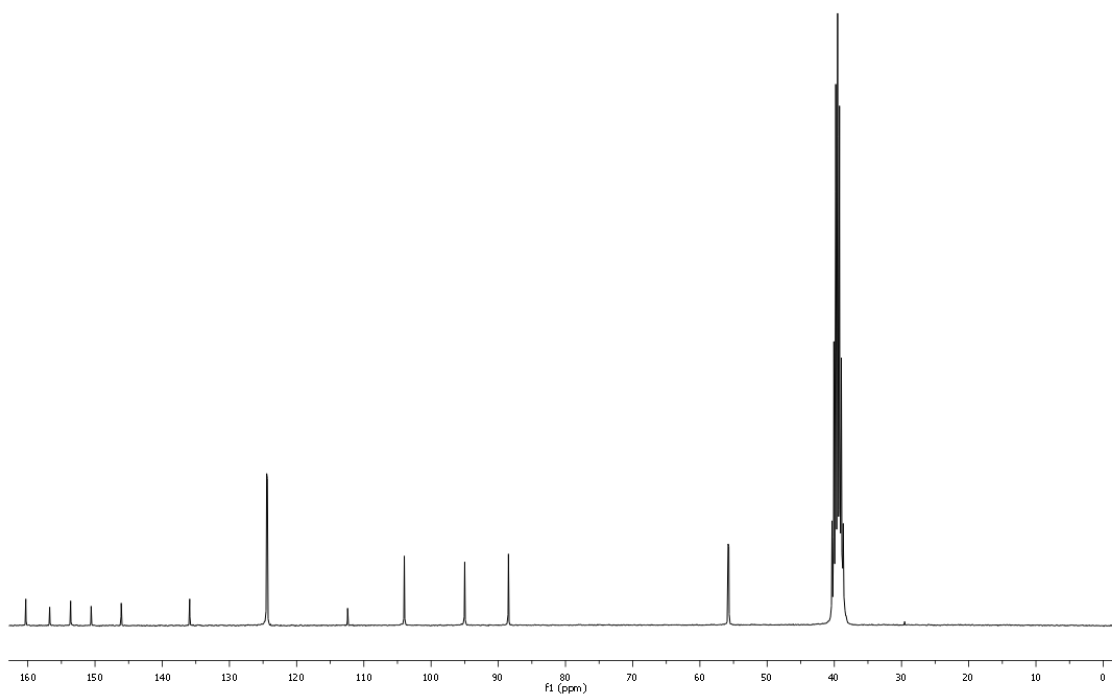


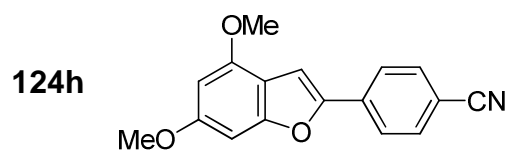


$^1\text{H-NMR}$ (CDCl_3)

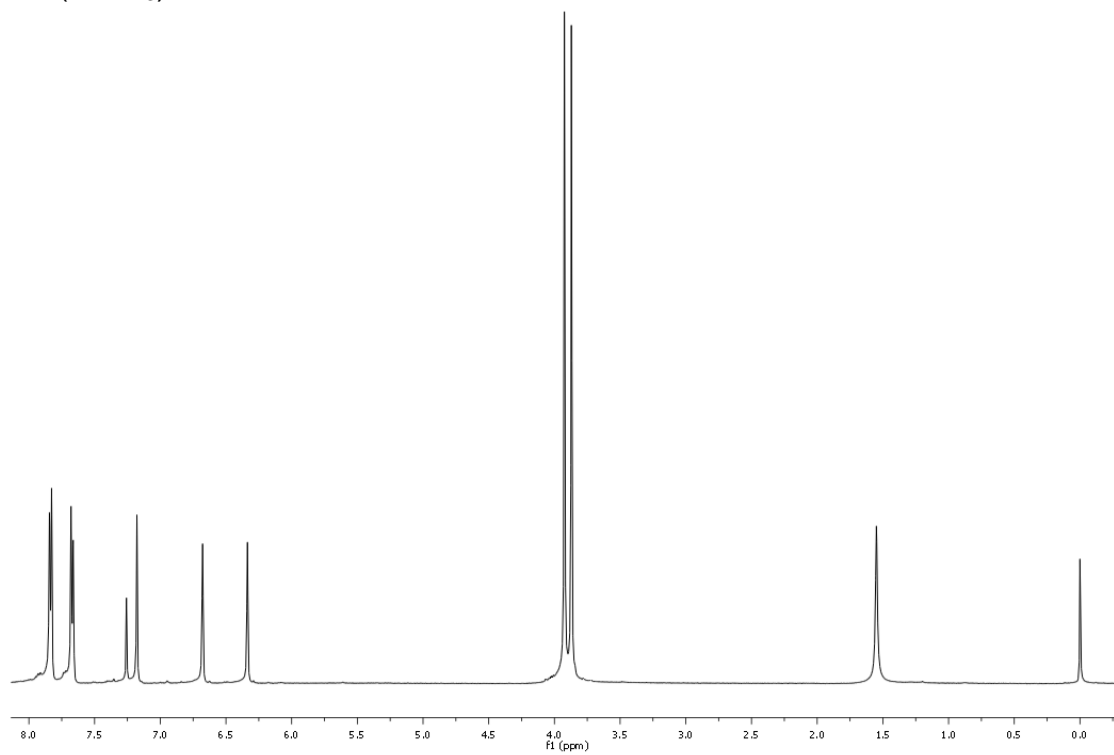


$^{13}\text{C-NMR}$ (DMSO-d_6)

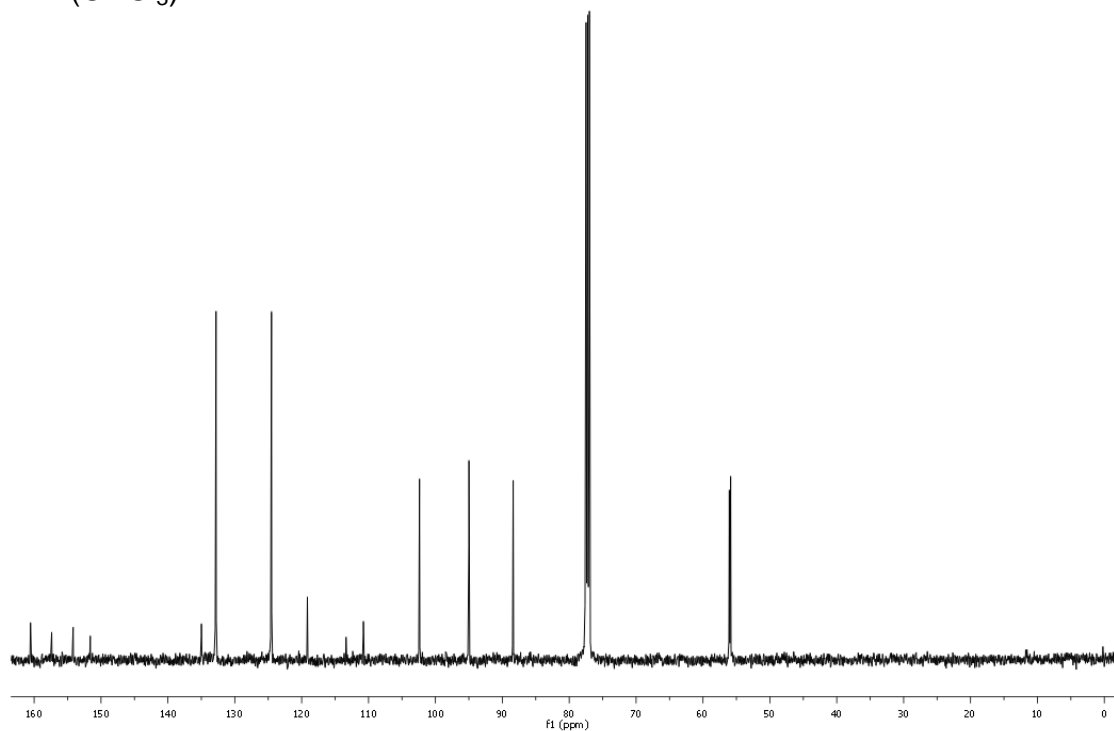


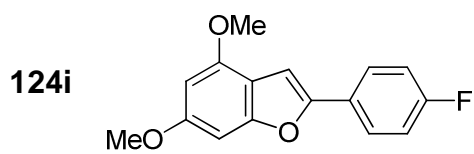


$^1\text{H-NMR}$ (CDCl_3)

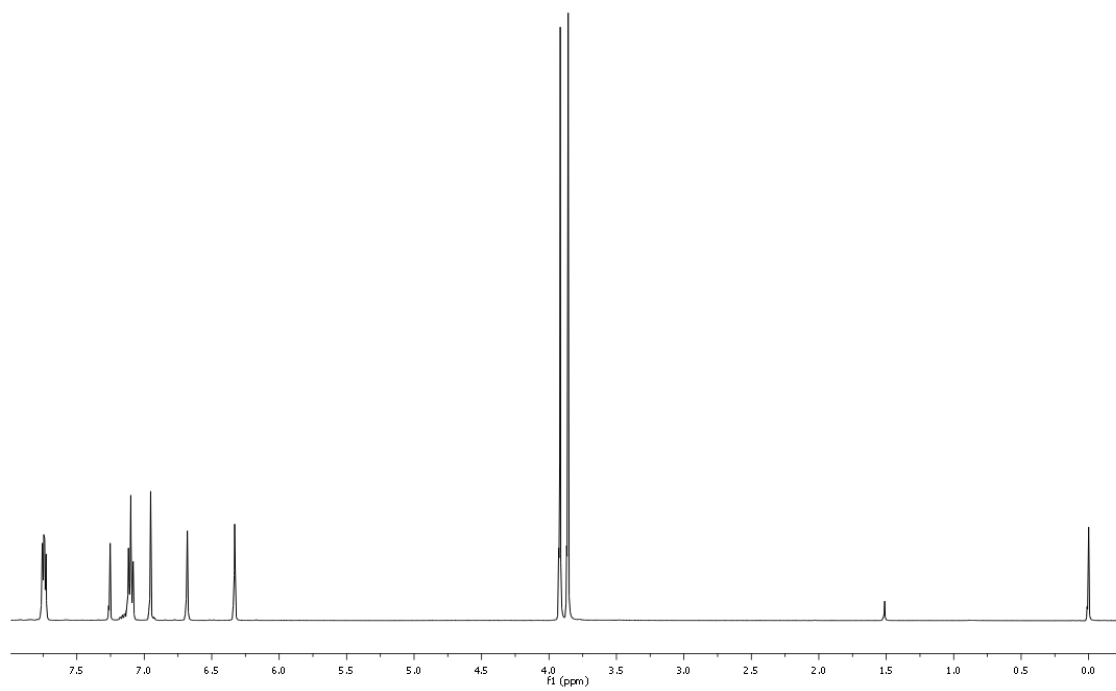


$^{13}\text{C-NMR}$ (CDCl_3)

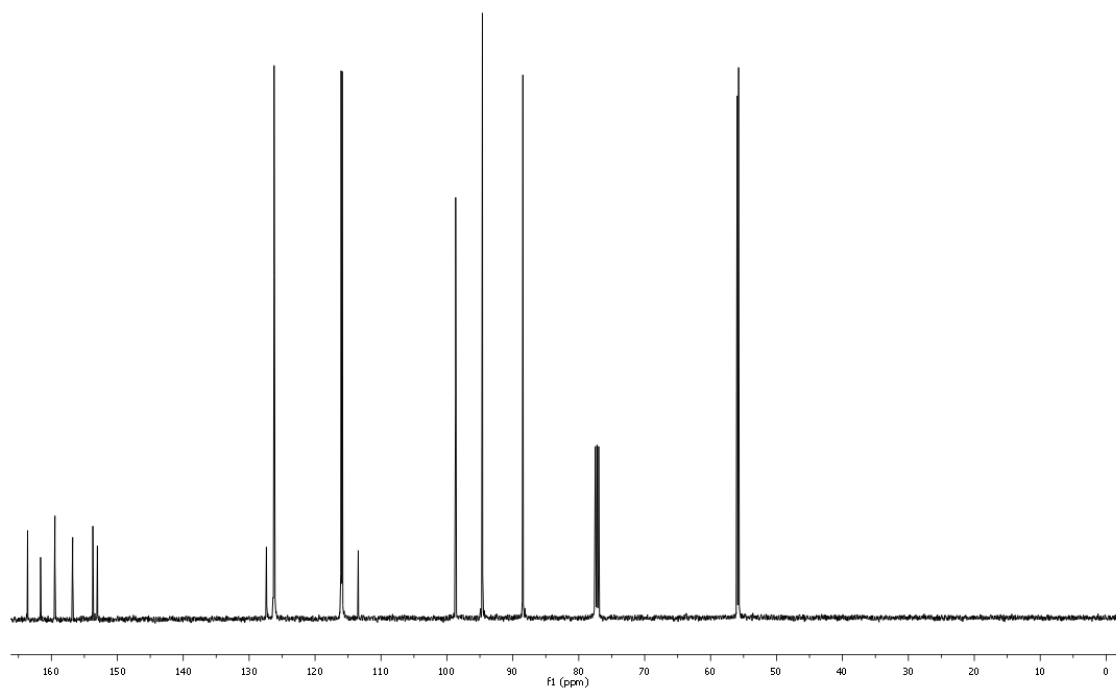


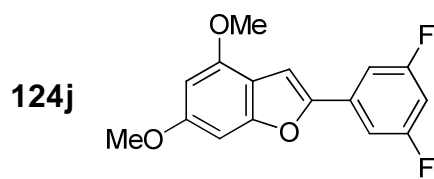


$^1\text{H-NMR}$ (CDCl_3)

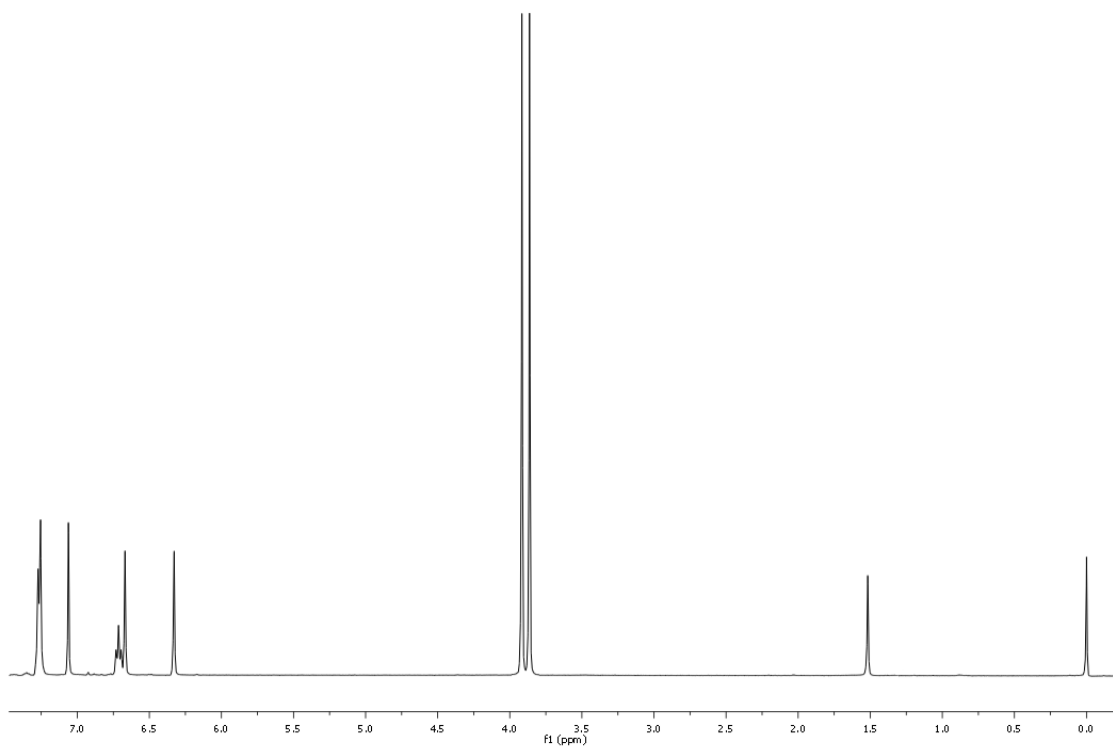


$^{13}\text{C-NMR}$ (CDCl_3)

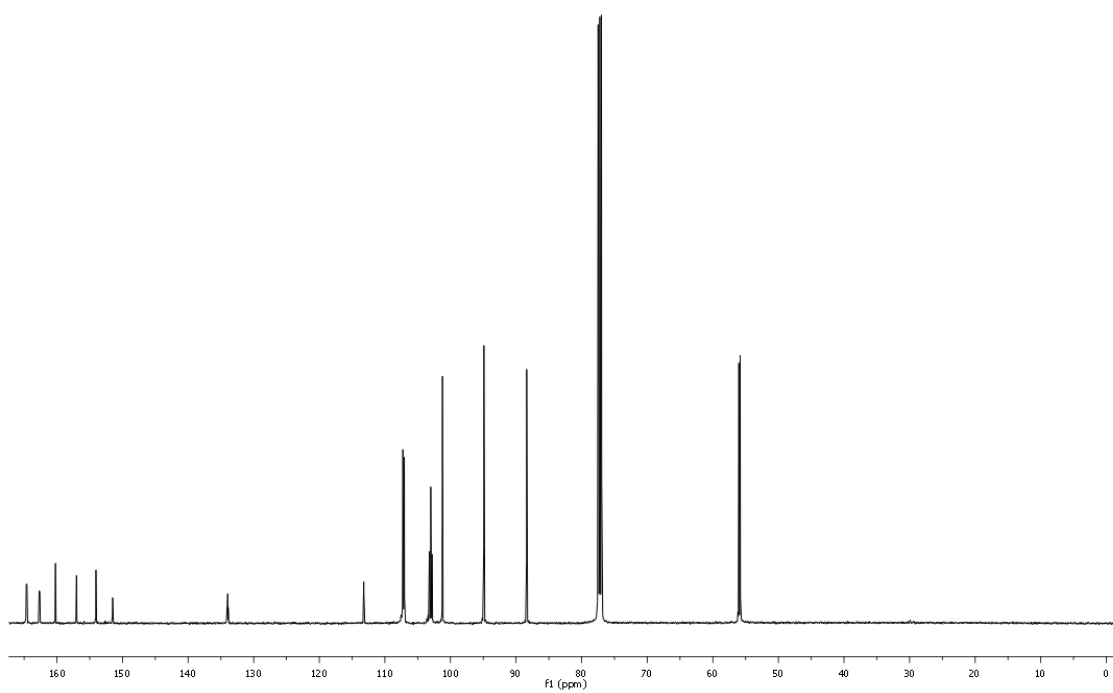


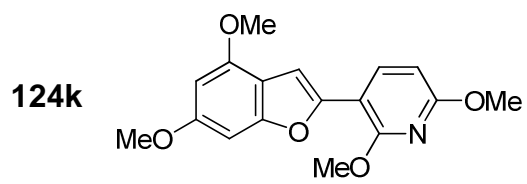


$^1\text{H-NMR}$ (CDCl_3)

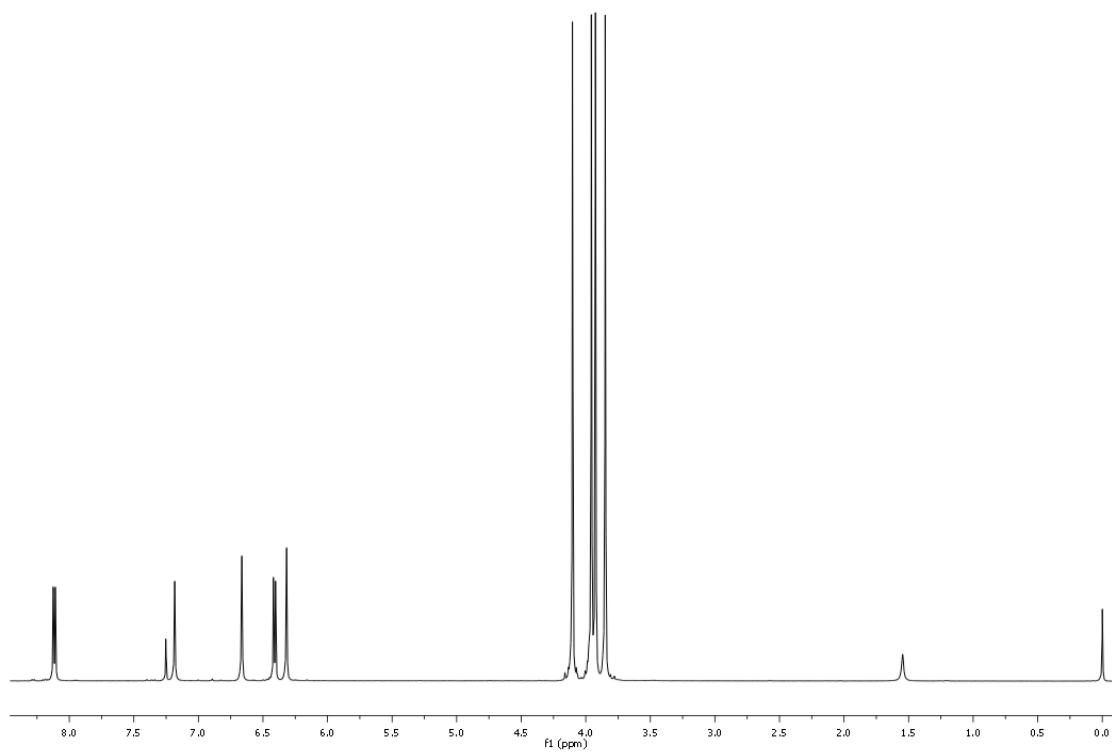


$^{13}\text{C-NMR}$ (CDCl_3)

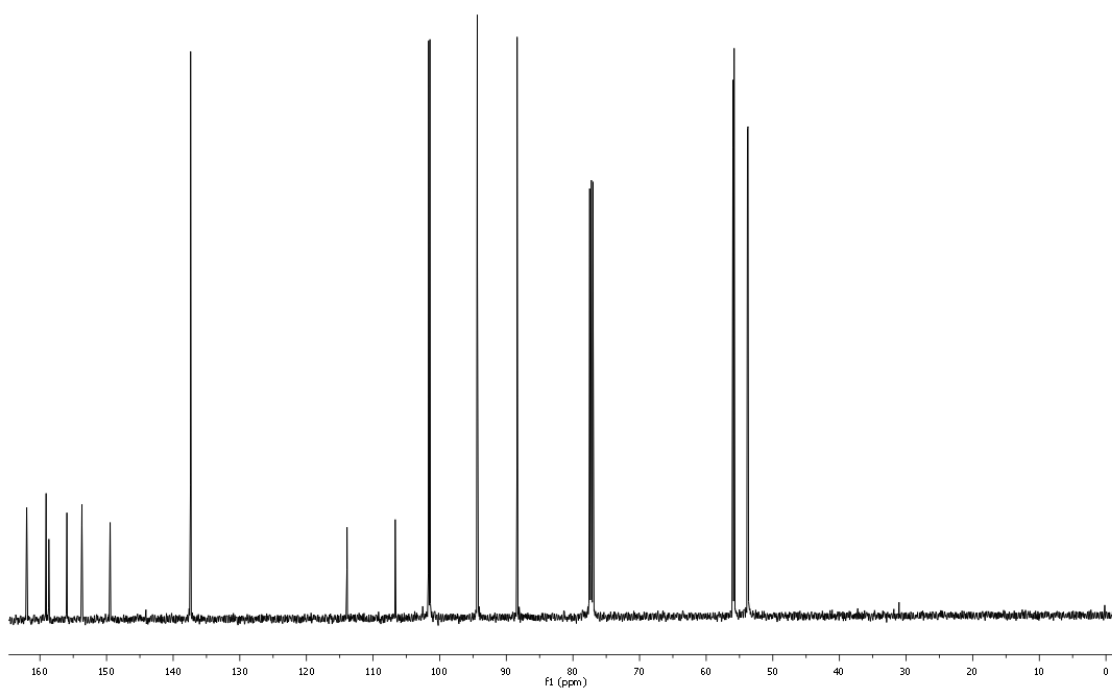


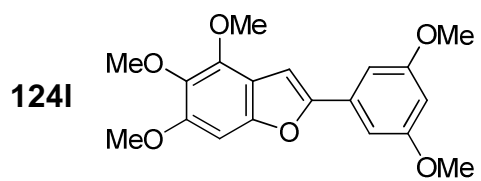


$^1\text{H-NMR}$ (CDCl_3)

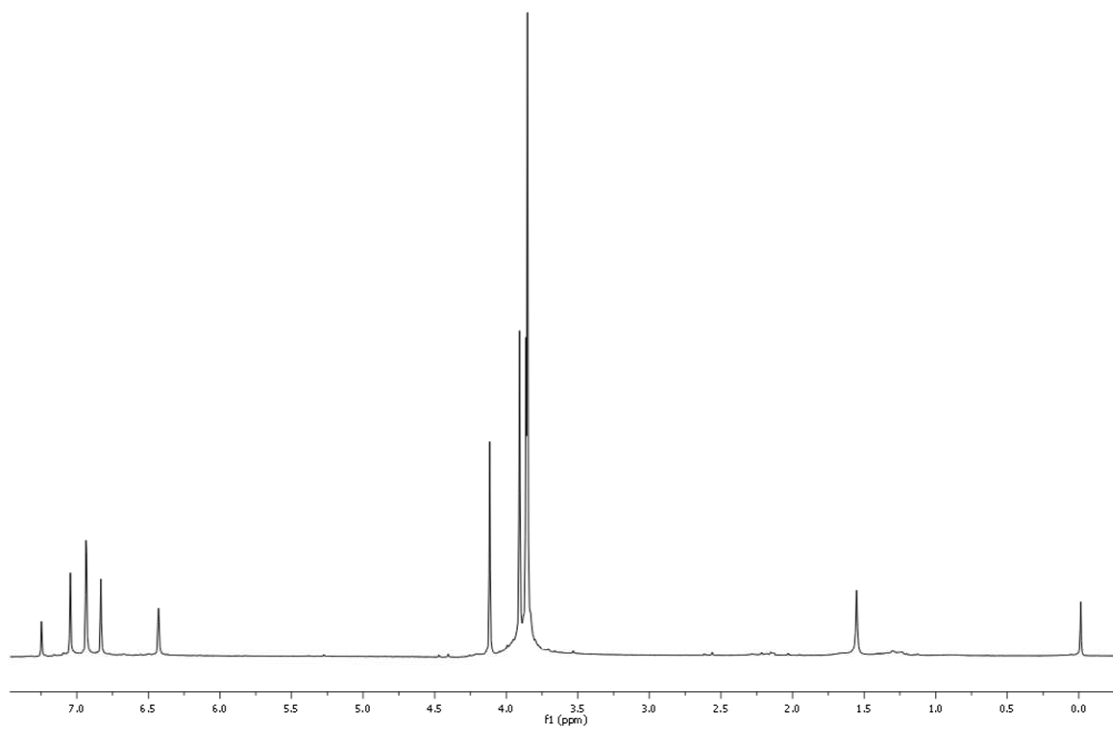


$^{13}\text{C-NMR}$ (CDCl_3)

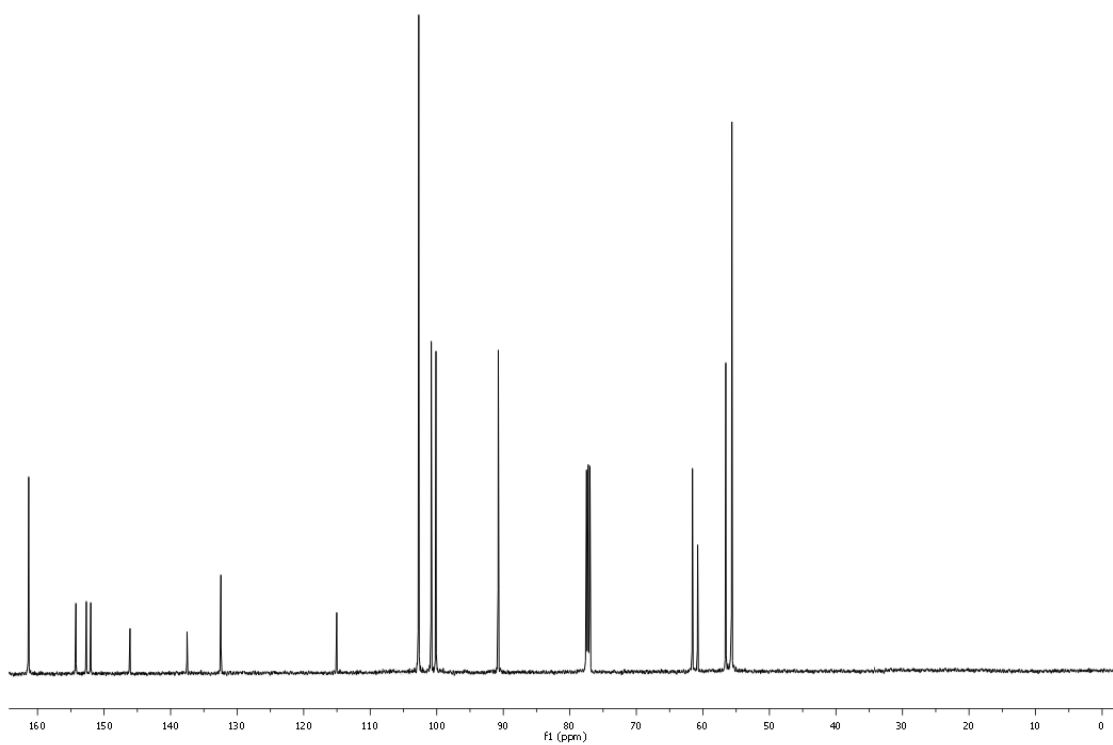


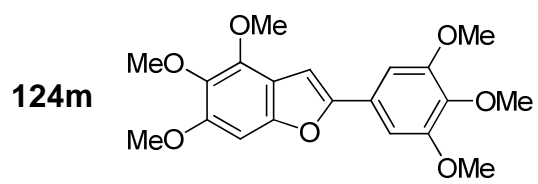


$^1\text{H-NMR}$ (CDCl_3)

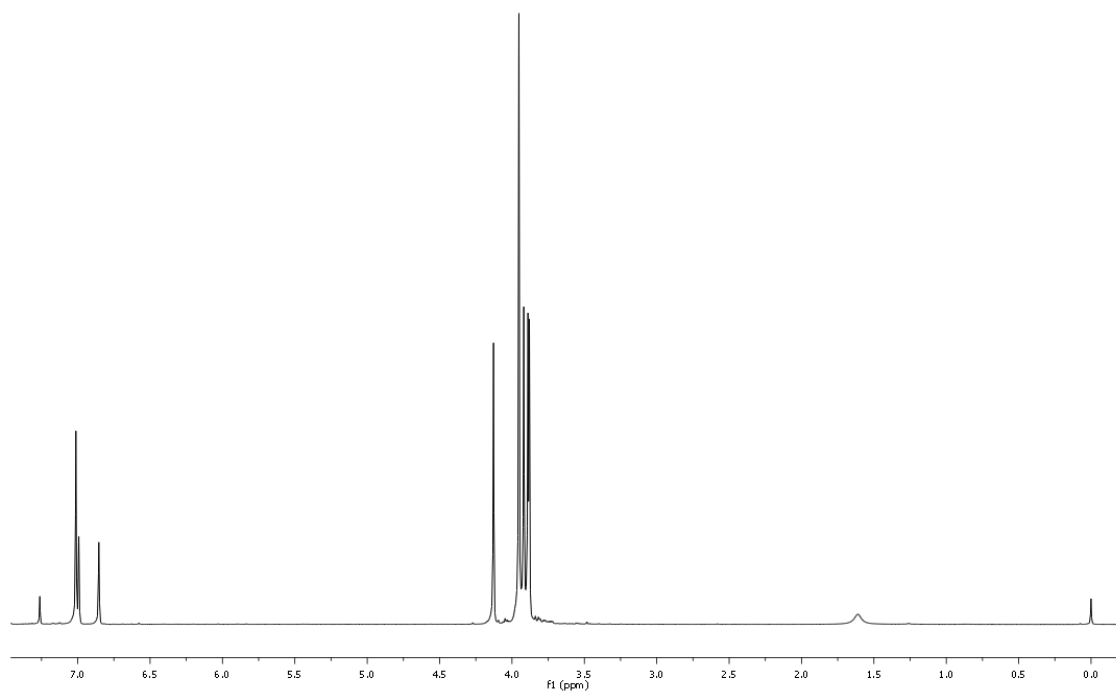


$^{13}\text{C-NMR}$ (CDCl_3)

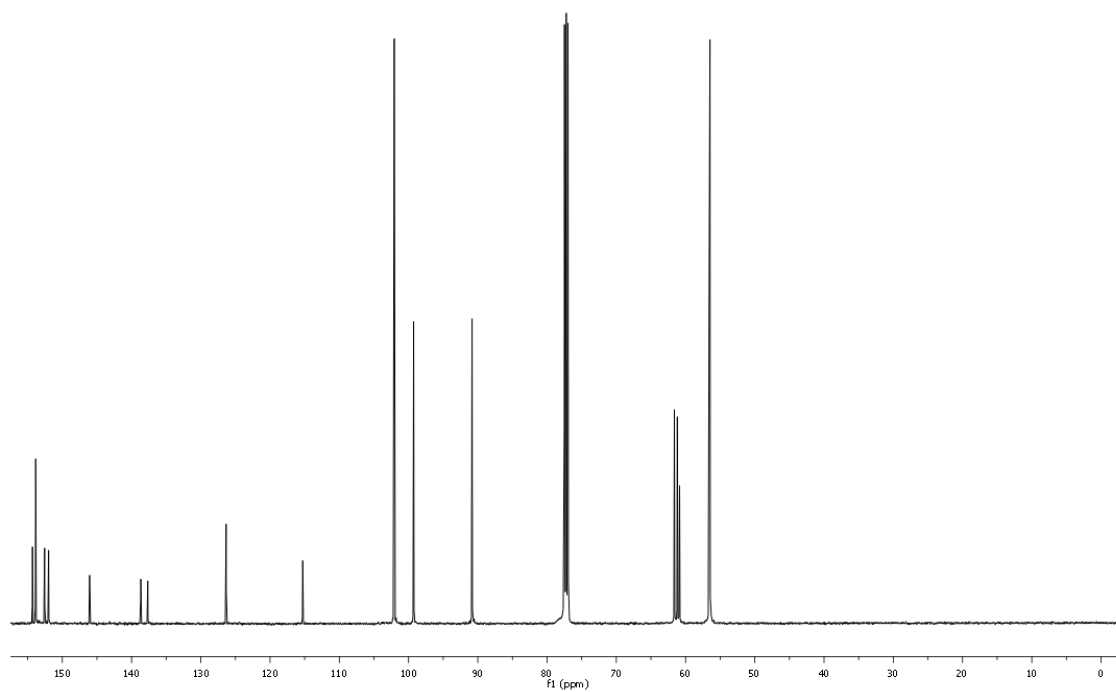


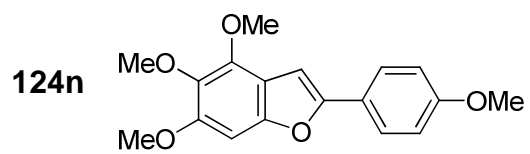


$^1\text{H-NMR}$ (CDCl_3)

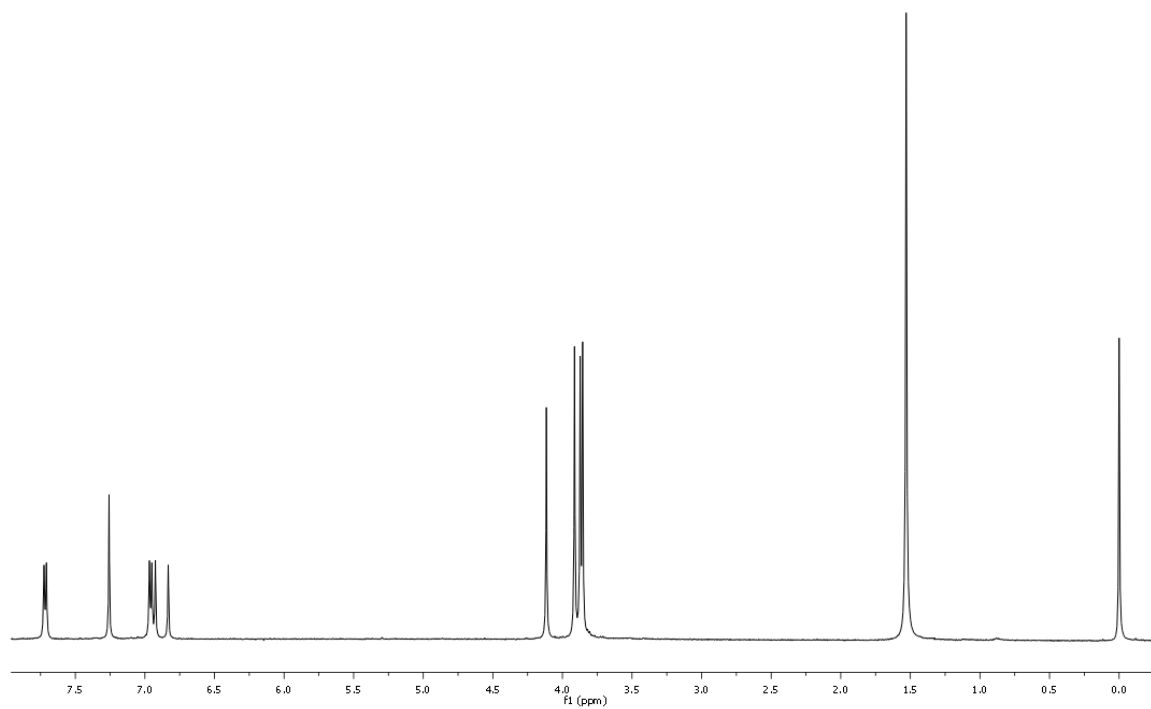


$^{13}\text{C-NMR}$ (CDCl_3)

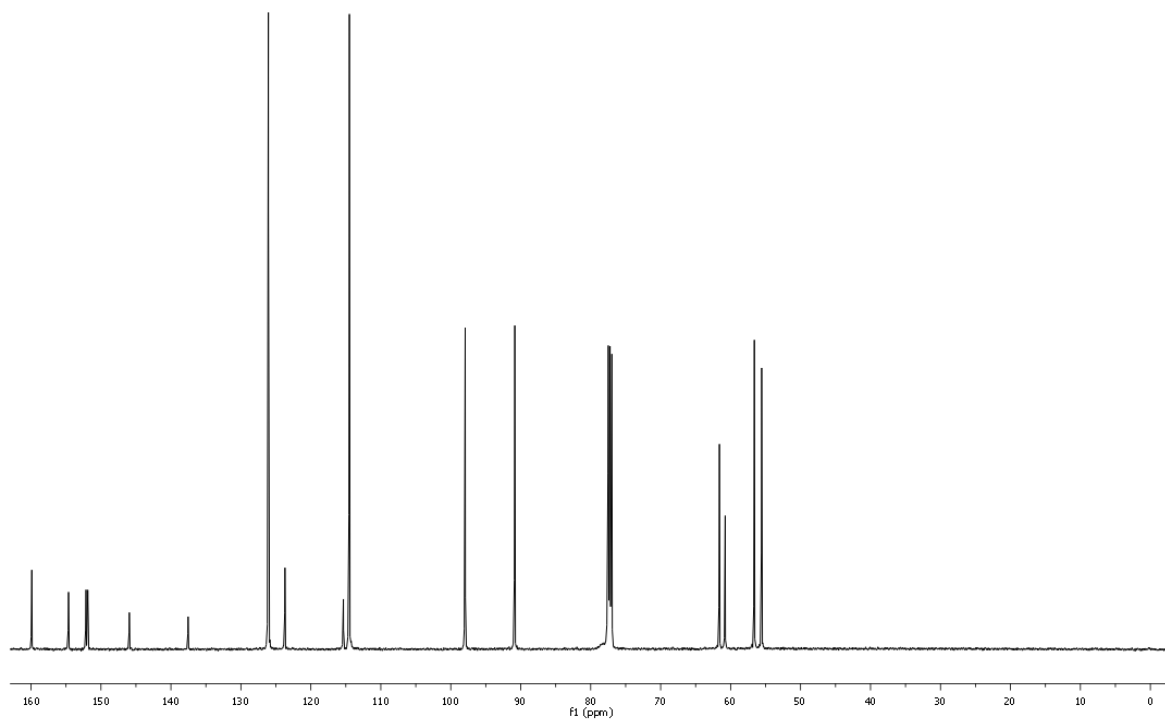




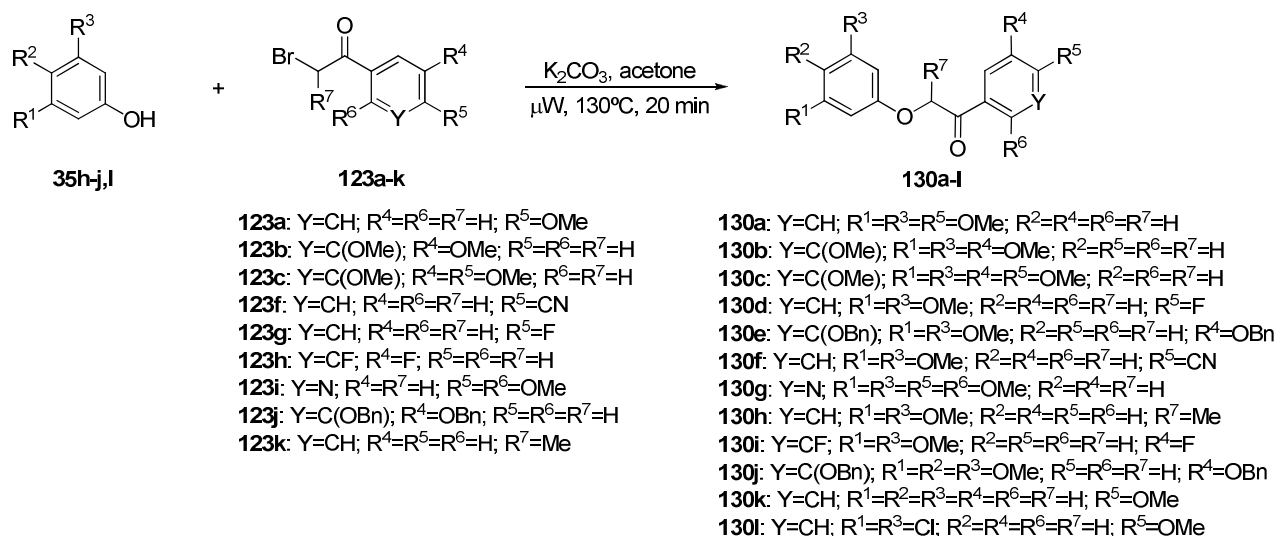
$^1\text{H-NMR}$ (CDCl_3)



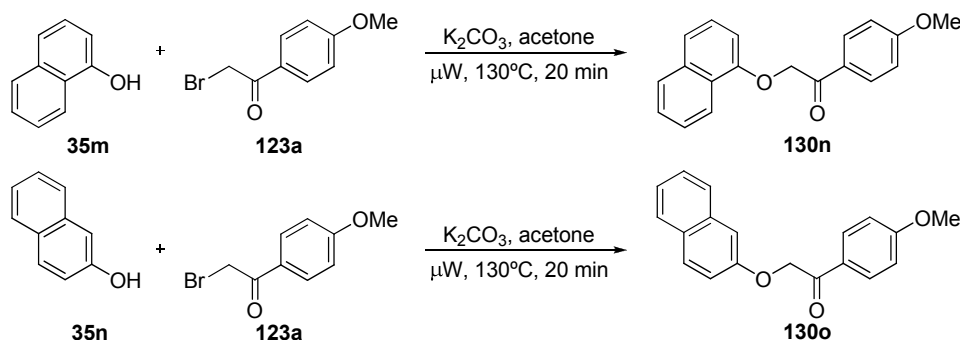
$^{13}\text{C-NMR}$ (CDCl_3)



5.2.3. Procedure for the preparation of α -phenoxyketones **130a-l** and α -naphthoxyketones **130n-o**

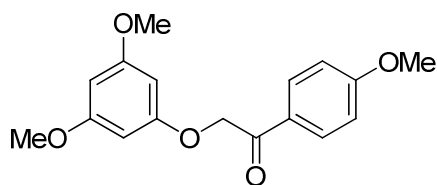


Scheme 5.4. Preparation of ethers **130a-l** from phenols **35h-j,l** and α -bromoacetophenones **123a-k**.



Scheme 5.5. Preparation of ethers **130n-o** from naphthols **35m-n** and α -bromoacetophenone **123a**.

As described in literature¹⁷⁵, phenol or naphthol **35** (2.0 mmol), α -bromoacetophenone **123** (2.0 mmol, 1 eq), K₂CO₃ (4.0 mmol, 2 eq) and 2 ml of acetone were placed in a microwave vessel and sealed. The mixture was irradiated with microwaves at 130 °C and 100-400 W for 20 minutes. The resulting mixture was left to cool until it reached room temperature. It was then filtered through a Celite pad and evaporated under reduced pressure. The crude obtained this way was purified by precipitation in Et₂O or, when necessary, by column chromatography on silica gel, using EtOAc/Hx mixtures as eluent to afford the corresponding pure products **130**.

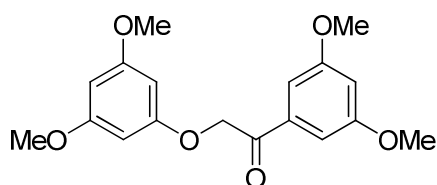
2-(3',5'-dimethoxyphenoxy)-1-(4'-methoxyphenyl)ethanone¹²⁷, 130a:Molecular formula: C₁₇H₁₈O₅

Molecular weight: 302.32 g/mol

Aspect: White solid

Yield: 99%

¹H-NMR (500 MHz, CDCl₃) δ = 7.98 (d, *J*=8.9 Hz, 2H), 6.96 (d, *J*=8.9 Hz, 2H), 6.13 (d, *J*=2.1 Hz, 2H), 6.11 (t, *J*=2.0 Hz, 1H), 5.15 (s, 2H), 3.88 (s, 3H), 3.75 (s, 6H).

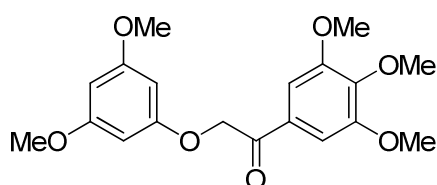
2-(3',5'-dimethoxyphenoxy)-1-(3',5'-dimethoxyphenyl)ethanone, 130b:Molecular formula: C₁₈H₂₀O₆

Molecular weight: 332.35 g/mol

Aspect: Yellow solid

Yield: 93%

m.p.: 104-105 °C. IR (KBr): 2931, 1709, 1209, 1160, 1023 cm⁻¹. ¹H-NMR (500 Hz, CDCl₃) δ = 7.11 (d, *J*=2.2 Hz, 2H), 6.69 (t, *J*=2.2 Hz, 1H), 6.13 (d, *J*=1.9 Hz, 2H), 6.12 (d, *J*=1.9 Hz, 1H), 5.18 (s, 2H), 3.84 (s, 6H), 3.76 (s, 6H). ¹³C-NMR (126 MHz, CDCl₃) δ = 194.0, 161.8, 161.3, 160.1, 136.6, 106.3, 106.1, 94.1, 71.0, 55.8, 55.6. Elemental analysis calculated for C₁₈H₂₀O₆: C, 65.0; H, 6.1. Found: C, 65.0; H, 6.1.

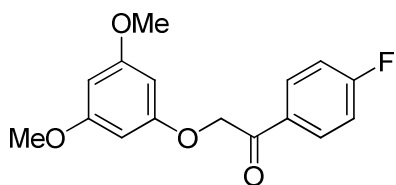
2-(3',5'-dimethoxyphenoxy)-1-(3',4',5'-trimethoxyphenyl)ethanone, 130c:Molecular formula: C₁₉H₂₇O₇

Molecular weight: 362.37 g/mol

Aspect: White solid

Yield: 99%

m.p.: 86-87 °C. IR (KBr): 2937, 1703, 1203, 1148, 1130, 1075 cm⁻¹. ¹H-NMR (500 MHz, CDCl₃) δ = 7.27 (s, 2H), 6.13 (d, *J*=1.9 Hz, 2H), 6.12 (d, *J*=1.9 Hz, 1H), 5.16 (s, 2H), 3.93 (s, 3H), 3.91 (s, 6H), 3.76 (s, 6H). ¹³C-NMR (126 MHz, CDCl₃) δ = 193.4, 161.8, 160.1, 153.5, 143.6, 129.9, 106.1, 94.1, 94.0, 71.1, 61.1, 56.6, 55.6. Calculated for C₁₉H₂₇O₇: C, 63.0; H, 6.1. Found: C, 62.8; H, 6.2.

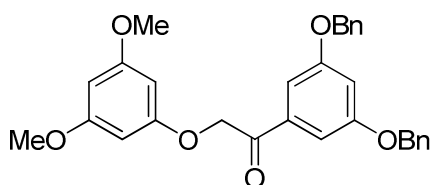
2-(3',5'-dimethoxyphenoxy)-1-(4'-fluorophenyl)ethanone³²³, 130d:Molecular formula: C₁₆H₁₅FO₄

Molecular weight: 290.29 g/mol

Aspect: White solid

Yield: 97%

¹H-NMR (500 MHz, CDCl₃) δ = 8.06 (dd, *J*=8.1, 5.6 Hz, 2H), 7.19 (t, *J*=8.4 Hz, 2H), 6.15 (s, 3H), 5.18 (s, 2H), 3.78 (s, 6H).

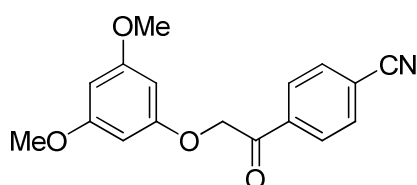
1-(3',5'-bis(benzyloxy)phenyl)-2-(3',5'-dimethoxyphenoxy)ethanone, 130e:Molecular formula: C₃₀H₂₈O₆

Molecular weight: 484.54 g/mol

Aspect: White solid

Yield: 99%

m.p.: 125 °C. IR (KBr): 2914, 1703, 1201, 1166, 1070 cm⁻¹. ¹H-NMR (500 MHz, CDCl₃) δ = 7.45–7.30 (m, 10H), 7.20 (d, *J*=2.2 Hz, 2H), 6.84 (t, *J*=2.2 Hz, 1H), 6.12 (s, 3H), 5.15 (s, 2H), 5.08 (s, 4H), 3.75 (s, 6H). ¹³C-NMR (126 MHz, CDCl₃) δ = 193.8, 161.8, 160.4, 160.1, 136.6, 136.5, 128.9, 128.4, 127.8, 107.9, 107.3, 94.1, 94.0, 70.9, 70.7, 55.6. Elemental analysis calculated for C₃₀H₂₈O₆: C, 74.4; H, 5.8. Found: C, 74.3; H, 5.8.

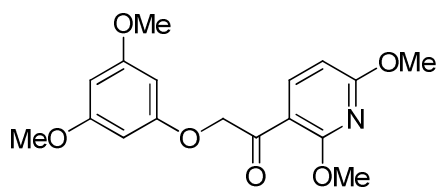
4-(2-(3',5'-dimethoxyphenoxy)acetyl)benzonitrile, 130f:Molecular formula: C₁₇H₁₅NO₄

Molecular weight: 297.31 g/mol

Aspect: Yellow solid

Yield: 99%

m.p.: 116–117 °C. IR (KBr): 2885, 2229, 1706, 1215, 1157 cm⁻¹. ¹H-NMR (500 MHz, CDCl₃) δ = 8.08 (d, *J*=8.3 Hz, 2H), 7.79 (d, *J*=8.3 Hz, 2H), 6.12 (d, *J*=1.8 Hz, 1H), 6.09 (d, *J*=1.8 Hz, 2H), 5.16 (s, 2H), 3.75 (s, 6H). ¹³C-NMR (75 MHz, CDCl₃) δ = 194.0, 162.0, 159.7, 137.8, 132.8, 129.0, 117.9, 117.3, 94.2, 94.0, 71.3, 55.6. Elemental analysis calculated for C₁₇H₁₅NO₄: C, 68.7; H, 5.1; N, 4.7. Found: C, 68.7; H, 5.0; N, 4.8.

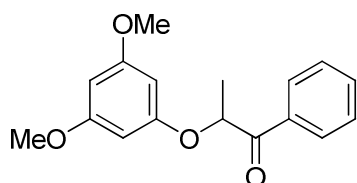
2-(3',5'-dimethoxyphenoxy)-1-(2',6'-dimethoxypyridin-3-yl)ethanone, 130g:Molecular formula: C₁₇H₁₉NO₆

Molecular weight: 333.34 g/mol

Aspect: White solid

Yield: 73%

m.p.: 108-109°C. IR (KBr): 2919, 1683, 1590, 1336, 1167, 1155, 1088 cm⁻¹. ¹H-NMR (500 MHz, CDCl₃) δ = 8.27 (d, *J*=8.4 Hz, 1H), 6.42 (d, *J*=8.4 Hz, 1H), 6.12 (d, *J*=1.9 Hz, 2H), 6.10 (d, *J*=1.9 Hz, 1H), 5.17 (s, 2H), 4.10 (s, 3H), 4.00 (s, 3H), 3.76 (s, 6H). ¹³C-NMR (126 MHz, CDCl₃) δ = 192.0, 166.4, 162.8, 161.7, 160.5, 143.4, 111.0, 103.7, 94.1, 93.6, 73.9, 55.5, 54.3, 54.2. Elemental analysis calculated for C₁₇H₁₉NO₆: C, 61.2; H, 5.8; N, 4.2. Found: C, 61.3; H, 5.7; N, 4.2.

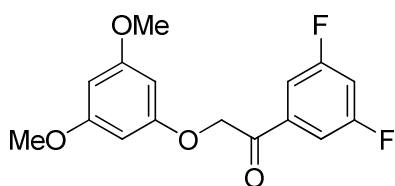
2-(3',5'-dimethoxyphenoxy)-1-phenylpropan-1-one³²⁴, 130h:Molecular formula: C₁₇H₁₈O₄

Molecular weight: 286.32 g/mol

Aspect: White solid

Yield: 84%

¹H-NMR (500 MHz, CDCl₃) δ = 8.05 (d, *J*=8.3 Hz, 2H), 7.61–7.53 (m, 1H), 7.46 (t, *J*=7.3 Hz, 2H), 6.06 (d, *J*=0.6 Hz, 3H), 5.45 (q, *J*=6.7 Hz, 1H), 3.71 (s, 3H), 3.70 (s, 3H), 1.68 (dd, *J*=6.8, 1.0 Hz, 3H).

1-(3',5'-difluorophenyl)-2-(3',5'-dimethoxyphenoxy)ethanone, 130i:Molecular formula: C₁₆H₁₄F₂O₄

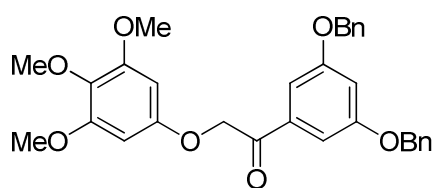
Molecular weight: 308.28 g/mol

Aspect: Yellow solid

Yield: 24%

m.p.: 92-93 °C. IR (neat): 2847, 1713, 1309, 1203, 1150, 1056 cm⁻¹. ¹H-NMR (500 MHz, CDCl₃) δ = 7.52 (d, *J*=5.6 Hz, 2H), 7.06 (t, *J*=8.2 Hz, 1H), 6.13 (s, 1H), 6.11 (s, 2H), 5.12 (s, 2H), 3.76 (s, 6H). ¹³C-NMR (126 MHz, CDCl₃) δ = 192.6, 163.3 (dd, *J*=251.5, 11.7 Hz), 161.9, 159.7, 137.5 (t, *J*=7.7 Hz), 111.5 (dd, *J*=20.1, 6.6 Hz), 109.4 (t, *J*=25.3 Hz), 94.3, 94.0, 71.2, 55.6. Elemental analysis calculated for C₁₆H₁₄F₂O₄: C, 62.3; H, 4.6. Found: C, 62.3; H, 4.5.

³²⁴ Dirania, M. K. M.; Hill, J. *J. Chem. Soc. C* **1969**, 16, 2144-2147

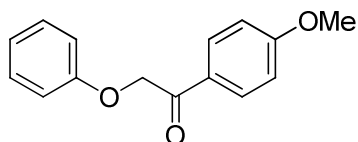
1-(3',5'-bis(benzyloxy)phenyl)-2-(3',4',5'-trimethoxyphenoxy)ethanone, 130j:Molecular formula: C₃₁H₃₀O₇

Molecular weight: 514.57 g/mol

Aspect: White solid

Yield: 20%

m.p.: 111 °C. IR (neat): 2942, 1704, 1289, 1152, 1020 cm⁻¹. ¹H-NMR (500 MHz, CDCl₃) δ = 7.50–7.29 (m, 10H), 7.22 (s, 2H), 6.86 (s, 1H), 6.19 (s, 2H), 5.16 (s, 2H), 5.08 (s, 4H), 3.82 (s, 6H), 3.78 (s, 3H). ¹³C-NMR (126 MHz, CDCl₃) δ = 194.1, 160.4, 154.8, 154.0, 136.5, 136.4, 133.3, 128.9, 128.5, 127.8, 107.7, 107.3, 93.1, 71.4, 70.6, 61.2, 56.4. Calculated for C₃₁H₃₀O₇: C, 72.4; H, 5.9. Found: C, 72.1; H, 5.6.

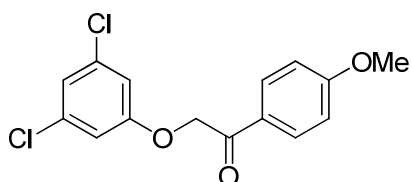
1-(4'-methoxyphenyl)-2-phenoxyethanone³²⁵, 130k:Molecular formula: C₁₅H₁₄O₃

Molecular weight: 242.27 g/mol

Aspect: Yellow solid

Yield: 99%

¹H-NMR (300 MHz, CDCl₃) δ = 8.00 (d, *J*=8.9 Hz, 2H), 7.32–7.23 (m, 2H), 7.02–6.88 (m, 5H), 5.20 (s, 2H), 3.88 (s, 3H).

2-(3',5'-dichlorophenoxy)-1-(4'-methoxyphenyl)ethanone 130l:Molecular formula: C₁₅H₁₂Cl₂O₃

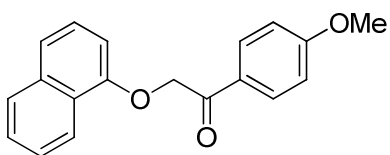
Molecular weight: 311.16 g/mol

Aspect: Pale pink solid

Yield: 99%

m.p.: 95-96 °C. IR (neat): 2838, 1691, 1241, 1085 cm⁻¹. ¹H-NMR (500 MHz, CDCl₃) δ = 7.95 (d, *J*=8.9 Hz, 2H), 6.96 (s, 1H), 6.96 (d, *J*=8.8 Hz, 2H), 6.82 (s, 2H), 5.20 (s, 2H), 3.88 (s, 3H). ¹³C-NMR (126 MHz, CDCl₃) δ = 191.8, 164.5, 159.4, 135.7, 130.6, 127.5, 122.1, 114.4, 114.2, 70.9, 55.7. Elemental analysis calculated for C₁₅H₁₂Cl₂O₃: C, 57.9; H, 3.9. Found: C, 58.1; H, 4.0.

³²⁵ Commercial product, CAS: 19513-78-1

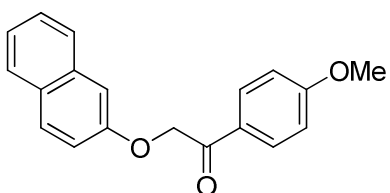
1-(4'-methoxyphenyl)-2-(naphthalen-1-yloxy)ethanone³²², 130n:Molecular formula: C₁₉H₁₆O₃

Molecular weight: 292.33 g/mol

Aspect: White solid

Yield: 70%

¹H-NMR (200 MHz, CDCl₃) δ = 8.44–8.27 (m, 1H), 7.85 (d, *J*=7.7 Hz, 2H), 7.76–7.64 (m, 1H), 7.47–7.30 (m, 3H), 7.21 (t, *J*=7.9 Hz, 1H), 6.74 (d, *J*=7.7 Hz, 2H), 6.62 (d, *J*=7.5 Hz, 1H), 5.16 (s, 2H), 3.62 (s, 3H).

1-(4'-methoxyphenyl)-2-(naphthalen-2-yloxy)ethanone³²⁶, 130o:Molecular formula: C₁₉H₁₆O₃

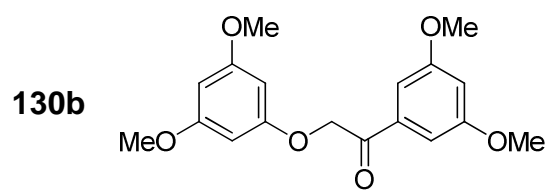
Molecular weight: 292.33 g/mol

Aspect: White solid

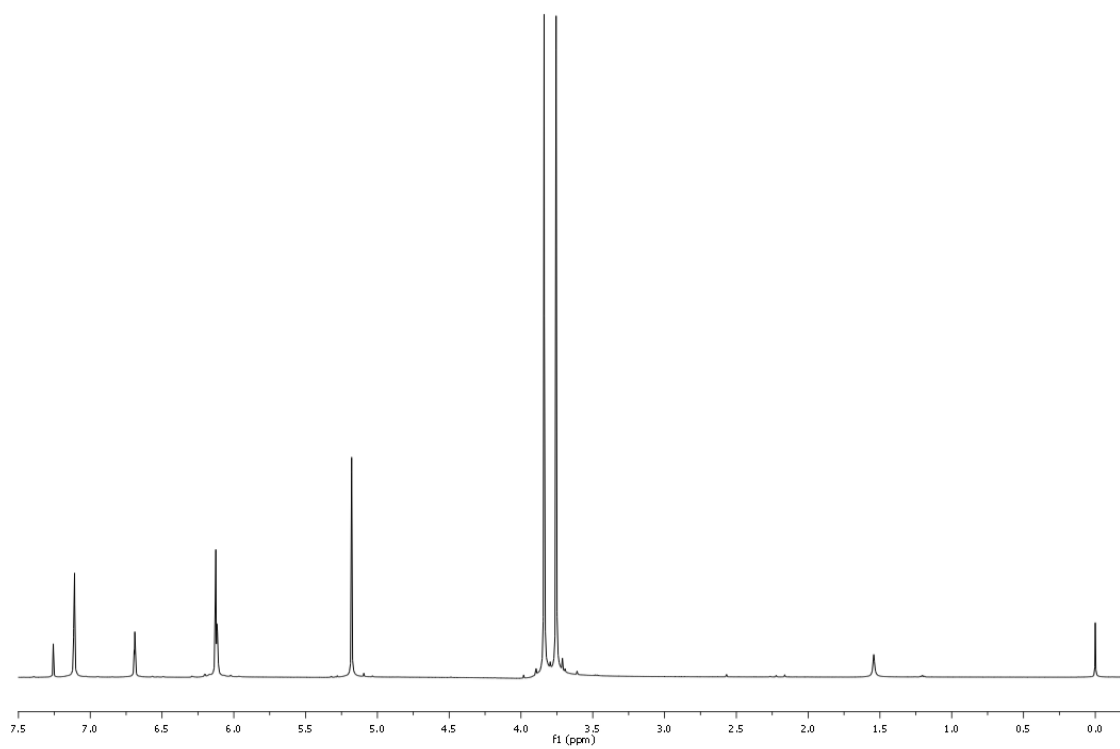
Yield: 95%

¹H-NMR (500 MHz, CDCl₃) δ = 8.04 (d, *J*=8.4 Hz, 2H), 7.76 (d, *J*=8.6 Hz, 2H), 7.70 (d, *J*=8.2 Hz, 1H), 7.42 (t, *J*=7.5 Hz, 1H), 7.34 (t, *J*=7.4 Hz, 1H), 7.26 (d, *J*=4.8 Hz, 1H), 7.13 (s, 1H), 6.97 (d, *J*=8.4 Hz, 2H), 5.31 (s, 2H), 3.88 (s, 3H).

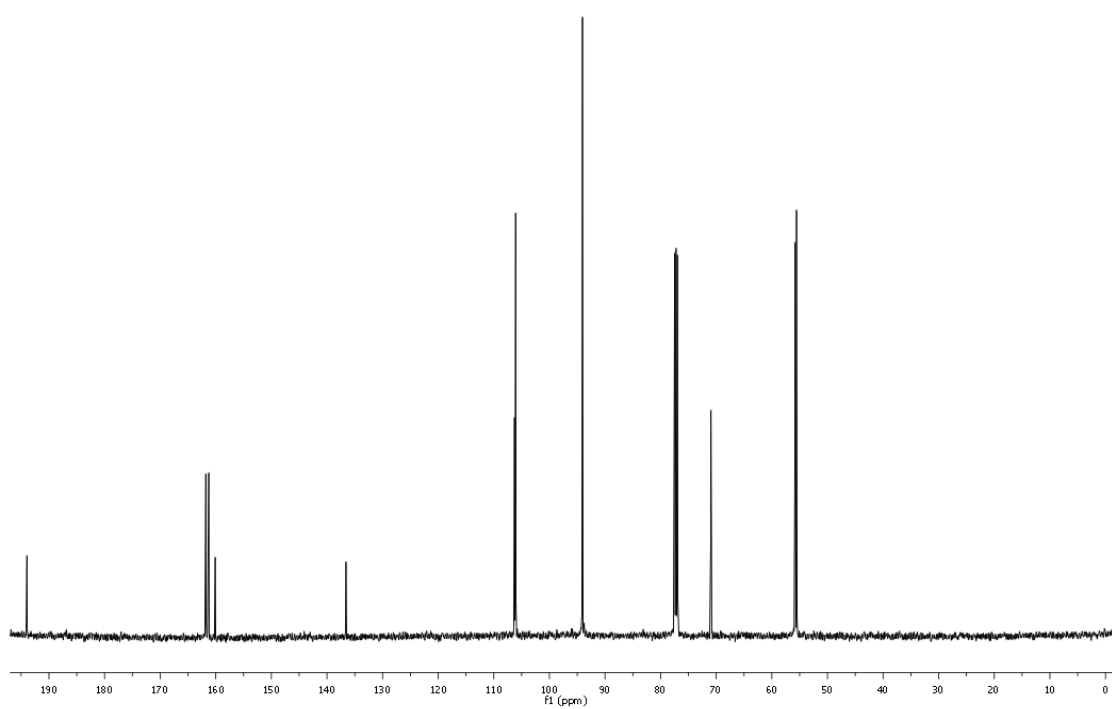
³²⁶ Tzeng, C.-C.; Lee, K.-H.; Wang, T.-C.; Han, C.-H.; Chen, Y.-L. *Pharm. Res.* **2000**, *17*, 715-719

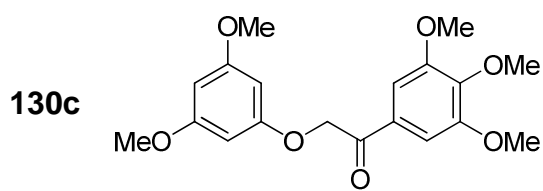


$^1\text{H-NMR}$ (CDCl_3)

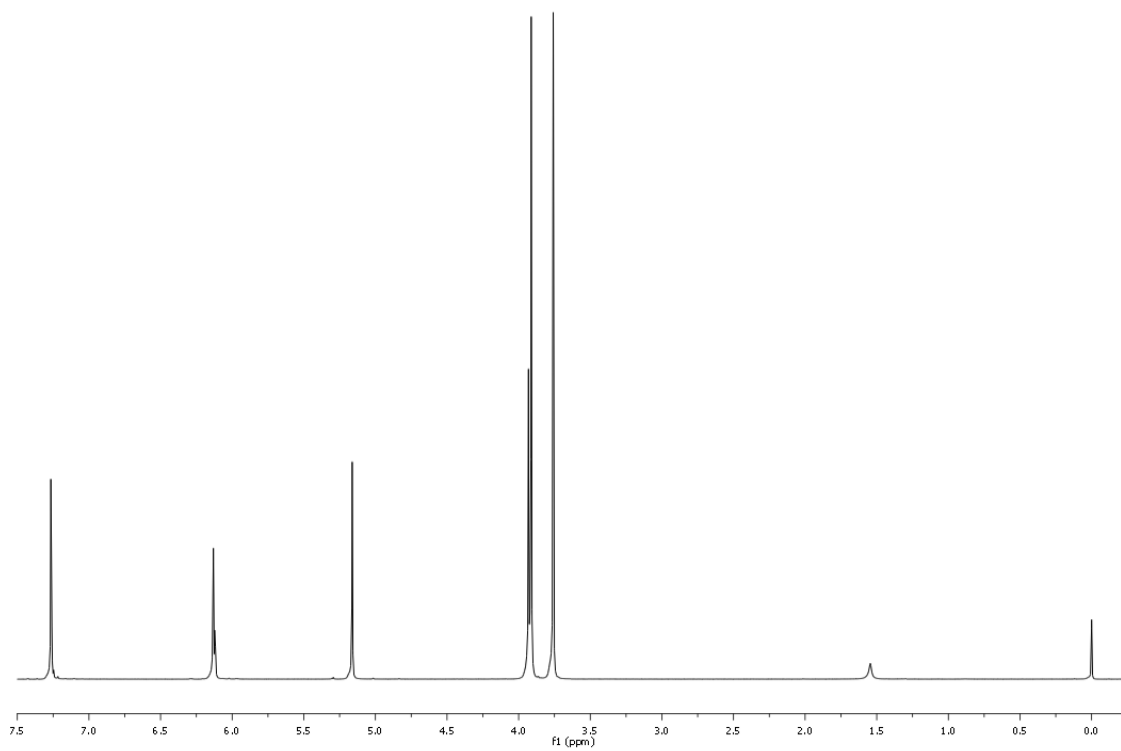


$^{13}\text{C-NMR}$ (CDCl_3)

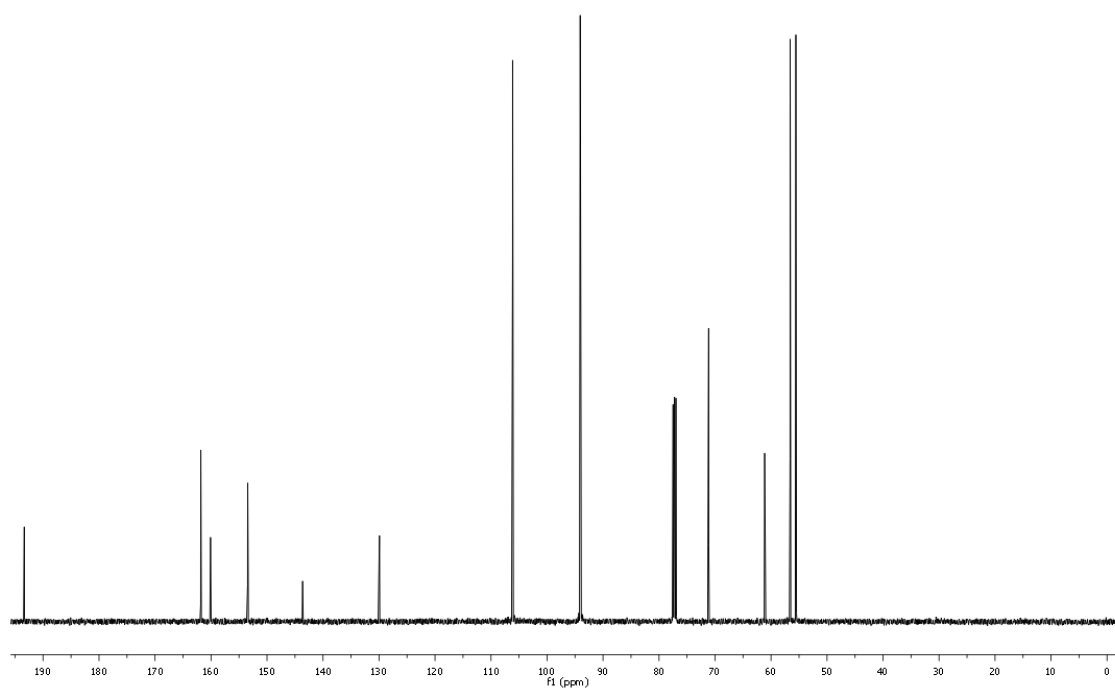


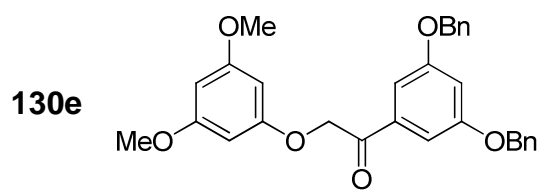


$^1\text{H-NMR}$ (CDCl_3)

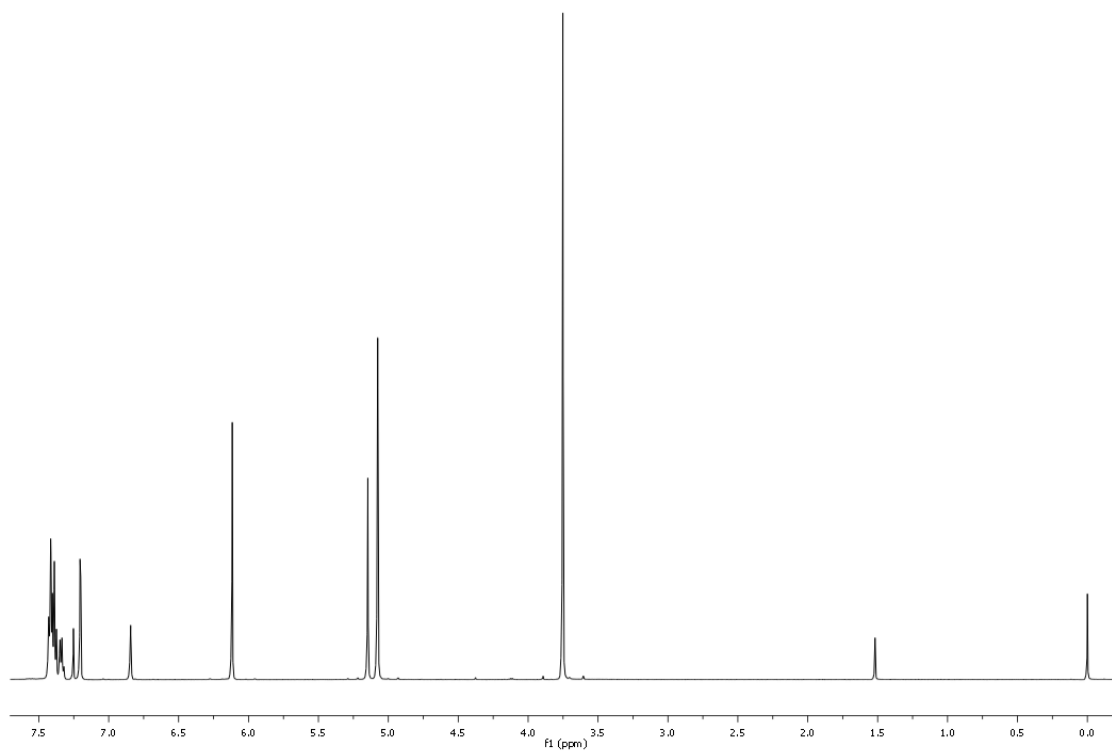


$^{13}\text{C-NMR}$ (CDCl_3)

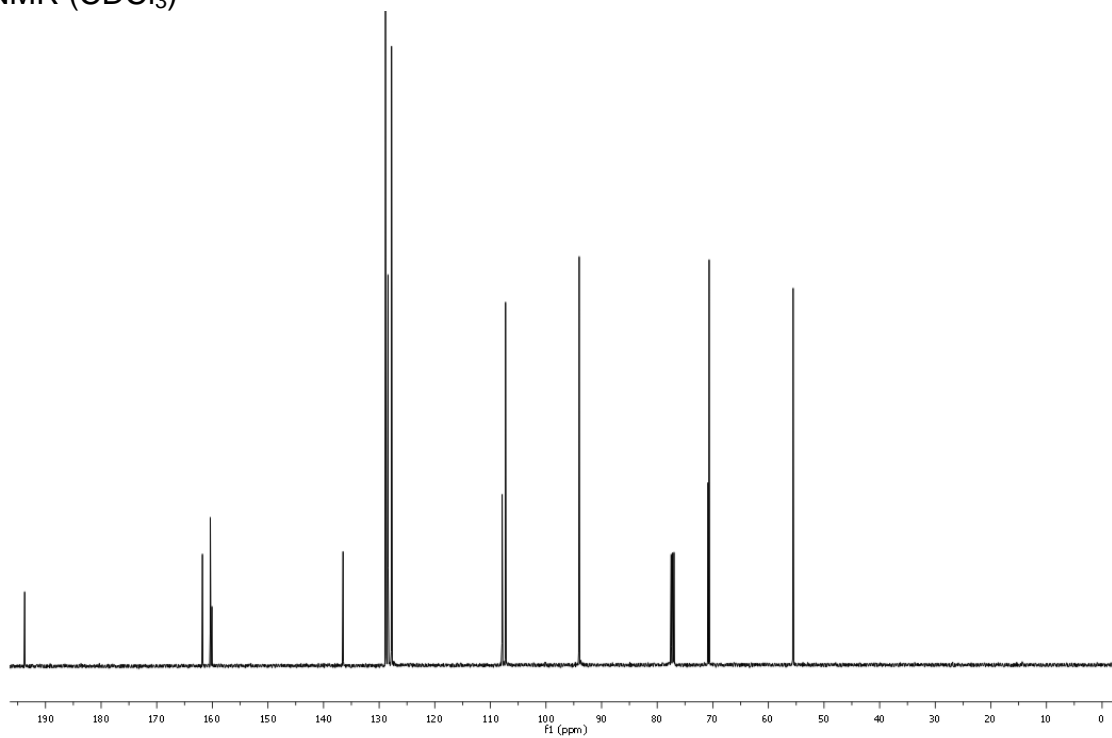


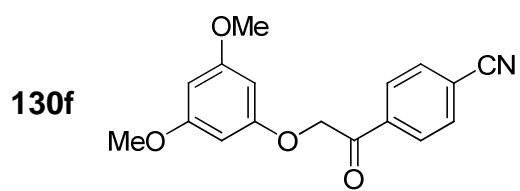


$^1\text{H-NMR}$ (CDCl_3)

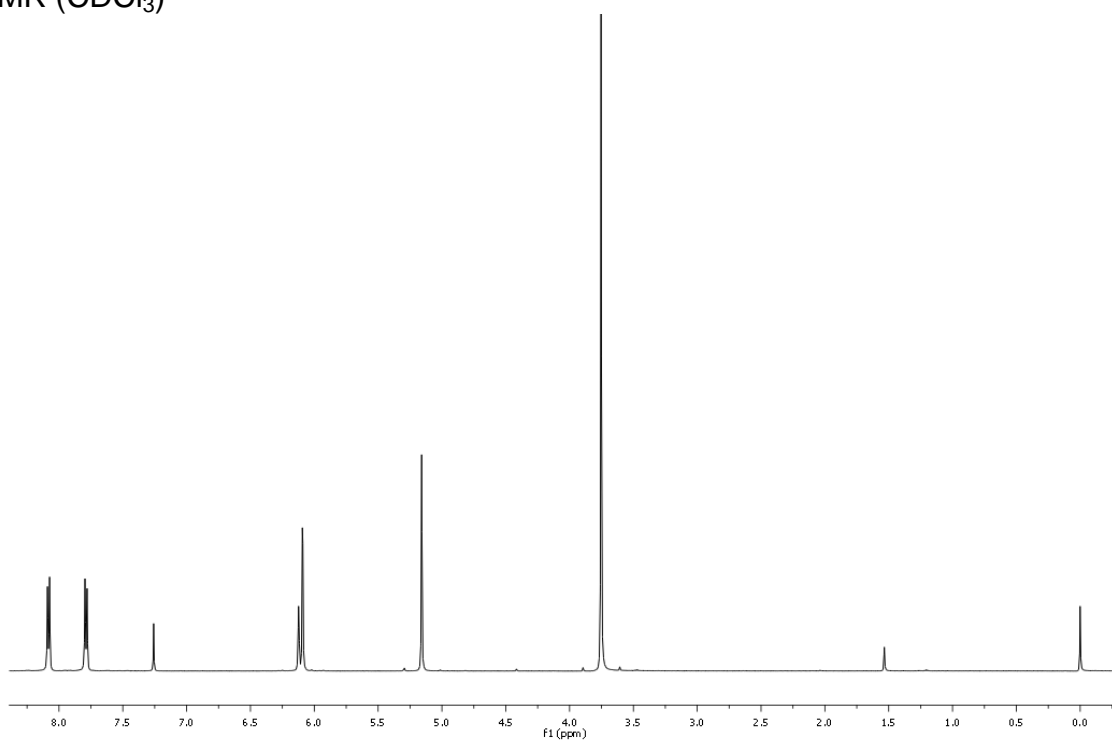


$^{13}\text{C-NMR}$ (CDCl_3)

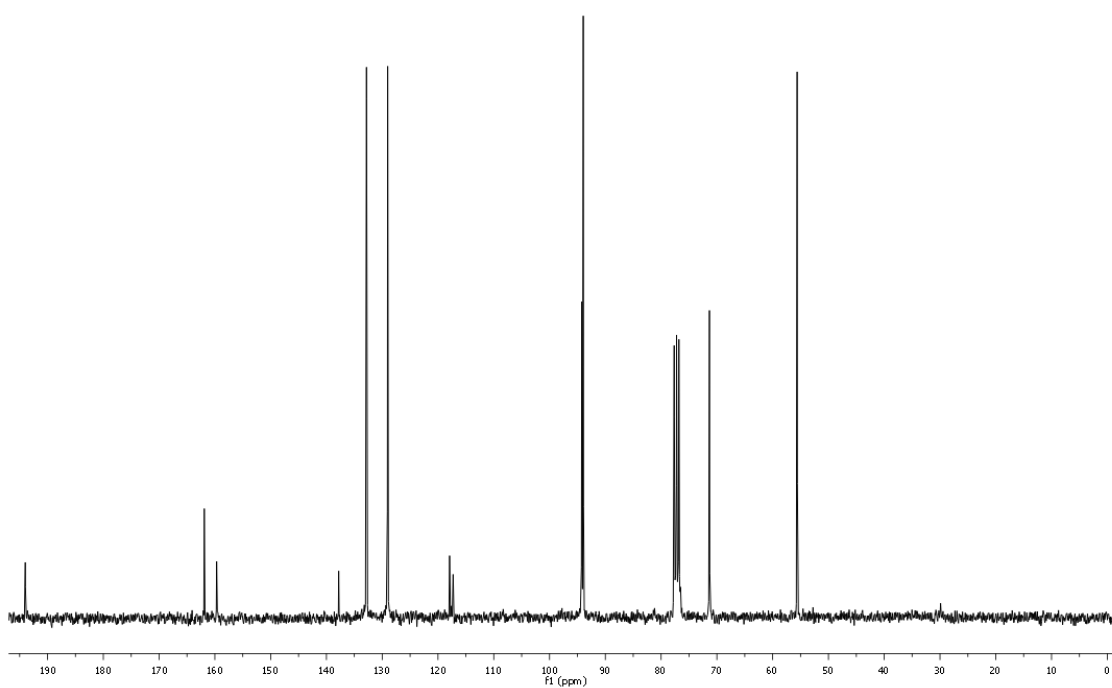


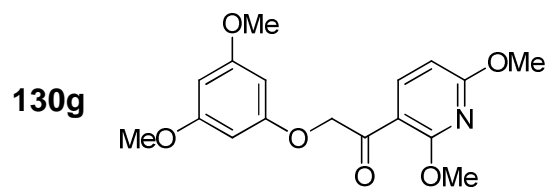


$^1\text{H-NMR}$ (CDCl_3)

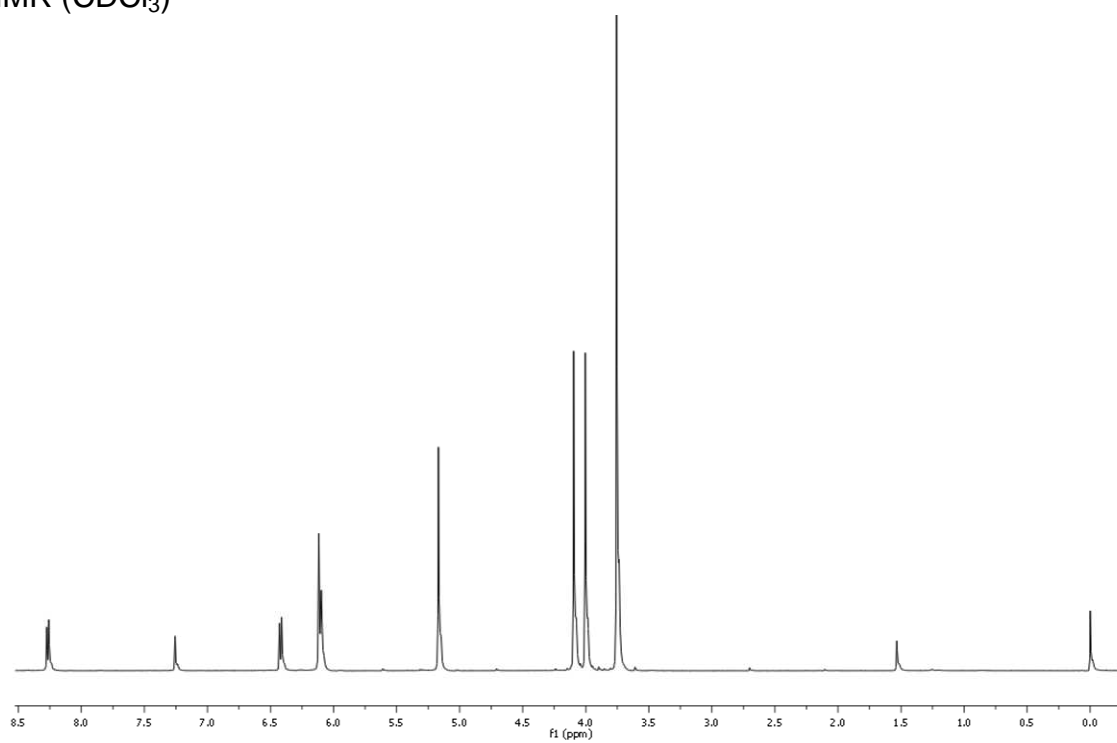


$^{13}\text{C-NMR}$ (CDCl_3)

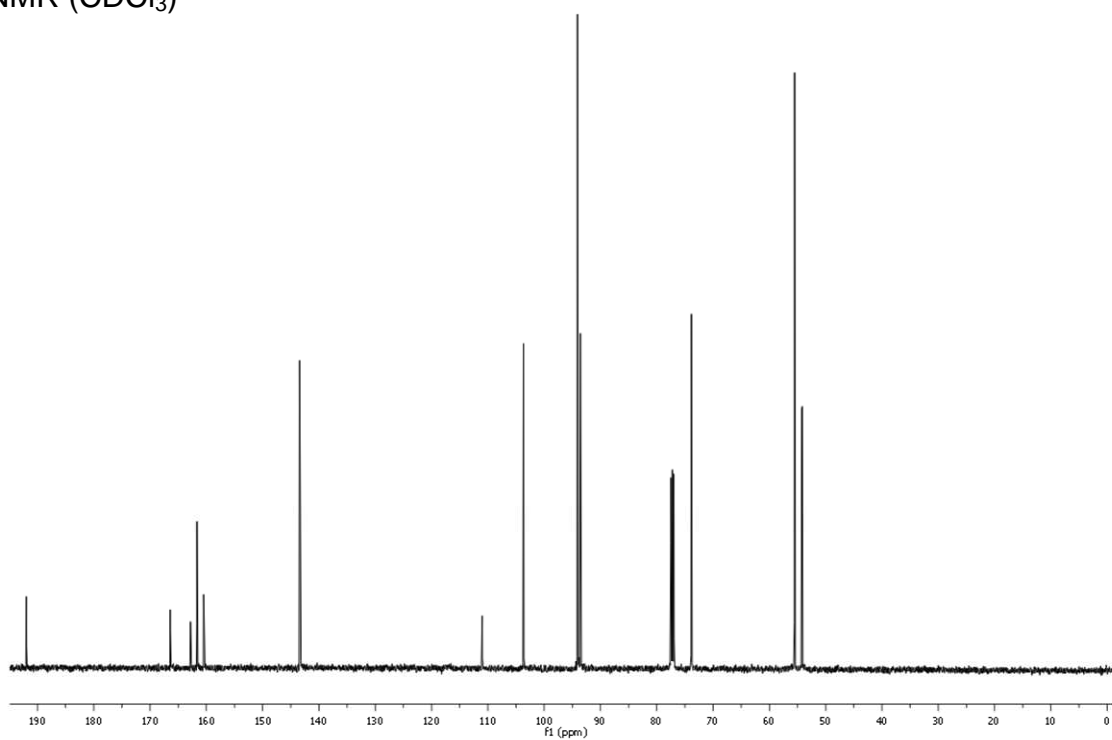


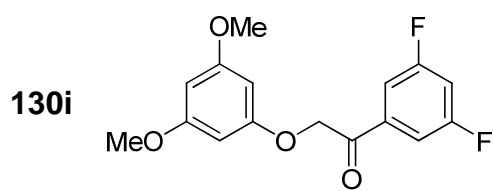


$^1\text{H-NMR}$ (CDCl_3)

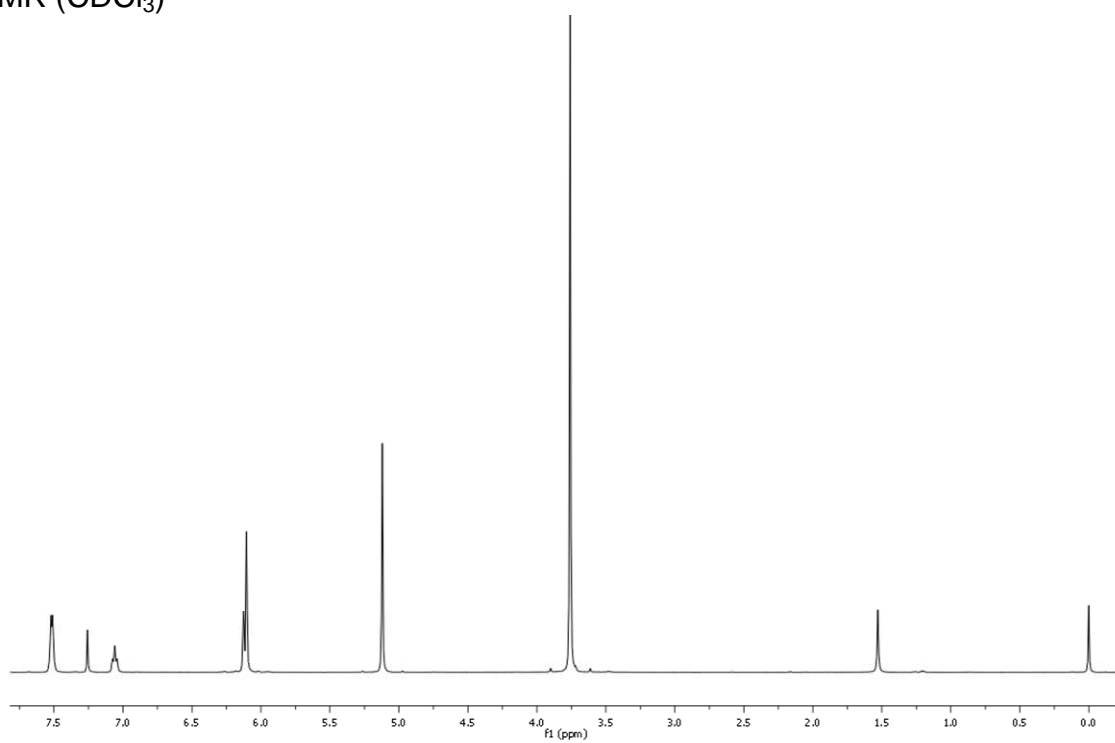


$^{13}\text{C-NMR}$ (CDCl_3)

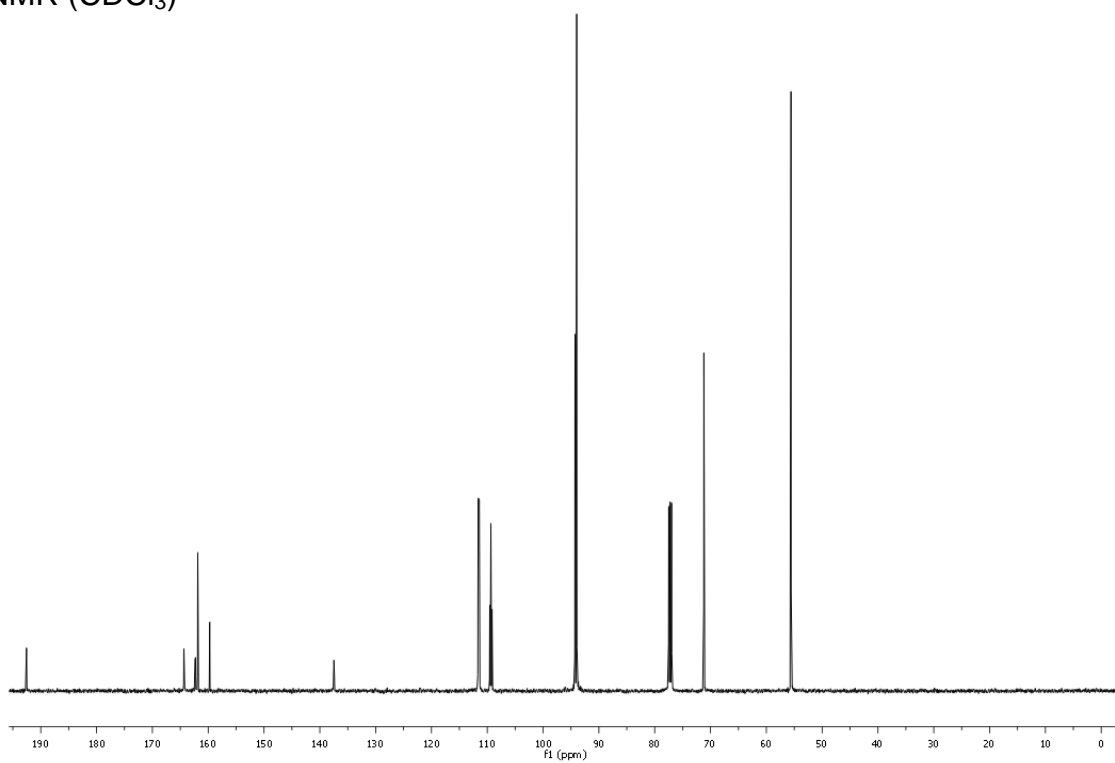


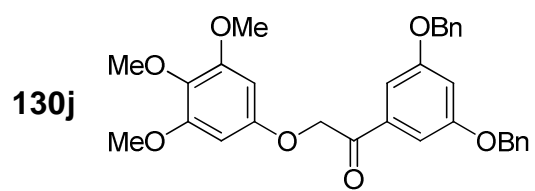


$^1\text{H-NMR}$ (CDCl_3)

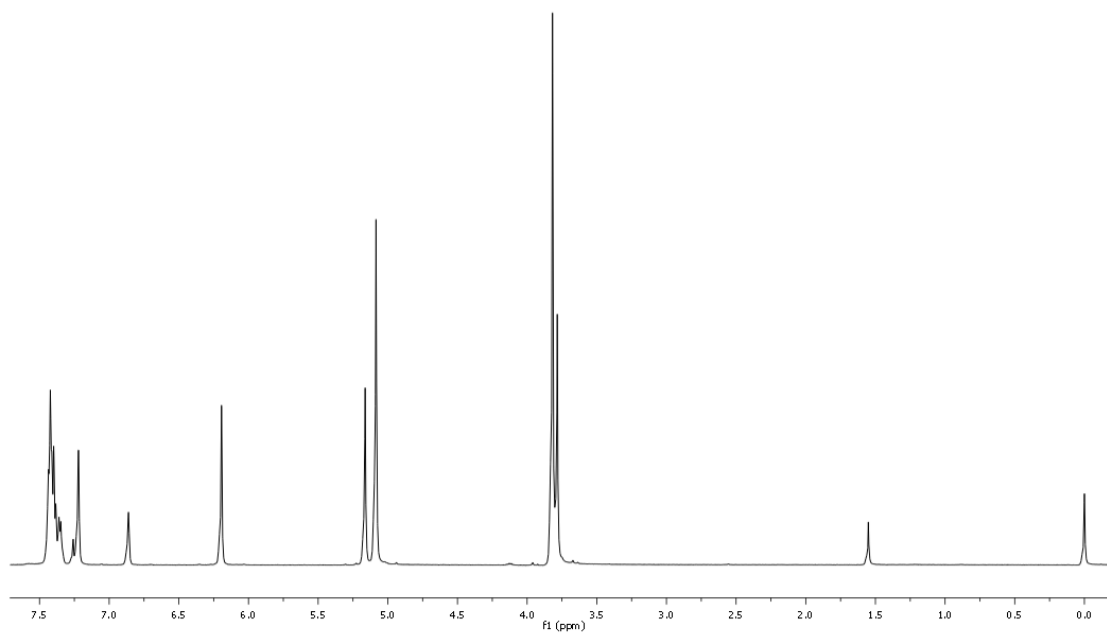


$^{13}\text{C-NMR}$ (CDCl_3)

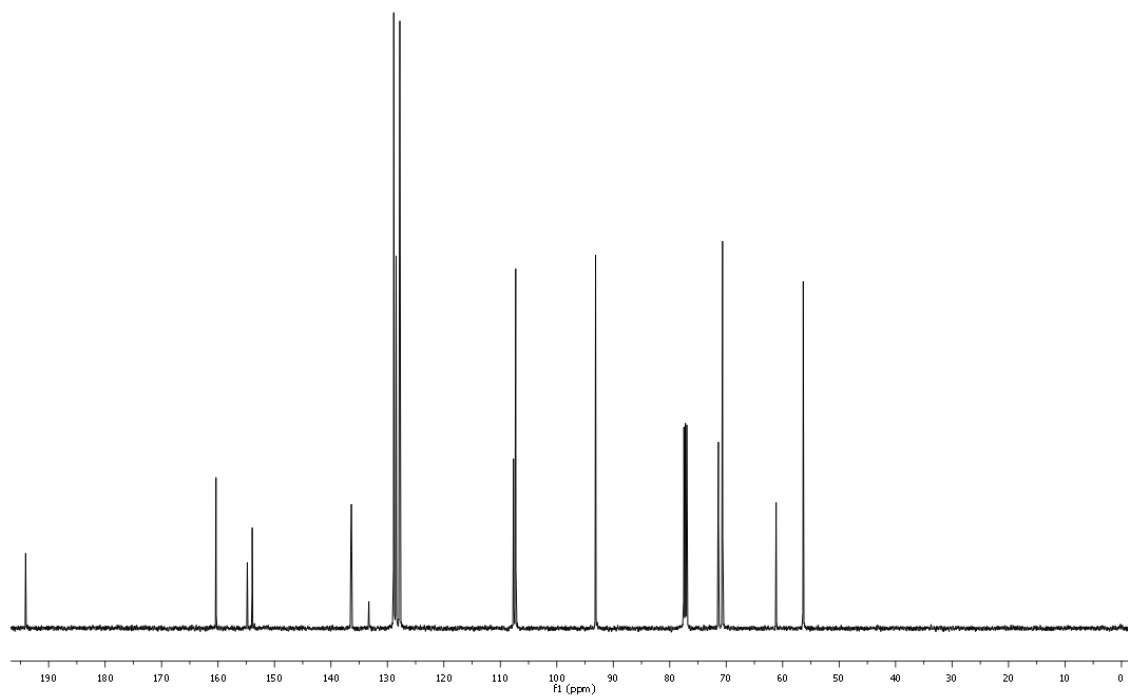


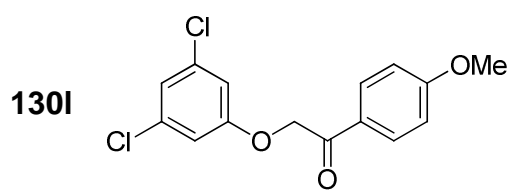


$^1\text{H-NMR}$ (CDCl_3)

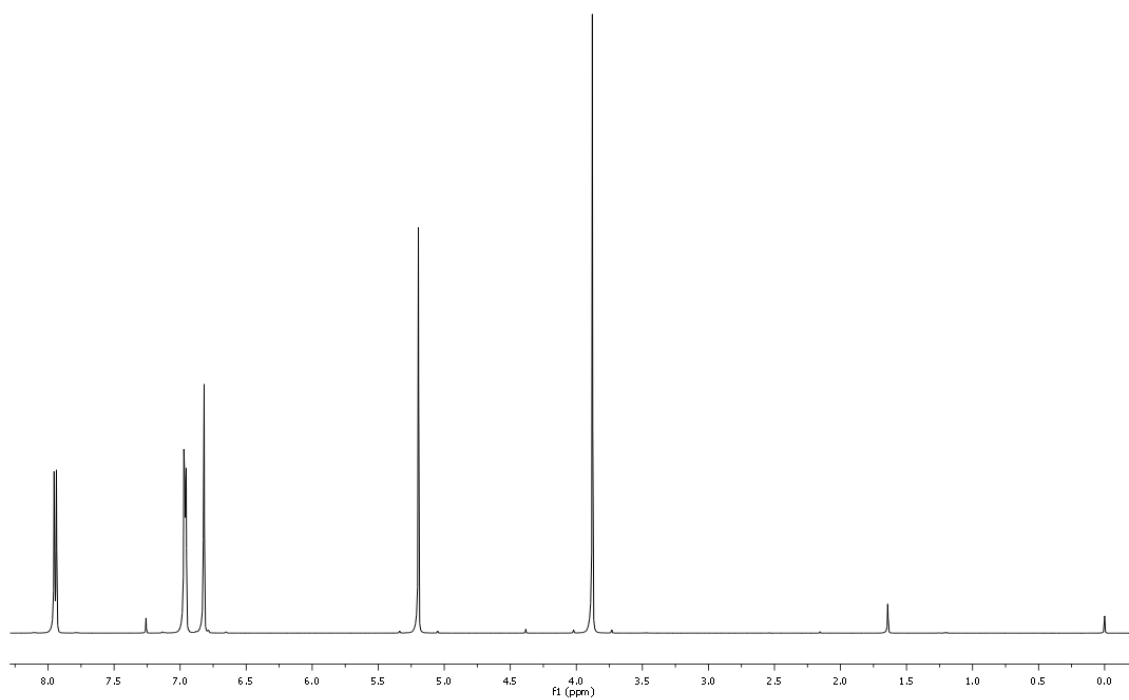


$^{13}\text{C-NMR}$ (CDCl_3)

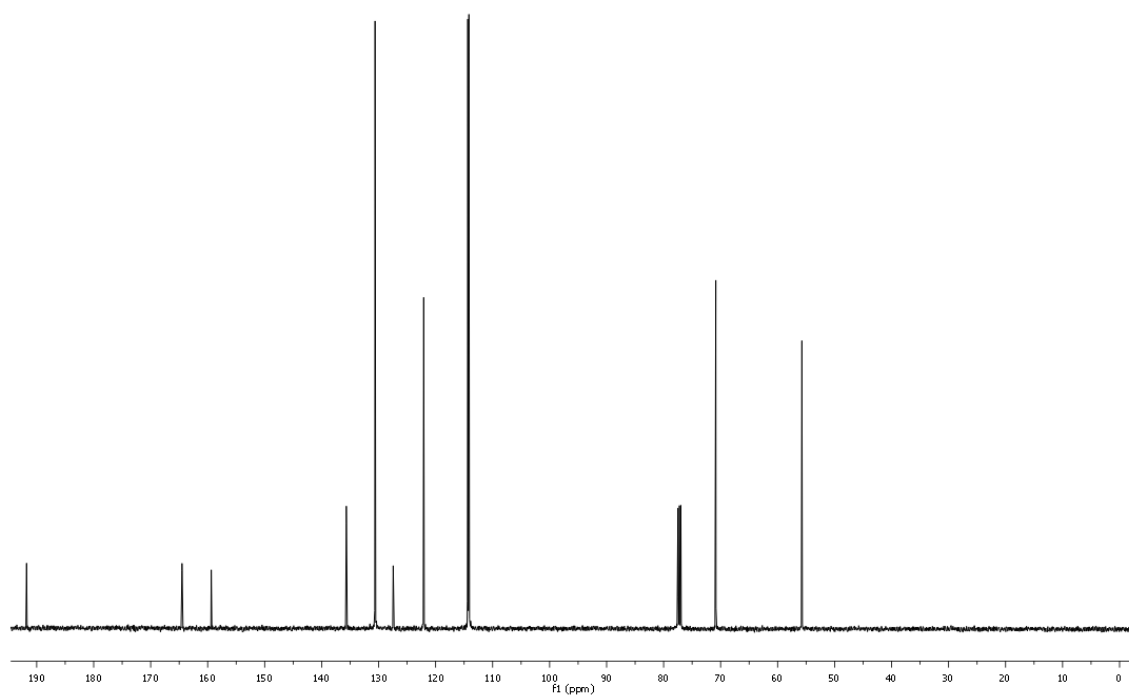




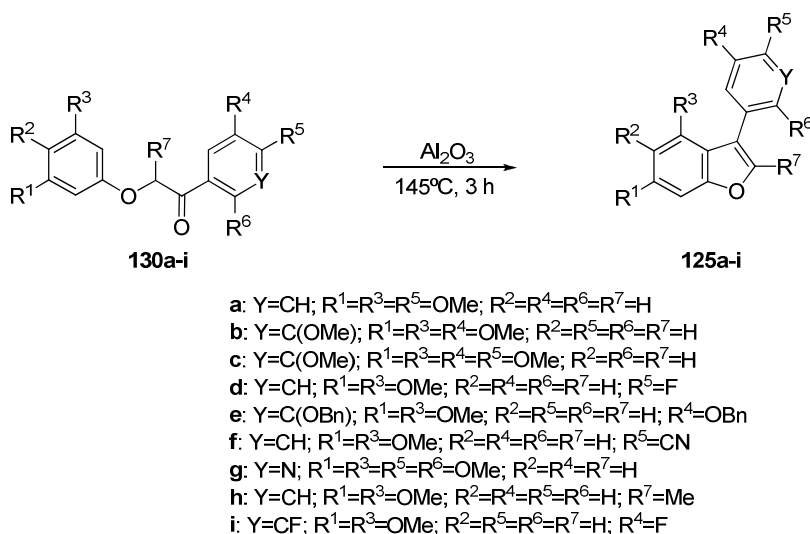
$^1\text{H-NMR}$ (CDCl_3)



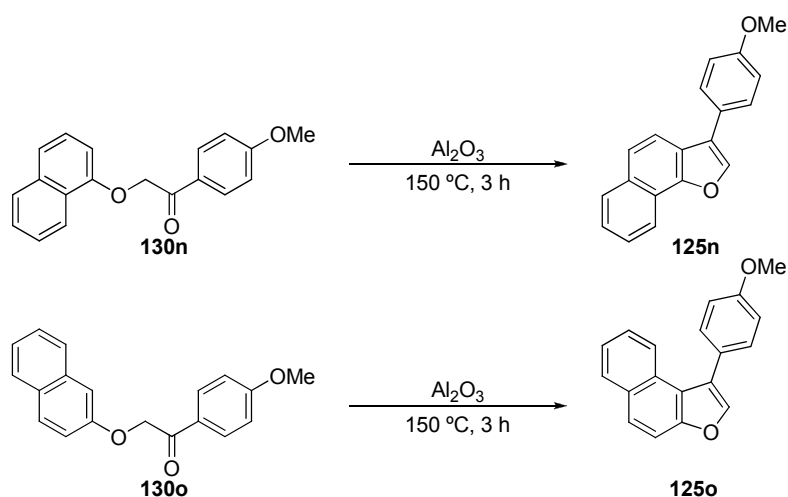
$^{13}\text{C-NMR}$ (CDCl_3)



5.2.4. Procedure for the preparation of 3-aryl benzo[*b*]furans **125a-i** and 3-aryl naphtho[1,2-*b*] and 3-aryl naphtho[2,1-*b*] furans **125n-o**

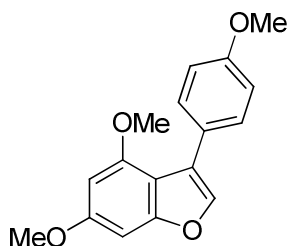


Scheme 5.6. Preparation of 3-aryl benzo[*b*]furans **125a-i** from ethers **130a-i**.



Scheme 5.7. Preparation of 3-aryl naphtho[*b*]furans **125n-o** from ethers **130n-o**.

α -Phenoxy- or α -naphthoxyketone **130** (2.0 mmol) was dispersed in alumina (34.0 mmol, 17 eq), placed in a round bottom flask capped with a silica gel desiccant containing bend. The mixture was heated in an oil bath at 150 °C (internal temperature monitored by a fibre-optic probe) for 3 hours. The resulting reaction mixture was left to cool until it reached room temperature. It was then filtered through a Celite pad and evaporated under reduced pressure. The crude obtained this way was purified by column chromatography on silica gel, using EtOAc/Hx mixtures as eluent to afford the corresponding pure products **125**. The alumina (aluminium oxide) employed was neutral (activated, Brockmann I, STD grade, approx. 150 mesh, 58 Å).

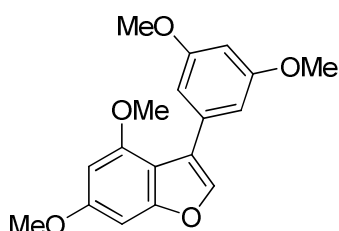
4,6-dimethoxy-3-(4'-methoxyphenyl)benzofuran¹²⁷, 125a:Molecular formula: C₁₇H₁₆O₄

Molecular weight: 284.31 g/mol

Aspect: Light yellow solid

Yield: 78%

¹H-NMR (500 MHz, CDCl₃) δ = 7.54 (d, *J*=8.7 Hz, 2H), 7.43 (s, 1H), 6.93 (d, *J*=8.7 Hz, 2H), 6.67 (d, *J*=1.8 Hz, 1H), 6.35 (d, *J*=1.7 Hz, 1H), 3.86 (s, 3H), 3.85 (s, 3H), 3.80 (s, 3H).

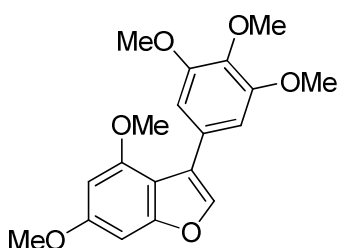
3-(3',5'-dimethoxyphenyl)-4,6-dimethoxybenzofuran, 125b:Molecular formula: C₁₈H₁₈O₅

Molecular weight: 314.33 g/mol

Aspect: White solid

Yield: 54%

m.p.: 92-93 °C. IR (neat): 2834, 1590, 1415, 1201, 1141, 1082 cm⁻¹. ¹H-NMR (500 MHz, CDCl₃) δ = 7.51 (s, 1H), 6.82 (s, 2H), 6.68 (s, 1H), 6.46 (s, 1H), 6.37 (s, 1H), 3.86 (s, 3H), 3.83 (s, 9H). ¹³C-NMR (126 MHz, CDCl₃) δ = 160.6, 159.4, 158.1, 154.8, 140.3, 134.4, 123.0, 109.9, 107.6, 99.9, 94.9, 88.7, 55.9, 55.6, 55.5. Elemental analysis calculated for C₁₈H₁₈O₅: C, 68.8; H, 5.8. Found: C, 68.7; H, 5.8.

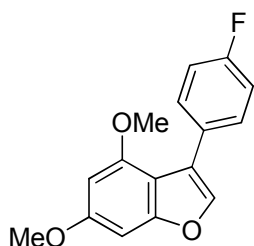
4,6-dimethoxy-3-(3',4',5'-trimethoxyphenyl)benzofuran, 125c:Molecular formula: C₁₉H₂₀O₆

Molecular weight: 344.36 g/mol

Aspect: Yellow oil

Yield: 50%

IR (neat): 2934, 1580, 1414, 1215, 1150, 1120 cm⁻¹. ¹H-NMR (500 MHz, CDCl₃) δ = 7.51 (s, 1H), 6.89 (s, 2H), 6.68 (d, *J*=1.9 Hz, 1H), 6.38 (d, *J*=1.9 Hz, 1H), 3.90 (s, 9H), 3.87 (s, 3H), 3.84 (s, 3H). ¹³C-NMR (126 MHz, CDCl₃) δ = 159.4, 158.2, 154.7, 153.0, 140.0, 128.0, 123.1, 109.8, 106.8, 94.9, 88.7, 61.2, 56.3, 56.0, 55.6.

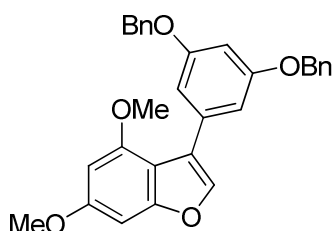
3-(4'-fluorophenyl)-4,6-dimethoxybenzofuran³²³, 125d:Molecular formula: C₁₆H₁₃FO₃

Molecular weight: 272.27 g/mol

Aspect: Green-grey solid

Yield: 72%

¹H-NMR (500 MHz, CDCl₃) δ = 7.56 (dd, *J*=8.2, 5.7 Hz, 2H), 7.44 (s, 1H), 7.07 (t, *J*=8.6 Hz, 2H), 6.67 (s, 1H), 6.35 (s, 1H), 3.85 (s, 3H), 3.79 (s, 3H).

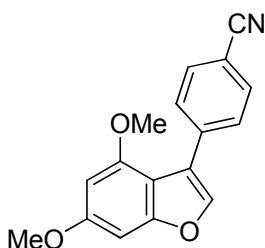
3-(3',5'-bis(benzyloxy)phenyl)-4,6-dimethoxybenzofuran, 125e:Molecular formula: C₃₀H₂₆O₅

Molecular weight: 466.52 g/mol

Aspect: Yellow oil

Yield: 26%

IR (neat): 2935, 1585, 1453, 1213, 1144, 1050 cm⁻¹. ¹H-NMR (500 MHz, CDCl₃) δ = 7.48 (s, 1H), 7.46–7.26 (m, 10H), 6.92 (d, *J*=2.2 Hz, 2H), 6.66 (d, *J*=1.9 Hz, 1H), 6.62 (t, *J*=2.2 Hz, 1H), 6.35 (d, *J*=1.8 Hz, 1H), 5.07 (s, 4H), 3.84 (s, 3H), 3.76 (s, 3H). ¹³C-NMR (126 MHz, CDCl₃) δ = 159.8, 159.4, 158.1, 154.8, 140.4, 137.3, 134.5, 128.8, 128.2, 127.7, 123.0, 109.9, 108.8, 101.6, 94.9, 88.7, 70.4, 56.0, 55.6.

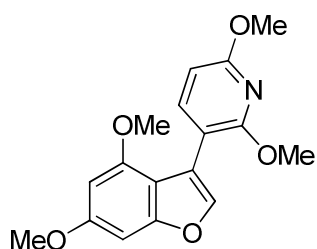
4-(4',6'-dimethoxybenzofuran-3-yl)benzonitrile, 125f:Molecular formula: C₁₇H₁₃NO₃

Molecular weight: 279.29 g/mol

Aspect: Yellow solid

Yield: 42%

m.p.: 151–152 °C. IR (neat): 2938, 2220, 1598, 1503, 1215, 1044, 1085 cm⁻¹. ¹H-NMR (500 MHz, CDCl₃) δ = 7.72 (d, *J*=8.0 Hz, 2H), 7.66 (d, *J*=8.2 Hz, 2H), 7.54 (s, 1H), 6.69 (s, 1H), 6.38 (s, 1H), 3.87 (s, 3H), 3.82 (s, 3H). ¹³C-NMR (126 MHz, CDCl₃) δ = 159.8, 158.3, 154.6, 140.9, 137.6, 131.9, 129.9, 121.9, 119.3, 110.7, 109.2, 95.2, 88.7, 56.0, 55.6. Elemental analysis calculated for C₁₇H₁₃NO₃: C, 73.1; H, 4.7; N, 5.0. Found: C, 73.1; H, 4.6; N, 5.1.

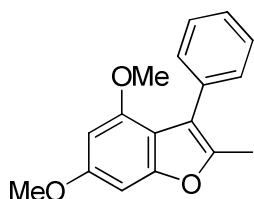
3-(4',6'-dimethoxybenzofuran-3-yl)-2,6-dimethoxypyridine, 125g:Molecular formula: C₁₇H₁₇NO₅

Molecular weight: 315.32 g/mol

Aspect: Light yellow solid

Yield: 12%

m.p.: 131 °C. IR (neat): 2943, 1586, 1481, 1315, 1080, 1023 cm⁻¹. ¹H-NMR (500 MHz, CDCl₃) δ = 7.72 (d, *J*=8.0 Hz, 1H), 7.58 (s, 1H), 6.67 (s, 1H), 6.36 (d, *J*=8.0 Hz, 1H), 6.32 (s, 1H), 3.97 (s, 3H), 3.95 (s, 3H), 3.85 (s, 3H), 3.76 (s, 3H). ¹³C-NMR (126 MHz, CDCl₃) δ = 162.3, 160.3, 159.2, 157.5, 154.8, 143.1, 141.4, 116.0, 110.9, 106.8, 100.1, 94.8, 88.6, 56.0, 55.6, 53.8, 53.6. Elemental analysis calculated for C₁₇H₁₇NO₅: C, 64.8; H, 5.4; N, 4.4. Found: C, 64.6; H, 5.5; N, 4.5.

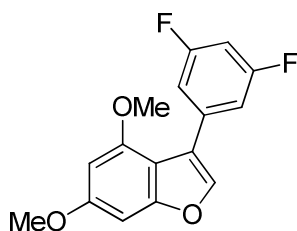
4,6-dimethoxy-2-methyl-3-phenylbenzofuran^{323,327}, 125h:Molecular formula: C₁₇H₁₆O₃

Molecular weight: 268.31 g/mol

Aspect: White solid

Yield: 40%

¹H-NMR (500 MHz, CDCl₃) δ = 7.47–7.27 (m, 5H), 6.63 (s, 1H), 6.30 (s, 1H), 3.84 (s, 3H), 3.70 (s, 3H), 2.39 (s, 3H).

3-(3',5'-difluorophenyl)-4,6-dimethoxybenzofuran, 125i:Molecular formula: C₁₆H₁₂F₂O₃

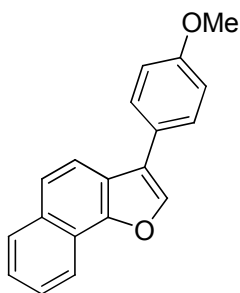
Molecular weight: 290.26 g/mol

Aspect: Light yellow solid

Yield: 68%

m.p.: 102-103 °C. IR (KBr): 2937, 1591, 1501, 1444, 1354, 1217, 1113 cm⁻¹. ¹H-NMR (300 MHz, CDCl₃) δ = 7.49 (s, 1H), 7.20–7.11 (m, 2H), 6.75 (tt, *J*=9.0, 2.3 Hz, 1H), 6.66 (d, *J*=1.9 Hz, 1H), 6.36 (d, *J*=1.9 Hz, 1H), 3.84 (s, 3H), 3.82 (s, 3H). ¹³C-NMR (75 MHz, CDCl₃) δ = 162.8 (dd, *J*=246.5, 13.3 Hz), 159.7, 158.2, 154.6, 140.7, 135.8 (t, *J*=10.6 Hz), 121.5, 112.2 (dd, *J*=8.1, 17.4 Hz), 109.2, 102.4 (t, *J*=25.5 Hz), 95.1, 88.6, 55.9, 55.5. Elemental analysis calculated for C₁₆H₁₂F₂O₃: C, 66.2; H, 4.2. Found: C, 66.2; H, 4.3.

³²⁷ Birch, H. F.; Flynn, D. G.; Robertson, A.; Curd, F. H. *J. Chem. Soc.* **1936**, 1834-1837

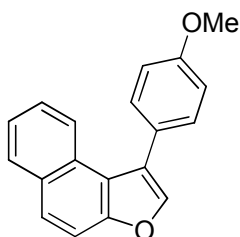
3-(4'-methoxyphenyl)naphtho[1,2-*b*]furan³²², 125n:Molecular formula: C₁₉H₁₄O₂

Molecular weight: 274.31 g/mol

Aspect: Yellow solid

Yield: 16%

¹H-NMR (500 MHz, CDCl₃) δ = 8.34 (d, *J*=8.2 Hz, 1H), 7.95 (d, *J*=8.1 Hz, 1H), 7.87 (s, 1H), 7.85 (d, *J*=8.7 Hz, 1H), 7.71 (d, *J*=8.6 Hz, 1H), 7.61 (t, *J*=9.0 Hz, 3H), 7.65–7.58 (m, 1H), 7.04 (d, *J*=8.5 Hz, 2H), 3.88 (s, 3H).

1-(4'-methoxyphenyl)naphtho[2,1-*b*]furan³²⁸, 125o:Molecular formula: C₁₉H₁₄O₂

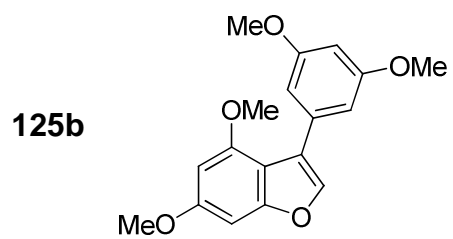
Molecular weight: 274.31 g/mol

Aspect: Yellow oil

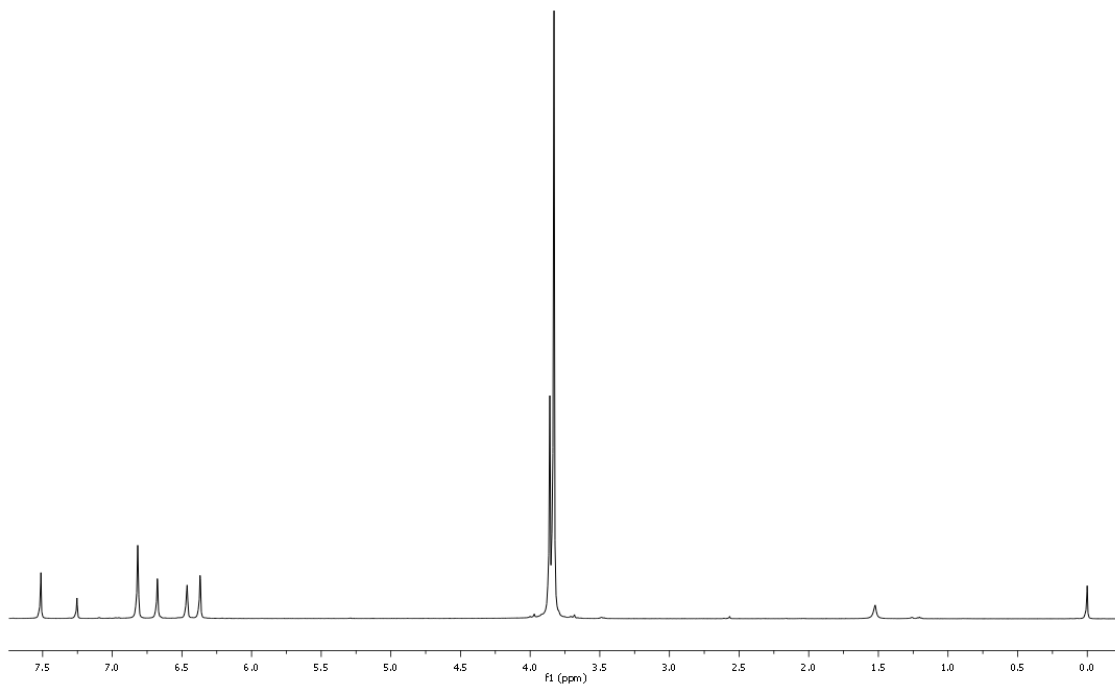
Yield: 15%

¹H-NMR (500 MHz, CDCl₃) δ = 8.00 (d, *J*=8.3 Hz, 1H), 7.92 (d, *J*=8.1 Hz, 1H), 7.74 (d, *J*=8.9 Hz, 1H), 7.67 (d, *J*=8.9 Hz, 1H), 7.64 (s, 1H), 7.50 (d, *J*=8.1 Hz, 2H), 7.42 (t, *J*=7.5 Hz, 1H), 7.35 (t, *J*=7.6 Hz, 1H), 7.04 (d, *J*=8.1 Hz, 2H), 3.89 (s, 3H).

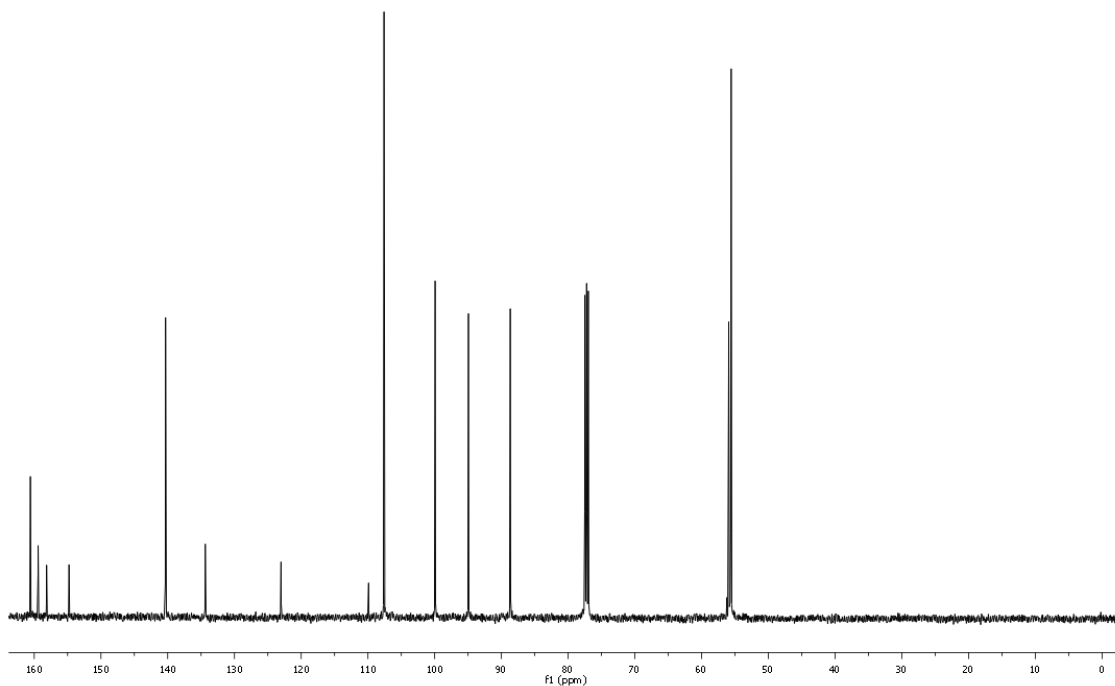
³²⁸ Mashraqui, S. H.; Patil, M. B.; Sangvikar, Y.; Ashraf, M.; Mistry, H. D.; Dâub. E. T. H.; Meetsma, A. J. *Heterocycl. Chem.* **2005**, *42*, 947-954

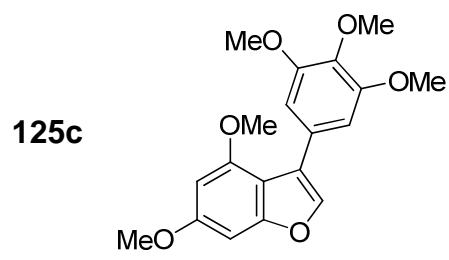


$^1\text{H-NMR}$ (CDCl_3)

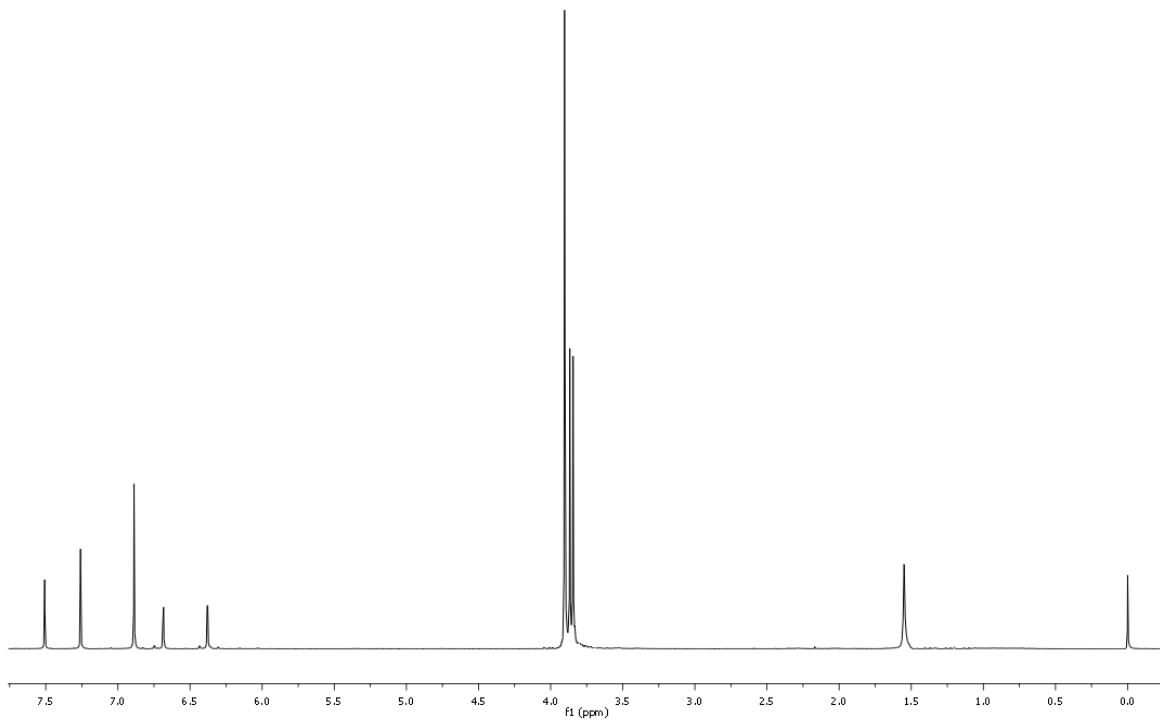


$^{13}\text{C-NMR}$ (CDCl_3)

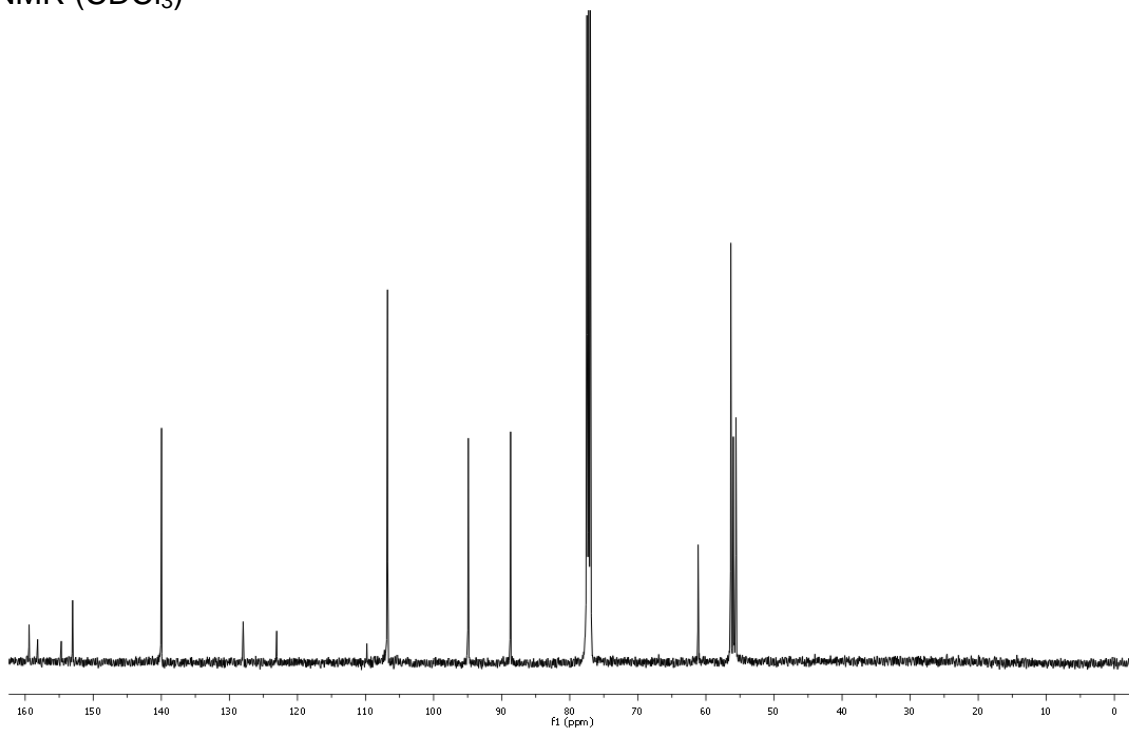


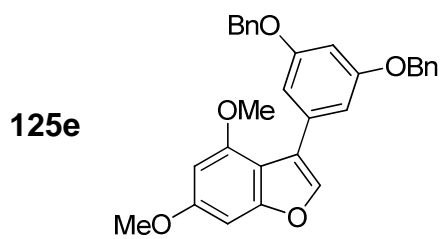


$^1\text{H-NMR}$ (CDCl_3)

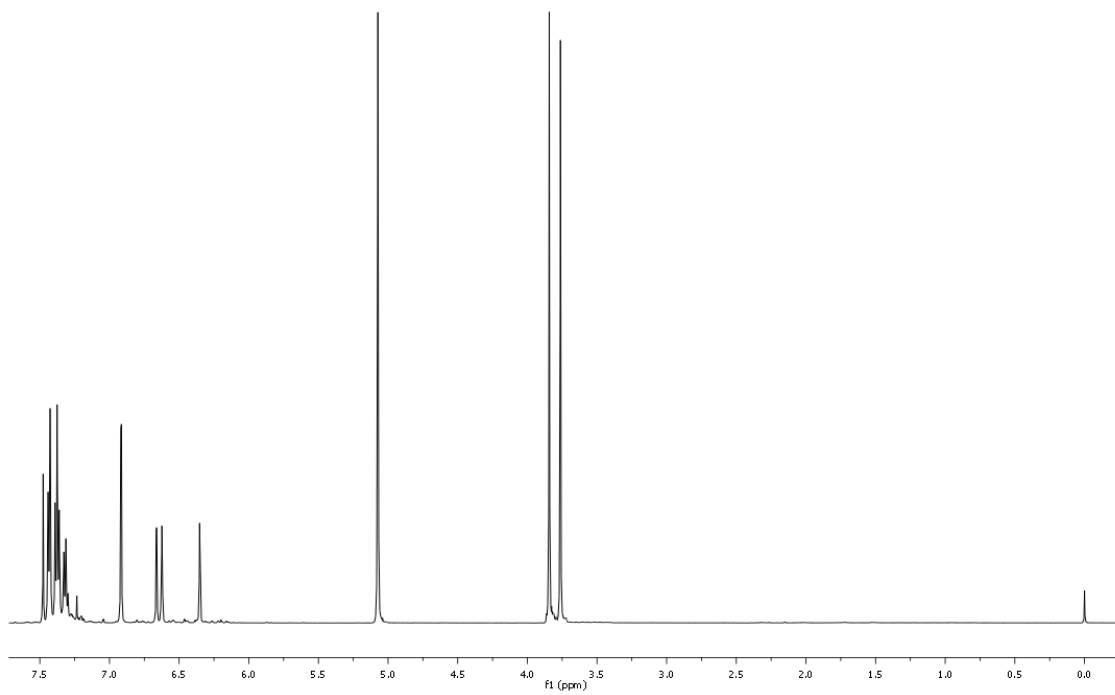


$^{13}\text{C-NMR}$ (CDCl_3)

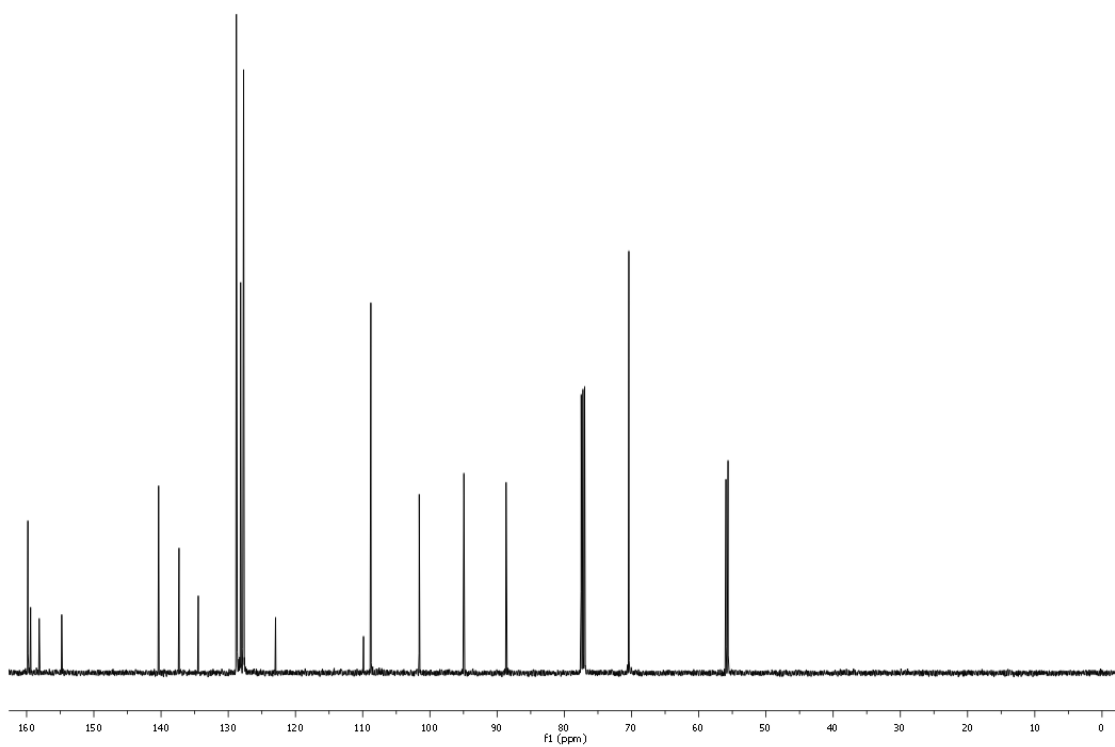


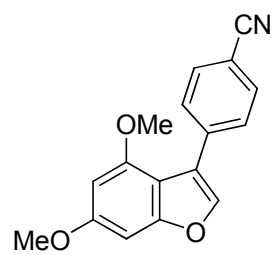
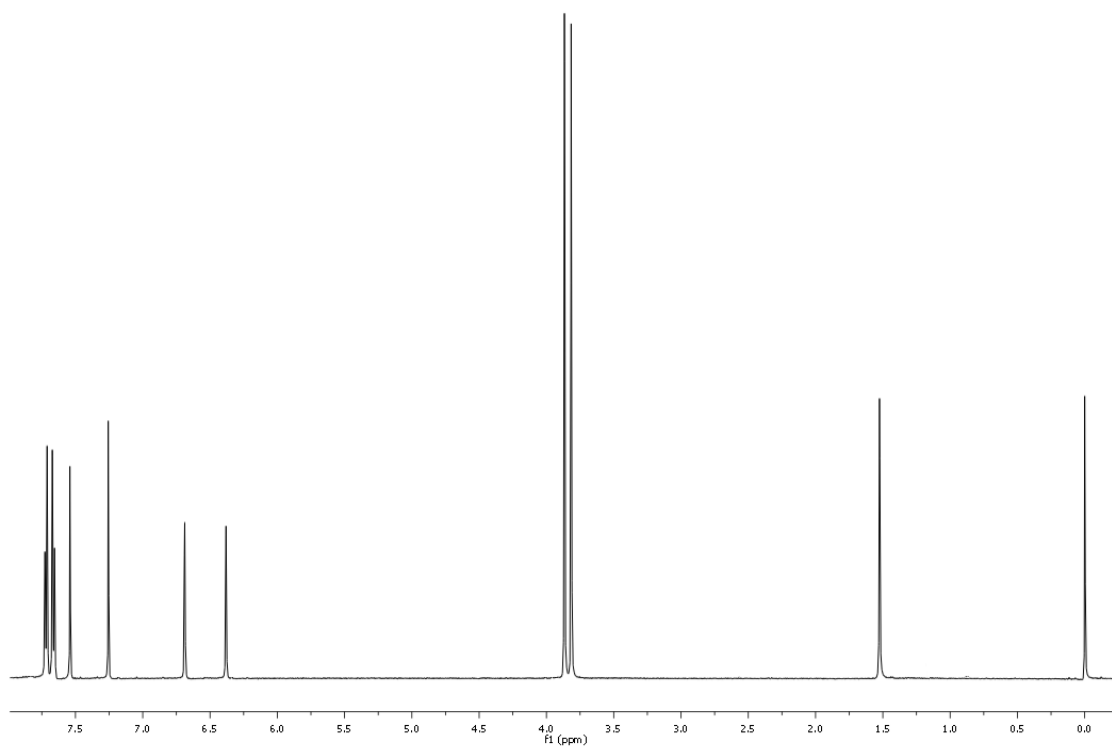
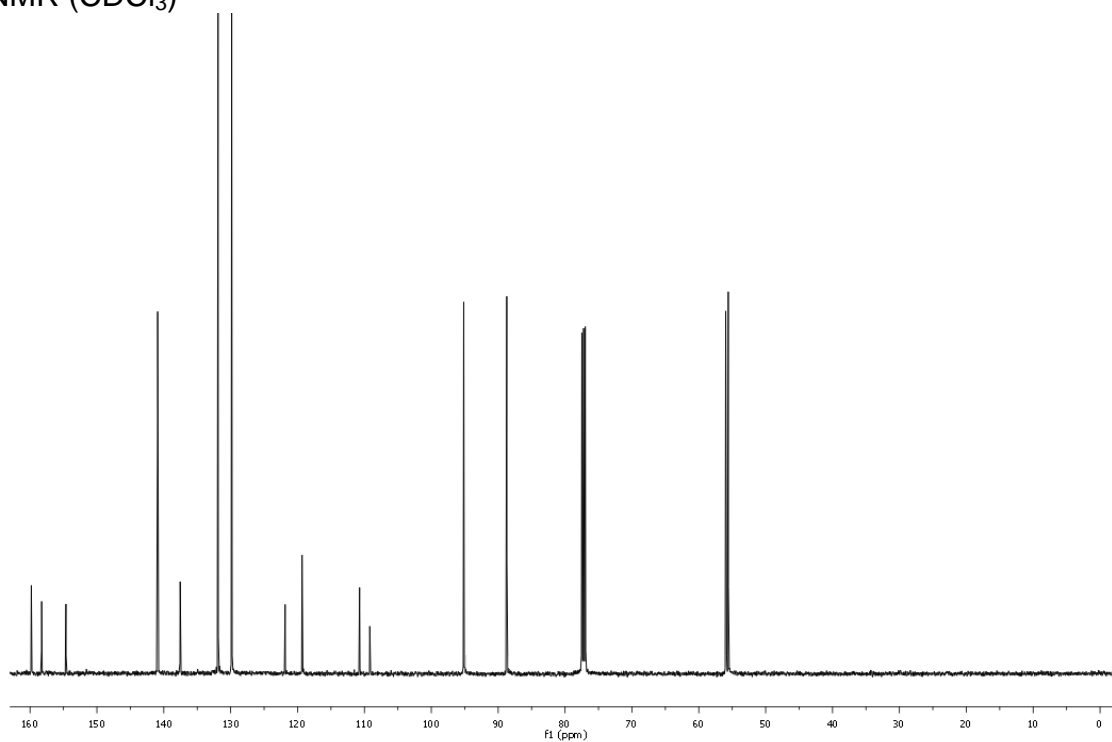


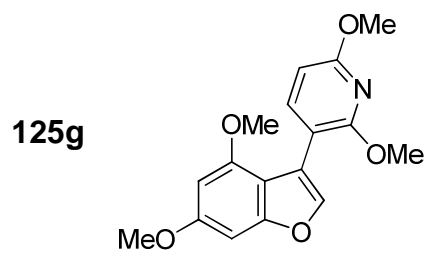
$^1\text{H-NMR}$ (CDCl_3)



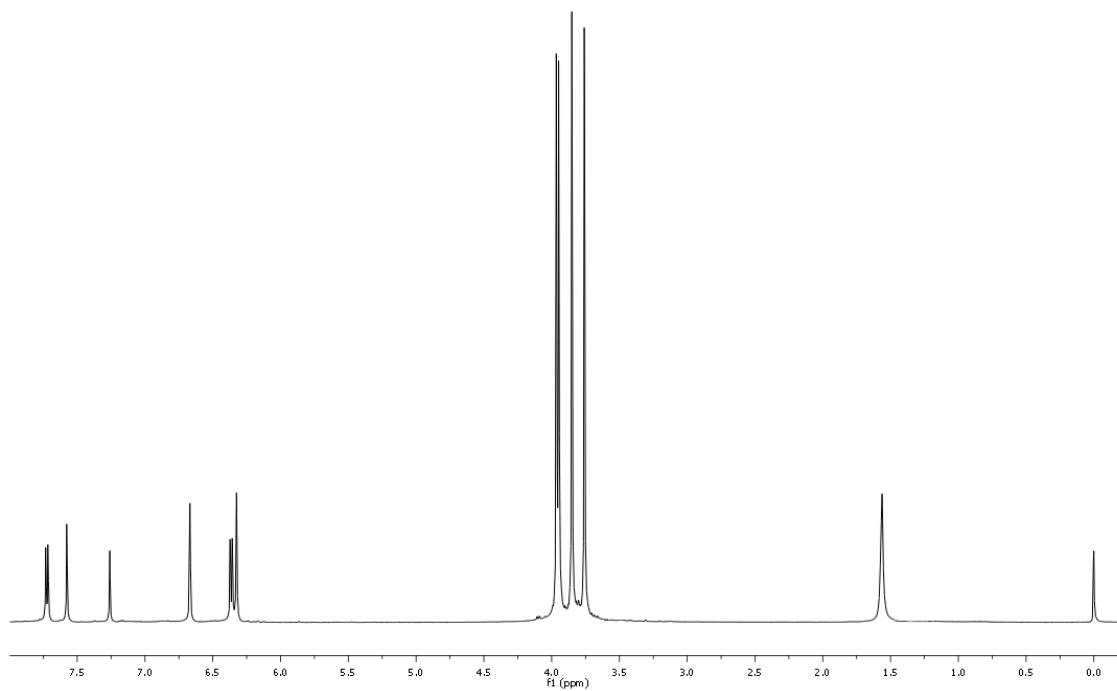
$^{13}\text{C-NMR}$ (CDCl_3)



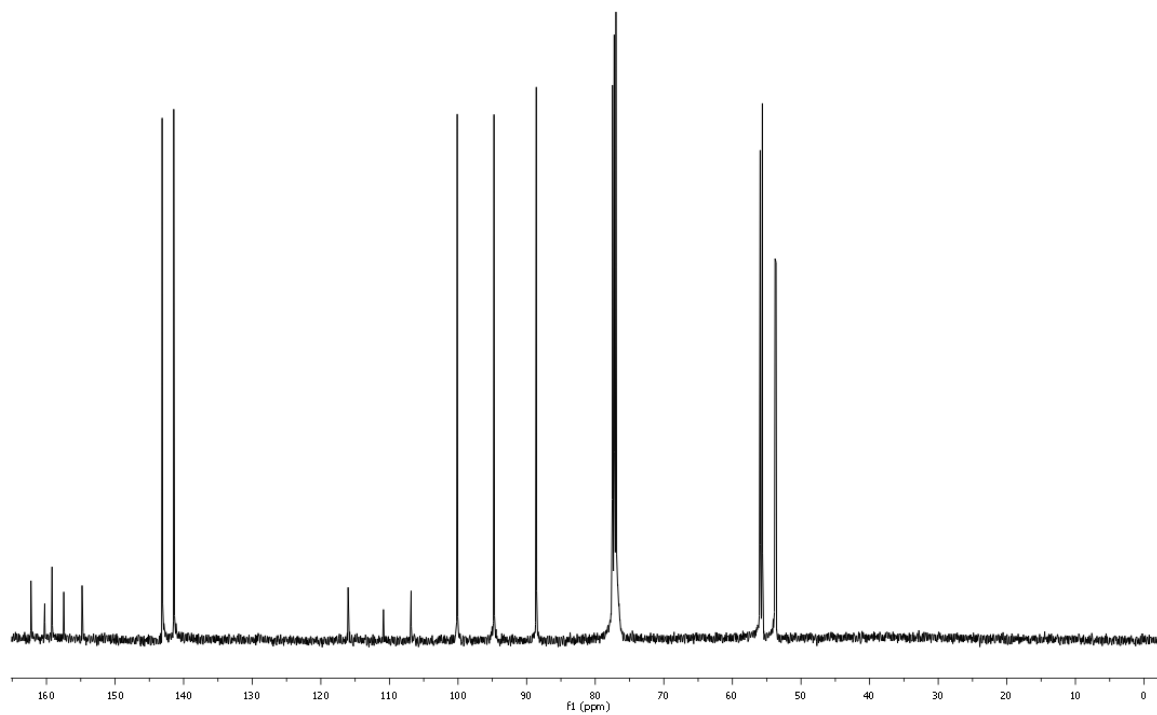
125f¹H-NMR (CDCl₃)¹³C-NMR (CDCl₃)

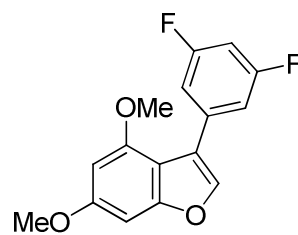
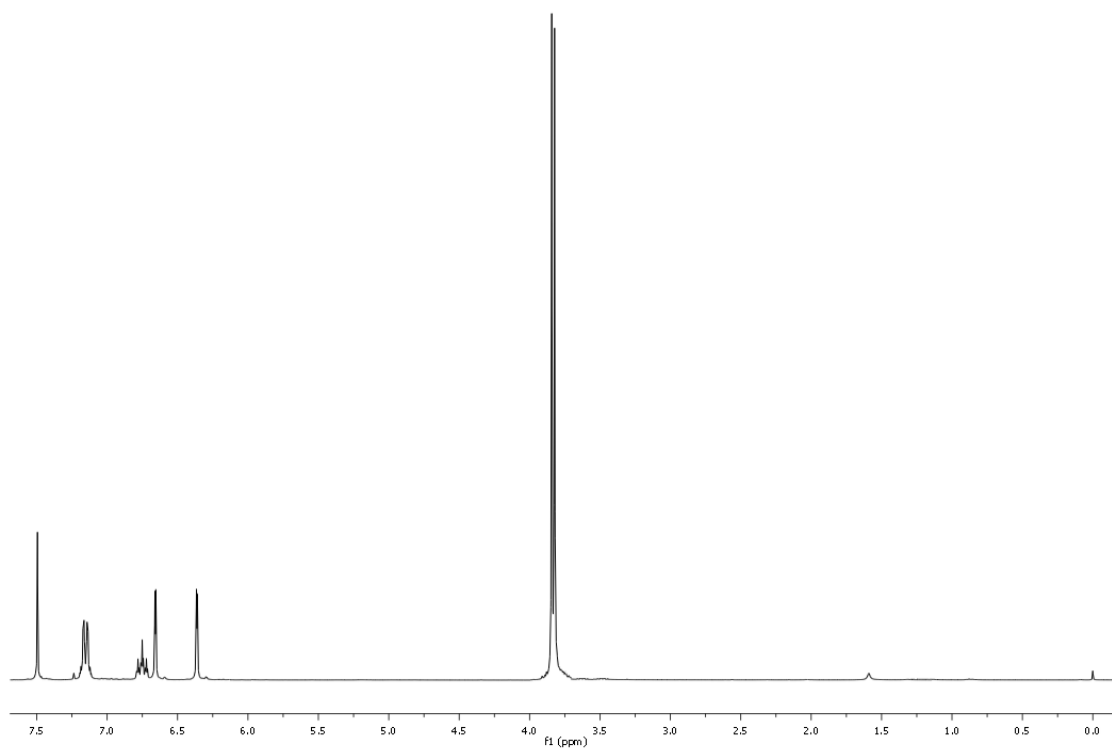
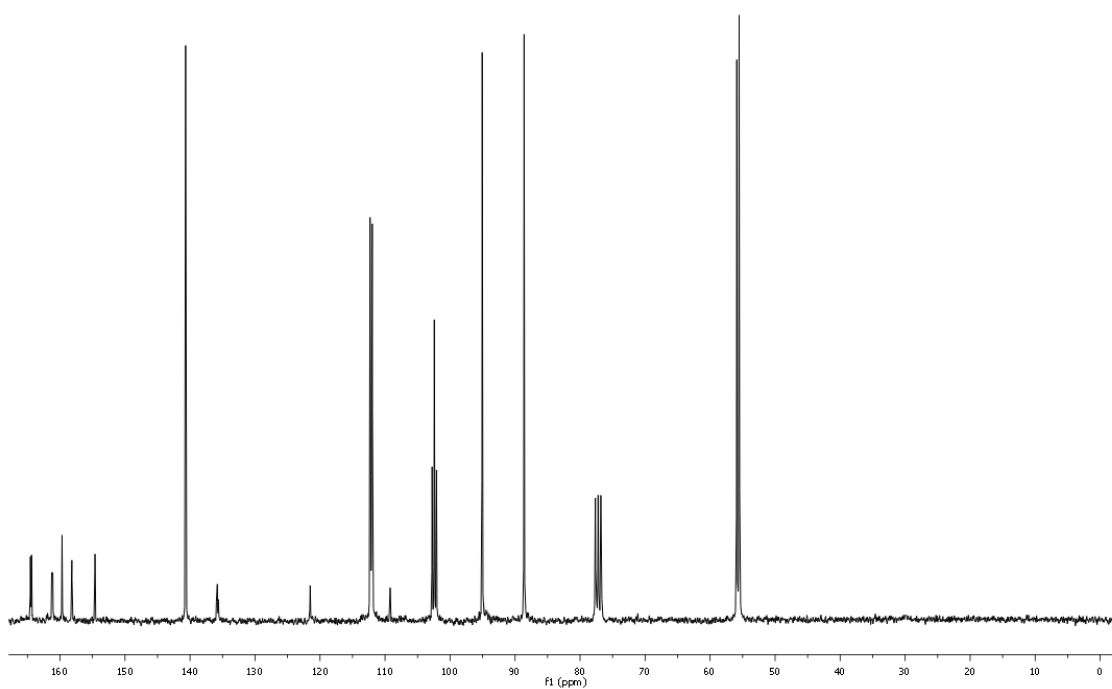


$^1\text{H-NMR}$ (CDCl_3)



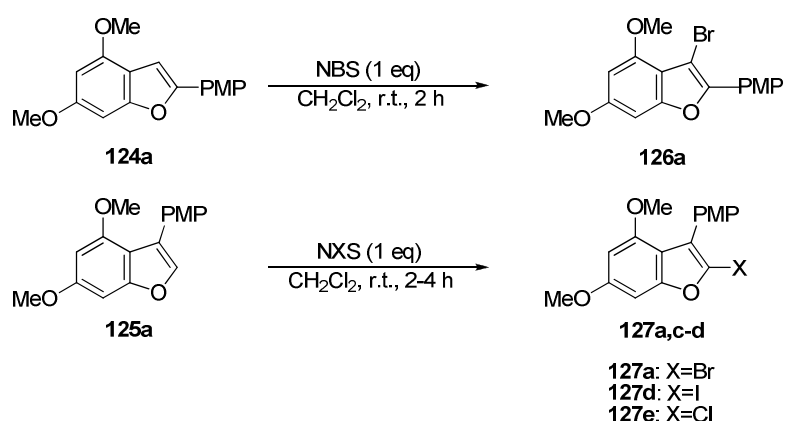
$^{13}\text{C-NMR}$ (CDCl_3)



125i¹H-NMR (CDCl₃)¹³C-NMR (CDCl₃)

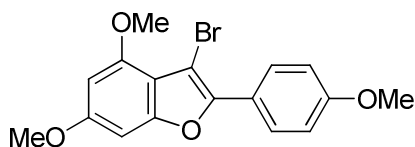
5.3. N-HALOSUCCINIMIDES (NXS)-MEDIATED REGIOSELECTIVE HALOGENATION of 2- and 3-ARYL BENZO[*b*]FURANS 124a and 125a

5.3.1. Procedure for the monohalogenation of 2-aryl benzo[*b*]furan 124a and 3-aryl benzo[*b*]furan 125a with NXS leading to products 126a and 127a,d-e



Scheme 5.8. Preparation of monohalogenated 2-aryl and 3-aryl benzo[*b*]furans **126a** and **127a,d-e** from benzo[*b*]furans **124a** and **125a**.

A solution of benzo[*b*]furan **124a** or **125a** (0.440 mmol) in 6.6 ml of CH_2Cl_2 and a solution of NXS (0.440 mmol, 1 eq) in 6.6 ml of CH_2Cl_2 were separately prepared by stirring the mixtures in round bottom flasks until total solution of the solids. The solution of the benzo[*b*]furan was then dropwise added over the solution of NXS and the round bottom flask was capped with a silica gel desiccant containing bend. The mixture was stirred at room temperature for 2-4 hours, until TLC revealed complete conversion of the reaction. The resulting reaction mixture was evaporated under reduced pressure and purified by column chromatography on silica gel, using EtOAc/Hx mixtures as eluent to afford the corresponding pure products **126a** and **127a,d-e**. Unfortunately product **127d** was unstable (progressively degraded), therefore only the data corresponding to its $^1\text{H-NMR}$ and IR are given.

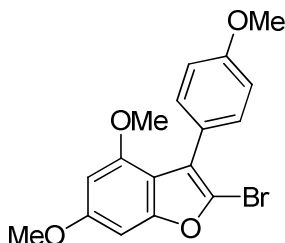
3-bromo-4,6-dimethoxy-2-(4'-methoxyphenyl)benzofuran, 126a:Molecular formula: C₁₇H₁₅BrO₄

Molecular weight: 363.20 g/mol

Aspect: White solid

Yield: 81%

m.p.: 125-126 °C. IR (neat): 2835, 1595, 1151, 1027, 833 cm⁻¹. ¹H-NMR (500 MHz, CDCl₃) δ = 8.02 (d, *J*=8.8 Hz, 2H), 6.98 (d, *J*=8.8 Hz, 2H), 6.64 (d, *J*=1.7 Hz, 1H), 6.33 (d, *J*=1.7 Hz, 1H), 3.92 (s, 3H), 3.86 (s, 3H), 3.85 (s, 3H). ¹³C-NMR (126 MHz, CDCl₃) δ = 159.7, 159.5, 155.3, 154.3, 148.7, 128.2, 122.8, 114.1, 112.2, 95.2, 89.8, 88.3, 55.9, 55.5. Elemental analysis calculated for C₁₇H₁₅BrO₄: C, 56.2; H, 4.2. Found: C, 55.9; H, 3.9.

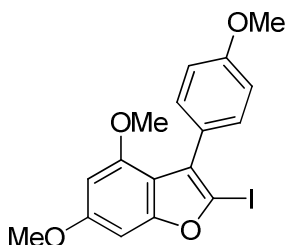
2-bromo-4,6-dimethoxy-3-(4'-methoxyphenyl)benzofuran, 127a:Molecular formula: C₁₇H₁₅BrO₄

Molecular weight: 363.20 g/mol

Aspect: White solid

Yield: 81%

m.p.: 114-115 °C. IR (neat): 2936, 1507, 1098, 816 cm⁻¹. ¹H-NMR (500 MHz, CDCl₃) δ = 7.48 (d, *J*=8.6 Hz, 2H), 6.96 (d, *J*=8.6 Hz, 2H), 6.63 (d, *J*=1.2 Hz, 1H), 6.32 (d, *J*=1.1 Hz, 1H), 3.87 (s, 3H), 3.85 (s, 3H), 3.72 (s, 3H). ¹³C-NMR (126 MHz, CDCl₃) δ = 159.2, 159.1, 157.3, 153.9, 131.7, 123.7, 122.9, 120.4, 113.3, 111.5, 95.1, 88.2, 56.0, 55.6, 55.4. Elemental analysis calculated for C₁₇H₁₅BrO₄: C, 56.2; H, 4.2. Found: C, 56.0; H, 4.0.

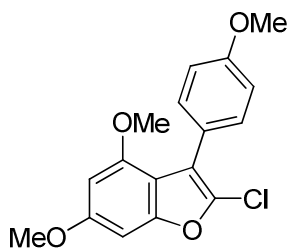
2-iodo-4,6-dimethoxy-3-(4'-methoxyphenyl)benzofuran, 127d (unstable product):Molecular formula: C₁₇H₁₅IO₄

Molecular weight: 410.20 g/mol

Aspect: Yellow oil

Yield: 41%

IR (neat): 2932, 1593, 1145, 1090, 813 cm⁻¹. ¹H-NMR (500 MHz, CDCl₃) δ = 7.47 (d, *J*=8.5 Hz, 2H), 6.99 (d, *J*=8.5 Hz, 2H), 6.68 (d, *J*=1.2 Hz, 1H), 6.32 (d, *J*=1.1 Hz, 1H), 3.90 (s, 3H), 3.87 (s, 3H), 3.73 (s, 3H).

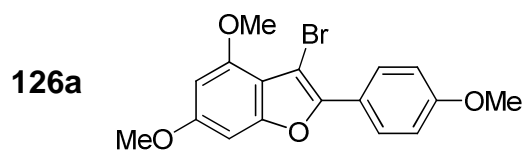
2-chloro-4,6-dimethoxy-3-(4'-methoxyphenyl)benzofuran, 127e:Molecular formula: C₁₇H₁₅ClO₄

Molecular weight: 318.75 g/mol

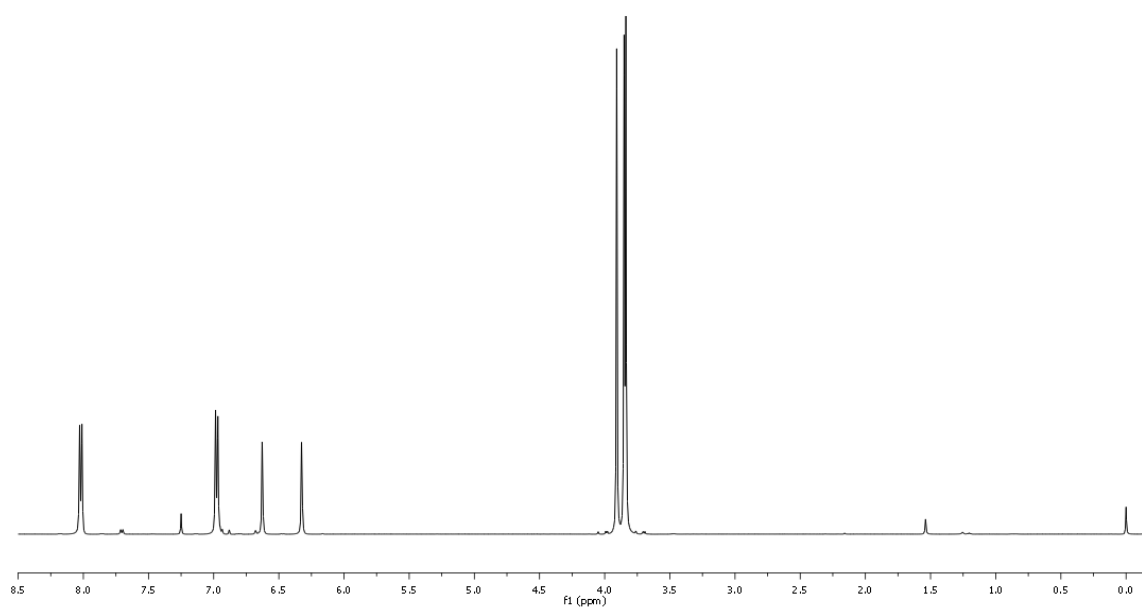
Aspect: White solid

Yield: 86%

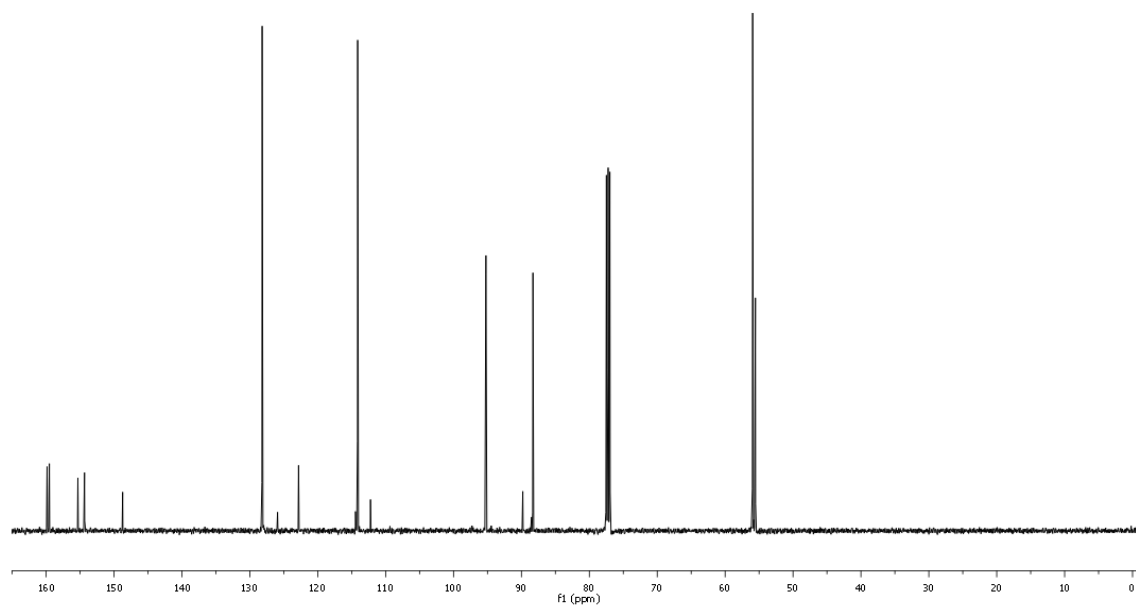
m.p.: 133-134 °C. IR (neat): 2937, 1510, 1101, 817 cm⁻¹. ¹H-NMR (500 MHz, CDCl₃) δ = 7.47 (d, *J*=8.6 Hz, 2H), 6.94 (d, *J*=8.7 Hz, 2H), 6.61 (d, *J*=1.7 Hz, 1H), 6.32 (d, *J*=1.6 Hz, 1H), 3.85 (s, 3H), 3.83 (s, 3H), 3.72 (s, 3H). ¹³C-NMR (126 MHz, CDCl₃) δ = 159.1, 155.3, 154.1, 134.7, 131.6, 123.2, 116.1, 113.3, 111.2, 95.2, 88.2, 55.9, 55.6, 55.4. Elemental analysis calculated for C₁₇H₁₅ClO₄: C, 64.1; H, 4.7. Found: C, 63.8; H, 5.0.

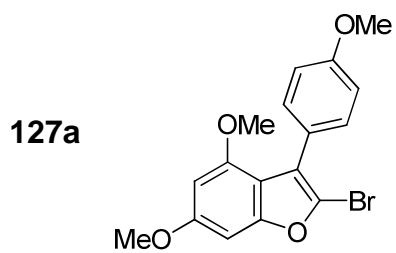


$^1\text{H-NMR}$ (CDCl_3)

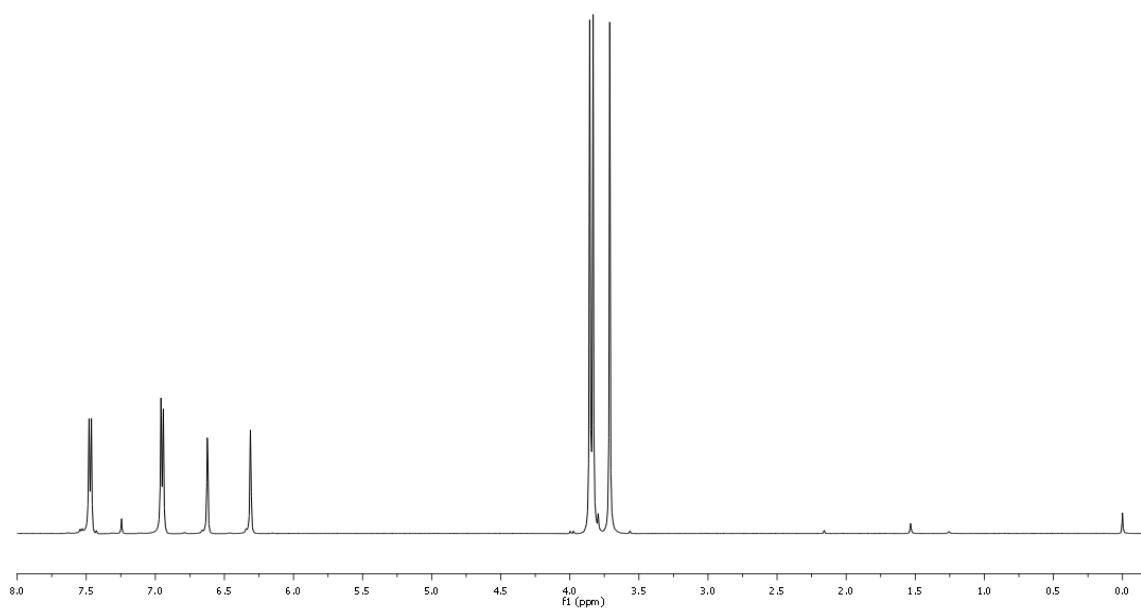


$^{13}\text{C-NMR}$ (CDCl_3)

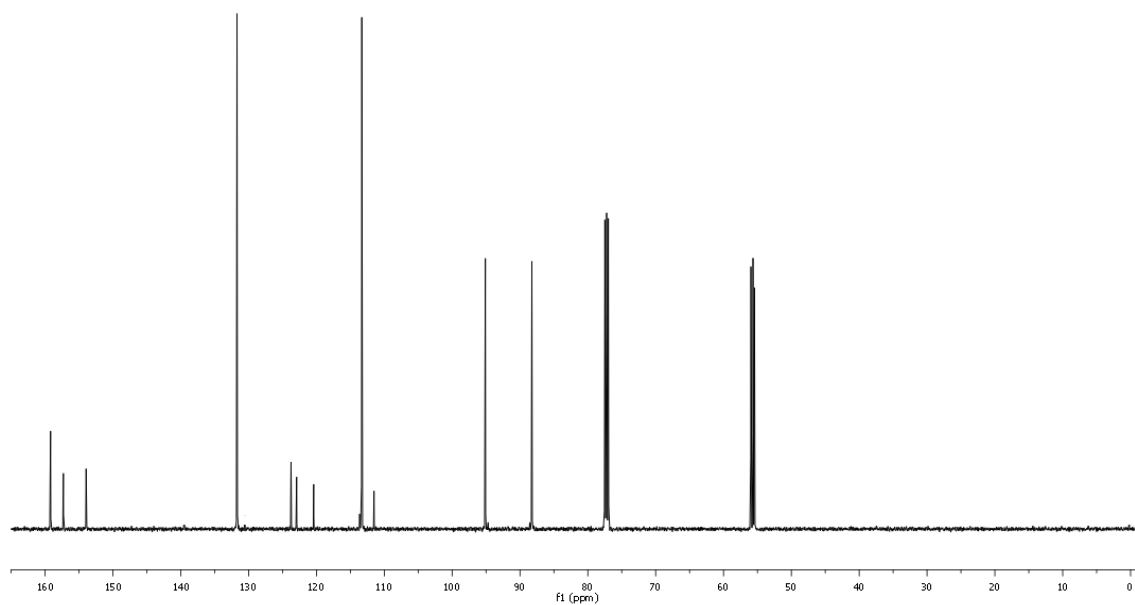


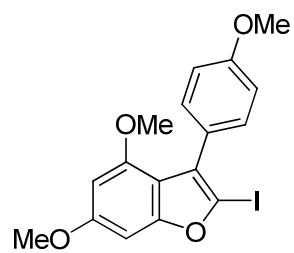
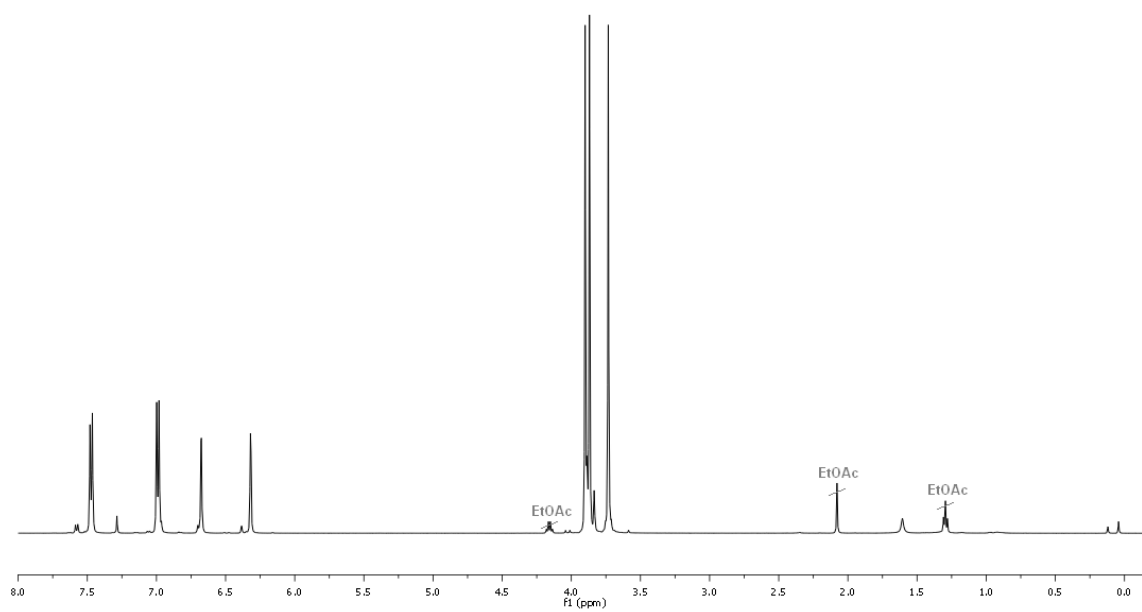


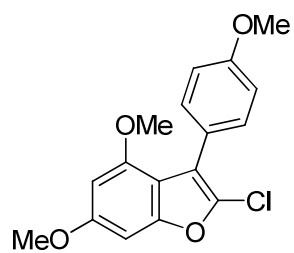
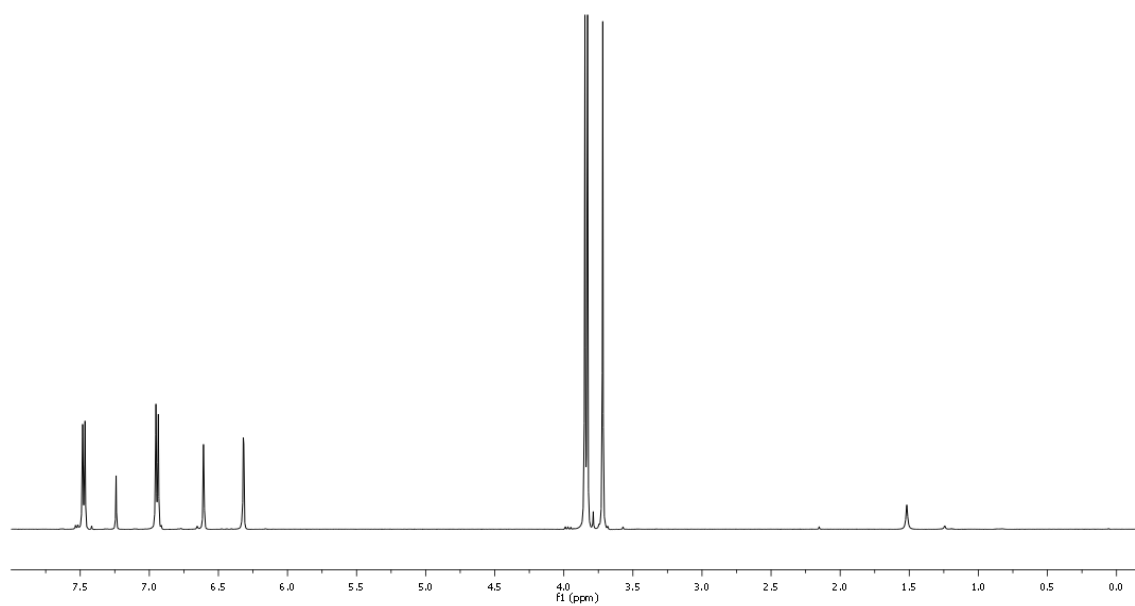
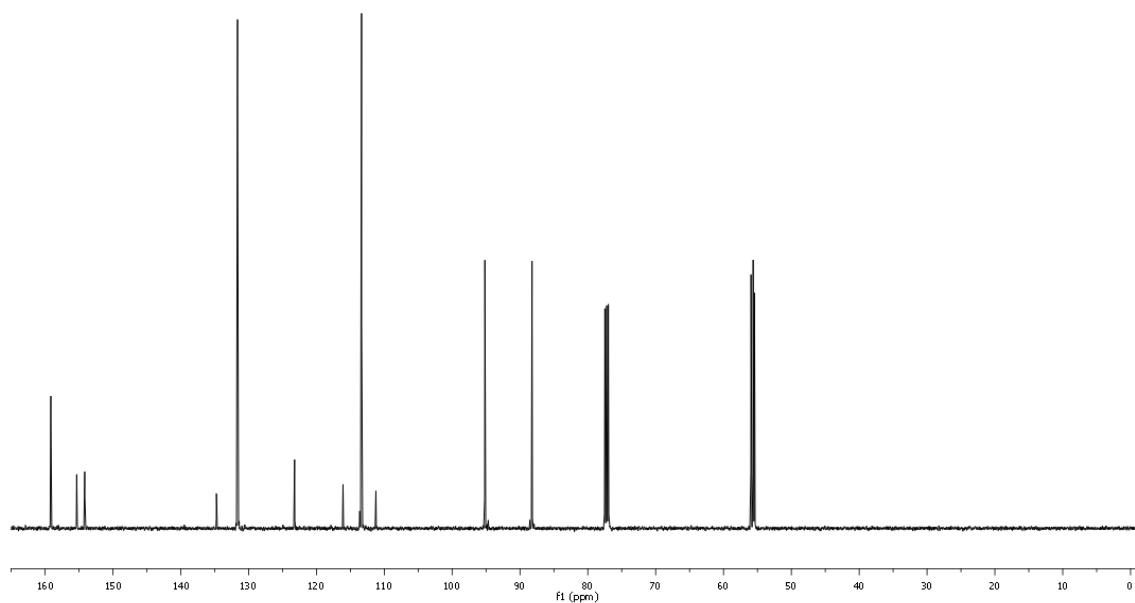
$^1\text{H-NMR}$ (CDCl_3)



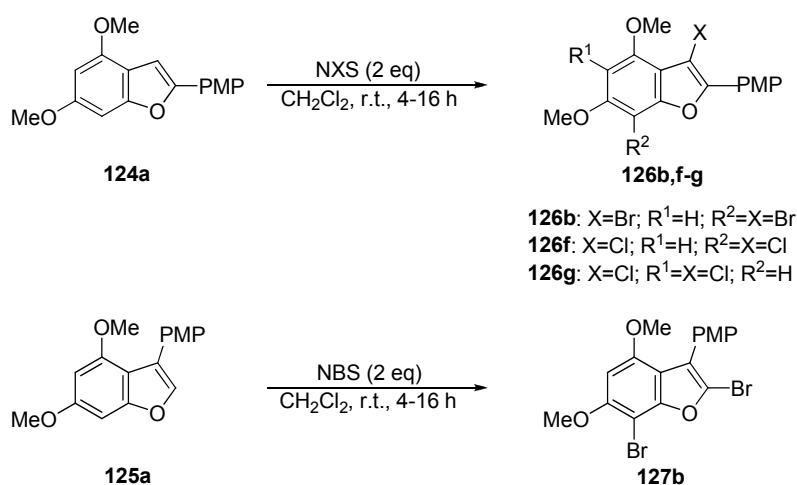
$^{13}\text{C-NMR}$ (CDCl_3)



127d $^1\text{H-NMR}$ (CDCl_3)

127e¹H-NMR (CDCl₃)¹³C-NMR (CDCl₃)

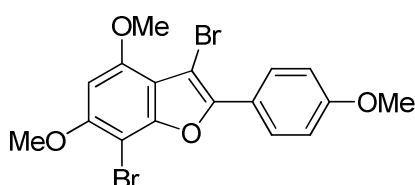
5.3.2. Procedure for the dihalogenation of 2-aryl benzo[*b*]furan 124a and 3-aryl benzo[*b*]furan 125a with NXS leading to products 126b,f-g and 127b



Scheme 5.9. Preparation of dihalogenated 2-aryl and 3-aryl benzo[*b*]furans **126b,f-g** and **127b** from benzo[*b*]furans **124a** and **125a**.

A solution of benzo[*b*]furan **124a** or **125a** (0.440 mmol) in 6.6 ml of CH₂Cl₂ and a solution of NXS (0.880 mmol, 2 eq) in 6.6 ml of CH₂Cl₂ were separately prepared by stirring the mixtures in round bottom flasks until total solution of the solids. The solution of the benzo[*b*]furan was then dropwise added over the solution of NXS and the round bottom flask was capped with a silica gel desiccant containing bend. The mixture was stirred at room temperature for 7-48 hours, until TLC revealed complete conversion of the reaction. The resulting reaction mixture was evaporated under reduced pressure and purified by column chromatography on silica gel, using EtOAc/Hx mixtures as eluent to afford the corresponding pure products **126b,f-g** and **127b**. Compound **127b** decomposes rather than melt upon heating.

3,7-dibromo-4,6-dimethoxy-2-(4'-methoxyphenyl)benzofuran, 126b:



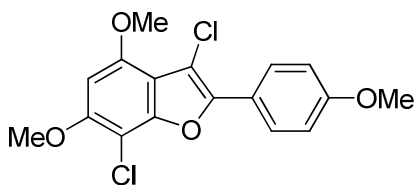
Molecular formula: C₁₇H₁₄Br₂O₄

Molecular weight: 442.10 g/mol

Aspect: White solid

Yield: 89%

m.p.: 141-142 °C. IR (neat): 2834, 1612, 1212, 1128, 823 cm⁻¹. ¹H-NMR (500 MHz, CDCl₃) δ = 8.07 (d, *J*=8.6 Hz, 2H), 6.98 (d, *J*=8.6 Hz, 2H), 6.37 (s, 1H), 3.94 (s, 3H), 3.93 (s, 3H), 3.85 (s, 3H). ¹³C-NMR (126 MHz, CDCl₃) δ = 160.1, 155.1, 153.4, 152.1, 149.7, 128.4, 122.2, 114.1, 113.2, 92.7, 89.7, 85.2, 57.4, 56.2, 55.5. Elemental analysis calculated for C₁₇H₁₄Br₂O₄: C, 46.2; H, 3.2. Found: C, 45.9; H, 3.1.

3,7-dichloro-4,6-dimethoxy-2-(4'-methoxyphenyl)benzofuran, 126f:Molecular formula: C₁₇H₁₄Cl₂O₄

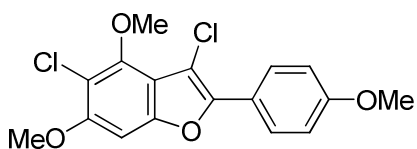
Molecular weight: 353.20 g/mol

Aspect: White solid

Yield: 57% of isolated regioisomer

(71% global yield, 4:1 ratio of regioisomers)

m.p.: 138-139 °C. IR (neat): 2838, 1509, 1132, 821 cm⁻¹. ¹H-NMR (500 MHz, CDCl₃) δ = 8.03 (d, *J*=8.9 Hz, 2H), 6.99 (d, *J*=8.9 Hz, 2H), 6.38 (s, 1H), 3.95 (s, 3H), 3.93 (s, 3H), 3.85 (s, 3H). ¹³C-NMR (126 MHz, CDCl₃) δ = 160.0, 154.2, 152.4, 150.3, 148.5, 127.8, 122.0, 114.2, 112.3, 105.5, 98.0, 92.7, 57.4, 56.3, 55.5. Elemental analysis calculated for C₁₇H₁₄Cl₂O₄: C, 57.8; H, 4.0. Found: C, 57.8; H, 4.0.

3,5-dichloro-4,6-dimethoxy-2-(4'-methoxyphenyl)benzofuran, 126g:Molecular formula: C₁₇H₁₄Cl₂O₄

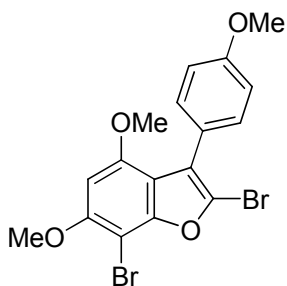
Molecular weight: 353.20 g/mol

Aspect: White solid

Yield: 14% of isolated regioisomer

(71% global yield, 4:1 ratio of regioisomers)

m.p.: 182-183 °C. IR (neat): 2943, 1504, 1243, 1093, 815 cm⁻¹. ¹H-NMR (500 MHz, CDCl₃) δ = 8.00 (d, *J*=8.8 Hz, 2H), 7.01 (d, *J*=8.8 Hz, 2H), 6.90 (s, 1H), 4.01 (s, 3H), 3.95 (s, 3H), 3.87 (s, 3H). ¹³C-NMR (126 MHz, CDCl₃) δ = 160.2, 154.5, 152.5, 149.9, 148.9, 127.9, 122.0, 115.6, 114.3, 113.3, 104.6, 92.3, 62.8, 57.0, 55.6. Elemental analysis calculated for C₁₇H₁₄Cl₂O₄: C, 57.8; H, 4.0. Found: C, 57.5; H, 3.7.

2,7-dibromo-4,6-dimethoxy-3-(4'-methoxyphenyl)benzofuran, 127b:

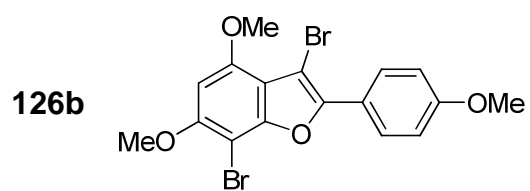
Molecular formula: C₁₇H₁₄Br₂O₄

Molecular weight: 442.10 g/mol

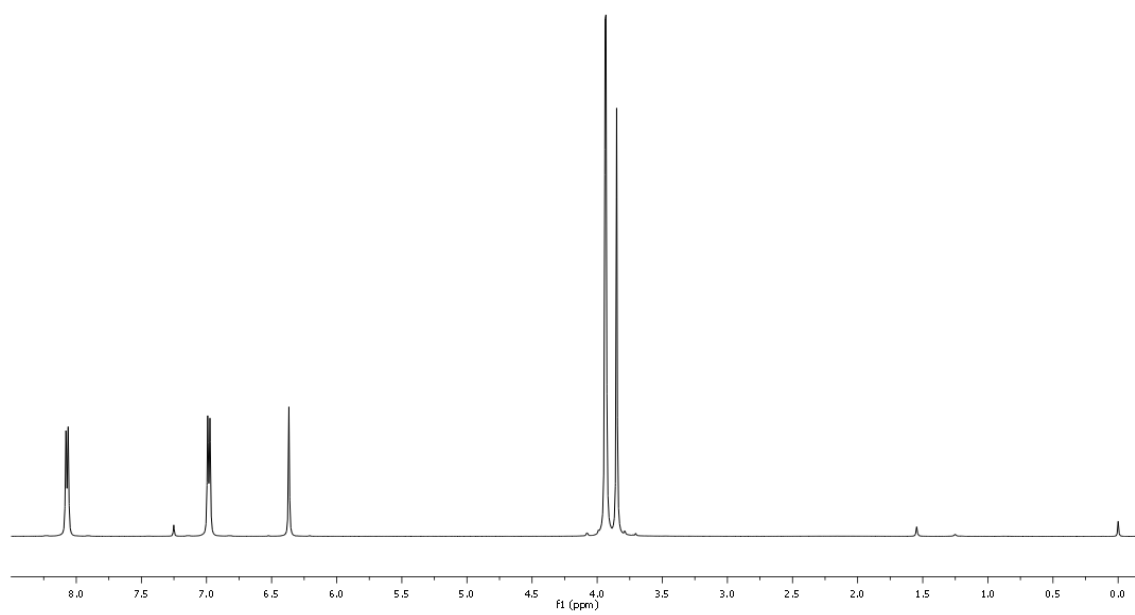
Aspect: White solid

Yield: 68%

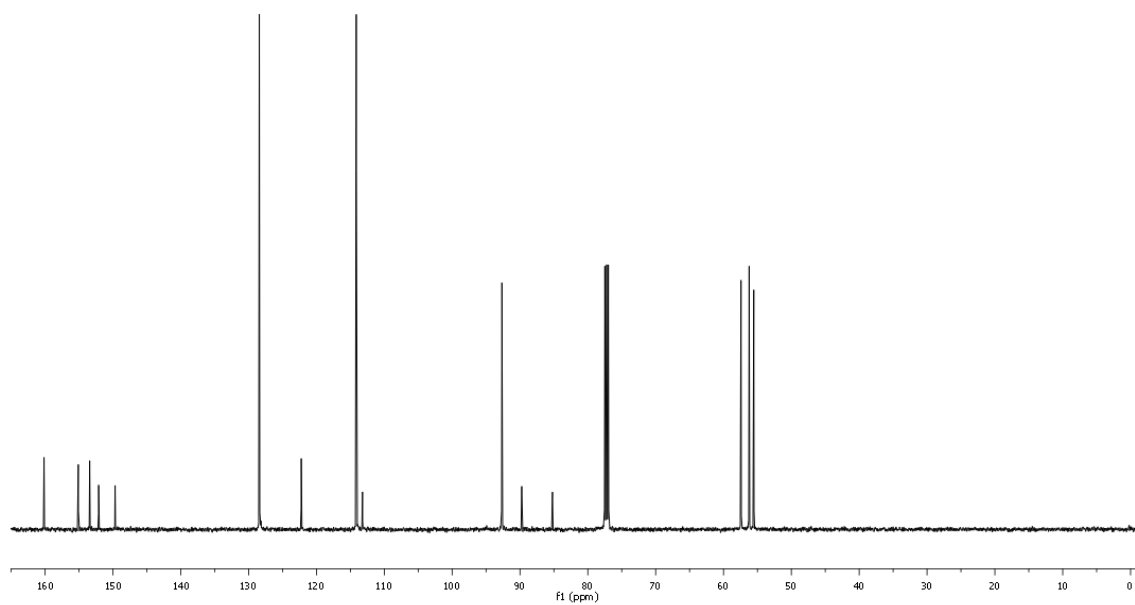
m.p.: 166 °C (dec.). IR (neat): 2930, 1506, 1109, 818 cm⁻¹. ¹H-NMR (500 MHz, CDCl₃) δ = 7.44 (d, *J*=8.6 Hz, 2H), 6.95 (d, *J*=8.6 Hz, 2H), 6.38 (s, 1H), 3.95 (s, 3H), 3.86 (s, 3H), 3.74 (s, 3H). ¹³C-NMR (126 MHz, CDCl₃) δ = 159.1, 154.7, 154.1, 152.8, 131.4, 124.1, 123.0, 120.9, 113.2, 112.4, 92.5, 85.0, 57.2, 55.8, 55.2. Elemental analysis calculated for C₁₇H₁₄Br₂O₄: C, 46.2; H, 3.2. Found: C, 46.1; H, 3.0.

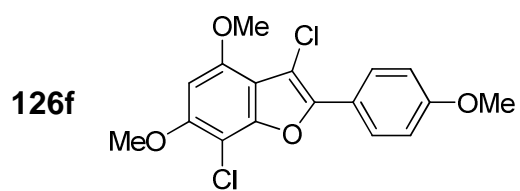


$^1\text{H-NMR}$ (CDCl_3)

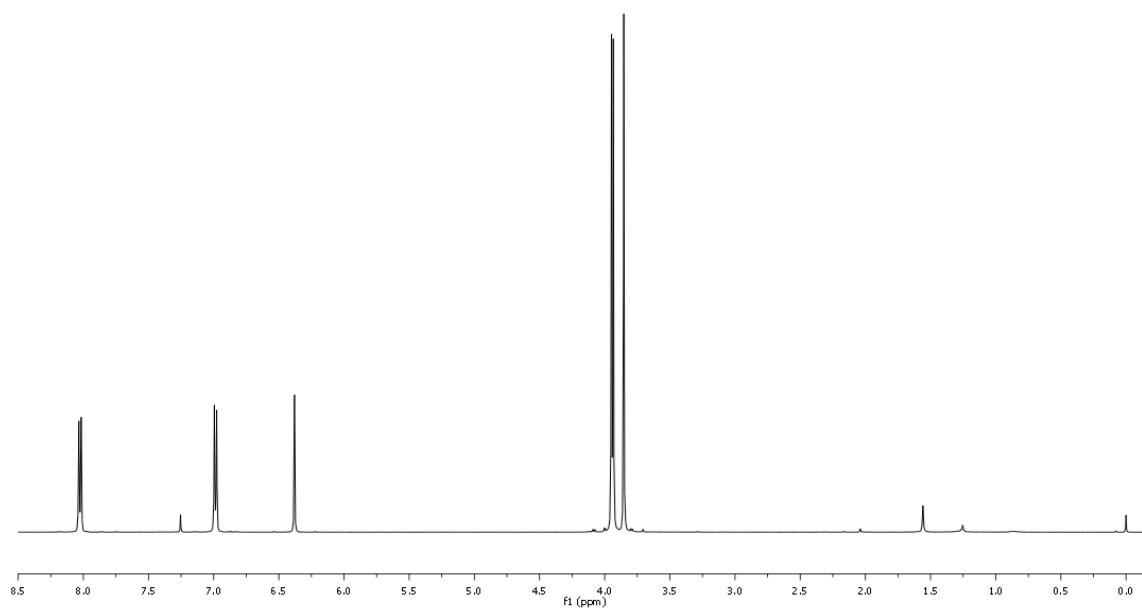


$^{13}\text{C-NMR}$ (CDCl_3)

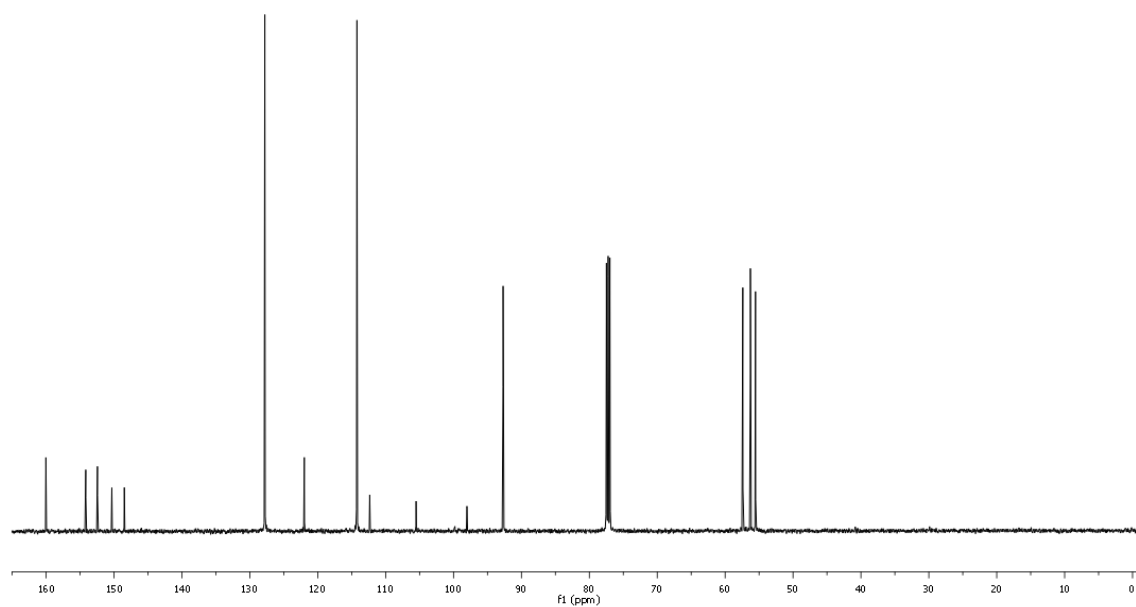


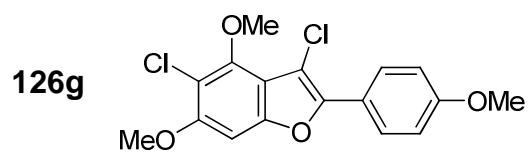


$^1\text{H-NMR}$ (CDCl_3)

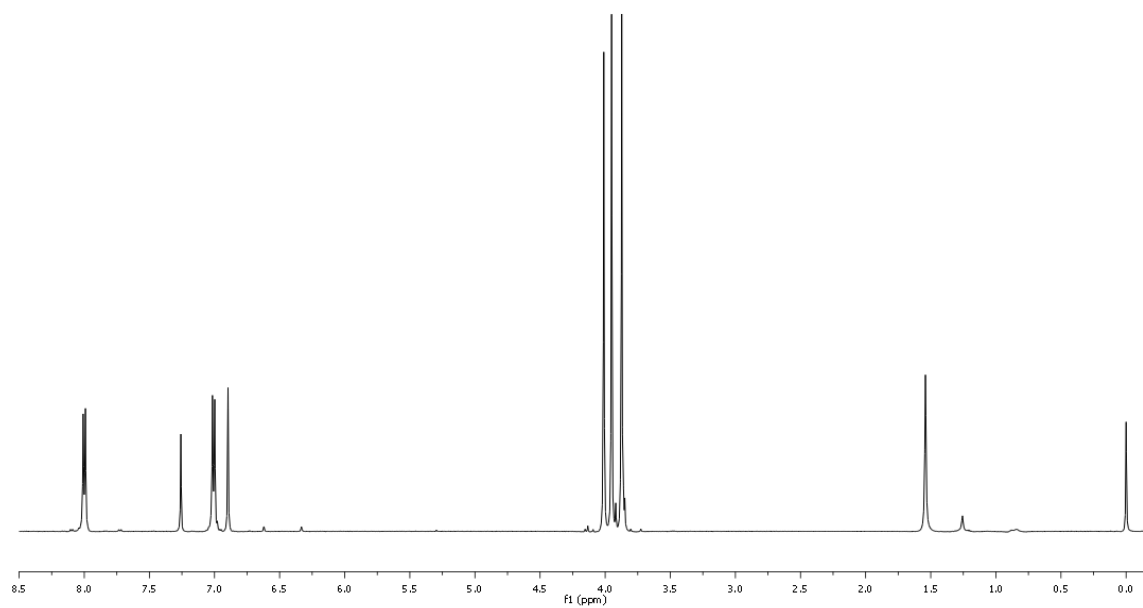


$^{13}\text{C-NMR}$ (CDCl_3)

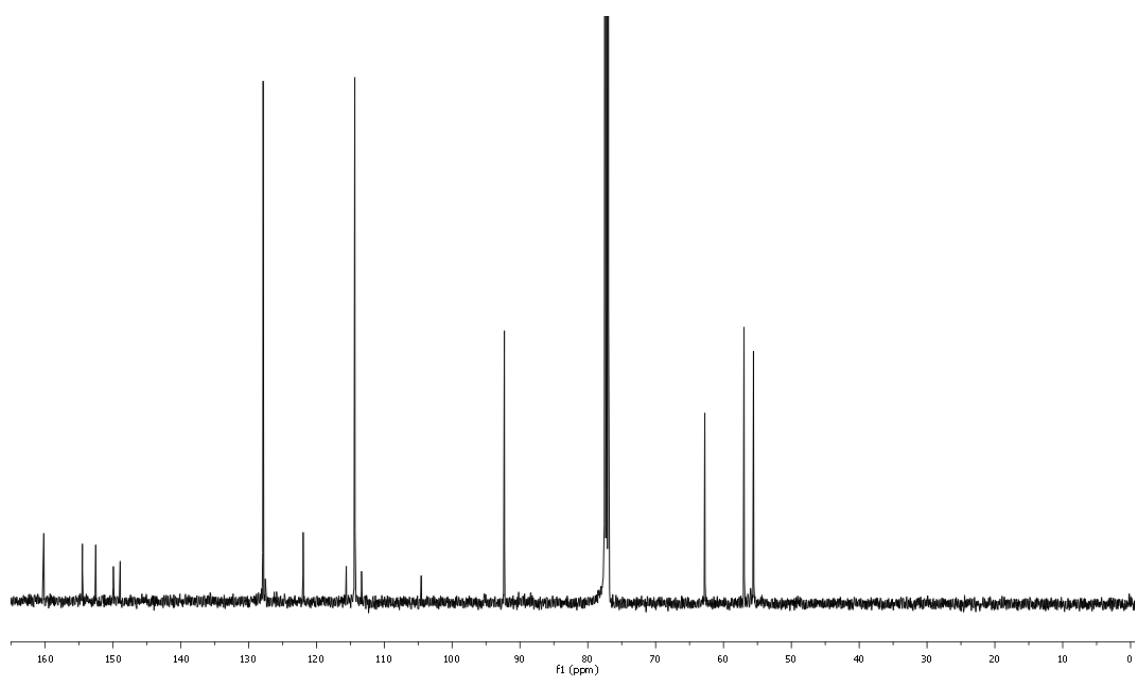


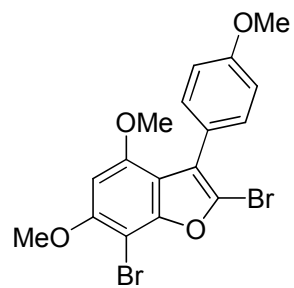
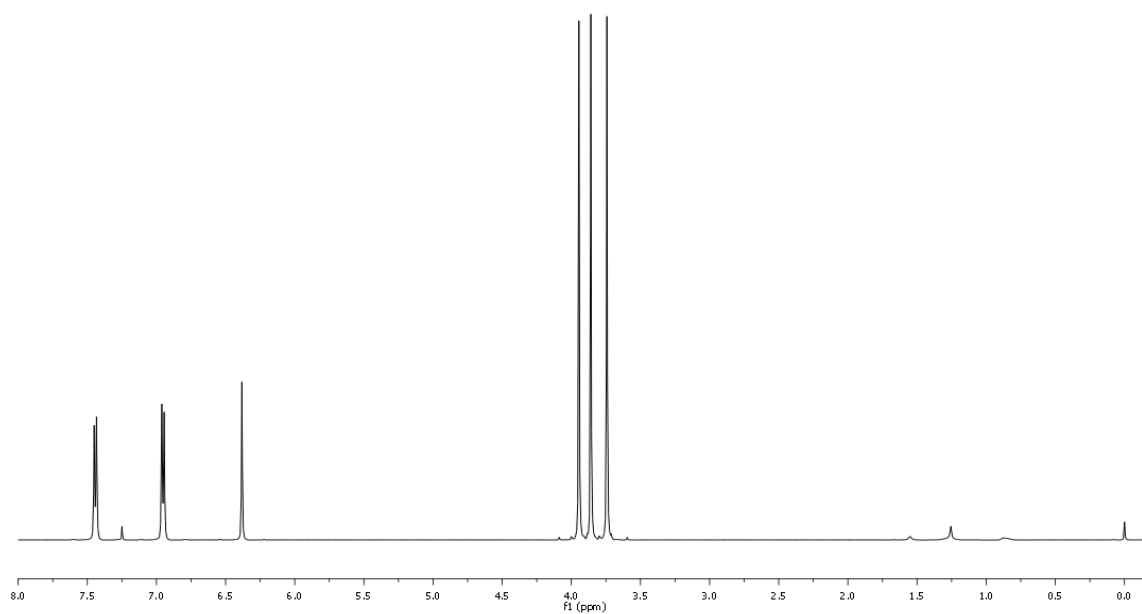
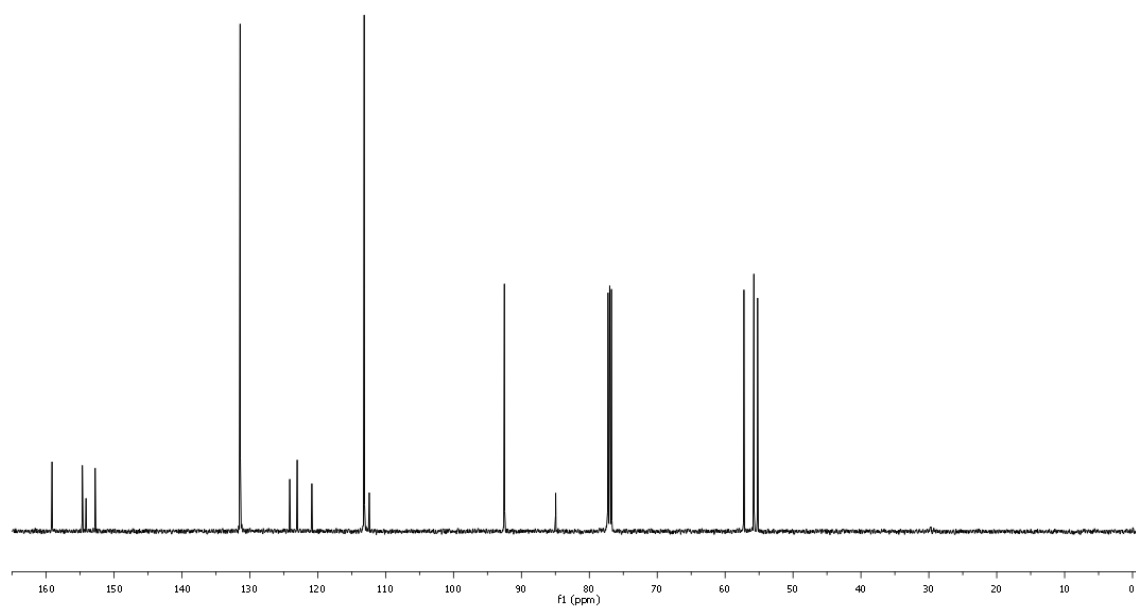


$^1\text{H-NMR}$ (CDCl_3)

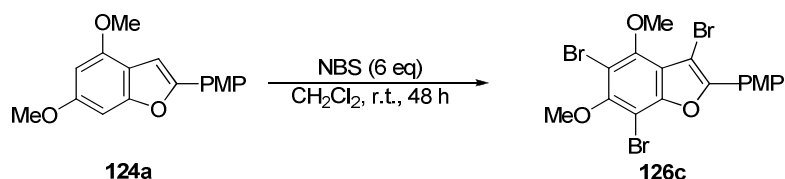


$^{13}\text{C-NMR}$ (CDCl_3)



127b¹H-NMR (CDCl₃)¹³C-NMR (CDCl₃)

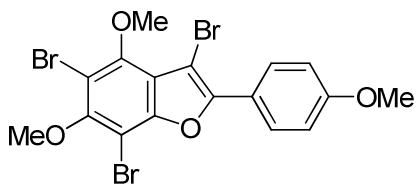
5.3.3. Procedure for the tribromination of 2-aryl benzo[*b*]furan **124a** with NBS leading to product **126c**



Scheme 5.10. Preparation of tribrominated 2-aryl benzo[*b*]furan **126c** from benzo[*b*]furan **124a**.

A solution of benzo[*b*]furan **124a** (0.176 mmol) in 3.0 ml of CH_2Cl_2 and a solution of NBS (1.056 mmol, 6 eq) in 3.0 ml of CH_2Cl_2 were separately prepared by stirring the mixtures in round bottom flasks until total solution of the solids. The solution of the benzo[*b*]furan was then dropwise added over the solution of NBS and the round bottom flask was capped with a silica gel desiccant containing bend. The mixture was stirred at room temperature and monitored by TLC for 48 hours, after which TLC revealed no further conversion of the reaction. The resulting reaction mixture was evaporated under reduced pressure and purified by column chromatography on silica gel, using EtOAc/Hx mixtures as eluent to afford the corresponding pure product **126c**.

3,5,7-tribromo-4,6-dimethoxy-2-(4'-methoxyphenyl)benzofuran, **126c**:



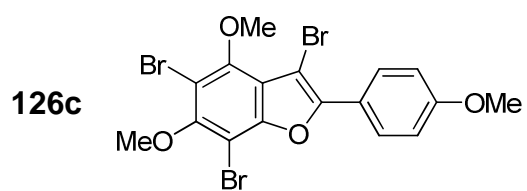
Molecular formula: $\text{C}_{17}\text{H}_{13}\text{Br}_3\text{O}_4$

Molecular weight: 520.99 g/mol

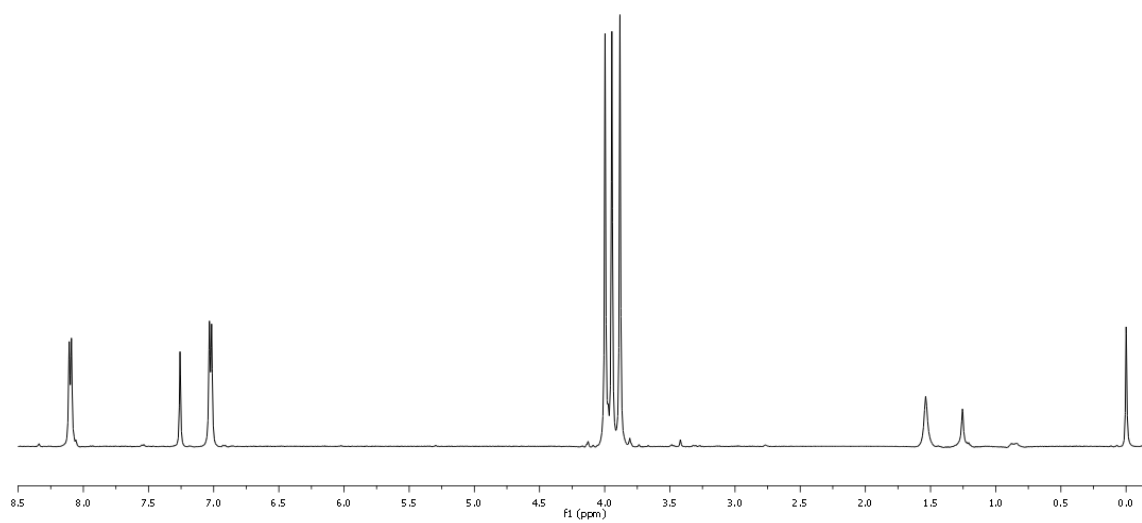
Aspect: White solid

Yield: 30%

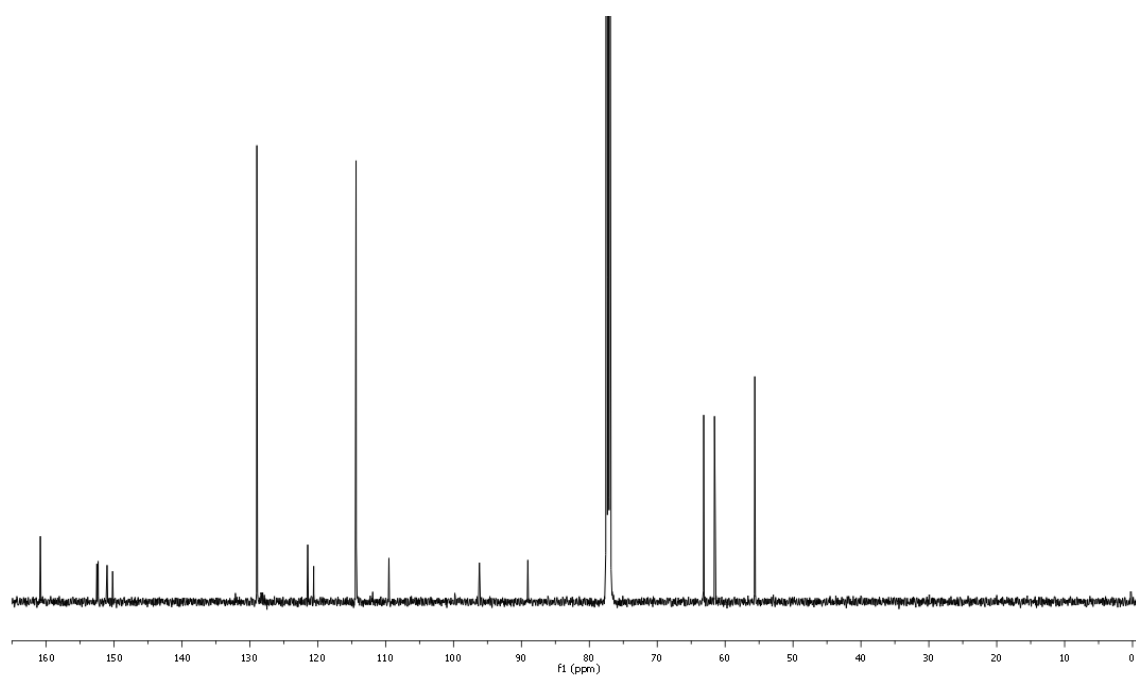
m.p.: 129-130 °C. IR (neat): 2942, 1501, 1087, 824 cm^{-1} . $^1\text{H-NMR}$ (500 MHz, CDCl_3) δ = 8.10 (d, $J=8.4$ Hz, 2H), 7.02 (d, $J=8.4$ Hz, 2H), 4.00 (s, 3H), 3.95 (s, 3H), 3.88 (s, 3H). $^{13}\text{C-NMR}$ (126 MHz, CDCl_3) δ = 160.8, 152.5, 152.3, 151.0, 150.2, 129.0, 121.5, 120.6, 114.4, 109.5, 96.2, 89.0, 63.2, 61.6, 55.6. Elemental analysis calculated for $\text{C}_{17}\text{H}_{13}\text{Br}_3\text{O}_4$: C, 39.2; H, 2.5. Found: C, 38.9; H, 2.2.



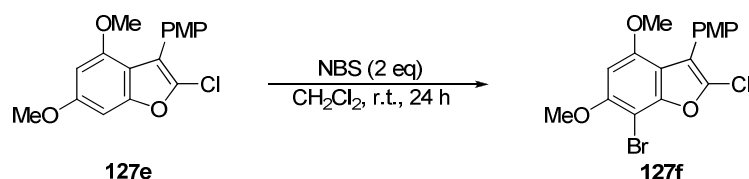
$^1\text{H-NMR}$ (CDCl_3)



$^{13}\text{C-NMR}$ (CDCl_3)



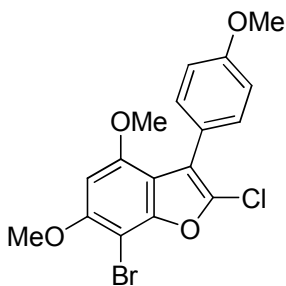
5.3.4. Procedure for the monobromination of 3-aryl-2-chlorobenzo[*b*]furan **127e** with NBS leading to product **127f**



Scheme 5.11. Preparation of dihalogenated 3-aryl benzo[*b*]furan **127f** from benzo[*b*]furan **127e**.

A solution of benzo[*b*]furan **127e** (0.125 mmol) in 2.0 ml of CH_2Cl_2 and a solution of NBS (0.125 mmol, 1 eq) in 1.0 ml of CH_2Cl_2 were separately prepared by stirring the mixtures in round bottom flasks until total solution of the solids. The solution of the benzo[*b*]furan was then dropwise added over the solution of NBS and the round bottom flask was capped with a silica gel desiccant containing bend. The mixture was stirred at room temperature for 8 hours. Then another equivalent of NBS (0.125 mmol) was added and the mixture was stirred until TLC revealed complete conversion of the reaction. The resulting reaction mixture was evaporated under reduced pressure and purified by column chromatography on silica gel, using EtOAc/Hx mixtures as eluent to afford pure product **127f**.

7-bromo-2-chloro-4,6-dimethoxy-3-(4'-methoxyphenyl)benzofuran, **127f**:



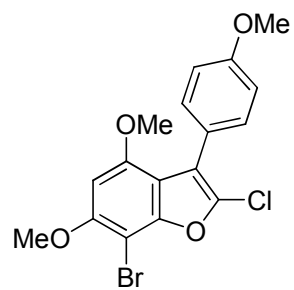
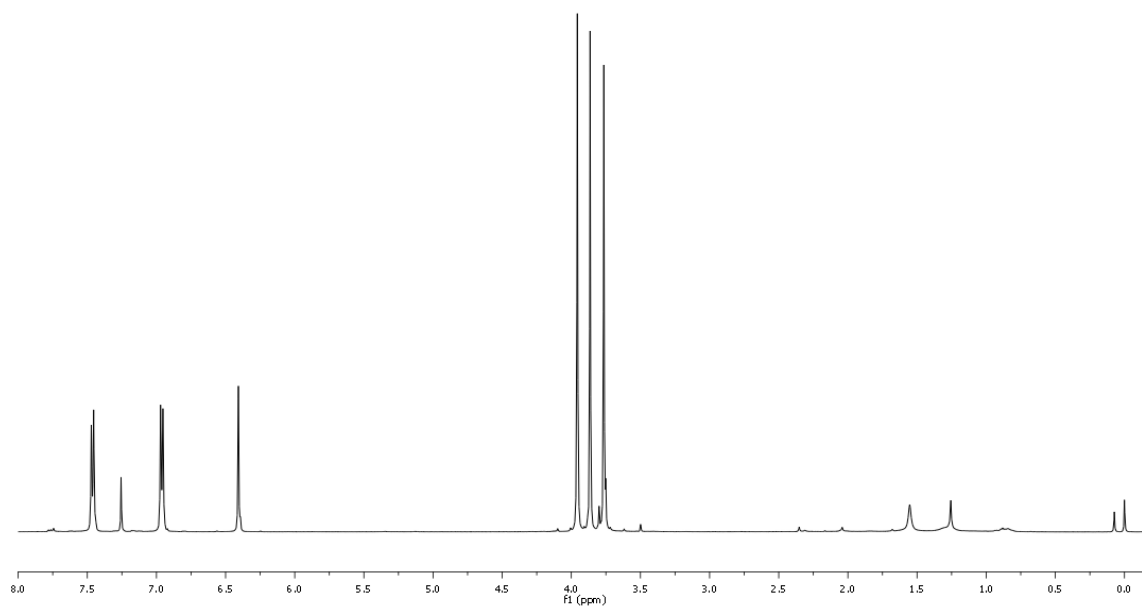
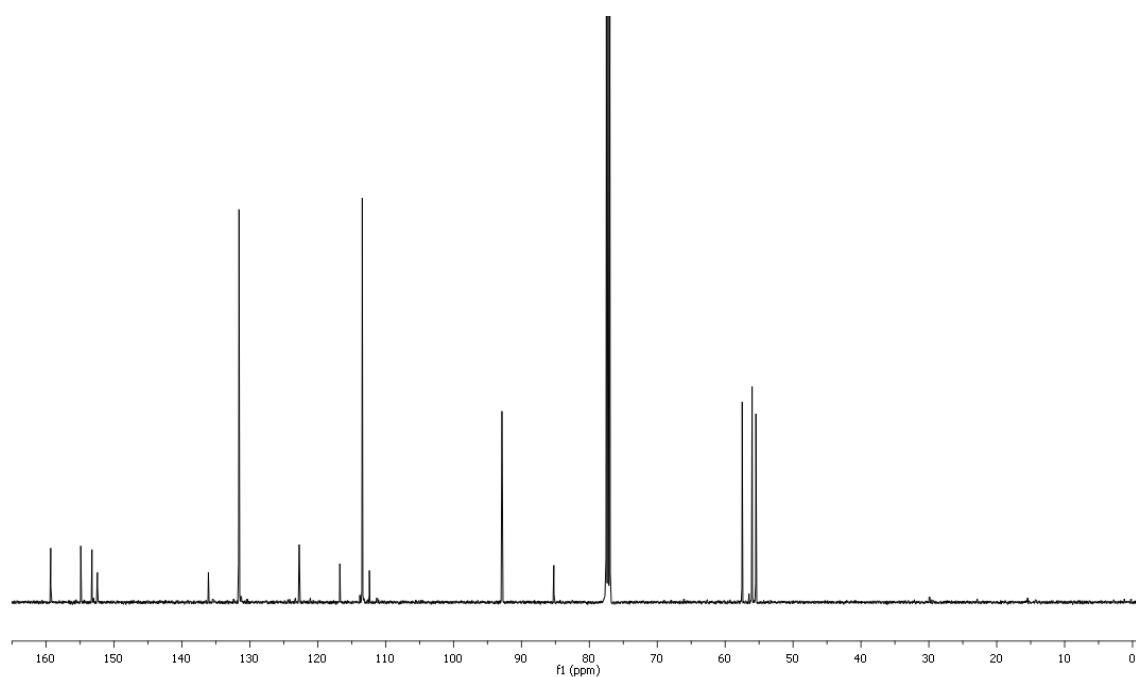
Molecular formula: $\text{C}_{17}\text{H}_{14}\text{BrClO}_4$

Molecular weight: 397.65 g/mol

Aspect: White solid

Yield: 44%

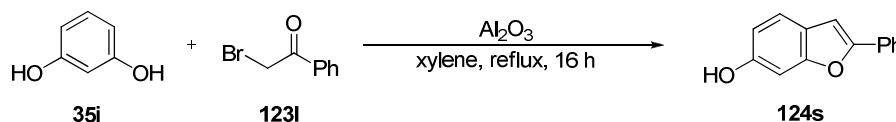
m.p.: 170-171 °C. IR (neat): 2948, 1509, 1115, 818 cm^{-1} . $^1\text{H-NMR}$ (500 MHz, CDCl_3) δ = 7.46 (d, $J=8.5$ Hz, 2H), 6.96 (d, $J=8.6$ Hz, 2H), 6.41 (s, 1H), 3.96 (s, 3H), 3.86 (s, 3H), 3.76 (s, 3H). $^{13}\text{C-NMR}$ (126 MHz, CDCl_3) δ = 159.3, 154.9, 153.2, 152.4, 136.1, 131.6, 122.7, 116.7, 113.4, 112.4, 92.9, 85.2, 57.5, 56.0, 55.5. Elemental analysis calculated for $\text{C}_{17}\text{H}_{14}\text{BrClO}_4$: C, 51.3; H, 3.6. Found: C, 51.0; H, 3.9.

127f $^1\text{H-NMR}$ (CDCl_3) $^{13}\text{C-NMR}$ (CDCl_3)

5.4. HYPERVALENT IODINE REAGENTS-MEDIATED OXIDATIVE DEAROMATIZATION of 2- and 3-ARYL BENZO[*b*]FURANS **124s** and **125p**

5.4.1. Procedure for the preparation of 2-phenylbenzofuran-6-ol **124s**

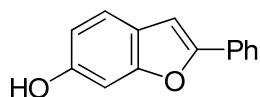
It was prepared following the procedure described in section 5.2.2.



Scheme 5.12. Preparation of 2-phenylbenzofuran-6-ol **124s** from resorcinol **35j** and 2-bromoacetophenone **123I**.

Resorcinol **35j** (15.0 mmol), 2-bromoacetophenone **123I** (21.0 mmol, 1.4 eq), alumina (105.0 mmol, 7 eq) and 60 ml of xylene were placed in a round bottom flask equipped with a reflux condenser. The mixture was heated under reflux for 16 hours. The resulting reaction mixture was left to cool until it reached room temperature. It was then filtered through a Celite pad and evaporated under reduced pressure. The crude obtained this way was purified by column chromatography on silica gel, using EtOAc/Hx mixtures as eluent to afford the pure product **124s**. The alumina (aluminium oxide) employed was neutral (activated, Brockmann I, STD grade, approx. 150 mesh, 58 Å) and the xylene, a mixture of isomers.

2-phenylbenzofuran-6-ol³²⁹, **124s**:



Molecular formula: C₁₄H₁₀O₂

Molecular weight: 210.23 g/mol

Aspect: White-yellow solid

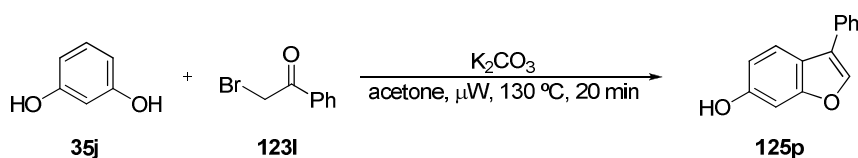
Yield: 36%

¹H-NMR (300 MHz, CDCl₃) δ = 7.81 (d, *J*=7.2 Hz, 2H), 7.45–7.39 (m, 3H), 7.31 (t, *J*=7.4 Hz, 1H), 7.01 (d, *J*=2.0 Hz, 1H), 6.94 (d, *J*=0.8 Hz, 1H), 6.77 (dd, *J*=8.4, 2.2 Hz, 1H), 4.78 (bs, 1H). ¹H-NMR (300 MHz, acetone-*d*₆) δ = 8.52 (s, 1H), 7.86 (d, *J*=7.2 Hz, 2H), 7.49–7.42 (m, 3H), 7.34 (t, *J*=7.4 Hz, 1H), 7.18 (s, 1H), 7.02 (d, *J*=2.0 Hz, 1H), 6.83 (dd, *J*=8.4, 2.1 Hz, 1H).

³²⁹ Commercial product, CAS: 24534-37-0

5.4.2. Procedure for the preparation of 3-phenylbenzofuran-6-ol **125p**

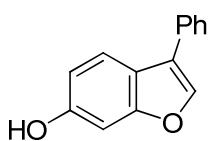
It was obtained as one of the products of the reaction procedure described in section 5.2.3 to prepare, in principle, its open-chain precursor **130p**, which was only obtained in traces amount.



Scheme 5.13. Preparation of 3-phenylbenzofuran-6-ol **125p** from resorcinol **35j** and 2-bromoacetophenone **123I**.

Resorcinol **35j** (7.8 mmol), 2-bromoacetophenone **123I** (7.8 mmol, 1 eq), K₂CO₃ (15.6 mmol, 2 eq) and 6 ml of acetone were placed in a microwave vessel and sealed. The mixture was irradiated with microwaves at 130 °C and 100-400 W for 20 minutes. The resulting mixture was left to cool until it reached room temperature. It was then filtered through a Celite pad and evaporated under reduced pressure. The crude obtained this way was purified by column chromatography on silica gel, using EtOAc/Hx mixtures as eluent to afford the **125p** (as the minor product of the reaction).

3-phenylbenzofuran-6-ol³³⁰, **125p**:



Molecular formula: C₁₄H₁₀O₂

Molecular weight: 210.23 g/mol

Aspect: White-yellow solid

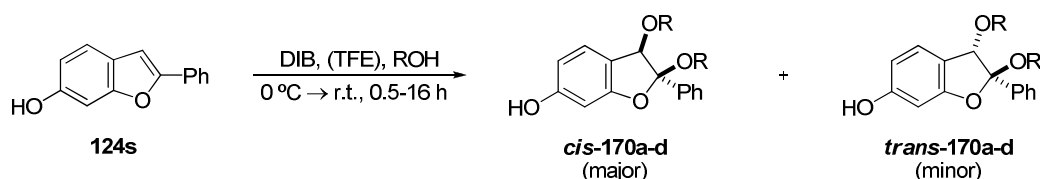
Yield: 27% of isolated product

(95% global yield, 2.5:1 ratio of products **130p**':**125p**)

¹H-NMR (500 MHz, CDCl₃) δ = 7.70–7.57 (m, 4H), 7.45 (t, *J*=7.6 Hz, 2H), 7.35 (t, *J*=7.4 Hz, 1H), 7.02 (d, *J*=2.1 Hz, 1H), 6.84 (dd, *J*=8.5, 2.2 Hz, 1H), 4.85 (bs, 1H). ¹H-NMR (300 MHz, acetone-d₆) δ = 8.56 (s, 1H), 7.97 (s, 1H), 7.77–7.67 (m, 3H), 7.48 (t, *J*=7.5 Hz, 2H), 7.36 (t, *J*=7.4 Hz, 1H), 7.02 (d, *J*=2.1 Hz, 1H), 6.92 (dd, *J*=8.5, 2.2 Hz, 1H).

³³⁰ Commercial product, CAS: 13196-08-2

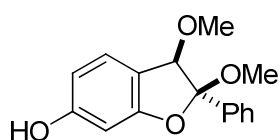
5.4.3. Procedure for the preparation of *cis/trans*-2,3-dialkoxy-2-phenyl-2,3-dihydrobenzofuran-6-ols *cis/trans*-170a-d



Scheme 5.14. Preparation of 2,3-dialkoxy-2-phenyl-2,3-dihydrobenzofuran-6-ols *cis/trans*-170a-d from 2-phenylbenzofuran-6-ol **124s**.

A solution of benzo[*b*]furan **124s** (0.714 mmol) in 15 ml of alcohol and a solution of DIB (0.785 mmol, 1.1 eq) in 5 ml of alcohol (MeOH for **170a**, EtOH for **170b**) or in 5 ml of TFE (for **170c-d**) were separately prepared under inert argon atmosphere by stirring the mixtures in round bottom flasks until total solution of the solids. The solution of **124s** was cooled to 0 °C in an ice-water bath and the solution of DIB was dropwise added over it. The bath was then removed, allowing the reaction slowly reach room temperature. The mixture was stirred for 0.5-16 hours until TLC revealed complete conversion of the reaction. It was then quenched by adding anhydrous NaHCO₃ (1.43 mmol, 2 eq), stirred for 15 more minutes and filtered through a medium flow rate filter paper. The resulting reaction mixture was evaporated under reduced pressure and purified by column chromatography on silica gel, using EtOAc/cyclohexane mixtures as eluent to afford pure products *cis*-**170a-b** and *trans*-**170a-b**, when using MeOH and EtOH as nucleophiles and the corresponding *cis/trans* mixture of products **170c-d** when using ⁿPrOH and ⁿBuOH.

cis-2,3-dimethoxy-2-phenyl-2,3-dihydrobenzofuran-6-ol, *cis*-170a:



Molecular formula: C₁₆H₁₆O₄

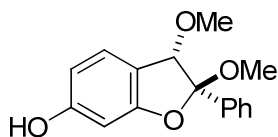
Molecular weight: 272.30 g/mol

Aspect: Yellow oil

Yield: 38% of isolated diastereomer

(43% global yield, 7:1 ratio of diastereomers)

IR (neat): 3338, 2943, 1607, 1078, 956 cm⁻¹. ¹H-NMR (500 MHz, acetone-d₆) δ = 8.59 (s, 1H), 7.50 (d, *J*=7.1 Hz, 2H), 7.40 (t, *J*=7.4 Hz, 2H), 7.35 (t, *J*=7.3 Hz, 1H), 7.10 (d, *J*=8.7 Hz, 1H), 6.50–6.42 (m, 2H), 4.68 (s, 1H), 3.54 (s, 3H), 3.36 (s, 3H). ¹³C-NMR (126 MHz, acetone-d₆) δ = 161.0, 160.5, 142.3, 129.4, 129.3, 127.7, 127.0, 117.8, 113.0, 109.6, 97.9, 88.2, 58.6, 52.3.

***trans*-2,3-dimethoxy-2-phenyl-2,3-dihydrobenzofuran-6-ol, *trans*-170a:**Molecular formula: C₁₆H₁₆O₄

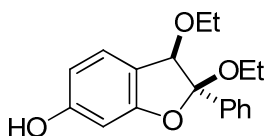
Molecular weight: 272.30 g/mol

Aspect: Yellow oil

Yield: 5% of isolated diastereomer

(43% global yield, 7:1 ratio of diastereomers)

IR (neat): 3326, 2932, 1601, 1073, 967 cm⁻¹. ¹H-NMR (500 MHz, acetone-d₆) δ = 8.60 (s, 1H), 7.57 (d, *J*=6.8 Hz, 2H), 7.46–7.37 (m, 3H), 7.27 (d, *J*=8.0 Hz, 1H), 6.55–6.46 (m, 2H), 4.57 (s, 1H), 3.13 (s, 3H), 2.91 (s, 3H). ¹³C-NMR (101 MHz, acetone-d₆) δ = 161.5, 160.9, 136.6, 129.4, 128.9, 128.7, 128.0, 119.1, 115.5, 109.4, 99.2, 87.1, 55.9, 50.7.

***cis*-2,3-diethoxy-2-phenyl-2,3-dihydrobenzofuran-6-ol, *cis*-170b:**Molecular formula: C₁₈H₂₀O₄

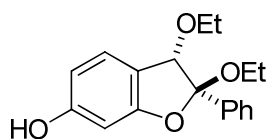
Molecular weight: 300.35 g/mol

Aspect: Yellow oil

Yield: 34% of isolated diastereomer

(42% global yield, 4:1 ratio of diastereomers)

IR (neat): 3270, 2973, 1610, 1094, 957 cm⁻¹. ¹H-NMR (500 MHz, acetone-d₆) δ = 8.58 (s, 1H), 7.50 (d, *J*=7.6 Hz, 2H), 7.39 (t, *J*=7.5 Hz, 2H), 7.34 (t, *J*=6.6 Hz, 1H), 7.08 (d, *J*=8.0 Hz, 1H), 6.46–6.38 (m, 2H), 4.76 (s, 1H), 3.96–3.87 (m, 1H), 3.81–3.74 (m, 1H), 3.68–3.60 (m, 1H), 3.55–3.47 (m, 1H), 1.24–1.14 (m, 6H). ¹³C-NMR (126 MHz, acetone-d₆) δ = 160.9, 160.5, 143.2, 129.3, 129.1, 127.5, 126.8, 118.2, 112.8, 109.5, 97.8, 86.9, 66.7, 60.8, 16.1, 15.9.

***trans*-2,3-diethoxy-2-phenyl-2,3-dihydrobenzofuran-6-ol, *trans*-170b:**Molecular formula: C₁₈H₂₀O₄

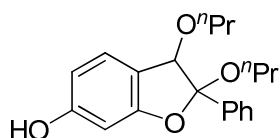
Molecular weight: 300.35 g/mol

Aspect: Yellow oil

Yield: 8% of isolated diastereomer

(42% global yield, 4:1 ratio of diastereomers)

IR (neat): 3209, 2969, 1604, 1066, 960 cm⁻¹. ¹H-NMR (500 MHz, acetone-d₆) δ = 8.55 (s, 1H), 7.58 (d, *J*=7.1 Hz, 2H), 7.45–7.35 (m, 3H), 7.22 (d, *J*=8.4 Hz, 1H), 6.48 (d, *J*=5.2 Hz, 2H), 4.64 (s, 1H), 3.62–3.51 (m, 1H), 3.42–3.34 (m, 1H), 3.29–3.20 (m, 1H), 3.03–2.94 (m, 1H), 1.06 (t, *J*=7.0 Hz, 3H), 0.65 (t, *J*=6.9 Hz, 3H). ¹³C-NMR (126 MHz, acetone-d₆) δ = 161.9, 161.2, 138.0, 129.7, 129.2, 129.0, 128.3, 120.1, 116.2, 109.8, 99.4, 86.7, 65.1, 60.1, 16.2, 15.8.

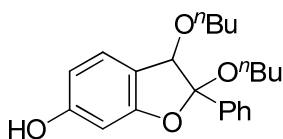
2-phenyl-2,3-dipropoxy-2,3-dihydrobenzofuran-6-ol, 170c (*cis/trans* mixture):Molecular formula: C₂₀H₂₄O₄

Molecular weight: 328.40 g/mol

Aspect: Yellow oil

Yield: 38%

The data corresponding to the 3.5:1 mixture of isomers obtained by column chromatography are shown. ¹H-NMR (500 MHz, acetone-d₆, major isomer) δ = 8.55 (s, 1H), 7.51 (d, *J*=7.3 Hz, 2H), 7.40 (m, 3H), 7.08 (d, *J*=7.8 Hz, 1H), 6.44 (m, 2H), 4.76 (s, 1H), 3.90–3.83 (m, 1H), 3.73–3.66 (m, 1H), 3.60–3.53 (m, 1H), 3.44–3.37 (m, 1H), 1.67–1.55 (m, 4H), 0.94 (m, 6H). ¹H-NMR (500 MHz, acetone-d₆, minor isomer) δ = 8.54 (s, 1H), 7.58 (d, *J*=7.1 Hz, 2H), 7.34 (m, 3H), 7.23 (d, *J*=8.4 Hz, 1H), 6.49 (m, 2H), 4.65 (s, 1H), 3.51–3.44 (m, 1H), 3.31–3.24 (m, 1H), 3.24–3.17 (m, 1H), 2.97–2.88 (m, 1H), 1.50–1.41 (m, 2H), 1.12–1.04 (m, 2H), 0.78 (t, *J*=7.4 Hz, 3H), 0.49 (t, *J*=7.4 Hz, 3H). HRMS calculated for C₂₀H₂₅O₄ [M+H]⁺: 329.1753. Found: 329.1765. Unfortunately our attempts to separate the two isomers met with no success and the mixture was not further characterized.

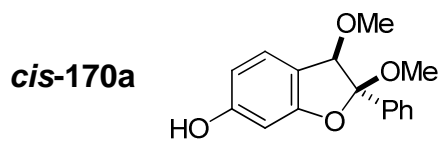
2,3-dibutoxy-2-phenyl-2,3-dihydrobenzofuran-6-ol, 170d (*cis/trans* mixture):Molecular formula: C₂₂H₂₈O₄

Molecular weight: 356.46 g/mol

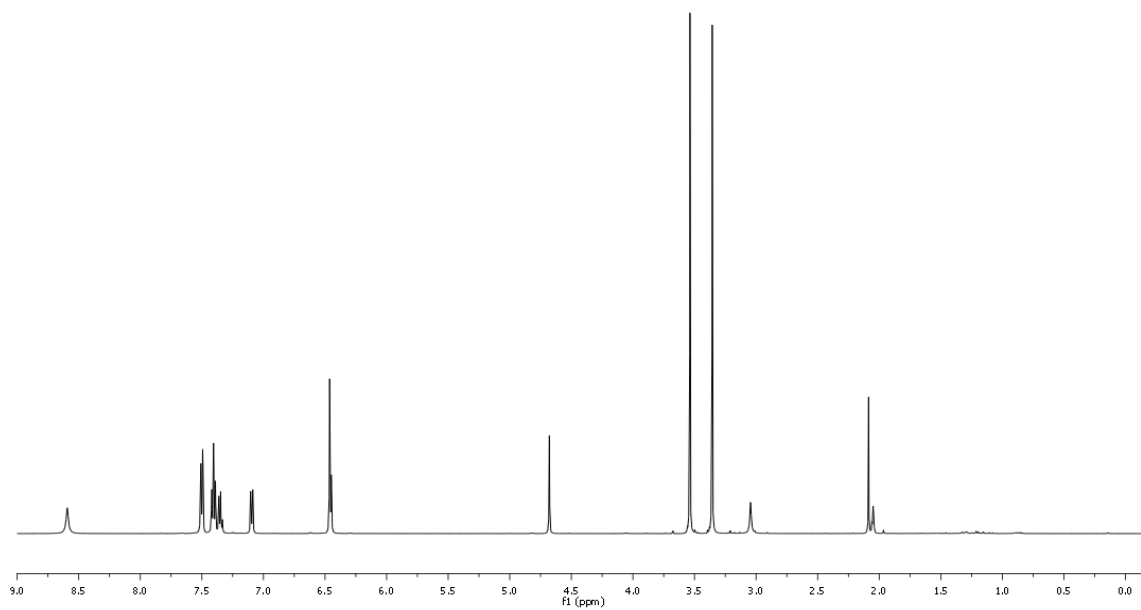
Aspect: Yellow oil

Yield: 24%

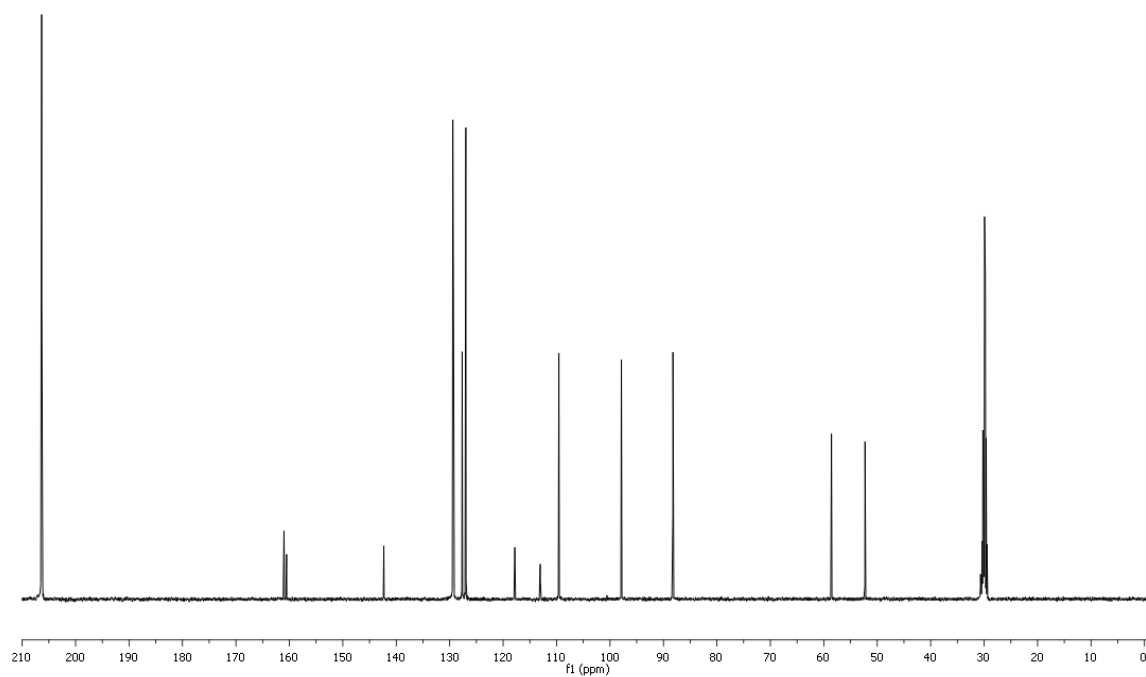
The data corresponding to the 2.8:1 mixture of isomers obtained by column chromatography are shown. ¹H-NMR (500 MHz, acetone-d₆, major isomer) δ = 8.53 (s, 1H), 7.51 (d, *J*=7.3 Hz, 2H), 7.44–7.36 (m, 3H), 7.08 (d, *J*=7.8 Hz, 1H), 6.46–6.40 (m, 2H), 4.75 (s, 1H), 3.94–3.88 (m, 1H), 3.78–3.69 (m, 1H), 3.64–3.57 (m, 1H), 3.48–3.40 (m, 1H), 1.63–1.53 (m, 4H), 1.48–1.36 (m, 4H), 0.91 (m, 6H). ¹H-NMR (500 MHz, acetone-d₆, minor isomer) δ = 8.52 (s, 1H), 7.58 (d, *J*=7.0 Hz, 2H), 7.34 (m, 3H), 7.22 (d, *J*=8.5 Hz, 1H), 6.48 (m, 2H), 4.64 (s, 1H), 3.55–3.49 (m, 1H), 3.35–3.29 (m, 1H), 3.27–3.21 (m, 1H), 3.02–2.95 (m, 1H), 1.28–1.19 (m, 4H), 1.09–1.01 (m, 4H), 0.80 (t, *J*=7.4 Hz, 3H), 0.64 (t, *J*=7.3 Hz, 3H). HRMS calculated for C₂₂H₂₉O₄ [M+H]⁺: 357.2066. Found: 357.2063. Unfortunately our attempts to separate the two isomers met with no success and the mixture was not further characterized.

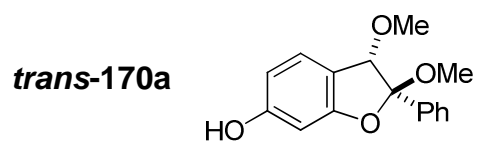


$^1\text{H-NMR}$ (acetone- d_6)

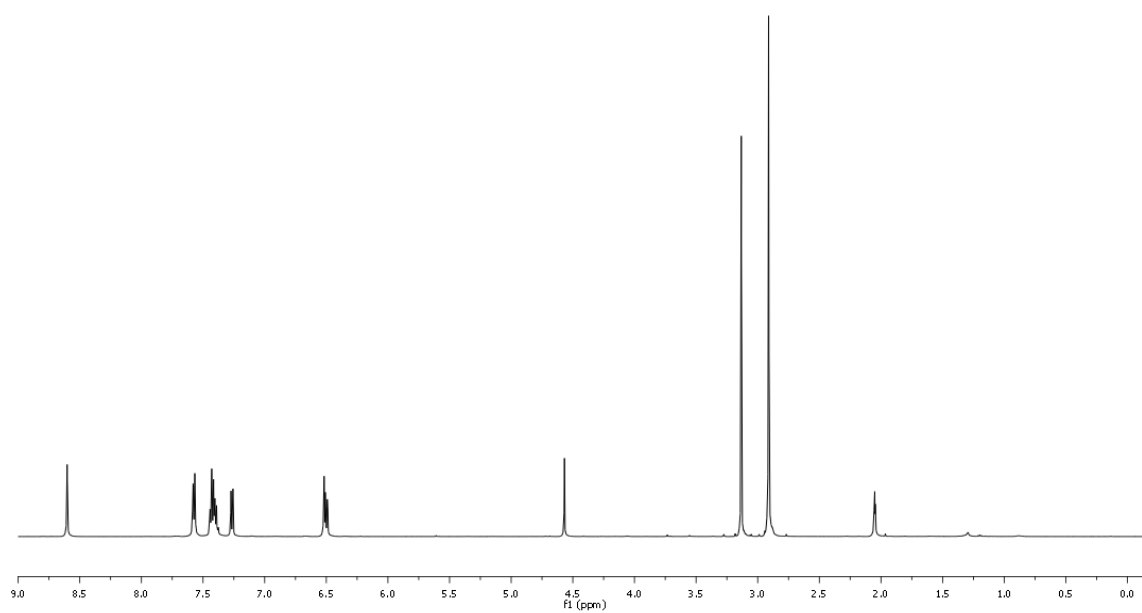


$^{13}\text{C-NMR}$ (acetone- d_6)

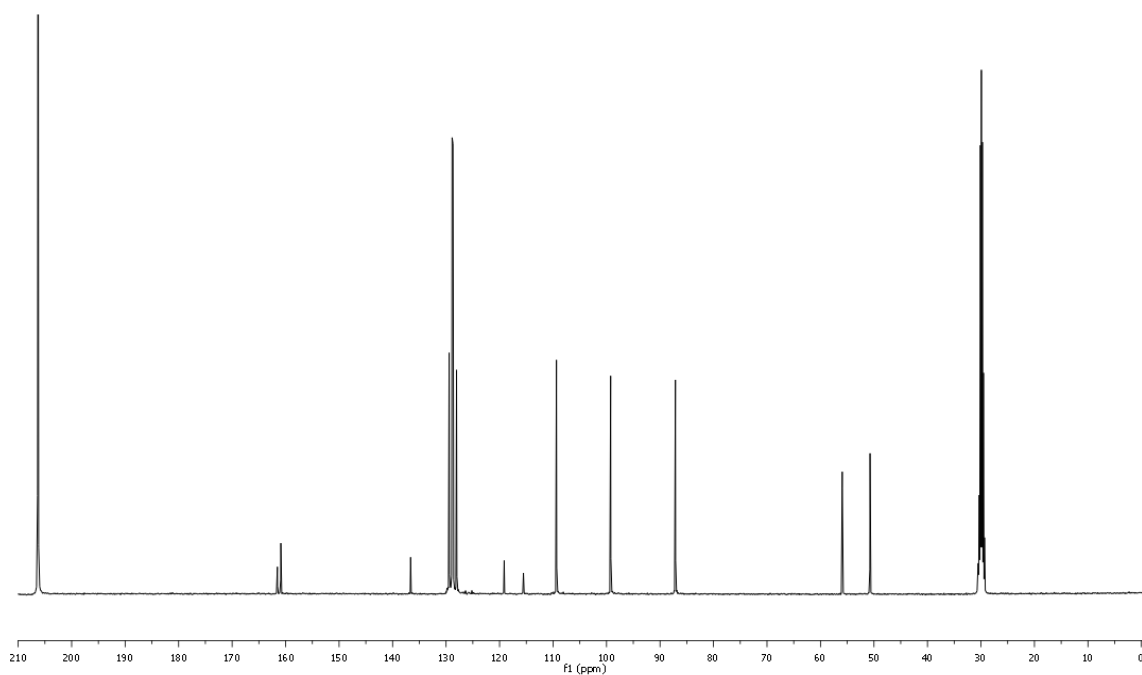


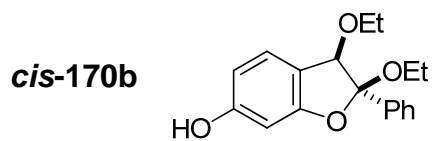


$^1\text{H-NMR}$ (acetone- d_6)

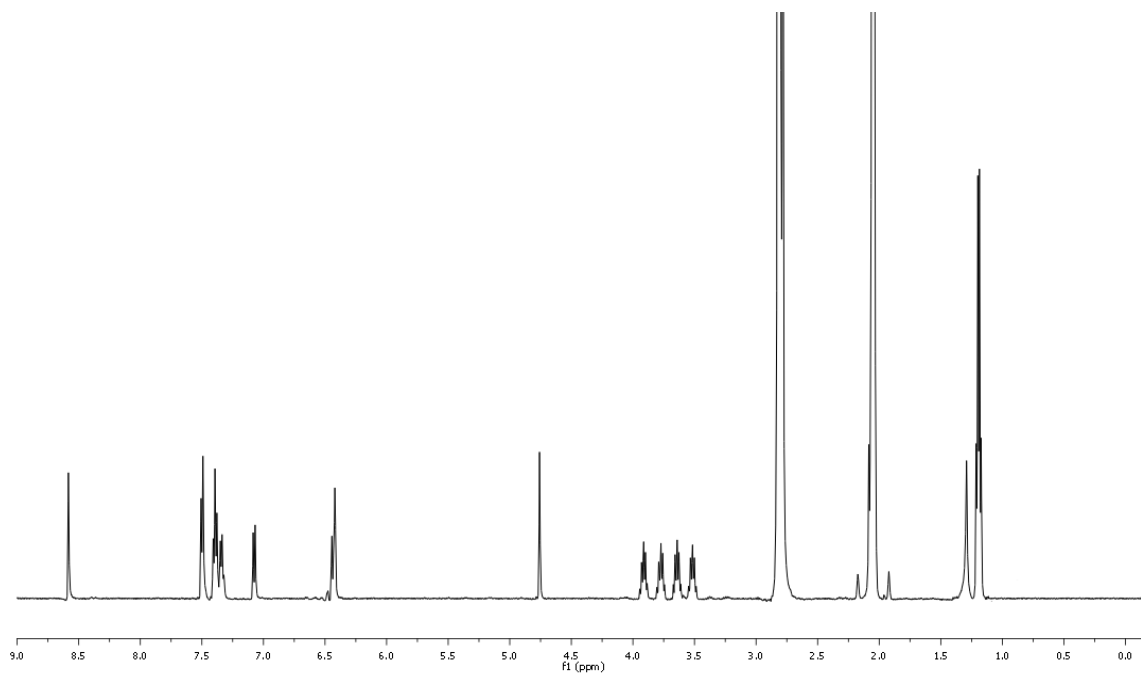


$^{13}\text{C-NMR}$ (acetone- d_6)

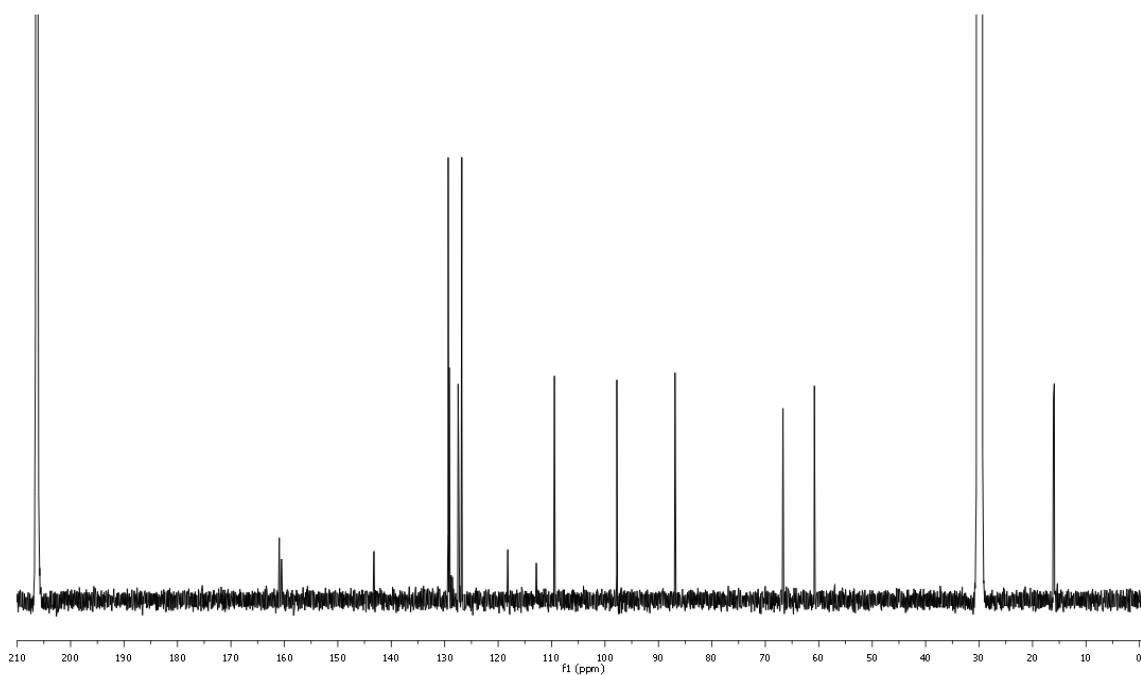


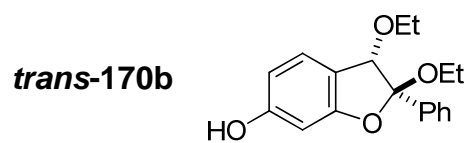


$^1\text{H-NMR}$ (acetone- d_6)

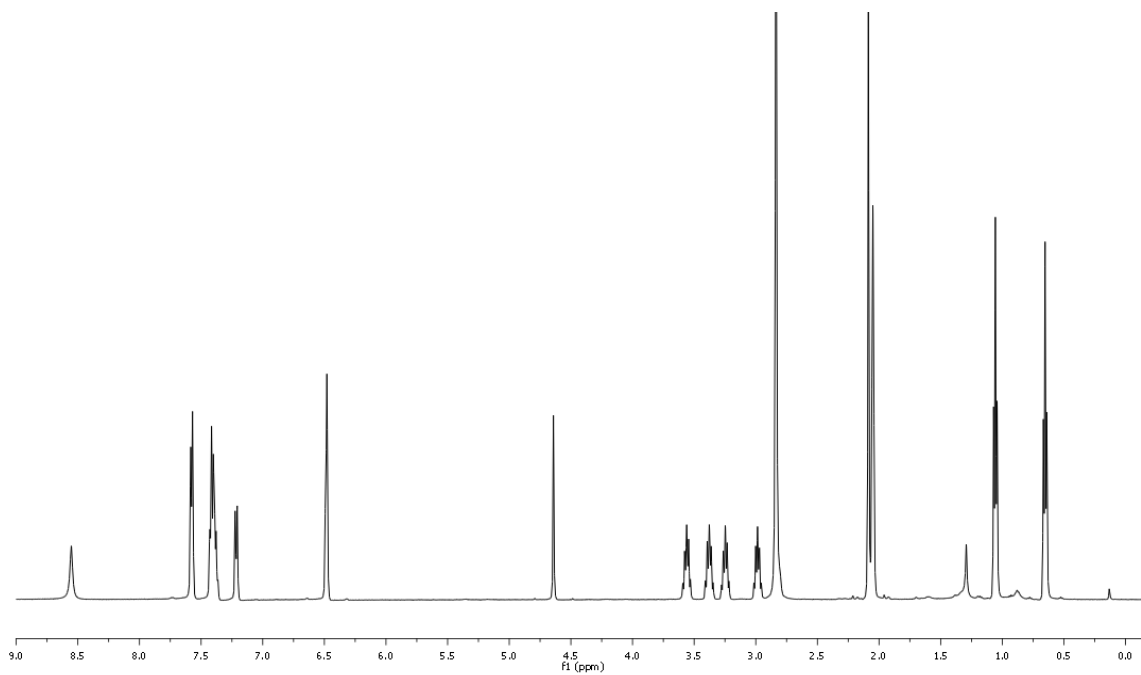


$^{13}\text{C-NMR}$ (acetone- d_6)

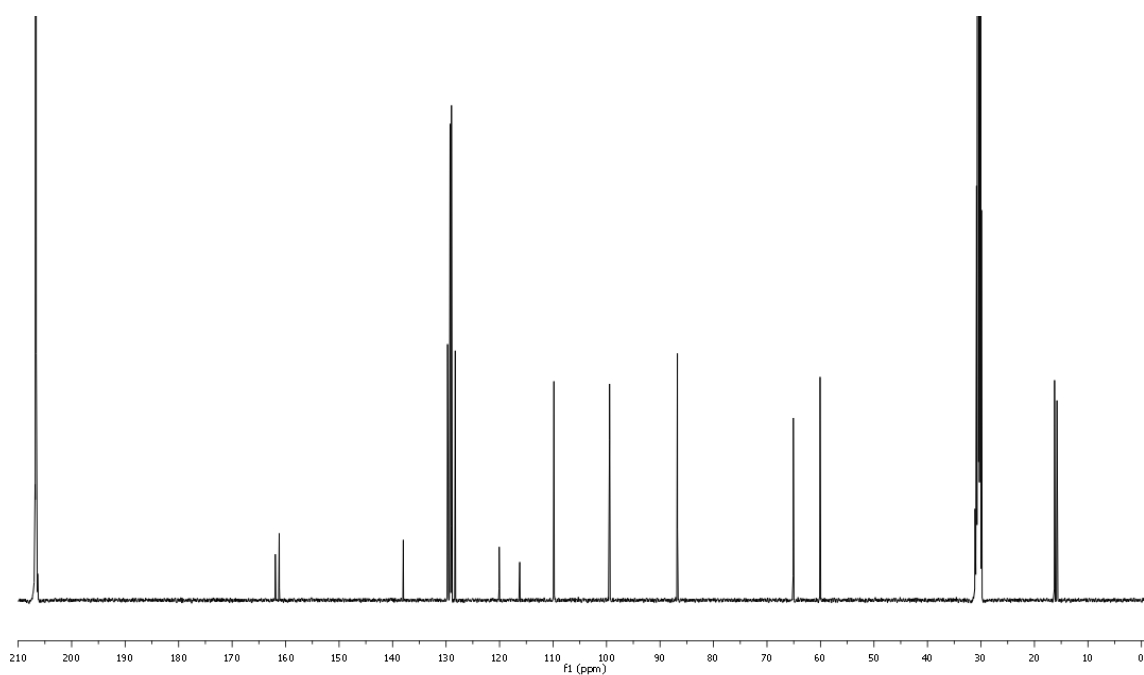


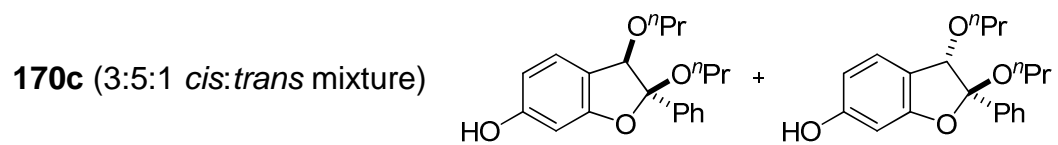


$^1\text{H-NMR}$ (acetone- d_6)

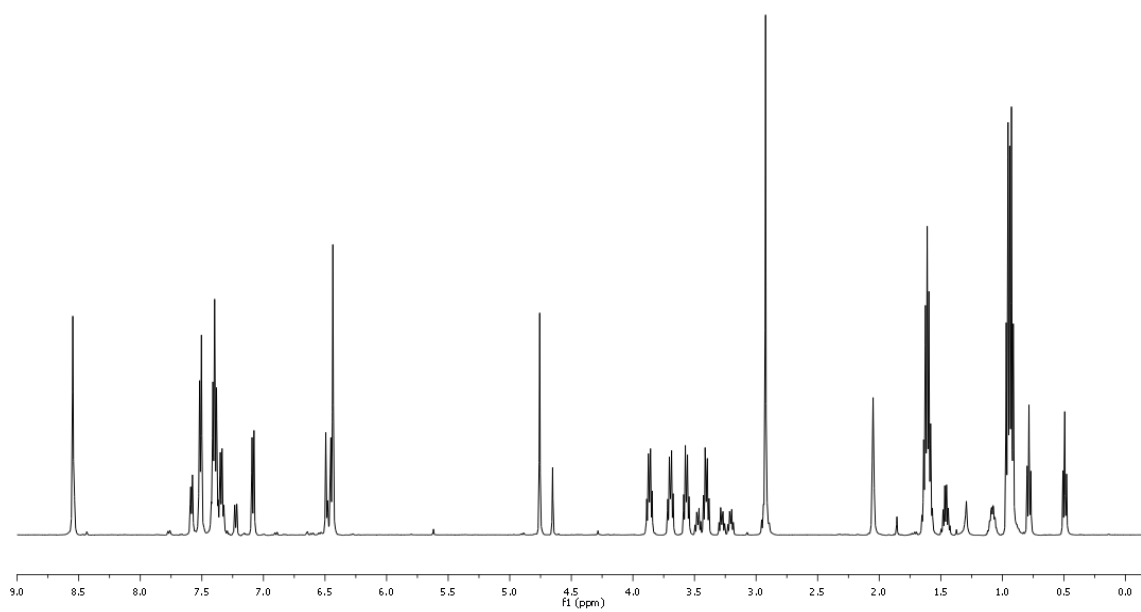


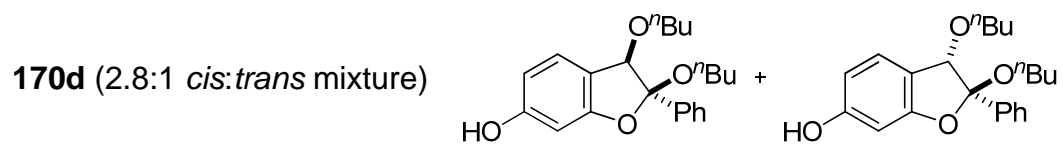
$^{13}\text{C-NMR}$ (acetone- d_6)



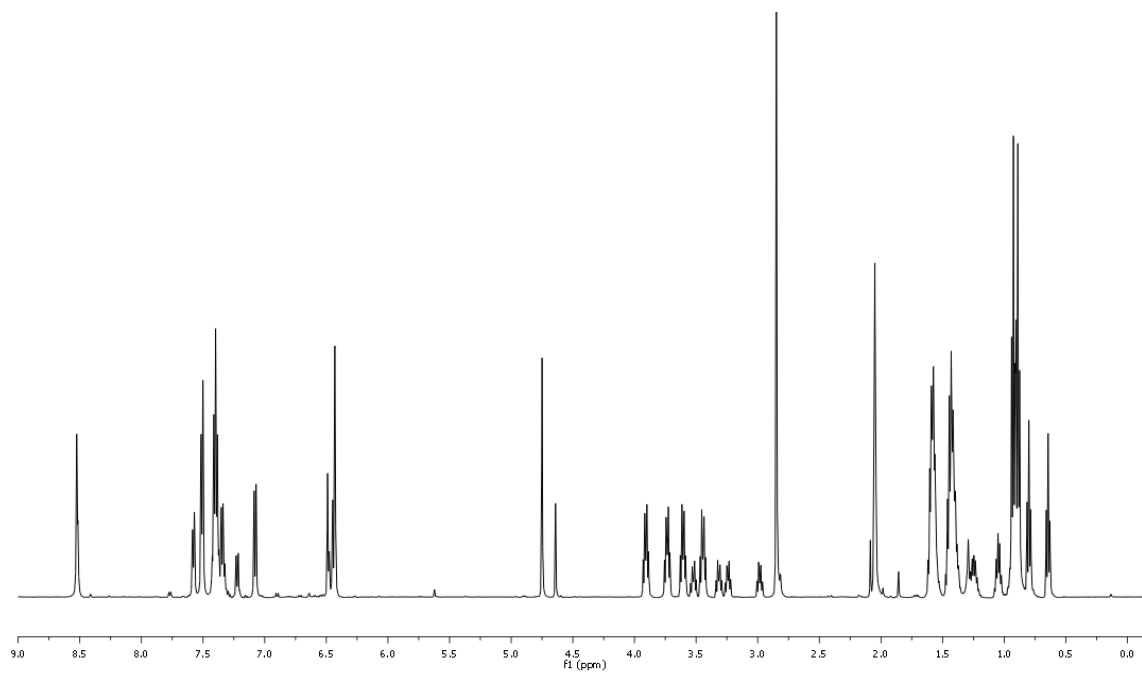


$^1\text{H-NMR}$ (acetone- d_6)

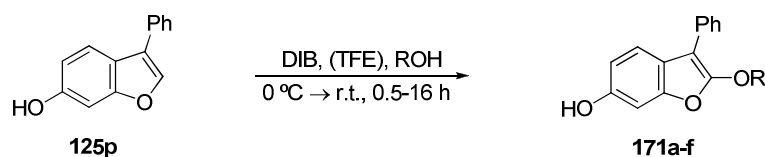




$^1\text{H-NMR}$ (acetone- d_6)



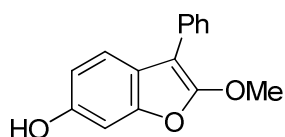
5.4.4. Procedure for the preparation of 2-alkoxy-3-phenylbenzofuran-6-ols **171a-f**



Scheme 5.15. Preparation of 2-alkoxy-3-phenylbenzofuran-6-ols **171a-f** from 3-phenylbenzofuran-6-ol **125p**.

A solution of benzo[*b*]furan **125p** (0.714 mmol) in 15 ml of alcohol and a solution of DIB (0.785 mmol, 1.1 eq) in 5 ml of alcohol (MeOH for **171a**, EtOH for **171b**) or in 5 ml of TFE (for **171c-f**) were separately prepared under inert argon atmosphere by stirring the mixtures in round bottom flasks until total solution of the solids. The solution of **125p** was cooled to 0 °C in an ice-water bath and the solution of DIB was dropwise added over it. The bath was then removed, allowing the reaction slowly reach room temperature. The mixture was stirred for 0.5-16 hours until TLC revealed complete conversion of the reaction. It was then quenched by adding anhydrous NaHCO₃ (1.43 mmol, 2 eq), stirred for 15 more minutes and filtered through a medium flow rate filter paper. The resulting reaction mixture was evaporated under reduced pressure and purified by column chromatography on silica gel, using EtOAc/cyclohexane mixtures as eluent to afford the corresponding pure products **171a-f**. Unfortunately products **171c** and **171d** were unstable (progressively degraded), therefore only the data corresponding to their ¹H-NMR and IR are given.

2-methoxy-3-phenylbenzofuran-6-ol, **171a**:



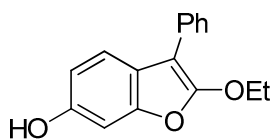
Molecular formula: C₁₅H₁₂O₃

Molecular weight: 240.25 g/mol

Aspect: Yellow oil

Yield: 61%

IR (neat): 3330, 2944, 1621, 1109 cm⁻¹. ¹H-NMR (500 MHz, acetone-d₆) δ = 8.40 (s, 1H), 7.71 (d, *J*=7.8 Hz, 2H), 7.55 (d, *J*=8.4 Hz, 1H), 7.44 (t, *J*=7.5 Hz, 3H), 7.26 (t, *J*=7.3 Hz, 1H), 6.97 (s, 1H), 6.88 (d, *J*=8.4 Hz, 1H), 4.09 (s, 3H). ¹³C-NMR (126 MHz, acetone-d₆) δ = 158.4, 155.1, 150.3, 133.1, 129.4, 128.2, 126.8, 121.5, 120.1, 112.9, 98.8, 95.5, 59.6.

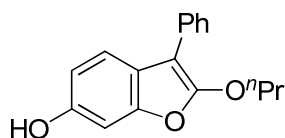
2-ethoxy-3-phenylbenzofuran-6-ol, 171b:Molecular formula: C₁₆H₁₄O₃

Molecular weight: 254.28 g/mol

Aspect: Yellow oil

Yield: 57%

IR (neat): 3341, 2980, 1619, 1109 cm⁻¹. ¹H-NMR (500 MHz, acetone-d₆) δ = 8.42 (s, 1H), 7.74 (d, *J*=7.2 Hz, 2H), 7.55 (d, *J*=8.4 Hz, 1H), 7.44 (t, *J*=7.8 Hz, 2H), 7.26 (t, *J*=7.4 Hz, 1H), 6.96 (d, *J*=2.1 Hz, 1H), 6.87 (dd, *J*=8.4, 2.2 Hz, 1H), 4.40 (q, *J*=7.1 Hz, 2H), 1.39 (t, *J*=7.1 Hz, 3H). ¹³C-NMR (126 MHz, acetone-d₆) δ = 157.8, 155.3, 150.5, 133.3, 129.5, 128.3, 126.9, 121.4, 120.2, 112.8, 98.8, 96.5, 69.4, 15.5.

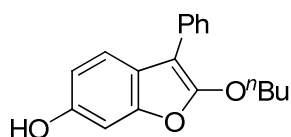
3-phenyl-2-propoxybenzofuran-6-ol, 171c (unstable product):Molecular formula: C₁₇H₁₆O₃

Molecular weight: 268.31 g/mol

Aspect: Yellow oil

Yield: 37%

IR (neat): 3319, 2965, 1618, 1111 cm⁻¹. ¹H-NMR (500 MHz, acetone-d₆) δ = 8.39 (s, 1H), 7.73 (d, *J*=7.2 Hz, 2H), 7.54 (d, *J*=8.4 Hz, 1H), 7.45 (t, *J*=7.8 Hz, 2H), 7.26 (t, *J*=7.4 Hz, 1H), 6.92 (d, *J*=2.1 Hz, 1H), 6.83 (dd, *J*=8.4, 2.2 Hz, 1H), 4.33 (t, *J*=6.5 Hz, 2H), 1.88 (sextet, *J*=7.0 Hz, 2H), 1.01 (t, *J*=7.4 Hz, 3H).

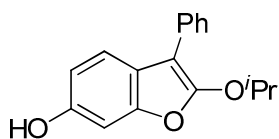
2-butoxy-3-phenylbenzofuran-6-ol, 171d (unstable product):Molecular formula: C₁₈H₁₈O₃

Molecular weight: 282.33 g/mol

Aspect: Yellow oil

Yield: 47%

IR (neat): 3363, 2959, 1622, 1112 cm⁻¹. ¹H-NMR (500 MHz, acetone-d₆) δ = 8.40 (s, 1H), 7.72 (d, *J*=7.2 Hz, 2H), 7.54 (d, *J*=8.4 Hz, 1H), 7.44 (t, *J*=7.8 Hz, 2H), 7.26 (t, *J*=7.4 Hz, 1H), 6.92 (d, *J*=2.1 Hz, 1H), 6.84 (dd, *J*=8.4, 2.2 Hz, 1H), 4.37 (t, *J*=6.5 Hz, 2H), 1.77 (pentet, *J*=7.0 Hz, 2H), 1.48 (sextet, *J*=7.5 Hz, 2H), 0.93 (t, *J*=7.4 Hz, 3H).

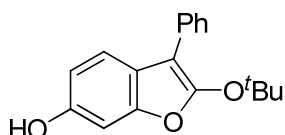
2-*iso*-propoxy-3-phenylbenzofuran-6-ol, 171e:Molecular formula: C₁₇H₁₆O₃

Molecular weight: 268.31 g/mol

Aspect: Yellow oil

Yield: 52%

IR (neat): 3352, 2978, 1620, 1093 cm⁻¹. ¹H-NMR (500 MHz, acetone-d₆) δ = 8.37 (s, 1H), 7.75 (d, *J*=7.3 Hz, 2H), 7.54 (d, *J*=8.4 Hz, 1H), 7.44 (t, *J*=7.7 Hz, 2H), 7.26 (t, *J*=7.4 Hz, 1H), 6.93 (d, *J*=2.0 Hz, 1H), 6.85 (dd, *J*=8.4, 2.2 Hz, 1H), 4.83 (septet, *J*=6.1 Hz, 1H), 1.37 (d, *J*=6.2 Hz, 6H). ¹³C-NMR (101 MHz, acetone-d₆) δ = 157.2, 155.3, 150.6, 133.3, 129.4, 128.2, 126.9, 121.3, 120.2, 112.7, 98.8, 97.9, 77.5, 22.7.

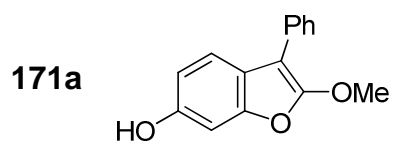
2-*tert*-butoxy-3-phenylbenzofuran-6-ol, 171f:Molecular formula: C₁₈H₁₈O₃

Molecular weight: 282.33 g/mol

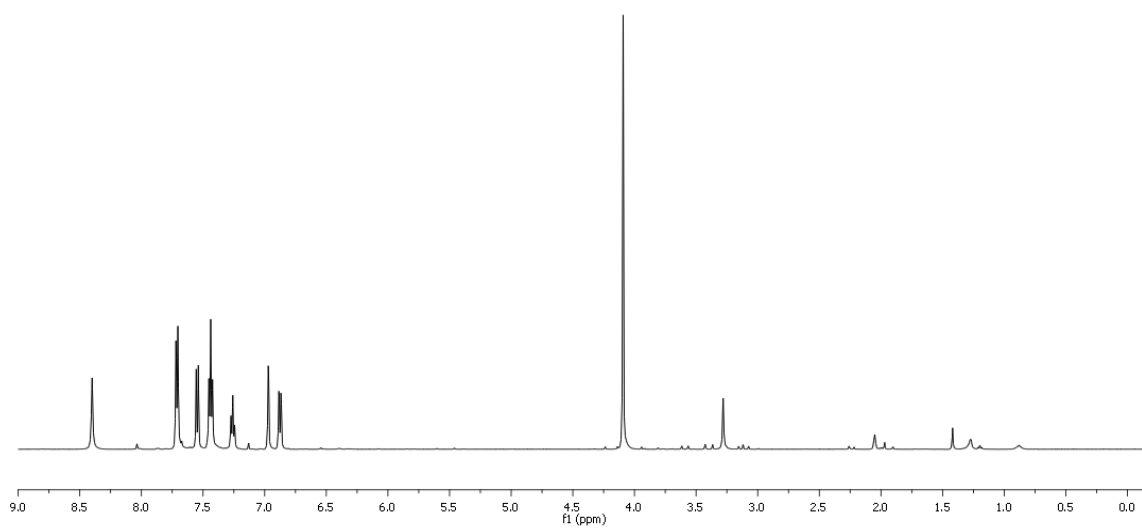
Aspect: Yellow oil

Yield: 49%

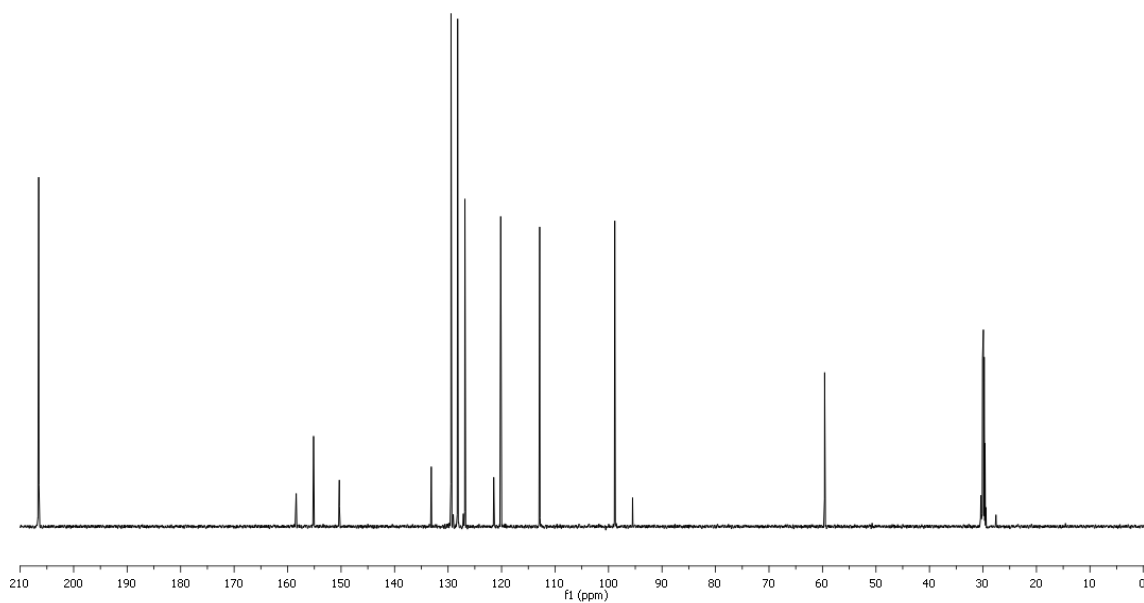
IR (neat): 3372, 2978, 1620, 1108 cm⁻¹. ¹H-NMR (500 MHz, acetone-d₆) δ = 8.39 (s, 1H), 7.75 (d, *J*=7.3 Hz, 2H), 7.54 (d, *J*=8.4 Hz, 1H), 7.45 (t, *J*=7.7 Hz, 2H), 7.27 (t, *J*=7.4 Hz, 1H), 6.94 (d, *J*=2.0 Hz, 1H), 6.85 (dd, *J*=8.4, 2.1 Hz, 1H), 1.39 (s, 9H). ¹³C-NMR (126 MHz, acetone-d₆) δ = 156.2, 155.6, 150.9, 133.6, 129.4, 128.6, 127.1, 120.9, 120.4, 112.6, 102.0, 98.7, 86.0, 29.1.

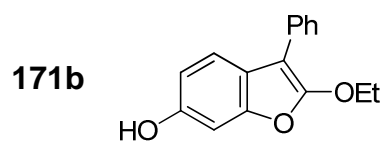


$^1\text{H-NMR}$ (acetone- d_6)

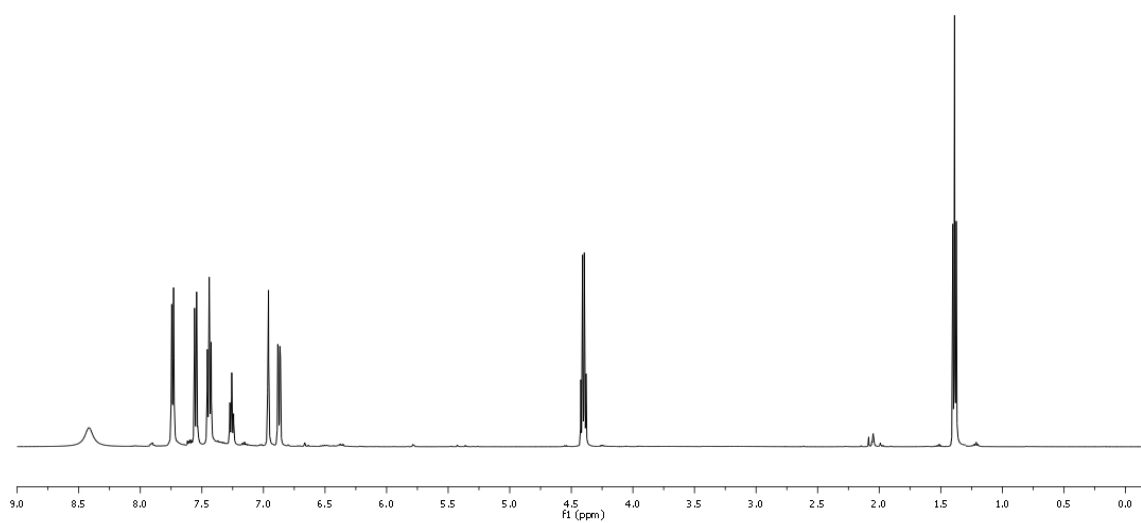


$^{13}\text{C-NMR}$ (acetone- d_6)

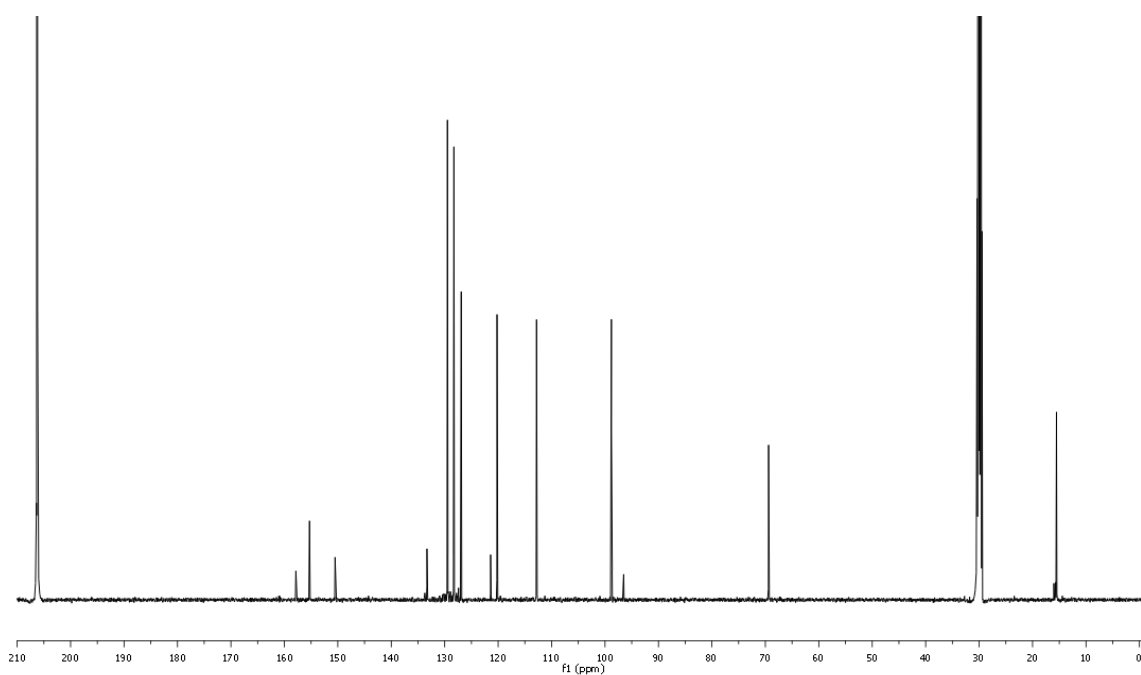


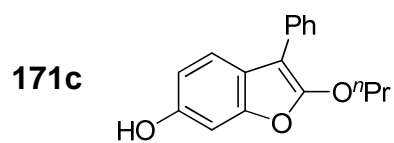


$^1\text{H-NMR}$ (acetone- d_6)

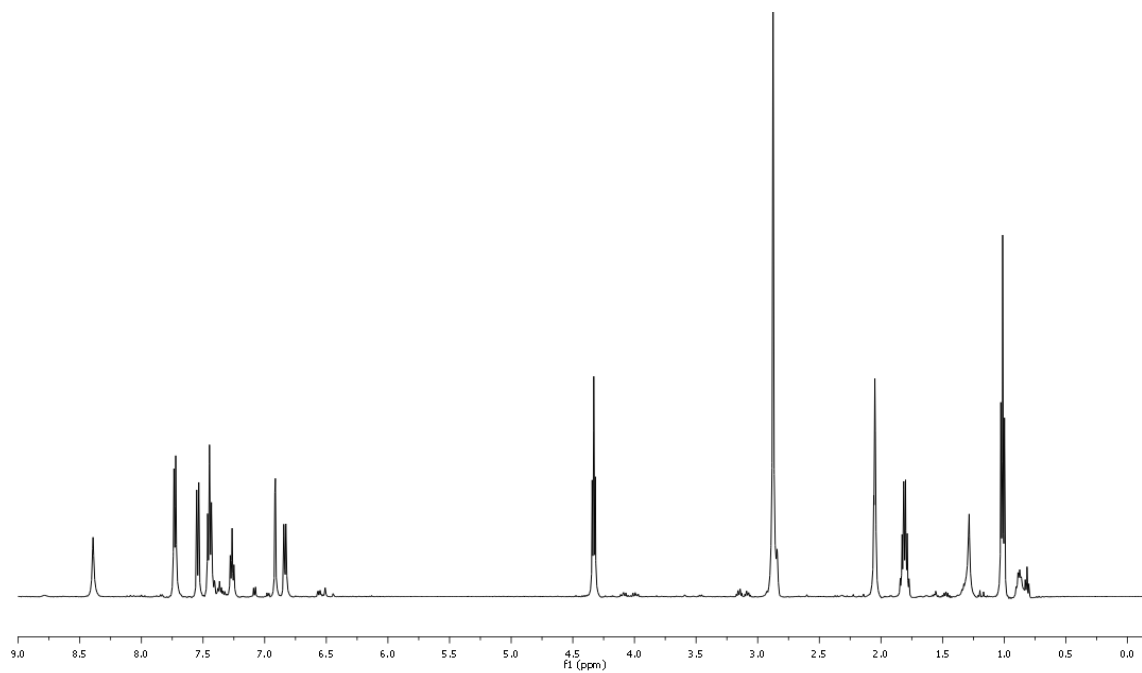


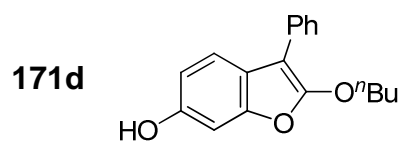
$^{13}\text{C-NMR}$ (acetone- d_6)



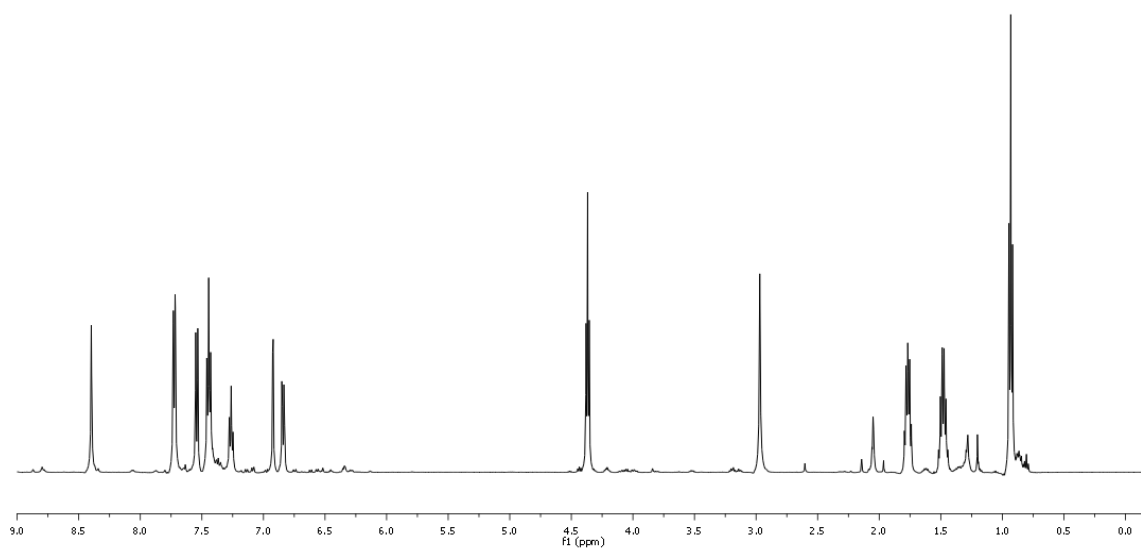


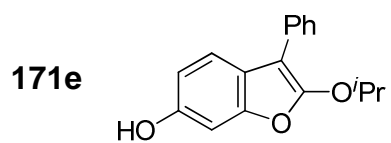
¹H-NMR (acetone-d₆)



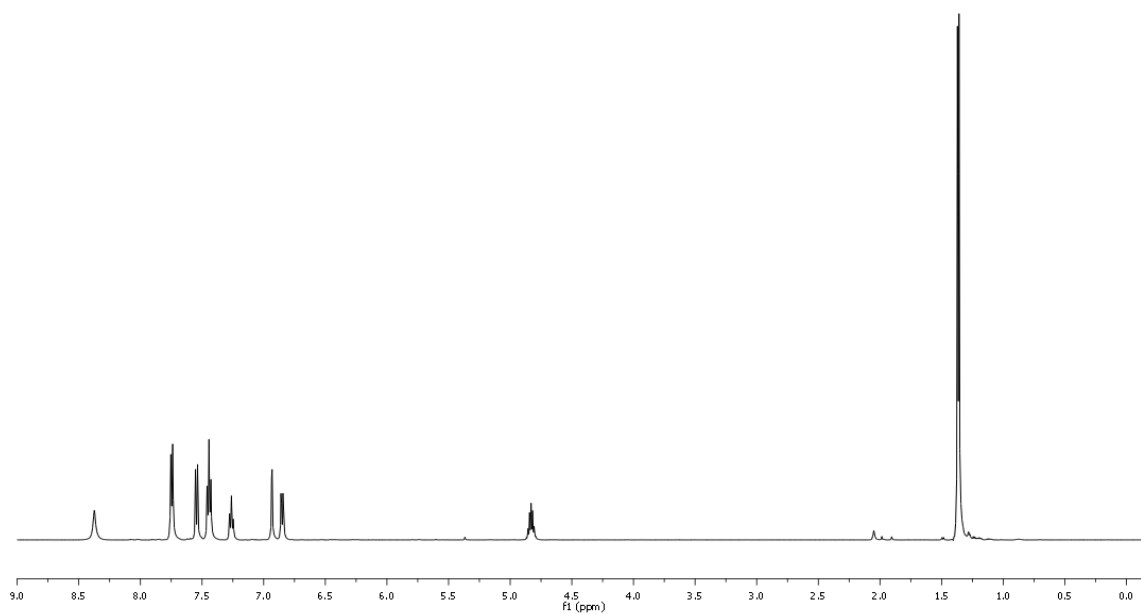


$^1\text{H-NMR}$ (acetone- d_6)

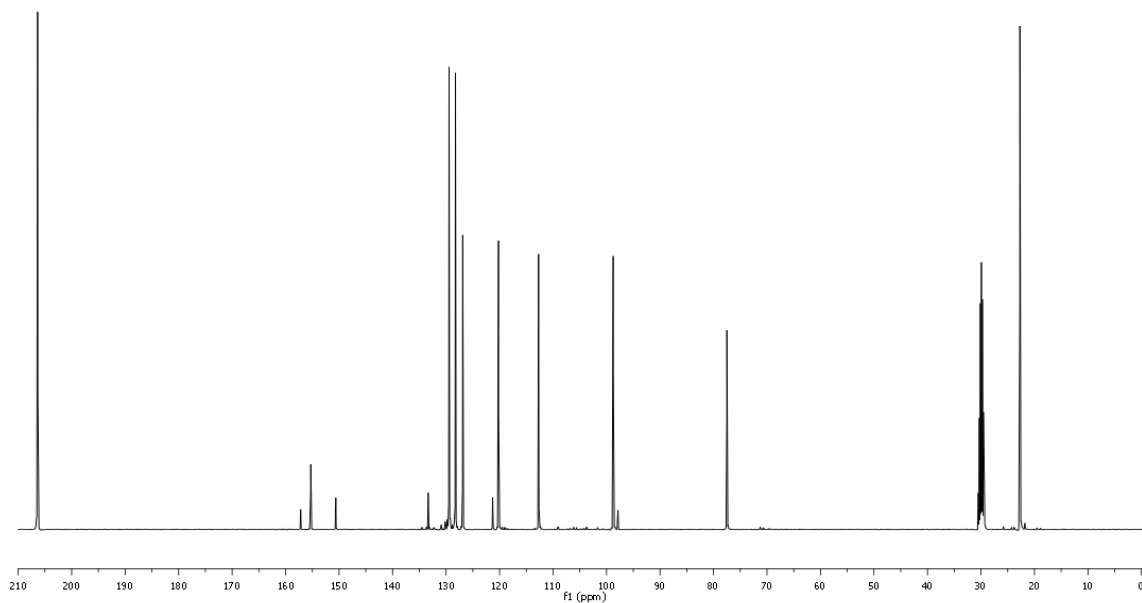


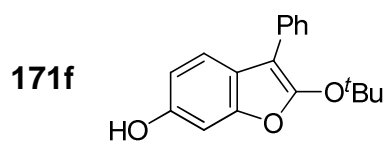


$^1\text{H-NMR}$ (acetone- d_6)

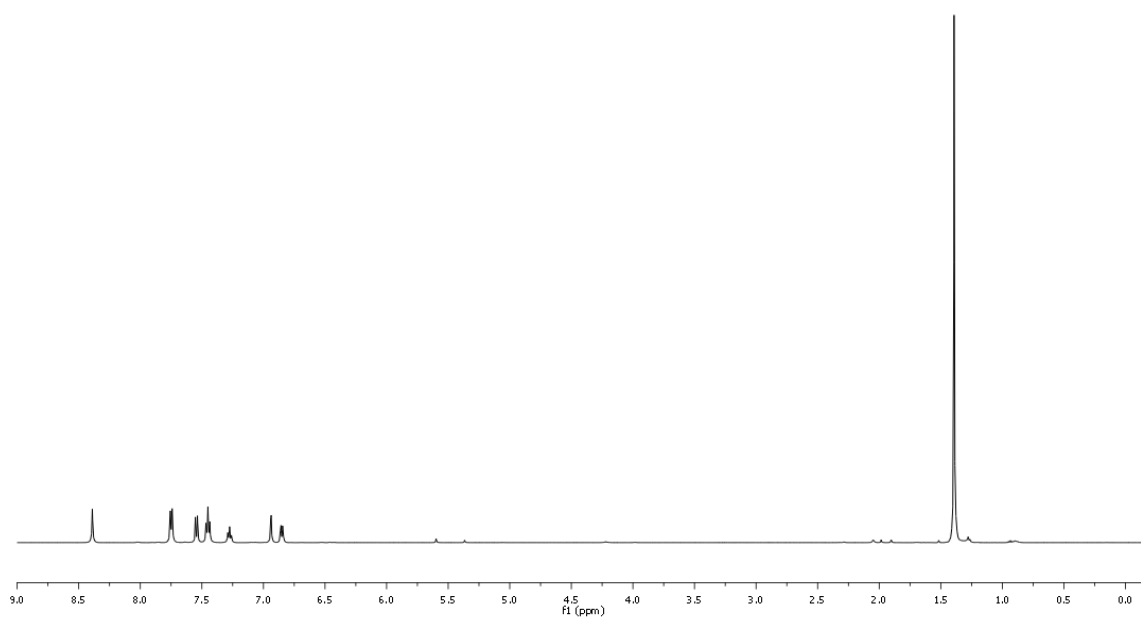


$^{13}\text{C-NMR}$ (acetone- d_6)

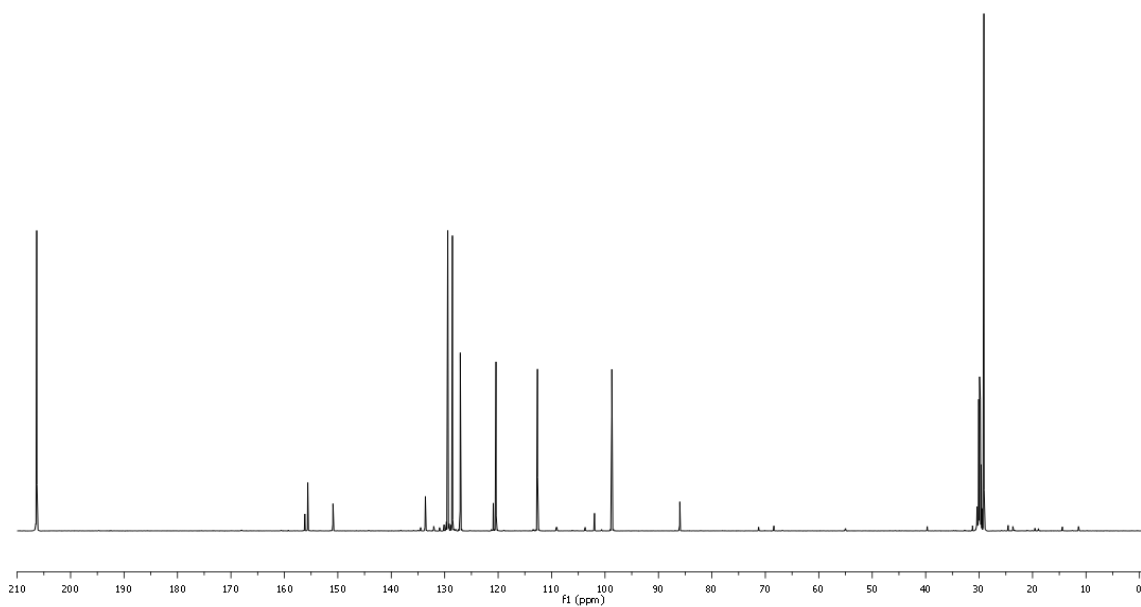




$^1\text{H-NMR}$ (acetone- d_6)

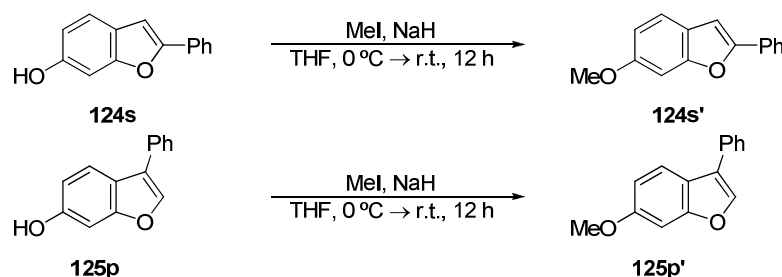


$^{13}\text{C-NMR}$ (acetone- d_6)



5.4.5. Methylation of 2- and 3-phenyl benzo[*b*]furans 124s and 125p with methyl iodide

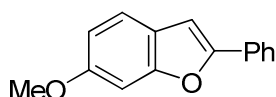
Benzo[*b*]furan-6-ols **124s** and **125p** were transformed into 6-methoxybenzo[*b*]furans **124s'** and **125p'** following a standard methylation procedure described in the literature²³⁹.



Scheme 5.16. Preparation of 6-methoxy-2-phenylbenzofuran **124s'** and 6-methoxy-3-phenylbenzofuran **125p'** via methylation of 2-phenylbenzofuran-6-ol **124s** and 3-phenylbenzofuran-6-ol **125p**, respectively.

NaH (0.714 mmol, 1.5 eq, 60% dispersion in mineral oil) was introduced in a round bottom flask under inert argon atmosphere and 1 ml of anhydrous THF was added. The suspension was cooled in an ice-water bath, and a solution of benzo[*b*]furan **124s** or **125p** (0.476 mmol) in 4 ml of anhydrous THF (under inert argon atmosphere) was dropwise added. Then, methyl iodide (0.714 mmol, 1.5 eq) was added and the mixture was stirred for 12 hours allowing it gradually reach room temperature. After this stirring time, the reaction was set at 0 °C and MeOH and H₂O (0.2 ml of each) were added to eliminate the excess of NaH and MeI. Solvents were evaporated under reduced pressure and the crude reaction mixture was dissolved in Et₂O and washed with H₂O and brine. Organic phase was then dried over anhydrous Na₂SO₄, filtered through a silica pad and evaporated under reduced pressure yielding the corresponding methylated product in excellent yield.

6-methoxy-2-phenylbenzofuran³³¹, **124s'**:



Molecular formula: C₁₅H₁₂O₂

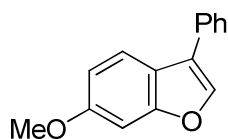
Molecular weight: 224.25 g/mol

Aspect: Salmon solid

Yield: 93%

¹H-NMR (500 MHz, acetone-*d*₆) δ = 7.87 (d, *J*=7.9 Hz, 2H), 7.47 (m, 3H), 7.35 (t, *J*=7.4 Hz, 1H), 7.16 (s, 2H), 6.90 (d, *J*=8.5 Hz, 1H), 3.86 (s, 3H).

³³¹ Commercial product, CAS: 33973-14-7

6-methoxy-3-phenylbenzofuran³³², 125p':Molecular formula: C₁₅H₁₂O₂

Molecular weight: 224.25 g/mol

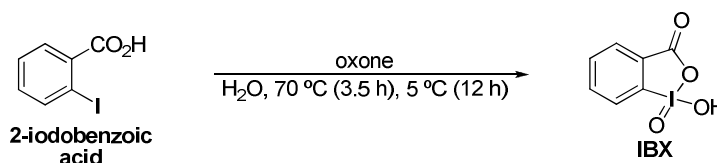
Aspect: Yellow oil

Yield: 92%

¹H-NMR (500 MHz, acetone-d₆) δ = 7.99 (s, 1H), 7.76 (d, *J*=8.6 Hz, 1H), 7.71 (d, *J*=8.0 Hz, 2H), 7.48 (t, *J*=7.5 Hz, 2H), 7.36 (t, *J*=7.1 Hz, 1H), 7.17 (s, 1H), 6.98 (d, *J*=8.6 Hz, 1H), 3.87 (s, 3H).

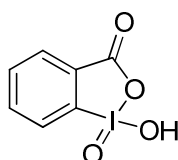
5.4.6. Synthesis of o-iodoxybenzoic acid IBX

IBX was prepared following a procedure described in the literature²⁴⁰.



Scheme 5.17. Preparation of IBX from 2-iodobenzoic acid.

A solution of oxone (123.50 mmol, 3.05 eq) in 400 ml of H₂O was prepared in a round bottom flask and 2-iodobenzoic acid (40.32 mmol) was added. The suspension was heated at 70 °C and stirred at this temperature for 3.5 hours, when TLC revealed no presence of starting 2-iodobenzoic acid. The suspension obtained this way was cooled to 5 °C (in a household fridge) for 12 hours, to allow the precipitation of the solid IBX. It was then filtered through a medium porosity sintered-glass funnel, and the solid was repeatedly rinsed with water (6 x 20 ml) and acetone (6 x 20 ml). The IBX, which was obtained as a white, crystalline solid, was left to dry at room temperature for at least 16 hours.

o-iodoxybenzoic acid^{240,333}, IBX:Molecular formula: C₇H₅IO₄

Molecular weight: 280.02 g/mol

Aspect: White solid

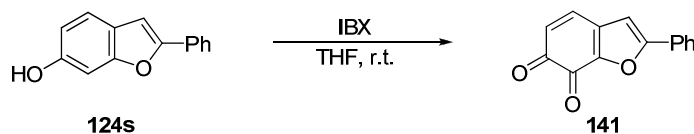
Yield: 77%

¹H-NMR (300 MHz, DMSO-d₆) δ = 8.13 (t, *J*=7.3 Hz, 1H), 8.07–7.90 (m, 2H), 7.84 (td, *J*=7.3, 0.9 Hz, 1H).

³³² Commercial product, CAS: 58468-44-3

³³³ Giuffredi, G. T.; Purser, S.; Sawicki, M.; Thompson, A. L.; Gouverneur, V. *Tetrahedron: Asymmetry* **2009**, *20*, 910-920

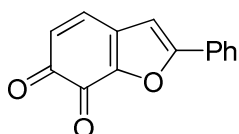
5.4.7. Procedure for the preparation of 2-phenylbenzofuran-6,7-dione **141**



Scheme 5.18. Preparation of the benzofurandione **141** via IBX-mediated oxidative dearomatization of **124s**.

A solution of benzo[*b*]furan **124s** (0.951 mmol) in 20 ml of anhydrous THF was prepared in a sealed round bottom flask covered with aluminium foil (as a prevention against light degradation) under inert argon atmosphere. 1.046 mmol (1.1 eq) of IBX were added and the reaction was stirred at room temperature. The conversion of the reaction was monitored by TLC and portions of 1.046 mmol (1.1 eq) of IBX were sequentially added every 8-12 hours until TLC revealed complete conversion (5.5 eq of IBX). The reaction mixture was then filtered through a medium flow rate filter paper and most of the solvent was evaporated at room temperature under reduced pressure. Then cold *n*-pentane was added (10 ml) and the round bottom flask was introduced in the freezer to precipitate product **141** in a 70% yield. The product was covered with aluminium foil throughout the whole process (to avoid a possible light degradation). Unfortunately product **141** was unstable (progressively degraded), therefore only the data corresponding to its ¹H-NMR and IR are given.

2-phenylbenzofuran-6,7-dione, 141 (unstable product):



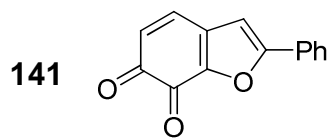
Molecular formula: C₁₄H₈O₃

Molecular weight: 224.21 g/mol

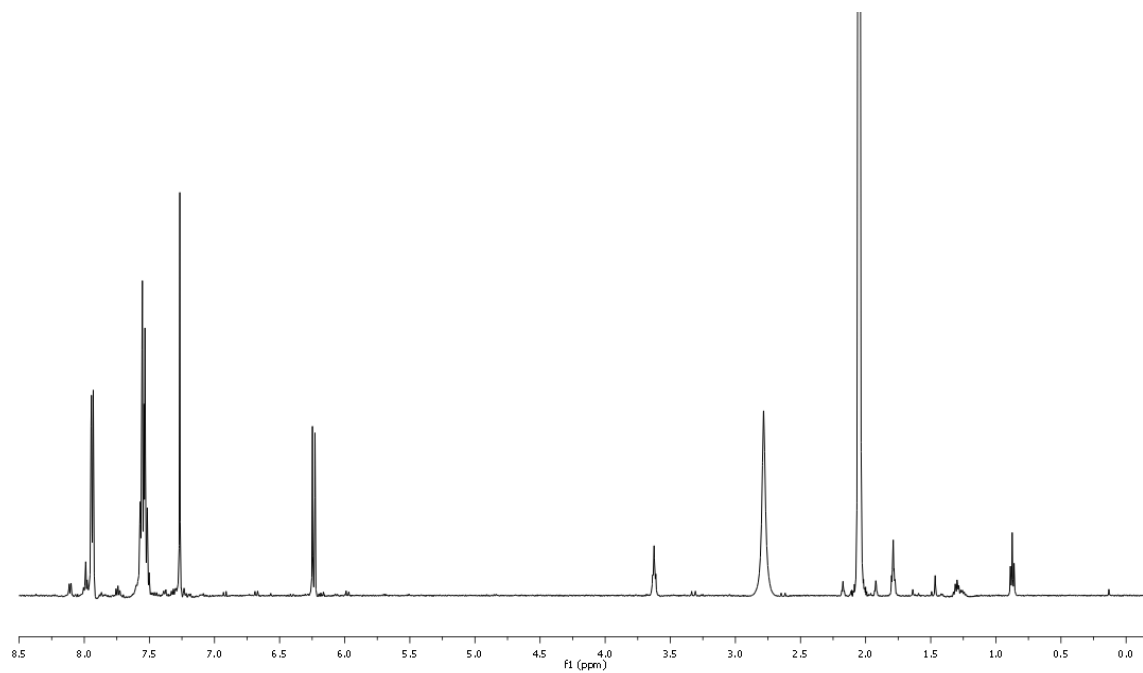
Aspect: Dark red solid

Yield: 70%

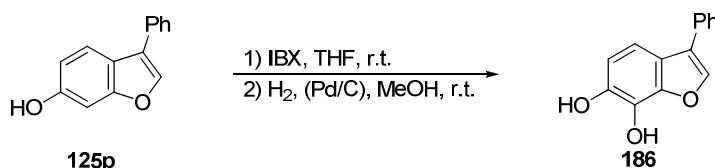
IR (neat): 2954, 1640, 1451, 762 cm⁻¹. ¹H-NMR (500 MHz, acetone-d₆) δ = 7.94 (d, *J*=6.9 Hz, 2H), 7.62–7.49 (m, 4H), 7.27 (s, 1H), 6.24 (d, *J*=9.9 Hz, 1H).



$^1\text{H-NMR}$ (acetone- d_6)



5.4.8. Procedure for the preparation of 3-phenylbenzofuran-6,7-diol **186**

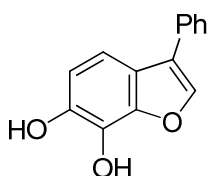


Scheme 5.19. Preparation of the benzofurandiol **186** via IBX-mediated oxidative dearomatization of **125p** followed by catalytic hydrogenation with Pd/C.

A solution of benzo[*b*]furan **125p** (0.951 mmol) in 20 ml of anhydrous THF was prepared in a sealed round bottom flask covered with aluminium foil (as a prevention against light degradation) under inert argon atmosphere. 1.046 mmol (1.1 eq) of IBX were added and the reaction was stirred at room temperature. The conversion of the reaction was monitored by TLC and portions of 1.046 mmol (1.1 eq) of IBX were sequentially added every 8-12 hours until TLC revealed complete conversion (3.3 eq of IBX). The reaction mixture was then filtered through a medium flow rate filter paper and the solvent was evaporated at room temperature under reduced pressure.

The obtained crude reaction mixture (enriched in 3-phenylbenzofuran-6,7-dione, **142**) was dissolved in 10 ml of MeOH (approximately 0.05 M) and filtered through a 0.20 μm pore filter. The resulting solution was made to react in the H-Cube® hydrogenation reactor at room temperature, with a 1 ml/minute flow in the presence of Pd/C catalyst. The crude obtained this way was evaporated under reduced pressure and purified by column chromatography on silica gel, using EtOAc/Hx mixtures as eluent to afford product **186**. The solution was covered with aluminium foil throughout the whole process in order to protect the product from possible light degradation.

3-phenylbenzofuran-6,7-diol, **186**:



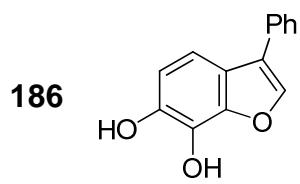
Molecular formula: $\text{C}_{14}\text{H}_{10}\text{O}_3$

Molecular weight: 226.23 g/mol

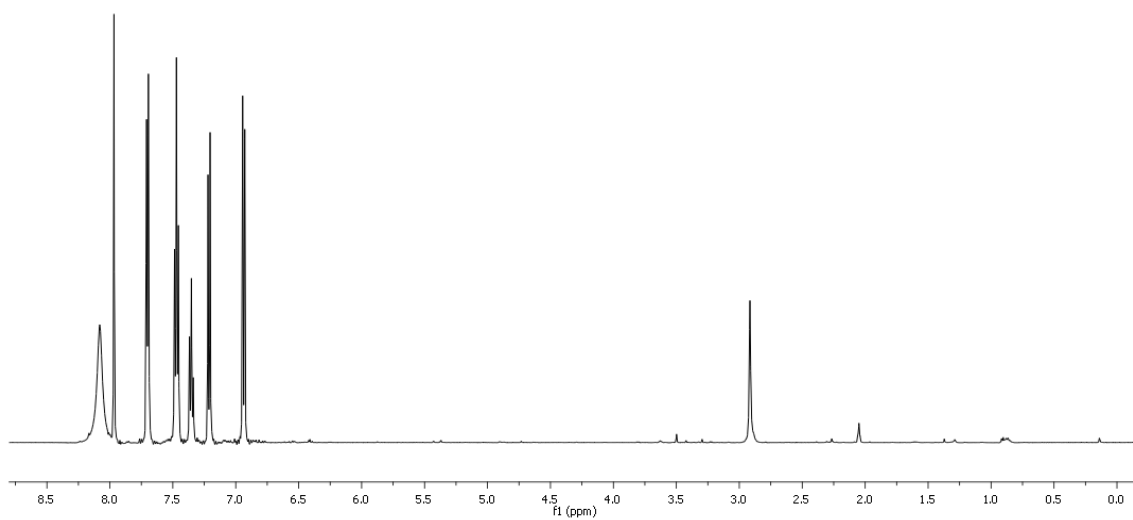
Aspect: Yellow oil

Yield: 23% (2 steps)

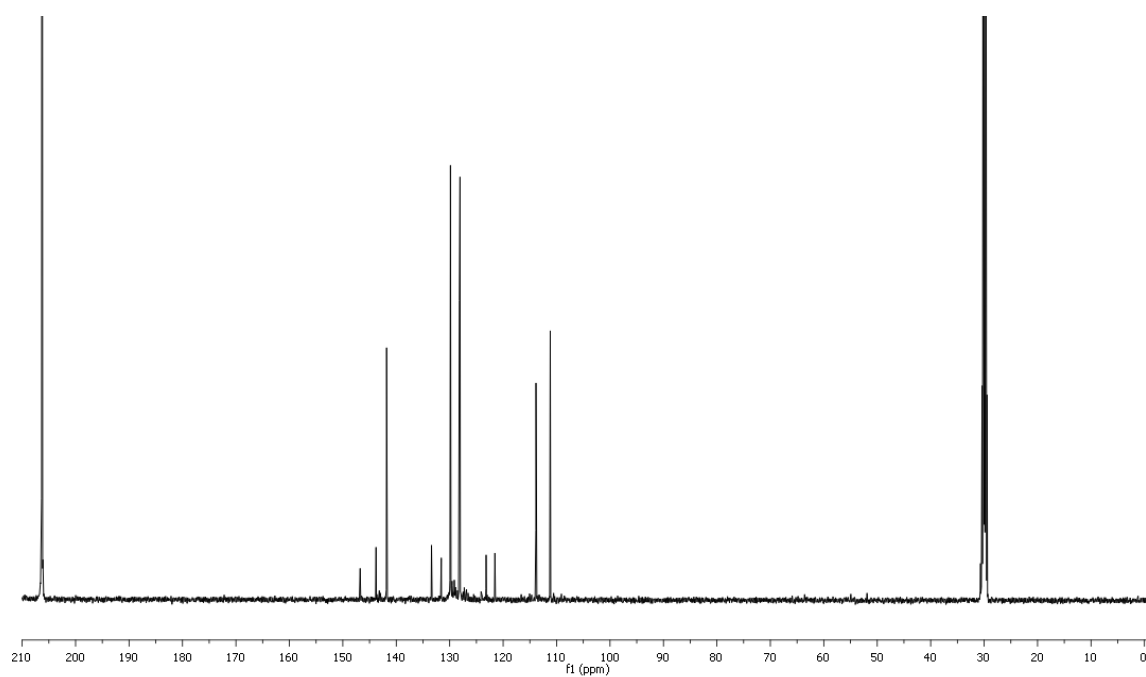
IR (neat): 3055, 1597, 1275, 696 cm^{-1} . $^1\text{H-NMR}$ (500 MHz, acetone- d_6) δ = 8.08 (bs, 2H), 7.97 (s, 1H), 7.70 (d, $J=7.2$ Hz, 2H), 7.47 (t, $J=7.7$ Hz, 1H), 7.35 (t, $J=7.4$ Hz, 0H), 7.21 (d, $J=8.4$ Hz, 1H), 6.94 (d, $J=8.4$ Hz, 1H). $^{13}\text{C-NMR}$ (126 MHz, acetone- d_6) δ = 146.8, 143.8, 141.8, 133.4, 131.6, 129.9, 128.2, 128.1, 123.2, 121.5, 113.9, 111.2.



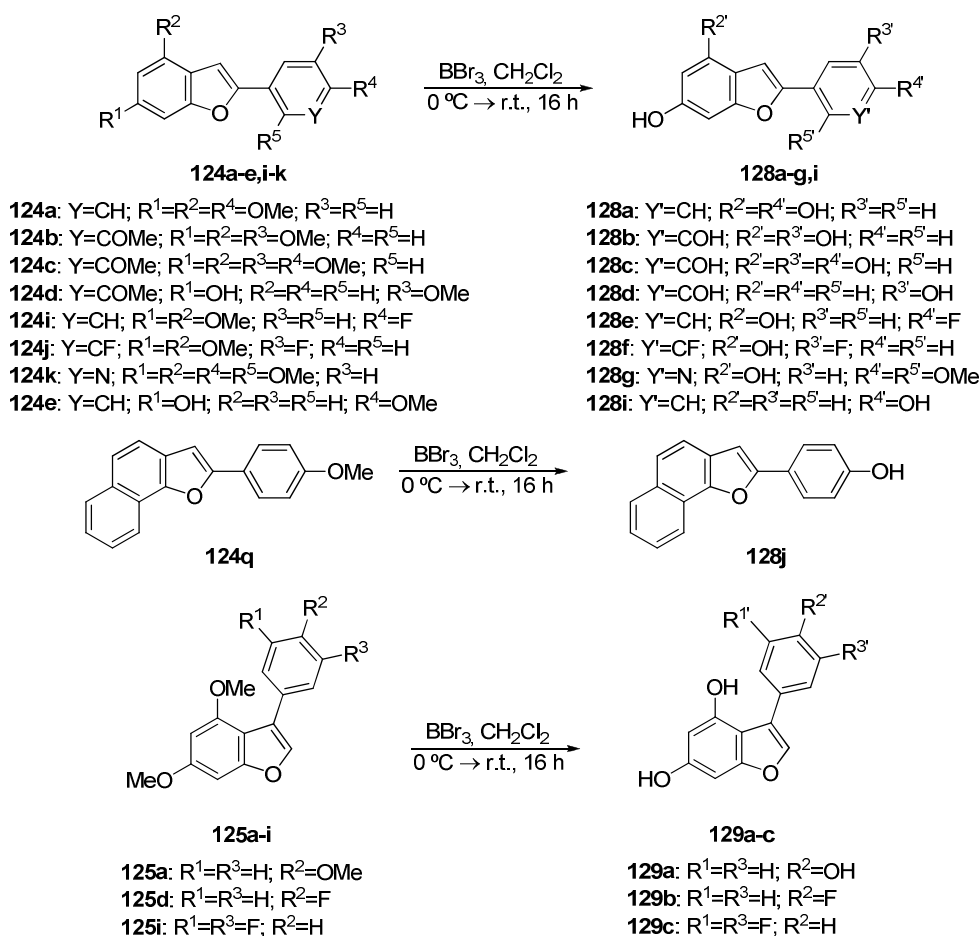
$^1\text{H-NMR}$ (acetone- d_6)



$^{13}\text{C-NMR}$ (acetone- d_6)

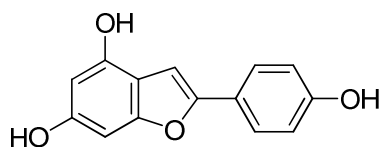


5.5. BORON TRIBROMIDE-MEDIATED DEMETHYLATION of METHOXY GROUPS of 2- and 3-ARYL BENZO[b]FURANS **124a-e,i-k** and **125a,d,i**



Scheme 5.20. Preparation of (poly)hydroxylated 2-arylbenzofurans **128a-g,i**, 2-arylnaphthofuran **128j** and 3-arylbenzofurans **129a-c** via demethylation of the corresponding 2-arylbenzofurans **124a-e,i-k**, 2-arylnaphthofuran **124q** and 3-arylbenzofurans **125a,d,i**.

A solution of benzo[b]furan (or naphthofuran) **124** or **125** (0.3 mmol) in 10 ml of anhydrous CH₂Cl₂ was prepared in a sealed round bottom flask under inert argon atmosphere and cooled to 0 °C in a ice-water bath. A 1M solution of BBr₃ in CH₂Cl₂ (2 eq per methoxy group to be demethylated) was dropwise added at 0°C. The bath was then removed, allowing the reaction slowly reach room temperature. The mixture was stirred for 16 hours after which TLC revealed complete conversion of the reaction. Then MeOH (1 ml per mmol of BBr₃ employed) was dropwise added at 0 °C (ice-water bath) to quench the reaction. The resulting crude reaction mixture was evaporated under reduced pressure and immediately purified by column chromatography on silica gel, using EtOAc/Hx mixtures as eluent to afford the corresponding pure products **128** and **129**. Compounds **128b-c,g** and **129a-b** decompose rather than melt upon heating.

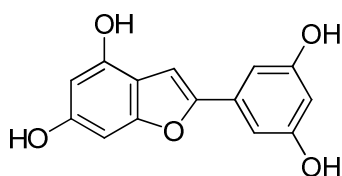
2-(4'-hydroxyphenyl)benzofuran-4,6-diol, 128a:Molecular formula: C₁₄H₁₀O₄

Molecular weight: 242.23 g/mol

Aspect: White solid

Yield: 93%

m.p.: 216-217 °C. IR (KBr): 3309, 1613, 1510, 1439, 1241, 1134, 1064 cm⁻¹. ¹H-NMR (500 MHz, DMSO-d₆) δ = 9.76 (s, 1H), 9.67 (s, 1H), 9.28 (s, 1H), 7.59 (d, *J*=8.7 Hz, 2H), 6.97 (s, 1H), 6.83 (d, *J*=8.7 Hz, 2H), 6.39 (d, *J*=0.8 Hz, 1H), 6.16 (d, *J*=1.8 Hz, 1H). ¹³C-NMR (126 MHz, CD₃OD) δ = 158.7, 158.4, 157.3, 154.8, 152.1, 126.8, 124.3, 116.7, 113.1, 98.8, 97.4, 90.9. Elemental analysis calculated for C₁₄H₁₀O₄: C, 69.4; H, 4.2. Found: C, 69.3; H, 4.2.

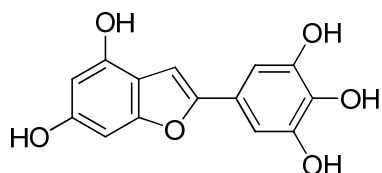
2-(3',5'-dihydroxyphenyl)benzofuran-4,6-diol, 128b:Molecular formula: C₁₄H₁₀O₅

Molecular weight: 258.23 g/mol

Aspect: Light brown solid

Yield: 74%

m.p.: 244 °C (dec.). IR (KBr): 3349, 2920, 1610, 1442, 1252, 1134 cm⁻¹. ¹H-NMR (500 MHz, DMSO-d₆) δ = 9.78 (s, 1H), 9.33 (s, 2H), 9.32 (s, 1H), 7.01 (s, 1H), 6.62 (d, *J*=2.0 Hz, 2H), 6.39 (s, 1H), 6.19–6.15 (m, 2H). ¹³C-NMR (126 MHz, CD₃OD) 160.0, 158.6, 157.9, 154.5, 152.4, 134.1, 112.9, 103.9, 103.4, 99.8, 98.8, 90.8. Elemental analysis calculated for C₁₄H₁₀O₅: C, 65.1; H, 3.9. Found: C, 64.9; H, 3.9.

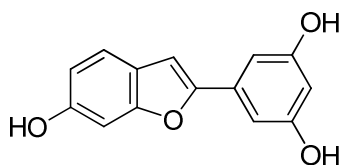
5-(4',6'-dihydroxy-1-benzofuran-2-yl)benzene-1,2,3-triol, 128c:Molecular formula: C₁₄H₁₀O₆

Molecular weight: 274.23 g/mol

Aspect: Yellow-brown solid

Yield: 62%

m.p.: 260 °C (dec.). IR (KBr): 3442, 3326, 1600, 1539, 1470, 1313, 1197, 1072, 1037 cm⁻¹. ¹H-NMR (500 MHz, DMSO-d₆) δ = 9.67 (s, 1H), 9.22 (s, 1H), 8.97 (s, 2H), 8.29 (s, 1H), 6.81 (s, 1H), 6.69 (s, 2H), 6.37 (s, 1H), 6.14 (s, 1H). ¹³C-NMR (75 MHz, CD₃OD) δ = 158.3, 157.3, 155.0, 151.9, 147.4, 134.8, 123.8, 113.1, 104.8, 98.7, 97.7, 90.8. Elemental analysis calculated for C₁₄H₁₀O₆: C, 61.3; H, 3.7. Found: C, 61.0; H, 3.6.

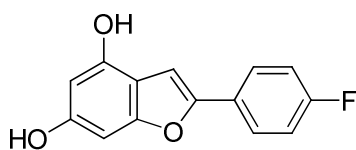
5-(6'-hydroxybenzofuran-2-yl)benzene-1,3-diol (moracin M)³³⁴, 128d:Molecular formula: C₁₄H₁₀O₄

Molecular weight: 242.23 g/mol

Aspect: Yellow-brown solid

Yield: 25%

¹H-NMR (500 MHz, DMSO-d₆) δ = 9.52 (s, 1H), 9.37 (s, 2H), 7.38 (d, *J*=8.4 Hz, 1H), 7.06 (s, 1H), 6.92 (s, 1H), 6.74 (d, *J*=8.3 Hz, 1H), 6.68 (s, 2H), 6.21 (s, 1H).

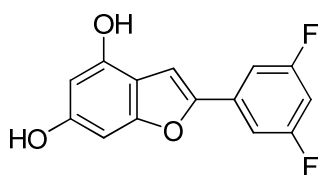
2-(4'-fluorophenyl)benzofuran-4,6-diol, 128e:Molecular formula: C₁₄H₉FO₃

Molecular weight: 244.22 g/mol

Aspect: Purple solid

Yield: 80%

m.p.: 189-190 °C. IR (KBr): 3332, 1614, 1500, 1243, 1125, 1072 cm⁻¹. ¹H-NMR (500 MHz, DMSO-d₆) δ = 9.85 (s, 1H), 9.36 (s, 1H), 7.82 (dd, *J*=8.7, 5.4 Hz, 2H), 7.27 (t, *J*=8.9 Hz, 2H), 7.21 (s, 1H), 6.42 (s, 1H), 6.19 (d, *J*=1.7 Hz, 1H). ¹³C-NMR (126 MHz, CD₃OD) δ = 163.8 (d, *J*=246.0 Hz), 158.8, 158.0, 153.3, 152.5, 129.0 (d, *J*=3.3 Hz), 127.1 (d, *J*=8.1 Hz), 116.8 (d, *J*=22.2 Hz), 112.9, 99.7, 98.9, 90.9. Elemental analysis calculated for C₁₄H₉FO₃: C, 68.8; H, 3.7. Found: C, 68.9; H, 3.9.

2-(3',5'-difluorophenyl)benzofuran-4,6-diol, 128f:Molecular formula: C₁₄H₈F₂O₃

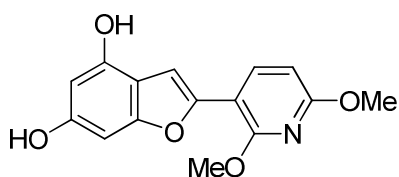
Molecular weight: 262.21 g/mol

Aspect: White solid

Yield: 60%

m.p.: 208-209 °C. IR (KBr): 3353, 3092, 1615, 1780, 1432, 1349, 1125 cm⁻¹. ¹H-NMR (500 MHz, DMSO-d₆) δ = 10.05 (s, 1H), 9.54 (s, 1H), 7.49 (d, *J*=6.8 Hz, 2H), 7.47 (s, 1H), 7.15 (t, *J*=8.6 Hz, 1H), 6.43 (s, 1H), 6.21 (s, 1H). ¹³C-NMR (126 MHz, CD₃OD) δ = 165.1 (dd, *J*=246.3, 13.3 Hz), 159.0, 158.9, 152.9, 151.6, 135.7 (t, *J*=10.6 Hz), 112.7, 107.7 (dd, *J*=21.0, 6.8 Hz), 103.3 (t, *J*=26.1 Hz), 102.6, 99.2, 90.8. Elemental analysis calculated for C₁₄H₈F₂O₃: C, 64.1; H, 3.1. Found: C, 64.3; H, 3.2.

³³⁴ Commercial product, CAS: 56137-21-6

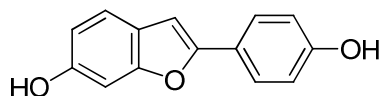
2-(2',6'-dimethoxypyridin-3-yl)benzofuran-4,6-diol, 128g:Molecular formula: C₁₅H₁₃NO₅

Molecular weight: 287.27 g/mol

Aspect: Grey solid

Yield: 47%

m.p.: 97°C (dec.). IR (KBr): 3434, 2958, 1587, 1471, 1319, 1265, 1084, 1020 cm⁻¹. ¹H-NMR (500 MHz, DMSO-d₆) δ = 9.77 (s, 1H), 9.30 (s, 1H), 8.07 (d, *J*=8.3 Hz, 1H), 7.13 (s, 1H), 6.51 (d, *J*=8.3 Hz, 1H), 6.40 (s, 1H), 6.16 (s, 1H), 4.08 (s, 3H), 3.92 (s, 3H). ¹³C-NMR (126 MHz, CD₃OD) δ = 163.3, 159.7, 157.8, 157.5, 152.3, 149.5, 138.2, 113.3, 107.8, 102.8, 102.6, 98.7, 90.7, 54.2, 54.1. Elemental analysis calculated for C₁₅H₁₃NO₅: C, 62.7; H, 4.6; N, 4.9. Found: C, 62.4; H, 4.5; N, 4.9.

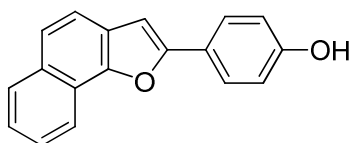
2-(4'-hydroxyphenyl)benzofuran-6-ol³³⁵, 128i:Molecular formula: C₁₄H₁₀O₃

Molecular weight: 226.23 g/mol

Aspect: White-yellow solid

Yield: 71%

¹H-NMR (300 MHz, DMSO-d₆) δ = 9.70 (s, 1H), 9.45 (s, 1H), 7.64 (d, *J*=8.6 Hz, 2H), 7.35 (d, *J*=8.4 Hz, 1H), 7.00 (s, 1H), 6.91 (d, *J*=1.4 Hz, 1H), 6.85 (d, *J*=8.7 Hz, 2H), 6.71 (dd, *J*=8.4, 2.1 Hz, 1H).

4-(naphtho[1,2-*b*]furan-2-yl)phenol, 128j:Molecular formula: C₁₈H₁₂O₂

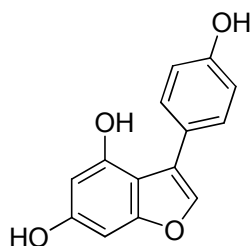
Molecular weight: 260.29 g/mol

Aspect: Pink solid

Yield: 97%

m.p.: 158-159 °C. IR (neat): 3196, 1233, 812 cm⁻¹. ¹H-NMR (300 MHz, DMSO-d₆) δ = 9.81 (s, 1H), 8.32 (d, *J*=8.1 Hz, 1H), 8.02 (d, *J*=8.2 Hz, 1H), 7.85 (d, *J*=8.6 Hz, 2H), 7.77-7.70 (m, 2H), 7.65 (t, *J*=7.1 Hz, 1H), 7.52 (t, *J*=7.0 Hz, 1H), 7.31 (s, 1H), 6.92 (d, *J*=8.7 Hz, 2H). ¹³C-NMR (101 MHz, CD₃OD) δ = 159.3, 157.5, 151.0, 132.8, 129.6, 127.5, 127.4, 126.7, 125.8, 124.6, 123.8, 122.6, 120.7, 120.6, 116.9, 101.4. Elemental analysis calculated for C₁₈H₁₂O₂: C, 80.1; H, 4.6. Found: C, 80.2; H, 4.5.

³³⁵ (a) Lions, F.; Willison, A. M. *J. & Proc. Roy. Soc. New South Wales* **1940**, 73, 240-252 (b) Goldenberg, C.; Gillyns, E.; Wandestrack, R.; Binon, F.; Broekhuysen, J.; Barchewitz, G.; Pacco, M.; Sion, R.; Charlier, R. *Chim. Ther.* **1973**, 8, 398-411

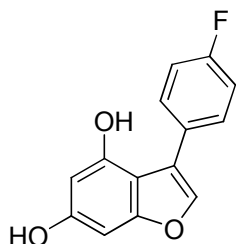
3-(4'-hydroxyphenyl)benzofuran-4,6-diol, 129a:Molecular formula: C₁₄H₁₀O₄

Molecular weight: 242.23 g/mol

Aspect: Yellow solid

Yield: 38%

m.p.: 220 °C (dec.). IR (KBr): 3460, 3373, 2914, 1635, 1518, 1229, 1133, 1055 cm⁻¹. ¹H-NMR (500 MHz, DMSO-d₆) δ = 9.75 (s, 1H), 9.36 (s, 1H), 9.33 (s, 1H), 7.62 (s, 1H), 7.46 (d, *J*=8.5 Hz, 2H), 6.75 (d, *J*=8.5 Hz, 2H), 6.37 (d, *J*=1.7 Hz, 1H), 6.21 (d, *J*=1.6 Hz, 1H). ¹³C-NMR (126 MHz, CD₃OD) δ = 160.2, 157.7, 157.5, 153.6, 139.7, 131.4, 125.4, 124.1, 115.9, 109.6, 99.0, 90.9. Elemental analysis calculated for C₁₄H₁₀O₄: C, 69.4; H, 4.2. Found: C, 69.5; H, 4.2.

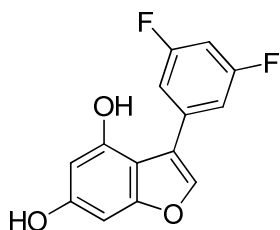
3-(4'-fluorophenyl)benzofuran-4,6-diol, 129b:Molecular formula: C₁₄H₉FO₃

Molecular weight: 244.22 g/mol

Aspect: Green-brown solid

Yield: 58%

m.p.: 125 °C (dec.). IR (KBr): 3508, 1612, 1508, 1455, 1240, 1121, 1090, 1048 cm⁻¹. ¹H-NMR (500 MHz, DMSO-d₆) δ = 9.84 (s, 1H), 9.36 (s, 1H), 7.77 (s, 1H), 7.70 (dd, *J*=8.1, 5.9 Hz, 2H), 7.20 (t, *J*=8.8 Hz, 2H), 6.41 (s, 1H), 6.25 (s, 1H). ¹³C-NMR (126 MHz, CD₃OD) δ = 163.7 (d, *J*=243.9 Hz), 160.2, 157.7, 153.6, 140.4, 132.0 (d, *J*=7.9 Hz), 130.4 (d, *J*=3.3 Hz), 123.3, 115.6 (d, *J*=21.6 Hz), 109.2, 99.1, 91.0. Elemental analysis calculated for C₁₄H₉FO₃: C, 68.8; H, 3.7. Found: C, 69.0; H, 3.6.

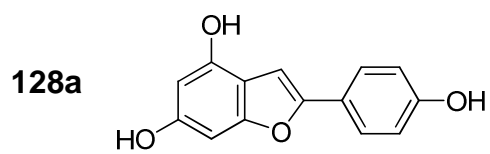
3-(3',5'-difluorophenyl)benzofuran-4,6-diol, 129c:Molecular formula: C₁₄H₈F₂O₃

Molecular weight: 262.21 g/mol

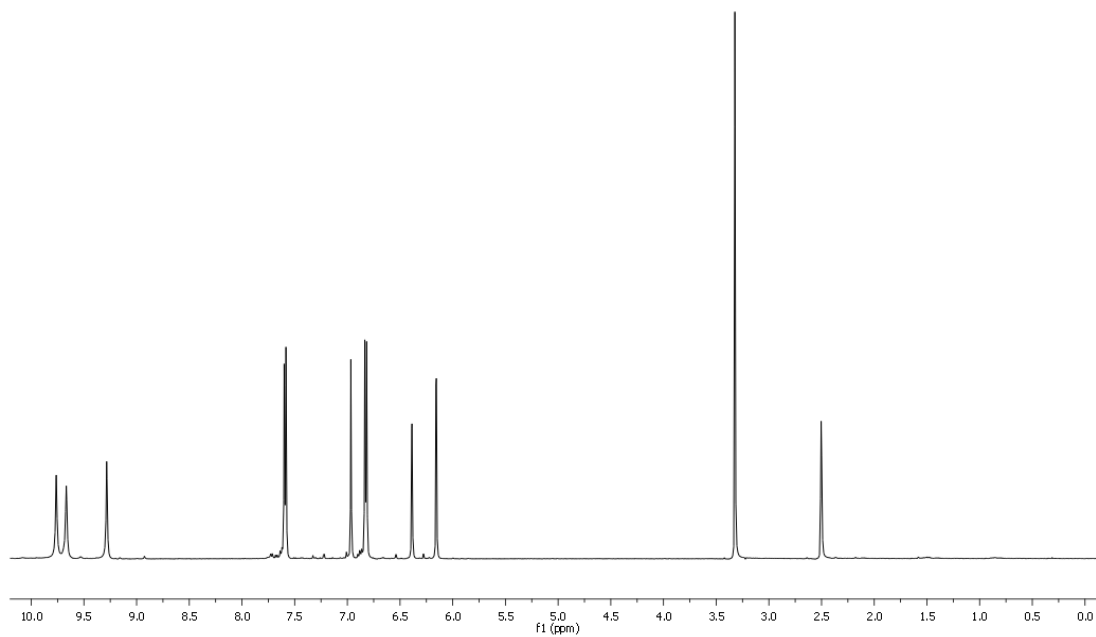
Aspect: White solid

Yield: 70%

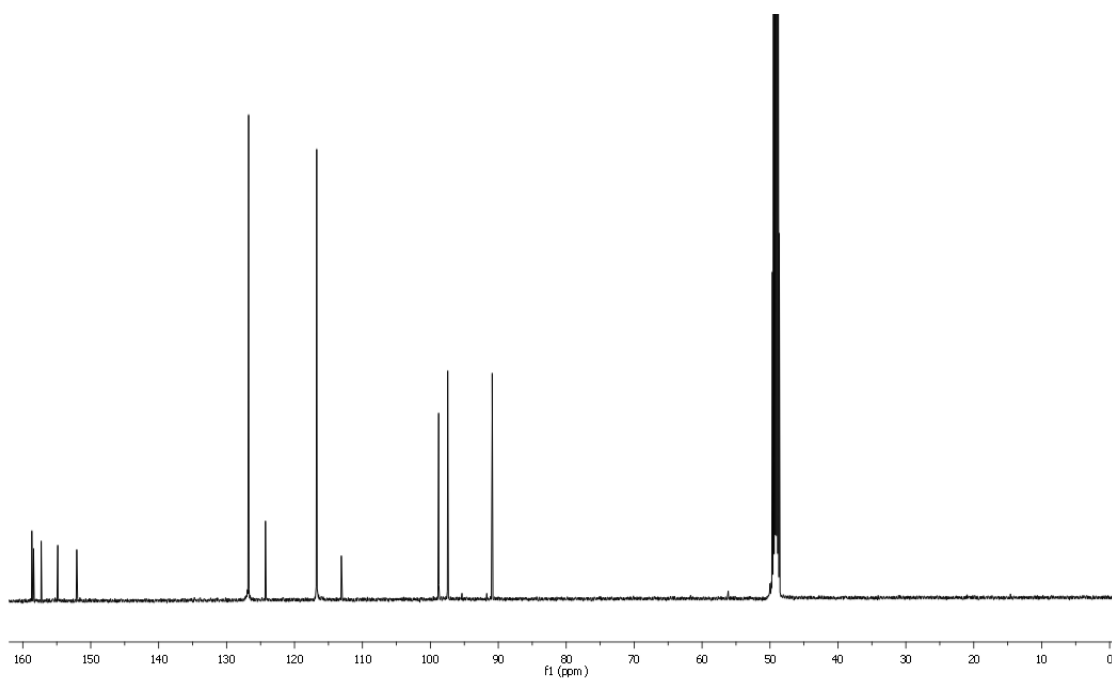
m.p.: 149-151 °C. IR (KBr): 3373, 1629, 1507, 1359, 1255, 1157, 1123, 1031 cm⁻¹. ¹H-NMR (500 MHz, DMSO-d₆) δ = 10.08 (s, 1H), 9.45 (s, 1H), 8.02 (s, 1H), 7.49 (d, *J*=7.7 Hz, 2H), 7.13 (t, *J*=9.4 Hz, 1H), 6.43 (s, 1H), 6.28 (s, 1H). ¹³C-NMR (75 MHz, CD₃OD) δ = 164.3 (dd, *J*=244.8, 13.4 Hz), 160.4, 158.1, 153.5, 141.7, 137.8 (t, *J*=10.7 Hz), 122.6, 112.8 (dd, *J*=8.1, 17.6 Hz), 108.4, 102.6 (t, *J*=25.9 Hz), 99.4, 91.0. Elemental analysis calculated for C₁₄H₈F₂O₃: C, 64.1; H, 3.1. Found: C, 64.4; H, 3.3.

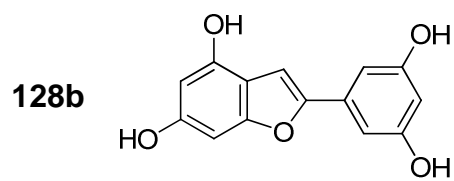


$^1\text{H-NMR}$ (DMSO-d_6)

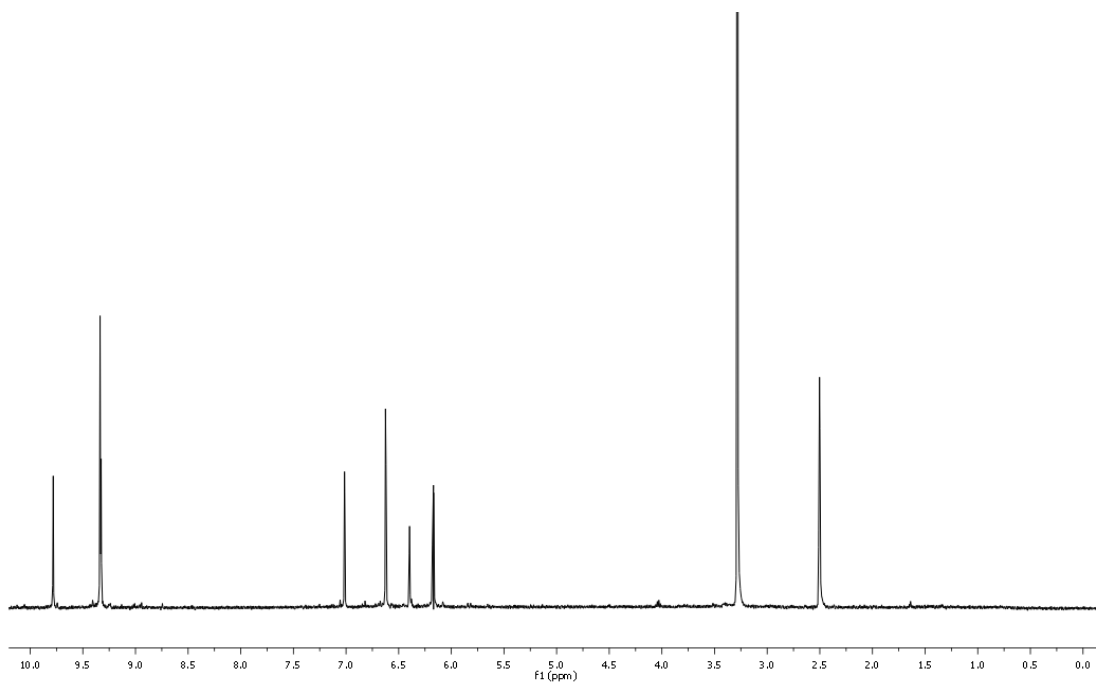


$^{13}\text{C-NMR}$ (CD_3OD)

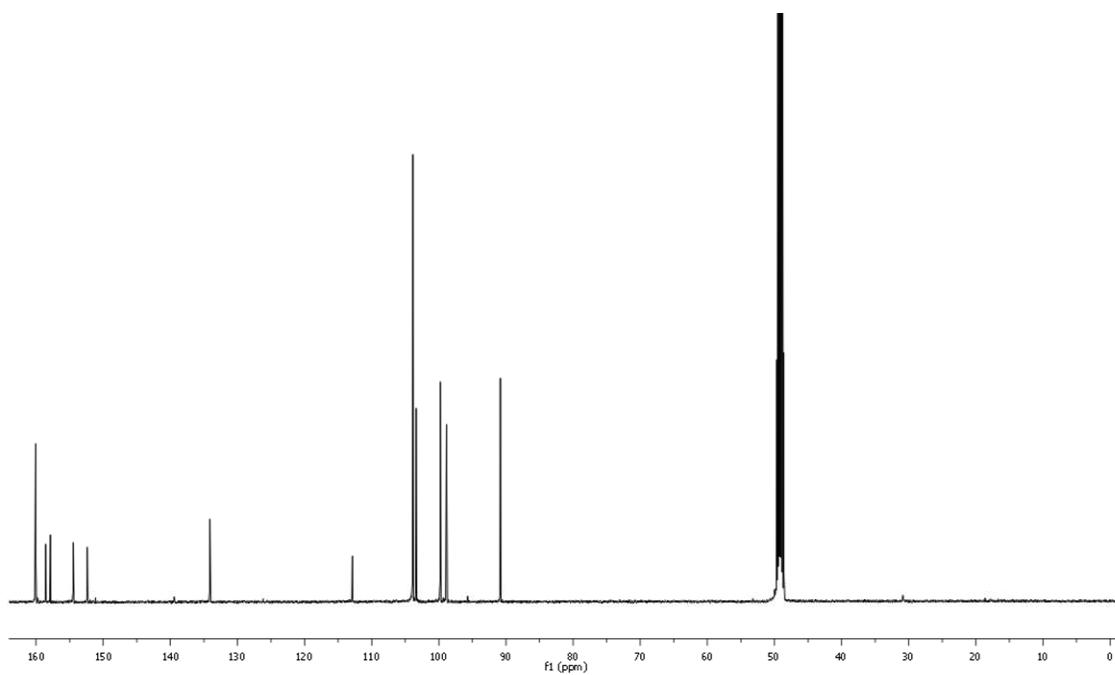


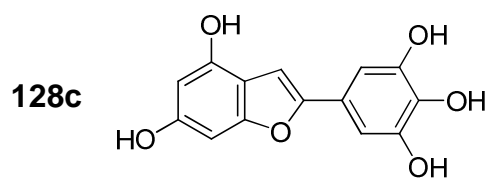


$^1\text{H-NMR}$ (DMSO- d_6)

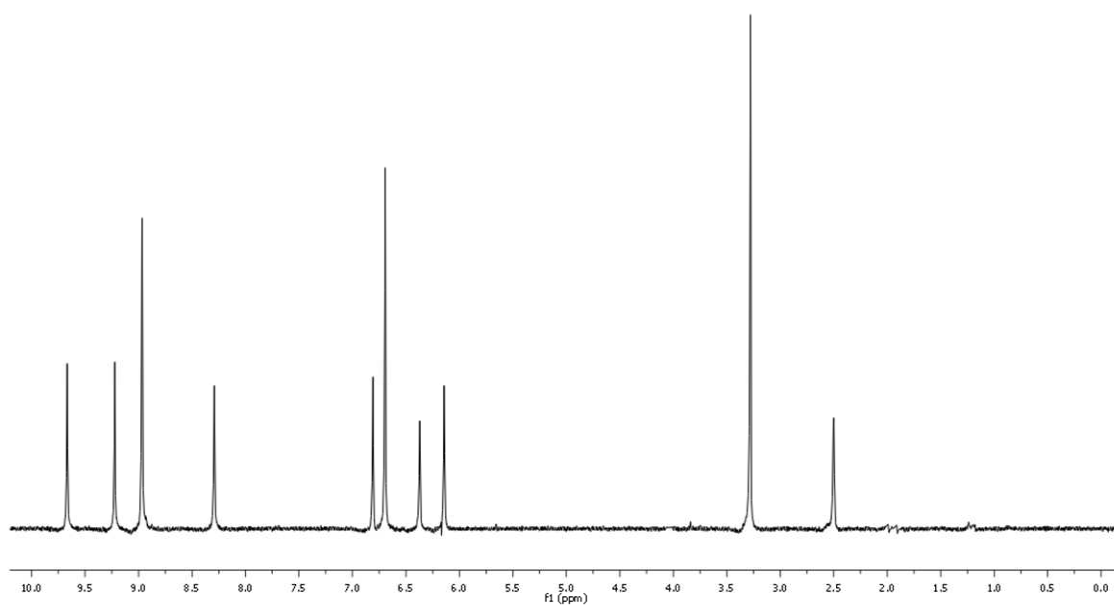


$^{13}\text{C-NMR}$ (CD_3OD)

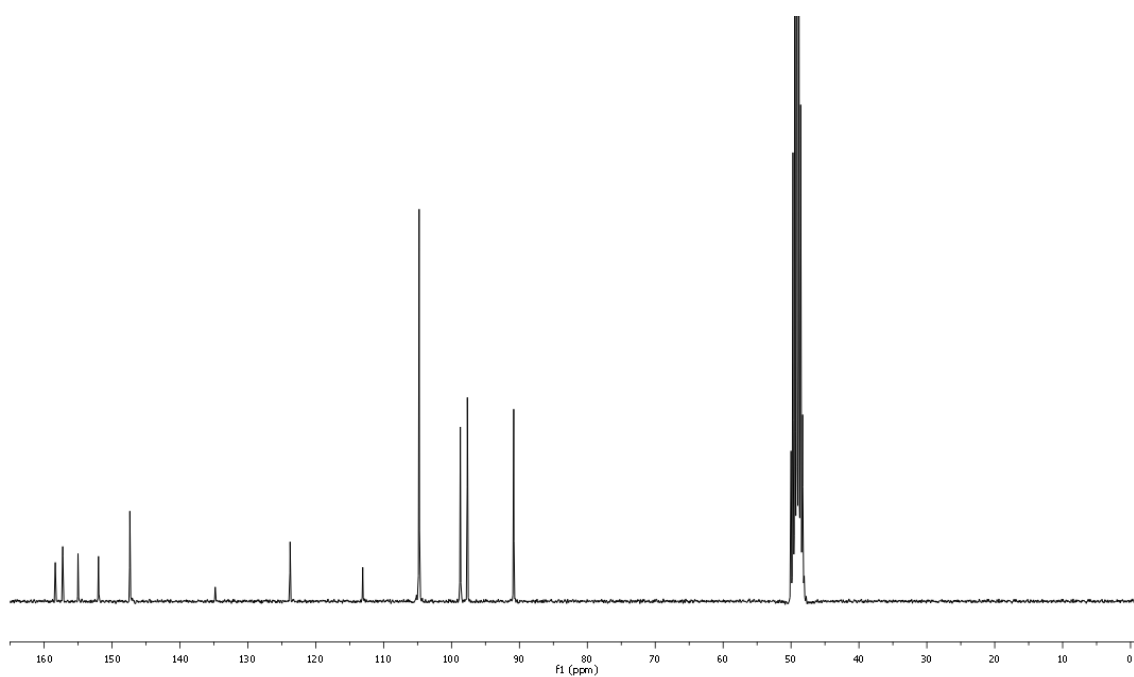


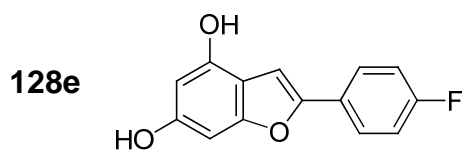


$^1\text{H-NMR}$ (DMSO-d_6)

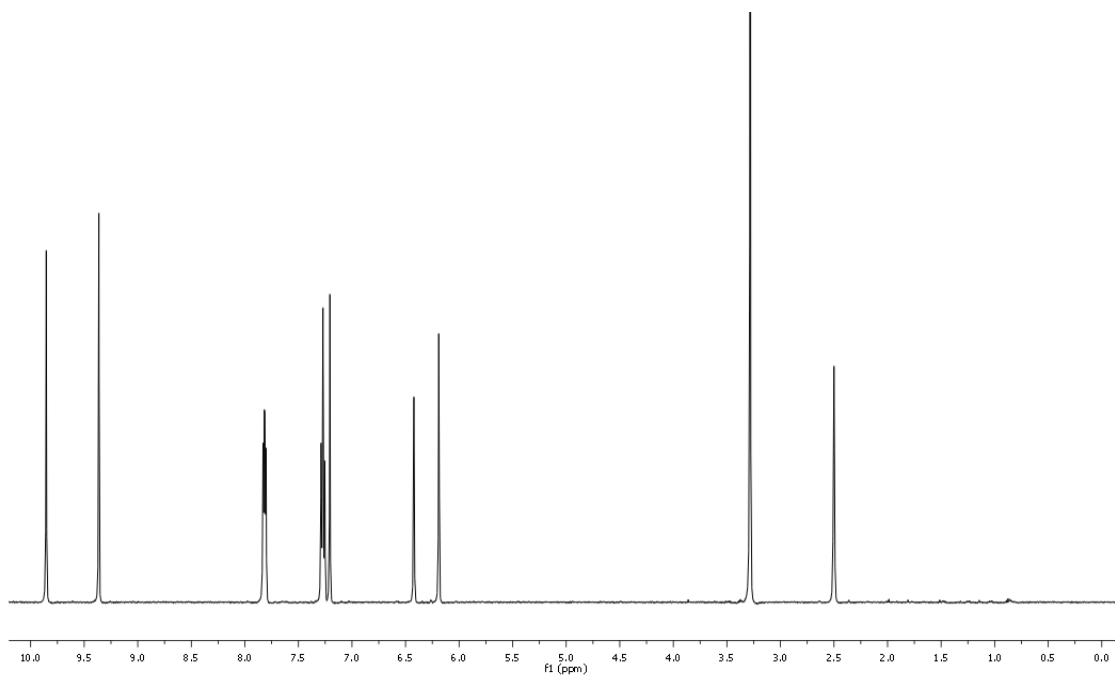


$^{13}\text{C-NMR}$ (CD_3OD)

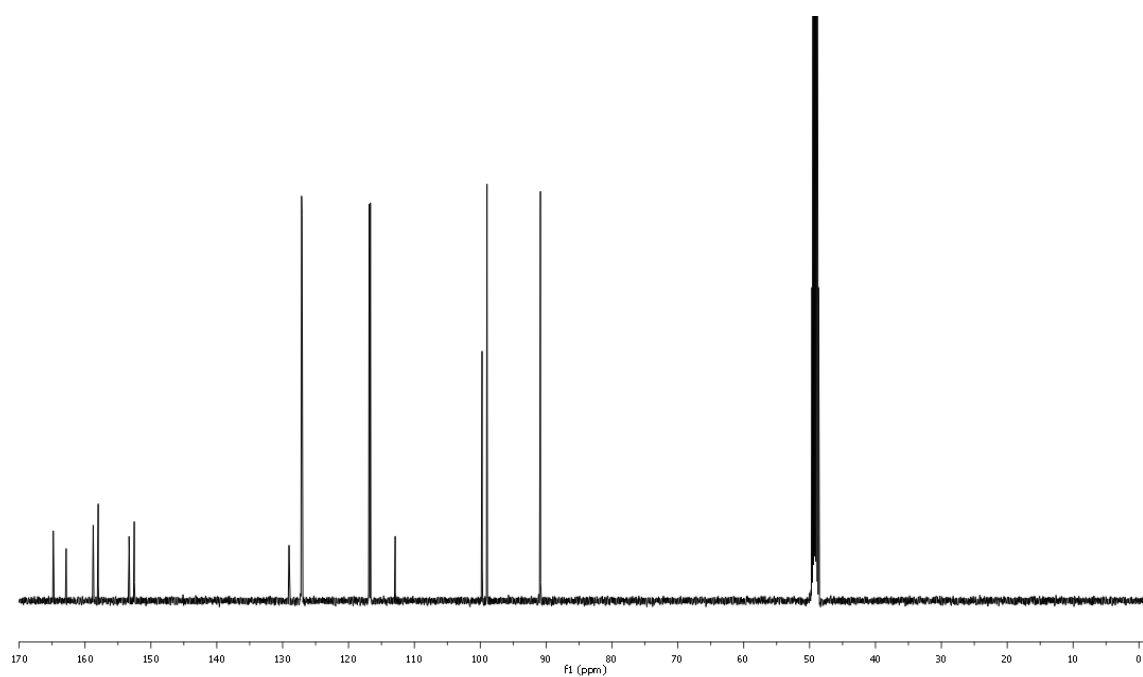


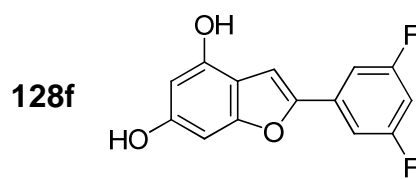


$^1\text{H-NMR}$ (DMSO- d_6)

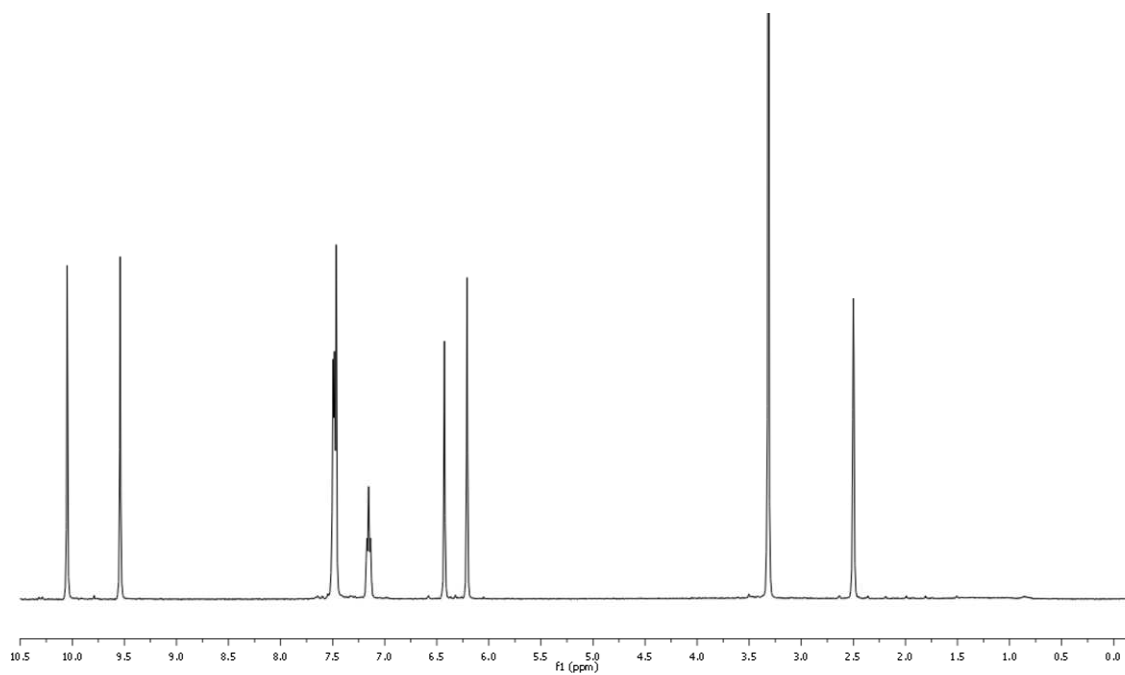


$^{13}\text{C-NMR}$ (CD_3OD)

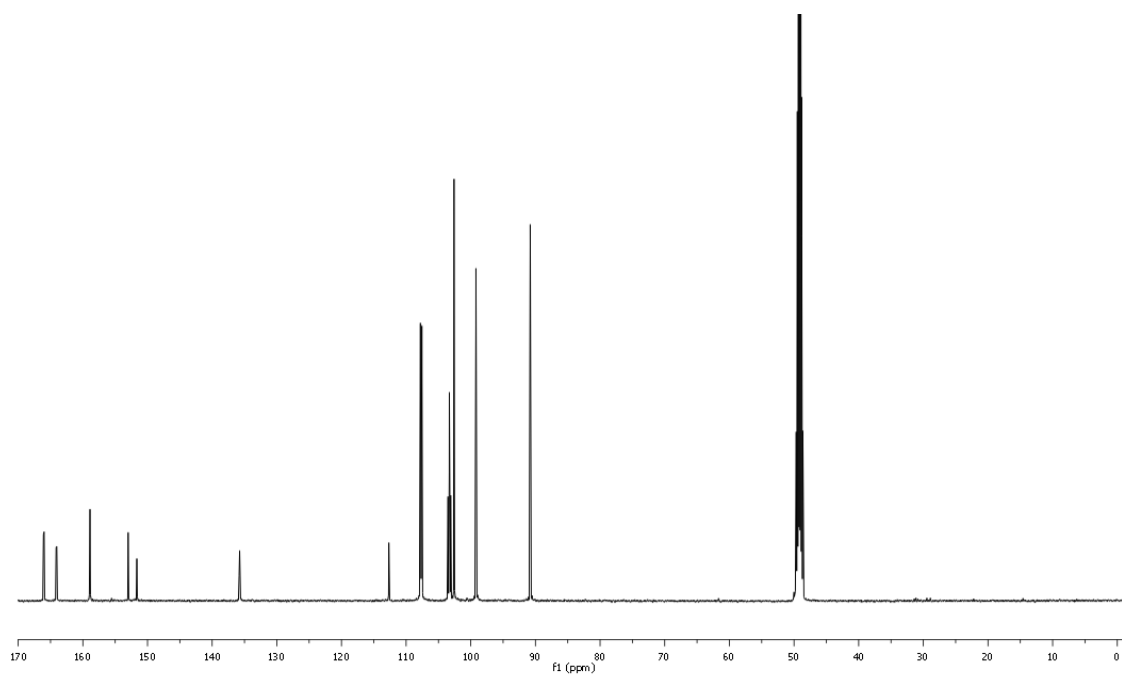




$^1\text{H-NMR}$ (DMSO-d_6)

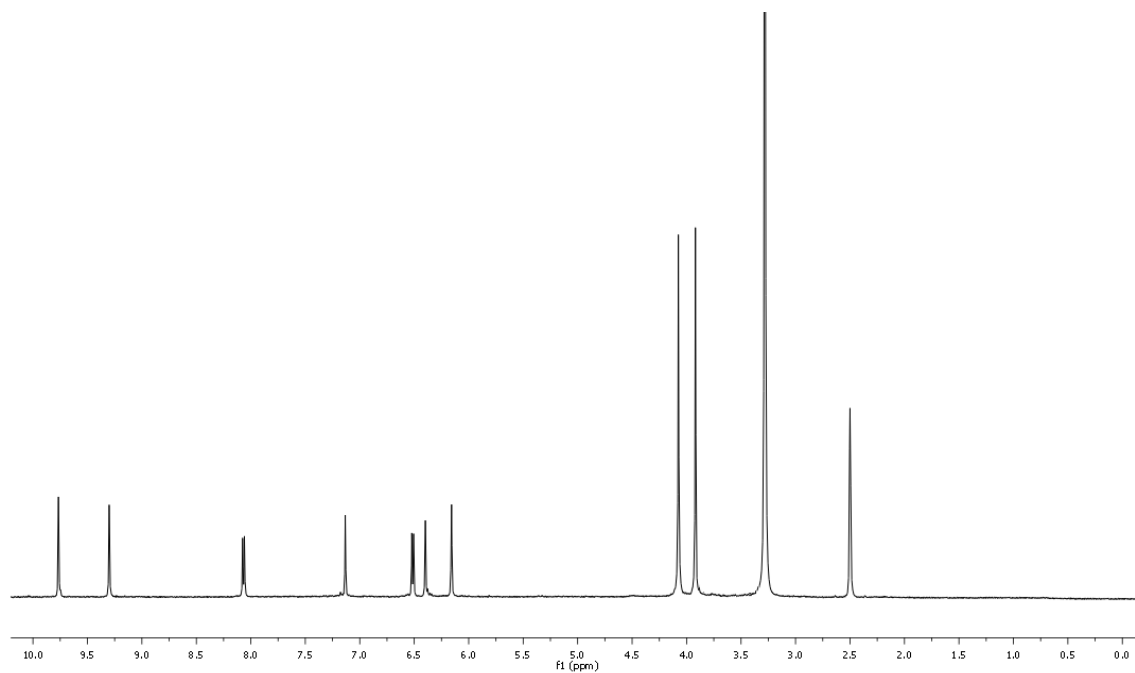


$^{13}\text{C-NMR}$ (CD_3OD)

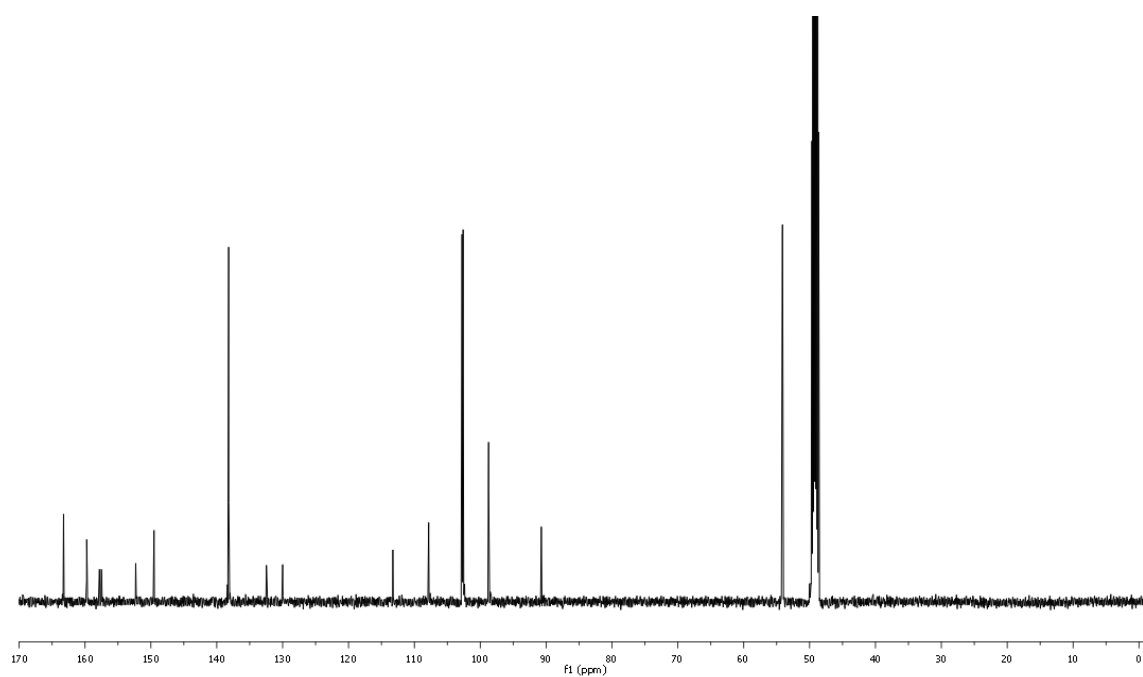


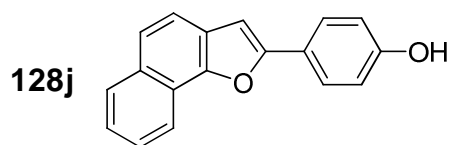


$^1\text{H-NMR}$ (DMSO- d_6)

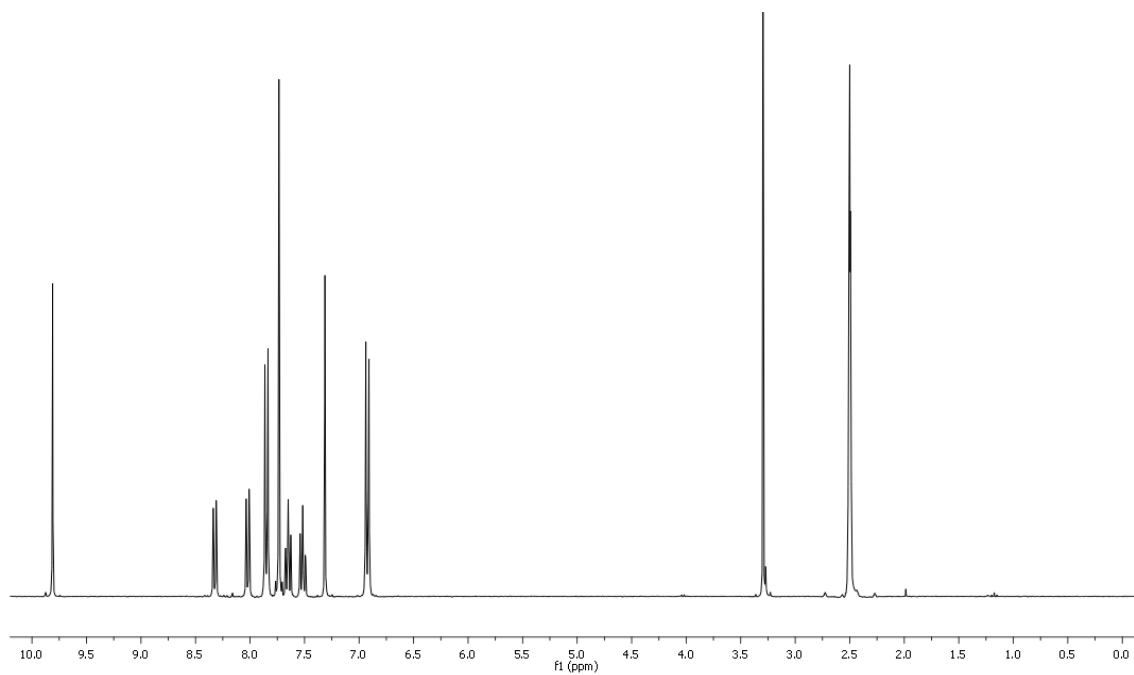


$^{13}\text{C-NMR}$ (CD_3OD)

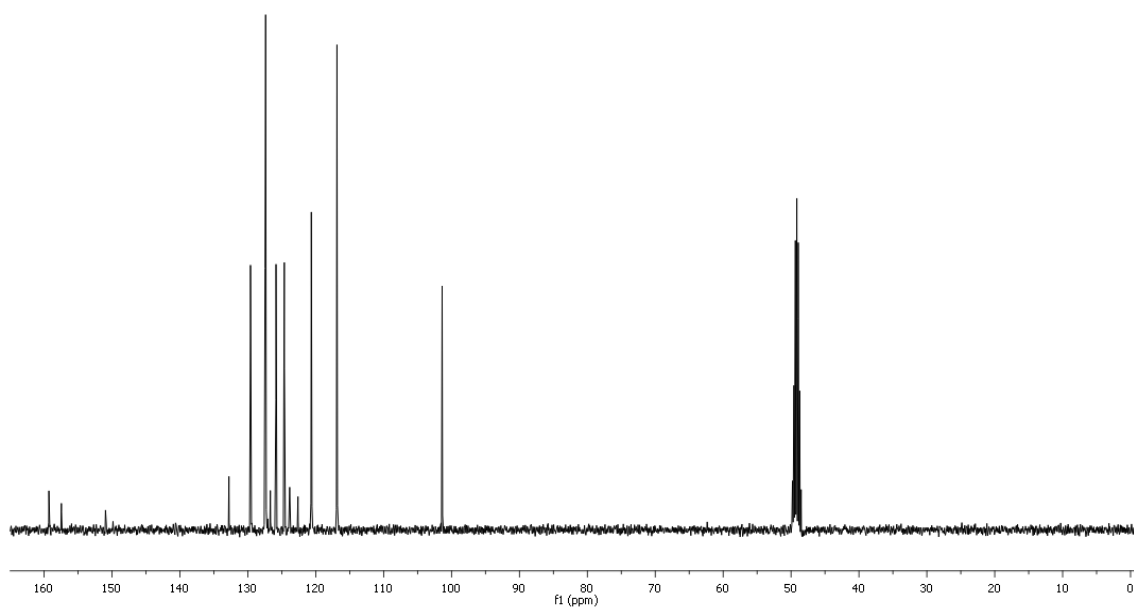


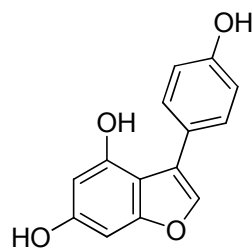
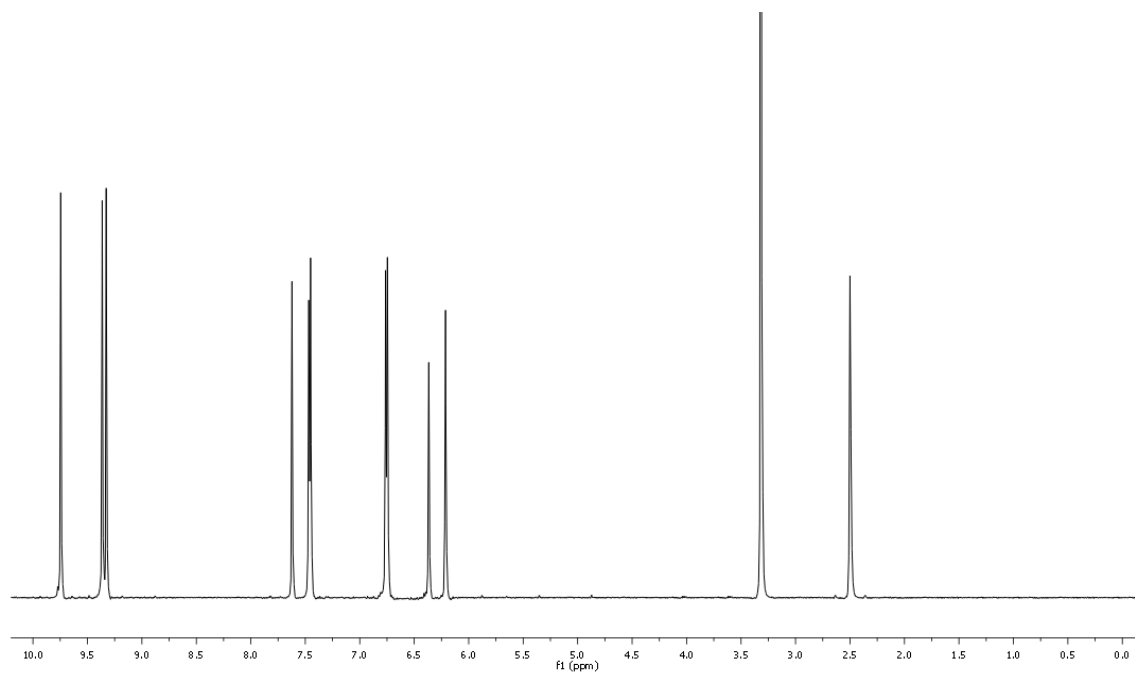
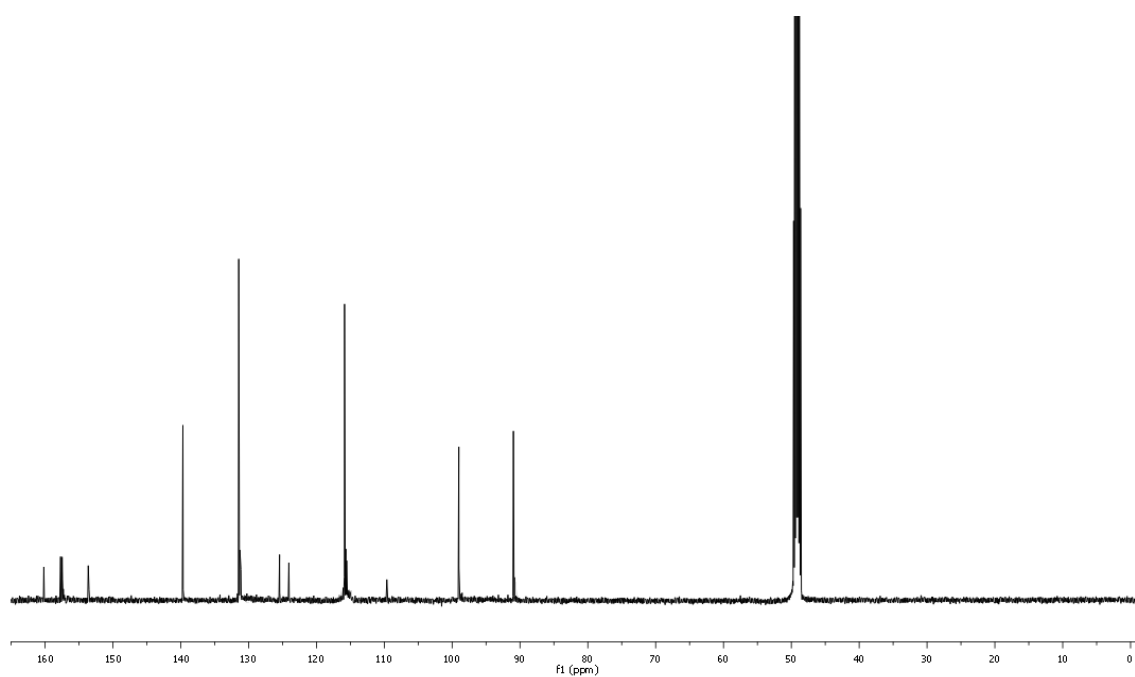


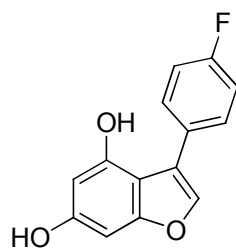
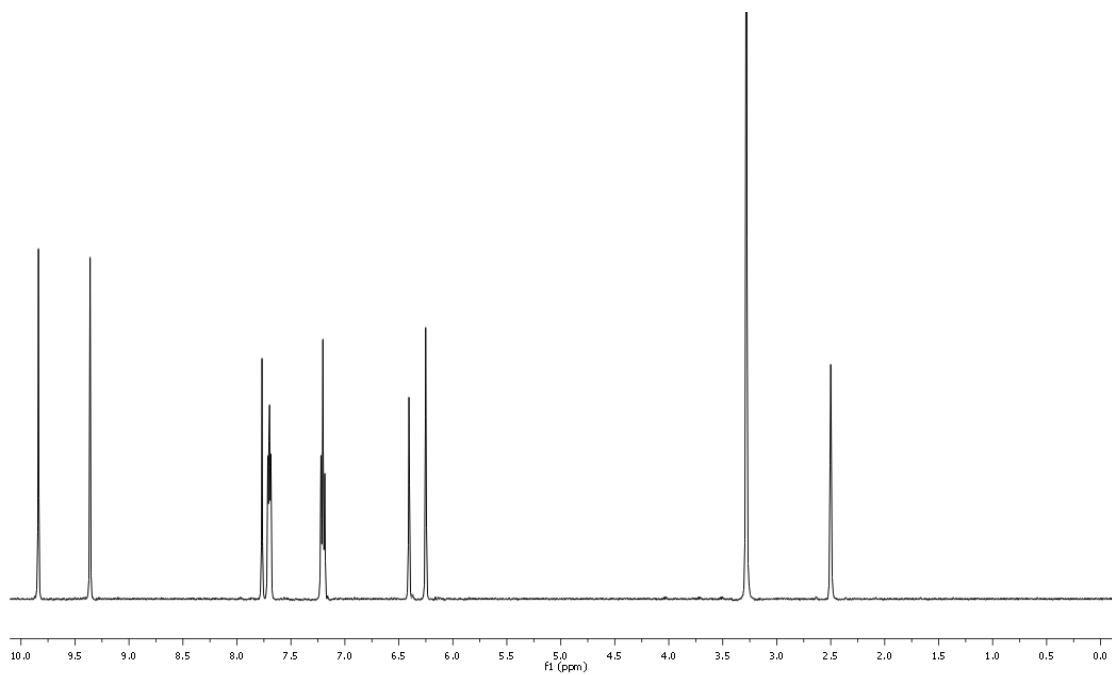
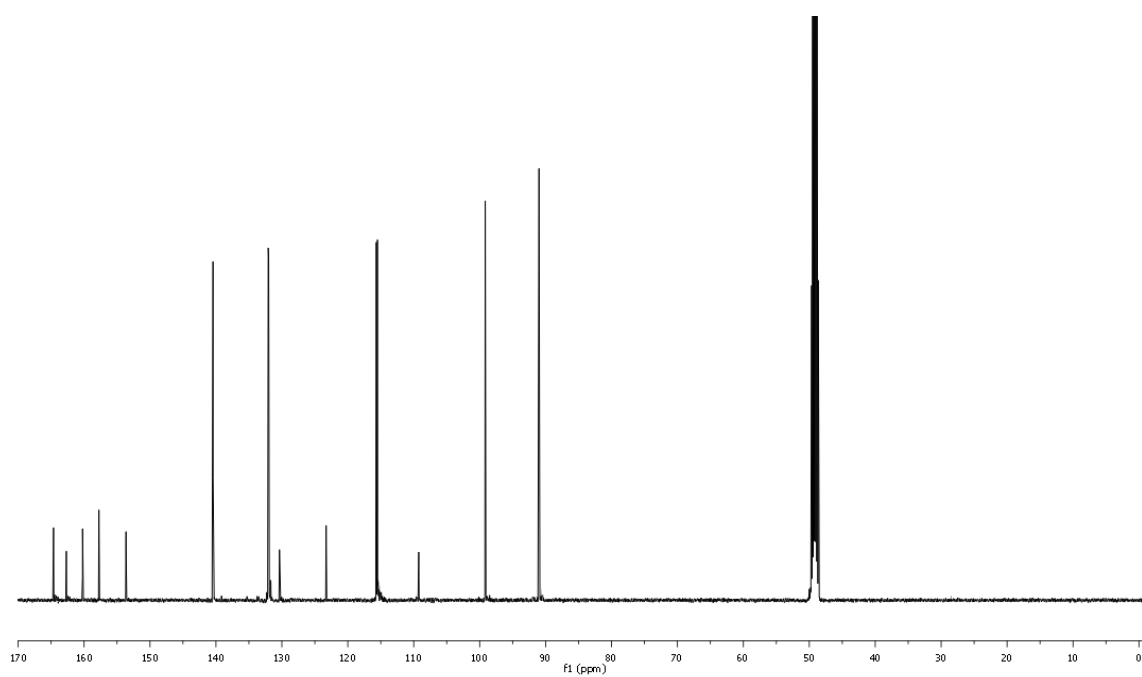
$^1\text{H-NMR}$ (DMSO- d_6)

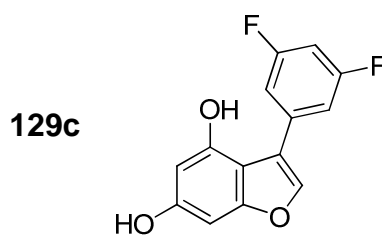


$^{13}\text{C-NMR}$ (CD_3OD)

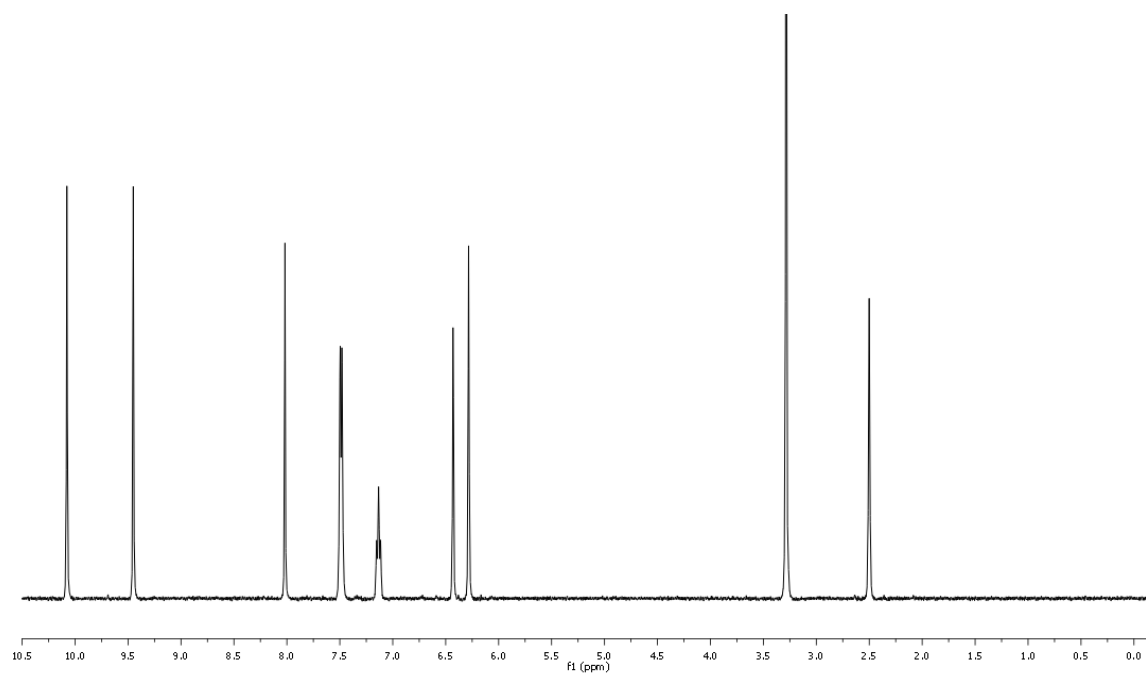


129a $^1\text{H-NMR}$ (DMSO-d_6) $^{13}\text{C-NMR}$ (CD_3OD)

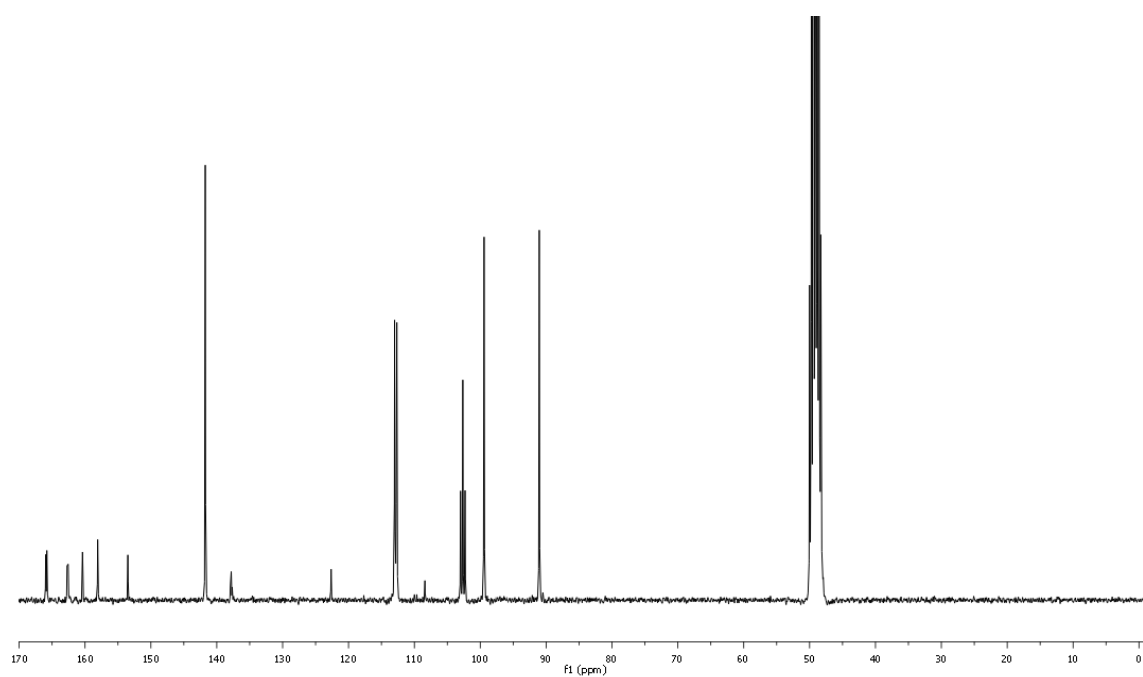
129b $^1\text{H-NMR}$ (DMSO- d_6) $^{13}\text{C-NMR}$ (CD_3OD)



$^1\text{H-NMR}$ (DMSO-d_6)



$^{13}\text{C-NMR}$ (CD_3OD)



5.6. CHARACTERIZATION REPORTS

5.6.1. X-ray diffraction analysis report of compound 124a

(124a is denoted as dendrilS35 in the report)



SERVICIO GENERAL RAYOS X Unidad de Moléculas y Materiales


☑ Servicios Generales de Investigación (SGIker)
Facultad de Ciencia y Tecnología, Edificio CD3
UPV/EHU.
B° Sarriena, s/n - 48940 Leioa (Bizkaia)

sgiker

Irakurtzeko Zentzu Orokorak
Servicio General de Investigación

Fax: 946013500
☎ 946015334, 946012599
✉ pablo.vitoria@ehu.es

Cristal: dendrilS35 **Técnico:** Pablo Vitoria **Fecha de la medida:** 5 Diciembre 2008

Datos Físicos y Cristalográficos		Condiciones de Registro y Afinamiento	
Fórmula	C ₁₇ H ₁₆ O ₄	Difractómetro	Xcalibur 2
M _r (g·mol ⁻¹)	284.3	Detector	CCD (Saphire 2)
Sistema cristalino	Triclinico	Temperatura (K)	297(2)
Grupo espacial	P-1	λ (MoKα) (Å)	0.71073
a (Å)	10.0851(4)	Monocromador	Grafito
b (Å)	10.1437(3)	Colimador (mm)	0.8
c (Å)	15.5003(7)	Modo de barrido	Rotación ω
α (°)	71.158(4)	Anchura de barrido (°)	1.0
β (°)	71.357(4)	Tiempo por placa (s) (Total, h)	45 (15)
γ (°)	87.168(3)	Intervalo de θ (°)	2.78-26.00
V (Å ³)	1419.40(10)	(hkl) mínimo	(-12 -12 -19)
Z	4 (Z'=2)	(hkl) máximo	(12 12 19)
F (000)	600	Reflexiones medidas	11862
μ (MoKα) (mm ⁻¹)	0.095	Reflexiones independientes (R _{int})	5547 (0.033)
D _x (g·cm ⁻³)	1.330(1)	Reflexiones observadas [I>2σ(I)]	2559
Morfología	Prisma	Corrección de absorción	Multi-scan
Color	Incoloro	Solución	Superflip
Tamaño (mm)	0.64x0.38x0.1	Refinamiento	SHELXL97
		Número de variables	386
		Número de restricciones	0
		Δ/σ máximo	0.001
		Δ/σ media	0.001
		Δρ máximo (eÅ ⁻³)	0.25
		Δρ mínimo (eÅ ⁻³)	-0.25
		S (GOF)	0.851
		R(F) (I>2σ _I , todos los datos)	0.0535, 0.1208
		R _w (F ²) ^[a] (I>2σ _I , todos los datos)	0.1104, 0.1309

[a] Esquema de pesado: $1/[\sigma^2(F_o^2) + (0.0690P)^2]$ donde $P = [\text{Max}(F_o^2, 0) + 2F_c^2]/3$.

Comentario:

La toma de datos se ha realizado a temperatura ambiente, puesto que los cristales parecían degradarse a baja temperatura.

Se confirma la estructura molecular propuesta por el usuario del servicio.

En la unidad asimétrica hay dos moléculas ($Z'=2$), y se ha adoptado una nomenclatura relacionada en ambas para facilitar la comparación. Ambas moléculas son prácticamente planas e idénticas, excepto por el sentido de rotación del grupo fenilo respecto al resto de la molécula, el cual está girado $19.98(9)$ y $19.19(9)^\circ$ en las moléculas 1 y 2. De hecho la diferencia cuadrática media (RMS) entre ambas en distancias y ángulos de enlace es de sólo 0.057 \AA y 0.29° , respectivamente

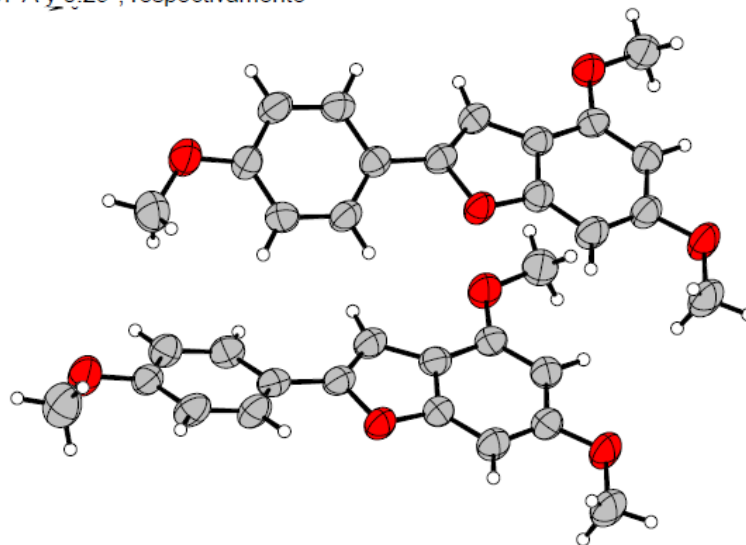
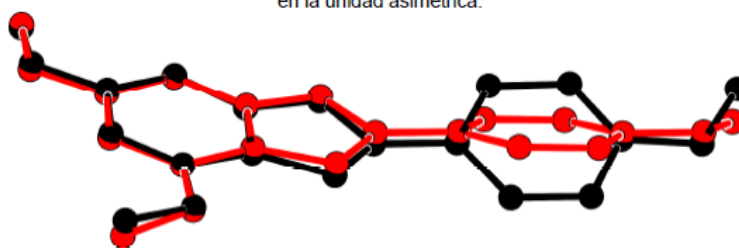
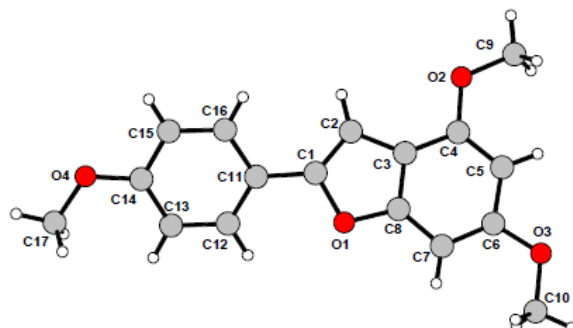


Diagrama ORTEP con los elipsoides térmicos al 50% de probabilidad de las dos moléculas ($Z'=2$) presentes en la unidad asimétrica.

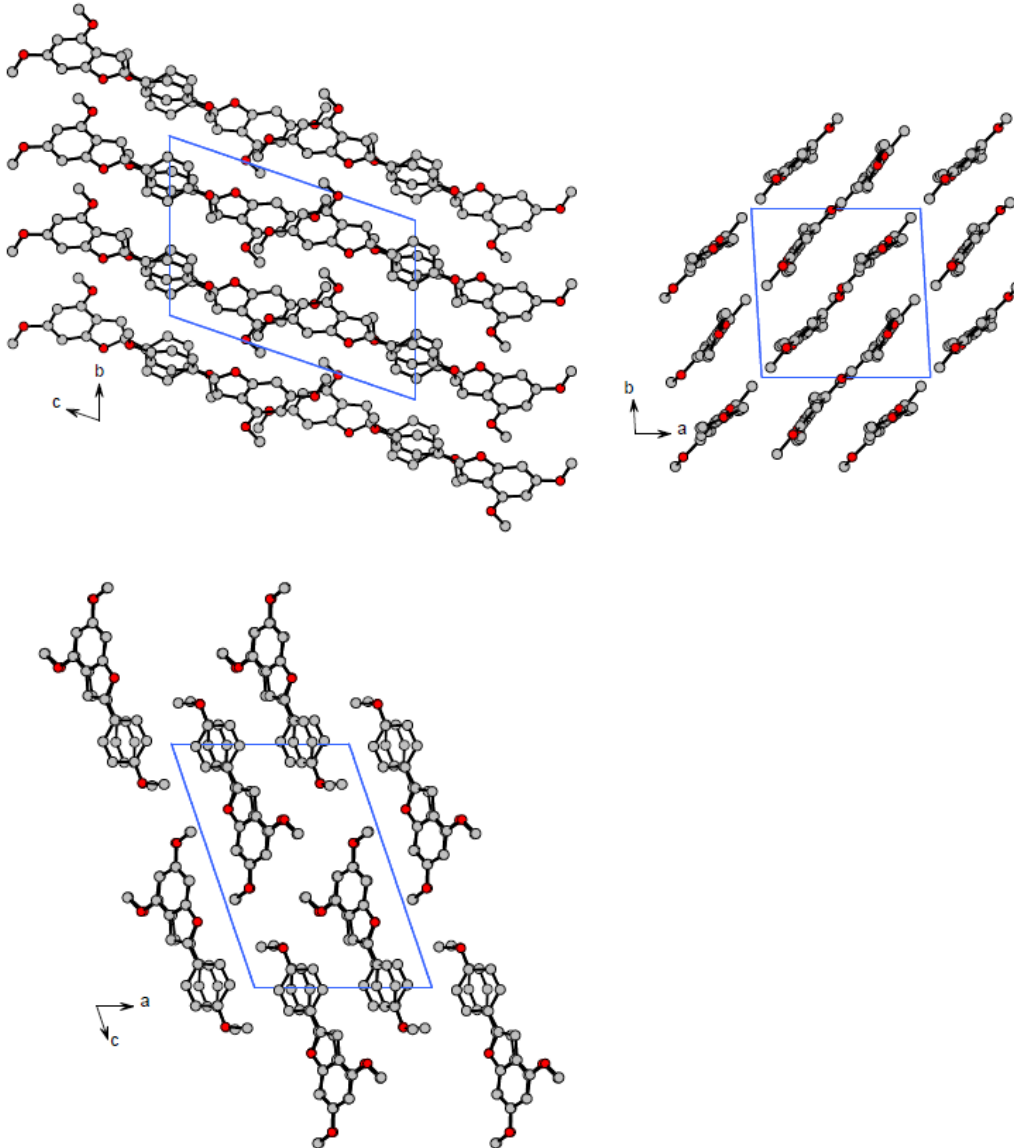


Superposición de las dos moléculas en la unidad asimétrica



Nomenclatura de la molécula 1. Para obtener el número de los átomos de la molécula 2 basta sumar 10 ó 20 para oxígeno o carbono, respectivamente.

En la estructura cristalina no se observan interacciones significativas entre las moléculas, las cuales forman capas con los planos moleculares paralelos.



Vistas de la estructura a lo largo de los ejes cristalinos.

Tabla 1. Distancias de enlace (Å)

<i>Molécula 1</i>		<i>Molécula 2</i>	
O1–C1	1.400(3)	O11–C21	1.394(3)
O1–C8	1.365(3)	O11–C28	1.368(3)
O2–C4	1.365(3)	O12–C24	1.363(3)
O2–C9	1.419(3)	O12–C29	1.422(3)
O3–C6	1.374(3)	O13–C26	1.369(3)
O3–C10	1.434(3)	O13–C30	1.435(3)
O4–C14	1.364(3)	O14–C34	1.365(3)
O4–C17	1.406(4)	O14–C37	1.412(4)
C1–C2	1.337(3)	C21–C22	1.340(3)
C1–C11	1.448(3)	C21–C31	1.450(3)
C2–C3	1.423(3)	C22–C23	1.428(3)
C3–C4	1.395(3)	C23–C24	1.395(3)
C3–C8	1.387(3)	C23–C28	1.389(3)
C4–C5	1.378(3)	C24–C25	1.374(3)
C5–C6	1.404(3)	C25–C26	1.409(3)
C6–C7	1.368(3)	C26–C27	1.374(3)
C7–C8	1.396(3)	C27–C28	1.386(3)
C11–C16	1.406(3)	C31–C36	1.397(3)
C11–C12	1.376(3)	C31–C32	1.387(3)
C12–C13	1.387(3)	C32–C33	1.383(3)
C13–C14	1.382(3)	C33–C34	1.373(3)
C14–C15	1.383(3)	C34–C35	1.394(3)
C15–C16	1.371(3)	C35–C36	1.371(3)

Tabla 2. Ángulos de enlace (°)

<i>Molécula 1</i>		<i>Molécula 2</i>	
C1–O1–C8	106.01(16)	C21–O11–C28	106.21(16)
C4–O2–C9	117.75(16)	C24–O12–C29	117.83(17)
C6–O3–C10	117.02(17)	C26–O13–C30	116.97(18)
C14–O4–C17	119.18(18)	C34–O14–C37	119.20(18)
O1–C1–C2	110.08(18)	O11–C21–C22	110.47(18)
C2–C1–C11	133.5(2)	O11–C21–C31	116.57(18)
O1–C1–C11	116.42(18)	C22–C21–C31	132.9(2)
C1–C2–C3	108.06(19)	C21–C22–C23	107.58(19)
C2–C3–C8	105.48(19)	C22–C23–C24	136.2(2)
C4–C3–C8	118.18(19)	C22–C23–C28	105.68(18)
C2–C3–C4	136.3(2)	C24–C23–C28	118.12(19)
O2–C4–C3	115.15(18)	O12–C24–C23	115.22(19)
O2–C4–C5	125.62(19)	O12–C24–C25	125.7(2)
C3–C4–C5	119.2(2)	C23–C24–C25	119.0(2)
C4–C5–C6	120.4(2)	C24–C25–C26	120.7(2)
O3–C6–C7	124.1(2)	O13–C26–C25	113.99(19)
C5–C6–C7	122.28(19)	O13–C26–C27	124.1(2)
O3–C6–C5	113.65(19)	C25–C26–C27	121.9(2)
C6–C7–C8	115.6(2)	C26–C27–C28	115.6(2)
C3–C8–C7	124.2(2)	O11–C28–C23	110.05(18)
O1–C8–C3	110.37(18)	O11–C28–C27	125.31(19)
O1–C8–C7	125.40(19)	C23–C28–C27	124.7(2)
C1–C11–C16	119.18(19)	C21–C31–C32	123.15(19)
C12–C11–C16	117.10(19)	C21–C31–C36	119.61(19)
C1–C11–C12	123.69(19)	C32–C31–C36	117.14(19)
C11–C12–C13	122.18(19)	C31–C32–C33	122.1(2)
C12–C13–C14	119.6(2)	C32–C33–C34	119.6(2)
O4–C14–C13	125.1(2)	O14–C34–C33	125.2(2)
O4–C14–C15	115.57(19)	O14–C34–C35	115.19(19)

C13–C14–C15	119.3(2)	C33–C34–C35	119.6(2)
C14–C15–C16	120.5(2)	C34–C35–C36	120.0(2)
C11–C16–C15	121.2(2)	C31–C36–C35	121.5(2)

Tabla 3. Ángulos de torsión (°)

<i>Molécula 1</i>		<i>Molécula 2</i>	
C8–O1–C1–C2	0.4(2)	C28–O11–C21–C31	–177.91(18)
C8–O1–C1–C11	178.69(18)	C21–O11–C28–C27	–178.6(2)
C1–O1–C8–C7	178.2(2)	C28–O11–C21–C22	–0.2(2)
C1–O1–C8–C3	–0.6(2)	C21–O11–C28–C23	0.9(2)
C9–O2–C4–C3	–174.9(2)	C29–O12–C24–C25	–0.7(3)
C9–O2–C4–C5	4.9(3)	C29–O12–C24–C23	179.4(2)
C10–O3–C6–C5	–178.3(2)	C30–O13–C26–C25	–172.0(2)
C10–O3–C6–C7	1.6(3)	C30–O13–C26–C27	8.2(3)
C17–O4–C14–C15	176.9(2)	C37–O14–C34–C35	178.3(2)
C17–O4–C14–C13	–3.8(3)	C37–O14–C34–C33	–0.6(3)
O1–C1–C11–C12	–19.1(3)	C22–C21–C31–C36	17.5(4)
C11–C1–C2–C3	–178.0(2)	O11–C21–C31–C36	–165.35(19)
O1–C1–C11–C16	162.98(19)	C22–C21–C31–C32	–158.6(2)
C2–C1–C11–C12	158.6(2)	O11–C21–C22–C23	–0.6(2)
C2–C1–C11–C16	–19.3(4)	C31–C21–C22–C23	176.6(2)
O1–C1–C2–C3	–0.1(3)	O11–C21–C31–C32	18.5(3)
C1–C2–C3–C8	–0.3(2)	C21–C22–C23–C24	–178.4(3)
C1–C2–C3–C4	177.8(3)	C21–C22–C23–C28	1.1(2)
C2–C3–C4–C5	179.1(2)	C22–C23–C28–O11	–1.3(2)
C2–C3–C4–O2	–1.1(4)	C28–C23–C24–C25	2.0(3)
C2–C3–C8–C7	–178.3(2)	C22–C23–C28–C27	178.2(2)
C4–C3–C8–O1	–177.95(18)	C24–C23–C28–C27	–2.2(3)
C8–C3–C4–C5	–3.1(3)	C28–C23–C24–O12	–178.12(19)
C4–C3–C8–C7	3.2(3)	C22–C23–C24–O12	1.3(4)
C8–C3–C4–O2	176.75(19)	C24–C23–C28–O11	178.35(19)
C2–C3–C8–O1	0.5(2)	C22–C23–C24–C25	–178.6(2)
O2–C4–C5–C6	–178.7(2)	C23–C24–C25–C26	–0.6(3)
C3–C4–C5–C6	1.1(3)	O12–C24–C25–C26	179.5(2)
C4–C5–C6–O3	–179.2(2)	C24–C25–C26–C27	–0.7(3)
C4–C5–C6–C7	0.9(3)	C24–C25–C26–O13	179.5(2)
C5–C6–C7–C8	–0.9(3)	C25–C26–C27–C28	0.6(3)
O3–C6–C7–C8	179.3(2)	O13–C26–C27–C28	–179.6(2)
C6–C7–C8–C3	–1.3(3)	C26–C27–C28–O11	–179.7(2)
C6–C7–C8–O1	–179.9(2)	C26–C27–C28–C23	0.9(3)
C12–C11–C16–C15	0.9(3)	C21–C31–C36–C35	–177.3(2)
C1–C11–C16–C15	179.0(2)	C32–C31–C36–C35	–0.9(3)
C1–C11–C12–C13	–179.0(2)	C21–C31–C32–C33	177.1(2)
C16–C11–C12–C13	–1.0(3)	C36–C31–C32–C33	0.8(3)
C11–C12–C13–C14	–0.4(3)	C31–C32–C33–C34	–0.7(3)
C12–C13–C14–C15	2.0(3)	C32–C33–C34–C35	0.7(3)
C12–C13–C14–O4	–177.3(2)	C32–C33–C34–O14	179.5(2)
C13–C14–C15–C16	–2.1(3)	O14–C34–C35–C36	–179.7(2)
O4–C14–C15–C16	177.2(2)	C33–C34–C35–C36	–0.8(3)
C14–C15–C16–C11	0.7(3)	C34–C35–C36–C31	0.9(3)

5.6.2. X-ray diffraction analysis report of compound 125a

(125a is denoted as iksr81 in the report)


SERVICIO GENERAL RAYOS X
Unidad de Moléculas y Materiales

✉ Servicios Generales de Investigación (SGIker)
 Facultad de Ciencia y Tecnología, Edificio CD3
 UPV/EHU.
 B° Sarriena, s/n - 48940 Leioa (Bizkaia)

sgiker

Barikuntzarako Zerbizuko Oinokorak
 Servicio General de Investigación
 Fax: 946013500
 ☎ 946015334, 946012599
 ✉ pablo.vitoria@ehu.es

Cristal: iksr81**Técnico:** Pablo Vitoria**Fecha de la medida:** 9 Junio 2009

Datos Físicos y Cristalográficos		Condiciones de Registro y Afinamiento	
Fórmula	<chem>C17H16O4</chem>	Difractómetro	Xcalibur 2
		Detector	CCD (Saphire 2)
		Temperatura (K)	100(1)
M_r (g·mol ⁻¹)	284.3	λ (MoK α) (Å)	0.71073
Sistema cristalino	Triclinico	Monocromador	Grafito
Grupo espacial	P-1	Colimador (mm)	0.8
a (Å)	7.2747(5)	Modo de barrido	Rotación ω
b (Å)	8.8758(5)	Anchura de barrido (°)	1.0
c (Å)	11.9601(9)	Tiempo por placa (s) (Total, h)	15 (8)
α (°)	109.342(6)	Intervalo de θ (°)	3.54-28.3
β (°)	105.211(6)	(hkl) mínimo	(-9 -11 -15)
γ (°)	92.871(5)	(hkl) máximo	(8 9 14)
V (Å ³)	695.13(9)	Reflexiones medidas	5537
Z	2 (Z'=1)	Reflexiones independientes (R_{int})	3448 (0.025)
F (000)	300	Reflexiones observadas [$I > 2\sigma(I)$]	2634
μ (MoK α) (mm ⁻¹)	0.097	Corrección de absorción	Multi-scan
D_x (g·cm ⁻³)	1.358(1)	Solución	SIR2004
Morfología	Prisma cortado	Refinamiento	SHELXL97
Color	Incoloro	Número de variables	193
Tamaño (mm)	0.51x0.27x0.22	Número de restricciones	0
		Δ/σ máximo	0.001
		Δ/σ media	0.000
		$\Delta\rho$ máximo (eÅ ⁻³)	0.37
		$\Delta\rho$ mínimo (eÅ ⁻³)	-0.26
		S (GOF)	0.977
		R(F) ($I > 2\sigma_i$, todos los datos)	0.0413, 0.0537
		$R_w(F^2)^{[a]}$ ($I > 2\sigma_i$, todos los datos)	0.1059, 0.1109

[a] Esquema de pesado: $1/[\sigma^2(F_o^2) + (0.0702P)^2]$ donde $P = [\text{Max}(F_o^2, 0) + 2F_c^2]/3$.

Detalles técnicos:

Las toma de datos se han realizado a una temperatura de 100K, usando un Cryostream 700 de Oxford Cryosystems alimentado con nitrógeno líquido.

Los átomos de hidrógeno se han localizado todos (incluidos los grupos metilo) en el mapa de densidad residual y se han refinado con el modelo *riding* de SHELXL97, con la geometría fijada a la ideal a 100K.

Puesto que el compuesto es un regioisómero de dendrilS35, se ha adoptado la misma nomenclatura de los átomos para facilitar comparaciones.

Comentario:

Se confirma la estructura molecular propuesta por el usuario del servicio.

El grupo 4,6-dimetoxibenzofurano es prácticamente plano, y el grupo metoxifenilo está girado $43.37(5)^\circ$ respecto a él.

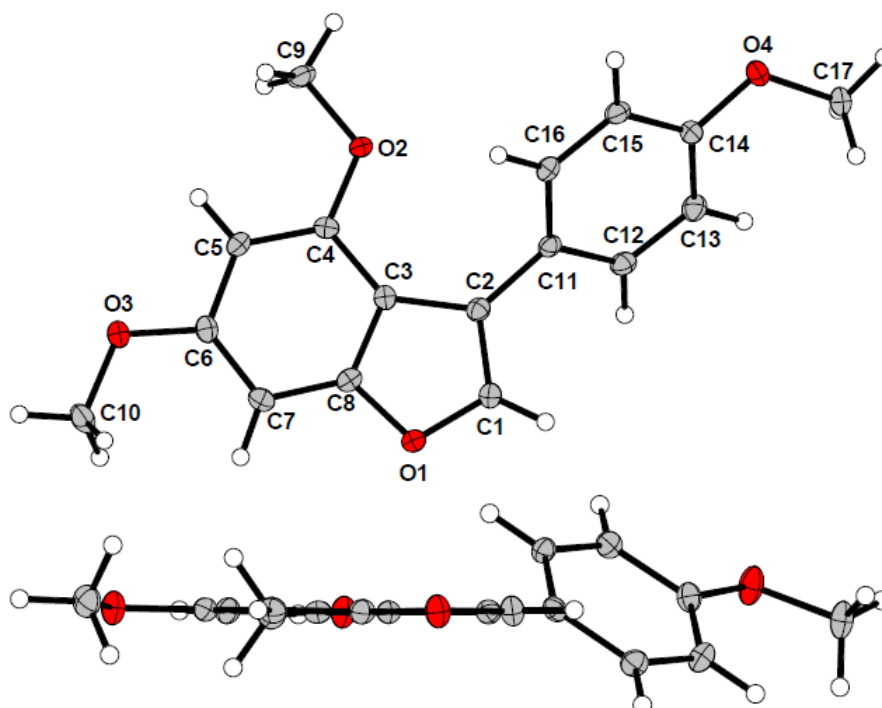
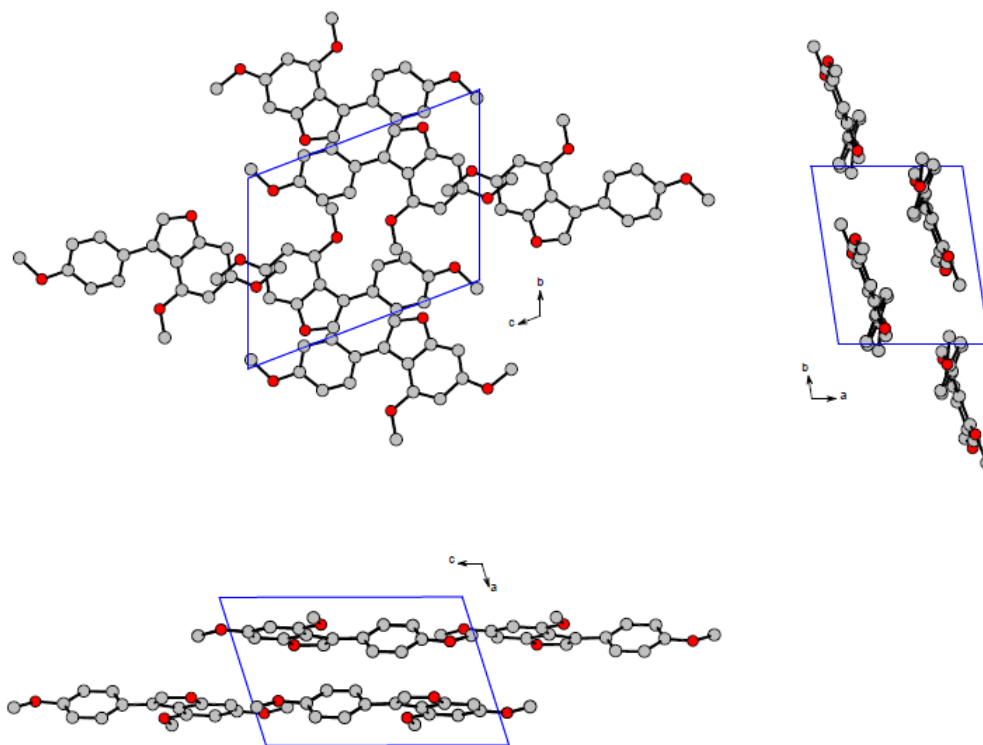


Diagrama ORTEP (vistas superior y frontal) con los elipsoides térmicos al 50% de probabilidad. Y nomenclatura de la molécula

En la estructura cristalina no se observan interacciones significativas entre las moléculas, las cuales forman capas con los planos moleculares paralelos.



Vistas de la estructura a lo largo de los ejes cristalinicos.

Tabla 1. Distancias de enlace (Å)

O1-C1	1.3776(14)	C3-C8	1.3954(17)
O1-C8	1.3718(15)	C4-C5	1.3800(16)
O2-C4	1.3626(14)	C5-C6	1.4094(17)
O2-C9	1.4311(15)	C6-C7	1.3816(18)
O3-C6	1.3653(14)	C7-C8	1.3893(17)
O3-C10	1.4295(15)	C11-C12	1.3970(17)
O4-C14	1.3736(14)	C11-C16	1.4009(17)
O4-C17	1.4305(15)	C12-C13	1.3930(17)
C1-C2	1.3500(18)	C13-C14	1.3919(18)
C2-C3	1.4538(17)	C14-C15	1.3946(17)
C2-C11	1.4759(17)	C15-C16	1.3802(17)
C3-C4	1.4134(17)		

Tabla 2. Ángulos de enlace (°)

C1-O1-C8	105.62(9)	O3-C6-C7	124.31(10)
C4-O2-C9	117.08(9)	C5-C6-C7	121.75(11)
C6-O3-C10	116.25(10)	C6-C7-C8	115.02(11)
C14-O4-C17	116.64(10)	O1-C8-C3	110.30(10)
O1-C1-C2	112.97(11)	O1-C8-C7	123.61(11)
C1-C2-C3	105.12(10)	C3-C8-C7	126.08(12)
C1-C2-C11	123.96(11)	C2-C11-C12	120.33(11)
C3-C2-C11	130.88(11)	C2-C11-C16	121.79(11)
C2-C3-C4	137.20(11)	C12-C11-C16	117.81(11)
C2-C3-C8	105.98(10)	C11-C12-C13	121.74(12)
C4-C3-C8	116.82(10)	C12-C13-C14	119.15(11)
O2-C4-C3	117.04(10)	O4-C14-C13	124.19(11)
O2-C4-C5	123.99(11)	O4-C14-C15	115.88(11)
C3-C4-C5	118.96(11)	C13-C14-C15	119.93(11)
C4-C5-C6	121.37(11)	C14-C15-C16	120.22(11)
O3-C6-C5	113.94(11)	C11-C16-C15	121.12(11)

Tabla 3. Ángulos de torsión (°)

C8-O1-C1-C2	-0.48(14)	C4-C3-C8-C7	-0.56(19)
C1-O1-C8-C7	-178.75(12)	C8-C3-C4-O2	179.65(11)
C1-O1-C8-C3	0.35(13)	C2-C3-C4-O2	0.3(2)
C9-O2-C4-C3	179.27(11)	C4-C3-C8-O1	-179.64(10)
C9-O2-C4-C5	-1.70(17)	C2-C3-C4-C5	-178.75(14)
C10-O3-C6-C5	-176.51(11)	C3-C4-C5-C6	-0.11(19)
C10-O3-C6-C7	3.77(17)	O2-C4-C5-C6	-179.11(11)
C17-O4-C14-C13	-15.39(18)	C4-C5-C6-C7	-0.46(19)
C17-O4-C14-C15	164.79(11)	C4-C5-C6-O3	179.80(11)
O1-C1-C2-C3	0.41(14)	C5-C6-C7-C8	0.48(18)
O1-C1-C2-C11	178.32(11)	O3-C6-C7-C8	-179.81(11)
C1-C2-C11-C16	-133.47(14)	C6-C7-C8-O1	178.99(11)
C11-C2-C3-C8	-177.88(12)	C6-C7-C8-C3	0.04(19)
C1-C2-C11-C12	43.41(18)	C2-C11-C16-C15	176.13(12)
C1-C2-C3-C4	179.20(14)	C12-C11-C16-C15	-0.83(18)
C1-C2-C3-C8	-0.17(14)	C2-C11-C12-C13	-175.21(12)
C11-C2-C3-C4	1.5(2)	C16-C11-C12-C13	1.79(19)
C3-C2-C11-C12	-139.25(14)	C11-C12-C13-C14	-1.04(19)
C3-C2-C11-C16	43.87(19)	C12-C13-C14-C15	-0.70(19)
C2-C3-C8-O1	-0.12(13)	C12-C13-C14-O4	179.48(12)
C8-C3-C4-C5	0.58(17)	O4-C14-C15-C16	-178.52(11)
C2-C3-C8-C7	178.96(12)	C13-C14-C15-C16	1.64(19)
		C14-C15-C16-C11	-0.86(19)

5.6.3. X-ray diffraction analysis report of compound *cis-170a*

(*cis-170a* is denoted as LAA043 in the report)



SERVICIO GENERAL RAYOS X Unidad de Moléculas y Materiales

✉ Servicios Generales de Investigación (SGIker)
Facultad de Ciencia y Tecnología, Edificio CD3
UPV/EHU.
B° Sarriena, s/n - 48940 Leioa (Bizkaia)

sgiker

Irakuntzerako Zerbiztu Osoak
Servicios Generales de Investigación

☎ 946015334, 946012599
Fax: 946013500
✉ pablo.vitoria@ehu.es

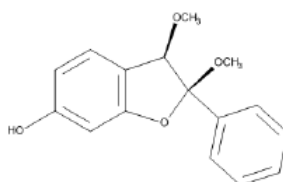
Cristales: LAA043 **Técnico:** Pablo Vitoria

Fecha de la medida: 23 de febrero de 2011

Comentario:

El usuario envió una muestra del compuesto LAA043 (un único cristal muy grande ligeramente amarillo, entregado en mezcla de cristalización hexanol/acetato de etilo) para determinar su estructura molecular. Puesto que el cristal era de gran tamaño ha sido necesario cortar un fragmento de tamaño aprox. $0,37 \times 0,22 \times 0,14$ mm³ para realizar la toma de datos

El usuario había propuesto un par de posibles estructuras moleculares, pero la estructura correcta no es ninguna de ellas, variando la posición de los grupos -OCH₃ (ver esquema molecular). El compuesto es quiral, pero la estructura cristalina determinada es centrosimétrica (grupo espacial P2₁/c), y por tanto ambos enantiómeros están presentes en el cristal (cristal racémico)

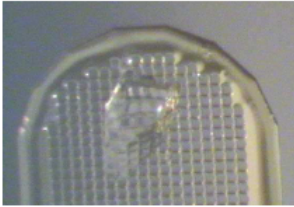


Detalles técnicos:

La toma de datos se ha realizado en el difractor Oxford Diffraction Xcalibur 2, equipado con detector de tipo CCD modelo Sapphire 2, a una temperatura de 100K, usando un Cryostream 700 de Oxford Cryosystems alimentado con nitrógeno líquido.

Todos los átomos se han refinado con parámetros térmicos (ADP) anisotrópicos, excepto los de hidrógeno, que se han localizado todos en el mapa de densidad residual y se han refinado con la geometría restringida a la ideal y los parámetros térmicos isotrópicos proporcionales a los del átomo al que están enlazados (modelo *riding* de SHELXL97).

Cristal LAA043

Datos Físicos y Cristalográficos		Condiciones de Registro y Afinamiento	
Fórmula	C ₁₆ H ₁₆ O ₄	Difractómetro	OD Xcalibur 2
M _r (g·mol ⁻¹)	272.29	Detector	CCD (Sapphire 2)
Sistema cristalino	Monoclínico	Temperatura (K)	100(1)
Grupo espacial	P2 ₁ /c	λ (MoKα) (Å)	0.71073
a (Å)	12.3139(5)	Monocromador	Grafito
b (Å)	9.1592(3)	Colimador (mm)	0.5
c (Å)	13.4356(6)	Modo de barrido	Rotación ω
α (°)	90	Anchura de barrido (°)	1.0
β (°)	113.465(5)	Tiempo por placa (s) (Total, h)	60 (8)
γ (°)	90	Intervalo de θ (°)	2.77-26.5
V (Å ³)	1390.03(10)	(hkl) mínimo	(-15 -10 -16)
Z	4 (Z'=1)	(hkl) máximo	(15 11 13)
F (000)	576	Reflexiones medidas	10117
μ (MoKα) (mm ⁻¹)	0.093	Reflexiones independientes (R _{int})	2890 (0.034)
D _x (g·cm ⁻³)	1.3011(1)	Reflexiones observadas [I>2σ(I)]	2251
Morfología	Prisma cortado	Corrección de absorción	Análítica (caras)
Color	Amarillo claro	Solución	SIR2004
Tamaño (mm)	0.37x0.22x0.14	Refinamiento	SHELXL97
		Número de parámetros	184
		Número de restricciones	0
		Δ/σ máximo	0.001
		Δ/σ media	0.000
		Δρ máximo (eÅ ⁻³)	0.35
		Δρ mínimo (eÅ ⁻³)	-0.25
		S (GOF)	1.005
		Coefficiente extinción secundaria ^[b]	0
		R(F) (I>2σ _i , todos los datos)	0.0371, 0.0477
		R _w (F ²) ^[a] (I>2σ _i , todos los datos)	0.0932, 0.0957

[a] Esquema de pesado: $1/[\sigma^2(F_o^2)+(0.0609P)^2]$ donde $P = [\text{Max}(F_o^2,0)+2F_o^2]/3$.

[b] Expresión de extinción secundaria tipo SHELXL: $F_o^* = kF_o[1+0.001F_o^2\lambda^3/\text{sen}(2\theta)]^{-1/4}$

Estructura molecular y cristalina de LAA043

En la unidad asimétrica de LAA043 hay una molécula del compuesto (Figura 1).

El anillo 3H-benzofuran-6-ol es prácticamente plano, ya que las mayores desviaciones respecto al plano medio son de sólo $-0.059(1)$ y $0.057(1)\text{\AA}$ para los átomos C2 y C3, respectivamente. Los dos grupos metoxi se encuentran en *cis* (Figura 2)

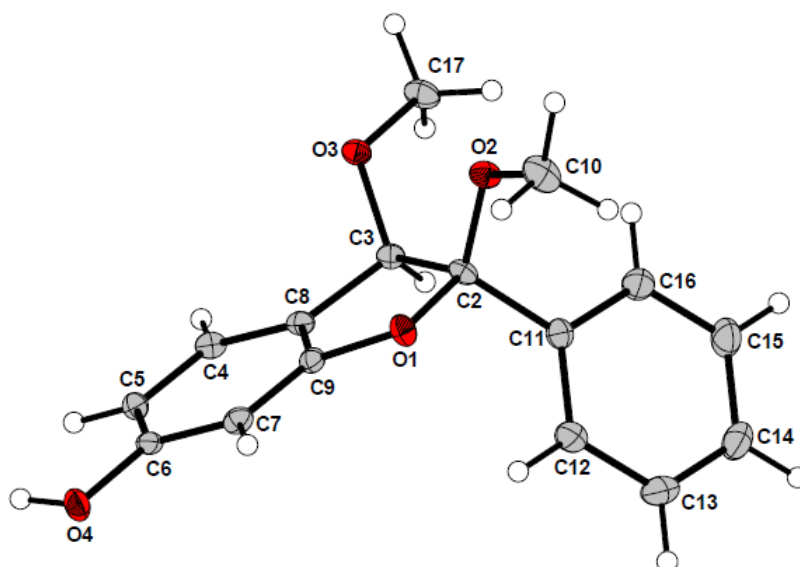


Figura 1. Diagrama ORTEP con los elipsoides térmicos al 50% de probabilidad de la molécula de LAA043 con la nomenclatura atómica utilizada.

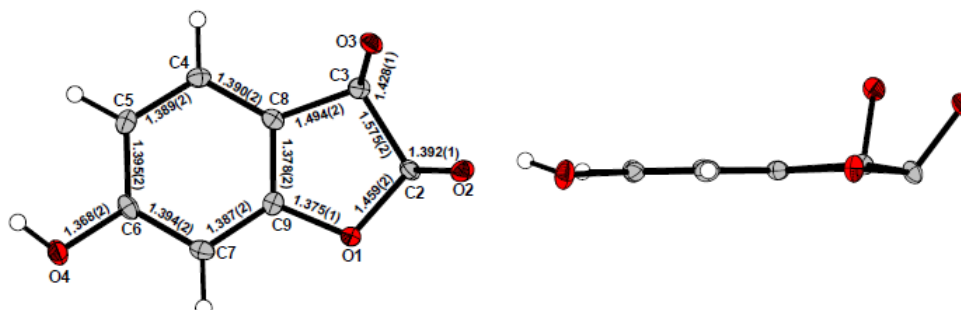


Figura 2. Vistas superior y frontal con detalle de las distancias de enlace (Å)

La única interacción intermolecular destacable (Tabla 4) es un enlace de hidrógeno $\text{O}-\text{H}\cdots\text{O}$ entre el grupo hidroxilo y el oxígeno O3 de uno de los grupos metoxi. El oxígeno del otro metoxi (O2) se haya a una distancia sólo ligeramente mayor del grupo hidroxilo, lo que podría dar lugar a un enlace de hidrógeno bifurcado; pero el hidrógeno localizado en el mapa de densidad residual apunta claramente a O3.

Los enlaces de hidrógeno dan lugar a cadenas helicoidales de moléculas a lo largo del eje cristalográfico y (b). (Figura 3)

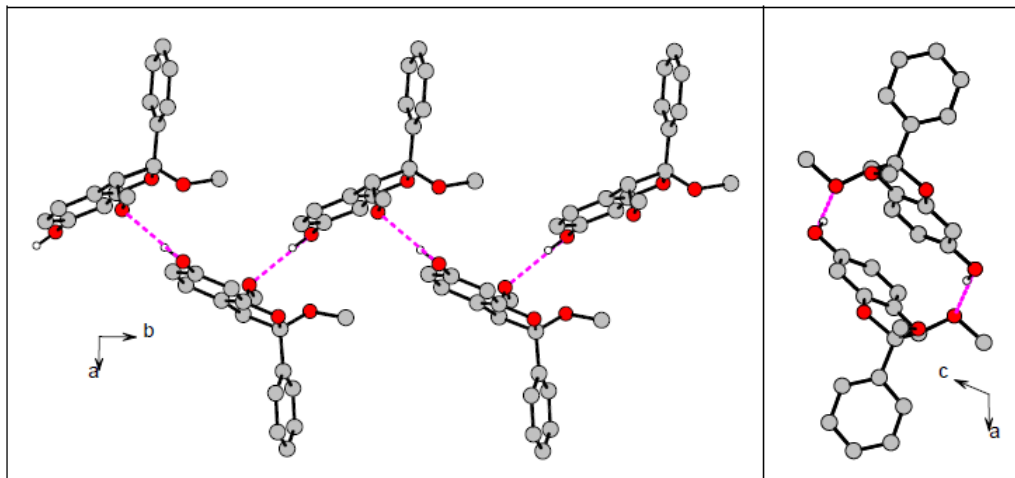


Figura 3. Vistas lateral (izada.) y frontal (dcha.) de las cadenas helicoidales formadas por enlaces de hidrógeno.

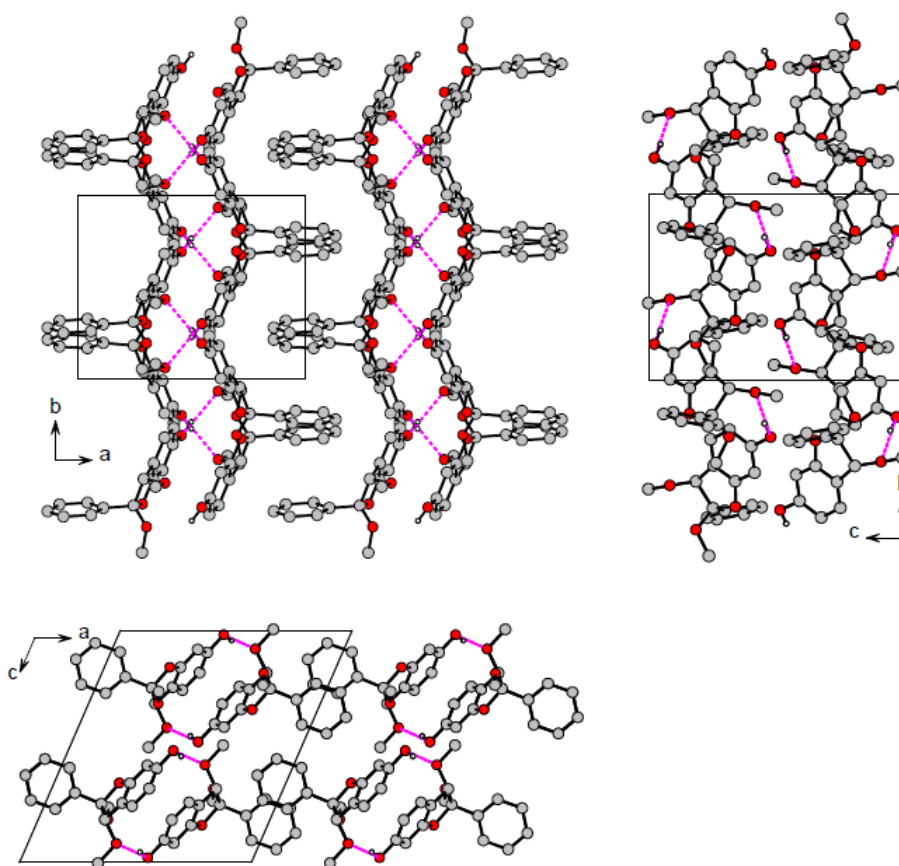


Figura 4. Vistas de la estructura cristalina de LAA043 a lo largo de los ejes cristalográficos. Los átomos de hidrógeno, excepto el del grupo hidroxilo, han sido eliminados por claridad.

Tabla 1. Distancias de enlace (Å)

O1–C2	1.4588(16)	C2–C11	1.521(2)	C8–C9	1.3778(17)
O1–C9	1.3752(15)	C2–C3	1.5746(17)	C11–C16	1.396(2)
O2–C2	1.3923(14)	C3–C8	1.4938(18)	C11–C12	1.3813(18)
O2–C10	1.4340(15)	C4–C5	1.3886(18)	C12–C13	1.396(2)
O3–C3	1.4277(15)	C4–C8	1.3904(17)	C13–C14	1.382(2)
O3–C17	1.4332(16)	C5–C6	1.3953(18)	C14–C15	1.384(2)
O4–C6	1.3676(16)	C6–C7	1.3937(18)	C15–C16	1.382(2)
O4–H4O	0.84	C7–C9	1.3869(18)		

Tabla 2. Ángulos de enlace (°)

C2–O1–C9	108.20(9)	C2–C3–C8	101.69(10)	O1–C9–C7	123.51(11)
C2–O2–C10	115.22(9)	O3–C3–C8	109.55(10)	C7–C9–C8	123.20(12)
C3–O3–C17	112.76(10)	C5–C4–C8	118.94(11)	O1–C9–C8	113.28(11)
C6–O4–H4O	109	C4–C5–C6	120.17(11)	C2–C11–C12	122.76(12)
O1–C2–C3	106.39(10)	O4–C6–C7	117.03(11)	C12–C11–C16	118.96(13)
O1–C2–C11	108.67(10)	C5–C6–C7	121.66(12)	C2–C11–C16	118.25(11)
O2–C2–C3	107.13(10)	O4–C6–C5	121.30(11)	C11–C12–C13	120.38(13)
O2–C2–C11	113.01(10)	C6–C7–C9	116.41(11)	C12–C13–C14	120.22(14)
C3–C2–C11	112.21(10)	C3–C8–C9	109.70(10)	C13–C14–C15	119.56(14)
O1–C2–O2	109.19(10)	C4–C8–C9	119.62(11)	C14–C15–C16	120.32(13)
O3–C3–C2	113.98(10)	C3–C8–C4	130.54(11)	C11–C16–C15	120.56(13)

Tabla 3. Ángulos de torsión (°)

C9–O1–C2–O2	122.94(10)	C2–C3–C8–C9	6.57(14)
C9–O1–C2–C3	7.63(13)	C2–C3–C8–C4	–177.84(13)
C9–O1–C2–C11	–113.39(10)	C5–C4–C8–C3	–176.26(13)
C2–O1–C9–C7	177.51(12)	C5–C4–C8–C9	–1.03(19)
C2–O1–C9–C8	–3.64(14)	C8–C4–C5–C6	0.73(19)
C10–O2–C2–C11	–62.36(14)	C4–C5–C6–O4	–178.83(12)
C10–O2–C2–O1	58.71(14)	C4–C5–C6–C7	0.2(2)
C10–O2–C2–C3	173.53(11)	O4–C6–C7–C9	178.28(11)
C17–O3–C3–C2	92.94(12)	C5–C6–C7–C9	–0.77(19)
C17–O3–C3–C8	–153.90(10)	C6–C7–C9–C8	0.47(19)
C11–C2–C3–O3	–131.96(11)	C6–C7–C9–O1	179.21(12)
O2–C2–C3–O3	–7.36(15)	C3–C8–C9–O1	–2.28(15)
O2–C2–C3–C8	–125.14(11)	C4–C8–C9–C7	0.4(2)
O1–C2–C11–C16	–167.59(11)	C3–C8–C9–C7	176.58(12)
O2–C2–C11–C12	136.13(12)	C4–C8–C9–O1	–178.43(11)
O2–C2–C11–C16	–46.23(15)	C2–C11–C12–C13	177.80(12)
C3–C2–C11–C12	–102.59(14)	C16–C11–C12–C13	0.18(19)
C3–C2–C11–C16	75.05(14)	C2–C11–C16–C15	–177.74(12)
C11–C2–C3–C8	110.27(11)	C12–C11–C16–C15	0.0(2)
O1–C2–C11–C12	14.77(15)	C11–C12–C13–C14	–0.2(2)
O1–C2–C3–C8	–8.45(12)	C12–C13–C14–C15	0.1(2)
O1–C2–C3–O3	109.33(11)	C13–C14–C15–C16	0.1(2)
O3–C3–C8–C9	–114.36(11)	C14–C15–C16–C11	–0.1(2)
O3–C3–C8–C4	61.24(17)		

Tabla 4. Posibles enlaces de hidrógeno (Å, °)

D–H...A	D–H	H...A	D...A	D–H...A
O4–H4O...O3'	0.84	2.04	2.8697(13)	169
O4–H4O...O2'	0.84	2.52	2.9436(13)	112
C4–H4...O4''	0.95	2.56	3.4382(15)	154
C12–H12...O1	0.95	2.41	2.7632(17)	101

Operaciones de simetría: (i) 1–x, –1/2+y, 1/2–z, (ii) x, –1/2–y, 1/2+z

5.6.4. X-ray diffraction analysis report of compound *trans*-170a

(*trans*-170a is denoted as LAA043B in the report)



SERVICIO GENERAL RAYOS X Unidad de Moléculas y Materiales

✉ Servicios Generales de Investigación (SGIker)
Facultad de Ciencia y Tecnología, Edificio CD3
UPV/EHU.
B° Sarriena, s/n - 48940 Leioa (Bizkaia)

sgiker

Heriotzarako Zentzu Orokorak
Servicio General de Investigación

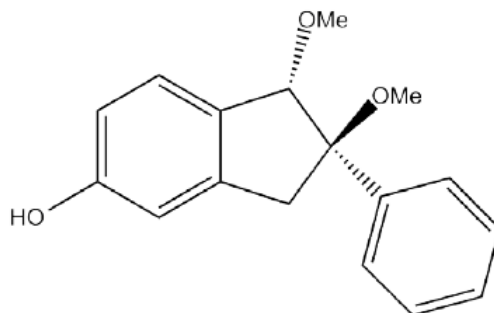
☎ 946013488
Fax: 946013500
✉ leire.sanfelices@ehu.es

Cristales: LAA043B **Técnico:** Leire San Felices
Fecha de la medida: 14 de Noviembre 2011

Comentario:

El usuario envió una muestra del compuesto LAA043B (prismas grandes incoloros) para determinar su estructura molecular. Los cristales eran grandes, pero se pudo seleccionar uno de ellos de tamaño 0,11x0,07x0,02 mm³ para realizar la toma de datos, sin necesidad de fragmentarlos.

Se confirma la estructura molecular que se muestra en la figura y coincide con la propuesta por el usuario. La estructura cristalina determinada presenta el grupo espacial P2₁/n.



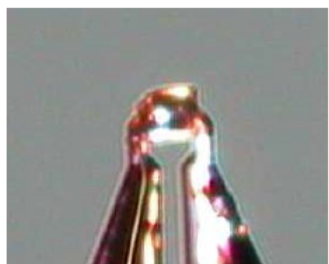
Detalles técnicos:

La toma de datos se ha realizado en el difractor Agilent SuperNova Cu, equipado con detector de tipo CCD modelo Atlas, a una temperatura de 100K, usando un Cryostream 700 de Agilent Cryosystems alimentado con nitrógeno líquido.

Todos los átomos se han refinado con parámetros térmicos (ADP) anisotrópicos, excepto los de hidrógeno, que se han localizado todos en el mapa de densidad residual y se han refinado con la geometría restringida a la ideal y los parámetros térmicos isotrópicos proporcionales a los del átomo al que están enlazados (modelo riding de SHELXL97).

Cristal LAA043B

Datos Físicos y Cristalográficos		Condiciones de Registro y Afinamiento	
Fórmula	C ₁₆ H ₁₆ O ₄	Difractómetro	Agilent SuperNova Cu
M _r (g·mol ⁻¹)	272.29	Detector	CCD (Atlas)
Sistema cristalino	Triclínico	Temperatura (K)	100(1)°
Grupo espacial	P-1	λ (CuKα) (Å)	1.54184
a (Å)	6.7539(4)	Monocromador	Óptica multicapa
b (Å)	9.7194(6)	Colimador (mm)	0.5
c (Å)	10.9633(5)	Modo de barrido	Rotación ω
α (°)	67.333(5)	Anchura de barrido (°)	1.0
β (°)	80.928(5)	Tiempo por placa (s) (Total, h)	8;32(20)
γ (°)	87.131(5)	Intervalo de θ (°)	4.42-69.96
V (Å ³)	655.73(6)	(hkl) mínimo	(-8 -11 -13)
Z	2 (Z'=1)	(hkl) máximo	(7 10 13)
F (000)	288	Reflexiones medidas	4896
μ (CuKα) (mm ⁻¹)	0.813	Reflexiones independientes (R _{int})	2480(0.020)
D _x (g·cm ⁻³)	1.379 (1)	Reflexiones observadas [I>2σ(I)]	2139
Morfología	Prisma	Corrección de absorción	Multi-scan
Color	incoloro	Solución	SIR92
Tamaño (mm)	0,11x0,07x0,02	Refinamiento	SHELXL97
		Número de parámetros	184
		Número de restricciones	0
		Δ/σ máximo	0.000
		Δ/σ media	0.000
		Δρ máximo (eÅ ⁻³)	0.199
		Δρ mínimo (eÅ ⁻³)	-0.24
		S (GOF)	1.043
		Coefficiente extinción secundaria ^[b]	0
		R(F) (I>2σ _I , todos los datos)	0.0348, 0.0414
		R _w (F ²) ^[a] (I>2σ _I , todos los datos)	0.0881, 0.0938



[a] Esquema de pesado: $1/[\sigma^2(F_o^2)+(0.0390P)^2]$ donde $P = [\text{Max}(F_o^2,0)+2F_o^2]/3$.

[b] Expresión de extinción secundaria tipo SHELXL: $F_o^* = kF_o^2[1+0.001F_o^2\lambda^3/\text{sen}(2\theta)]^{-1/4}$

Estructura molecular y cristalina de LAA043B

En la unidad asimétrica de LAA043B hay una molécula coincidente con la propuesta por el usuario (Figura 1). Además existe una molécula de metanol de cristalización.

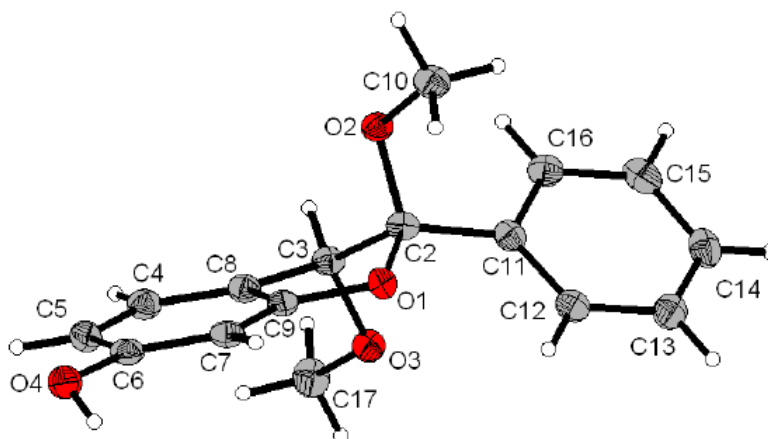
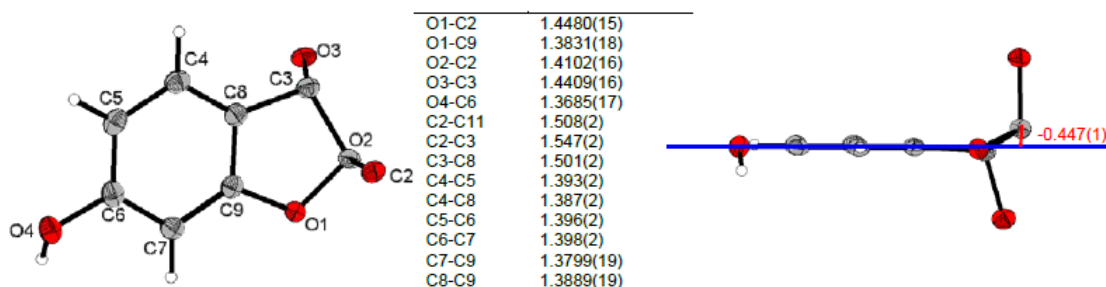


Figura 1. Vista del diagrama ORTEP con los elipsoides térmicos al 50% de probabilidad de la molécula (coincidente con la propuesta) presente en la estructura de LAA043B con la nomenclatura atómica utilizada.

Todos los átomos del anillo 3H-benzofuran-6-ol a excepción del átomo C2 se encuentran prácticamente en el mismo plano, siendo las mayores desviaciones respecto al plano medio de sólo 0.045(1) Å para el átomo C4 el resto de desviaciones del plano son en valor absoluto inferiores a 0.030(1) Å. El átomo C2 se desvía mucho del plano intermedio del resto de átomos del anillo siendo el valor de dicha distancia de -0.447(1) Å. Los dos grupos metoxi se encuentran en *trans* (Figura 2)

El empaquetamiento cristalino de la estructura a lo largo de los ejes cristalográficos a, b y c puede visualizarse en la figura 3.

La única interacción intermolecular destacable (Tabla 4) es un enlace de hidrógeno O–H...O entre el grupo hidroxilo y el oxígeno O3 de uno de los grupos metoxi. El oxígeno del otro metoxi (O2) se haya apuntando hacia el hidrogeno de uno de los carbonos asimétricos del anillo 3H-benzofuran-6-ol a una distancia ligeramente mayor que el enlace anterior dando lugar a un contacto de hidrogeno más débil.



Los enlaces de hidrógeno dan lugar a cadenas de moléculas a lo largo del eje cristalográfico z (c). (Figura 4) La cadenas se apilan en las direcciones de los otros dos ejes cristalográficos y están distanciadas entre ellas el valor del parámetro de dichos ejes

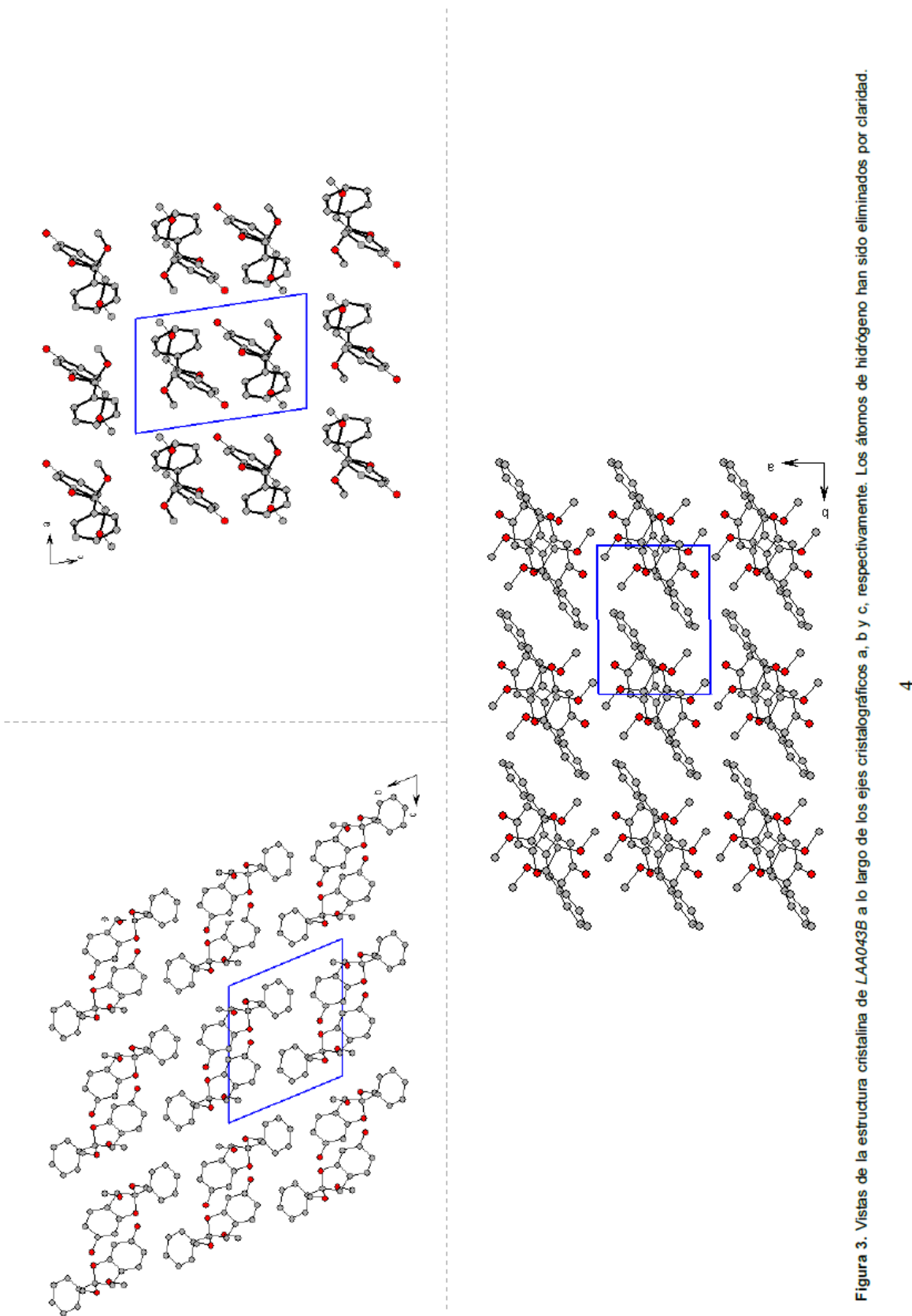


Figura 3. Vistas de la estructura cristalina de L-AA043B a lo largo de los ejes cristalográficos a, b y c, respectivamente. Los átomos de hidrógeno han sido eliminados por claridad.

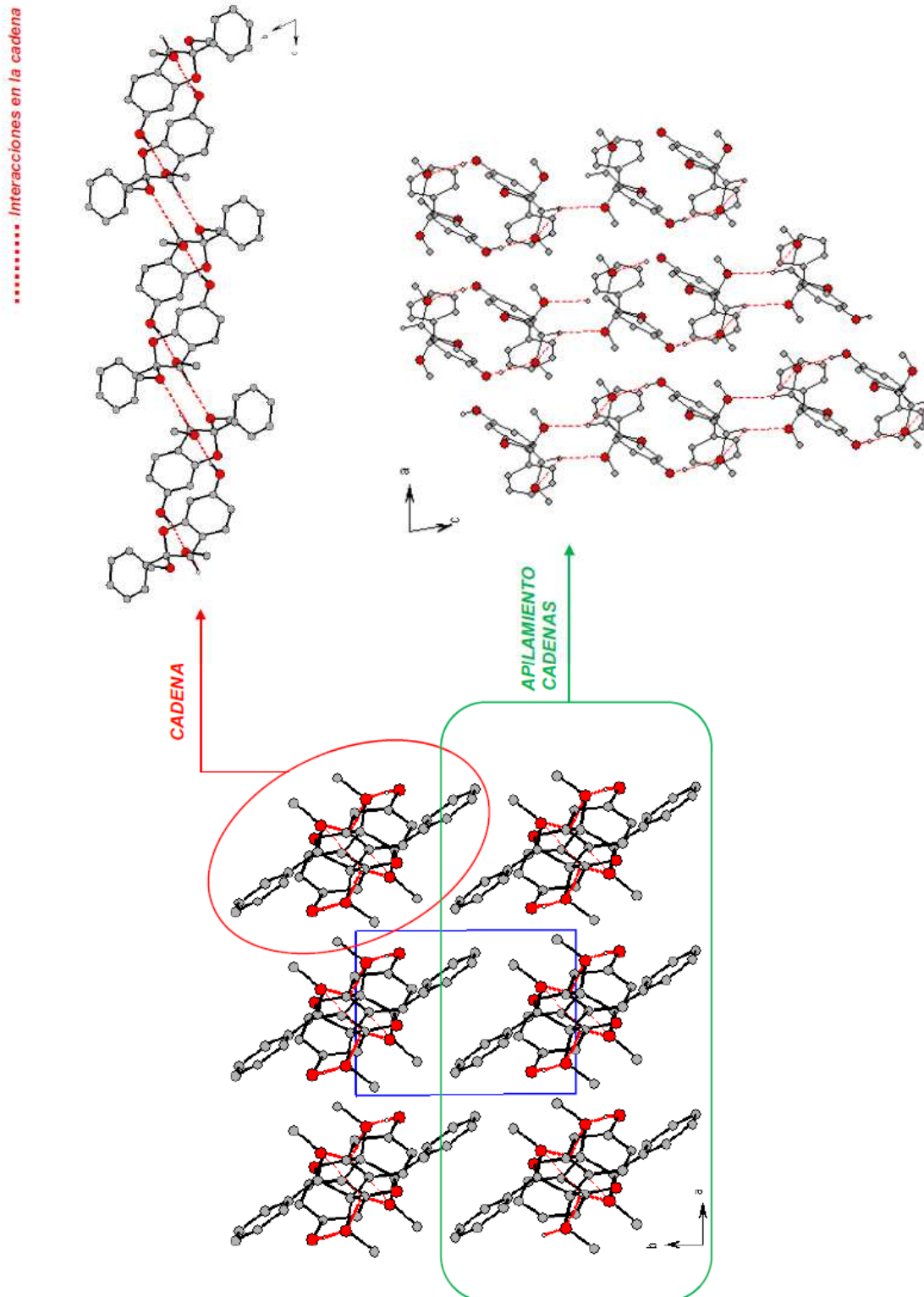


Figura 3. Visualización de las interacciones presentes en la estructura cristalina de NC011 con detalles de las cadenas y las capas formadas.

Tabla 1. Distancias de enlace (Å)

ÁTOMOS	DIST.(Å)	ÁTOMOS	DIST.(Å)
O1-C2	1.4480(15)	C4-C8	1.387(2)
O1-C9	1.3831(18)	C5-C6	1.396(2)
O2-C2	1.4102(16)	C6-C7	1.398(2)
O2-C10	1.4354(18)	C7-C9	1.3799(19)
O3-C3	1.4409(16)	C8-C9	1.3889(19)
O3-C17	1.4269(18)	C11-C16	1.3975(19)
O4-C6	1.3685(17)	C11-C12	1.3898(19)
C2-C11	1.508(2)	C12-C13	1.391(2)
C2-C3	1.547(2)	C13-C14	1.390(2)
C3-C8	1.501(2)	C14-C15	1.389(2)
C4-C5	1.393(2)	C15-C16	1.384(2)

Tabla 2. Ángulos de enlace (°)

ÁTOMOS	ANG.(°)	ÁTOMOS	ANG.(°)
O1-C9-C8	112.33(12)	C3-O3-C17	112.87(10)
O1-C9-C7	124.27(12)	C3-C2-C11	115.74(11)
O1-C2-O2	108.73(10)	C3-C8-C9	107.44(13)
O1-C2-C3	104.58(11)	C3-C8-C4	133.32(12)
O1-C2-C11	110.82(10)	C4-C5-C6	120.29(14)
O2-C2-C3	104.45(10)	C4-C8-C9	119.19(13)
O2-C2-C11	111.98(11)	C5-C4-C8	119.13(13)
O3-C3-C2	107.86(10)	C5-C6-C7	121.36(13)
O3-C3-C8	111.55(11)	C6-C7-C9	116.62(12)
O4-C6-C7	121.66(12)	C7-C9-C8	123.40(14)
O4-C6-C5	116.97(13)	C11-C16-C15	120.18(13)
C2-C11-C16	117.05(12)	C11-C12-C13	119.89(13)
C2-C11-C12	123.24(12)	C12-C11-C16	119.71(13)
C2-C3-C8	100.05(10)	C12-C13-C14	120.23(13)
C2-O1-C9	105.52(10)	C13-C14-C15	119.87(14)
C2-O2-C10	113.77(10)	C14-C15-C16	120.10(13)

Tabla 3. Ángulos de torsión (°)

ÁTOMOS	ANG.(°)	ÁTOMOS	ANG.(°)
O1-C2-C11-C12	12.18(18)	C4-C8-C9-O1	-179.21(11)
O1-C2-C11-C16	-168.57(11)	C4-C8-C9-O1	-179.21(11)
O1-C2-C3-C8	30.43(12)	C5-C4-C8-C3	175.71(14)
O1-C2-C3-O3	-86.25(11)	C5-C4-C8-C9	-1.1(2)
O2-C2-C11-C12	133.78(13)	C5-C6-C7-C9	-1.41(19)
O2-C2-C11-C16	-46.97(16)	C6-C7-C9-C8	0.50(19)
O2-C2-C3-C8	-83.76(11)	C6-C7-C9-O1	-179.54(12)
O2-C2-C3-O3	159.56(10)	C8-C4-C5-C6	0.2(2)
O3-C3-C8-C4	-83.80(18)	C9-O1-C2-C11	-155.26(10)
O3-C3-C8-C9	93.29(13)	C9-O1-C2-C3	-29.88(12)
O4-C6-C7-C9	-179.69(12)	C9-O1-C2-O2	81.25(12)
C2-C11-C12-C13	178.61(13)	C10-O2-C2-C11	-60.22(14)
C2-C11-C16-C15	-179.15(13)	C10-O2-C2-C3	173.79(10)
C2-C3-C8-C4	162.32(15)	C10-O2-C2-O1	62.57(14)
C2-C3-C8-C9	-20.59(13)	C11-C12-C13-C14	0.1(2)
C2-O1-C9-C7	-162.61(12)	C11-C2-C3-C8	152.64(11)
C2-O1-C9-C8	17.36(14)	C11-C2-C3-O3	35.96(14)
C3-C2-C11-C12	-106.66(14)	C12-C11-C16-C15	0.1(2)
C3-C2-C11-C16	72.60(15)	C12-C13-C14-C15	0.9(2)
C3-C8-C9-C7	-176.82(12)	C13-C14-C15-C16	-1.4(2)
C3-C8-C9-O1	3.21(15)	C14-C15-C16-C11	0.9(2)
C4-C5-C6-C7	1.1(2)	C16-C11-C12-C13	-0.6(2)
C4-C5-C6-O4	179.43(12)	C17-O3-C3-C2	-172.42(11)
C4-C8-C9-C7	0.8(2)	C17-O3-C3-C8	78.65(13)

Tabla 4. Posibles enlaces de hidrógeno (Å, °)

	<i>D—H...A</i>	<i>D—H</i>	<i>H...A</i>	<i>D...A</i>	<i>D—H...A</i>
<i>INTERACCIONES</i>	C10-H10A...O1	0.9800	2.4100	2.8227(17)	105.00
<i>INTRAMOLECULARES</i>	C12-H12...O1	0.9500	2.4700	2.8033(18)	101.00
<i>INTERACCIONES EN LA</i>	O4-H4...O3 ⁱ	0.8400	1.9800	2.8018(13)	167.00
<i>CADENA</i>	C3-H3...O2 ⁱⁱ	1.0000	2.4500	3.4420(15)	172.00

Operaciones de simetría: (i)= 1-x,-y,1-z; (ii)= 1-x,-y,2-z

5.6.5. HRMS report of *cis/trans* mixtures of compounds 170c and 170d

(170c and 170d are denoted as LAB001 and LAB002, respectively, in the report)



Servicio Central de Análisis de Bizkaia, Facultad de Ciencia y Tecnología
Barrio Sarriena s/n, 48940 Leioa-Bizkaia. C.I.F.: Q-4818001B

14.10.2009

SCAB.FR.01.PR.11.01

INFORME TÉCNICO DE RESULTADOS

Dra. Beatriz Abad García
Telf. (34) 94 601 31 97-
Fax: (34) 94 601 35 00

Leioa, 20 de Febrero de 2012

Cliente: Leire Arias
Técnica de medida: UPLC-DAD-QTOF
N Registro: 20111223182400
ID SGA: 1424-1425

ÍNDICE

1.	OBJETO DEL INFORME	2
2.	DESARROLLO DEL ESTUDIO	2
2.1.	REFERENCIA Y DESCRIPCIÓN DE LA MUESTRA	2
2.2.	FECHA DE RECEPCIÓN	2
2.3.	PERIODO DE ESTUDIO	2
2.4.	PERSONAL PARTICIPANTE	2
2.5.	EQUIPO INSTRUMENTAL	2
2.6.	RESUMEN DEL MÉTODO ANALÍTICO Y REFERENCIAS	2
3.	RESULTADOS	2
4.	DISCUSIÓN Y CONCLUSIÓN	4
5.	ANEXOS	4

Importante: La persona a quien se dirige el presente informe debe comunicar al servicio su conformidad con los resultados presentados en un plazo máximo de 15 días. Si transcurrido este tiempo, no se hubiese comunicado dicha conformidad, el servicio entenderá que se ha aceptado el informe completo.

En caso de que los datos recogidos en este informe sean utilizados para algún tipo de publicación científica, comunicación a congreso o tesis doctoral, deberá citarse la utilización del servicio en el apartado de agradecimientos con uno de los siguientes textos:

Los autores agradecen el apoyo técnico y humano de los SGiker (UPV/EHU, MICINN, GV/EJ, FSE).

SGIker technical and human support (UPV/EHU, MICINN, GV/EJ, ESF) is gratefully acknowledged.

1. OBJETO DEL INFORME

Determinación de la masa exacta del ión molecular protonado $[M+H]^+$.

2. DESARROLLO DEL ESTUDIO

2.1. REFERENCIA Y DESCRIPCIÓN DE LA MUESTRA

Referencia de la muestra: 1424

Descripción: vial transparente que contiene 8.0 mg del compuesto LAB001

Referencia de la muestra: 1425

Descripción: vial transparente que contiene 3.0 mg del compuesto LAB002

2.2. FECHA DE RECEPCIÓN

18/01/2012

2.3. PERIODO DE ESTUDIO

17/02/12

2.4. PERSONAL PARTICIPANTE

Dra. Beatriz Abad

2.5. EQUIPO INSTRUMENTAL

Cromatografía Líquida Ultrarápida (modelo UPLC ACQUITY de Waters) acoplado a un Detector de Fotodiodos (modelo PDA detector de Waters) un Espectrómetro de Masas de tipo QTOF (Synapt G2 de Waters).

2.6. RESUMEN DEL MÉTODO ANALÍTICO Y REFERENCIAS

Preparación de la muestra: Se prepara una disolución de cada compuesto de concentración 10 $\mu\text{g/mL}$ en acetonitrilo

Técnica:

- Fuente de ionización: ESI
- Modo de ionización positivo.
- Modo de barrido TOF MS^E
- Voltaje de cono 15 V. Función 1: Trap 6 eV y Transfer Off. Función 2: Trap rampa 20-30 eV y Transfer Off.

Calibrado: el equipo se calibra con formiato sódico introducido directamente en la fuente de ionización y se autocompensa la diferencia de masa durante la adquisición empleando como lockmass leucina enkephalin.

3. RESULTADOS

Las muestra introdujeron el Espectrómetro de Masas a través cromatografía líquida utilizando para este fin una columna Acquity UPLC BEH C18 1.7 μ m 50 x 2.1 mm y como fases móviles: A. H₂O:HCOOH (99.9:0.1, v/v) y B. MeOH:HCOOH (99.9:0.1, v/v). El gradiente usado fue: 0-2.5 min, gradiente de 5 a 100 % B; 2.5-4.0 min, isocrático 100 % B; 4.0-4.1 min, gradiente de 100 a 5 %B; 4.1-5 min, isocrático 5%B. El volumen de inyección fue de 1 μ L. La columna se termostató a 30° C y el inyector a 10 °C.

Muestra	Fórmula	Masa exacta detectada	Masa exacta teórica	mDa	ppm
LAB001	C20H25O4	329.1765	329.1753	1.2	3.6
LAB002	C22H29O4	357.2063	357.2066	-0.3	-0.8

NOTA: en cromatografía líquida acoplada a la espectrometría de masas la formación de aductos con Na es frecuente. El Na procede del vidrio de los viales o de los disolventes utilizados y es imposible evitarlo. La tendencia a formar $[M+Na]^+$ depende de la molécula analizada.

En Leioa, a 20 de Febrero de 2012



Servicio Central de Análisis de Bizkaia, Facultad de Ciencia y Tecnología
Barrio Sarriena s/n, 48940 Leioa-Bizkaia. C.I.F.: Q-4818001B

14.10.2009

SCAB.FR.01.PR.11.01

4. DISCUSIÓN Y CONCLUSIÓN

“No aplica”

5. ANEXOS



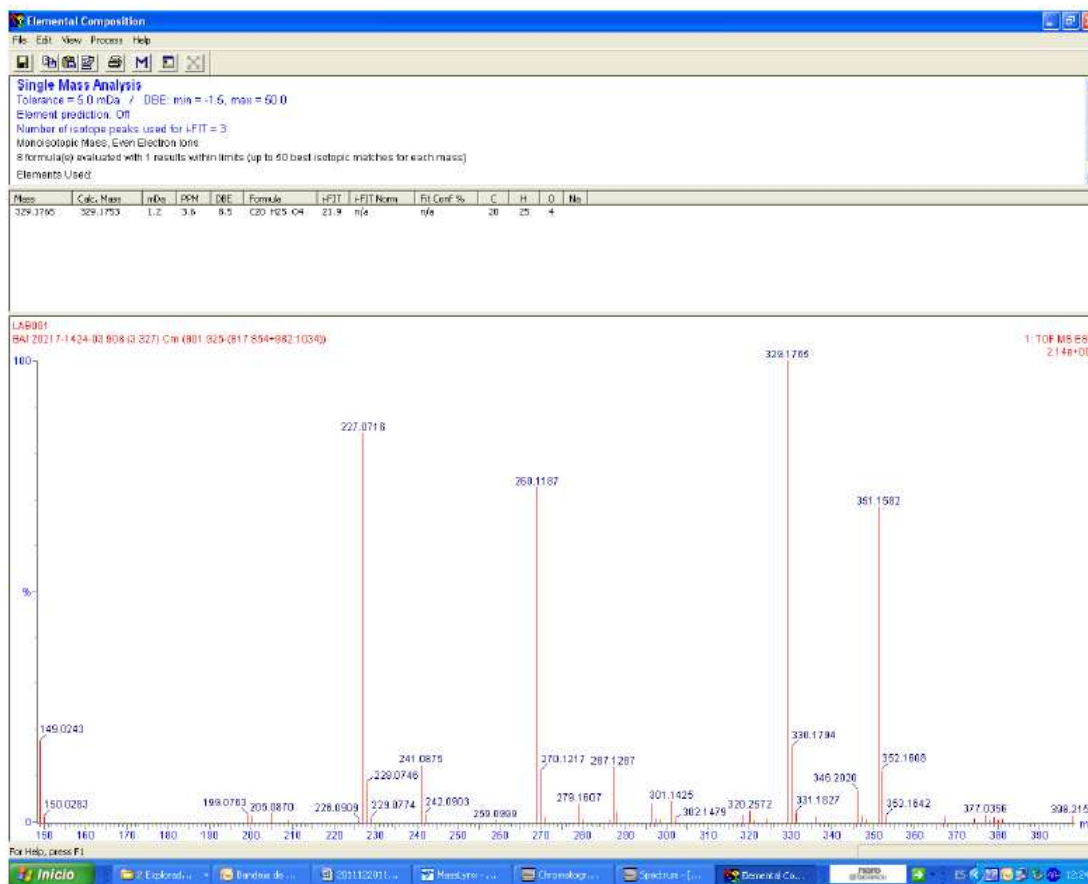
Servicio Central de Análisis de Bizkaia, Facultad de Ciencia y Tecnología
 Barrio Sarriena s/n, 48940 Leioa-Bizkaia. C.I.F.: Q-4818001B

14.10.2009

SCAB.FR.01.PR.11.01

LAB001

Composición elemental





Universidad Euskal Herriko
del País Vasco Unibertsitatea

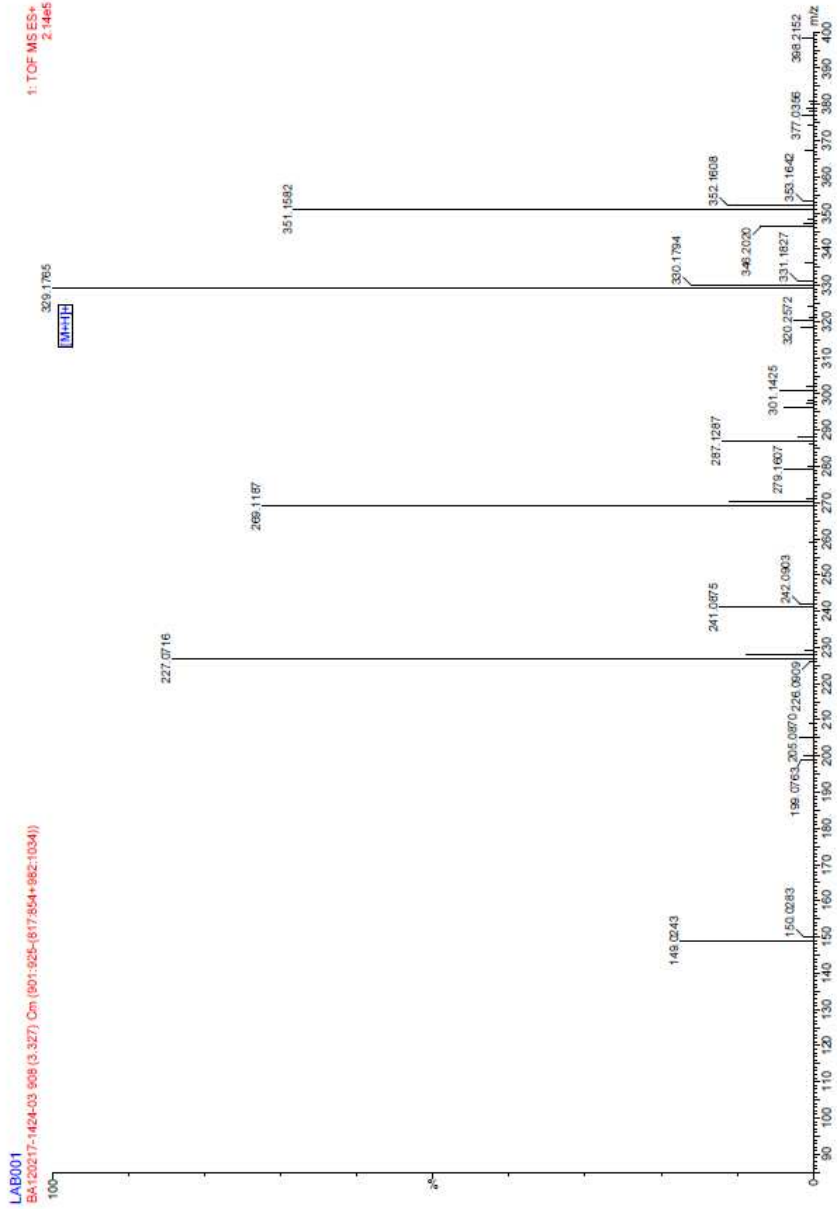


sgiker
SERVICIO CENTRAL DE ANÁLISIS QUÍMICOS
DE INVESTIGACIÓN

Servicio Central de Análisis de Bizkaia, Facultad de Ciencia y Tecnología
Barrio Sarrrena s/n, 48940 Leioa-Bizkaia. C.I.F.: Q-4818001B

14.10.2009 SCAB.FR.01.PR.11.01

Espectro de masas





Servicio Central de Análisis de Bizkaia, Facultad de Ciencia y Tecnología
Barrio Sarriena s/n, 48940 Leioa-Bizkaia. C.I.F.: Q-4818001B

14.10.2009

SCAB.FR.01.PR.11.01

Listado de masas

LAB001

BA120217-1424-03 908 (3.327) Cm (901:925-(817:854+982:1034))

1: TOF MS ES+

No	Mass	Inten	%BPI	%TIC	No	Mass	Inten	%BPI	%TIC	No	Mz
1:	149.0243	3.74e4	17.44	2.93	59:	346.2020	1.47e4	6.87	1.15		
2:	150.0283	2.56e3	1.20	0.20	60:	347.2052	2.70e3	1.26	0.21		
3:	177.0924	6.38e2	0.30	0.05	61:	348.1474	1.30e3	0.61	0.10		
4:	199.0763	3.30e3	1.54	0.26	62:	348.2089	7.15e2	0.33	0.06		
5:	200.0820	3.70e2	0.17	0.03	63:	348.6534	6.01e2	0.28	0.05		
6:	200.2022	2.70e3	1.26	0.21	64:	351.1582	1.46e5	68.25	11.46		
7:	201.2045	3.87e2	0.18	0.03	65:	352.1608	2.40e4	11.22	1.88		
8:	204.5761	2.46e2	0.12	0.02	66:	353.1642	2.62e3	1.22	0.21		
9:	205.0870	3.93e3	1.83	0.31	67:	363.2238	3.27e2	0.15	0.03		
10:	206.0905	5.58e2	0.26	0.04	68:	365.1144	5.79e2	0.27	0.05		
11:	209.0805	8.13e2	0.38	0.06	69:	367.1303	2.26e3	1.05	0.18		
12:	222.1824	2.73e2	0.13	0.02	70:	368.1391	3.70e2	0.17	0.03		
13:	226.0909	8.30e2	0.39	0.07	71:	369.0420	5.62e2	0.26	0.04		
14:	227.0716	1.81e5	84.30	14.15	72:	374.2324	1.52e3	0.71	0.12		
15:	228.0746	1.89e4	8.81	1.48	73:	375.2340	2.61e2	0.12	0.02		
16:	229.0774	2.18e3	1.02	0.17	74:	376.2334	2.53e2	0.12	0.02		
17:	230.0811	2.72e2	0.13	0.02	75:	377.0356	2.99e3	1.39	0.23		
18:	241.0875	2.63e4	12.27	2.06	76:	378.0393	8.09e2	0.38	0.06		
19:	241.1237	2.05e3	0.96	0.16	77:	379.0358	1.80e3	0.84	0.14		
20:	242.0903	3.64e3	1.70	0.29	78:	379.0496	2.16e2	0.10	0.02		
21:	242.1230	2.21e2	0.10	0.02	79:	380.0363	7.43e2	0.35	0.06		
22:	243.0898	2.28e2	0.11	0.02	80:	381.0331	1.06e3	0.49	0.08		
23:	259.0999	9.69e2	0.45	0.08	81:	382.0346	2.26e2	0.11	0.02		
24:	259.1911	3.28e2	0.15	0.03	82:	387.0838	2.42e2	0.11	0.02		
25:	269.1187	1.55e5	72.46	12.16	83:	397.1513	2.55e2	0.12	0.02		
26:	269.2079	2.67e2	0.12	0.02	84:	398.2152	2.89e3	1.35	0.23		
27:	270.1217	2.34e4	10.92	1.83	85:	399.2248	4.61e2	0.22	0.04		
28:	271.1255	2.00e3	0.93	0.16							
29:	273.1168	2.70e2	0.13	0.02							
30:	279.1607	8.21e3	3.83	0.64							
31:	279.2303	3.48e2	0.16	0.03							
32:	280.1635	1.37e3	0.64	0.11							
33:	286.1459	9.46e2	0.44	0.07							
34:	287.1287	2.56e4	11.94	2.01							
35:	288.1334	4.26e3	1.99	0.33							
36:	289.1364	4.13e2	0.19	0.03							
37:	296.2596	8.24e3	3.84	0.65							
38:	297.2626	1.75e3	0.82	0.14							
39:	298.2753	1.31e3	0.61	0.10							
40:	301.1425	9.49e3	4.43	0.74							
41:	302.1479	1.75e3	0.82	0.14							
42:	304.9806	3.80e2	0.18	0.03							
43:	306.9754	2.99e2	0.14	0.02							
44:	310.2357	2.65e2	0.12	0.02							
45:	313.1225	2.94e2	0.14	0.02							
46:	318.2413	3.24e3	1.51	0.25							
47:	319.2442	5.97e2	0.28	0.05							
48:	320.2572	5.36e3	2.50	0.42							
49:	321.2606	8.22e2	0.38	0.06							
50:	323.0666	3.50e2	0.16	0.03							
51:	324.2169	1.58e3	0.74	0.12							
52:	329.1765	2.14e5	100.00	16.79							
53:	330.1794	3.44e4	16.07	2.70							
54:	331.1827	4.25e3	1.98	0.33							
55:	332.1857	3.16e2	0.15	0.02							
56:	336.2517	2.28e3	1.06	0.18							
57:	336.9869	2.22e2	0.10	0.02							
58:	337.2534	2.52e2	0.12	0.02							



Universidad Euskal Herriko
del País Vasco Unibertsitatea

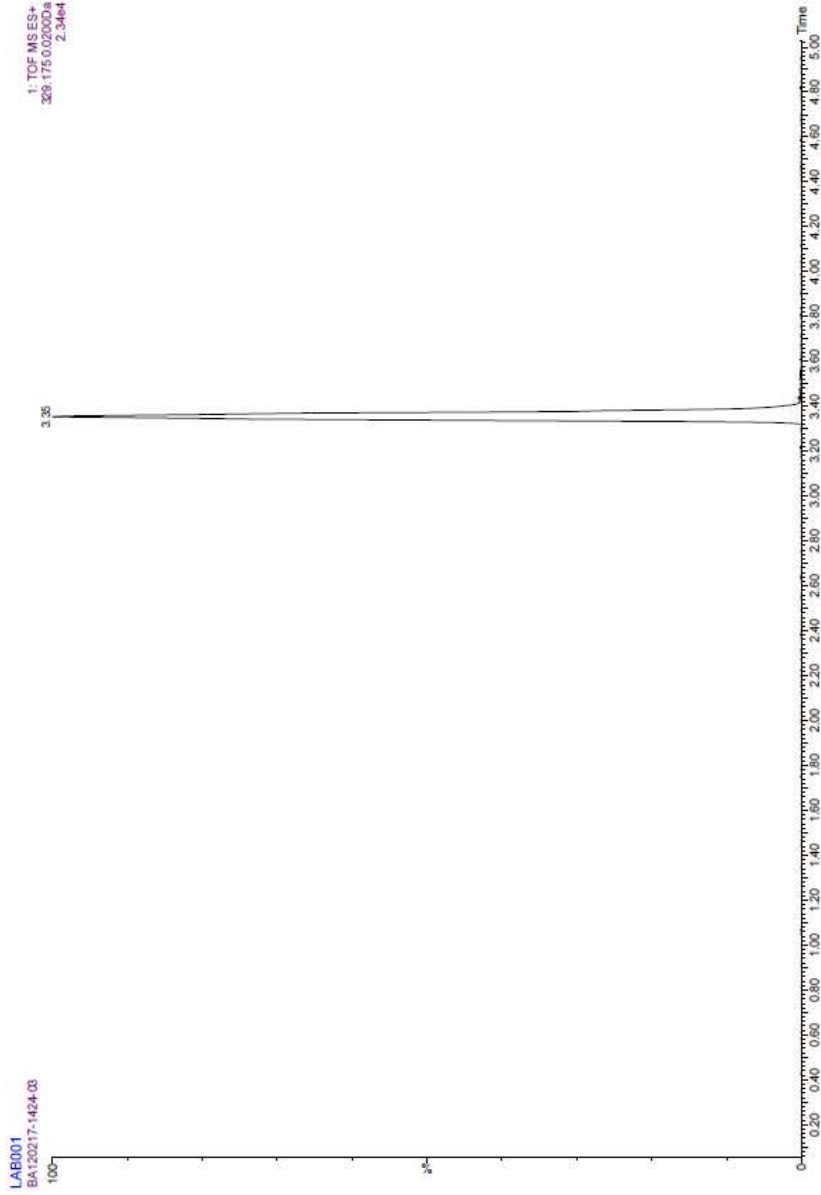


sgiker
Servicio Central de Análisis de Biotecnología

Servicio Central de Análisis de Biotecnología, Facultad de Ciencia y Tecnología
Barrio Sarriena s/n, 48940 Leioa-Bizkaia. C.I.F.: Q-481 800 1B

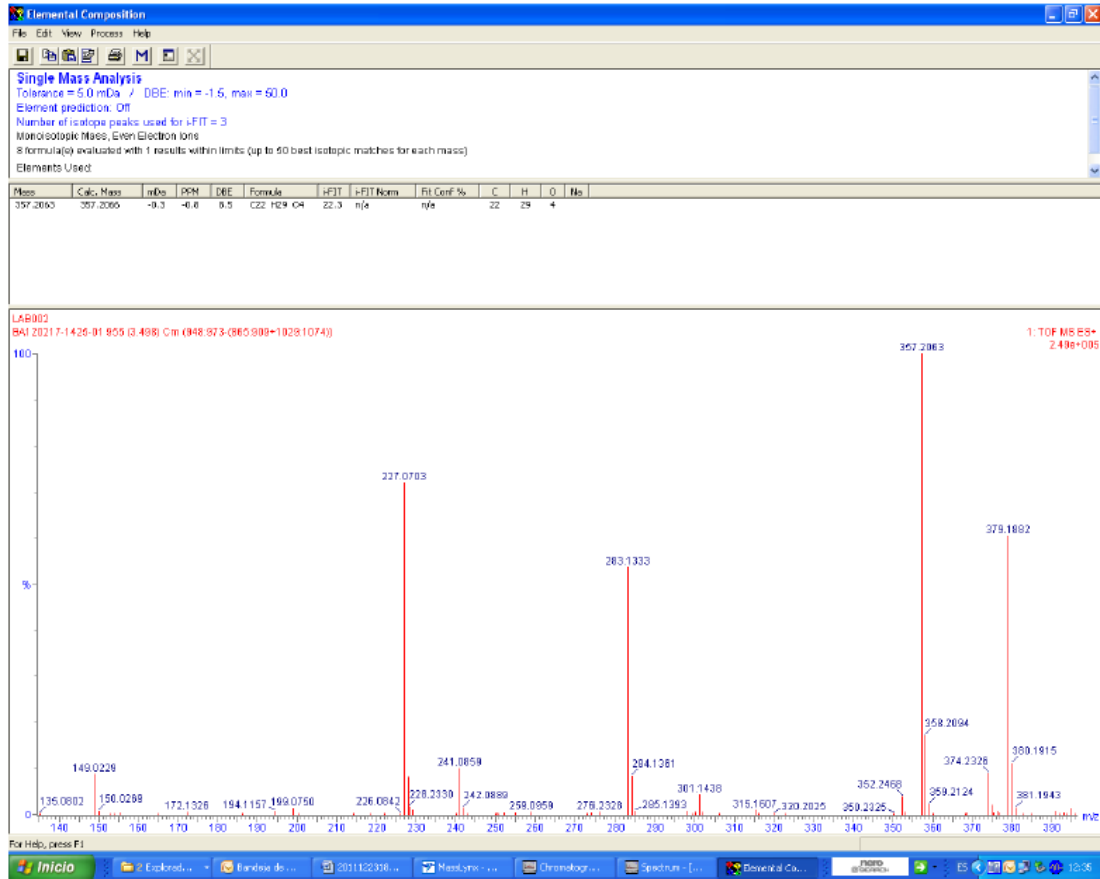
14.10.2009 SCAB.FR.01.PR.11.01

Cromatograma TIC



LAB002

Composición elemental





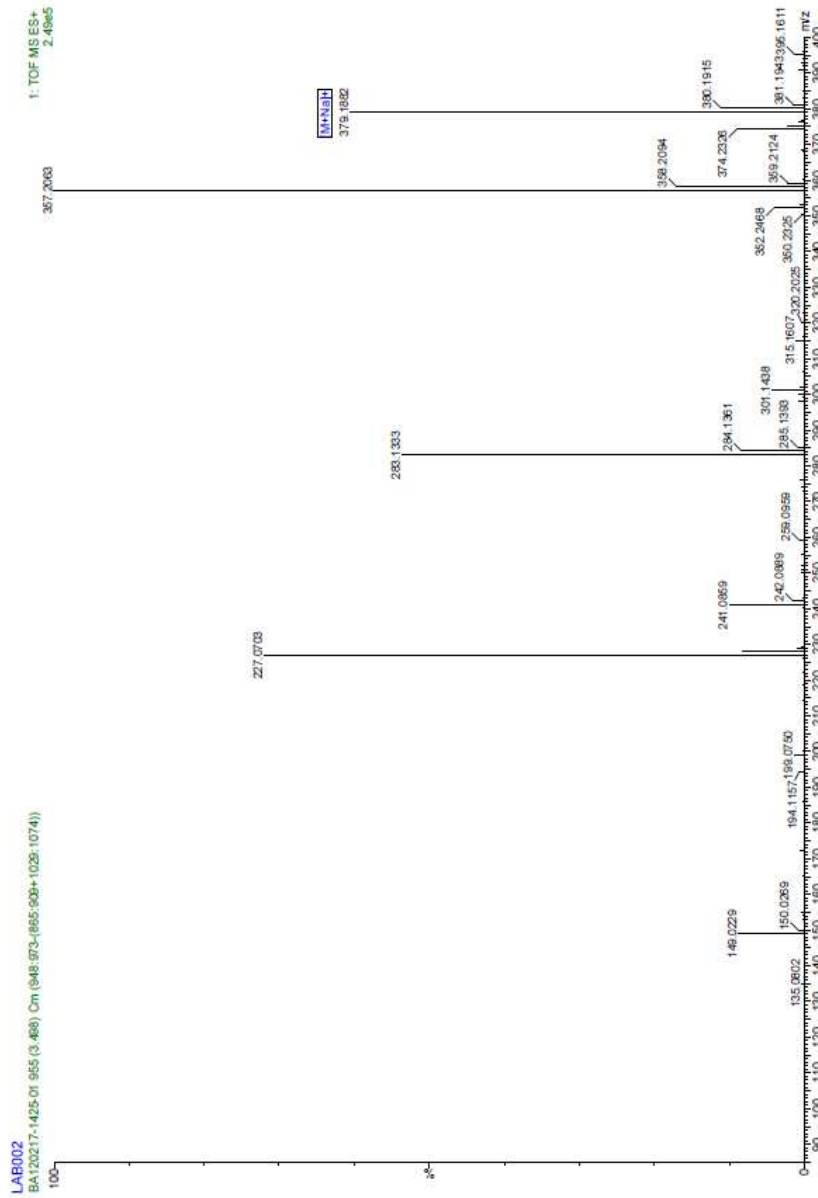
Universidad Euskal Herriko del Pais Vasco Unibertsitatea



Servicio Central de Análisis de Bizkaia, Facultad de Ciencia y Tecnología Barrio Surrutia s/n, 48940 Lezua-Bizkaia. C.I.F.: Q-4818001B

14.10.2009 SCAB.FR.01.PR.11.01

Espectro de masas





Universidad del País Vasco Euskal Herriko Unibertsitatea



Servicio Central de Análisis de Bizkaia, Facultad de Ciencia y Tecnología
Barrio Sarriena s/n, 48940 Leioa-Bizkaia. C.I.F.: Q-4818001B

14.10.2009

SCAB.FR.01.PR.11.01

Listado de masas

LAB002

BA120217-1425-01 955 (3.498) Cm (948:973-(865:909+1029:1074))

1: TOF MS ES+

No	Mass	Inten	%BPI	%TIC	No	Mass	Inten	%BPI	%TIC	No	Mi
1:	135.0802	6.16e2	0.25	0.04	59:	374.2326	2.24e4	8.99	1.62		
2:	149.0229	2.17e4	8.72	1.57	60:	375.2356	5.24e3	2.11	0.38		
3:	150.0269	1.91e3	0.77	0.14	61:	375.3221	1.01e3	0.41	0.07		
4:	153.0910	4.24e2	0.17	0.03	62:	376.1788	1.93e3	0.77	0.14		
5:	154.0538	2.60e2	0.10	0.02	63:	376.2381	5.93e2	0.24	0.04		
6:	155.1060	9.00e2	0.36	0.07	64:	376.6804	7.56e2	0.30	0.05		
7:	165.1112	5.40e2	0.22	0.04	65:	379.1340	6.55e2	0.26	0.05		
8:	172.1326	1.31e3	0.53	0.10	66:	379.1882	1.50e5	60.45	10.90		
9:	186.1505	2.57e2	0.10	0.02	67:	380.1915	2.75e4	11.04	1.99		
10:	194.1157	1.76e3	0.71	0.13	68:	381.1943	3.57e3	1.43	0.26		
11:	199.0750	3.17e3	1.27	0.23	69:	383.0520	3.27e2	0.13	0.02		
12:	200.1636	5.04e2	0.20	0.04	70:	385.1538	3.04e2	0.12	0.02		
13:	214.1829	2.84e2	0.11	0.02	71:	391.0539	1.69e3	0.68	0.12		
14:	218.5888	3.11e2	0.12	0.02	72:	392.0510	3.37e2	0.14	0.02		
15:	222.1465	3.59e2	0.14	0.03	73:	393.0509	7.31e2	0.29	0.05		
16:	226.0842	4.37e2	0.18	0.03	74:	394.0522	3.57e2	0.14	0.03		
17:	227.0703	1.79e5	71.94	12.97	75:	395.0466	6.91e2	0.28	0.05		
18:	228.0739	2.05e4	8.25	1.49	76:	395.1611	3.09e3	1.24	0.22		
19:	228.2330	4.00e3	1.61	0.29	77:	396.1675	4.54e2	0.18	0.03		
20:	229.0757	2.15e3	0.86	0.16							
21:	229.2348	5.73e2	0.23	0.04							
22:	240.2320	4.57e2	0.18	0.03							
23:	241.0859	2.49e4	9.99	1.80							
24:	242.0889	3.54e3	1.42	0.26							
25:	243.0932	2.76e2	0.11	0.02							
26:	250.1438	2.82e2	0.11	0.02							
27:	250.2147	8.84e2	0.36	0.06							
28:	251.0475	5.55e2	0.22	0.04							
29:	252.2313	9.95e2	0.40	0.07							
30:	255.1399	8.27e2	0.33	0.06							
31:	259.0959	1.41e3	0.57	0.10							
32:	273.1123	3.48e2	0.14	0.03							
33:	274.2144	7.46e2	0.30	0.05							
34:	276.2328	1.24e3	0.50	0.09							
35:	283.1333	1.33e5	53.62	9.66							
36:	284.1361	2.06e4	8.29	1.49							
37:	285.1393	1.93e3	0.77	0.14							
38:	298.2140	8.65e2	0.35	0.06							
39:	298.2737	1.70e3	0.68	0.12							
40:	299.2760	2.80e2	0.11	0.02							
41:	300.1579	5.79e2	0.23	0.04							
42:	300.2306	1.53e3	0.62	0.11							
43:	301.1438	1.06e4	4.27	0.77							
44:	302.1474	1.41e3	0.57	0.10							
45:	306.2408	3.13e2	0.13	0.02							
46:	315.1607	2.52e3	1.01	0.18							
47:	316.1638	4.85e2	0.19	0.04							
48:	320.2025	7.27e2	0.29	0.05							
49:	323.0649	3.84e2	0.15	0.03							
50:	350.2325	6.68e2	0.27	0.05							
51:	352.2468	9.89e3	3.97	0.72							
52:	353.2505	1.28e3	0.51	0.09							
53:	357.2063	2.49e5	100.00	18.02							
54:	358.2094	4.23e4	16.98	3.06							
55:	359.2124	5.38e3	2.16	0.39							
56:	360.2141	4.20e2	0.17	0.03							
57:	368.2176	3.42e2	0.14	0.02							
58:	368.4226	7.43e2	0.30	0.05							



Universidad Euskal Herriko
del País Vasco Unibertsitatea

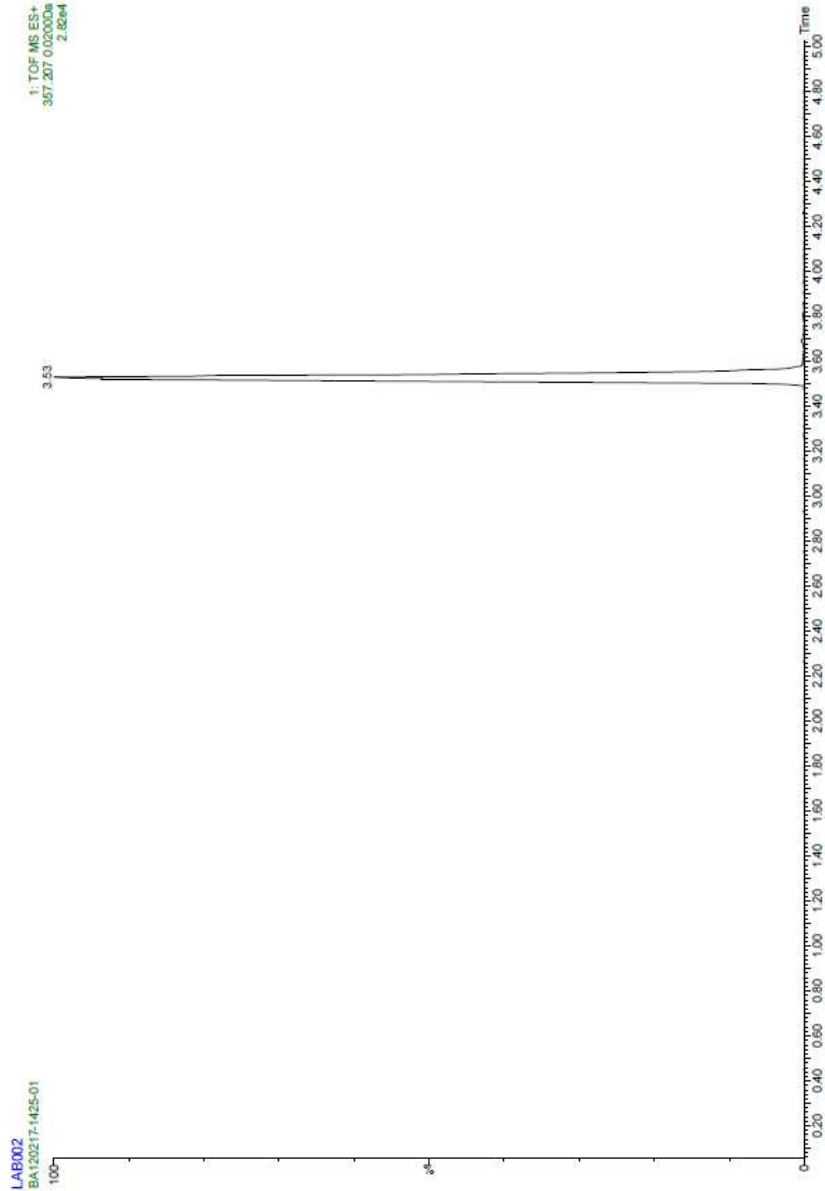


sgiker
SERVICIO CENTRAL DE ANÁLISIS
DE INVESTIGACIÓN

Servicio Central de Análisis de Bizkaia, Facultad de Ciencia y Tecnología
Barrio Surtenea s/n, 48940 Leioa-Bizkaia. C.I.F.: Q-4818001B

14.10.2009 SCAB.FR.01.PR.11.01

Cromatograma TIC








Servicio Central de Análisis de Bizkaia, Facultad de Ciencia y Tecnología
Barrio Sarriena s/n, 48940 Leioa-Bizkaia. C.I.F.: Q-4818001B

14.10.2009

SCAB.FR.01.PR.11.01

"No aplica"

<p>Firma Técnico SGIker</p>  <p>Dra. Beatriz Abad</p>	<p>Firma Dirección del Servicio</p>  <p>Prof. Rosa María Alonso Rojas</p>	<p>Sello</p>  <p>Servicio Centra de Análisis UPV/EHU</p>
---	---	--

